Corrosion Prevention and Protection
Practical Solutions

V. S. SASTRI
Sai Ram Consultants, Ottawa, Ontario, Canada

EDWARD GHALI
Department of Metallurgical Engineering, Laval University, Quebec, Canada

MIMOUN ELBOUJDAINI
Materials Technology Laboratory, CANMET, Ottawa, Canada

John Wiley & Sons, Ltd

Corrosion Prevention and Protection

Corrosion Prevention and Protection
Practical Solutions

V. S. SASTRI
Sai Ram Consultants, Ottawa, Ontario, Canada

EDWARD GHALI
Department of Metallurgical Engineering, Laval University, Quebec, Canada

MIMOUN ELBOUJDAINI
Materials Technology Laboratory, CANMET, Ottawa, Canada

John Wiley & Sons, Ltd

John Wiley & Sons Ltd, The Atrium, Southern Gate, Chichester,
West Sussex PO19 8SQ, England
Telephone (+44) 1243 779777

Email (for orders and customer service enquiries): cs-books@wiley.co.uk
Visit our Home Page on www.wileyeurope.com or www.wiley.com

Other Wiley Editorial Offices

John Wiley & Sons Inc., 111 River Street, Hoboken, NJ 07030, USA
Jossey-Bass, 989 Market Street, San Francisco, CA 94103-1741, USA
Wiley-VCH Verlag GmbH, Boschstr. 12, D-69469 Weinheim, Germany
John Wiley & Sons Australia Ltd, 42 McDougall Street, Milton, Queensland 4064, Australia
John Wiley & Sons (Asia) Pte Ltd, 2 Clementi Loop #02-01, Jin Xing Distripark, Singapore 129809
John Wiley & Sons Canada Ltd, 6045 Freemont Blvd, Mississauga, ONT, L5R 4J3

Wiley also publishes its books in a variety of electronic formats. Some content that appears in print may not be available in electronic books.

Library of Congress Cataloging-in-Publication Data

Sastri, V. S.
Corrosion prevention and protection : practical solutions / V. S. Sastri, Edward Ghali, Mimoun Elboujdaini.
p. cm.
Includes index.
ISBN-13: 978-0-470-02402-7
ISBN-10: 0-470-02402-X
1. Corrosion and anti-corrosives. I. Ghali, Edward. II. Elboujdaini, Mimoun. III. Title.
TA462.S3185 2006
620.1′1223–dc22 2006022728

British Library Cataloguing in Publication Data

A catalogue record for this book is available from the British Library

ISBN 10: 0 470 02402 X (HB) ISBN 13: 978 0 470 02402 7 (HB)

Typeset in 10/12 pt Times by Thomson Digital, India
Printed and bound in Great Britain by Antony Rowe, Chippenham, Wiltshire
This book is printed on acid-free paper responsibly manufactured from sustainable forestry
in which at least two trees are planted for each one used for paper production

I am grateful for the blessings of Sri Vighneswara, Sri Venkateswara, Sri Anjaneya, Sri Satya Sai Baba, my parents and teachers. I am also thankful for the support of my wife, Bonnie, and my children, Anjali and Martin Anil Kumar Sastri. We also recognise Anjali Sastri for her help with the figures, and to Gerry Burtenshaw for assistance in the preparation of the manuscript.

V. S. Sastri

I cannot adequately explain my gratitude to my wife, Helen, and Doctors Rafik and Sonia Ghali, whose encouragement, patience and love played an indispensable part in my career as Professor and participant in this book.

Edward Ghali

I would like to express my gratitude to my employer and my colleagues at CANMET Materials Technology Laboratory. I sincerely appreciate the exceptional understanding of my wife, Manon, along with my children Anaïs, Ismaël, and Gabriel, who sometimes did not get the attention they deserved.

Mimoun Elboujdaini

Contents

Preface

There are many books and monographs on corrosion, such as *Corrosion and Corrosion Control* by H. H. Uhlig and R. W. Revie; *Corrosion Engineering* by M. G. Fontana and N. D. Greene; *Principles and Prevention of Corrosion* by D. A. Jones; *An Introduction to Corrosion and Protection of Metals* by G. Wranglen; and *Corrosion for Science and Engineering* by K. R. Trethewey and J. Chamberlain. The present title differs from existing books in more ways than one, such as the chapters dealing with practical solutions. The title was chosen to reflect the content of the subject matter, which is presented in two parts.

The first chapter presents the historical development of corrosion concepts, such as the electrochemical theory of corrosion, the economic significance of corrosion and its impact, cathodic protection, Faraday's laws, the role of oxygen, passivity, inhibitors and their classification, the role of thermodynamics, the historical development of the corrosion literature, and the establishment of scientific organizations dealing with corrosion, and centres and laboratories for studies on corrosion phenomena, progressive development of the scientific literature on corrosion, safety and its impact. The role of thermodynamics and kinetics in corrosion, electrochemical principles of corrosion, Pourbaix diagrams, the Helmholtz double layer and its significance in corrosion, electrochemical polarization, Tafel plots, activation polarization, hydrogen overvoltage, mixed potential theory of corrosion, AC impedance and potential noise in corrosion phenomena, high-temperature corrosion, corrosion prevention strategies such as design factors, corrosion-based life prediction analysis of materials, corrosion inhibitors and their role in corrosion prevention, coatings and their role in corrosion control, cathodic protection and impressed current protection are presented.

The second chapter deals with corrosion testing for environmentally assisted cracking, atmospheric corrosion, galvanic corrosion, tests for degradation of polymeric materials, refractories and ceramic materials and corrosion inhibitors. This is followed by a discussion of corrosion detection and monitoring by methods such as visual examination, laser inspection, replication microscopy, radiographic inspection, neutron radiography, liquid penetrant method, eddy current method, ultrasonic testing, acoustic emission testing, finite element analysis, strain gage methods and thermal methods of inspection. Failure analysis consisting of various modes of failure by different damage mechanisms are presented, including microfractography, fracture mechanics, determination of

residual stress by X-ray diffraction, role of surface analysis techniques in failure analysis, including failure in polymeric and ceramic materials.

The next chapter deals with regulations, specification and safety. The regulations and specifications of materials used in industry are briefly discussed. This is followed by safety considerations to be observed both in the corrosion laboratory and field inspection. Hazard identification techniques at different stages of the project, a checklist for process hazard analysis, safety procedures in the corrosion laboratory, including a model chemical hygiene plan, guidelines in using radiation sources including lasers and safety considerations in the design stage and field plant inspection are presented.

Materials such as metals, alloys, steels and plastics form the theme of the fourth chapter. The behavior and use of cast irons, low alloy carbon steels and their application in atmospheric corrosion, fresh waters, seawater and soils are presented. This is followed by a discussion of stainless steels, martensitic steels and duplex steels and their behavior in various media. Aluminum and its alloys and their corrosion behavior in acids, fresh water, seawater, outdoor atmospheres and soils, copper and its alloys and their corrosion resistance in various media, nickel and its alloys and their corrosion behavior in various industrial environments, titanium and its alloys and their performance in various chemical environments, cobalt alloys and their applications, corrosion behavior of lead and its alloys, magnesium and its alloys together with their corrosion behavior, zinc and its alloys, along with their corrosion behavior, zirconium, its alloys and their corrosion behavior, tin and tin plate with their applications in atmospheric corrosion are discussed. The final part of the chapter concerns refractories and ceramics and polymeric materials and their application in various corrosive media.

Corrosion economics and corrosion management forms the theme of the fifth chapter. Discounted cash flow calculations, depreciation, the declining balance method, double declining method, modified accelerated cost recovery system and present worth calculation procedures are given, together with examples. In the second part, corrosion management, including the people factor in corrosion failure is briefly presented. Some of the expert systems presently available in the literature are briefly discussed.

The second part of the book consists of two chapters; namely the forms of corrosion and practical solutions. The chapter, 'Forms of Corrosion' consists of a discussion of corrosion reactions, corrosion media, active and active–passive corrosion behavior, the forms of corrosion, namely, general corrosion, localized corrosion, metallurgically influenced corrosion, microbiologically influenced corrosion, mechanically assisted corrosion and environmentally induced cracking, the types and modes of corrosion, the morphology of corroded materials along with some published literature on corrosion.

The last chapter is a collection of case histories or practical solutions the authors have provided to various clients. These solutions span a wide range of industrial problems in a variety of environments frequently encountered.

It is the experience of the authors that the material in the first part of the book can be covered in one semester lasting 12 weeks. The second part of the book can be covered in a subsequent semester lasting 12 weeks. It is also possible that some laboratory work can be carried out by the students when the instructor is teaching the second part of the book.

The authors have received their education in universities in North America and Europe and have a combined experience of approximately 100 years in corrosion and its mitigation. The present monograph is a product of this rich experience.

Acknowledgments

I cannot adequately express my gratitude to my wife, Bonnie Sastri whose efforts and encouragement played the greatest role in sustaining me through the challenge of writing this book. Our children, Anjali and Martin Sastri, also deserve my appreciation for their help and understanding. Grateful appreciation is expressed to the American Chemical Society, the American Society of Metals, Plenum Publishing, EG&G Princeton Applied Research, and Longman Publishers, NACE International, Houston, Texas, John Wiley & Sons, N.Y., USA, McGraw-Hill, N.Y., Elsevier, Oxford, UK for their permission to reproduce figures or tables from the literature.

V. S. Sastri
E. Ghali
M. Elboujdaini

Please note that figures 7.53 (Plate 2), 7.54 (Plate 3), 7.55 (Plate 4), 7.56 (Plate 5), 7.57 (Plate 6), 7.58 (Plate 7), 7.59, 7.60 and 7.61 are © Crown in Right of Canada, sourced from Failure Investigation Report #0505007 (Report on Copper Pipe or Sprinkler Pipes Experiencing MIC), Mr. Nick Dawe, P. Eng, D/Chief Building Services - PSEPC.

Part I

1

Introduction and Principles of Corrosion

The term corrosion has its origin in Latin. The Latin term *rodere* means 'gnawing' and *corrodere* means 'gnawing to pieces'. It is rather interesting to examine the historical aspects of the developments of corrosion. Metallic corrosion has no doubt been a problem since common metals were first put to use. Most metals occur in nature as compounds, such as oxides, sulfides, silicates or carbonates (very few metals occur in native form). The obvious reason is the thermodynamic stability of the compounds as opposed to the metals. The process of extraction of a metal from the ore is reduction.

$$2\,Fe_2O_3 + 3\,C \rightarrow 4\,Fe + 3\,CO_2$$

In the extraction of iron, the oxide is reduced to metallic iron. On the other hand, the oxidation of iron to produce the brown iron oxide commonly known as rust is the opposite reaction to the production of the metal from the oxide. The extraction of iron from the oxide, must be conducted with utmost careful control of the conditions, such that the backward reaction is prevented.

During the Gupta Dynasty (320–480 A.D.) the production of iron in India achieved a remarkable degree of sophistication as attested by the Dhar Pillar, a seven-tonne, one-piece iron column made in the fourth century A.D. This implies that the production of metallic iron from the ores was a well-established process, and the people involved at that time were aware of the reverse reaction involving the oxidation of iron to produce the oxide (the familiar rusting of iron).

Other examples involve the use of copper nails coated with lead by the Greeks in the construction of lead-covered decks for ships.[1] They probably realized that metallic couples of common metals are undesirable in seawater. Protection of iron by bitumen, tar, etc., was known and practiced by the Romans.

The earliest published accounts of the causes of corrosion are the two publications by Robert Boyle (1627–1691) entitled 'Of the Mechanical Origin of Corrosiveness' and

Corrosion Prevention and Protection: Practical Solutions V. S. Sastri, E. Ghali and M. Elboujdaini

'Of the Mechanical Origin of Corrodibility', which appeared in 1675 in London.[2] It was not until the turn of the19th century[3,4] that some of the basic principles were understood, soon after the discovery of the galvanic cell and Davy's theory on the close relationship between electricity and chemical changes.[5]

The impetus for further developments was the recognition of the economic significance of corrosion phenomenon during the 19th century that led the British Association for the Advancement of Science to sponsor corrosion testing projects such as the corrosion of cast and wrought iron in river and seawater atmospheres in 1837. Early academic interest in corrosion phenomenon (up to the First World War) was followed by industrial interest due to the occurrence of equipment failures. An example of this is the corrosion-related failure of condenser tubes as reported by the Institute of Metals and the British Non-ferrous Metals Research Association in 1911. This initiative led to the development of new corrosion-resistant alloys, and the corrosion related failure of condenser tubes in the Second World War was an insignificant problem.

Corrosion and its control mean the corrosion process and the measures taken to control or keep in check the corrosion process. Sometimes it is also referred to as corrosion, prevention and protection. Although the terms 'prevention' and 'protection' appear to be synonymous, prevention means measures taken to control corrosion to a limited extent while protection means extensive or more comprehensive measures taken to control the corrosion process. In more general terms preventive measures are knowledge-based while protection involves both known and unknown factors, such as natural disasters.

The heart of corrosion science has been identified as electrochemical science coupled with the thermodynamic and kinetic values. Other limbs are oxidation and high-temperature oxidation of metals, protective coatings, passivity, inhibitors, microbial-induced corrosion, corrosion fatigue, hydrogen embrittlement and corrosion-resistant alloys. Having identified the limbs of corrosion science, it is instructive to examine how the various aspects came into existence over a period of time.

The French chemist Louis Jacques Thenard first enunciated electrochemical nature of corrosion phenomenon explicitly in 1819. Some research activities that led to the firm electrochemical foundations of corrosion process are summarized below:

Sir Humphry Davy	1824	Principle of cathodic protection
Auguste de la Rive	1830	Established best quality of zinc for galvanic batteries
Michael Faraday	1834–1840	Provided relations between chemical action and generation of electric currents based on Faraday's laws
Svante Arrhenius	1901–	Postulated the formation of microcells
W.R. Whitney	1903	Confirmed the theory of microcells
A.S. Cushman	1907	
Walker	1907	Established role of oxygen in corrosion as a cathodic stimulator
Cederholm		
Bent		
William Tilden	1908	

Corey, Finnegan, Kay Thompson	1939, 1940	Investigated attack of iron by oxygen-free water
A. Thiel, Luckmann	1928	Investigated attack of iron by dilute alkali with liberation of hydrogen
Heyn and Bauer	1908	Corrosion studies of iron and steel, both alone and in contact with other metals, leading to the concept that iron in contact with nobler metal increased the corrosion rate, while in contact with a base metal resulted in partial or complete protection
Whitman and Russell, U. Evans, G.V. Akimov	1924, 1928, 1935	Observed increased corrosion rate when a small anode is connected to a large cathode

Other important and related phenomena in corrosion and their historical development are summarized below:

John Stewart MacArthur	1887	Process of cyanide dissolution of gold (gold is not soluble in hot acids)
P.F. Thompson	1947	Dissolution of gold in dilute cyanide solutions recognized as electrochemical process
Concept of passivity		
James Keir	1790	Observed that iron in conc. nitric acid altered in its properties
Christian Friedrich Schönbein	1799–1868	Suggested the state of iron in conc. HNO_3 as passivity
W. Müller (Konopicky and Willi Machu)	1927	Posulated the mathematical basis of the mechanism of anodic passivation
Bengough (Stuart, Lee and Wormweil)	1927	Systematic and carefully controlled experimental work on passivity
Role of oxygen		
	~1900	Hydrogen peroxide was detected during the corrosion of metals
	~1905	The view that acids are required for corrosion to occur was dispelled by the observation of rusting of iron in water and oxygen

Marianini	1830	The research work of these scientists indicated the electric currents due to the variations in oxygen concentrations
Adie	1845	
Warburg	1889	
V.A. Kistiakowsky	1908	
Aston	1916	Role of local differences in oxygen concentration in the process of rusting of iron
McKay	1922	Currents due to a single metal of varying metal ion concentrations
U.R. Evans	1923	Differential aerations and their role in metallic corrosion
Evans and co-workers	1931–1934	Electric currents due to corrosion of metal in salt solutions were measured and a quantitative electrochemical basis of corrosion was propounded. The oxygen-rich region becomes cathodic and the metal is protected, and the lower oxygen region, being anodic, is attacked
Inhibitors		
Roman civilization	—	Protection of iron by bitumen, tar, extracts of glue, gelatin and bran to inhibit corrosion of iron in acid
Murangoni Stephanelli	1872	
Chyzewski	1938	Classified inhibitors as cathodic and anodic inhibitors
—	—	Distinction between inhibitive paints and mechanically excluding paints was made based on laboratory, and field tests
—	—	Development of paints containing zinc dust
John Samuel Frost Roetheli and Brown	1930	Protective property of coating varied and depended on the rate of supply of oxygen to the surface
Friend	1920	Colloidal solution of ferric hydroxide acts as an oxygen carrier, passing between ferrous and ferric states
Herzog	1936	Posulated that iron, on long exposure to water, becomes being covered by a magnetite overlaid with ferric hydroxide. Magnetite layer acts as cathode and ferric hydroxide is cathodically converted to hydrated

		magnetite. Hydrated magnetite may lose water and reinforce the pre-existing magnetite or absorb oxygen from air to give ferric hydroxide
V.S. Sastri	1990	Modern classification of inhibitors as hard, soft and borderline inhibitors (*11th International Corrosion Congress*, V. 3, p. 55)
V.S. Sastri	1988	Classification of corrosion inhibition mechanisms such as interface inhibition, interphase inhibition, intraphase inhibition and precipitation coating (*Corrosion '88*, Paper 155)
V.S. Sastri, J.R. Perumareddi and M. Elboujdaini	1994	Novel theoretical method of selection of inhibitors (*Corrosion*, **50**, 432, 1994)
V.S. Sastri, J.R. Perumareddi and M. Elboujdaini	2005	Sastri equation relating the percent inhibition to the fractional electronic charge on the inhibitor. (*Corrosion Eng. Sci. & Tech.*, **40**, 270, 2005)

High-temperature oxidation

Gustav Tammann	1920	Enumerated 'Parabolic Law' (i.e., rate of oxidation of metal decreases as oxide layer thickness increases)
	1922	Logarithmic law of oxidation of metals
N.B. Pilling and R.E. Bedworth	1923	Distinction between porous and non-porous oxide layer
Leonard B. Pfeil	1929	Concept of movement of metal outward rather than oxygen inward into the oxide layer
Portevin Prétet Jolivet	1934	Extensive studies on the oxidation of iron and its alloys
Carl Wagner	~1934	High-temperature oxidation involves passage of ions and electrons through the growing oxide layer. Postulated an equation relating oxidation rate with the electrical properties of the oxide layer
Hoar, Price	1938	Derivation of Wagner's equation
Mott, Cabrera	1939, 1948	Oxide film growth controlled by ions jumping from site to site over intervening energy barriers

Karl Houffe Ilschner	—	Significant work on the oxidation of alloys. Also criticism of Mott's theory
Tammann	1920–1926	Interference method of obtaining thickness of oxide films
Constable	1927	Spectroscopic method to obtain thickness of oxide film
Finch Quarrell	1933	X-ray and electron diffraction methods to study oxide films
Microbiological corrosion		
R.H. Gaines	1910	Sulfate-reducing bacteria in soils produce H_2S and cause corrosion
Corrosion fatigue	~1900	Alternating stresses and chemical environment together cause corrosion fatigue
Stress–corrosion cracking	~1900	Applied stress and chemical environment causing stress–corrosion cracking
Hydrogen embrittlement		
Haber–Bosch process for synthesis of ammonia	1916	Microcracks in the steel reactor were observed due to the reaction of hydrogen with carbon in the steel to produce methane. Mo and Cr were found to prevent hydrogen embrittlement
Role of thermodynamics		
—	—	Corrosion of metal obeys the laws of thermodynamics. This was recognized in the early development of corrosion science
Marcel Pourbaix	1940	Pourbaix diagrams involving pH and potential give regions of corrosion, immunity and passivity
Kinetics		
Evans, Hoar	1932	Quantitative correlation of corrosion rates with measured electrochemical reaction rates
F. Habashi	1965	Validity of a single kinetic law irrespective of the metal, composition of aqueous phase, and evolution of hydrogen when no insoluble products, scales or films are formed

The number of published scientific papers through 1907–2003 illustrates development of the corrosion science in the form of published scientific literature as shown below:

Title	1907	1950	2000	2003
Corrosion	35	922	10985	10655
Corrosion and protection	3	122	1162	1050
Corrosion and prevention	3	320	1639	1358

The journals that came into existence are given below:

Title	Year
Corrosion	1945
Corrosion Science	1961
British Corrosion Journal	1965
Werkstoffe und Korrosion	1950
Corrosion Prevention and Control	1954
Anti-corrosion Methods and Materials	1962
Materials Performance	1962

Some of the leading organizations championing corrosion science, which were founded, are detailed below. This list does not include academic institutions.

American Society for Testing Materials (ASTM)	1898
American Society of Metals (ASM)	1913
Corrosion Division of the Electrochemical Society	1942
National Association of Corrosion Engineers	1943
Comité International de Thermodynamique et Cinétique Électrochimique (CITCE)	1949
International Society of Electrochemistry (ISE)	1971
International Corrosion Council	1961
The Corrosion Group of the Society of Chemical Industry	1951
Belgium Center for Corrosion Study (CEBELCOR)	1951
Commission of Electrochemistry	1952
National Corrosion Centre (Australia)	
Australian Corrosion Association	~1980
Chinese Society of Corrosion and Protection	~1980
National Association of Corrosion Engineers (in Canada)	—

Research groups, which became active in the field of corrosion in the early stages, are shown below. It is prudent to state that the list is by no means exhaustive.

Massachusetts Institute of Technology
National Bureau of Standards

Ohio State University
University of Texas
University of California, Los Angeles
National Research Council, Ottawa
Cambridge University
Technical University, Vienna

Industrial laboratories such as U.S. Steel, International Nickel company and Aluminum Company of America, DuPont have also initiated their own corrosion research.

The progress made in the scientific approach and the degree of sophistication attained over the years becomes evident from the following title papers:

1. A.S. Cushman, Corrosion of Iron as an Electrolytic Phenomenon, *U.S. Bur. Agr.*, *Electrochemical Metallurgy Industry*, Vol. 5, No. 256, C.A., 1907, p. 2360.

   Hydrogen ions are the primary cause of rusting and oxygen the secondary cause. Iron passes into solution in the form of ferrous ions as the result of galvanic action; the ferrous ions are then oxidized by the oxygen of the air to ferric ions. Alkaline solutions prevent rusting because they contain no hydrogen ions. Chromic acid and its salts prevent rusting because an oxygen film is formed, and the iron becomes polarized in the sense of becoming an oxygen electrode.

2. R.H. Brown, G.C. English and R.D. Williams, The Role of Polarization in Electrochemical Corrosion, *NACE Conference*, St. Louis, Missiouri, USA, 4–7 April 1950.

   In its most practical aspects as well as in its fundamental mechanisms electrochemical corrosion is almost always associated with irreversible electrode phenomena. The multitude of factors involved in these phenomena may be defined as electrochemical polarization. Idealized schematic as well as actual polarization diagrams are discussed. Methods of correlating polarization with corrosion data such as weight loss are shown. A method for obtaining the contribution made by the polarization of each electrode reaction to the total polarization observed at an electrode is described along with the implications, thereof in the evaluation of the true over-voltage values. In addition, other factors, which may fall within a broad definition of polarization, are treated. The relationship of the so-called IR drop or true ohmic resistance at metal liquid interfaces to polarization diagrams, and to over voltage concept is discussed.

3. R. Balasubramanium, A.V. Ramesh Kumar, Corrosion Resistance of the Dhar Iron Pillar, *Corrosion Science*, *45*, 2451–2465, 2003.

   The corrosion resistance of the 950 year old Dhar iron pillar has been addressed. The microstructure of a Dhar pillar iron sample exhibited characteristics typical of ancient Indian iron. Intergranular cracking indicated P segregation to the grain boundaries. The potentiodynamic polarization behaviour of the Dhar pillar iron and mild steel, evaluated in solutions of pH 1 and 7.6, indicate that the pillar iron is inferior to mild steel under complete immersion conditions. However, the excellent atmospheric corrosion resistance of the phosphoric Dhar pillar iron is due to the formation of a protective passive film on the surface. Rust analysis revealed the presence of crystalline magnetite (Fe_3-xO_4), α-Fe_2O_3 (hematite), goethite (α-FeOOH), lepidocrocite (γ-FeOOH), akaganeite (β-FeOOH) and phosphates, and amorphous δ-FeOOH phases. The rust cross-section revealed a layered structure at some locations.

The experimental techniques used are optical and scanning electron microscopes, electron microprobe, potentiodynamic polarization, X-ray diffraction, Fourier transform infrared spectroscopy and transmission Mössbauer spectroscopy.

Some significant titles, which are worth noting are shown below:

Gustav Tammann	Lehrbuch der Metallkunde	1914
	Die Aggregatzüstande	1922
	Lehrbuch der heterogenen Gleichgewichte	1924
Ulick R. Evans	The Corrosion of Metals	1924
	Metallic Corrosion, Passivity and Protection	1937
	An Introduction to Metallic Corrosion	1948
	The Corrosion and Oxidation of Metals	1960
	(first supplementary volume)	1968
	(second supplementary volume)	1976
Marcel Pourbaix	Thermodynamics of Dilute Aqueous Solutions	
	Atlas of Electrochemical Equilibria in Aqueous solutions	
	Atlas of Chemical and Electrochemical Equilibria in the presence of Gaseous Phase	
	Lectures on Electrochemical Corrosion	
Herbert H. Uhlig		1948
	Uhlig's Corrosion Handbook (2nd edn)	2000
	Corrosion and Corrosion Control	1963
H.H. Uhlig, R.W. Revie	Corrosion and Corrosion Control (revised)	1986
Mars Guy Fontana	Corrosion	1957
N.D. Greene	Corrosion Engineering	1967
		1986
J.I. Bregman	Corrosion Inhibitors	1963
V.S. Sastri	Corrosion Inhibitors Principles and Applications	1998
I.L. Rozenfeld	Corrosion Inhibitors	1982
H. Van Droffelar	Corrosion and its Control	1995
J.T.N. Atkinson	An introduction to the subject	
Kenneth R. Trethewey	Corrosion	1988, 1995
John Chamberlain	for Science and Engineering	
G. Wranglen	An introduction to Corrosion and Protection of Metals	1972
D.A. Jones	Principles and Prevention of Corrosion	1992
P.R. Roberge	Handbook of Corrosion Engineering	1999
P.R. Roberge	Corrosion Doctor website on Internet	1999
K. Seymour Coburn	Corrosion	1984
L.S. Van Delinder	Corrosion Basics – an introduction	1984
A.R. Troiano	Hydrogen Embrittlement and Stress Corrosion Cracking	1984

G. Charles Munger	Corrosion Prevention by Protective Coatings	1984, 1999
W.H. Ailor	Atmospheric Corrosion	1982
J. Yahalom	Stress Corrosion Cracking	1980
J.M. West	Basic Corrosion and Oxidation	1980
E. Mattsson	Basic Corrosion Technology for Scientists and Engineers	1989
F. Hine	Localized Corrosion	1988
J. Toucek	Theoretical Aspects of the Localized Corrosion of Metals	1985
P.A. Schweitzer	Encyclopedia of Corrosion Technology	1998
G. Welsch	Oxidation and Corrosion of Intermetallic Alloys	1996
J.B. Little	Microbiologically Influenced Corrosion	1997
Y.I. Kuznetsov	Organic Inhibitors for Corrosion of Metals	1996
P.A. Schweitzer	Encyclopedia of Corrosion Technology	1998
L.L. Shreir	Corrosion	1994
R.S. Munn	Computer Modeling in Corrosion	1992
R.H. Jones	Stress–Corrosion Cracking	1992
A.J. McEvily	Atlas of Stress–Corrosion and Corrosion Fatigue Curves	1990
G. Prentice	Perspectives on Corrosion	1990
A.S. Bradford	Corrosion Control	2001
R. Baboian	NACE Corrosion Engineer's Reference Book	2002

1.1 Impact of Corrosion

There are three areas of concern when corrosion and its prevention are considered. The three major factors are economics, safety and environmental damage.

Metallic corrosion, although seemingly innocuous, indeed affects many sectors of a nation's economy. The National Bureau of Standards (NBS) in collaboration with Battelle Columbus Laboratory (BCL) studied the costs of corrosion in USA using the input/output model.[7] Some elements of the costs of corrosion used in the model are shown below:

Capital costs

- Replacement of equipment and buildings
- Excess capacity
- Redundant equipment

Control costs

- Maintenance and repair
- Corrosion control

Table 1.1 *Corrosion costs in the United States (billions of dollars)*

Industry		1975	1995	2005
	Total	82.0	296	403
All industries	Avoidable	33.0	104	142
Automotive	Total	31.4	94.0	125.3
	Avoidable	23.1	65.0	86.7
Aircraft	Total	3.0	13.0	18.0
	Avoidable	0.7	3.0	4.2
Others	Total	47.6	159.0	260
	Available	9.3	36.0	50

Design costs

- Materials of construction
- Corrosion allowance
- Special processing

Associated costs

- Loss of product
- Technical support
- Insurance
- Parts and equipment inventory

The data resulting from the calculations using I/O model are given in Table 1.1. The data given for the year 2005 are olny estimates.

The corrosion costs in Canada[8] as of 2003, along with the various sectors are given in Tables 1.2 and 1.3.

The cost of corrosion in other countries in the world is given in Table 1.4.

The staggering costs of corrosion affect the national economy significantly and it is meaningful and justified that the corrosion scientists involved should adopt corrosion control measures so that significant savings are achieved. Reference in this regard may be made to a report[17] of the NACE Task Group T-3C-1 entitled, 'Economics of Corrosion' which deals with: (i) economic techniques that can be used by personnel as a decision making tool; (ii) facilitating communications between corrosion scientists and the management; and (iii) justifying the investments in corrosion preventive measures to achieve long-term benefits.

Table 1.2 *Corrosion costs in Canada*

Sector	$ billion
Utilities	8.2
Transportation	5.1
Infrastructure	3.8
Government	3.5
Production and manufacturing	3.0
Total	23.6

Table 1.3 *Total corrosion costs in Canada*

	$ billion
Total direct cost of corrosion	23.6
Cost of corrosion (extrapolated to Canada economy)	46.4
Estimated savings by corrosion control	14.00

It is evident from the data presented on the economics of corrosion that corrosion costs amount to about 2–4% of GNP, and about 25% of the costs are avoidable by adopting corrosion control measures. The measures taken to combat corrosion in UK, USA, Australia, China and Canada have been discussed.[18] The following is a short summary of the activities in various parts of the world to combat corrosion.

UK National Corrosion Service	1975	UK National corrosion service Educating engineering undergraduates in corrosion awareness. Published and distributed 15 guides on corrosion, and 6 booklets on 'controlling corrosion'. Assembled corrosion prevention directory of corrosion personnel
National Corrosion Coordination Centre		Multiclient 50/50 cost-shared research on high-temperature corrosion, metal finishing, microbial corrosion and expert systems in corrosion engineering
United States	~1980	National Association of corrosion engineers in collaboration with National Bureau of Standards developed corrosion data program
Australia	1982	National Corrosion Centre. Established nationwide – referral service for corrosion problems

Table 1.4 *Corrosion costs*

Country	Year	Corrosion costs ($)	Percent of GNP	Avoidable cost $	Reference
UK	1969–1970	3.2 billion	3.5	0.73 billion	9
West Germany	1968–1969	1.5 billion	3.0	0.375 billion	10
Sweden	1964	58–77 million		15–19 million 20–27 million	11
Finland	1965	47–62 million			12
Russia	1969	6.7 billion	2.0		13
Australia	1973	A $470 million	1.5		14
India	1960–1961	$320 million			15
Japan	1976–1977	9.2 billion	1.8		16

Peoples Republic of China	1980	Educating and training of personnel in corrosion. Organized 15 technical courses. Established 11 institutes of higher learning to give courses in corrosion
Canada		So far no organization has been established to implement corrosion control methods to achieve savings of the order of several millions of dollars. Proposal to establish a national corrosion secretariat[19–21] to educate industrial personnel, operate a referral service, assemble directory of corrosion experts, initiate site visits and show movies on corrosion and establish 50/50 cost-shared research projects was submitted in 1994

The most important factor of impact of corrosion is safety. This factor must be uppermost in the minds of personnel working in industry. Although corrosion of materials is as severe as cancer or AIDS in its economic and safety consequences to a nation, the issue has not received much attention from the governmental organizations and it continues to be conveniently ignored. It is now useful to turn our attention to some common industries, which have contributed to the so-called modern way of life of comfort and examine the role of corrosion, and its consequences in these industries.

Industry	Corrosion Problems	Remedy
Aircraft	Pitting and crevice corrosion develop intergranular stress–corrosion cracking and corrosion fatigue	Damage tolerance standards introduced into the design; corrosion inhibiting primers and sealants are used.
	Fatal crashes in early times due to fatigue	Titanium alloys are used. Fiber-reinforced plastics are used. Nondestructive inspection such as ultrasonic, eddy current, optical and radiography methods are used periodically
Automotive	General corrosion of the body of cars due mainly to deicing salts; car scrapped due to accidents, obsolescence and corrosion, correlation between injuries in accidents and age of the car	Improvement in the body of the car and its resistance to corrosion. Rustproofing treatments were developed

(*contd.*)

(*contd.*)

Industry	Corrosion Problems	Remedy
Chemicals	Chemicals such as HF and hot NaOH among others, cause severe corrosion problems. Severe corrosion and stress–corrosion cracking. Accidents involving cyclohexene (Flixborough) and HCN (Bhopal) caused deaths of several thousands	Corrosion-resistant materials must be chosen along with periodic inspection
Defense	Failure of weapons due to corrosion. Examples can be torpedo or missile (generally made of lightweight alloys). An example is failure of ammunition	Periodic tests to ensure the safe operation
Construction	Corrosion of steel bars in reinforced structures. Corrosion of suspension bridge over Severn River, Pelham bridge in Lincoln, bridges in New York state and other areas containing deicing salts. This is an expensive problem that needs immediate attention	Protective coatings
Marine	Corrosion of metal structures due to the most aggressive environment. Corrosion of iron hulls observed in ~1800. Many accidents due to loss of ships resulting in loss of many lives	Selection of corrosion resistant materials and proper coatings.
Electronics	Galvanic corrosion between Al and Au. Corrosion of power cables due to sheath damage caused by lightning, rodents, etc.	Sheathing of coated Al and clad metals of copper adjacent to steels
Medicine	Medical implants suffer corrosion. Fatigue failure of heart valve. Hip joints made of titanium and steel may fail in warm serum solutions	Improved designs

(*contd.*)

Industry	Corrosion Problems	Remedy
Nuclear	Unique corrosion problems although Zr and its alloys are used. Loss in capacity of the reactors due to corrosion. Radiation hazards. Long-term storage of spent fuel causes serious problems	Progress has been made in long-term storage of spent fuel. Hydrogen-induced cracking continues to be a significant problem
Fossil fuels	Corrosion due to SO_2 in coal-fired power plants	Flue gas scrubber system eliminates SO_2
Energy, oil and gas	H_2S, CO_2, NaCl are corrosive. Hydrogen induced cracking, pitting, sulphide-stress cracking, stress-corrosion cracking and SOHIC occur. Pipeline failures have occurred. The effect is pollution of environment	Inhibitors are used in existing pipelines, clean steels devoid of MnS inclusions are chosen for new pipelines

The foregoing discussion of the industries, with the associated corrosion-related accidents or failures, emphasizes the importance of safety to personnel involved in the industries as the most important factor that is reflected as the impact of corrosion.

Corrosion has a tremendous effect on the environment in the sense corrosion-related failure of oil pipelines or gas pipelines or oil tankers can have very detrimental effect on the environment in the form of water and air pollution, leading to the demise of aquatic life. Corrosion-related accidents can in principle destroy natural fauna or flora since these are irreplaceable.

Another aspect of concern is the limit of resources in the world. Some decades ago, the term recycling was almost unknown. At the present time recycling is a household term and recycling of metal products, paper and plastics has been recognized for the important role it plays in conserving our resources. We have reached a level of maturity to be able to recognize that our natural resources are limited and finite in our world, and that methods to conserve these resources by recycling and other methods have a prominent role to play.

Corrosion prevention and protection arrests the degradation of metals/materials and contributes in a significant way to the conservation of resources with minimum damage to the ecosystems. Since materials are prone to corrosion it is useful to know the factors both direct and indirect, which affect the choice of materials and their related corrosion resistance of paramount importance in the design of an engineering structure.

Materials selection	
Direct factors	Indirect factors
Cost	Mechanical properties
Appearance	Corrosion resistance
Ease of availability	Metallurgical
Ease of fabrication	Safety
Application	
Environmental	

In the design of a new plant the first step involves selection of materials, which should have reasonable corrosion-resistance properties in the environment of chosen application. This requires the corrosion studies of the material. The corrosion framework encompasses electrochemistry, corrosion modes, environments, inhibitors, metallurgical factors, coatings, design considerations, corrosion detection, monitoring, and testing and failure analysis. Within the framework of materials, knowledge of economics, safety, specifications and corrosion management is essential. It is also necessary for the corrosion scientist to have knowledge of the various forms of corrosion encountered in some familiar environments along with the recommended solutions. To this end, efforts are made in the following sections to discuss as succinctly as possible the required material for both students and practicing corrosion scientists.

1.2 Preliminary Aspects of Thermodynamics and Kinetics

Before embarking on the discussion of corrosion and the electrochemical nature of corrosion it is useful to examine corrosion process from the point of view of energetics. Thermodynamics deals with energy and its changes in reactions. Reactions are viewed in terms of changes in free energy. According to the first law of thermodynamics energy can be neither created nor destroyed. The second law states that the free energy is released from the system to surroundings in all spontaneous changes. Corrosion reactions are spontaneous and are governed by the laws of thermodynamics.

Consider the reaction:

$$\mathrm{A} + \mathrm{B} \underset{k_b}{\overset{k_f}{\rightleftharpoons}} \mathrm{C} + \mathrm{D}$$

where k_f is the forward reaction rate constant and k_b the rate constant for the backward reaction. From the point of view of transition state theory, A and B react to form an activated complex $(\mathrm{A}\cdots\mathrm{B})$, which leads to the products C and D, depending upon energetically favourable conditions. The energy profile of the reaction is represented in Figure 1.1.

ΔG is the energy difference between the reactants and products, and since the reaction is spontaneous ΔG must have a negative value. Note that $\Delta G^{\neq}$ is the energy barrier that A and B have to surmount to give products C and D. This arises from the internal energy of A and B. Once the activated complex $(\mathrm{A}\cdots\mathrm{B})$ is formed is can revert to A and B or give C and D, and the latter is energetically favoured because the reaction under

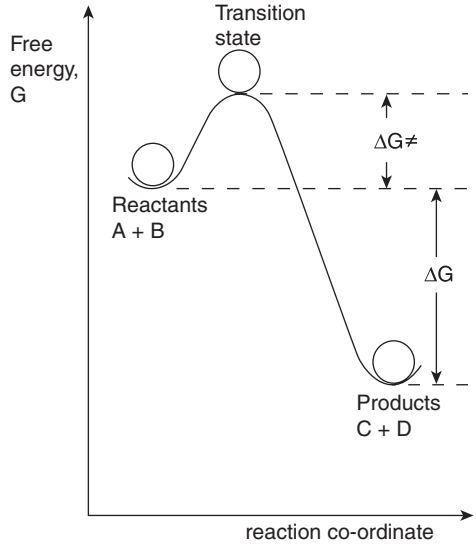

Figure 1.1 *Energy profile of a reaction*

consideration is spontaneous, and the transition state with the complex (A···B) reaches lower energy by giving C and D.

$$\text{Rate of forward reaction} = k_f[\text{A}]\ [\text{B}]$$
$$\text{Rate of reverse reaction} = k_b[\text{C}]\ [\text{D}]$$

At equilibrium we have $k_f[\text{A}]\ [\text{B}] = k_b[\text{C}]\ [\text{D}]$

$$K = \frac{k_f}{k_b} = \frac{[\text{C}]\ [\text{D}]}{[\text{A}]\ [\text{B}]}$$

When $k_f \gg k_b$ we have a large value for K and the forward reaction is predominant and the reverse reaction is negligible. On the other hand when $k_f \ll k_b$ the reverse reaction is favoured and the value of K is very small.

For the forward reaction the temperature dependence is given by the Arrhenius equation.

$$k_f = A\text{e}^{-\Delta G^{\neq}/RT}$$

where A and R are constants, T the temperature and $\Delta G^{\neq}$ the activation energy. The rate constant increases with increase in temperature.

For the reverse reaction (i.e., conversion of C and D into A and B), the activation energy required will be greater than $\Delta G^{\neq}$, and the reverse reaction is not favored.

From thermodynamics we have the relationship between free energy and equilibrium constant for a reaction:

$$\Delta G^{\circ} = -RT \ln K$$
$$\Delta G^{\circ} = -2.303\, RT \log K$$

ΔG° for the reaction can be calculated by using the values for reactants and products.

$$\Delta G^\circ_{298} = [G^\circ_{298}(\mathrm{C}) + G^\circ_{298}(\mathrm{D})] - [G^\circ_{298}(\mathrm{A}) + G^\circ_{298}(\mathrm{B})]$$

When the equilibrium constant is known it is possible to obtain ΔG°. ΔG° can also be calculated from G° values of products and reactants given in thermochemical tables. When ΔG° is negative the reaction is favoured in the forward direction. Thus for corrosion reactions to occur the ΔG° values have to be negative. For copper and gold the oxidation reactions are:

$$\mathrm{Cu} + \mathrm{H_2O} + {}^1\!/_2\,\mathrm{O_2} \rightarrow \mathrm{Cu(OH)_2} \quad \Delta G^\circ = -119\,\mathrm{kJ\ mol^{-1}}$$

$$\mathrm{Au} + \frac{3}{2}\,\mathrm{H_2O} + {}^3\!/_4\,\mathrm{O_2} \rightarrow \mathrm{Au(OH)_3} \quad \Delta G^\circ = +66\,\mathrm{kJ\ mol^{-1}}$$

and ΔG° values of -119 and $+66\,\mathrm{kJ\ mol^{-1}}$, show that corrosion of copper can occur whereas gold resists corrosion. These predictions are in agreement with the experimental observations (i.e., tarnishing of copper occurring and gold not tarnishing). It should be pointed out that these free energy values indicate whether a reaction as written will occur or not, but do not give any idea as to the rate at which it will occur. The rates of the corrosion are given by kinetic studies. It should also be pointed out that the environment of exposure has a decisive role in determining the occurrence of corrosion of the metal. This is exemplified by the fact that gold is resistant to atmospheric oxidation, and resistant to acid attack, but it is well known that gold dissolves in aerated cyanide solutions. In fact the cyanide process for extraction of gold and its assay is well known. Thus it is important to note that the environment also plays an important role in corrosion phenomena. Another example is the ease of rusting of iron by atmospheric attack, and the preservation of iron (free from corrosion) by keeping the metal in peat bogs.

1.3 Nature of Corrosion Reactions

Consider the system in which metallic iron is immersed in a solution of copper sulfate. In course of time metallic copper begins to appear. This process is known as a cementation reaction. The species present initially and after a lapse of time are as follows:

Initial	$\mathrm{Fe^\circ}$	$\mathrm{Cu^{2+}}$
Final	$\mathrm{Fe^{2+}}$	$\mathrm{Cu^\circ}$

Then, we may write the reactions occurring as:

$$\mathrm{Fe^\circ} \rightarrow \mathrm{Fe^{2+}} + 2\mathrm{e^-} \qquad \text{Oxidation (anodic)}$$

$$\mathrm{Cu^{2+}} + 2\mathrm{e^-} \rightarrow \mathrm{Cu^\circ} \qquad \text{Reduction (cathodic)}$$

$$\mathrm{Fe^\circ} + \mathrm{Cu^{2+}} \rightarrow \mathrm{Fe^{2+}} + \mathrm{Cu^\circ}$$

The equilibrium constant K and the free energy change in the overall cementation reaction may be written as:

$$\Delta G = \Delta G^\circ + RT \ln \frac{[Fe^{2+}][Cu^\circ]}{[Fe^\circ][Cu^{2+}]}$$

Since the corrosion of iron in copper sulfate solution involves an oxidation and reduction reactions with exchange of electrons, the reaction must involve an electrochemical potential difference, related to the equilibrium constant. This relationship may be written as:

$$\Delta G = -n\,FE$$

and is known as the Faraday's law. Here F (the Faraday) = 96 494 coulombs, E is the potential difference, n, the number of electrons transferred. Under standard state conditions,

$$\Delta G^\circ = -n\,FE^\circ$$

Neglecting solids we may write, for the reaction of iron in copper sulfate solution

$$-nFE = -nFE^\circ + RT \ln \frac{[Fe^{2+}]}{[Cu^{2+}]}$$

Division by nF leads to

$$E = E^\circ - \frac{RT}{nF} \ln \frac{[Fe^{2+}]}{[Cu^{2+}]}$$

In general terms

$$E = E^\circ - \frac{RT}{nF} \ln \frac{[\text{Products}]}{[\text{Reactants}]}$$

Converting to log and $T = 298$, and inserting numerical F, R values

$$E = E^\circ - \frac{0.059}{n} \log \frac{[\text{Products}]}{[\text{Reactants}]}$$

This equation is known as the Nernst equation, and is extensively used in electrochemical measurements. Under equilibrium conditions $E = E^\circ$ and the experimentally obtained values of E° are tabulated in the literature. E° values can be used to determine whether a reaction will occur or not.

Having established the criterion for the reaction, such as oxidation of a metal, in terms of the oxidation potential value and its sign and magnitude, it is useful to learn as to how these potentials are experimentally determined. The oxidation potentials are obtained by measuring against a standard hydrogen electrode, consisting of a platinium electrode immersed in 1 M HCl with hydrogen gas at 1 atmosphere pressure passing through it. The standard hydrogen electrode is assigned a value of 0.0 for the reaction

$$2H^+ + 2e^- \rightarrow H_2$$

and the measured potential of the metal in question, say copper or zinc, is obtained with respect to the standard hydrogen electrode. In the following electrochemical cell operation and measurement of standard electrode potentials is briefly discussed.

1.3.1 Electrochemical Cells

Consider the redox reaction

$$Zn(s) + Cu^{2+}_{(aq)} \rightarrow Zn^{2+}_{(aq)} + Cu_{(s)}$$

Zinc transfers two electrons to cupric ion. Thus zinc is the reducing agent. Cupric ion is the oxidizing agent. By separating the zinc (reducing agent) and the cupric ion (oxidizing agent) physically, the transfer of electrons can occur through an external conducting medium and as a result electricity is generated due to the progress of the redox reaction.

An electrochemical cell is an experimental apparatus for generating electricity by using a redox reaction. The Daniel cell for the system $Zn(s) + Cu^{2+}_{(aq)} \rightarrow Zn^{2+}_{(aq)} + Cu_{(s)}$ is shown in Figure 1.2.

Zinc, anode, positive	$Zn(s) \rightarrow Zn^{2+}_{(aq)} + 2e^-$	Oxidation
Copper, cathode, negative	$Cu^{2+}_{(aq)} + 2e^- \rightarrow Cu(s)$	Reduction

A salt bridge enables the movement of ions from one container to another and acts a conducting medium and completes the circuit. During the redox reaction electrons flow from the zinc anode through the wire and voltmeter to the copper cathode. In solution cations Zn^{2+}, Cu^{2+} and K^+ move toward the copper cathode and anions SO_4^{2-}, Cl^- move toward the zinc anode.

In the electrochemical cell an electric current flows from the zinc anode to the copper cathode. The difference in electrical potential between the anode and cathode is measured by the voltmeter, and is known as the cell voltage. The cell voltage is also

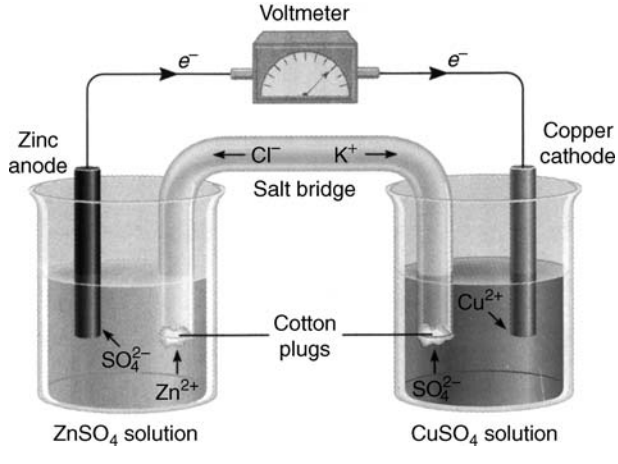

Figure 1.2 *The Daniel electrochemical cell*

known as the cell potential or electromotive force (emf). The cell voltage also depends on the concentration of the ions. Electrochemical cells are represented as cell diagrams. For the Daniel cell, assuming the solutions are 1.0 *M*, we may write:

$$\mathrm{Zn(s)|\,Zn^{2+}(1M)||\,Cu^{2+}(1M)|Cu(s)}$$

The single vertical line denotes a boundary between solid electrode and solution, and the double vertical lines signify the salt bridge. By convention the anode is on the left and the cathode is on the right of the salt bridge.

1.3.2 Standard Electrode Potentials

The measured voltage of the Daniel cell is 1.10 V. This is the overall voltage of the cell consisting of two half-reactions, namely the oxidation of zinc and the reduction of cupric ion. The individual potentials of the half-reactions cannot be measured. The potentials of the half-reactions can be obtained relative to a standard. The standard is a hydrogen electrode. This consists of a platinum electrode immersed in 1 *M* HCl with hydrogen gas bubbling through at 1 atmosphere pressure. The reaction is:

$$\mathrm{2H^{+}}(1\,M) + \mathrm{2e^{-}} \rightarrow \mathrm{H_2}(1\,\mathrm{atm})E^{\circ} = 0\,\mathrm{V}$$

and the potential of this is zero. The hydrogen electrode is known as standard hydrogen electrode (SHE) with a reduction potential of 0. Now we connect the zinc electrode system to a standard hydrogen electrode system with a salt bridge, as shown in Figure 1.3. The cell diagram is as follows:

$$\mathrm{Zn_{(s)}||\,Zn^{2+}(1M)\,||\,H^{+}(1M)\,||\,H_2(1\,atm)|Pt_{(s)}}$$

Zinc is the anode,

$$\mathrm{Zn_{(s)} \rightarrow Zn^{2+}_{(aq)} + 2e^{-}} \qquad \text{oxidation} \qquad E^{\circ}_{\mathrm{zn/Zn^{2+}}} = 0.76\,\mathrm{V}$$

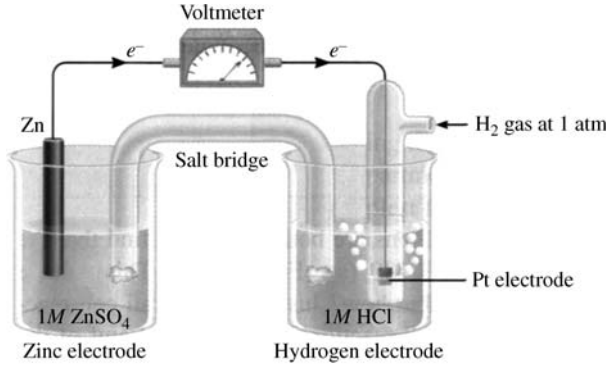

Figure 1.3 *An electrochemical cell consisting of zinc and hydrogen electrodes*

At the Pt electrode

$$2H^+_{(aq)} + 2e^- \rightarrow H_{2(g)} \qquad \text{reduction} \qquad E^\circ_{H^+/H_2} = 0.0\,V$$

When $Zn^{2+} = 1\,M, H^+ = 1\,M, H_{2(g)}$ at 1 atm (i.e., standard state conditions) the emf of the cell = 0.76 V at 25°C.

$$E^\circ_{cell} = E^\circ_{ox} + E^\circ_{red}$$
$$E^\circ_{cell} = E^\circ_{zn/zn^{2+}} + E^\circ_{H^+/H_2}$$
$$0.76 = E^\circ_{zn/zn^{2+}} + 0$$

The standard oxidation potential of zinc = 0.76 V. The overall reaction is the sum of oxidation and reduction potentials (see Figure 1.3).

The standard electrode potential can be obtained by connecting a hydrogen electrode system to a copper electrode system through a U-bridge and a voltmeter, as shown in Figure 1.4. In this system copper is the cathode since reduction occurs.

$$Cu^{2+}_{(aq)} + 2e^- \rightarrow Cu(s)$$

For this system the cell diagram may be written as:

$$Pt_{(s)} \,|\, H_2(1\,atm) \,|\, H^+(1M) \,\|\, Cu^{2+}(1M) \,|\, Cu(s)$$

The half-cell reactions are:

Anode (oxidation)	$H_2(1\,atm) \rightarrow 2H^+(1\,M) + 2e^-$	$E^\circ_{H_2/H^+}$
Cathode(reduction)	$Cu^{2+}(1\,M) + 2e^- \rightarrow Cu(s)$	$E^\circ_{Cu^{2+}/Cu}$
Overall	$H_2(1\ atm) + Cu^{2+}(1\,M) \rightarrow 2H^+(1\,M) + Cu(s)$	E°_{cell}

The potential under standard conditions is 0.34 V at 25°C.

$$E^\circ_{cell} = E^\circ_{H_2/H^+} + E^\circ_{Cu^{2+}/Cu}$$
$$0.34\,V = 0 + E^\circ_{Cu^{2+}/Cu}$$

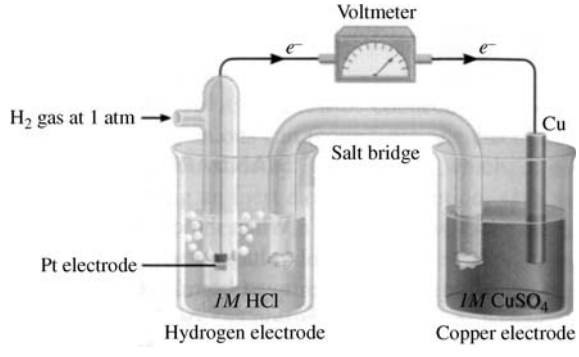

Figure 1.4 *An electrochemical cell consisting of copper and hydrogen electrodes*

Thus, the standard reduction potential of copper $E^{\circ}_{Cu^{2+}/Cu}$ is 0.34 V. Hence, the standard oxidation potential, $E^{\circ}_{Cu^{2+}/Cu} = -0.34\,V$.

Now we consider the Daniel cell:

Anode (oxidation)	$Zn_{(s)} \rightarrow Zn^{2+}(1\,M) + 2\,e^-$	$E^{\circ}_{Zn/Zn^{2+}}$
Cathode (reduction)	$Cu^{2+}(1\,M) + 2\,e^- \rightarrow Cu(s)$	$E^{\circ}_{Cu^{2+}/Cu}$
Overall	$Zn_{(s)} + Cu^{2+}(1\,M) \rightarrow Zn^{2+}(1\,M) + Cu_{(s)}$	E°_{cell}

The emf of the cell

$$\begin{aligned} E^{\circ}_{cell} &= E^{\circ}_{Zn/Zn^{2+}} + E^{\circ}_{Cu^{2+}/Cu} \\ &= 0.76\,V + 0.34\,V = 1.10\,V \end{aligned}$$

The standard potential series obtained is given in Table 1.5.

In the table, potential values given are reduction potentials and when the potential values are reversed in sign we have the oxidation potentials. The sign and magnitude of the potentials give a rough idea as to the ease of oxidation or reduction as the case may be.

Table 1.5 *Standard potential series*

Electrode	Reaction	E°_{red} (V)
Li^+, Li	$Li^+ + e^- \rightarrow Li$	−3.024
K^+, K	$K^+ + e^- \rightarrow K$	−2.924
Ca^{2+}, Ca	$Ca^{2+} + 2\,e^- \rightarrow Ca$	−2.87
Na^+, Na	$Na^+e^- \rightarrow Na$	−2,714
Mg^{2+}, Mg	$Mg^{2+} + 2\,e^- \rightarrow Mg$	−2.34
Ti^{2+}, Ti	$Ti^{2+} + 2\,e^- \rightarrow Ti$	−1.75
Al^{3+}, Al	$Al^{3+} + 3\,e^- \rightarrow Al$	−1.67
Mn^{2+}, Mn	$Mn^{2+} + 2\,e^- \rightarrow Mn$	−1.05
Zn^{2+}, Zn	$Zn^{2+} + 2\,e^- \rightarrow Zn$	−0.761
Cr^{3+}, Cr	$Cr^{3+} + 3e^- \rightarrow Cr$	−0.71
Fe^{2+}, Fe	$Fe^{2+} + 2\,e^- \rightarrow Fe$	−0.441
Co^{2+}, Co	$Co^{2+} + 2\,e^- \rightarrow Co$	−0.277
Ni^{2+}, Ni	$Ni^{2+} + 2\,e^- \rightarrow Ni$	−0.250
Sn^{2+}, Sn	$Sn^{2+} + 2\,e^- \rightarrow Sn$	−0.140
Pb^{2+}, Pb	$Pb^{2+} + 2\,e^- \rightarrow Pb$	−0.126
Fe^{3+}, Fe	$Fe^{3+} + 3e^- \rightarrow Fe$	−0.036
H^+, H_2	$2\,H^+ + 2\,e^- \rightarrow H_2$	−0,000
Saturated calomel	$Hg_2Cl_2 + 2\,e^- \rightarrow 2\,Hg + 2\,Cl^-$ (Sat. KCl)	0.244
Cu^{2+},Cu	$Cu^{2+} + 2\,e^- \rightarrow Cu$	0.344
Cu^+,Cu	$Cu^+ + e^- \rightarrow Cu$	0.522
Hg_2^{2+}, Hg	$Hg_2^{2+} + 2\,e^- \rightarrow 2\,Hg$	0.798
Ag^+, Hg	$Ag^{2+} + 2\,e^- \rightarrow 2\,Hg$	0.799
Pd^+, Pd	$Pd^+ + 2\,e^- \rightarrow Pd$	0.83
Hg^+, Hg	$Hg^+ + e^- \rightarrow Hg$	0.854
Pt^{2+}, Pt	$Pt^{2+} + 2\,e^- \rightarrow Pt$	1.2 (ca)
Au^{3+}, Au	$Au^{3+} + 3e^- \rightarrow Au$	1.42
Au^+, Au	$Au^+ + e^- \rightarrow Au$	1.68

From the values given for copper and gold for the reduction, we have:

$$Cu^{2+} + 2e^- \rightarrow Cu \qquad 0.344\,V$$
$$Au^{3+} + 3e^- \rightarrow Au \qquad 1.42\,V$$

and it is easy to note that gold has a higher value than copper, indicating that the reduction is more favored. In general, as one goes down the table we have increasing positive values, indicating the ease of reduction. By the same token the ease of oxidation is indicated by increasing negative values as one goes upwards in the table. It should be pointed out that the potential values given in the table are with respect to hydrogen electrode, which is difficult to use in routine measurements. A common standard electrode routinely used is the calomel electrode.

Now let us recall the two examples of copper and gold, which were shown to be feasible, and not feasible, respectively, with respect to corrosion, based on the free energy values, calculated for the respective reactions. The same conclusion can be reached based on the electrochemical potentials for the reactions of copper and gold.

$$2\,Cu_{(s)} + 2H_2O_{(l)} + O_{2(g)} \rightarrow 2\,Cu(OH)_{2(s)} \qquad E = 0.63\,V$$
$$4\,Au_{(s)} + 3\,02_{(g)} + 6\,H_2O_{(l)} \rightarrow 4\,Au(OH)_3 \qquad E = -0.23\,V$$

Using the above values for the potentials and the relationship between the potential and free energy,

$$\Delta G^\circ = -nFE$$

we get -120 kJ/mole and 66.5 kJ/mole for the reactions of copper and gold, which are in good agreement with the value obtained earlier.

It is well known that gold is extracted and also assayed by the familiar cyanide leaching.

$$8NaCN + 4Au + O_2 + 2H_2O \rightarrow 4Na\,Au(CN)_2 + 4NaOH$$

The potential for the reaction is 1.0 V, and using this value one obtains a value -96.5 kJ/mole for the free energy of the reaction, showing the feasibility of this reaction as well as the important role that the environment plays in these reactions.

Now that corrosion phenomenon has been firmly established as electrochemical in nature, we will examine the all too familiar rusting of iron due to corrosion. The mechanism of corrosion is complex and a simplistic mechanism is as follows. The iron metal surface consists of a region, which acts as an anode. Oxidation occurs at the anodic site.

$$Fe(s) \rightarrow Fe^{2+}(aq) + 2e^- \qquad \text{oxidation}$$

Since there is oxygen in the atmosphere, reduction occurs at another region of the metal surface.

$$O_{2(g)} + 4H^+ + 4e^- \rightarrow 2H_2O(l) \qquad \text{reduction}$$

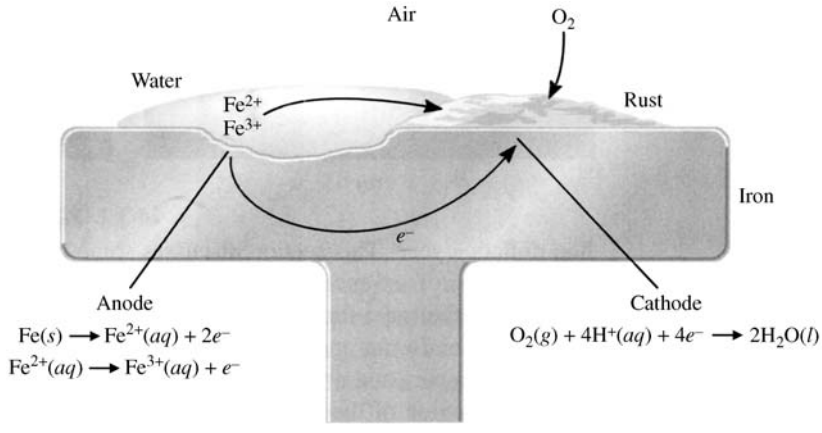

Figure 1.5 *The electrochemical process involved in rust formation*

The source of H^+ can be dissolved CO_2 or SO_2 in industrial areas. The overall reaction is:

$$2Fe_{(s)} + O_{2(g)} + 4H^+_{(aq)} \rightarrow 2Fe^{2+}_{(aq)} + 2H_2O(l)$$

The brown rust observed is hydrated iron oxide, $Fe_2O_3\, nH_2O$ (Figure 1.5).

The sodium chloride used in deicing roads accelerates the corrosion due to the fact chloride ion is aggressive and promotes the electrochemical process.

The standard potential series can be used as only a rough guide with respect to the ability of a metal to resist corrosion. In most of the corrosion reactions, the potential values shown in the table are not applicable because of the presence of a film on the metal surface, and the change in potential because the activity of metal ions is less than unity.

An alternate guide to the corrosion resistance of metals and alloys is the galvanic series. When two metals are coupled together and immersed in an electrolyte, an electrode potential difference is observed due to exchange of electrons and ions. Using this procedure galvanic series in seawater has been developed and is given in Figure 1.6. From the galvanic series shown in the figure it is possible to assess the behavior of metals and alloys with respect to corrosion in flowing seawater. It is clear from the figure that magnesium and zinc with negative potentials at the top portion of the figure with tendency to corrosion while platinium and graphite at the bottom of the figure with positive potentials and exhibiting greater resistance to corrosion.

The potentials of various metals shown in Table 1.5 are with respect to the standard hydrogen electrode (SHE). The hydrogen electrode is not very convenient to use in practice as a reference electrode in the context of measuring electrode potentials. Some of the reference electrodes used in practice are detailed below (see Table 1.6).

The measured electrode potential with respect to calomel electrode is added to the value of calomel electrode to obtain the value of the potential with respect to the standard hydrogen electrode.

$$E_{\text{SHE}} = E_{\text{meas}} + E_{\text{cal}}$$

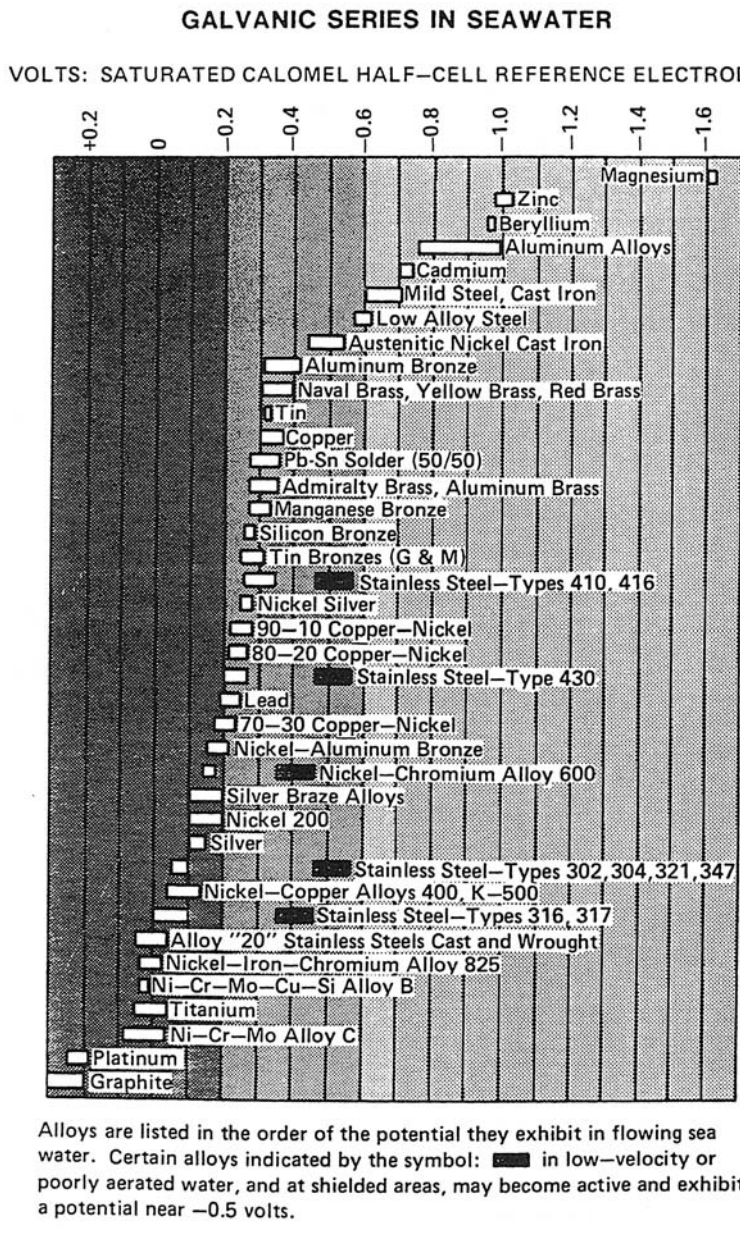

Figure 1.6 *The galvanic series in seawater*

1.3.3 Pourbaix Diagrams

When an electrochemical reaction is perturbed from its equilibrium state, the relative stabilities of the species in the reaction are changed. The change due to the perturbation is reflected in the measured electrode potential, which differs from the equilibrium

Table 1.6 *Reference electrodes*

System at 25°C	Electrolyte	Potential (V vs SHE)
$2Hg + 2Cl^- = Hg_2Cl_2 + 2e$	0.01 *M* KCl	0.389
Calomel	0.1 *M* KCl	0.333
	1.0 *M* KCl	0.280
	Sat. KCl	0.241
$Cu = Cu^{2+} + 2e$	0.1 *M* $CuSO_4$	0.284
Copper – copper sulfate	0.5 *M* $CuSO_4$	0.294
	Sat. $CuSO_4$	0.298
$Ag + Cl^- = AgCl + e$	0.001 *M* KCl	0.400
	0.001 *M* KCl	0.343
	0.1 *M* KCl	0.288
	1.0 *M* KCl	0.234
Platinized platinum	0.1 *M* NaCl	−0.12 (approx.)
Gold	0.1 *M* NaCl	−0.25 (approx.)
Zinc	Seawater	−0.79 (approx.)

electrode potential of the reaction. If the measured electrode potential is positive with respect to the equilibrium electrode potential, the reaction proceeds irreversibly from left to right.

$$\text{Reduced species} = \text{oxidized species} + ne$$

When the measured potential is negative with respect to the equilibrium value, the reaction favours the reduced form.

Consider water, which is an electrochemically active species. The electrochemical reactions involving water are:

$$2H_2O = 4H^+ + O_2 + 4e$$
$$H_2 + 2OH^- = 2H_2O + 2e$$

For solutions in which the activity of water and the fugacities of oxygen and hydrogen gases are unity, the equilibrium electrode potentials for the above reactions at 25°C are:

$$E_{0,H_2O/O_2} = +1.23 - 0.059\,pH$$
$$E_{0,H_2/H_2O} = -0.059\,pH$$

The electrode potentials given are with respect to SHE.

Pourbaix has shown that plotting electrode potentials of electrochemical reactions against pH of the solution is useful in identifying regions of stability of various chemical species in solution. These plots are commolny known as Pourbaix diagrams. These diagrams are extremely useful in corrosion science. The Pourbaix diagram for the system H_2O–H_2–O_2–H^+–OH^- will be considered (Figure 1.7). The lines (1) and (2) represent plots of $E_{0,H_2O/O_2}$ and $E_{0,H_2/H_2O}$ vs pH respectively. Inspection of line (1) and the reaction

$$2H_2O = 4H^+ + O_2 + 4e$$

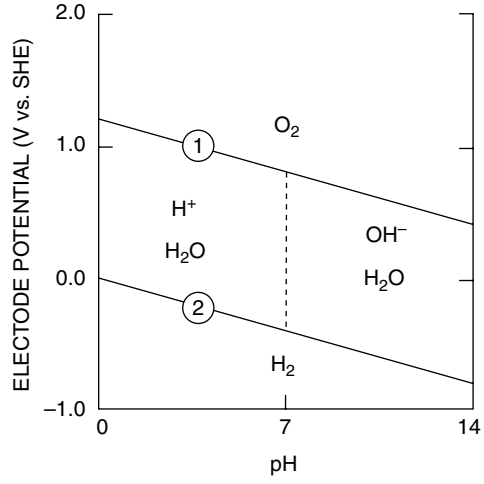

Figure 1.7 *Pourbaix diagram for the system: water–hydrogen–oxygen–hydrogen ion–hydroxyl ion. Activity of water is unity; fugacities of hydrogen and oxygen are unity. Temperature 25° C*

shows that water is a stable entity at potentials below this line and conversely, unstable at potentials above this line. Similar analysis of line (2) and the reaction,

$$H_2 + 2OH^- = 2H_2O + 2e$$

shows that water is a stable entity at electrode potentials above line (2) and unstable below this line. The Pourbaix diagram for this system (Figure 1.7) is similar to a phase diagram. This can be considered as a form of electrochemical phase diagram. The region where a species is stable is identified with the chemical symbol of the species.

The Pourbaix diagram is extremely useful in determining stable chemical species for metals in contact with aqueous solutions. When the Pourbaix diagram for water is superimposed on the metal of interest, two types of behavior are observed. This behavior classification of metals is based on the relationship between the metal–metal ion equilibrium reaction and the region of stability of water. In one class of metals, the metal–metal ion equilibrium potential falls within the region of stability of water. In these cases, it is possible to measure the equilibrium electrode potential of metal–metal ion reaction in aqueous solution and devise a method by which the kinetic properties of the reaction may be obtained with minimal kinetic complexity. In the second class of metals, the metal–metal ion equilibrium electrode potentials fall below the region of stability of water. These metals form mixed potential systems with solvent water. Therefore, the equilibrium electrode potential of the metal–metal ion reaction cannot be measured in aqueous solution, and the kinetics of the complete reaction cannot be determined with ease. Copper is an example of the first type and iron is an example of the second class of metals. Figure 1.8 is the Pourbaix diagram for copper and some of its ionic species and compounds in aqueous solution at 25°C.

The equilibrium electrode potential for the copper–cupric ion reaction is located within the region of stability of water represented by dashed lines. Thus, the

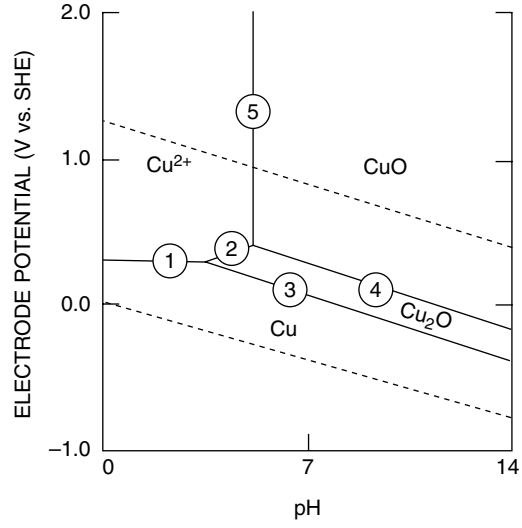

Figure 1.8 *Pourbaix diagram for the system copper–cupric ion–cuprous oxide–water. Activity of cupric ion is .01. The dashed lines denote the stability range of water.The temperature is 25° C. The reactions considered: 1. copper going to cupric ion and two electrons; 2. cuprous oxide reacting with hydrogen ion to give cupric ion, water and two electrons. 3. cuprous oxide reacting with water to give cupric oxide, hydrogen ion and two electrons; 4. copper metal reacting with water to give cuprous oxide, hydrogen ion and electrons; 5. cupric ion reacting with water to give cupric oxide and hydrogen ion*

measurement of the equilibrium electrode potential is possible and the kinetics of the copper–cupric ion system can be studied without interference from reactions involving solvent decomposition. All the reactions involved in this system are electrochemical except the reaction,

$$Cu^{2+} + H_2O \equiv CuO + 2H^+$$

and can be studied by standard electrochemical techniques. If the measured electrode potential and pH are known, this figure may be used to determine the stable form of copper and its compounds under those conditions.

Figure 1.9 is the Pourbaix diagram for iron and some of its compounds in an aqueous system at 25°C. The equilibrium potential of the reaction $Fe^\circ = Fe^{2+} + 2e$ falls outside the stability region of water represented by dashed lines. Hence, measurement of the equilibrium electrode potential is complicated by the solvent undergoing a reduction reaction, while the iron is undergoing electrochemical oxidation. This is the basis of the mixed potential model of corrosion.

In the potential–pH region where iron metal is the stable species, corrosion cannot occur since the reactions are not thermodynamically favorable. Pourbaix calls these regions ‘immune’ to corrosion. However, in the broader sense of corrosion, iron may corrode in this region, such as the fracture of iron alloys in the presence of hydrogen. Hence, it is not sufficient for a metal to be ‘immune’ for it to be free of corrosion.

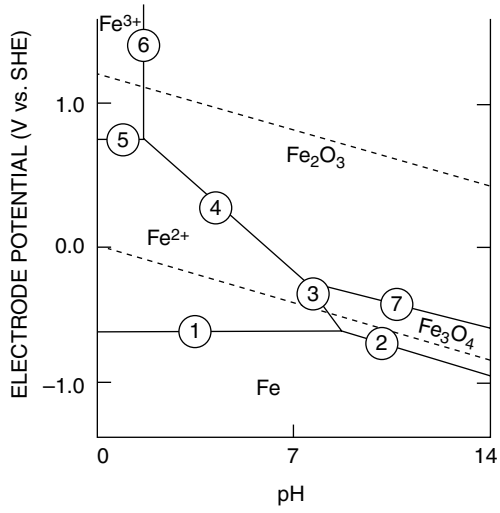

Figure 1.9 *Pourbaix diagram for the system iron–ferrous ion–ferric ion–haematite–ferric oxide. Activities of ferrous and ferric ions are 10^{-6}. The temperature is 25° C. The reactions considered: 1. iron metal giving ferrous ion and two electrons; 2. iron reacting with water to give haematite, hydrogen ion and electrons; 3. ferrous ion reacting with water to give haematite, hydrogen ion and electrons; 4. ferrous ion reacting with water to give ferric oxide, hydrogen ion and electrons; 5. ferrous ion giving rise to ferric ion and electron; 6. ferric ion reacting with water to give ferric oxide and hydrogen ion; 7. haematite reacting with water to give ferric oxide, hydrogen ion and electrons*

Considering the Pourbaix diagram for iron, the region of stability of iron oxide shows that the film of iron oxide on the metal surface forms a barrier between the metal and the environment. This condition is called passivity and is characterized by the measured electrode potentials in the regions where the passive oxide film is stable. Figure 1.10 is a simplified Pourbaix diagram for iron. The diagram clearly distinguishes the regions of immunity, corrosion and passivity.

Use of Pourbaix diagrams. Consider copper metal at +0.150 V vs SCE in an aqueous solution of pH 2.5 and a cupric ion activity of 0.01 at 25°C. In order to use the Pourbaix diagram, the potential is converted to SHE scale.

$$E_2 = +0.150 + 0.241 = 0.391\,\text{V vs SHE}$$

Reference to the Pourbaix diagrams for water and copper shows the stable species to be Cu^{2+}, H^+ and H_2O. Corrosion is possible under these conditions. Let us consider the case of iron metal at −0.750 V vs SCE in a solution of pH 5.0 and a ferrous ion activity of 10^{-6} at 25°C. The electrode potential with respect to SHE is −0.509 V and reference to Pourbaix diagrams for water and iron shows the stable species to be Fe^{2+} and H_2, and that corrosion is possible under these conditions.

It is needless to emphasize that Pourbaix diagrams reveal information on stability of species and whether corrosion is likely to occur under a given set of conditions.

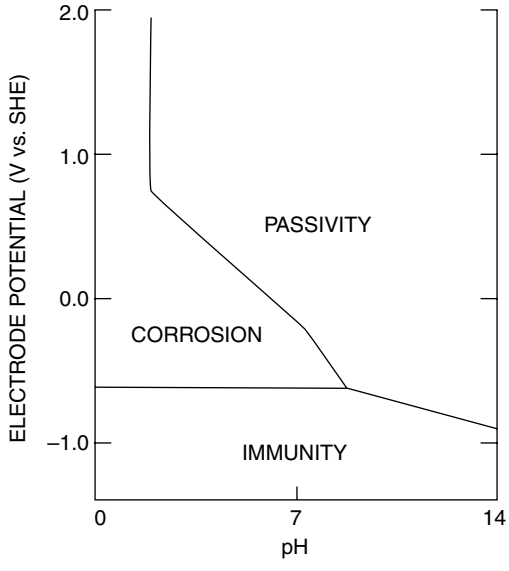

Figure 1.10 *Pourbaix diagram for iron in terms of corrosion, passivity and immunity*

1.3.4 Dynamic Electrochemical Processes

The potential series and the Pourbaix diagrams involving equilibrium conditions discussed thus far led to determine the feasibility of the corrosion process based on thermodynamics. These concepts do not give any information on the rates of corrosion processes. In order to ascertain the corrosion rates it is imperative to understand the intimate dynamical processes occurring at the metal exposed to an electrolyte solution.

Let us consider an electrode immersed in an electrolyte. A potential difference arises at the interface between the electrode and the surrounding electrolyte solution. The potential difference arises due to charge separation. If electrons leave the electrode and reduce the cations in solution, the electrode acquires a positive charge, the solution loses electroneutrality and anions would move closer to the positively charged electrode. The situation is depicted in Figure 1.11. Thus, we have a pair of positive and negative sheets, which is known as the electrical double layer.

The process of contact adsorption of an ion consists of desolvation of anion, removal of solvent water molecule from the surface of the electrode and the desolvated anion taking the vacant position on the electrode as a result of departure of water molecule from the electrode surface. The steps of anion adsorption in terms of energy are:

$$E(\text{electrode}-\text{anion}) > E(\text{water on electrode}) + E(\text{desolvation of anion})$$

The disposition of water molecules attached to positive ions and negative ions with metal–oxygen and anion–hydrogen interactions are shown in Figures 1.12 and 1.13, respectively.

The first-row water molecules near the electrode surface of an electrode play an important role in the sense that they have to allow either an anion or a solvated cation to

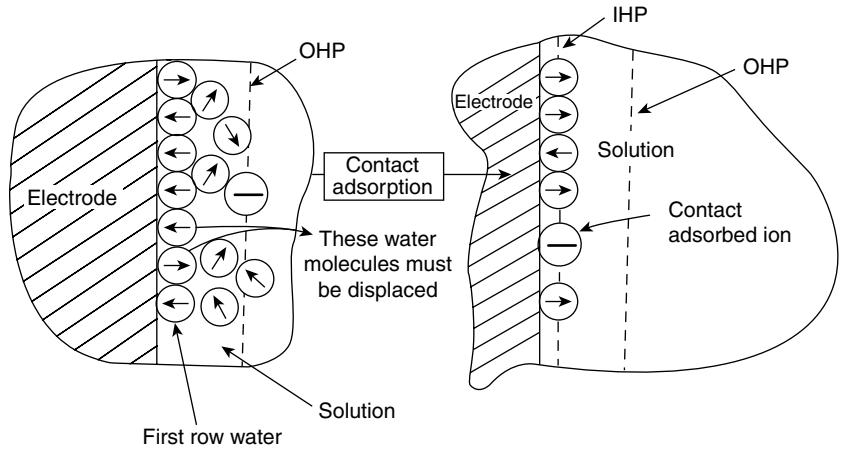

Figure 1.11 *Process of contact adsorption in which a negative ion can lose its hydration and displace first-row water. The locus of the centers of the ions defines the inner Helmholtz plane*

come close to the electrode surface. The locus of the centre of the first-row molecules on the electrode surface defines the inner Helmholtz plane, and the distance between the inner Helmholtz plane and the electrode is ~3 Å. Similarly the locus of the center of the water molecules adjacent to the first row is the outer Helmholtz plane, and this plane is about 5–6 Å from the electrode surface.

The solvation of cations and anions by water molecules is possible due to the dipolar nature of water in the sense that oxygen and hydrogen have partial negative and positive charges respectively.

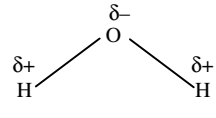

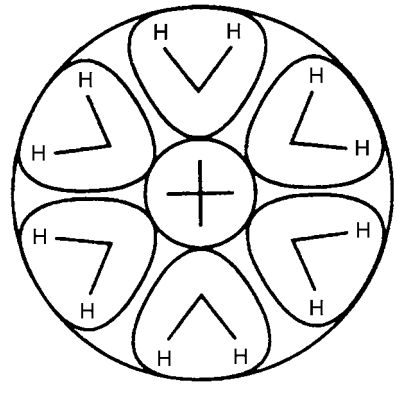

Figure 1.12 *Schematic of a positive ion surrounded by a sheet of apex-inward water dipoles*

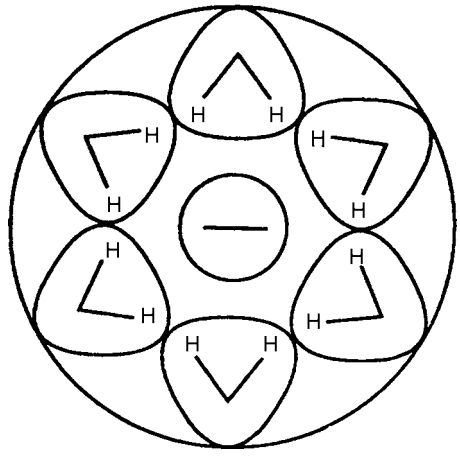

Figure 1.13 *Schematic of a negative ion surrounded by a sheet of apex-outward water dipoles*

It should also be noted that the bonding between a cation and water dipole is stronger than an anion and a water dipole.

Now we turn to the situation when the electrode is negatively charged as shown in Figure 1.14. It is important to note that the solvated cations lie at the outer Helmholtz plane, unlike the situation in which the anions adsorb on the positive electrode surface. In terms of interaction forces the cation–water interactions are stronger than the negatively charged electrode – water interactions. In terms of more intimate mechanism the water molecules attached to the cation do not exchange with water molecules adsorbed on the electrode surface. The solvated cation is situated at the outer Helmholtz plane.

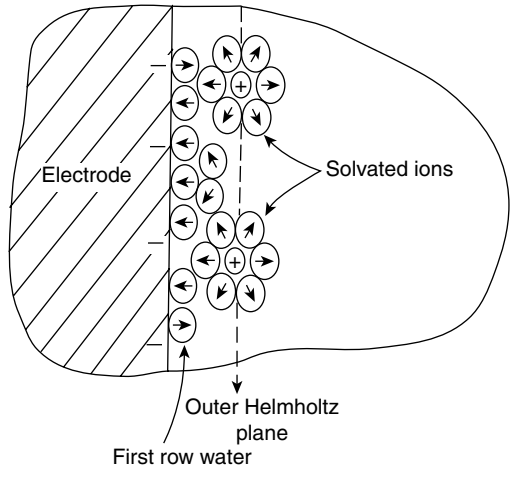

Figure 1.14 *A layer of hydrated positive ions whose hydration sheath cannot be stripped, on the first layer of water molecules. The locus of the centers of these ions define the outer Helmholtz plane*

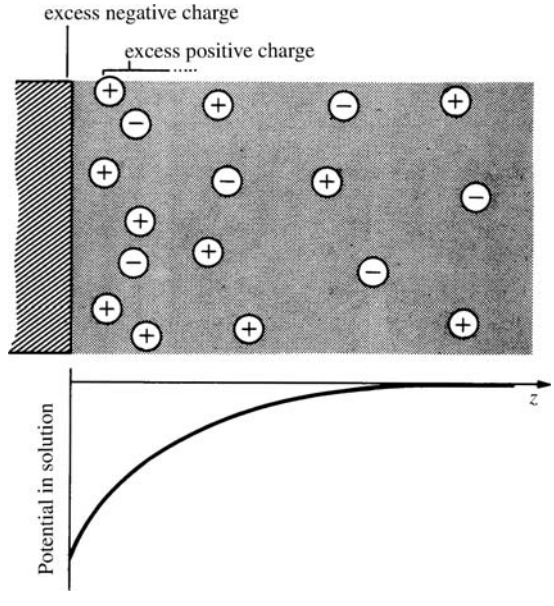

Figure 1.15 *Gouy–Chapman model of the double layer*

The double layer model of Helmholtz assumes fixed layer of charges on the electrode and the outer Helmholtz plane. This model has been modified by Guoy–Chapman analysis, which assumes that the ions of charge opposite of the charge on the electrode distribute themselves in a diffuse manner as shown in Figure 1.15.

The variation of potential with distance is exponential according to this model, while it is linear according to the Helmholtz model. Another modification of the double layer theory is due to Stern, who proposed a synthesis of the Helmholtz and Guoy–Chapman models in that both the fixed layer of charges and diffuse layer of charges are taken into consideration. Stern's model, showing charge distribution and the variation of potential with distance, is shown in Figure 1.16. The figure also shows that by assuming the layer of charges as parallel plate capacitor, the relationship between the total differential capacity and the capacitances due to Helmholtz (C_H) and Guoy–Chapman (C_G). The variation of potential with distance shows both linear and nonlinear portions, confirming that this model embraces both Helmholz, and Guoy–Chapman models.

The variation of potential with distance when a test charge located at a distance from the electrode approaches the electrode surface passing through the electrolyte solution is shown in Figure 1.17. It should be borne in mind that this trend in potential variation is the predicted trend. It should also be noted that the potential difference between the metal and the solution is $\Delta\phi$ and is given by:

$$\Delta\phi = \phi_M - \phi_s$$

where ϕ_M and ϕ_s are the potentials of metal and solution. The potential difference $\Delta\phi$ (M, S) is the measured parameter when an electrode is immersed in an electrolyte.

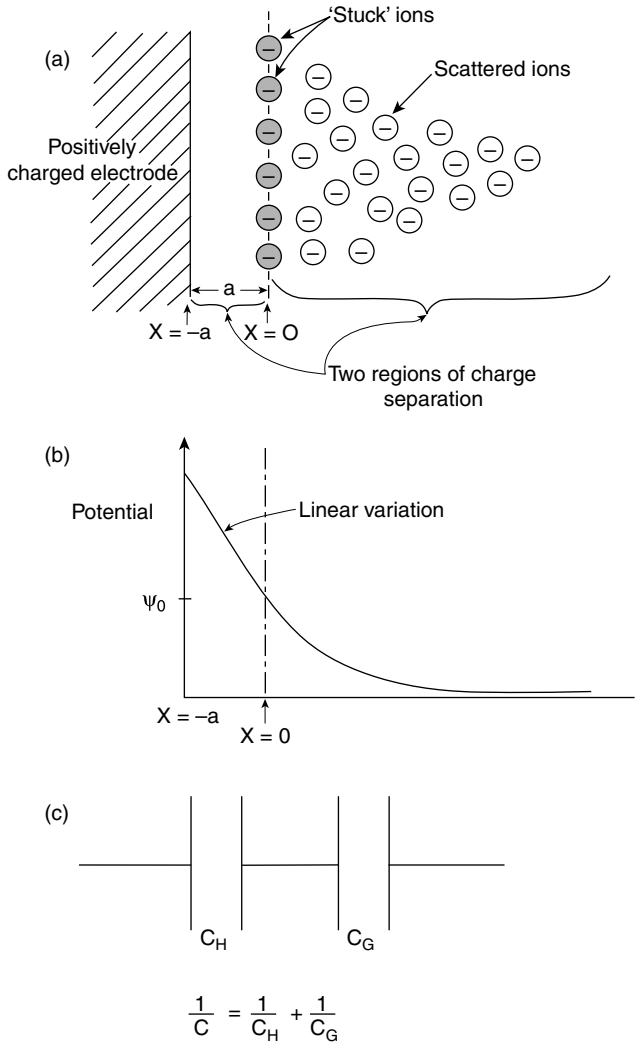

Figure 1.16 *The Stern model. (a) A layer of ions stuck to the electrode and the remainder scattered in cloud fashion; (b) the potential variation according to this model; (c) the corresponding total differential capacity C is given by the Helmholtz and Gouy capacities in series*

In corrosion the dynamic electrochemical processes are of importance and hence considerations of the consequences of perturbation of a system at equilibrium are considered. Let us consider the familiar Daniel cell consisting of copper metal in copper sulfate, and zinc metal in zinc sulfate solution. This, as depicted in Figure 1.18 gives an electromotive force of 1.1 V when there is no current flow. When a small current flows through the resistance R, the potential decreases below 1.1 V. On continued flow of current, the potential difference between the electrodes approaches a value near zero, and

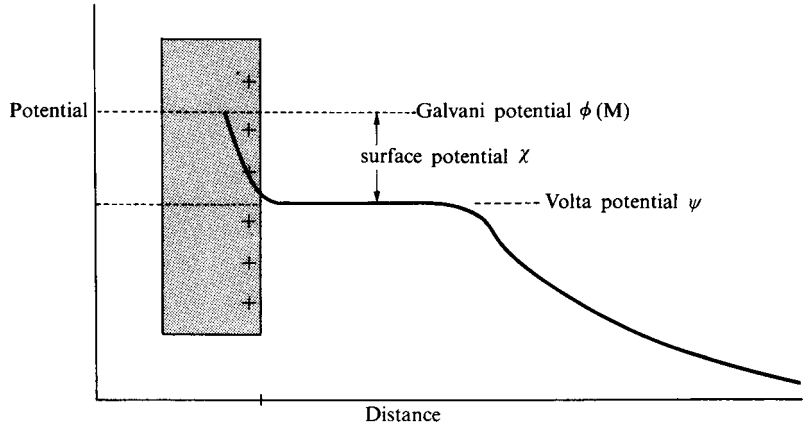

Figure 1.17 *Variation of potential with distance from an electrode*

the potential difference continues to decrease as the current increases since the electrodes polarize. The effect of net current flow on the voltage of the Daniel cell can be represented by plotting the individual potentials of copper and zinc electrodes against the current, as shown in Figure 1.19. This is known as the polarization diagram. When there is no net current flow, we have ϕ_{Cu} and ϕ_{Zn}, the potential values of copper and zinc known as open-circuit potentials. The zinc electrode polarizes along a–b–c, and the copper electrode along d–e–f. At a current value of I_1 the polarization of zinc is the potential at b minus ϕ_{Zn} (or the open-circuit potential at a). Similarly in the case of copper we have ϕ at e minus ϕ at d or ϕ_{Cu}. The potential difference of the polarized electrodes i.e., zinc at b and copper at e is equal to $I_1(R_e + R_m)$ where R_e and R_m are electrolytic and metal resistance in series. At a point c the current is maximum and we have potential difference at a minimum and equal to I_{max} R_e. The potential

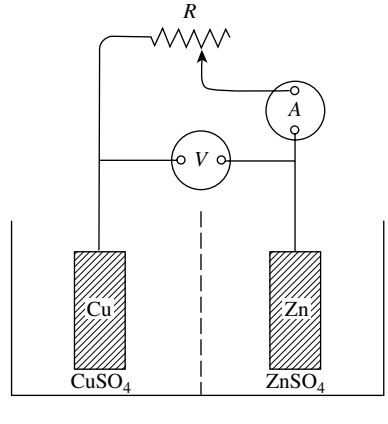

Figure 1.18 *Polarized copper–zinc cell*

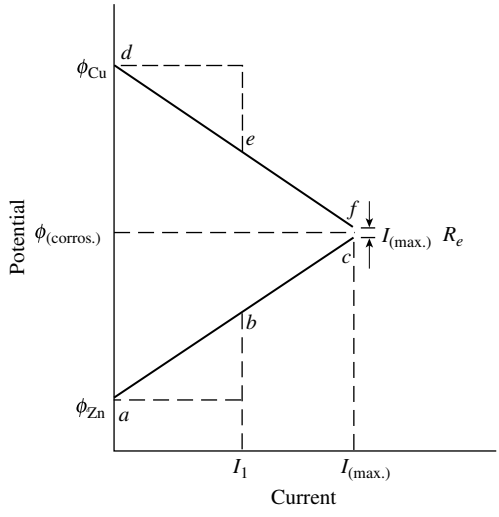

Figure 1.19 *Polarization diagram for copper–zinc cell*

corresponding to I_{max} is known as the corrosion potential. Using the equivalent weight of zinc (65.32/2), the Faraday equal to 96 500 coulombs/equivalent, and the value of I_{max}, the amount of zinc corroding in unit time may be calculated. Similarly an equivalent amount of copper will be deposited during the cathodic reaction. The lines (a–b–c) and (d–e–f) are known as the anodic and cathodic branches of the polarization diagram.

Note that Faraday's law has been used to determine the rate of corrosion of zinc in the case of a polarized Daniel cell (i.e., Faraday's law relates the charge Q created by ionization of M moles metal such as zinc).

$$Q = zFM$$

where Z is the valence, F, the Faraday and M, the number of moles

$$\frac{dQ}{dt} = zF\frac{dM}{dt}$$

Noting that $dM/dt = J$ the flux of the substance, I the current flowing through unit area of cross-section, i is the current density, we can write:

$$i = zFJ$$

Thus the flux of the material is the corrosion rate and we arrive at the corrosion rate equated to the current density.

Polarization is defined as a type of perturbation, which results in disturbing the equilibrium and producing a dynamic situation. The three types of polarization are concentration polarization, activation polarization, and *IR* drop.

Let us consider metallic copper sample immersed in water and let us suppose the metallic copper in contact with water gives rise to cupric ions and the energy profile for

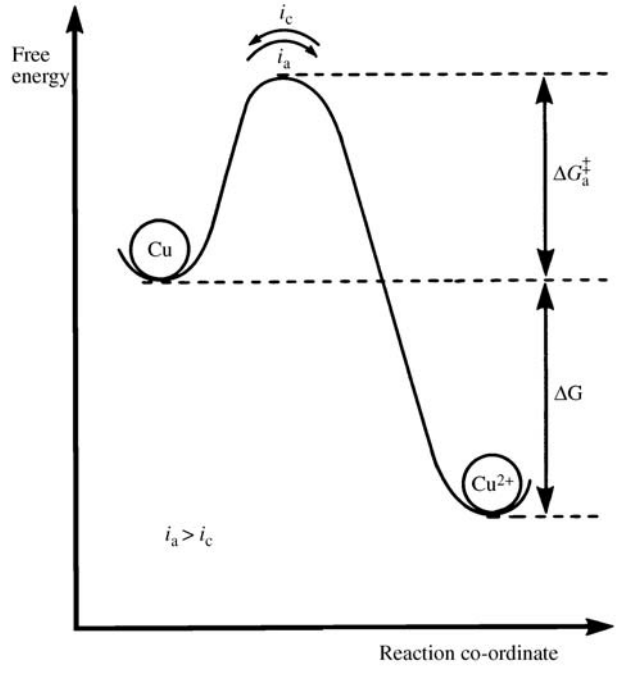

Figure 1.20 *Energy profile for oxidation of copper. (Reproduced from Corrosion for Science and Engineering, Tretheway and Chamberlain, Copyright Pearson Education Ltd)*

the system will be as shown in Figure 1.20.

$$Cu \rightarrow Cu^{2+} + 2e^{-}$$

The environment must be capable of providing sufficient energy to aid metallic copper to corrode and give cupric ions, i.e., the metal must overcome the barrier $\Delta G^{\neq}$. For some time there will be corrosion and as a result cupric ion concentration increases. This tendency of copper to corrode will decrease as the current increases from zero, and the value of ΔG decreases, along with potential in conformity with Faraday's law. The thermodynamic energies of the metal atoms and the ions approach each other. After a lapse of time an equilibrium state is reached when the rate of metallic copper producing cupric ions will equal the rate of reduction of cupric ions to produce metallic copper. The energy profile for such an equilibrium state is depicted in Figure 1.21. We note that the energy of activation $\Delta G^{\neq}$ and that for the case of copper we may write.

$$Cu \underset{i_c}{\overset{i_a}{\rightleftharpoons}} Cu^{2+} + 2e^{-}$$

and in more general terms

$$M \underset{i_c}{\overset{i_a}{\rightleftharpoons}} M^{2+} + 2e^{-}$$

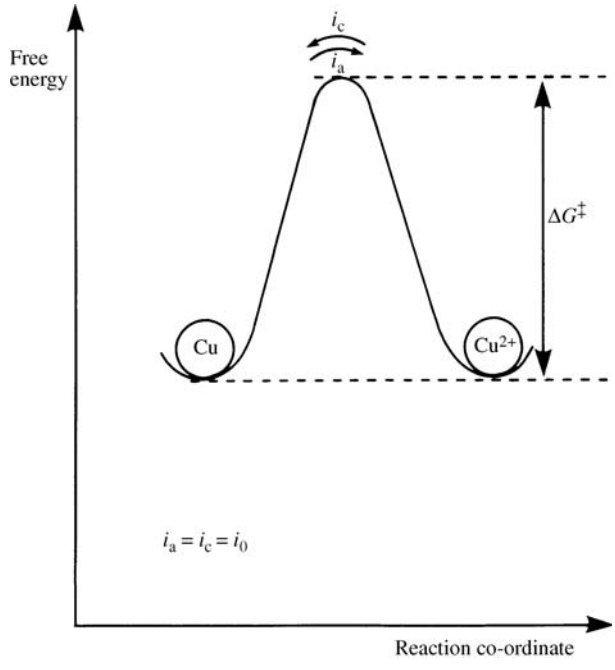

Figure 1.21 *An energy profile for copper in equilibrium with a solution of its divalent ions; $i_a = i_c = i_0$ (Reproduced from Corrosion for Science and Engineering, Tretheway and Chamberlain, Copyright Pearson Education Ltd)*

At equilibrium, $i_a = i_c$ and the measured current density $i_{meas} = i_a - i_c$ and no net current flows. There is current flow, but it is equal and opposite and cannot be measured. This quantity is known as exchange current denoted by I_0 and when divided by area, it is i_0.

Thus we note that current density gives a measure of corrosion rate. Corrosion rates are generally expressed in practice as mpy (mils per year), ipy (inches per year), ipm (inches per month) and mdd (loss of weight in milligrams per square decimetre per day), and a nomograph for interconversion of one unit into another unit is depicted in Figure 1.22.

Perturbation of a system at equilibrium in terms of potential is known as polarization. The polarization of the equilibrium is also termed as overpotential or overvoltage denoted by η: consider the system.

$$M \underset{i_c}{\overset{i_a}{\rightleftharpoons}} M^{2+} + 2e^-$$

for which the corrosion rate r may be written as:[75]

$$r = k_{corr}[\text{reactants}]$$

where $k_{corr} = Ae^{-\Delta G^{\neq}/RT}$ and A is a constant

$$r = Ae^{-\Delta G^{\neq}/RT}[\text{reactants}]$$

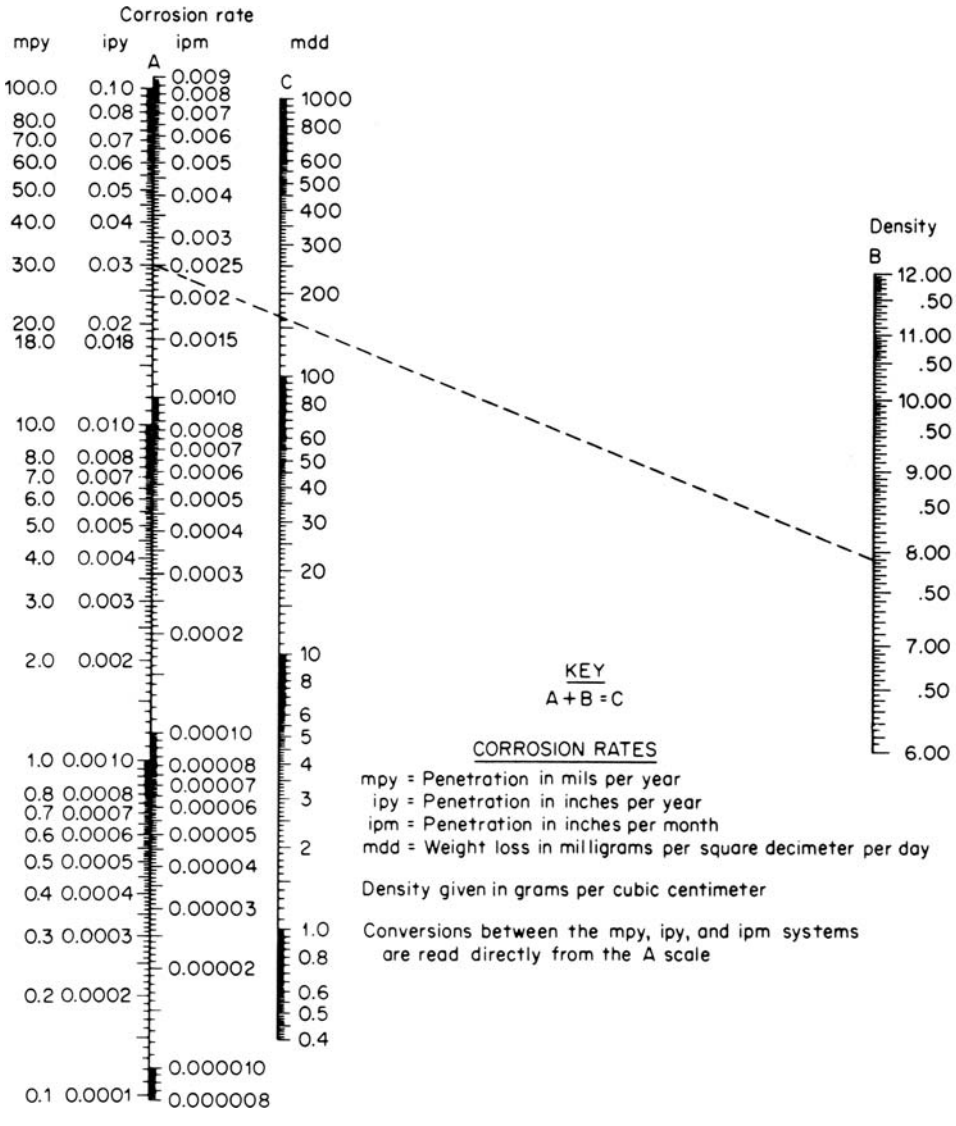

Figure 1.22 *Nomograph for mpy, ipy, ipm, and mdd*

At equilibrium $k_f = k_r$ or $i_a = i_c = i_0$. Since solid metal is corroding, it may be taken as constant,

$$i_a = i_0 = A_0\, e^{-\Delta G/RT}$$

The energy profile for the system at equilibrium along with anodic polarization of the equilibrium state is shown Figure 1.23.

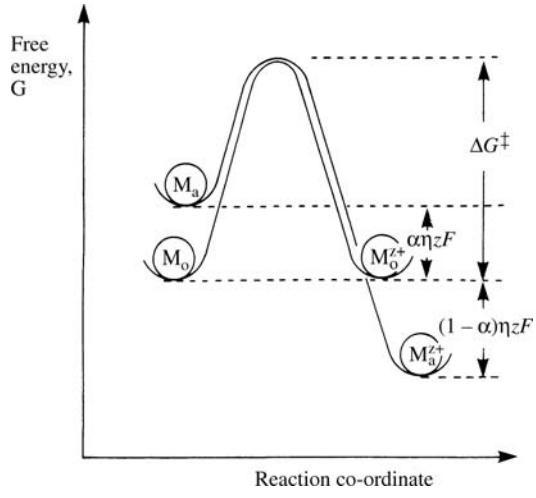

Figure 1.23 *An energy profile for an anode at equilibrium and a similar profile for anodic activation polarization (Reproduced from Corrosion for Science and Engineering, Tretheway and Chamberlain, Copyright Pearson Education Ltd)*

By denoting the anodic polarization as $\alpha\eta$ and cathodic polarization as $(1-\alpha\eta)$, we can write:[75]

$$i_a = A_0\, e^{-\Delta G^{\neq} + \alpha\eta F/RT}$$
$$= A_0\, e^{-\Delta G^{\neq}/RT} e^{\alpha\eta zF/RT}$$
$$i_a = i_0\, e^{\alpha\eta zF/RT}$$
$$i_c = i_0\, e^{(1-\alpha)\eta zF/RT}$$

Since bulk current flow, $i_{meas} = i_a - i_c$,

$$i_{meas} = i_0[e^{\alpha\eta zF/RT} - e^{(1-\alpha)\eta zF/RT}]$$

This equation is known as Butler–Volmer equation. By letting $\alpha zF/RT = A'$

$$i_a = i_0 e^{(A'\eta)}$$

By taking logarithms

$$\ln i_a = \ln i_0 + A'\eta$$
$$\ln i_a = \ln i_0 + A'\eta$$
$$\ln\left(\frac{i_a}{i_0}\right) = A'\eta$$

or

$$\eta = \frac{2.303}{A'}\log(i_a/i_0)$$

If

$$\beta = \frac{2.303}{A'} = \frac{2.303RT}{\alpha zF}$$
$$\eta_a = \beta_a \log(i_a/i_0)$$

In general terms $\eta = c \log i + D$. This is known as Tafel equation. For the anodic and cathodic processes we have:

$$\eta_a = \beta_a \log i_a - \beta_a \log i_0$$
$$\eta_c = \beta_c \log i_c - \beta_c \log i_0$$

where

$$\beta_a = \frac{2.303RT}{\alpha zF} \qquad \beta_c = \frac{2.303RT}{(1 - \alpha zF)}$$

In the Tafel equations β_a and β_c are known as the anodic and cathodic Tafel constants. Tafel plots are useful in obtaining corrosion rates. Consider a sample of metal polarized 300 mV anodically and 300 mV cathodically from the corrosion potential E_{corr}. The potential scan rate may be 0.1–1.0 mV/s. The resulting current is plotted on a logarithmic scale. The plot is shown in Figure 1.24. The corrosion current i_{corr} is obtained from the

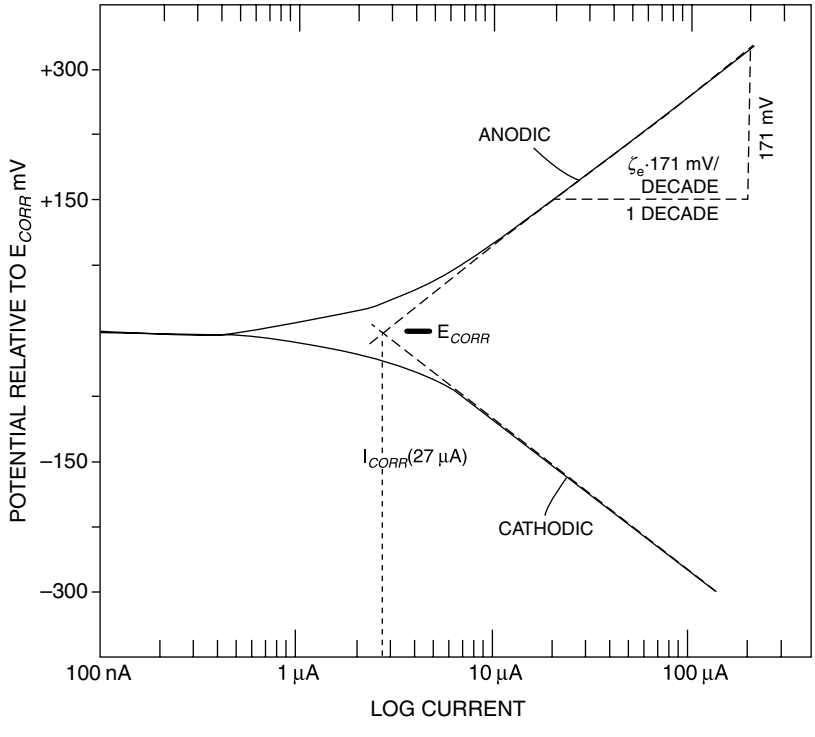

Figure 1.24 *Experimentally measured Tafel plot*

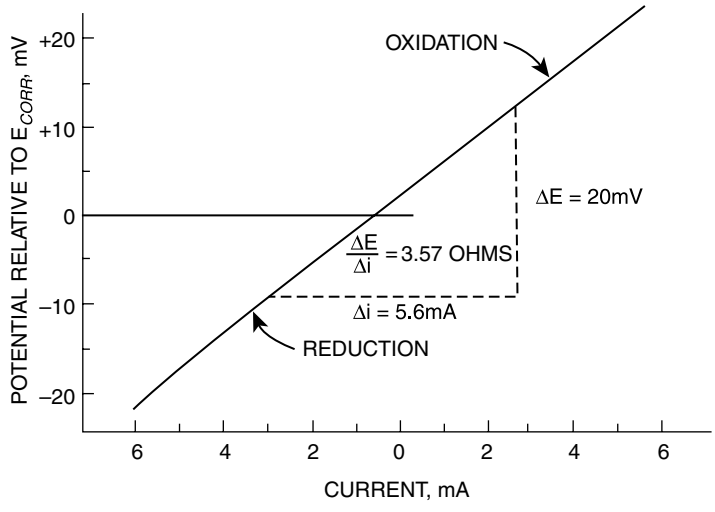

Figure 1.25 *Experimentally measured polarization resistance*

plot by extrapolation of the linear portions of the anodic and cathodic branches of the curve to the corrosion potential E_{corr}. The corrosion current may then be used to calculate the corrosion rate using the following equation:

$$\text{Corrosion rate (mpy)} = \frac{0.13\, i_{\text{corr}}(\text{Eq wt})}{d}$$

where i_{corr} is corrosion current density, (A/cm^2), d, the density of the corroding metal (g/cm^3) and Eq wt is the equivalent weight of the corroding metal in grams.

The linear polarization technique is rapid and gives corrosion rate data, which correlate reasonably well with weight loss method. The technique involves scanning through 25 mV above and below the corrosion potential and plotting the resulting current against potential as shown in Figure 1.25. The corrosion current i_{corr} is related to the slope of the line.

$$\frac{\Delta E}{\Delta i} = \frac{\beta_{\text{A}} + \beta_{\text{c}}}{2.3(i_{\text{corr}})(\beta_{\text{A}} + \beta_{\text{c}})}$$

$$i_{\text{corr}} = \frac{\beta_{\text{A}}\beta_{\text{c}}}{2.3(\beta_{\text{A}} + \beta_{\text{c}})}\left(\frac{\Delta i}{\Delta E}\right)$$

$$\text{corrosion rate (mpy)} = \frac{0.13 i_{\text{corr}}(\text{Eq wt})}{d}$$

Polarization experiments on a corrosion system are carried out by using a potentiostat. The experimental arrangement of the cell consists of a working electrode, reference electrode and a counter-electrode. The counter-electrode is used to apply a potential on the working electrode both in the anodic and the cathodic direction, and measure the resulting currents. The electrochemical cell is depicted in Figure 1.26.

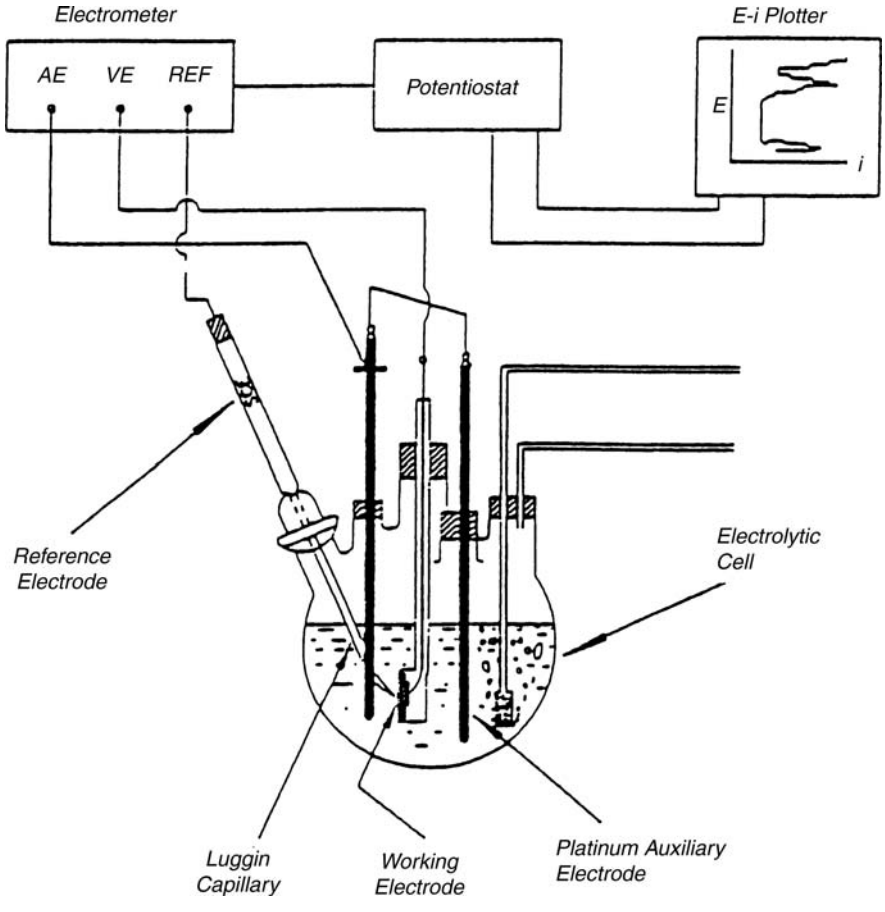

Figure 1.26 *Electrochemical cell used for potentiodynamic polarization studies*

1.3.5 Concentration Polarization

Concentration polarization may be illustrated by considering copper cathode in copper sulfate solution as an example. Using the Nernst equation we have for the oxidation potential.

$$E_1 = -0.337 - \frac{0.059}{2}\log(\mathrm{Cu}^{2+})$$

Upon current flow, copper is deposited, thereby reducing the amount of cupric ions to a new value $(\mathrm{Cu}^{2+})_s$, when,

$$E_2 = -0.337 - \frac{0.059}{2}\log(\mathrm{Cu}^{2+})_s$$

The difference in potential

$$E_2 - E_1 = \frac{0.059}{2} \log \frac{[Cu^{2+}]}{[Cu^{2+}]_s}$$

As the current flow increases, the smaller is the $(Cu)_s$ value and the larger is the polarization; this is known as concentration polarization. When $[Cu]_s$ approaches zero, the current density is known as the limiting current density.

When the limiting current density is i_L for the cathodic reaction, as i approaches i_L an expression is obtained of the form,

$$E_2 - E_1 = \frac{-RT}{nF} \ln \frac{i_L}{i_L - i}$$

The limiting current density is obtained from:

$$i_L = \frac{DnF}{\delta t} c \times 10^{-3}$$

where D is the diffusion coefficient, F, the Faraday, δ the thickness of the electrode layer and n is the number of electrons.

It is to be noted that the Helmholtz double layer plays a significant role in concentration polarization since the concentration of the ions on the electrode surface, and the diffusion of ions from the bulk of the solution into the Helmholtz plane are contributing factors to the limiting current density. This situation may be visualized as shown below:

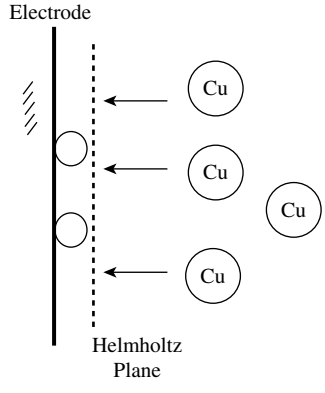

Activation polarization involves a slow step in the electrode reaction. The reduction of hydrogen at the cathode involves:

$$H^+ + e^- \rightarrow H, H + H \rightarrow H_2$$

and this is also known as the hydrogen overvoltage.
Another example is:

$$2\,OH^- \rightarrow \tfrac{1}{2}O_2 + H_2O + 2e^-$$

and this is known as the oxygen overvoltage.

Table 1.7 *Hydrogen reaction*[22]

Metal	Exchange current density (A/cm^2)
Pb, Hg	10^{-13}
Zn	10^{-11}
Sn, Al, Be	10^{-10}
Fe	10^{-6}
Ni, Ag, Cu and Cd	10^{-7}
Pd, Rh	10^{-4}
Pt	10^{-2}

The smaller the value for the exchange current density, the more polarizeable the metal.

Activation polarization, η in general terms may be given by:

$$\eta = \beta \log i/i_0$$

where β and i_0 are constants for a metal and a particular medium. The significance of the hydrogen overvoltage lies in the fact that acids attack most metals, and it is useful to know the exchange current densities and the hydrogen overpotentials of some common metals (see Table 1.7). The smaller the exchange current density the greater the polarizability.

Some data on hydrogen overvoltage for some metals at current density of 1 mA/cm^2 are given in Table 1.8.

In the first instance the equilibrium oxidation potential determines whether corrosion is likely or not. Then the hydrogen overpotential determines the corrosion rate of the metal in question.

Mixed potential theory can be illustrated by considering the two metals iron and zinc in an acid solution. The two factors to be considered are the anodic polarization line of the metal and the exchange current density for hydrogen evolution on the metal. Although zinc is expected to corrode according to its position in the galvanic series, it is the iron that corrodes in this system because the exchange current density for hydrogen evolution is higher on iron than on zinc. A mixed potential diagram for the iron, zinc system is shown in Figure 1.27. The lines a and b, refer to zinc alone and a″ and b″ are those of iron corroding in an isolated condition. The lines (a + a′) and (b + b′) represent the mixed electrode system of iron and zinc.[75]

Table 1.8 *Overvoltage data*[23]

Metal	i_0 (A/cm^2)	η, V (1 mA/cm^2)
Pt	10^{-3}	0.00
Pd	2×10^{-4}	0.02
Ni	8×10^{-7}	0.31
Fe	10^{-7}	0.40
Cu	2×10^{-7}	0.44
Al	10^{-10}	0.70
Sn	10^{-8}	0.75
Zn	1.6×10^{-11}	0.94
Pb	2.0×10^{-13}	1.16

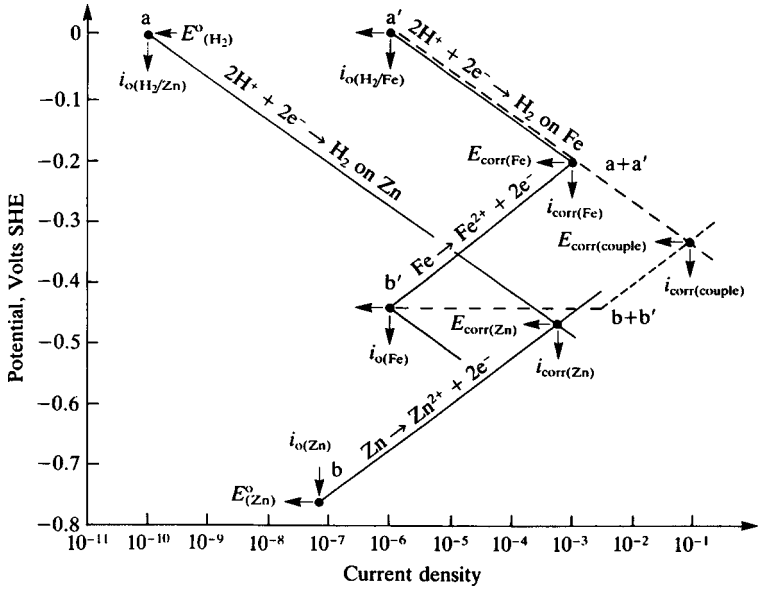

Figure 1.27 *A mixed potential plot for the bimetallic couple of iron and zinc. The figure also explains the higher corrosion rate of iron than zinc in hydrochloric acid solution. Despite the more positive reduction potential of iron, the evolution of hydrogen on iron has a high exchange current density (Reproduced from Corrosion for Science and Engineering, Tretheway and Chamberlain, Copyright Pearson Education Ltd)*

The example of the iron/zinc couple refers to an acid solution, if a neutral or alkaline (basic) solution is considered the cathodic reaction would be:

$$2\,H_2O + O_2 + 4e^- \rightarrow 4\,OH^-$$

and the rate of diffusion of oxygen to the surface of the metal has an important effect.

The electrochemical technique that is popular in corrosion studies is potentiodynamic polarization. This technique consists of using the sample specimen as the working electrode, with a reference electrode such as calomel electrode and a platinum counter- (auxiliary) electrode. A Luggin capillary is placed as close to the working electrode as possible to avoid or minimize the effect due to IR drop. The electrode assembly is immersed in the corrosive medium and the corrosion potential recorded. The potential is applied in the positive direction at a suitable rate (0.1 mV/s) and the resulting current recorded. Then the applied potential is in the negative direction to the corrosion potential and the resulting current noted. Thus, the potentiodynamic polarization gives the curves shown in Figure 1.28. The corrosion potential, the corrosion current obtained by drawing the anodic and the cathodic Tafel slopes, which interest at i_c and the various regions corresponding to activation polarization, concentration polarization and resistance polarization are labeled.

The experimental arrangement for potentiodynamic polarization experiment is shown in Figure 1.26. The experiment is done using the software, and polarization curves (both anodic and cathodic branches of polarization) are recorded at a suitable scan rate. The software performs the calculations and gives the data for corrosion potential and corrosion current density for the system on hand.

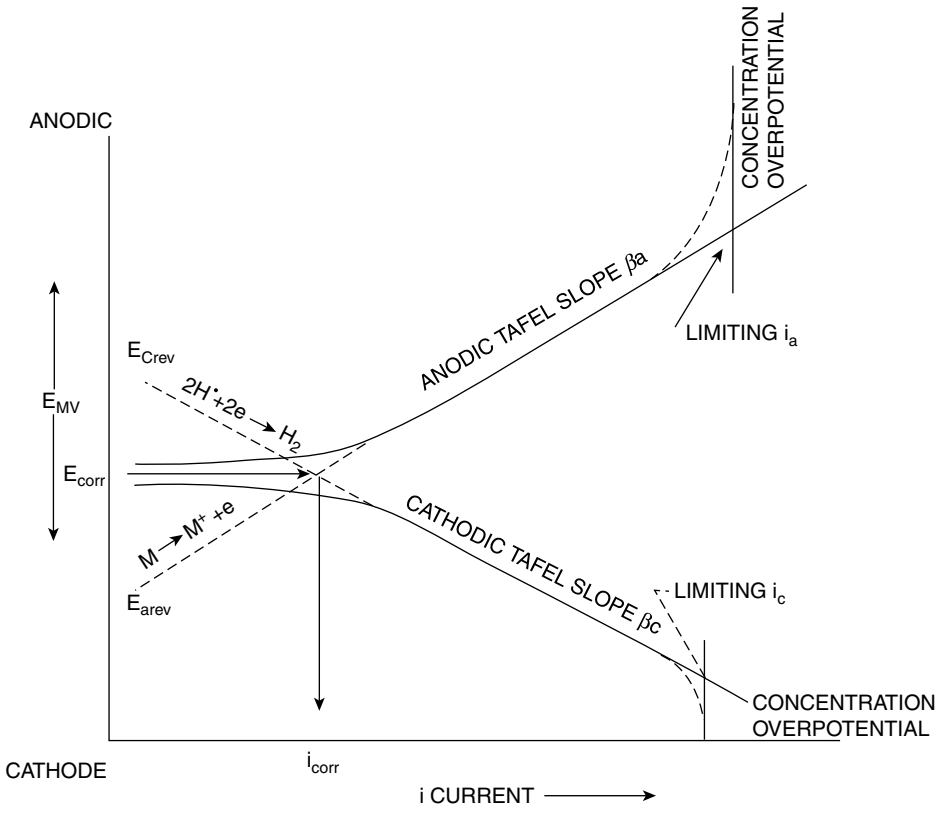

Figure 1.28 *Polarization diagram illustrating various parameters*

With the rapid developments of electrochemical techniques and the required instrumentation electrochemical impendance and electrochemical potential noise and current noise techniques are gaining prominence in corrosion studies.

Electrochemical impedance data give information on the kinetics and mechanism of the corroding system. Alternating current techniques have some advantages over DC techniques:

(i) AC techniques use very small excitation amplitudes in the range of 5–10 mV peak-to-peak;
(ii) data on electrode capacitance and charge transfer kinetics provide mechanistic information;
(iii) AC techniques can be applied to low-conductivity solutions while DC techniques are subject to serious potential errors in these media.

Consider the application of a small sinusoidal potential $(\Delta E \sin \omega t)$ on a corroding sample, which results in a signal along with the current flow of harmonics 2ω, 3ω, etc. Then the impedance $\Delta I \sin(\omega t + \phi)$ is the relation between $\Delta E/\Delta I$ and phase ϕ. In the case of corrosion studies, the sample is made part of a system known as equivalent circuit,[24] which consists of the solution resistance R_s, charge transfer resistance R_{CT} and the capacitance of the double layer C_{dl}. The measured impedance plot appears in the form of

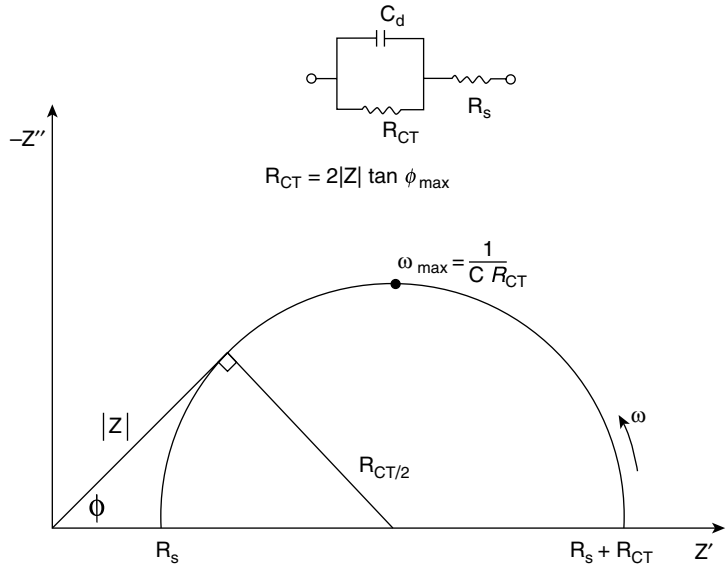

Figure 1.29 *Representation of equivalent circuit*[24]

semicircule (Nyquist plot). Both the equivalent circuit and the impedance plot are shown in Figure 1.29. The electrochemical experimental arrangement consisting of AC impedance analyzer, the electrochemical cell, and the computer to acquire the data over a period of time is depicted in Figure 1.30. It is useful to note that the polarization resistance data obtained can be used to calculate the corrosion rate of the corroding sample.

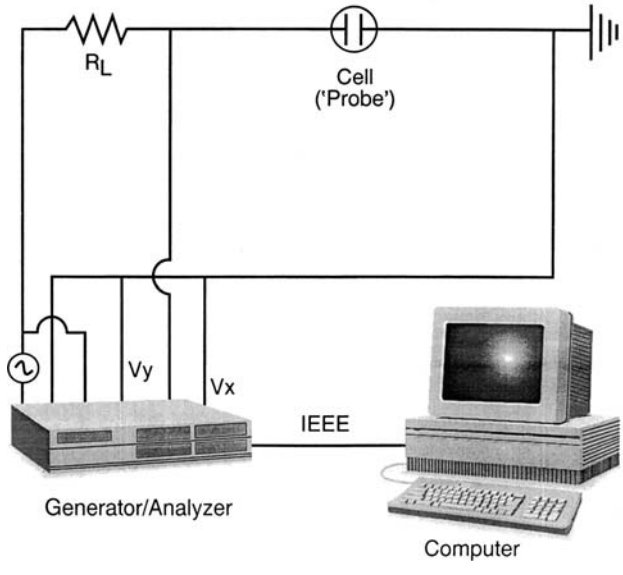

Figure 1.30 *Experimental set-up for AC impedance*

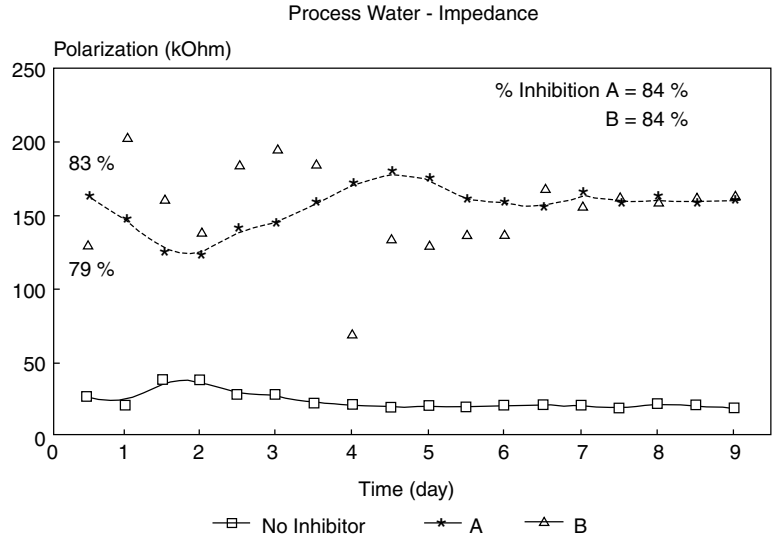

Figure 1.31 *Polarization resistance as a function of time*

Polarization resistance of the corroding sample may also be monitored over an extended duration. Thus, AC impedance may be used for online monitoring of a corrosion system such as on-line determination of corrosion inhibitor performance, as depicted in Figure 1.31.

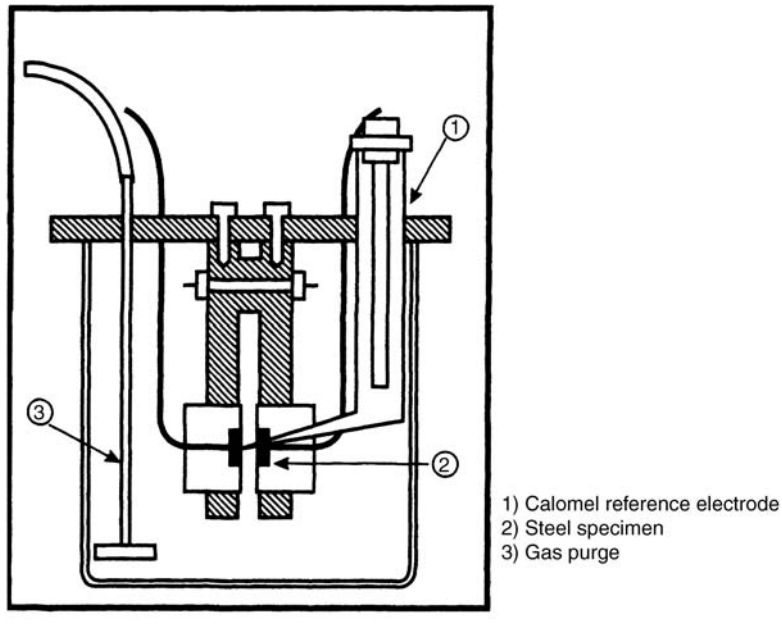

Figure 1.32 *Electrochemical cell*[24]

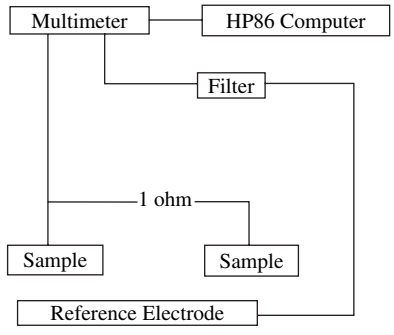

Figure 1.33 *Apparatus used for potential noise measurements*[24]

Electrochemical potential noise or current noise is gaining importance in monitoring corrosion processes, especially when localized corrosion such as pitting corrosion is involved. The electrochemical cell and the experimental arrangement for potential noise measurements are depicted in Figure 1.32 and 1.33, respectively. The figures clearly show the simplicity of the technique. This technique is particularly suited for on-line monitoring of corrosion processes for long durations and typical data obtained in the evaluation of the performance of corrosion inhibitors in a field study are shown in Figure 1.34. The AC impedance data given in Figure 1.31 and the potential noise data given in Figure 1.34 refer to the same system and shows an inhibition efficiency of 79–84%.

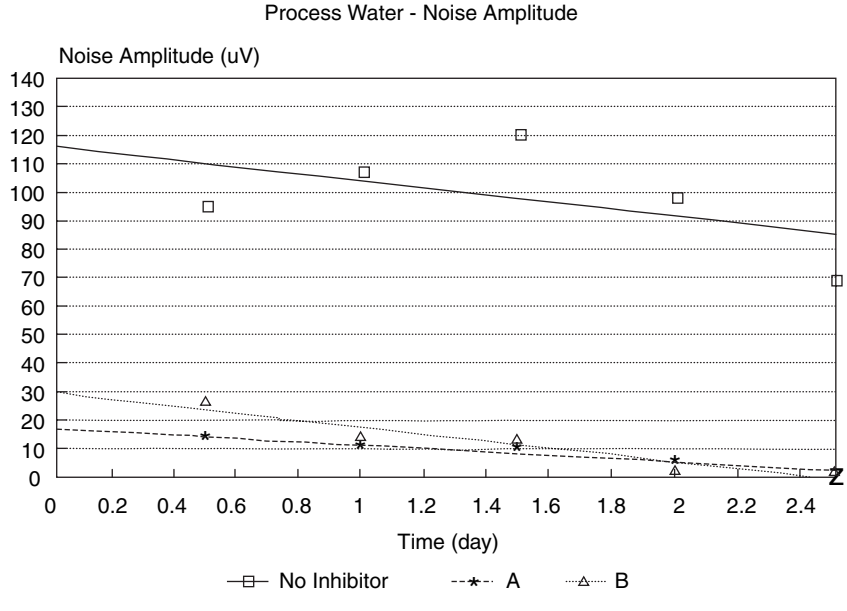

Figure 1.34 *Potential noise amplitude vs time*[24]

1.4 Oxidation and High-Temperature Corrosion

In the early part of this chapter winning metals by the reduction of oxides with reducing agent was cited:

$$2\,Fe_2O_3 + 3C \rightarrow 4\,Fe + 3\,CO_2$$

and the reverse reaction as oxidation of the metal,

$$4\,Fe + 3\,O_2 \rightarrow 2\,Fe_2O_3$$

otherwise known as corrosion of iron. In the oxidation of metal, we have:

$$M \rightarrow M^{n+} + ne^-$$
$$½\,O_2 = 2e^- \rightarrow O^{2-}$$

As a result of oxidation the product metal oxide is formed. In one of the earliest studies of oxide formation, Pilling and Bedworth[25] correlated oxidation resistance of metals with the volume ratio of oxide to metal per gram atom of metal. The oxide to metal volume ratios are given in Table 1.9. In a qualitative sense the ratio values of less than 1.0 and those between 2 to 3 are likely to be nonprotective oxides.

It should be noted that this ratio is olny empirical and indicates protective nature; other factors such as good adherence, high melting point, low vapor pressure, good high-temperature plasticity to fracture, low electrical conductivity or low diffusion coefficients for metal ions and oxygen define the protection nature.

Oxidation of metals occurs at the metal–scale interface and oxygen reduction at the scale–gas interface. This results in the formation of metal oxide scale on the surface. This is analogous to aqueous galvanic corrosion of metals. The oxide layer formed serves the

Table 1.9 *Values for the ratio volume of oxide produced/volume of metal consumed in producing the oxide*[26]

Metal	M_d/m_d
Li	0.57
Ca	0.64
Mg	0.81
Al	1.28
Ni	1.52
Zr	1.56
Cu	1.68
Ti	1.77
Fe	1.77
U	1.94
Cr	1.99
Mo	3.24
W	3.35

M_d = volume of oxide; m_d = volume of metal

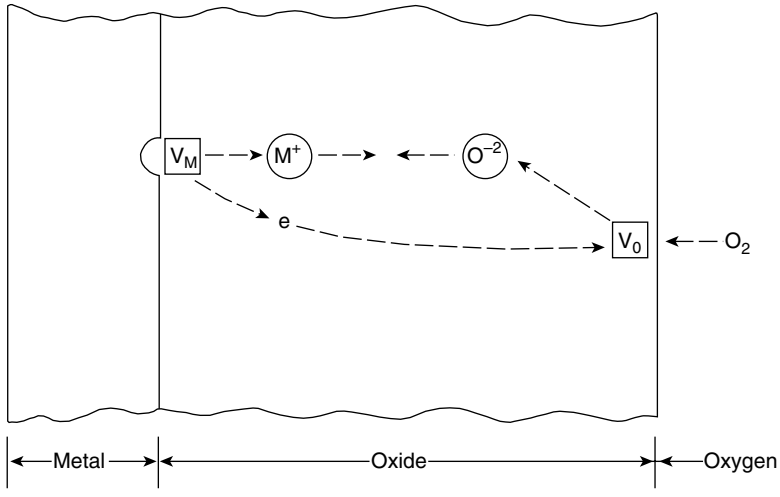

Figure 1.35 *Schematic illustration of electrochemical processes occurring during gaseous oxidation*

purpose of an ionic conductor (electrolyte), an electronic conductor, as an electrode at which oxygen is reduced and as a diffusion barrier through which electrons pass, and ions must migrate over defect lattice sites, indicated as V_M and V_o in Figure 1.35.

Kinetics of oxidation of metals forming oxides obeys different rate laws. The four different rate laws obeyed by metals during oxidation are illustrated in Figure 1.36. The oxidation of metals which form volatile oxides show a linear weight loss and these oxides are not protective. Oxidation of metals showing gain in weight may obey linear, parabolic and logarithmic kinetics. The oxidation of metal which results in weight gain and follows a parabolic kinetics is typified by an oxide film which remains intact on the metal surface, offering a uniform barrier to the diffusion of metal or oxide ions through the film. The parabolic rate law for the oxidation when the oxide thickness is x, t the time and c is constant.[75]

$$\frac{dx}{dt} = c_1/x$$

$$x^2 = c_1 t$$

Examples of this category are oxides of cobalt, copper, nickel and tungsten. The oxidation of metal at high temperature such as iron at 1000°C and magnesium at 500°C obey rectilinear rate law.

$$\frac{dx}{dt} = C$$

$$x = ct(\text{c is a constant})$$

In oxidation of this type the oxide is unable to offer a barrier to oxygen coming to the metal surface. If the oxide formed cracks or spalls due to internal stresses a few parabolic weight gain steps might occur which might appear linear overall.

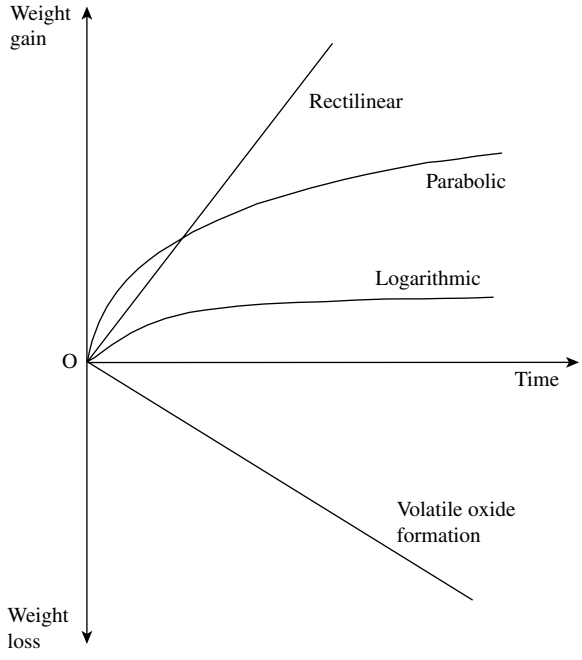

Figure 1.36 *Oxidation rate loss showing weight gain and weight loss with different kinetic forms. (Reproduced from Corrosion for Science and Engineering, Tretheway and Chamberlain, Copyright Pearson Education Ltd)*

In the case of some metals such as magnesium below a temperature of 200°C, a thin oxide layer is formed, which resists diffusion of oxygen and as a result an initial formation of oxide is followed by practically zero growth of the oxide. The rate law governing this type of oxide growth is logarithmic.[75]

$$x = C_0 \log(C_1 t + C_2)$$

where C_0, C_1 and C_2 are constants and x the thickness of the oxide layer. Another familiar example obeying the logarithmic rate law of oxide growth is aluminum below 50°C.

In some cases of oxidation of metals such as zirconium, the growth rate of oxide film has multiple stages of growth, as illustrated in Figure 1.37. The figure shows two points of change in curve A and one point of change in curve B where the oxide growth patterns change suddenly. These points are known as breakaway points, and are referred to as breakaway corrosion.

Curve A shows two breakaway stages while curve B shows one breakaway point. An example of such behavior is the oxidation of zirconium. Tin is added to zirconium to minimize breakaway corrosion.

Some examples of the phenomenon of breakaway corrosion are encountered in nuclear reactors used for power generation. In some reactors carbon dioxide is used as a coolant. Mild steel is chosen for use in gas-cooled reactors at 400°C, steel containing chrominum

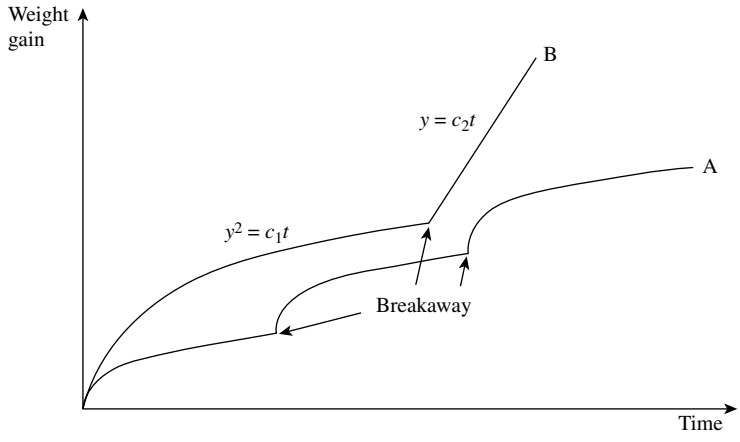

Figure 1.37 *Typical breakaway corrosion curves. (Reproduced from Corrosion for Science and Engineering, Tretheway and Chamberlain, Copyright Pearson Education Ltd)*

and molybdenum for temperatures at 400–500°C and austenitic stailness steel for temperatures greater than 550°C. In the nuclear reactors failure of bolts and nuts was observed due to breakaway corrosion. The mechanism of breakaway oxidation is complex and a simplistic explanation is as follows:

The protective oxide on ferritic steel consists of two layers, which are porous to carbon dioxide. The inner layer consists of crystallites of Cr and Si and the outer layer Fe_3O_4 (magnetite) formed by the reaction of metallic iron and CO_2 and the product CO giving elemental carbon.

$$3\,Fe + 4\,CO_2 \rightarrow Fe_3O_4 + 4\,CO$$

$$2\,CO \rightarrow CO_2 + C$$

The elemental carbon on reaching a level of 10% by weight in the inner oxide layer results in loss of protective action and initiation of breakaway corrosion.

We have so far dealt with the rate laws that govern the oxidation of metals and the empirical nature of the protective properties of the oxides. It has been pointed out earlier that the oxidation of metals at high temperatures is analogous to galvanic corrosion phenomena.

Metal oxides, the products of oxidation of metals are ionic compounds with the metal ions and oxide ions arranged in arrays in the crystal lattices. When the metal oxide contains excess metal ions in interstitial positions, they are known as n-type (or negative carrier type) oxides. When the metal oxides contain vacant sites (deficient in metal ions) in the lattice the oxides are known as p-type (positive carrier type).

n-type	ZnO	CdO	$A1_2O_3$
p-type	Cu_2O	NiO	Cr_2O_3

In the formation of metal oxides, both diffusion of oxygen inwards through the film on metal as well as diffusion of metal outwards may occur. Diffusion of oxide inwards to the metal/oxide interface is typified by titanium–oxygen and zirconium–oxygen systems.

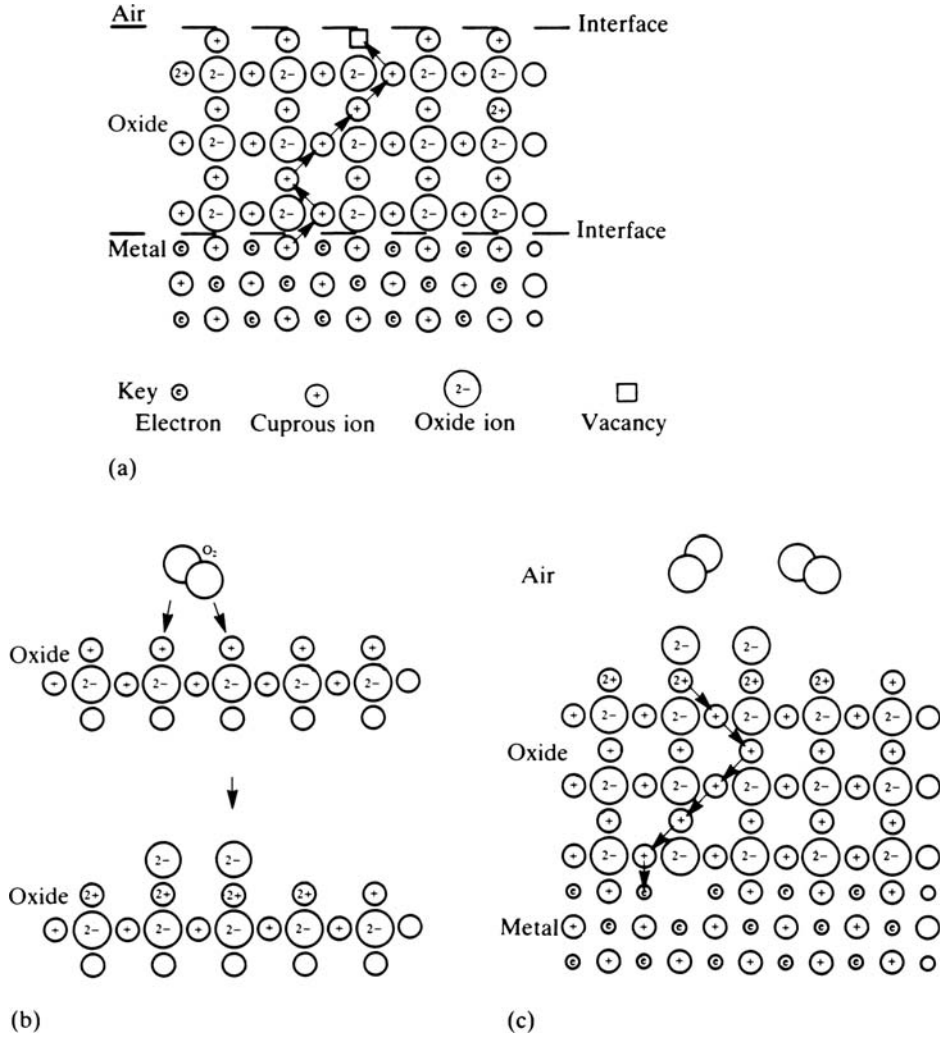

Figure 1.38 *Schematic diagram of the mechanism of oxidation of copper: (a) Diffusion of Cu^+ ions from the metal to the air/oxide interface via cation vacancies; (b) reaction of oxygen molecules with Cu^+ ions at the air/oxide interface; (c) diffusion of positive charge inwards to neutralize the excess of electrons in the metal. (Reproduced from Corrosion for Science and Engineering, Tretheway and Chamberlain, Copyright Pearson Education Ltd)*

Diffusion of metal outwards from the metal/oxide interface occurs in the copper–oxygen system.

The mechanism of oxidation of copper to produce cuprous oxide may be visualized as shown in Figure 1.38. Cuprous oxide is a p-type material and in Figure 1.38(a), the diffusion of cuprous ions to the metal to air/oxide through cation vacancies is shown with the path indicated by arrows. The oxygen molecules react with cuprous ions at the

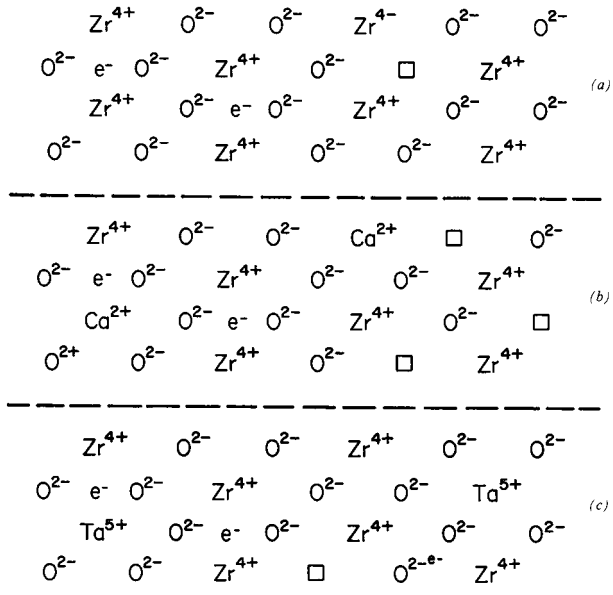

Figure 1.39 *Idealized lattice structure of zirconium oxide, an n-type semiconductor: (a) pure ZrO; (b) effect of Ca^{2+} addition; (c) effect of Ta^{5+} addition*

air/oxide interface as shown in Figure 1.38(b). The diffusion of positive charge inwards and electrons outwards to maintain electroneutrality occurs in the last step. One of the requirements of this type of mechanism is that the metal under consideration should have dual oxidation states. Examples of such metals are iron (II, III), Ni (II, III) and Cu (I, II).

In the case of NiO which is p-type metal-deficient material we have a structure with Ni^{2+}, O^{2-} and Ni^{3+} in nickel vacancy sites. Addition of lithium ion impurity to NiO makes it a p-type conductor and oxide growth rate is reduced compared with the Ni–O_2 system alone. On the other hand addition of Cr to Ni results in greater ease of oxidation than nickel alone due to higher cation diffusivity.

Zirconium oxide, an n-type oxide, has a monoclinic lattice and has excess metal. The vacant sites are compensated by electrons to maintain electroneutrality. In this case electron current is carried by the electrons and ion transport by the oxide ion. The addition of Ca^{2+} ions to the zirconium system results in a disposition such that Ca^{2+} ions fit into the monoclinic lattice, which is schematically shown in Figure 1.39.

In the case of calcium, anion vacancies are formed and charge compensation occurs. Substitution by addition of tantalum results in considerable changes in ionic diffusivity and electrical conductivity.

1.4.1 Oxidation of Alloys

Detailed systematic studies on the oxidation of alloys by Hauffe, Wagner *et al.*[27–29] led to some generalizations with respect to the role of minor elements on the oxide growth. In the case of Zn(n-type) addition of a small amount of Al results in considerable increase in oxidation rate of zinc. Addition of chrominum to nickel (which forms a p-type oxide)

Table 1.10 *The effect of alloying upon the rate of oxidation*[75]

Oxide type	Valency of alloying element compared with parent metal	Effect	Diffusion-controlled oxidation rate
p-type Cu_2O NiO FeO Cr_2O_3 CoO	Higher valency	Increases number of vacancies Decreases number of parent metal ions with a higher valency	Increases
Ag_2O MnO SnO	Lower valency	Decreases number of vacancies Increases number of parent metal ions with a higher valency	Decreases
n-type ZnO CdO Al_2O_3 TiO_2	Higher valency	Decreases concentration of interstitial metal ions Increases number of free electrons	Decreases
V_2O_5	Lower valency	Increases concentration of interstitial metal ions Decreases number of free electrons	Increases

results in increase in oxidation rate. On the other hand addition of lithium to nickel oxide results in reduced diffusion of nickel.

Some of the general rules deduced by Hauffe and Wagner with respect to oxidation of alloys, and the role of alloying elements on the oxidation rates are summarized in Table 1.10.

Over the years many alloys have been developed for applications in which the alloys resist oxidation and give good performance without failure. Table 1.11 gives the nominal compositions of some alloys for use in industrial environments. The performance of alloys in various industrial environments is summarized in Table 1.12.

Miscellaneous metal–gas reactions[30] other than metal–oxygen reactions may be referenced as follows. Decarburization and hydrogen attack. This is encountered when hydrogen removes the carbon from the steel resulting in loss of strength of the steel. Hydrogen combines with carbon to produce methane and causes decarburization. The reaction with hydrogen may also cause cracking of steel (HIC).

In the petroleum industry carbon monoxide and carbon dioxide reactions with steel are encountered which may also cause decarburization or carburization, depending upon the direction of the equilibrium.

$$C + CO_2 \rightleftharpoons 2CO$$

In the context of fossil fuels, sulfur compounds and their interaction with metals at high temperatures are important and this is termed sulfidation. The details of sulfidation attack are discussed in the literature[31]. The alloys which perform well in these atmospheres have already been cited (see Table 1.12).

Table 1.11 *Nominal compositions of high-temperature alloys for industrial environments*[75]

	Percent nominal weight										
Material	Ni	Co	Fe	Cr	Mo	W	Mn	Si	C	La	Others
Haynes 188	22	39	<3	22		14	<1.25	0.35	0.10	0.03	
214	75		3	16			<0.5	<0.2	0.05		4.5 Al, 0.01 Y, <0.1 Zr
230	57	<5	<3	22	2	14	0.5	0.4	0.10	0.02	0.3 Al
242	65	<2.5	<2	8	25		<0.8	<0.8	<0.03		<0.5 Al, <0.006 B, <0.5 Cu
556	20	18	31	22	3	2.5	1	0.4	0.10	0.02	0.6 Ta, 0.2 Al, 0.02 Zr
HR-120	37	<3	33	25	<2.5	<2.5	0.7	0.6	0.05		0.7 Cb, 0,2 N, 0.1 Al, 0.004 B
HR-160	37	30	<3.5	28	<1.0	<1.0	0.5	2.75	0.05		<1.0 Cb
Hastelloy N	71	<0.2	<5	7	16	<0.5	<0.8	<1	<0.08		<0.35 Cu, <0.5 (Al + Ti)
Hastelloy S	67	<2	<3	16	15	<1	0.5	0.4	<0.02	0.05	0.25 Al, <0.015 B
Hastelloy X	47	1.5	18	22	9	0.6	<1	<1	0.1		<0.008 B

Table 1.12 *Alloy performance in high-temperature industrial environments[75] (Copyright Pearson Education Ltd)*

Alloy*	Environment							
	Oxidizing	Sulfur-bearing	Carburizing	Nitriding	Molten chloride salts	Oxidizing chlorine-bearing	Reducing chlorine-bearing	Reducing fluorine-bearing
214	Excellent to 1250°C		Excellent	Excellent	Good	Excellent	Very good	
230	Excellent to 1150°C	Good	Very good	Excellent				Good
HR-160	Very good to 1100°C	Excellent	Very good	Very good	Very good	Excellent	Very good	Good
Hastelloy X	Very good to 1100°C	Good	Good	Good	Good	Very good	Good	
Hastelloy S	Very good to 1100°C		Good	Very good	Very good		Excellent	Very good
Hastelloy N								Very good
Haynes 188	Very good to 1100°C	Very good	Good	Very good	Excellent			
556	Very good to 1100°C	Very good	Very good		Very good	Excellent	Good	
HR-120	Very good to 975°C Good to 1100°C	Very good	Very good			Good	Good	
242				Excellent	Excellent		Excellent	Excellent

*Haynes, Hastelloy, 214, 230, 242, 556, HR-120 and HR-160 are trademarks of Haynes International Inc

Hot corrosion[32] is encountered in the operation of gas turbines between 730 and 1730°C. Operation of gas turbine engines in marine atmosphere is prone to hot corrosion, which involves oxidation and reaction with sulfur, sodium, vanadium and other contaminants present in the fuel or ilnet air. The consequence of this is the loss of protective action of chromium oxide on the blade and sometimes engine failure.

In marine atmospheres, the following reaction may occur:

$$2\,NaCl + S + 3/2\,O_2 \rightarrow Na_2SO_4 + 2HCl$$

and the sodium chloride and sodium sulfate form a slag. The slag on the surface melts at ~620°C and disrupts the protective action of chromium and aluminum oxides.

The elemental sulfur may also react with chromium to form sulfides and deplete the surface in chromium. Furthermore, the chromium sulfide releases sulfur by thermal decomposition, which in turn diffuses into the metal and depletes the chromium from the surface, which would otherwise offer protection. This mechanism of depletion of chromium due to sulfidation and increase in the rate of hot corrosion can be overcome by increasing the chromium content of the alloy to a high level.

Hot corrosion may also occur in breeder reactors when the fission products deposit on the stailness steel cladding as complex salts based on CsI and Cs_2O. This mode of corrosion occurs in boilers and turbines burning high-ash coal or residual fuel oil well as well as heat exchangers, alkali-carbonate-based fuel cells and carbonate storage systems.

It may be summarized that fused salt chemistry coupled with electrochemistry are operating in hot corrosion. High-temperature Pourbaix diagrams representing phase stabilities for Al in Na_2SO_4 at 906°C and NiO in Na_2SO_4 have been used to estimate corrosion rates.[33,34]

1.5 Corrosion Prevention

Corrosion prevention involves inherent factors, which are within the control of the metallurgist or engineer. The three main categories considered are materials selection, design factors and life prediction analysis.

Materials selection process can be depicted in terms of Figure 1.40. Materials selection involves many factors that have to be optimized for a particular application. The foremost consideration is the cost of the material and its applicability in the environmental conditions so that integrity can be maintained during the lifetime of the equipment. When the material of construction is metallic in nature, the chemical composition and the mechanical properties of the metal are significant. Some of the important mechanical properties are hardness, creep, fatigue, stiffness, compression, shear, impact, tensile strength and wear.

The cost considerations involve factors such as raw materials, quantities, production cost with respect to weldability, formability and machinability, labor requirements and anticipated service life. Ready availability of the material depends on whether the material is made to order, or readily bought from the manufacturer, or bought off the shelf, and whether any tooling is required to meet the specific standards.

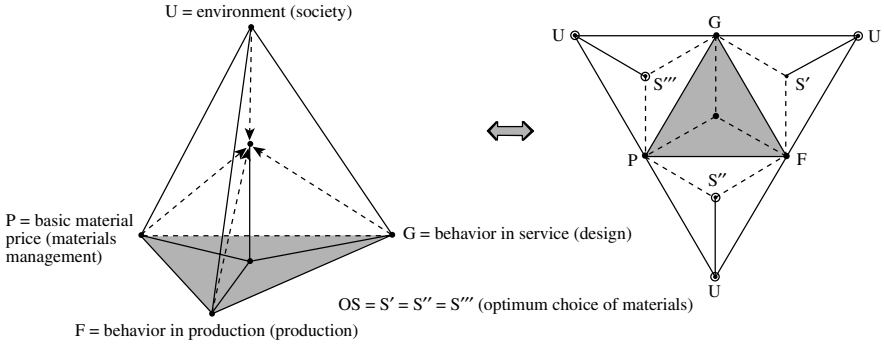

Figure 1.40 *The process of optimum material choice illustrated symbolically by a tetrahedron (industrial technology)*

Among the material properties of great importance and concern is design and choice of the material and its inherent resistance to corrosion. Significant and extensive experimental data on the corrosion rates of readily available metals and their alloys can be found in the literature.[35,36] The relative corrosion resistance of some steels, nickel, brass, nickel–copper alloys and Al–Cu alloys in chosen atmosphere[35] is shown in Table 1.13.

Table 1.13 *Relative corrosion resistance of some uncoated metals*[1]

Material	Industrial atmosphere	Fresh water	Seawater	Acid (H_2SO_4, 5–15% concentration)	Alkali (8%)
Low-carbon steel	1	1	1	1	5
Galvanized steel	4	2	4	1	1
Gray cast iron					
4–6% Cr steels	3	3	3	1	4
18–8 stainless steel	5	5	4	2	5
18–35 stainless steel	5	5	4	4	4
Monel (70% Ni, 30% Cu)	4	5	5	4	5
Nickel	4	5	5	4	5
Copper	4	4	4	3	3
Red brass (85% Cu, 15% Zn)	4	3	4	3	1
Aluminum bronze	4	4	4	3	3
Nickel silver (65% Cu, Ni, 17% Zn)	4	4	4	4	4
Al-Cu alloy (duralumin)	3	1	1	2	1

Key: 1 = poor–rapid attack; 2 = fair temperature use; 3 = good reasonable service; 4 = very good reliable service; 5 = excellent unlimited service

Table 1.14 *Compatible dissimilar metal couples*

Group	Metallurgical category	Emf (V)	Anodic index[1] (V)	Compatible couples[2]
1	Gold Au-Pt alloys wrought platinum	+0.15	0.10	○
2	Rhodium plated on silver-plated copper	+0.05	0.10	●
3	Silver, high-silver alloys	0	0.15	●●○
4	Nickel, nickel–copper alloys	−0.15	0.30	●●○
5	Copper, low brasses or bronze; silver solder; Ni–Cr alloys; austenitic corrosion-resistant steels	−0.20	0.35	●●●○
6	Commercial yellow brasses and bronzes	−0.25	0.40	●●●○
7	High brasses and bronzes, naval brass; Muntz metal	−0.30	0.45	●●●○
8	18% Cr stainless steels	−0.35	0.50	●●●●○
9	Chromium or tin plating, 12% Cr stainless steels	−0.45	0.60	●●●●○
10	Terne plate, tin-lead solder	−0.50	0.65	●●●●○
11	Lead, high-lead alloys	−0.55	0.70	●●●●○
12	Wrought 2000 series aluminum alloys	−0.60	0.75	●●●●○
13	Wrought gray or malleable iron, plain carbon and low-alloy steels, armco iron	−0.70	0.85	●●●●○
14	Wrought aluminum alloys except 2000 series, cast Al–Si alloys	−0.75	0.90	●●●●○
15	Cast aluminum alloys other than Al–Si, cadmium plating	−0.80	0.95	●●●●○
16	Hot-dip galvanized or electrogalvanized steel	−1.05	1.20	●○
17	Wrought zinc, zinc die-casting alloys	−1.10	1.25	●
18	Wrought and cast magnesium alloys	−1.60	1.75	●

[1]Anodic index is the absolute value of the potential difference between the noble (cathodic) metals listed (Group 1) and the metal or alloy in question

[2]Compatible means that the potential difference of the metals in question, which are connected by lines, is not more than 0.25 V. An open circle indicates the most cathodic member of a series; a closed circle indicates an anodic member. Arrows indicate the anodic direction

The compatible metallic couples of dissimilar metals along with the potentials taken from the literature[35] are shown in Table 1.14.

Some relevant data on stress–corrosion cracking in variety of environments are given in Table 1.15. The relative resistance of plastics and the environmental degradation of engineering plastics and the corrosion resistance of ceramic materials taken from the literature[35] are presented in Tables 1.16, 1.17 and 1.18, respectively. A typical format of presentation of corrosion performance data of ferrous alloys, austenitic stailness steels, copper-based alloys, nickel-based alloys and other miscellaneous metals in corrosive media such as hydrochloric acid is given in the literature.[36] Materials that have corrosion rates less than 20 mpy in different concentrations of hydrochloric acid, and temperatures are identified in the form of zones and depicted in Figure 1.41. The various metals in different zones are identified in Table 1.19.

Table 1.15 *Some environment/alloy combinations known to result in stress–corrosion cracking*

Environment	Aluminum alloys	Carbon steels	Cu alloys	Ni alloys	Austenitic	Duplex	Martensitic	Ti alloys	Zr alloys
Amines, aqueous		•	•						
Ammonia, anhydrous		•							
Ammonia, aqueous			•						
Bromine									•
Carbonates, aqueous		•							
Carbon monoxide, carbon dioxide and water mixture		•							
Chlorides, concentrated and boiling				•	•	•			
Chlorides, dry and hot				•				•	
Chlorinated solvents								•	•
Cyanides, aqueous and acidified		•							
Fluorides, aqueous				•					
Hydrochloric acid								•	
Hydrofluoric acid				•					
Hydroxides, aqueous		•			•	•	•		
Hydroxides, concentrated and hot				•	•	•	•		
Methanol plus halides								•	•
Nitrates, aqueous		•	•				•		
Nitric acid, concentrated									•
Nitric acid, fuming								•	
Nitrites, aqueous			•						
Nitrogen tetroxide								•	
Polythionic acids				•	•				
Steam			•						
Sulphides plus chlorides, aqueous					•	•	•		
Sulfurous acid					•				
Water, high-purity and hot	•			•					

Table 1.16 *Relative resistance of plastics to chemical exposure*[1]

Chemical media	PPS[2]	Nylon 6/6	PC[3]	PSO[4]	Mod. PPO[5]
Acids					
37% hydrochloric	100	0	0	100	100
30% sulfuric	100	0	100	100	100
Glacial acetic	98	0	67	91	78
Bases					
28% ammonium hydroxide	100	85	0	100	100
30% sodium hydroxide	100	89	7	100	100
N-butylamine	49	91	0	0	0
Aniline	96	85	0	0	0
Hydrocarbons					
Cyclohexane	100	90	75	99	0
Toluene	98	76	0	0	0
Diesel fuel	100	87	100	100	36
Gasoline	100	80	99	100	0
Organic solvents					
Chloroform	87	57	0	0	0
Chlorobenzene	100	73	0	0	0
Ethylene chloride	72	65	0	0	0
Butyl alcohol	100	87	94	100	84
Cyclohexanol	100	84	74	95	27
Phenol	100	0	0	0	0
Methyl ethyl ketone	100	87	0	0	0
Ethyl acetate	100	89	0	0	0

[1]Percent rentention of tensile strength after 24 h exposure at 200°F
[2]Polyphenylene sulfide
[3]Polycarbonate
[4]Polysulfone
[5]Modified polyphenylene oxide

Based on factors such as cast, mechanical properties, physical properties, ease of fabrication (design) and the corrosion resistance data available in the literature the choice of materials can lead to a short list of two or three materials. At this stage it is prudent that the engineer design prototype laboratory scale model equipment from the short-list of selected metals or alloys, and determine the corrosion rates in the environment of interest. These accelerated tests will enable the engineer to select the best candidate material, making proper allowance for the corrosion of the metal or alloy over the lifetime of the equipment.

1.6 Design Factors[37,38]

After selection of the material, the corrosion scientist must play a role in designing the equipment so that the design is appropriate, and avoids corrosion modes due to inappropriate design. Improper design may result in galvanic corrosion, crevice corrosion,

Table 1.17 *Environmental degradation[1] of engineering plastics*

Materials	Environment at 25 and 95°C																			
	Aromatic hydrocarbons		Aliphatic hydrocarbons		Halogenated solvents		Esters and Ketones		Alcohols		Amines		Weak bases and salt		Strong bases		Strong acids		Strong oxidants	
	25	95	25	95	25	95	25	95	25	95	25	95	25	95	25	95	25	95	25	95
Nylon (polyamide)	1	1	1	1	1	2	1	1	1	2	1	2	1	2	2	3	5	5	5	5
Polycarbonate (PC)	5	5	1	1	5	5	5	5		2		5	1	5	5	5	1	1	1	1
Polyesters	2	5	1	3–5	3	5	2	3–4					1	3–4	2	5	3	4–5	2	3–5
Polytetrafluor-eothylene (PTFE)	1	1	1	1	1	1	1	1	1	1	1	1	1	1	1	1	1	1	1	1
Polyimides	1	1	1	1	1	1	1	1					2	3	4	5	3	4	2	5
Polyphenylene oxide (PPO)	4	5	2	3	4	5	2	3		2–5		5	1	1	1	1	1	2	1	2
Polyphenylene sulphide (PPS)	1	2	1	1	1	2	1	1	1	1		1–3	1	1	1	1	1	1	1	3
Polysulfone (PSO)	4	4	1	1	5	5	3	4	1	1		5	1	1	1	1	1	1	1	1
Diallyl phthalate (DAP)	1–2	2–4	2	3	2	4	3–4	4–5					2	3	2	4	1–2	2–3	2	4
Phenolics	1	1	1	1	1	1	2	2	1	1	–	–	2	3	3	5	1	1	4	5

[1]No effect or inert; [2]slight effect; [3]mild effect

Table 1.18 *Corrosion of advanced ceramics in liquids*

Test environment[1]: conc. reagent, wt %	Temperature °C	(°F)	Corrosive weight loss, mg/cm^2 yr^2 Si/SiC composites (12% Si)	Tungsten carbide (6% Co)	Alumina (99%)	Silicon carbide (No free Si)
98% H_2SO_4	100	(212)	55.0	>1,000	65.0	1.8
50% NaOH	100	(212)	>1,000	5.0	75.0	2.5
53% HF	25	(77)	7.9	8.0	20.0	<0.2
85% H_3PO_4	100	(212)	8.8	55.0	>1,000	<0.2
70% HNO_3	100	(212)	0.5	>1,000	7.0	<0.2
45% KOH	100	(212)	>1,000	3.0	60.0	<0.2
25% HCl	70	(158)	0.9	85.0	72.0	<0.2
10% HF+ 57% HNO_3	25	(77)	>1,000	>1,000	16.0	<0.2

[1]Test time: 125–300 h submerged testing, continuously stirred
[2]Corrosion weight loss guide:

Rate	Comment
>1000 mg/cm^2 yr	Completely destroyed within days
100–999 mg/cm^2 yr	Not recommended for service greater than a month
50–100 mg/cm^2 yr	Not recommended for service greater than one year
10–49 mg/cm^2 yr	Caution recommended, based on the specific application
0.3–9.9 mg/cm^2 yr	Recommended for long-term service
<0.2 mg/cm^2 yr	Recommended for long-term service, no corrosion, other than as a result of surface cleaning, was evidenced.

concentration cells, erosion corrosion and base metal dissolution. Some of the design-related causes of corrosion are:

(i) use of dissimilar metals
(ii) poor drainage

Table 1.19 *Code for hydrochloric acid graph (Figure 1.41): materials with reported corrosion rates of <20 mpy*

Zone 1	Zone 2	Zone 3	Zone 4	Zone 5
20Cr 30Ni[1]	62 Ni 32Cu	62Ni 28Mo	66Ni 32Cu[2,6]	62Ni 28Mo[5]
66Ni 32Cu[2]	Molybdenum	Molybdenum	62Ni 28Mo[5]	Platinum
62Ni 28 Mo	Platinum	Platinum	Platinum	Silver
Copper[2]	Silicon bronze[2]	Silver	Silver	Tantalum
Nickel[2]	Silicon cast iron[3]	Tantalum	Tantalum	Zirconium
Platinum	Silver	Zirconium	Zirconium	
Silicon bronze[2]	Tantalum			
Silicon cast iron[3]	Zirconium			
Silver				
Tantalum				
Titanium[4]				
Tungsten				
Zirconium				

[1]<2% at 25°C
[2]No air
[3]No $FeC4_3$
[4]<10% at 25°C
[5]No chlorine
[6]<0.05% concentration

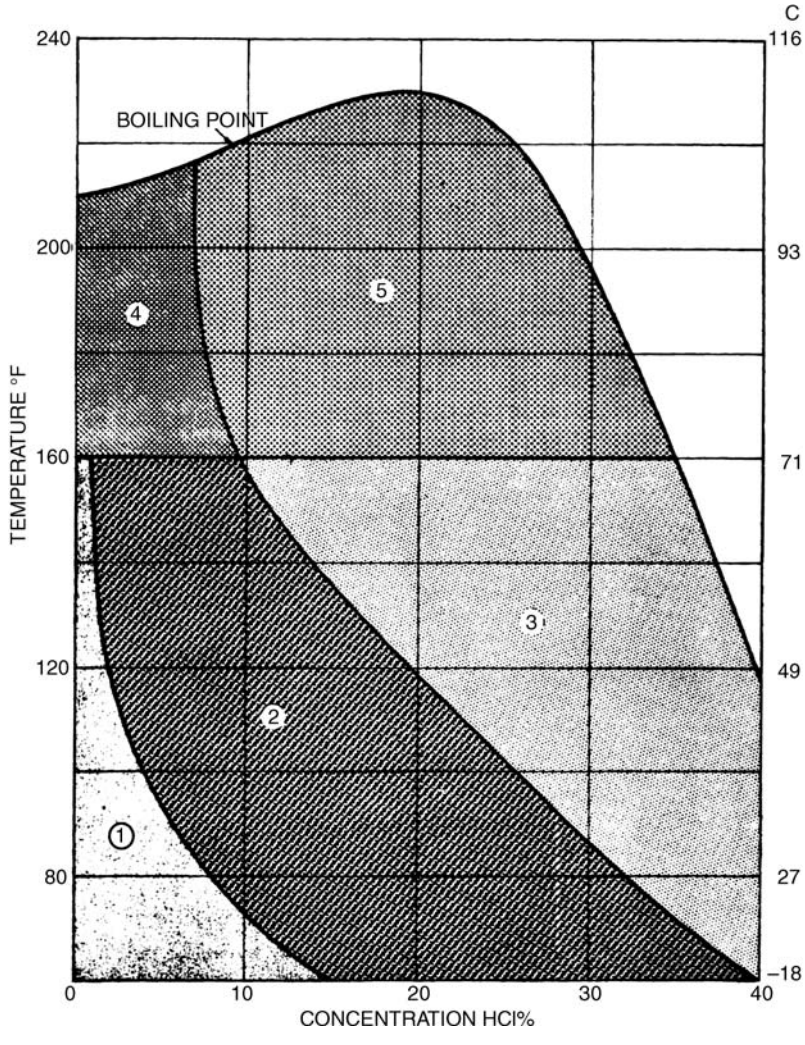

Figure 1.41 *Hydrochloric acid graph*

(iii) joints between metals and non-metals
(iv) presence of cevices
(v) stray currents
(vi) complex cells
(vii) relative motion between two interacting parts or between a metal and the environment
(viii) selective leaching of a metal in an alloy
(ix) inability to clean the surface thoroughly.

The galvanic series of metals and alloys in seawater has been given in Figure 1.6; whenever dissimilar metals are used, it is prudent to select a pair of metals with minimum difference in potential, in the particular environment and temperature of exposure.

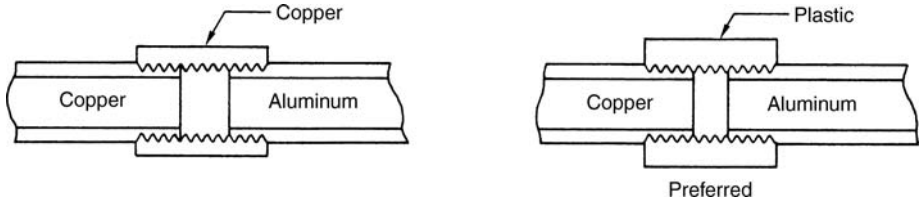

Figure 1.42 *Insulating material between dissimilar metals, such as copper and aluminum prevents galvanic corrosion*

In the case of aluminum and copper, aluminum will corrode in preference to copper. Galvanic corrosion (dissimilar metal corrosion) is affected by the relative areas of the two metals exposed to the corrosive medium. In most cases, the corrosion is under cathodic control, i.e., the size of the cathode controls the anodic current density. The larger the cathode area the larger will be the anodic current density. Thus, to minimize dissimilar metal corrosion the design should maximize anode area, and minimize cathode area. By insulating between copper and aluminum galvanic corrosion can be minimized, as shown in Figure 1.42. It is also desirable to avoid rivets that are anodic to the metal parts being joined in order to prevent corrosion of rivets and failure of the joints.

It is also necessary to provide an efficient drainage in the equipment through proper design. The stagnant areas in three improper designs which result in corrosion are shown in see Figure 1.43. A design for proper drainage of the liquid termed as

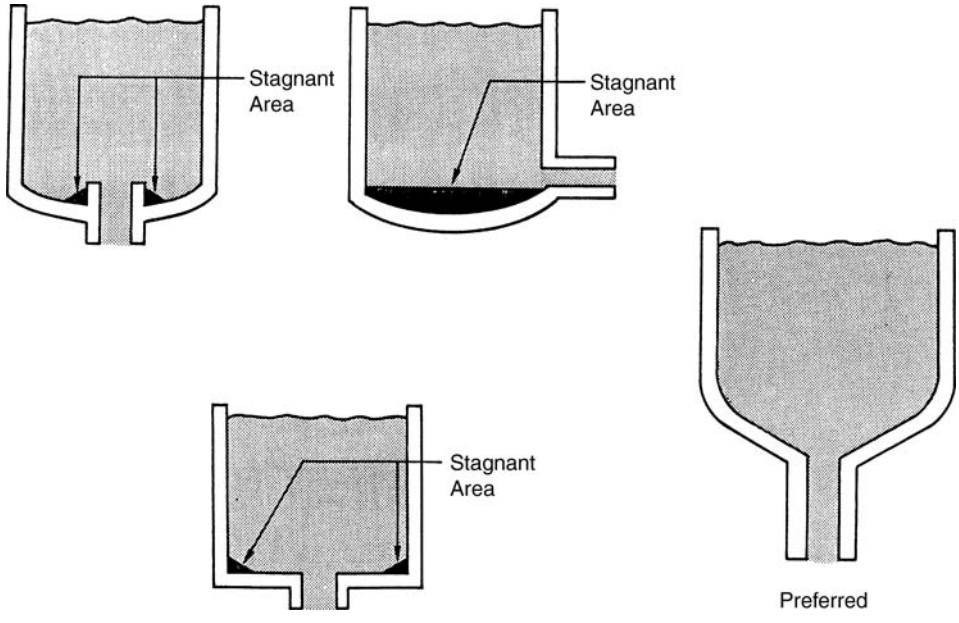

Figure 1.43 *Design for drainage*

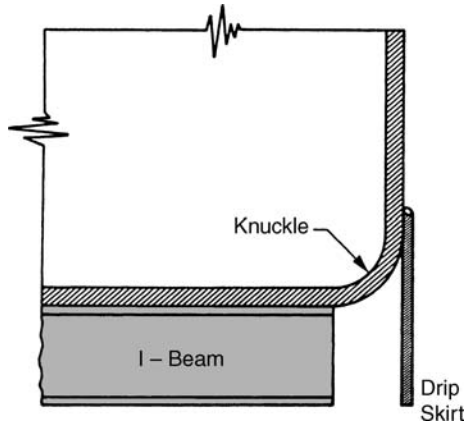

Figure 1.44 *A drip skirt reduces moisture collection under flat-bottom tanks*

preferred design is shown in Figure 1.43. In the case of flat-bottom tanks drip skirts are incorporated (Figure 1.44), which will direct the moisture to the ground instead of the moisture clinging to the sides and ending at the bottom of the tanks. The case of a pipe where water collects at the underside of pipe, and the same pipe with a metal support and a reinforcing saddle seal welded to the pipe are shown in Figure 1.45. In the preferred configuration, the moisture is not trapped, and as a result corrosive attack can be minimized.

Stanchions may be used for flat-bottom tanks in place of pads. For large tanks such as oil tanks, a cement ring is used to support the edge of the tank and the bottom is placed on

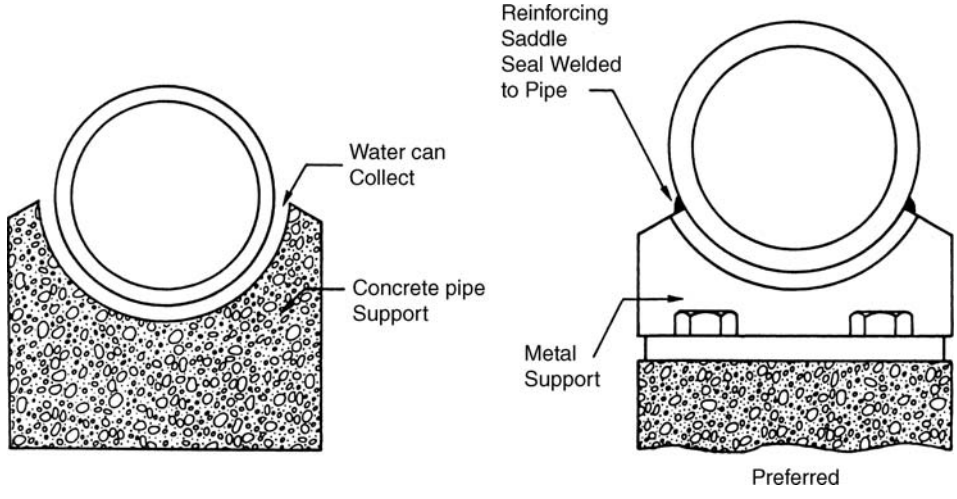

Figure 1.45 *Ceiling and a metal cradle avoid accumulation of water under a pipe in outdoor construction*

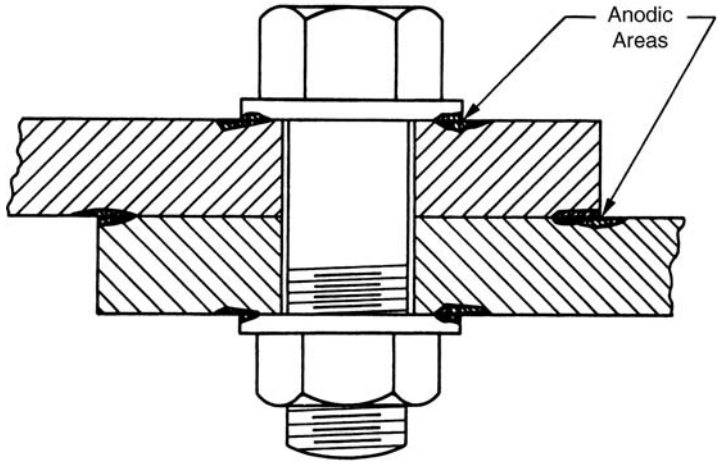

Figure 1.46 *Crevices lead to concentration cell corrosion*

compacted, crowned and oiled sand. The oiled sand gives corrosion protection for the underside of the tanks.

In the case of lap joints and other areas where crevices exist, the accumulated moisture leads to crevice corrosion. Crevice corrosion arises due to differential aeration cells. In the crevices less air causes the crevice region become anodic compared with the oxygen-rich regions which become cathodic. A typical case is illustrated in Figure 1.46. In some instances sealants are used and care needs to be exercised in the sense the sealants do not harden and cause a problem. In the place of sealants it is possible that galvanized steel parts or alclad aluminum parts may be used which can provide cathodic protection within the crevice. The configuration where a sealant or gasket may be used is illustrated in Figure 1.47.

When a system consists of a flowing component which impinges on a part or some parts of the structure we encounter erosion–corrosion, or abrasive wear and cavitation. The design must be such that localized constrictions are avoided or sharp directional

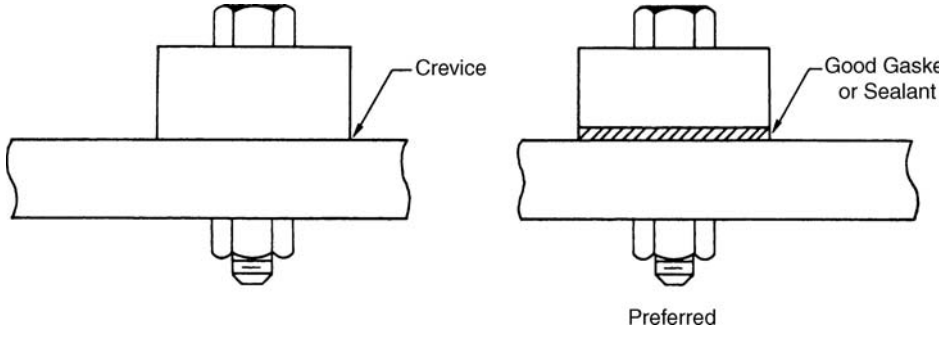

Figure 1.47 *Gasket or sealant to avoid crevices*

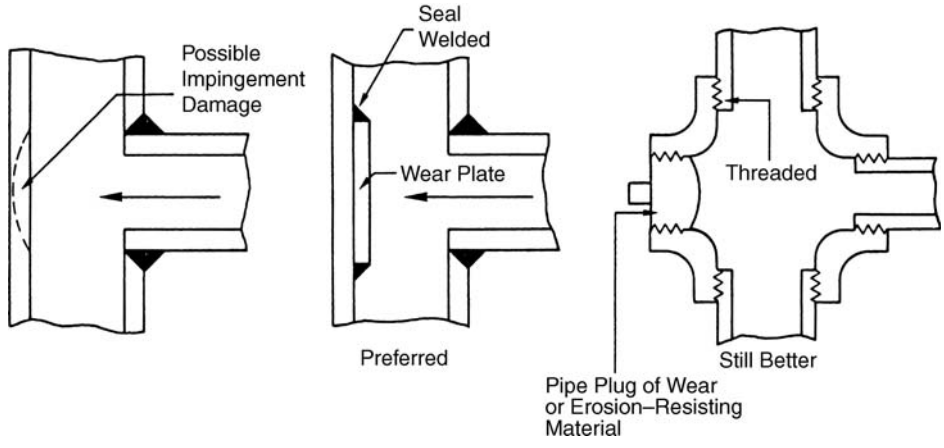

Figure 1.48 *Wear-resisting designs to minimize corrosive wear*

changes of the flow. Wear-resistant design to minimize corrosive wear is illustrated in Figure 1.48.

In some situations evaporation of solutions or localized condensation of vapors, which on further vaporization resulting in increase in concentration may cause corrosion. Such a localized concentration and the resulting corrosion can be mitigated through proper design as illustrated in Figure 1.49. The figure shows a preferred design to avoid evaporation and concentration of solutions resulting in corrosion.

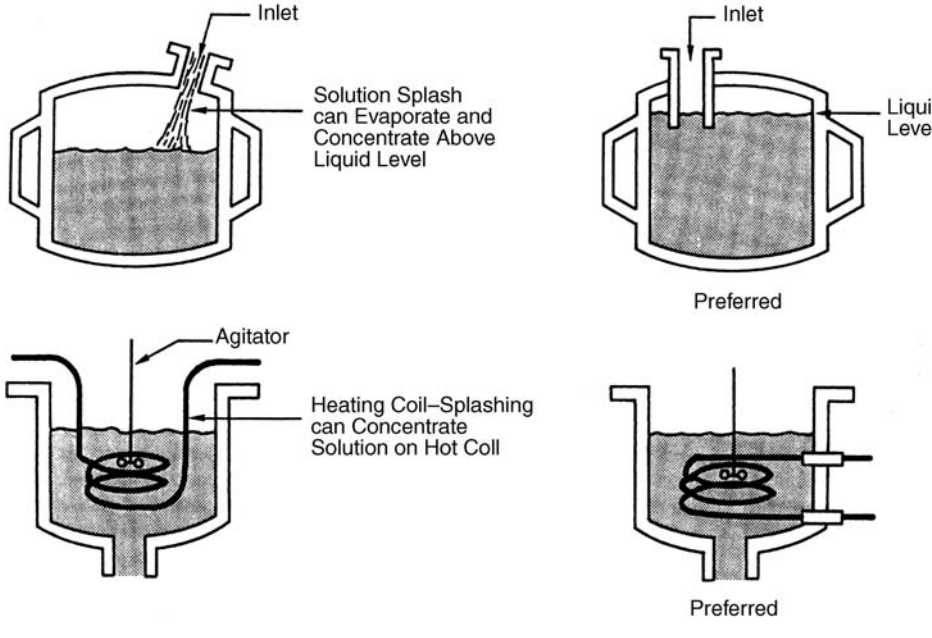

Figure 1.49 *Designs to minimize evaporation and concentration of solutions*

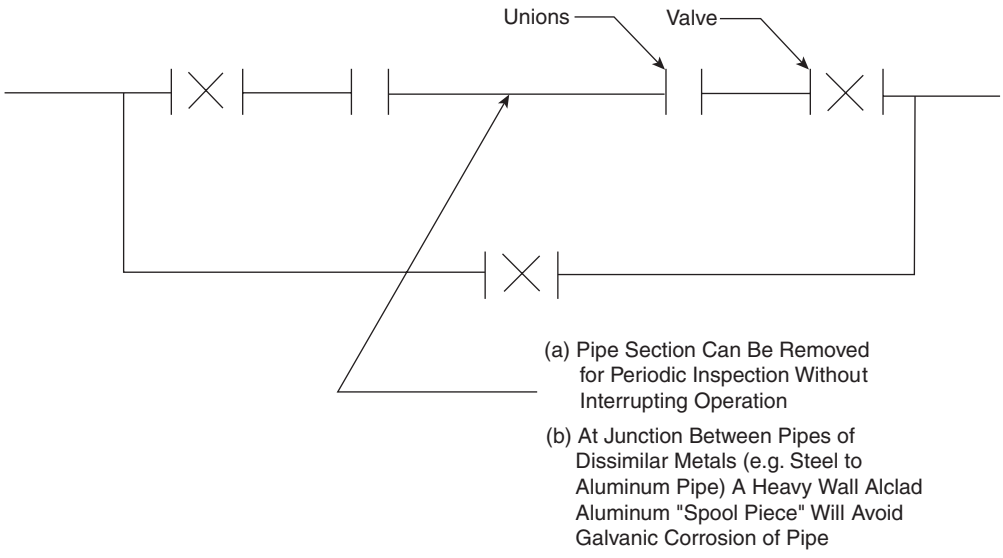

Figure 1.50 *Design that allows inspection to be carried out without interrupting operation*

In the design of heat exchangers and piping systems considerations must be given to a design that allows ease of periodic inspection as shown in Figure 1.50.

In some flow systems contamination of solutions with copper on lead ions may be removed through a trap containing aluminum filings which otherwise might cause corrosion and a typical trap is depicted in Figure 1.51.

In the case of welded joints consisting of carbon steel and stailness a design to avoid crevices is depicted in Figure 1.52. The design prevents base metal dilution.

The preferred design of joints in piping system to avoid crevices is depicted in Figure 1.53.

In the case of pressure vessels when attaching the dished heads to the sidewall of pressure vessel head the surface of the dished head need to be machined to accommodate the thickness transition, as shown in Figure 1.54.

Nonmetallics such as plastics are finding increasing use in place of metals and alloys. These materials are also subject to failure due to fatigue and other types, such as impact, chemical attack, pressure, fire and joint failures. The main types of failure along with the causes and recommended design for joints are given in Table 1.20 and Figure 1.55.

1.7 Life Prediction Analysis of Materials

Corrosion-based design analysis (CBDA) has been discussed extensively by Staehle.[39,40] This approach predicts the performance and assures the reliability of equipment or

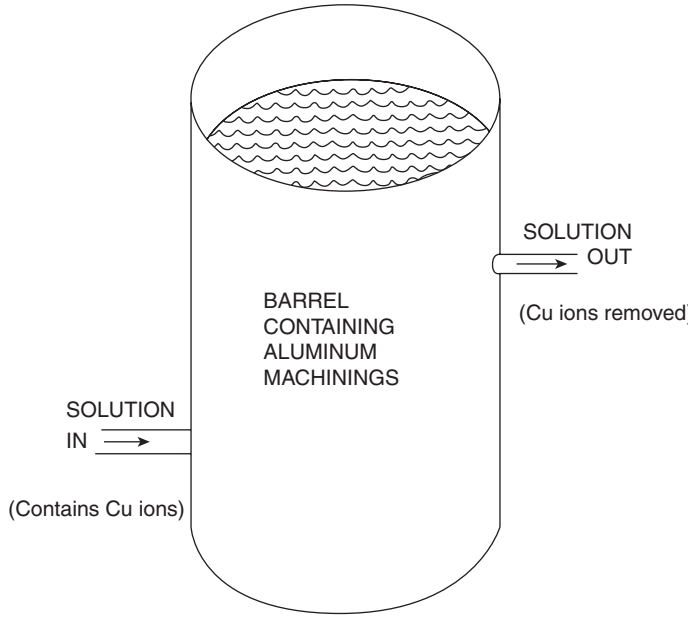

Figure 1.51 *Trap to remove heavy metals from a process stream*

structure in question. Related analysis procedures such as hazard operability (HAZOP) and hazard analysis (HAZAN) which is also known as probabilistic risk assessment (PRA) or quantitative risk assessment (QRA) are dealt with in the literature.[41–46]

The aim of CBDA is to assure the reliable operation of the chosen components in the intended application and for the intended life. The main steps involved in CBD analysis amount to the following ten steps:

(i) The environment in which the material selected can perform reliably. The environment considered is chemical as well as the thermal conditions and the operating stresses.

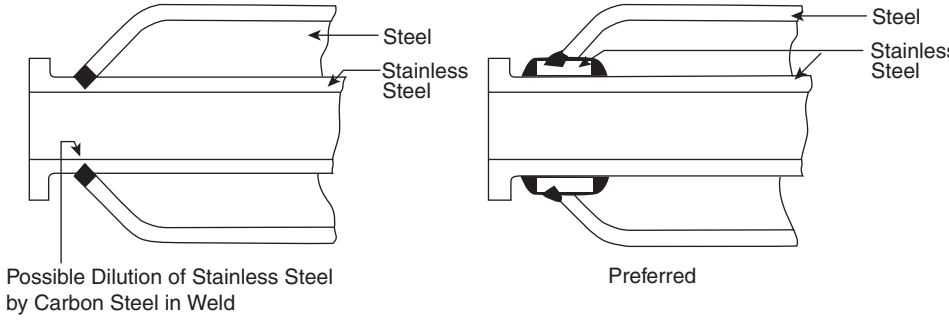

Figure 1.52 *Design to prevent base metal dilution*

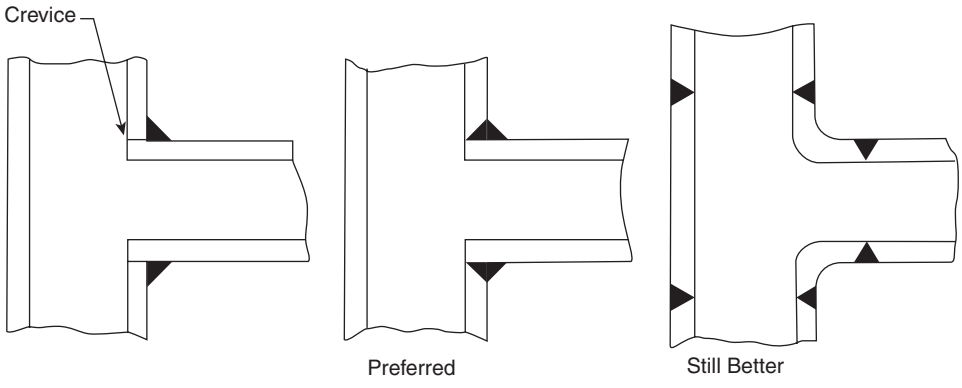

Figure 1.53 *Designs to avoid crevices caused by incomplete weld penetration*

(ii) Material is defined to include not only the type of alloy or metal, but also the impurities in grain boundaries, second phases, cold work, etc.

(iii) The 'mode' of corrosion is defined to include the morphology of degradation (corrosion) and its dependence on factors such as potential, pH, temperature, chemical species, alloy composition and stress.

(iv) Superposition involves comparison for the chosen material, the various possible modes of degradation and their dependence on the anticipated environmental conditions. If the chosen materials undergo degradation, change in conditions of overlap or change in design or material or modification of environment by the addition of inhibitors is warranted.

(v) Failure is a relative factor and in general means not meeting with the expected requirements. Since the term is relative it is imperative to define the requirements to be met at the design stage.

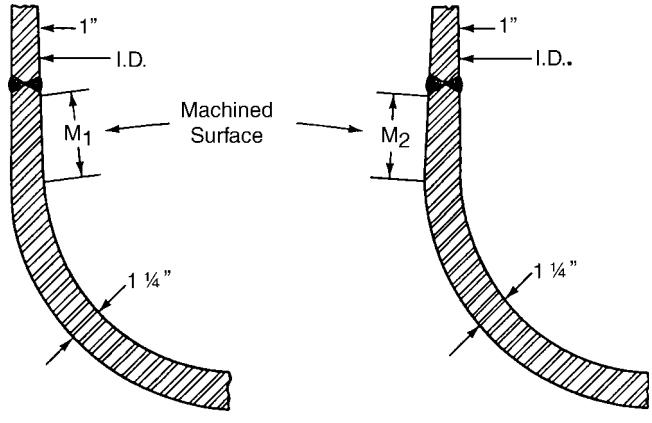

Figure 1.54 *Design of attachments to the side wall of pressure vessels so that the final machining operation is carried out on the exterior of the vessel*

Table 1.20 *Major types of failures in reinforced plastics and their causes*

System	Type of failure	Cause
Piping	Cemented joint	Failure to follow recommended practice
	Chemical attack	Poor resin selection or change in environmental conditions
	Impact damage	Various (generally, handling damage)
Tanks and process vessels	Chemical attack	Poor resin selection, or environmental data wrong
	Internal pressure	Operational errors and poor process design
	External pressure (vacuum)	Poor equipment design
	Secondary bond failure	Faulty fabrication
	Impact	Handling damage
Scrubbers and absorbers	Chemical attack	Service conditions wrong and change in process specifications
	Vacuum damage	Poor equipment design
	Impact	Handling damage
	Fire	Lack of maintenance, lack of adequate safeguards, lack of interlocks, possibility lack of employee training, or no scrubbing liquid
Ducts, fans and stacks	Joint failures	Generally, glue line
	Chemical attack	Poor resin selection, wrong, or changed service conditions
	Fire	80% of fires originate from an internal or process source, while 20% of fires originate externally. Lack of sprinkler protection is by far the largest single reason for large losses

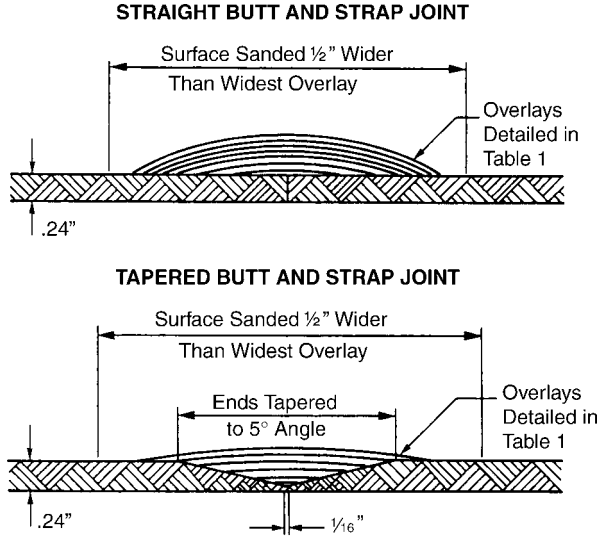

Figure 1.55 *Joint designs*

(vi) Development of a statistical framework of the corrosion modes and the extent of degradation.
(vii) Accelerated testing with the prototype equipment under the expected conditions must be done.
(viii) Based on the foregoing steps the prediction may be made on the performance of the chosen design and material and whether failure can occur.
(ix) The analysis also recommends corrosion monitoring, inspection and feedback of the results.
(x) Finally, depending upon the data accrued, modification in design, materials selection, operations, monitoring or inspection may be implemented as a result of comparison of operational data with the predictions.

It is beyond the scope of our objectives to delve into the details of the aforementioned steps of CBD analysis. The schematic relationships among hypothetical times-to-failure, design life and action levels are shown in Figure 1.56. The symbols DLO, DLCO, LEO and LECO stand for design life objective, life conservative objective; design life-extension objective and life-extension conservative objective, respectively. The symbol AL stands for action level.

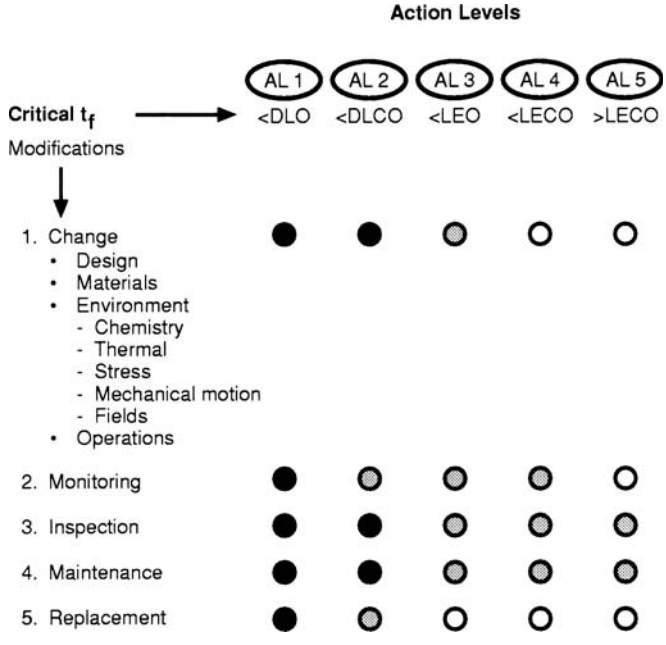

Figure 1.56 *Schematic view of relationships among hypothetical times-to-failure, targets for design life (DLO, DLCO, LEO, and LECO) action levels (AL 1, AL 2, AL 3, AL 4, and AL 5) and responses appropriate for each action level. Black dots indicate high priority actions, shaded dots indicate lower priority actions; open circles indicate no action*

1.8 Corrosion Protection

Corrosion protection refers to a situation in which all the inherent factors to prevent corrosion have been optimized and external intervention is deemed necessary to minimize the corrosion that is beyond the scope of corrosion-preventative factors such as metallurgical, design and life prediction analysis. Corrosion protection can be achieved by: (i) addition of inhibitors; and (ii) use of protective coatings.

1.8.1 Corrosion Inhibitors

A corrosion inhibitor is a chemical substance that, upon addition to a corrosive environment, results in reduction of corrosion rate to an acceptable level. Corrosion inhibitors are generally used in small concentrations. The principles and applications of corrosion inhibitors are discussed at great length in a recent monograph.[47] A corrosion inhibitor should not only mitigate the corrosion, but also be compatible with the environment in the sense that it should not cause any complications. Usually the corrosion inhibitor is rated in terms of inhibition efficiency I and is given by the relationship.

$$I = \frac{(\mathrm{CR})_{\mathrm{o}} - (\mathrm{CR})_{\mathrm{I}}}{(\mathrm{CR})_{\mathrm{o}}} \times 100$$

where CR refers to corrosion rate and the subscripts o and I refer to the absence and presence of the inhibitor.

A corrosion inhibitor can function in two ways. In some situations the added inhibitors can alter the corrosive environment into a noncorrosive or less corrosive environment through its interaction with the corrosive species. In other cases the corrosion inhibitor interacts with the metal surface and as a consequence inhibits the corrosion of the metal. Thus, based on the mode of interaction, there are two broad classes of inhibitors.

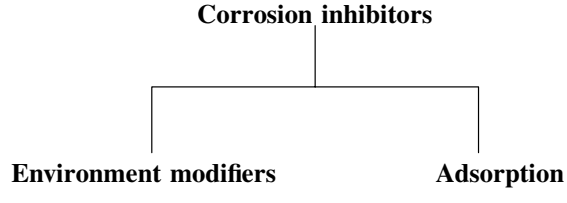

In the case of environment modifiers the action and mechanism of inhibition is a simple interaction with the aggressive species in the environment, and thus reduce the attack of the metal by the aggressive species. This is exemplified by oxygen scavengers such as hydrazine or sodium sulfite along with cobaltous nitrate and biocides used in inhibiting microbiological corrosion. In the case of corrosion in neutral and alkaline solutions, oxygen reduction is the cathodic reaction which can be countered by the oxygen scavengers and thus inhibit the corrosion.

$$\mathrm{O_2 + 2H_2O + 4e^- \rightarrow 4OH^-} \qquad \text{cathodic reaction}$$

$$\mathrm{5O_2 + 2N_2H_4 \rightarrow 2H_2O + 4H^+ + 4NO_2} \qquad \text{oxygen scavenging}$$

$$\mathrm{2SO_3^{2-} + O_2 \rightarrow 2SO_4^{2-}}$$

In the case of inhibitors which adsorb on the metal surface and inhibit the corrosion there are two steps, namely: (i) transport of inhibitor to the metal surface; and (ii) metal – inhibitor interactions. The process is analogous to drug molecule transport transported in the body to the required site and its interaction with the site to provide relief from the ailments. The most important step involves the interaction of the metal with the inhibitor molecule. These are chemical interactions and will be dealt with later.

Depending upon whether the cathodic reaction or the anodic reaction is suppressed by the added inhibitor, inhibitors have been further classified as follows:

Adsorption inhibitors

- Cathodic inhibitors
- Anodic inhibitors
- Mixed type inhibitors (both cathodic and anodic)

Cathodic inhibitors inhibit the hydrogen evolution in acidic solutions or the reduction of oxygen in neutral or alkaline solutions. It is also observed that the cathodic polarization curve is affected when a cathodic inhibitor is added to a system, as shown in Figure 1.57. Distinct differences are seen in the cathodic branch of the uninhibited and inhibited systems.[48] Substances with high overpotential for hydrogen in acidic solutions and those that form insoluble products in alkaline solutions are generally effective cathodic inhibitors. Some examples of such inhibitors are inorganic phosphates, silicates or borates in alkaline solutions which inhibit the oxygen reduction at the cathodic sites. Substances such as carbonates of calcium and magnesium, due to limited solubility, block the cathodic sites.

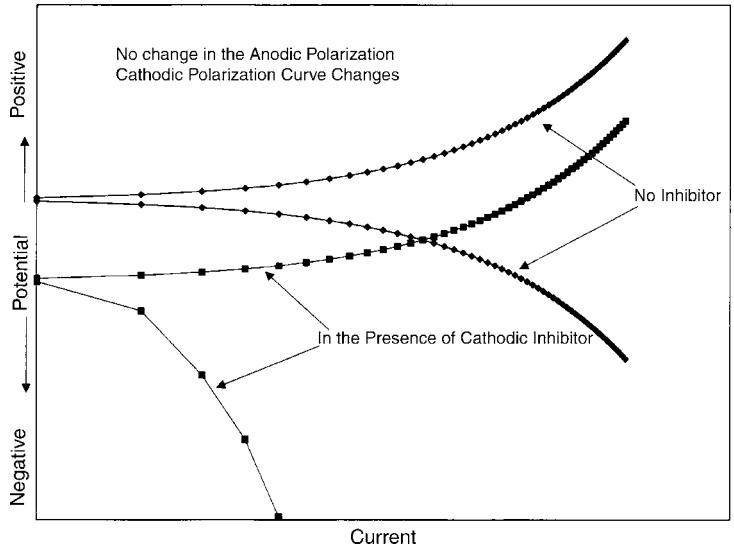

Figure 1.57 *Polarization curve in the presence of cathodic inhibitor*[48]

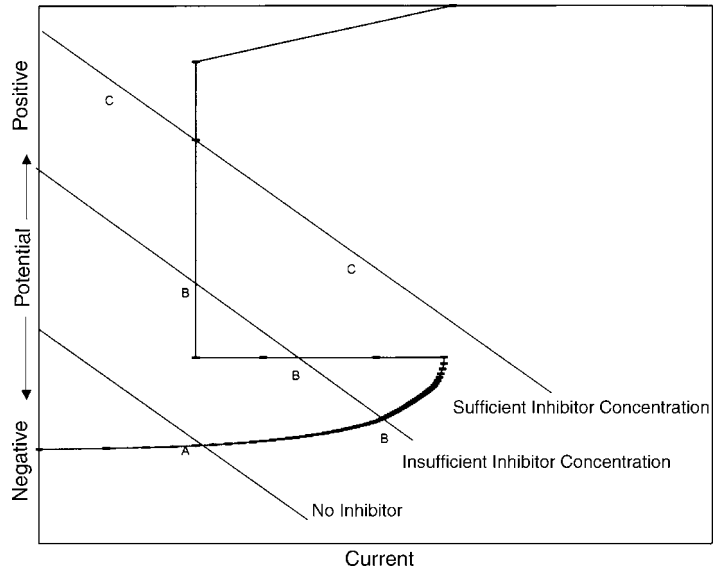

Figure 1.58 *Polarization diagram of an active–passive metal showing the dependence of the current on concentration of passivation-type inhibitor*[48]

Anodic inhibitors are generally effective in the pH range of 6.5–10.5 (near neutral to basic). Basically, oxyanions such as chromates, molybdates, tungstates and also sodium nitrite are very effective anodic inhibitors. These oxyanions are thought to play a role of repairing the defects in the passive iron oxide film on the iron surface. In the case of chromate or dichromate the concentration of the inhibitor used is critical. A potentiodynamic polarization diagram showing the effect of the concentration of the inhibitor is depicted in Figure 1.58. The diagram clearly illustrates the critical aspect of the concentration of the inhibitor. Protection is rendered when sufficient amount is used and conversely the corrosion is accelerated when the inhibitor is insufficient. This behavior is displayed by dichromate as an inhibitor.

Mixed type of inhibitors are generally represented by organic compounds. Irrespective of the type of inhibitor, the inhibition process involves transport of inhibitor to the metal site followed by interaction of the inhibitor with the surface of the metal, resulting in protection. We now recall the electrical double layer consisting of inner and outer Helmholtz planes and the distribution of anions (A^-), cations and water dipoles. This is schematically shown in Figure 1.59. When an inhibitor is added the structure of the double layer is affected, with the inhibitor displacing the adsorbed water molecules on the metal surface and taking their place on the metal surface.

$$M(n\,H_2O)_{ads} + I_{(sol)} \rightarrow MI_{ads} + n\,H_2O_{(sol)}$$

The variation of the potential in the double layer is shown in Figure 1.60. The adsorption of an inhibitor can be obtained by determining the electrokinetic potential

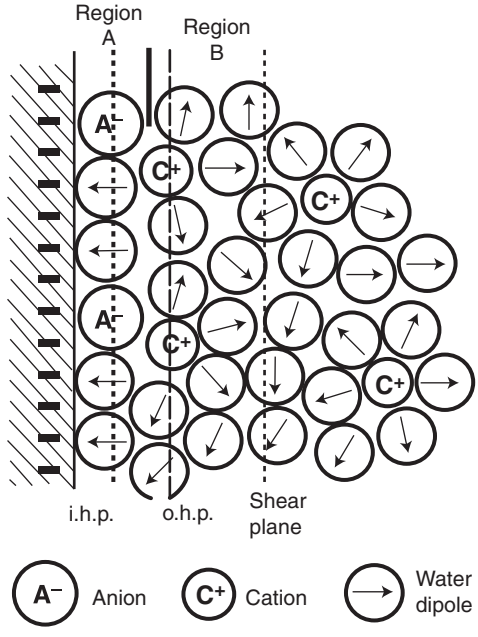

Figure 1.59 *Schematic representation of the electric double layer*

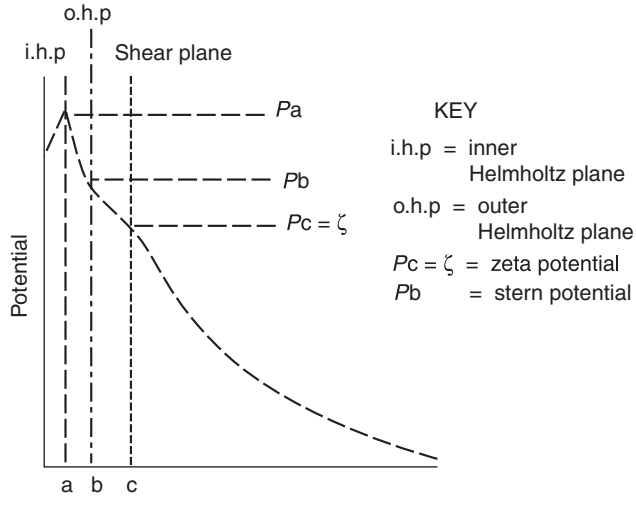

Figure 1.60 *Variation of potential in the double layer*

Table 1.21 *Adsorption isotherms*[50–53]

Name	Isotherm*	Verification plot
Langmuir	$\theta/(1-\theta) = \beta c$	$\theta/(1-\theta)$ vs $\log c$
Frumkin	$[\theta/(1-\theta)]e^{f\theta} = \beta c$	θ vs $\log c$
Bockris–Swinkels	$\theta/(1-\theta)^n[[\theta + n(1-\theta)]^{n-1}/n^n = ce^{-\beta}/55.4$	$\theta/(1-\theta)$ vs $\log c$
Temkin	$\theta = (1/f)\ln Kc$	θ *vs* $\log c$
Virial Parson	$\theta e^{2f\theta} = \beta c$	θ vs $\log(\theta/c)$

*θ, % P/100, surface coverage; β, $\Delta G/2.303\,RT$; ΔG, free energy of adsorption; R, gas constant; T, temperature; c, bulk inhibitor concentration; n, number of water molecules replaced per inhibitor molecule; f, inhibitor interaction parameter (0, no interaction; + attraction; and -, repulsion); K, constant; and % $P = 1$ inhibited corrosion rate/uninhibited corrosion rate.

or by determining the capacitance before and after the adsorption of the inhibitor by considering the system as a parallel plate capacitor. For effective adsorption of an inhibitor on a metal surface the forces of interaction of the metal and an inhibitor must be greater than the interaction forces of metal and water molecules.

The adsorption of an inhibitor affects the dielectric constant since the double layer structure is affected. This effect is exemplified by the corrosion of iron in 10% HCl by quinolinium compounds.[49] The inhibition by quinolinuim compounds has been attributed to the ordering effect by the π-electron system of the inhibitor molecules on the water molecules located at the metal interface.

Adsorption of inhibitors can be due to either physisorption or chemisorption. Inhibitors involved in physisorbtion can be desorbed with ease while inhibitors involved in chemisorption are difficult to desorb. Adsorption isotherms are shown to reflect the performance of inhibitors. The adsorption isotherms,[50–53] which describe the surface coverage and performance of the inhibitors are given in Table 1.21.

The surface charge on the metal is defined by the position of free corrosion potential E_{corr} of the metal with respect to its potential of zero charge E_{PZC}. When E_{corr}-E_{PZC} is negative, cations are adsorbed and when it is positive, negative ions are adsorbed and this adsorption is electrostatic in nature. Physical adsorption forces are relatively weak and have low activation energy. Some data on the values of zero charge potentials of metals are given in Table 1.22.

Chemisorption of inhibitor molecules on metals is slow and involves interaction forces stronger than the forces in physisorption. A coordinate type of bond between the metal and the inhibitor is thought to be present with charge transfer from the inhibitor to the metal.[55] An opposing view is that a chemical bond is not necessarily present in chemisorption of an inhibitor on the metal surface.[56] In some cases the temperature dependence shows higher inhibition efficiency and higher activation energy than physisorption.

Most of the organic inhibitors belonging to the mixed type or class have reactive functional groups which latch on to the metal. The inhibitor efficiency of organic inhibitors containing different donor atoms is in the sequence,

$$\text{Se} > \text{S} > \text{N} > \text{O}$$

Table 1.22 *Values of zero charge potentials*[54]

Metal	Zero-charge potential, mV (SHE)
Ag	−440
Al	−520
Au	+180
Bi	−390
Cd	−720
Co	−450
Cr	−450
Cu	+90
Fe	−350
Ga	−690
Hg	−190
In	−650
Ir	−40
Nb	−790
Ni	−300
Pb	−620
Pd	0
Pt	+20
Rh	−20
Sb	−140
Sn	−430
Ta	−850
Ti	−1050
Ti	−750
Zn	−630

and can be rationalized on the basis of electronegativity and polarizability. Systematic work on corrosion inhibition of metals by organic inhibitors has resulted in identifying some factors such as: (a) the electron density on the donor atom of the inhibitor; (b) inductive effects due to the substituent groups in the organic inhibitor molecule; (c) hydrophobicity of the substituent groups in the inhibitor; (d) molecular area, molecular weight and molecular configuration of the inhibitor; (e) chain length of the inhibitor; and (f) steric effects.

From the foregoing discussion it is evident that substituent groups in the organic inhibitor are likely to have a profound effect on the metal–inhibitor interactions and hence the inhibition efficiency. Thus structure–activity relationships in corrosion inhibition have evolved based on principles of physical organic chemistry. According to Hammett equation we have

$$\log \frac{k_I}{k_o} = \rho\sigma$$

where k_I and k_o refer to corrosion rates in presence of substituted and parent inhibitors, respectively, ρ is a constant and σ is the Hammett substituent constant reflecting the electronic effect of the substituent on the reaction centre of the inhibitor with the metal. This relationship is borne out by the inhibition of substituted pyridines on the corrosion of iron as depicted in Figure 1.61. The increasing negative value of σ is a measure of the

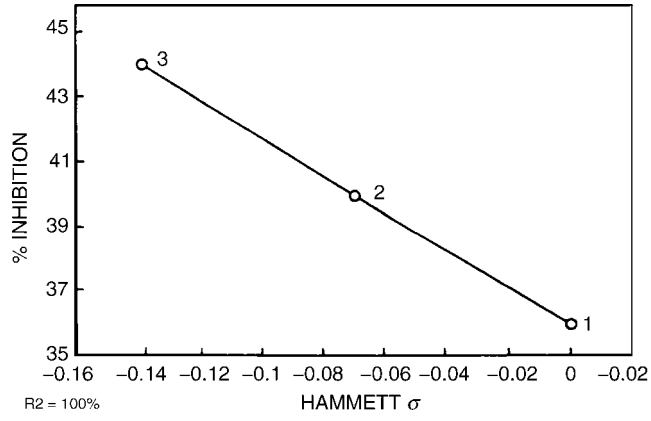

Figure 1.61 *Percentage inhibition for meta substituted methyl pyridines as a function of Hammett σ values: 1. pyridine; 2. 3-methylpyridine; 3. 3,5-dimethyl pyridine*

greater electron density on the basic pyridine nitrogen atom due to the particular substituent in the pyridine inhibitor molecule.

The charge density on the donor atom of the inhibitor molecule, ionization potential, the degree of softness of the inhibitor and the fractional charge transferred from the inhibitor to the metal, and heat of reaction are parameters obtained from quantum chemical calculational methods such as EHT, MNDO, ZINDO methods. Software is available for these computational methods. These methods have been applied[57,58] in the case of pyridines, benzotriazoles, anilines, ethanediamines, ethane diols, mercapto triazolines, biguanides, oxadiazoles with metals such as iron, copper, zinc, aluminum, and correlations such as inhibition efficiency with: (i) energy of the highest molecular orbital ($-E_{HOMO}$) (ionization energy); (ii) energy gap (E_{LUMO}–E_{HOMO}) or softness of the inhibitor; (iii) fraction of charge transferred from the inhibitor to the metal (ΔN); (iv) heat of reaction (ΔH). Some typical correlations of inhibition efficiency with the fractional charge transferred from the inhibitor to the metal (ΔN) and the negative values of heats of reaction (ΔH) are presented in Figure 1.62 and Table 1.23, respectively.

Metal–inhibitor interactions can be viewed in terms of acid–base reactions. This type of rationalization has been done by Sastri in terms of the hard and soft acid–base principle (HSAB) at great length.[18] The characteristics of hard acids, soft acids, hard bases and soft bases along with borderline acids are given below.

	Hard acids	Soft acids
Size	Small	Large
Electronegativity	High	Low
Polarizability	Low	High
Positive charge	High	Low
Electronegativity	High	Low
Polarizability	Low	High
Ease of oxidation	Hard	Easy

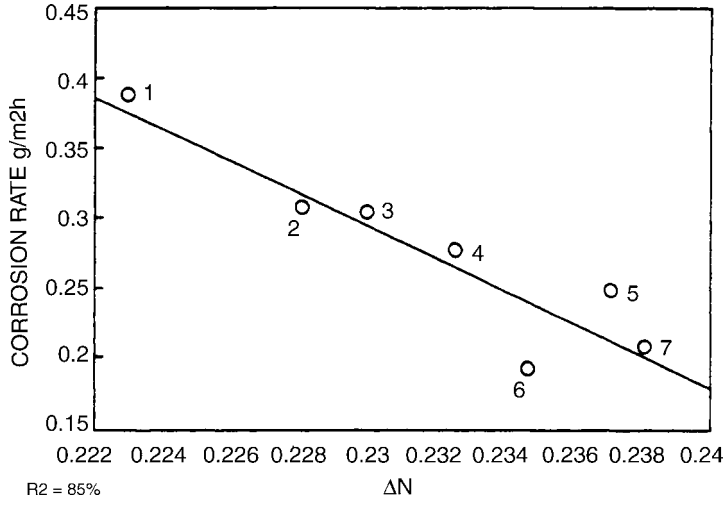

Figure 1.62 *Correlation of ΔN with corrosion rates of pyridine derivatives: 1. pyridine; 2. 3-methylpyridine; 3. 2-methylpyridine; 4. 3,5-dimethylpyridine; 5. 2,6-dimethylpyridine; 6. 2,5-dimethylpyridine; 7. 2,4,6-trimethylpyridine*

Corrosion inhibitors can be viewed from the point of view of the HSAB principle and described as either hard or soft inibitors. Inhibitors containing the following groups can be classified into hard, soft or borderline inhibitors.[59]

Sastri's classification of inhibitors

Hard inhibitor	Soft inhibitor	Borderline inhibitor
$CrO_4^{2-}, MoO_4^{2-}, PO_4^{3-}$	RSH, RS^-, R_3P	$C_6H_5NH_2, C_5H_5N$

Table 1.23 *Data on heats of reactions and percentage inhibition*[18]

System	Heat of reaction (kcal/mol)	% inhibition
Benzimidazole: Cu	−3467.17	92.11
2 Methyl benzimidazole: Cu	−4018.7	93.42
5,6 Dimethyl benzimidazole: Cu	−4547.8	96.71
Benzimidazole: Fe	−3471	29.0
2 Methyl benzimidazole: Fe	−4030.7	35.
2 Phenyl benzimidazole: Fe	−6001.4	95.0
1,2 Ethanediol: Fe	−299.538	2.0
1,2 Aminoethanol: Fe	−916.437	49.0
4-amino-3-*H*-5 mercapto 1,2,4 triazoline: Al	−1912.6	65.6
4-amino-3-methyl-5 mercapto-1,2,4 triazoline: Al	−2487.4	78.1
4-amino-3-*n*-propyl-5 mercapto-1,2,4 triazoline: Al	−3556.8	84.6
4-amino-3 isopropyl-5 mercapto-1,2,4 triazoline: Al	−3559.4	86.6

Metal atoms, metal ions and bulk metals are classified as follows:

Hard acids	Soft acids	Borderline acids
$Fe^{3+}, Cr^{3+}, MoO^{3+}, Al^{3+}$	Cu^{+}, M^{0}(metal atoms), bulk metals	$Fe^{2+}, Ni^{2+}, Cu^{2+}, Zn^{++}$

In accordance with the rules of the HSAB principle, hard acids tend to form complexes with hard bases, and soft acids form complexes with soft bases. Borderline acids form complexes with either soft or hard bases.

Using the HSAB principle, one can rationalize the corrosion inhibition of iron and aluminum by phosphate in which iron phosphate and aluminum phosphate are produced. Ferric and Al^{3+} are hard acids, and they react with phosphate, a hard inhibitor and give corrosion protection. Corrosion inhibition of Cu^{2+} and Zn^{2+} by amines can be rationalized by the formation of amine complexes of Cu^{2+} and Zn^{2+}, and this is in accord with the principle that Cu^{2+} and Zn^{2+} are borderline acids reacting with amines which belong to borderline inhibitors. Corrosion protection of copper (soft acid) by mercaptobenzothiazole (soft inhibitor) is also in keeping with the HSAB principle.

Hydrophobicity of an inhibitor and critical micelle concentrations of the inhibitor in forming micelles have been found[60] to play a significant role in the case of substituted imidazoles, imidazolines and fatty amines and these correlations do not take into account the electronic interactions. This correlation is based on Hansch's model of drug–receptor interactions based on transport of drug/inhibitor to the site followed by interaction at the site.

Selection of inhibitor. Inhibitor science and technology demands that the personnel involved have a good background in electrochemistry, physical, inorganic and organic chemistry and surface analytical techniques along with corrosion engineering. This requirement will become apparent as we examine the process of selection of inhibitors. It is mandatory that the corrosion engineer or scientist should have a knowledge of: (i) the corrosive species; (ii) corrosion reactions; (iii) the corrosion rates before embarking upon the selection of inhibitor. This is followed by: (i) thorough literature search of candidate inhibitors; (ii) identification of the family of inhibitors suitable to the system on hand; (iii) when the scientist encounters a wide choice of inhibitors, say twenty, it is imperative that quantum chemical calculations be performed to obtain data on $-E_{HOMO}$ (ionization potential, softness ($E_{LUMO}-E_{HOMO}$), ΔN, fraction of charge transferred from inhibitor to metal and, based on these parameters, narrow the choice to four or five best candidates. This novel method due to Sastri is successful and well established;[61–63] (iv) The next step involves novel and elegant coordinated surface analysis of the sample before and after exposure to the inhibitors as outlined by Sastri *et al.*[64,65]; (v) The final step involves unraveling the corrosion inhibition mechanism and deciding as to the type of mechanism, the various types according to Sastri's classification being[66] (a) interface inhibition, (b) interphase inhibition, (c) intraphase inhibition, and (d) precipitation coating.

Types of inhibitor. The inhibitors used commercially generally consist of a mixture of the active component along with a surfactant and a solvent. Organic inhibitors contain active functional groups which bond to the metal surface and offer protection. The functional

Table 1.24 *Some functional groups in organic inhibitors*

Structure	Name	Structure	Name
–OH	Hydroxy	$-CONH_2$	Amide
–C≡C–	–yne	–SH	Thiol
–C–O–C–	Ether	–S–	Sulfide
–COOH	Carboxy	–S=O	Sulfoxide
–C–N–C–	Amine	–C=S–	Thio
$-NH_2$	Amino	–P=O	Phosphonium
–NH	Imino	–P–	Phospho
$-NO_2$	Nitro	–As–	Arsano
–N=N–N–	Triazole	–Se–	Seleno

groups of the organic inhibitors are listed in Table 1.24. Table 1.25 gives some examples of inhibitors containing different functional groups.

Industrial applications of corrosion inhibitors are too numerous to cover in the present context. The inhibitor industry amounts to several billion dollars annually. Applications of inhibitors in petroleum production, oil and gas wells and pipelines, potable water, water cooling towers, acid systems, automobile antifreeze systems, paints, boiler waters, fuel tanks, refrigeration brines, reinforcing steel in concrete and protection of artifacts are extensively discussed in the literature.[18]

It is also necessary to bear in mind that the proper application technique is used and also the dependence of the effectiveness of the inhibition on temperature, the secondary inhibitive function, poisoning nature, synergistic and antagonistic effects of mixtures of inhibitors before the actual application of an inhibitor for a specific purpose.

As is common with any industry environmental concerns have led to intense activity in the development of green inhibitors. The biological oxygen demand (BOD) is the time duration over which the inhibitor persists in the environment. Inhibitors should be nontoxic and the BOD is at least 60%. Toxicity is expressed as LC_{50} which is the concentration of the inhibitor needed to kill 50% of the test species. Some typical data are given in Table 1.26.

The inhibitors considered thus far are either liquids or solids dissolved in solvents. Other useful type of inhibitors are vapor-phase corrosion inhibitors. These are used to minimize corrosion in electronics, packaging, processing industries, reinforced concrete,

Table 1.25 *Some typical inhibitors*

Functional group	Example	Reference
Carboxyl	Benzoic acid	
	Substituted benzoic acids	67
Basic nitrogen	Benzotriazole	68
Sulphur	Thiourea and its derivatives	69
Electronically conducting polymers	Pyrrole, thiophene, aniline	70
Nitrogen and oxygen	8-hydroxyquinoline	71

Table 1.26 *Toxicity of corrosion inhibitors*

Compound	LC_{50} (mg/kg)
Propargyl alcohol	55
Hexynol	34
Cinnamaldehyde	2200
Fomaldehyde	800
Dodecylpyridinium bromide	320
Naphthylmethylquinolinium chloride	644
Nonylphenol-ethylene oxide surfactants	1310

coatings and metal working fluids. Vapor phase inhibitors[72] vaporize readily and cover the metal surface and give protection as shown in Figure 1.63.

1.8.2 Protective Coatings

The application of paints to metallic objects for corrosion control has been known for a long time. The mechanism of protection by paint films was viewed as a source of insulation of the metal from the corrosive environment such as oxygen and water and inhibiting the cathodic reaction. The idea of protective action of paint films by providing insulation of the metal from oxygen and water was questioned, based on the data given in the literature.

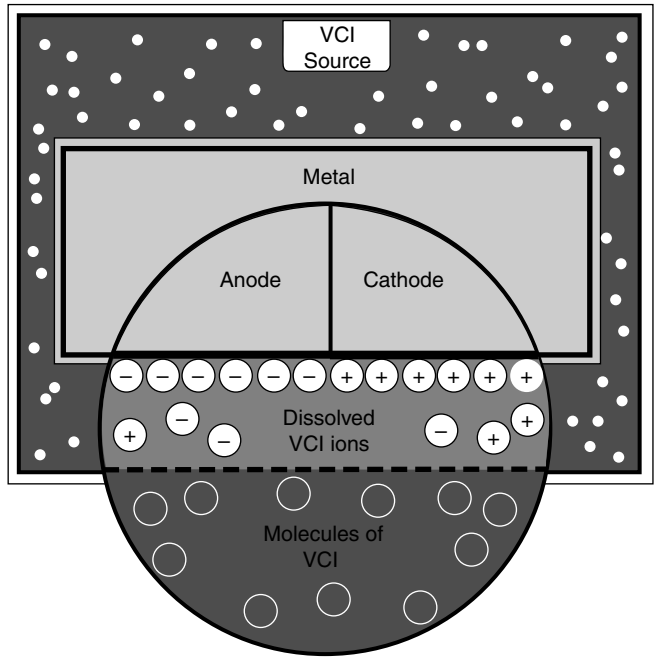

Figure 1.63 *Mechanism of protection by vapor phase inhibitors*

Table 1.27 *Data on amounts of water and oxygen transmitted through coatings (J.C. Hudson,* Corrosion of Iron and Steels, *Chapman & Hall, London, 1944)*

Coating	g water/m^2/day 25 m film, 95% R.H. 36°C	mL of O_2/m^2/day 100 :m film 85% RH 23°C, 1 atm O_2
Chlorinated Rubber primer	20 ± 3	30 ± 7
Chlorinated polymer	20 ± 5	33 ± 2
Coal tar epoxy	30 ± 1	213 ± 8
Aluminized Epoxy mastic	42 ± 6	110 ± 37
Titanium dioxide Pigmented alkyd	258 ± 6	595 ± 45
Red lead/linseed oil Primer	214 ± 3	734 ± 42
Threshold quantity of Water/oxygen to given corrosion rate of 70 mg Fe/cm^2/year	0.93	575

Corrosion control by coatings may be accomplished by: (i) barrier coatings which offer protection (a) by its high resistance which mitigates current transfer between anodic and cathodic sites, (b) by depriving oxygen diffusion and hence impede the cathodic reaction; (ii) cathodic protection as in the case of zinc-containing pigments (zinc is more anodic to iron); (iii) inhibitive primers which form passive films on the metal.

Paint or coating systems consists of many layers which are known as coats. The first coat applied on a structure is the primer and the last is known as finish or top coat. The coats between the primer and finish coat are intermediate coats.

A paint consists of: (i) vehicle; (ii) pigment; and (iii) additives or fillers. A vehicle renders the fluidity to the paint and upon drying leaves a film. A pigment suspended in the vehicle offers the corrosion protection. Additives or fillers enable the dry coating to withstand the environment. Corrosion control by barrier coatings may be envisaged as shown in Figure 1.64.

Barrier coatings need to: (i) be impermeable to ionic species; (ii) if possible be a barrier to oxygen; and (iii) maintain adhesion under wet conditions. The binders used in barrier coatings can be: (i) thermoplastic binders; or (ii) thermosetting binders. The molecular structure of the binder plays a significant role in rendering the coating impermeable. Some examples of thermoplastic binders are high-molecular-weight halogenated hydrocarbons (fluoropolymers, polyvinyl chlorides). Some examples of thermosetting binders are polymers such as epoxies, polyesters, vinyl esters and polyurethanes.

Pigments used in barrier coatings should also be hydrophobic in nature, and possess good adhesion across pigment–binder interfaces. Some typical pigments used are flat platey aluminum flakes, glass flakes, stailness steel flakes and micaceous iron oxide.

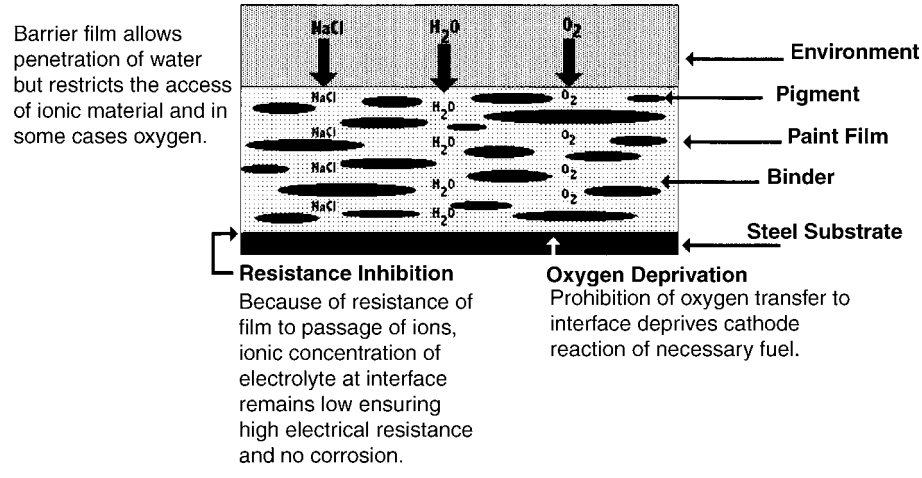

Figure 1.64 *Corrosion control by barrier coatings*

The solvents used in barrier coatings should be such that the lateral orientation of the pigment in the film is optimized, but at the same time the solvent should evaporate before the film is put in service.

For barrier coatings to be effective it is necessary to have: (i) good adhesion of the barrier film on the metal surface (this is generally accomplished by multicoat procedure to a certain extent); (ii) proper choice of the polymers to control the permeability of oxygen; and (iii) optimum film thickness achieved by multicoats or thin-film system, depending upon the envisaged application.

Sacrificial coatings consist of: (i) organic zinc-rich primers; (ii) inorganic zinc-rich primers. Corrosion control mechanism by zinc-rich primers may be visualized to occur as shown in Figure 1.65.

These coatings give the most effective corrosion protection. They contain high volumes of zinc pigment and are exclusively used as primers. The steel is protected

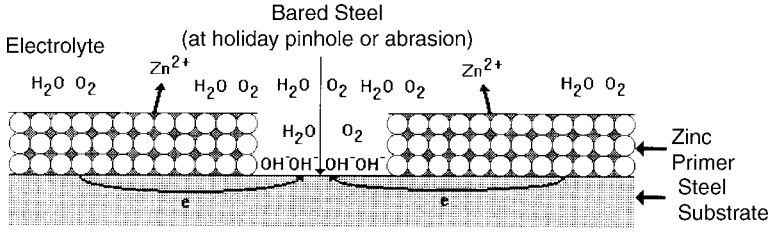

The presence of strongly electronegative zinc-pigmented coating short circuits all local cell activity on steel. The steel becomes totally cathodic to the anodic zinc coating. The zinc corrodes, but the steel will not corrode even at bare spots. it is mandatory that the zinc coating be in electrical contact with the steel surface; therefore, the steel must be stropped of all contamination.

Figure 1.65 *Fundamentals of zinc-rich protection*

cathodically, zinc in the form of spherical dust acts as the anode of the artificial galvanic cell.

Organic zinc-rich primers are based on epoxy/polyamides, high-molecular-weight linear epoxies, moisture-cured urethanes, high-styrene resins, chlorinated rubbers and epoxy esters. In this type of primer zinc is covered with a monomolecular layer of the binder which facilitates the adhesion of the film to the substrate.

Inorganic zinc-rich primers consist of zinc and a reactive binder such as an alkali metal silicate (sodium, potassium, lithium or quaternary ammonium silicate) or hydrolyzed ethyl silicate as binder. On mixing hard and cohesive films of silicate are formed. The structure of the inorganic zinc-rich silicate may appear as shown in Figure 1.66.

The zinc silicate film is porous and readily absorbs corrosive electrolyte. The film is harder, stronger than organic zinc-rich films. These films have better resistance to solvent and heat than the organic zinc-rich primers and may be used for tank linings and other applications up to 400°C.

In both organic zinc-rich and inorganic zinc-rich primers the duration of cathodic protection is finite and the effects of polarization of zinc and the production of zinc corrosion product on the surface results in a change of protection mechanism from

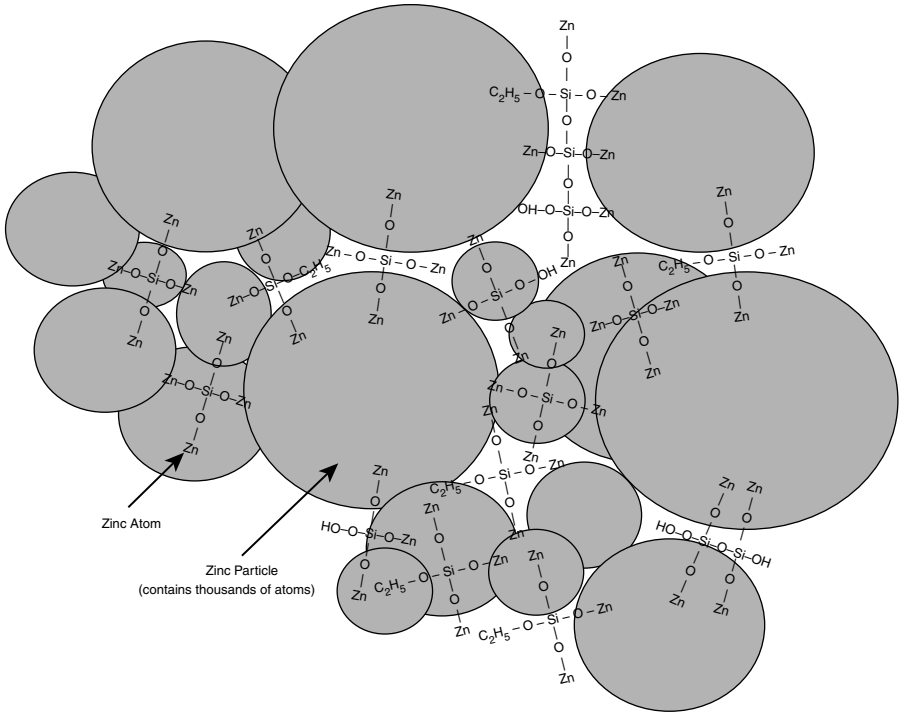

Figure 1.66 *Stylized representation of postulated structure of inorganic zinc-rich film in which silicate vehicle is primary valence bonded to zinc atoms on particles of zinc dust pigment. There is no encapsulation, and the film is porous to ingress of electrolyte. This affords good film strength, adhesion, electrical conductivity and cathodic protection*

galvanic to barrier film protection. The corrosion product of zinc is thought to block and seal the porosities of the film with a dense inorganic coat. Other mechanisms suggested include inhibition by zinc corrosion product, local high pH of the environment and control of oxygen reduction reaction.

Inhibitive Primers. The traditional primers are red lead and linseed oil, alkyd resins and zinc potassium chromate, proprietary epoxy, alkyd, urethane and latex systems with modified phosphate, borate and molybdate pigments. Chromate-based pigments, although in use in aircraft coatings, automotive primers and coil coating primers, are subject to environmental concern on the toxicity of hexavalent chromium which is likely to result in their replacement by innocuous products.

Chromates and molybdates protect the steel by passivation and form a chromium oxide–iron oxide in the case of chromate. While the oxide film of chromium may be several monolayers, molybdenum oxide film is of the order of a monolayer.[73]

Lead-based inhibitors and zinc phosphate inhibitors are thought to plug up the discontinuities in the natural oxide layer and hence offer protection. This is akin to the repair of an imperfect oxide film of iron by chromates, molybdates or tungstates.

Corrosion protection by an inhibitive primer may be envisaged as shown in Figure 1.67. Inhibitive metal primers are designed with relatively high pigment volumes to allow sufficient water absorption to dissolve the passivating inhibitor and yet prevent aggressive ions such as chloride which interfere in the passive oxide formation process.

Volatile organics in the coating film are deemed unacceptable from the environmental point of view and are giving way to water-based inhibitive primers. Some examples of water-based primers are of the acrylic latex type, as well as epoxies and water-borne

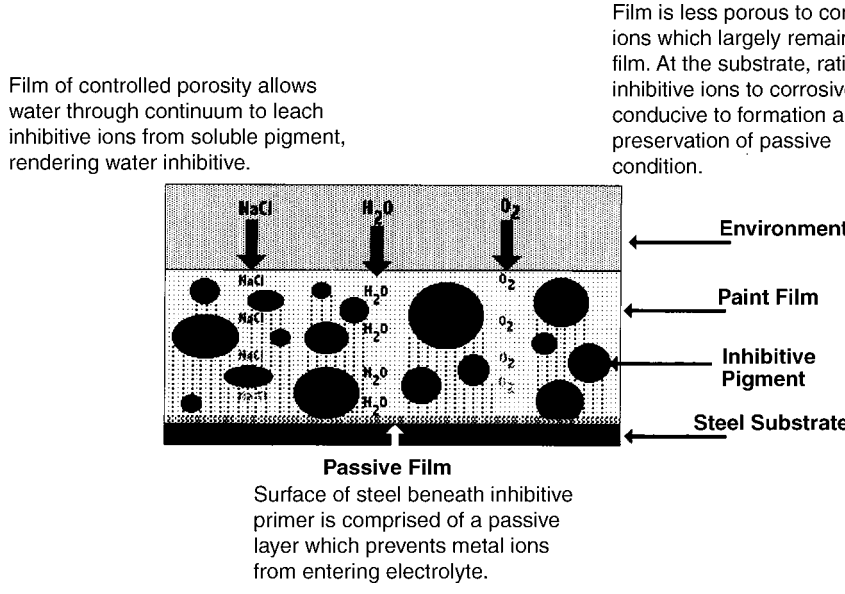

Figure 1.67 *Corrosion protection by inhibitive primer*

Table 1.28 *Prepainting cleaning and surface preparation processes*

Solubilization[a]	For removal of soluble inorganics with water and soluble organics with solvent
Emulsification[a]	For removal of insoluble and/or water-immiscible inorganics by emulsification with detergent solutions
Saponification[a]	For removal of ester and amide-based organics and inorganic salts by chemical hydrolysis with alkaline solutions
Chelation and sequestration[a]	For removal of metal ions from solutions and surfaces by chelation or complexation reactions
Deflocculation[a]	For wetting and dispersion of soils with surfactants, suspension of soil residues in order to prevent resedimentation and recontamination on metal surface
Pickling[b]	For removal of surface contaminations, rust scale, mill scale, and other bound moieties (including surface layers of metal itself) by chemical dissolution with acids or alkaline deoxidation with or without the application of an electric current
Mechanical scarification[c]	For removal of surface contamination, rust scale, mill scale, and other bound moieties by wet or dry abrasion (including surface layers of metal itself) by wet or dry abrasion, erosion, and/or cavitation processes

[a]Cleaning processes may involve spray, dip, wipe, and brush application. Solvent cleaning by vapor degreasing is very common and efficient. Processes generally become more efficient with increasing temperature and pressure (e.g., steam cleaning). Surface neutralization may be necessary with some processes (saponification). Final rinsing step with clean water or solvent is mandatory.
[b]Neutralization and/or rinsing with clean water is always necessary.
[c]Abrasive blasting (air nozzle or centrifugal) is preferable to hand tool grinding, brushing, and so on, which are slow and inefficient. Wet blasting without abrasive does not produce an anchor pattern.

alkyds. In these systems, the inhibitor is present in the water carrier in the can before application of the paint. Since the inhibitor is already in solution, the passivating film forms on the metal before the wet primer film begins to dry.

It is important that the utmost care is taken in the preparation of the surface of the sample to be coated since the performance of coating is only as good as the cleanliness of the surface. Some of the procedures involved in the preparation of a sample surface are given in Table 1.28.

Some of the paint types belonging to classes such as alkyds, coaltar epoxies, epoxy, heat-resistant, inorganic zinc types, polyurethanes, water-borne coatings as described by Sigma coatings are given in Table 1.29.

Plastic coatings are finding increasing use. Some of the commolny used plastic coatings along with a few characteristic features are given below:

Nylon	Can be used up to 120°C. Can be applied by dipping or spraying technique. Can be used in food industry since it can be sterilized. Coating may be up to 1 mm thick. Good bonding to steel and Al. For copper alloys primer is necessary
Polyethylene	Applied by either dipping or spraying in thin films. Subject to stress–corrosion cracking. Used in domestic ware, wire shelves, etc. High-density polythene used in ducting, chemical tanks, pipework, water purification plants

Table 1.29 *Paint types, applications and properties (courtesy of Sigma Coatings).*[75] *(Reproduced from Corrosion for Science and Engineering, Tretheway and Chamberlain, Copyright Pearson Education Ltd)*

Paint type	Percent solids content by volume (approx.)	Optimum dry film thickness (μm)	Touch dry after	Time before overcoat	Uses and properties
Alkyds					
Fast-dry enamel	32	38	1–2 h	6–8 h	Exterior exposure
Tank-finish aluminum	52	25	45 m	6 h	Experiors of steel storage tanks
Red oxide primer	42	38	2 h	24 h	Lead-free, general purpose, hard, water-resistant, anti-corrosive
Zinc phosphate primer	54	38	2 h	24 h	Lead and chromate-free, general purpose for steel in atmospheric exposure, can recoat conventional paint systems
General purpose gloss	55	38	1 h	16 h	Areas intermittently exposed to water immersion and atmospheric conditions
High-gloss, high-quality finish coat	54	38	1 h	16 h	High-gloss enamel for interior and exterior surfaces
Aluminum finishing coat	48	25	45 m	6 h	For dry cargo holds, good impact resistance
All purpose primer	32	25	10 m	30 m	Fast-drying, anticorrosive
Coaltar epoxies					
Polyamide cured coaltar	80	400	7 h	24 h	Two components, one coat, high build, outstanding oil and water resistance, cures to 10°C and resistant to 93°C in dry exposure
Polyamine-adduct-cured coal tar	71	125–500	4 h	6 h	Two components, high build, cures down to −5°C when substrate ice-free
Epoxy coatings					
Solvent-free epoxy (spray or trowel)	100	500–625	2 h	6 h	High resistance against tidal and impact actions, good oil and water resistance, good adhesion to many surfaces

Weather-resistant epoxy acrylic	44	50	2 h	2-3 h	Two components, topcoat, excellent weathering resistance, color and gloss retention, isocyanate-free
Nonskid epoxy	72	500–1000	20 h	24 h	Helidecks, ramps, walkways and concrete floors, resistant to chemical spillage
High-build, high-solids epoxy	85	75–200	5 h	16 h	Potable water systems, resistant to cathodic disbondment
High-solids epoxy primer	73	75–150	3 h	16 h	Tenacious adhesion to steel and concrete as primer for epoxies, urethanes and vinyls, good chemical resistance suitable for food contact
Armour epoxy	100	3000–5000	6 h	24 h	Solvent-free, quartz-reinforced
Zinc-rich epoxy primer	46	25-63	10 m	6 h	Two components, fast-drying, useful for a holding primer for rapid turnaround
High-build, anticorrosive epoxy	61	125–150	2 h	3 h	Two components, for land and marine structures, unlimited overcoating time, good impact resistance and flexibility
Multipurpose epoxy primer	52	50–125	30 m	8 h	Two components, holding primer, can be overcoated with many other paints
Epoxy-based adhesion primer/sealer	57	38	1 h	8 h	Two components for atmospheric and underwater systems, excellent adhesion to and sealing of aged zinc coatings, resists temperatures up to 175°C in dry exposure
Micaceous iron oxide epoxy primer	61	75–150	2 h	3 h	Two components, for land and marine structures
High-build epoxy lining	78	250	3 h	8 h	Useful tank coating in two-coat system, resistant to wide range of chemicals
Epoxy high build/finish coat	55	75–150	3 h	10 h	Two components, topcoat on primed steel and concrete for atmospheric conditions, seals inorganic zincs
Solvent-free epoxy	100	300	4 h	24 h	For crude oil/ballast tanks and aliphatic petroleum products
High-build abrasion-resistant epoxy	88	250–500	3 h	16 h	Amine-adduct-cured, glass-flake-reinforced
Acid-resistant epoxy	55	75-150	3 h	20 h	Two components, polyamine-cured
High-build, recoatable epoxy	62	150	2 h	12 h	Two components, general purpose
Solvent-free epoxy	100	>300	5 h	40 h	One coat, long-life protection for steel structures and storage tanks, suitable for ballast, crude oil and aliphatic petroleum products

(*contd.*)

Table 1.29 (*contd.*)

Paint type	Percent solids content by volume (approx.)	Optimum dry film thickness μm	Touch dry after	Time before overcoat	Uses and properties
High-build, surface-tolerant epoxy	80	125–200	2.5 h	6 h	For maintenance where blast cleaning is not possible
Phenolic epoxy	60	50–100	45 min	18 h	Two components for low friction on inside of pipes; resistant to crude oil containing H_2S and CO_2
Phenolic epoxy lining	55	75–150		12 h	For sweet and sour crude, brine, processed petroleum products, CO_2– and H_2S-containing CO_2
Phenolic epoxy tank lining primer/intermediate and finish formulations	66	100	2 h	24 h	Two components, good resistance to chemicals and higher temperatures
Heat-resistant coatings					
Heat-resisting aluminum	28	35	30 m	8 h	Two-coat system or overcoat for inorganic zinc primer, good up to 360°C
Heat-resisting aluminum finish	50	25	60 m	16 h	Good up to 175°C
Moisture-cured inorganic silicate	50	25	60 m	5 h	Finish coat over inorganic zinc primer, good from −90°C to 600°C
Inorganic zincs					
Water-based inorganic zinc primer	65	100–125	15 min	8 h	Self-curing alkali silicate primer under most paint systems, good from −90°C to 400°C, withstands rain 60 min after application, fair flexibility, good abrasion resistance when cured
Polyurethanes					
High-solids aliphatic acrylic	60	51–76	1 h	12 h	Two components, unlimited recoatability, excellent resistance to chemicals such as water, oil and solvents, tough, flexible and abrasion resistant, excellent hiding power

Aliphatic acrylic polyurethane	41	50	30 min	4 h	Two components, excellent color finish, excellent resistant to atmospheric exposure, resistant to mineral oils, paraffin and gasoline
Water-borne coatings					
Water-borne primer	43	50–75	10 min	2 h	Single-component primer as base for complete water-borne system on steel
Water-borne rust converting primer	43	50–75	30 min	6–8 h	For lightly rusted steel, eliminates the need for blasting, suitable for epoxy topcoats
Water-borne finish	42	50–75	30 min	1 h	For use over water-borne primer; for light to moderate chemical or high humidity exposure; good resistance to mechanical damage
Water-borne aluminum	45	50–75	15 min	2 h	For primer, intermediate or topcoats, excellent aluminum appearance and durability
Miscellaneous					
Polyvinyl butyral etch primer	10	13	5 min	1 h	Adhesion primer for ferrous and nonferrous metals
Vinyl finish	35	50	60 min	16 h	Durable finish coat over high build chlorinated rubber and vinyl systems applied to interior and exterior surfaces in marine and industrial environments
Water-based decorative wall paint	42	38	15 min	2 h	Flat, decorative finish on walls and ceilings, for interior and exterior use
Low-viscosity solvent-free epoxy sealer	100			16 h	Excellent penetrating sealer and adhesion promoter for concrete and prior to application of coatings, excellent chemical resistance

Polyvinyl chloride	Versatile coating. Applied by spraying and fluidized bed techniques. Temperature ranges 60–70°C
Polytetrafluoreethylene	Costly, but highly corrosion–resistant. Stable up to 250°C. Resistant to acids, alkalis and solvents

Concrete-coated structures contain reinforcing steel, which may be protected by injecting calcium nitrite on dieyclohexylamine nitrite or by cathodic protection. Metallic coatings such as nickel, chromium, zinc, cadmium, aluminum and tin were common before plastic appeared on the market. These have been applied by electroplating, hot dipping, spraying, clad coating and diffusion coating procedures.

Corrosion resistance of metallic coatings is dependent on the composition and nature of the electrolyte, oxygen concentration, polarization characteristics, ratio of cathodic to anodic area and the surface contaminants. If the corrosion potentials of two metals such as iron and aluminum are close to each other in a particular environment there may be reversal of the galvanic couple.

1.8.3 Cathodic Protection[75]

This method of corrosion protection consists of: (i) the sacrificial anode method; and (ii) impressed current cathodic protection. The other related impressed current protection method is anodic protection.

The principle of the cathodic protection may be elucidated for the case of carbon steel. The Pourbaix diagram for iron in water consisting of the plot E (potential) vs pH is shown in Figure 1.68. The regions of passivity, immunity and corrosion are seen in the figure.

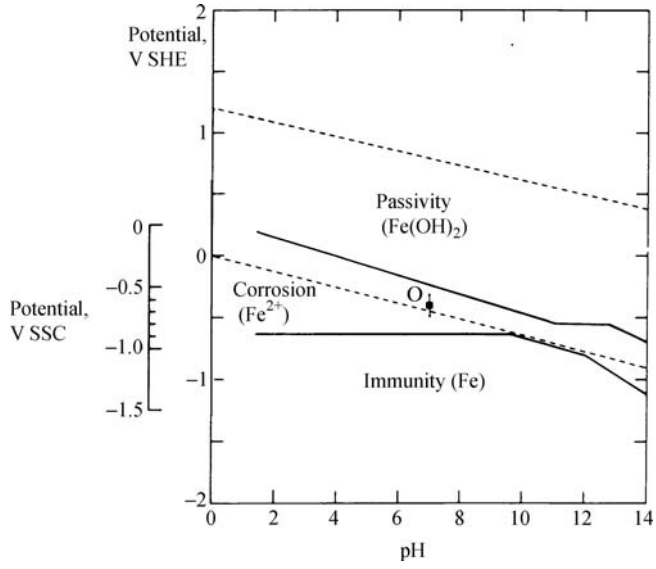

Figure 1.68 *E–pH diagram for iron in water. (Reproduced from Corrosion for Science and Engineering, Tretheway and Chamberlain, Copyright Pearson Education Ltd)*

The corrosion potential, E_{corr} for iron in aerated water is in the range of -600 to -700 mV at pH 7 against the silver–silver chloride reference electrode (Point 0). By decreasing the pH below 7.0 the system is unaffected and corrosion persists. Increase in pH moves the system into a passive region, but this type of perturbation of the system is not the focus of the present discussion. By applying a more negative potential it is possible to move the system into the region of immunity which means the corrosion susceptibility is reduced.

The more negative the potential, the greater the cathodic reaction and the smaller the anodic reaction; the metal is more cathodic, which is the basis of cathodic protection of metals. By applying more positive potentials the system moves into the passive region where the corrosion rate may be reduced. This is particularly the case for some steels in particular environments and other metals, which forms the basis of anodic protection of metals. Thus, it is seen that changing the potential of a system in an environment which cannot be altered leads to effective corrosion control by cathodic or anodic protection as the case may be.

A practical illustration of the application of more negative (cathodic) potential to carbon steel in seawater to reduce the corrosion rate is provided in Figure 1.69. The figure shows that the more cathodic the applied potential, the lower is the corrosion rate. In the figure r_p is the maximum acceptable (or allowed) corrosion rate with a corrosion current density of i_p and protection potential of E_p. For this particular case the protection potential range is -800 to -900 mV. The corrosion rate i_p may be written as:[75]

$$i_p = i_{corr.} e \frac{\alpha \eta z F)}{RT}$$

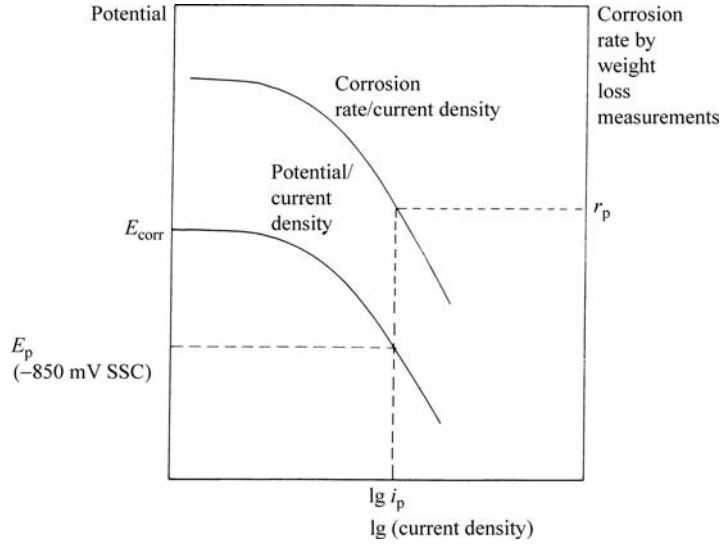

Figure 1.69 *Schematic diagram showing the variation of cathodic potential with current density for steel in seawater, and the correlation of corrosion rate measured by weight loss. (Reproduced from Corrosion for Science and Engineering, Tretheway and Chamberlain, Copyright Pearson Education Ltd)*

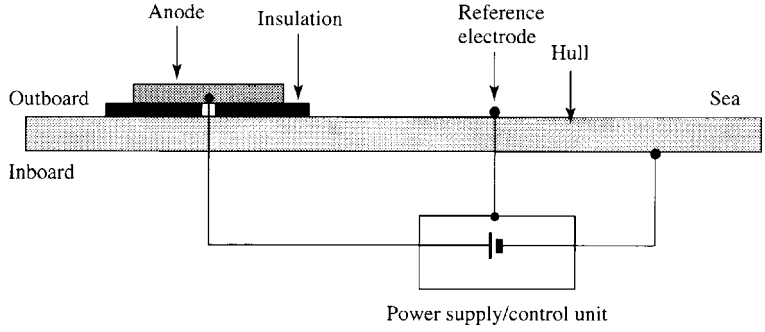

Figure 1.70 *The principle of impressed current cathodic protection using a potentiostat. (Reproduced from Corrosion for Science and Engineering, Tretheway and Chamberlain, Copyright Pearson Education Ltd)*

and with $\alpha = 0.5$, $z = 2$ for iron, $F = 96\,494\,\text{C mol}^{-1}$, $R = 8.314\,\text{J mol}^{-1}\,\text{K}^{-1}$ and $T = 273 + 10$ (seawater temperature) and for a polarization of $-200\,\text{mV}$

$$i_\text{p} = 0.00027 i_\text{corr}$$

$$i_\text{p} = i_\text{corr.} \text{e} \frac{(0.5(-0.2) \times 2 \times 96.494)}{8.314 \times 283}$$

Assuming E_corr in seawater is $-650\,\text{mV}$, then the corrosion rate at $-850\,\text{mV}$ is only 0.03% of the unprotected rate.

The experimental arrangement for the cathodic protection system is schematically shown in Figure 1.70 and is self-explanatory.

Impressed current cathodic protection has the following advantages and disadvantages. Adjustable output, availability of large current, applicability to bare or poorly coated structures, applicability to non-isolated structures and low-cost methods of replacing spent galvanic anodes are some of the advantages. Required constant power, frequent maintenance and inspections, possible cathodic interference and the need for experienced technical personnel may prove to be disadvantages.

The sacrificial anode system consists of a galvanic cell system in which the anode is made of a more active metal than the structure. The anode is attached to the structure and the anode output current may be measured. Magnesium and zinc anodes are commonly use in underground operations, zinc and aluminum alloy anodes in salt water.

Some advantages of galvanic system are: (i) no external power required; (ii) little maintenance; (iii) ease of installation; (iv) little cathodic interference; and (v) infrequent inspection.

The disadvantages to note are: (i) lack of adjustment without resistors in anode circuits; (ii) limited current output; (iii) high replacement costs; (iv) need for good coating; and (v) need for electrical isolation of the protected structure.

The structure to be protected is the cathode and, based on the galvanic series, a metal is chosen as an anode and coupled to the metallic structure to be protected. If the

structure to be protected is steel then one can choose any of the metals zinc or magnesium or aluminum which has more active potentials than iron for protection of steel. By attaching zinc to iron one can accomplish protection of iron, at the expense of corrosion of zinc.

It has been shown earlier that in the working of a Daniel cell consisting of copper and zinc the potential on the copper cathode becomes more negative as current is drawn while the potential of zinc becomes more positive. With time the potentials converge to the corrosion potential at which there is negligible resistance in the cell and limiting current flows. In galvanic corrosion the relative surface areas of the cathode anode are important. The actual potential depends upon the two metals as well as the relative areas. For the protection of large structures the distribution of potential over the surface is an important parameter. When the potential is more negative than E_{corr}, the corrosion potential the anodic reaction occurs to a very small extent and a negative potential more negative than E_{corr} known as E_p the protection potential may be defined for any system. E_p in the case of steel in seawater is ~ -800 mv vs SSC.

Cathodic protection of a hot water tanks using magnesium as the sacrificial anode is shown in Figure 1.71. Some characteristic properties of zinc, magnesium and aluminum anodes are listed in Table 1.30.

The two ways of protecting a system are: (i) to define the protection potential E_p and maintain the potential of the structure; and (ii) the current density required to protect the structure along with the area are used together with the output of the anode materials and use the calculated weight of the anode material. The amount of anode material required for protection of a structure.

$$\text{Anodes required} = \frac{\text{Current requirement}}{\text{Anode output}}$$

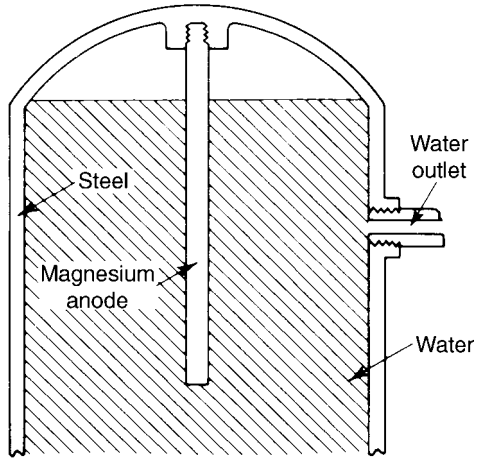

Figure 1.71 *Cathodic protection of a domestic hot water tank using a sacrificial anode*

Table 1.30 *Galvanic anode characteristics[a] [75] (Copyright Pearson Education Ltd)*

Material	Theoretical output (A h/kg)	Actual output (A h/kg)	Efficiency(%)	Consumption	
				Rate (kg/A yr)	Potential vs CSE[b]
Zinc					
Type I Zinc	860	781	90	11	1.06
Type II Magnesium	816	739	90	12	1.10
H-1 Alloy	2205	551–1279	25–58	6.8–16	1.40–1.60
Magnesium					
High potential	2205	992–1191	45–54	7.3–8.6	1.70–1.80
Al/Zn/Hg	2977	2822	95	3.1	1.06
Al/Zn/In	2977	2591	87	3.3	1.11

[a]Data adapted from Advanced Course Text, Chapter 6, Appalachian Underground Corrosion Short Course, West Virginia University, Morgantown, WV, 1993, 1988
[b]Copper/copper sulfate electrode

The capacity of an anode is the number of ampere-hours supplied by 1 kg of anode. Two other important parameters of anodes are: (i) wastage rates which are the rates of loss of metal by volume or mass; and (ii) throwing power which is a function of the distance between the anode and the structure being protected.

The total weight of anode material required to protect a structure for a projected life is given by:

$$W = \frac{i_{\mathrm{av}} AL \times 8760}{C}$$

where W is the total anode material (kg), i_{av} mean current density (A m^{-2}) A area (m^2), C anode capacity (A h Kg^{-1}), L is design life (yr). In practice the total anode material used in a practical situation must be greater than the calculated value. The anode capacity values are given in Table 1.30 and may be used in the calculations.

It is necessary that the anodes supply current demands consistently during the life of the system. It is necessary to bear in mind that the current output of the anode varies with the shape of the anode because of the difference in surface area/weight ratio. The anode output I depends on the anode shape, resistivity of the environment, the protection potential E_{p} and the anode operating potential E_{a} and may be written as:

$$I = \frac{(E_{\mathrm{p}} - E_{\mathrm{a}})}{R_{\mathrm{a}}}$$

where R_{a} is the resistance of the anode and formula for various shapes of anodes may be found in the literature.[75] The life of an anode L in years may be calculated by the equation

$$L = \frac{\mathrm{Th} \times WE \times \mathrm{UF}}{\mathrm{h} \times \mathrm{I}}$$

where Th is the theoretical output, A h/kg, W is the anode weight in kg, E is current efficiency and UF is the utilization factor, h is hours per year and I is the anode output in amperes. The utilization factor is generally chosen as 0.85 (85%).

Galvanic anode systems are generally used in well-coated electrically isolated structures, offshore structures, ship hulls, hot-spot pipeline protection, heat exchanger water boxes and other environments of resistivity below ~10000 Ω cm.

1.8.4 Impressed Current Protection[75]

Common uses of the impressed current method of protection include long transmission pipelines, complex underground structures, marine structures, ship hulls, and replacement for dissipated galvanic systems, large condenser water boxes, reinforcing steel in concrete, bare or poorly coated structures, unisolated structures and water storage tank interiors.

This method is especially suitable when large currents are involved, possibly as high as 500 A. The current requirement is calculated as:

$$I_{\text{req}} = A \times \%\,\text{bare} \times m\,\text{A/m}^2$$

Anode materials and their properties along with the recommended uses are noted in Table 1.31. For a number of anodes required for an impressed current ground bed, we calculate the weight required by the equation,

$$W = DI_{\text{req}}L$$

Table 1.31 *Impressed current anode materials and their properties[75] (Copyright Pearson Education Ltd)*

Material	Consumption (kg Ay^{-1})	Recommended uses and references
Platinized tantalum and niobium	8×10^{-6}	Marine environments, potable water, carbonaceous backfill and high purity liquids
Platinized titanium	8×10^{-6}	Marine environments and potable water
High-silicon iron	0.25–1.0	Potable waters and soil or carbonaceous backfill
Steel	6.8–9.1	Marine environments and carbonaceous backfill
Cast iron	4.5–6.8	Marine environments and carbonaceous backfill
Lead–platinum	0.09	Marine environments
Lead–silver	0.09	Marine environments
Graphite	0.1–1.0	Potable waters and carbonaceous backfill 75

Marine structures	Cathodic protection	76
Heat exchangers	Cathodic protection	76, 77
Steel in concrete	Cathodic protection	76
Water storage tanks	Cathodic protection	78, 79
Above-ground storage tank bottoms	Cathodic protection	76

where W is the weight, D is the dissipation rate in kg/A yr, I_{req} is the current required and L the life in years. The total resistance is the sum of anode to ground, cable and structure to ground

$$R = R_a + R_c + R_s$$

and the required driving voltage

$$E = \frac{I_{req}}{R_t}$$

Table 1.31 provides a list of applications with literature references.

1.8.5 Anodic Protection[75]

In the discussion of E the vs pH diagram for iron in water depicted in Figure 1.70, we noted that, with application of high positive potentials, the system moves into a region of passivity and results in a reduced corrosion rate. The passive film formed should be coherent and insulating to withstand corrosion and mechanical breakdown. Upon formation of the passive state the corrosion rate is reduced. Thus by polarization and applying more positive potentials than corrosion potentials the metal attains passivity and is protected. This is the principle of anodic protection. It is necessary that the potential of passivation be maintained at all times, since deviations outside the range would result in severe corrosion.

It is important to note that passive behavior of the metal also depends upon the electrolytic environment. As an example mild steel is passivated in pure nitric acid, but not in dilute aqueous nitric acid. The current density required to passivate i_{pass} can be high and the current density to maintain the film i_{film}, may be small.

Anodic protection is often used to protect Fe, Ni, Al, Ti, Mo, Zr, Hf and Nb and their alloys. Environments can vary from highly acidic to highly alkaline in nature. This method is used for storing acids in the chemical and fertilizer industry. Because of the aggressive nature of the environments reference electrodes suitable for use are noble metals such as platinium. Some of the advantages are low operating costs and controlled conditions. Cheaper alloys with anodic protection may be used in place of expensive alloys. Failure of electrical supply is hazardous and inapplicability to organic liquids is an obvious disadvantage.

References

1. J. Cousteau, *Nat. Geo. Mag.*, **105**, 1 (1954).
2. N. Hackerman, *Corrosion 93, Plenary and Keynote Lectures*, R.D. Gundry (ed.), NACE International, Houston, Texas, 1993, pp. 1–5.
3. U.R. Evans, *Chem. Ind.*, 986 (1952).
4. W. Lynes, *J. Electrochem. Soc.*, **98C**, 3–10 (1951).
5. H. Davy, *Nicholson's J.*, **4**, 337 (1800).
6. W.H. Wollaston, *Phil. Mag.*, **11**, 206 (1801).
7. L.H. Bennett, J. Kruger, R.I. Parker, E. Passaglia, C. Reimann, A.W. Ruff, H. Yakowitz and E.B. Berman, *Economic Effects of Metallic Corrosion in the United States – A Three Part Study for*

Congress; a) Part I NBS Special Publication 511-1, SD Stock No. SN-003-003-01926-7; b) Part II NBS Special Publication 511-2 Appendix B. A report to NBS by Battelle Columbus Laboratories, SD Stock No. SN-003-003-01927-5, US Govt. Printing Office, Washington, DC, 1978; c) Part III, Appendix C, Battelle Columbus Input/Output Tables, NBs GCR 78-122, PB-279 430, National Technical Information Service, Springfield, VA, 1978.

8. V.S. Sastri, M. Elboujdaini and J.R. Perumareddi, Economics of Corrosion and Wear in Canada, *Proceedings of the International Conference on Environmental Degradation of Metals*, Metallurgical Society of Canadian Institute of Mining held at Vancouver, BC, Canada, Jingli Li and M. Elboudjaini (eds.), 23–27 August 2003.
9. T.P. Hoar, *Report of the Committee on Corrosion and Protection*, Department of Trade and Industry, H.M.S.O., London, UK, 1971.
10. D. Behrens, *Br. Corros. J.*, **10**(3), 122 (1975).
11. K.F. Trädgäidh, *Tekn. Tedskrift, Sweden*, **95**(43), 1191 (1965).
12. V. Vläsaari, *Talouselämä, Economy*, (14/15), 351 (1965).
13. Y. Kolotyrkin, *Sov. Life*, **9**, 168 (1970).
14. R.W. Revie and H.H. Uhlig, *J. Inst. Eng. Austr.*, **46**(3–4), 3 (1976).
15. K.S. Rajagopalan, *The Hindu*, Madras, India, Nov. 12, 1973.
16. 'Committee on Corrosion and Protection', *Corr. Eng., Japanese*, **26**(7), 401 (1977).
17. NACE Technical Committee Report, Task Group T-3C-1 on Industrial Economic Calculational Techniques, *Economics of Corrosion*, NACE, Houston, Texas, 1972.
18. V.S. Sastri, *Corrosion Inhibitors*, John Wiley & Sons, Ltd, Chichester, UK, 1998, pp. 5–10.
19. V.S. Sastri, M. Elboudjaini and J.R. Perumareddi, *CIM Bulletin*, **90**(63), (1997).
20. V.S. Sastri, M. Elboudjaini and J.R. Perumareddi, *International Conference of the Metallurgical Society of CIM on Wear and Corrosion of Metals, Proceedings*, Sudbury, Ontario, August 1997.
21. V.S. Sastri, M. Elboudjaini and J.R. Perumareddi, 'Economics of Corrosion and Wear in Aerospace Industry,' *Proc. of the International Conference on Aerospace Materials*, Metallurgical Society of CIM, Montreal, 12–15 August 2002.
22. J.O.M. Bockris and B.E. Conway, *Modern Aspects of Electrochemistry*, London, Butterworths, 1954.
23. B.E. Conway, *Electrochemical Data*, Elsevier, New York, 1952.
24. P.R. Roberge and V.S. Sastri, 'Electrochemical Impedance Spectroscopy as a Reliable and Powerful Technique for Olnine Corrosion Monitoring', Paper No. 396, CORROSION 93.
25. N.B. Pilling and R.E. Bedworth, *J. Institute Metals*, **29**, 529 (1923).
26. B. Chalmers, *Physical Metallurgy*, John Wiley & Sons, Inc., NY, 1959, p. 445.
27. C. Gensch and K. Hauffe, *Z. Physik Chem.*, **196**, 427 (1950).
28. C. Wagner and K.E. Zimens, *Acta Chem. Scand.*, **1**, 547 (1947).
29. H. Pfeiffer and K. Hauffe, *Z. Metalkunder*, **43**, 364 (1952).
30. M.G. Fontana, *Corrosion Engineering*, McGraw-Hill, NY, 1980.
31. Z.A. Foroulis, *High Temperature Metallic Corrosion by Sulphur and its Compounds*, The Electrochemical Society, Princeton, New Jersey, 1970.
32. J.R. Nichols and P. Hancock, *Industrial Corrosion*, **5**(47), 17 (1987).
33. D.A. Shores, *Corrosion*, **24**, 434 (1975).
34. D.K. Gupta and R.A. Rapp, *J. Electrochem. Soc.*, **127**, 2194–2656 (1980).
35. *Metal Progress Data Book and Advanced Materials and Processes*, American Society for Metals, Metals Park, Ohio.
36. N.E. Hamner (ed.), *NACE Corrosion Data Survey*, Houston, TX, NACE, 1974.
37. H. Van Droffelar and J.T.N. Atkinson, *Corrosion and its Control*, NACE International, 1995.
38. E.D. Verink, Jr., *Uhlig's Corrosion Handbook*, 2nd edn, John Wiley & Sons, Inc., NY, 2000.
39. R.W. Staehle, *Life Prediction of Corrodible Structures*, R.N. Parkins (ed.), NACE, Vol. 3, Texas, 1994.
40. R.W. Staehle, *Environmental Definition, Materials Performance Maintenance*, R.W. Revie, V.S. Sastri, M. Elboudjaini, E. Ghali, D. Piron, P.R. Roberge and P. Meyer (eds.), Ottawa, Ontario, 1991, pp. 3–43.
41. *Guidelines for Chemical Process Quantitative Risk Analysis, Centre for Chemical Process Safety*, American Institute of Chemical Engineers, NY, 1989.

42. *Tools for Making Acute Risk Decisions with Chemical Process Safety Applications, Centre for Chemical Process Safety*, American Institute of Chemical Engineers, NY, 1995.
43. *Guidelines for Investigating Chemical Process Incidents, Centre for Chemical Process Safety*, American Institute of Chemical Engineers, NY, 1989.
44. *Guidelines for Chemical Process Quantitative Risk Analysis, Centre for Chemical Process Safety*, American Institute of Chemical Engineers, NY, 1989.
45. T.A. Kletz, *Hazop and Hazon: Identifying and Assessing Process Industry Hazards*, 3rd edn, Institution of Chemical Engineers, Rugby, Warwickshire, 1992.
46. T.A. Kletz, *Improving Chemical Engineering Practice: A New Look at the Old Myths of the Chemical Industry*, 2nd edn, Hemisphere Publishing Corporation, NY, 1990.
47. V.S. Sastri, *Corrosion Inhibitors, Principles and Applications*, John Wiley & Sons, Ltd, Chichester, UK, 1998.
48. N. Hackerman and E.S. Snavely, *Corrosion Basics*, L.S.V. Delinder (ed.), NACE, Houston, TX, 1984.
49. G. Schmidt and K. Bedbur, *Werkst und Korros*, **36**, 273 (1985).
50. Z.S. Smialowska and G. Wieczorek, *Corrosion Science*, **11**, 843 (1971).
51. S. Trassati, *J. Electroanal. Chem.*, **53**, 335 (1974).
52. J.O.M. Bockris and D.A. Swinkels, *J. Electrochem. Soc.*, **111**, 736 (1964).
53. I. Langmuir, *J. Am. Chem. Soc.*, **39**, 1848 (1947).
54. S. Trassali, *J. Electro Anal. Chem. Interf. Electrochem.*, **33**, 351 (1971).
55. N. Hackerman and R.M. Hurd, *Proc. Int. Congress on Metallic Corrosion*, London, Butterworth, 1962, p. 166.
56. J.O.M. Bockris, N. Bonciocat and F. Gutman, *An Introduction to Electrochemical Science*, London, Wykeham Pub. Ltd., 1974, p. 44.
57. V.S. Sastri and J.R. Perumareddi, *Corrosion*, **50**, 432 (1994).
58. V.S. Sastri and J.R. Perumareddi, *Corrosion*, **53** (1997).
59. V.S. Sastri and P.R. Roberge, *11th International Corrosion Congress*, Florence, Italy, Vol. 3, 1990, p. 55.
60. P. Dupin, A. de Savignac and Al. Lattes, *Information Chimie*, (228/229), 169 (1982).
61. V.S. Sastri, J.R. Perumareddi and M. Elboudjaini, *NACE Conference*, Ottawa, Ontario, 15–17 September 2003.
62. V.S. Sastri and J.R. Perumareddi, *Corrosion*, **53**, 617 (1997).
63. V.S. Sastri and J.R. Perumareddi, *Corrosion*, **50**, 432 (1994).
64. V.S. Sastri, *Corrosion*, **52**, 447 (1996).
65. V.S. Sastri, *British Corrosion J.*, **24**, 30 (1989).
66. V.S. Sastri and R.H. Packwood, *Werkstoffe und Korrosion*, **38**, 77 (1987).
67. A. Akiyama and R. Nobe, *J. Electrochem. Soc.*, **117**, 999 (1970).
68. P.G. Fox and G. Lewis, P.J. Boden, *Corrosion Science*, **19**, 457 (1979).
69. I. Singh, *Corrosion*, **49**, 473 (1993).
70. T.A. Skothaim (ed.), *Handbook of Conducting Polymers*, Marcel Dekker, NY, Vols. 1 and 2, 1986.
71. A. Weisstuch, D.A. Carter and C.C. Nathan, *Material Performance*, **10**(4), 11 (1971).
72. B. Mikisic, R. Boyle and B. Wuertz, *Corrosion*, **60**, 515 (2004).
73. V.S. Sastri, J. Bednar and R.H. Packwood, *Br. Corr. Journal*, **24**, 30 (1989).
74. F.L. Laque, *Marine Corrosion: Causes and Prevention*, John Wiley & Sons, Inc., NY, 1975, p. 203.
75. K.R. Tretheway and J. Chamberlain, *Corrosion for Science and Engineering*, Longman, 1995.
76. J.H. Morgan, *Cathodic Protection*, Chapter 7, 2nd edn, NACE International, TX, 1993.
77. R.W. Lane, *Control of Scale and Corrosion in Building Water Systems*, McGraw Hill, NY, 1993.
78. J.B. Bushman and D.H. Kroon, *J. AWWA*, January 1984.
79. A. Kumar, J.B. Bushman, J.H. Fitzgerald, A.E. Brown and T.M. Kelly, *Impressed Current Cathodic Protection Systems Utilizing Ceramic Anodes*, US Army Res. Labs, Champaign, Inc., 1990.
80. R. Walker and A. Ward, *Metals Review*, **137**, 143–151 (1969).

2

Corrosion Testing, Detection, Monitoring and Failure Analysis

Corrosion testing is an important step in the process of materials selection. It is necessary to carry out corrosion tests on materials of interest in the anticipated environments such as immersion, buried, or atmosphere or industrial in nature. The corrosion testing should also take into effect the role of the mechanical properties of the chosen materials and the consequent phenomena such as stress corrosion cracking. In the case of corrosion of general nature the weight loss method of testing is still the best and the most reliable method although it is slow and time consuming.

In systems involving finishing, rust staining, discoloration, chalking, gloss retention and sometimes pitting are applicable. It is useful to note that when pitting is involved it is mandatory to use large samples and obtain statistically valid data.

It is preferable to carry out laboratory corrosion tests and to validate the data with service tests for the selection of materials. It is needless to note that the chosen test method be reliable and cost effective. Some of the test methods in use in industry are service tests, field tests, laboratory tests, and rapid electrochemical methods such as potentiodynamic polarization, linear polarization, electrochemical impedance and electrochemical noise.

2.1 Corrosion Testing

The main purposes of corrosion testing are: (i) evaluation and selection of materials for a given application; (ii) evaluation of new or old materials to determine the environments which are suitable; (iii) control of corrosion resistance of the material or corrosivity of the environment; and (iv) study of the corrosion mechanism.

Corrosion Prevention and Protection: Practical Solutions V. S. Sastri, E. Ghali and M. Elboujdaini

The chemical composition, fabrication history, metallurgical history and positive identification of the samples should be known before testing. Established polishing procedures such as polishing with standard No. 120 abrasive cloth or paper should be used in preparing the sample surface. Samples are weighed after surface preparation and the dimensions are measured to obtain the surface area of the sample. Some of the considerations for exposure are ease of access of the corrosive to the sample, the supports holding the samples should not fail, samples must be insulated (isolated from electrical contact wit another metal), and proper positioning of sample and the samples must be readily accessible in plant tests.

The duration of test should be based on the nature of corrosion and the rule of thumb is:

$$\frac{2000}{\text{mils per year}} = \text{hours (duration of test)}$$

Two weeks to a month is recommended for plant tests. Atmospheric corrosion and soil corrosion involving low-corrosion rates require periods of the order of several years of exposure.

Aeration or the presence of oxygen is an important factor in corrosion testing. In normal procedures air is bubbled into the liquid during testing or nitrogen gas bubbling is used when testing requires exclusion of dissolved oxygen or air.

The corroded samples may be cleaned by: (i) mechanical means such as scraping, brushing, scrubbing with abrasives, sandblasting or the rubber-stopper method; (ii) chemical or solvent use; (iii) electrolytic methods in which the sample is made the cathode under an impressed current in a solution of acid (5% H_2SO_4) containing an inhibitor such as rhodine. This procedure requires a blank sample to run through the cleaning procedure. Some clearing reagents in common use are:

Al and their alloys – 70% nitric acid
Cu and its alloys – 10% H_2SO_4 or 20% HCl
Iron and steel – warm 20% HCl or H_2SO_4
Stain steel – hot 70% HNO_3
Lead and its alloys – boiling 1% acetic acid
Mg and its alloys – boiling 1% silver chromate and 15% chromic acid
Ni and its alloys – immerse in 15–20% HCl or 10% H_2SO_4
Zn and its alloys – immerse in saturated ammonium acetate solution

In general corrosion is accelerated by an increase in temperature with the exception when dissolved oxygen is the corrosive agent. Careful control of temperature in corrosion testing is mandatory. Sometimes high temperatures are used in accelerated corrosion tests.

The standard expression for corrosion rates may be written as:

$$\begin{matrix}\text{mils per year} \\ \text{(mpy)}\end{matrix} = \frac{534W}{DAT}$$

where W is weight loss in milligrams, D density of sample, g/cm^2, A is area of sample in square inches, and T the exposure time in hours. Corrosion rates are also expressed in units other than mils per year in which case the conversion may be made from other units to mpy as follows:

Multiply	By
inches/year	1000
inches/month	12 100
mg/dm^2/day (mdd)	1.44/specific gravity

Metric system corrosion rates may be written as:

$$1 \text{ mpy} = 0.0254 \frac{\text{mm}}{\text{yr}} = 25.4 \frac{\mu\text{m}}{\text{year}} = 2.90 \frac{\text{nm}}{\text{hr}} = 0.805 \frac{\text{pm}}{\text{s}}$$

Weight loss data may be used to convert into mm/yr or μm/yr.

$$\frac{\mu\text{m}}{\text{yr}} = 87\,600 \frac{W}{DAT}$$

$$\frac{\text{mm}}{\text{yr}} = 87.6 \frac{W}{DAT}$$

In the determination of corrosion rates by electrochemical techniques the corrosion current density i_{corr} in μa/cm^2 is measured which is written as:

$$\text{corrosion rate} = K \frac{a i_{\text{corr}}}{nD}$$

where a is the atomic weight, n the number of electrons involved, D the density of the metal, g/cm^3, K is a constant which assumes the values 0.129, 3.27 and 0.00327 for the corrosion rates in mpy, μm/yr and mm/yr, respectively.

Some typical comparative data in various units are shown in Table 2.1.

2.1.1 Testing for Environmentally Assisted Cracking (EAC)

This is a very extensive topic involving many variables. It involves the evaluation of the inherent compatibility between a material and the environment under applied or residual stress. Factors such as material type, process history, product form, active cracking mechanisms, loading configuration and geometry and exposure environments can have an impact on the type of sample and test conditions for the evaluation of EAC.

Table 2.1 *Some typical corrosion rate data based on typical ferrous and nickel base alloys*

Corrosion restistance rating	mpy	mm/yr
Outstanding	<1	<0.02
Excellent	1 to 5	0.02 to 0.1
Good	5 to 20	0.1 to 0.5
Fair	20 to 50	0.5 to 1
Poor	50 to 200	1 to 5
Unacceptable*	>200	>5

*Rates greater than 200 mpy are some times acceptable for cheap materials such as cast–iron of thick cross sections(e.g., cast-iron pump body).

The first and foremost step in the selection of test methods is a literature survey of the published literature on the previous tests and methodologies in anticipated environments. The types of EAC are stress–corrosion cracking, hydrogen embrittlement, and liquid metal embrittlement. Stress–corrosion cracking (SCC) involves formation of cracks through the simultaneous action of tensile stress and the corrosive environment. When crack propagation occurs along grain boundaries, the phenomenon is known as intergranular SCC. When the cracking is along specific crystallographic planes within the grains, it is termed transgranular SCC.

Hydrogen embrittlement is caused by reduction of hydrogen ion to atomic hydrogen followed by combining of hydrogen atoms. In the absence of hydrogen recombination poisons (S, P, As, Sn) hydrogen atoms combine to produce molecular hydrogen. When hydrogen atom recombination poisons are present hydrogen atoms can cause hydrogen embrittlement. This combined with stress results in stress oriented hydrogen damage. Liquid metal embrittlement shows many characteristics of both SCC and hydrogen embrittlement cracking (HEC). Schematic comparison of anodic SCC and HEC cracking is shown in Figure 2.1.

Testing of EAC involves constant load–deflection techniques, dynamic tests, and fracture mechanics tests. In a constant load test a tension sample is used and samples are loaded to various levels of applied stress as defined by 1–3 ISO 7539 - Part 4, ASTM G-49 and NACE TMO 177. A typical test cell is shown in Figure 2.2. The stress s is calculated by the formula P/A where P is the load and A is the sample cross-sectional area. The constant load is usually applied using a dead-weight fixture. For the case of dead-weight loading, a constant load is produced on the sample. Once cracking initiates in the sample, the cross-sectional area decreases and the applied stress increases. The sample fails after crack initiation and hence the information on crack propagation cannot be obtained. The effect of corrosion and stress can be seen at a location by the single notch in the sample gauge section. In the majority of studies multiple samples and stress levels are used, and a typical threshold stress curve obtained as shown in Figure 2.3.

Alternative to the constant load tensile test, a spring or proof ring is used in place of dead-weight and the load/deflection relationship for the particular geometry is

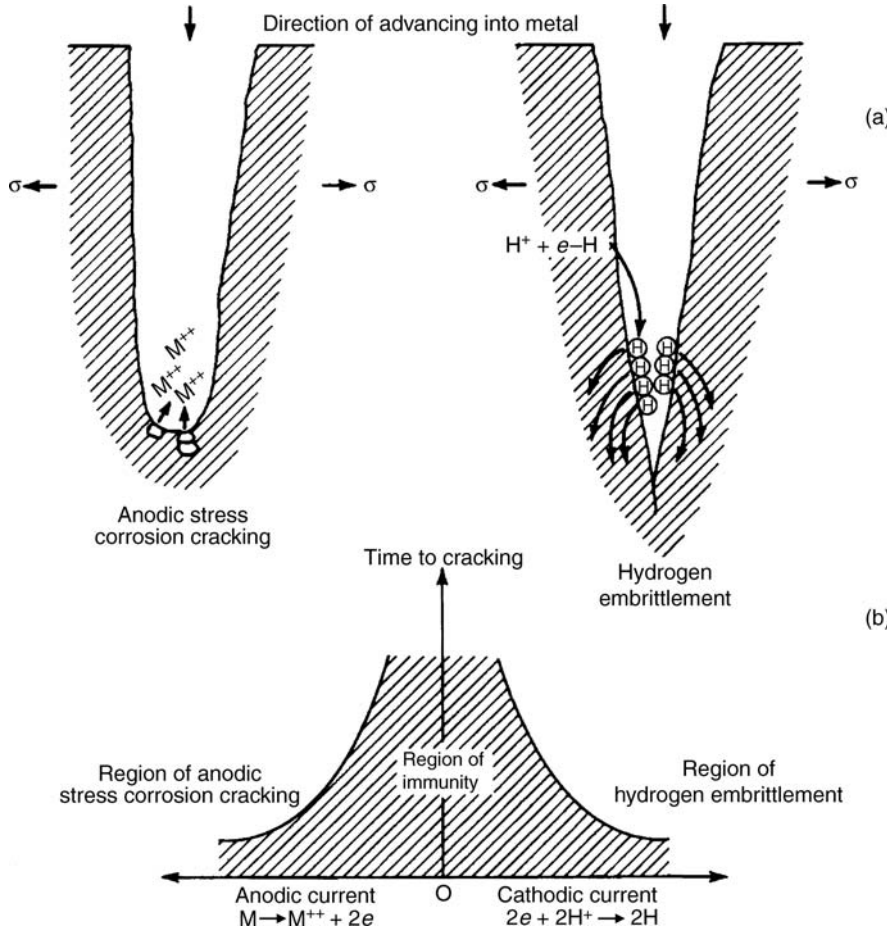

Figure 2.1 *Schematic comparison of: (a) anodic SCC; (b) hydrogen embrittlement cracking (HEC) mechanisms*

established. Some important points are that the deflections before and after the tests should be recorded, the sample to be checked for subcritical crack growth, periodic calibration for loads vs deflection, when limited compliance is available, the samples are broken in air after testing to locate any subcritical cracks, and the resulting reduction in load-carrying capacity of the test samples. This method of pulling non-failed samples to break failure is known as a breaking load test[4] (ASTM G139). Samples of different geometry used are:

Bent beam samples (two-, three-, and four-point loading) in ISO 7539 Part 2, ASTMG[5]38, NACE TM0177 Method B;

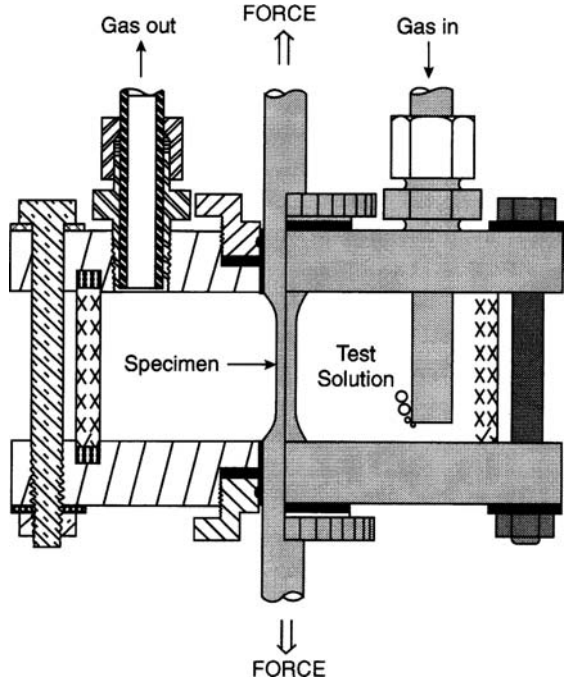

Figure 2.2 *Typical smooth tension specimen in test cell*

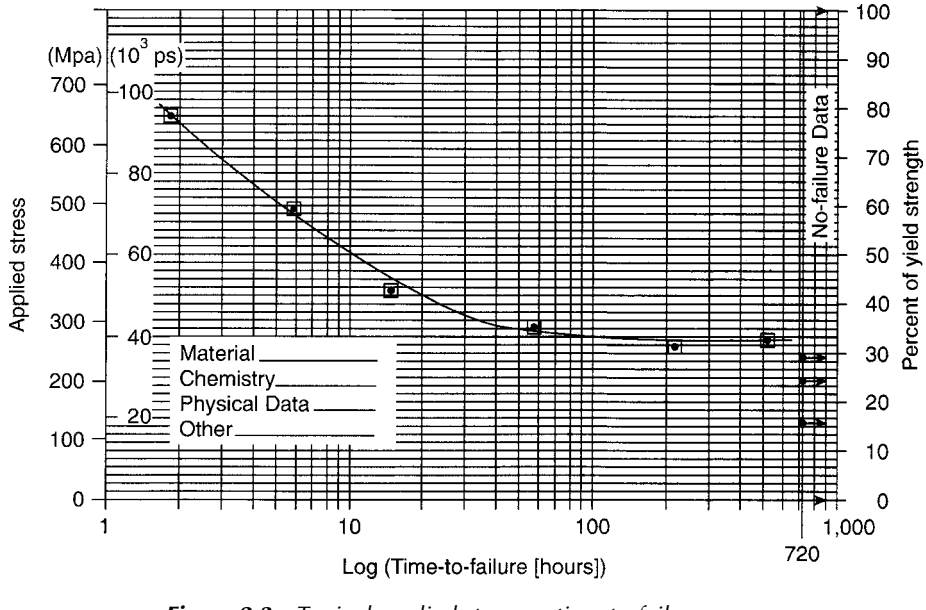

Figure 2.3 *Typical applied stress vs time-to-failure curve*

C-ring samples per ISO 7539 Part-5, ASTM[6] G38, TM0177 Method C;
U-bend samples per ISO 7539 Part 3, ASTM[7] G30,

Dynamic tests involve slow strain rate (SSR) or constant extension rate (CERT) tests. The principle of the test involves a slow extension of the sample that produces a ramping load (increasing stress) on the sample until failure occurs. Detailed descriptions of the test procedures are given[8,9] in ASTM G129, NACE TM0198 and ISO 7539-7. The main advantage of this method is that the test gives results within a short period (1–2 days). Another advantage of this method is that metallurgical variables such as alloy composition, heat treatment and processing, environmental variables such as aeration, concentration and inhibition can be evaluated. The main drawback of SSC is that the plastic strain used to cause an accelerated disruption of the surface films can cause complications in the interpretation of the test data since most of the materials are not subject to this high degree of straining in service applications. Cracking susceptibility of materials is overestimated by this technique.

The cyclic slow strain rate (CSSR) test overcomes the deleterious effect of plastic strain in the SSR technique by loading the sample to a relatively high percentage of its yield strength in tension and the stress is then varied by about $\pm$ 10% of the value. The number of cycles used is typically of the order of 100–200 and the test duration is between a few days to two weeks. Cyclic SSR technique is better than SSR technique for material/environment systems where excessive straining produces a large increase in susceptibility to cracking. Some examples of this type of behavior are ferritic and martensitic steels in hydrogenation atmospheres, duplex stainless steels, due to their ferritic/austenitic microstructure subject to a concentration of strain in the ferrite due to its lower work hardening coefficient than that of austenite.

Fracture mechanics testing techniques are generally used for evaluation of the metallurgical factors on environmentally assisted cracking where the sample contains a sharp crack. Constant-load or constant-deflection samples in combination with a precracked sample are used in fracture mechanics techniques. The most common types of specimens used for the evaluation of environmentally assisted cracking are compact tension (CT), precracked double-beam (PDB)/double-cantilever beam (DCB) or single-edge notched bend (SENB). It is a usual practice to fatigue-precrack the samples or to slot the samples using controlled electrodischarge machining (EDM) and then use in the environment of interest.

The stress intensity at the tip of the crack can be calculated using standard equations given in the literature, ASTME399 for CT and SENB samples[10], ASTM GXXX or NACE TM0177-Method D for the PDB samples[11]. The fracture mechanics test configurations are shown in Figure 2.4. It is generally recognized that EAC testing should involve more than one type of test specimen, various configurations of the same specimen, and alternative test techniques with the same specimen (i.e., crevices, applied potential, constant load, slow strain rate). As is often the case with testing it is also necessary to conduct integrated laboratory and field tests, correlation of laboratory data with service experience, and reviews of published literature on the service performance of similar materials.

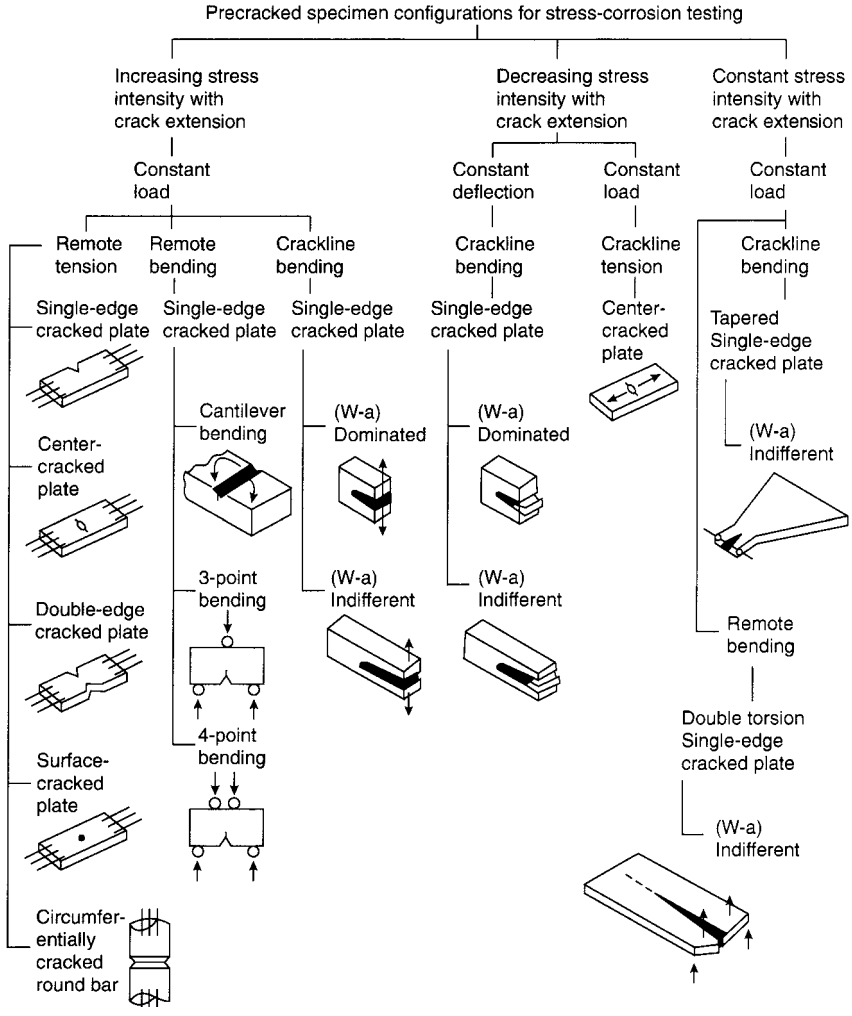

Figure 2.4 *Fracture mechanics test configurations*

Tests for aluminum and its alloys consist of intergranular corrosion, stress corrosion cracking; and corrosion fatigue as detailed below:

Alloy	Test	Exposure	Technique	References
Al–Cu–Mg (2XXX)	Intergranular corrosion	NaCl–H_2O_2 solution	Metallography Electrochemical	[1] [2]
Al–Mg–Si (6XXX)	Intergranular corrosion	NaCl–H_2O_2 solution	Metallography	[1]

(*contd.*)

(*contd*.)

Alloy	Test	Exposure	Technique	References
Al–Zn–Mg–Cu (7XXX)	Intergranular corrosion	$NaCl–H_2O_2$ solution	Electrochemical	[2]
	Corrosion fatigue	Distilled or deionized water or brine	Cyclic stress method	

[1] J.E. Hatch, *Aluminum: Properties Physical Metallurgy*, American Society for Metals, Ohio, 1984, Vol. 263, pp. 248–319, 263, 307.

[2] *Annual Book of ASTM Standards, Standard Practice for Measurement of Corrosion Potentials of Aluminum Alloys*, ASTM, Philadelphia, PA, 1994, G 69–81.

Magnesium and its alloys	Salt spray test		ASTM	
Used in automotive	Automotive cycle	Salt water	B117	[1]
Applications	Tests	Drying, high humidity		

[1] *Annual Book of ASTM Standards, Practice for Operating Salt Spray (Fog) Testing Apparatus*, B117-95, ASTM, Philadelphia, PA, 1995.

2.1.2 Atmospheric Corrosion Testing

Atmospheric corrosion is recognized as the single most severe form of corrosion on a tonnage basis. The following is a list of materials that are subject to atmospheric corrosion:

Bridges	Highway guard rails	Utility poles
Powerlines	Electrical switchgear cabinets	Automatic teller machine cabinets
Building siding and roofs	Automotive body	Airplane skins
Refrigerator back plates	Outboard motor housings	Oil derricks
Mail boxes	Chain link fences	Stadium seats and decks

The parameters to be determined during testing are as follows:

- Weight loss
- Thickness loss
- Loss of impact strength
- Loss of tensile strength
- Loss of ductility
- Pitting tendency
- Perforation
- Coating life
- Discoloration
- Contact resistance

Most of the atmospheres encountered should be defined by three principal conditions, namely[12] dampness, temperature and contaminants. Based on the three factors, the

atmospheres may be characterized as:

Dampness	Temperature	Contaminants
Dry	Tropical	Rural
Humid	Temperate	Urban
Marine	Arctic	Industrial

Every single factor in the three columns defines a particular atmosphere. Attempts to classify and characterize various atmospheres based on predicted corrosivity by measurement of time-of-wetness and contaminants[13,14] and actual determination of corrosion rates using standard metal samples[13,15,16] are part of the international program ISO CORRAG (ISO Technical Committee 156, Working Group 4).

The time-of-wetness τ, the amount of pollution P and the amount of chloride S are defined to estimate the corrosion rates of carbon steel, zinc, copper and aluminum and the resulting values for an exposure duration were obtained. Use of the different degrees of time of wetness, various values of pollution along with different amounts of contaminant such as chloride, the estimated corrosion rates[13] of steel, zinc, copper and aluminum for exposure duration of one year are given in Table 2.2.

The American Society for Testing and Materials provides the standards given below:

- Site characterization[17]
- Time-of-wetness monitoring[18]
- Pollution monitoring[19,20]
- CLIMAT (classification of Industrial and Marine Atmospheres,[21] gives data on uniform or galvanic corrosion of aluminum wire wound around threaded bolts made of steel or copper in an atmosphere of interest)

All the atmospheric corrosion tests discussed thus far should be used as guides, and suitable tests should be devised and conducted in the environment of interest to assess the corrosivity of the environment.

The utmost care and attention must be taken in choosing the test site located in a well-secured area without external disturbance, specimen racks must be corrosion-resistant with lifetimes longer than test periods, the bottom edge of the racks should be at least 75 cm above the ground, periodic check of the mounting of samples is necessary to make sure they are in fixed position, the samples attached to the rack via insulators to avoid galvanic corrosion, metal sheet samples are mounted facing skyward at 30°, in sea exposure the samples face the surf, samples with unusual shapes should be placed in such a manner as in-service conditions, and good record keeping is mandatory.

It is also mandatory to observe the principles of replication, randomization and blocking.[22–24] Replication overcomes the problems associated with attrition of samples. Nonuniformity of time-of-wetness on samples is minimized by randomization of sample mounting location. In the absence of randomization it is possible to create statistical blocks and processed statistically.

Some useful and pertinent information on atmospheric corrosion test site plans, hardware and other relevant information in the literature[25–30] may be used in planning atmospheric corrosion testing program.

Table 2.2 *Time-of-wetness, pollution, chloride, estimated corrosion rates*

Category	Time-of-wetness (%)
τ_1	<0.1
τ_2	0.1–3
τ_3	3–30
τ_4	30–60
τ_5	>60
Category	**Pollution (SO_2, $\mu g/m^2$)**
P_0	<12
P_1	12–40
P_2	40–90
P_3	90–250
Category	**Chloride (mg/m^2 day)**
S_0	<3
S_1	3–60
S_2	60–300
S_3	300–1500

	Corrosion rate (μm/yr)			
Category	Steel	Zinc	Copper	Aluminum
C_1	<1.3	<0.1	<0.1	Negligible
C_2	1.3–25	0.1–0.7	0.1–0.6	<0.6
C_3	25–50	0.7–2.1	0.6–1.3	0.6–2
C_4	50–80	2.1–4.2	1.3–2.8	2–5
C_5	80–200	4.2–8.4	2.8–5.6	5–10

2.1.3 Galvanic Corrosion Testing

Testing for galvanic corrosion throws light on compatibility of materials and predicts the extent and spatial distribution of corrosion damage. Geometry of samples plays an important role in galvanic corrosion and it is not possible to define a particular geometric configuration as a standard for testing. Thus the experimental design for galvanic corrosion testing is unique and variable from one situation to another.[31] A variety of cell designs have been documented in the literature.[31] These designs may be used as guides to design a cell suitable for the problem on hand. The geometry of the design should ensure uniform distribution of the potential over the surface of the anode and the cathode. This requires that the distance between the metals be larger than the sizes of the samples.

Electrochemical methods used in testing give data on potentials under coupled and uncoupled conditions, polarity of the bimetallic couple, and galvanic current, which gives the degree of galvanic corrosion. Other methods used include weight loss, determination of changes in thickness and visual and microscopic examination of the corroded

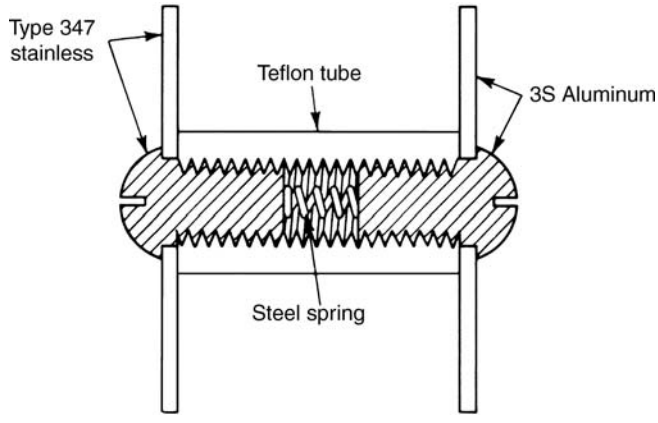

Figure 2.5 *Galvanic test couple assembly*

samples.[31] The foregoing discussion describes the difficulties in designing standardized tests. In spite of this ASTM provides guidelines[32,33] for galvanic corrosion testing with the titles ASTM Standard Guide 71 and ASTM Standard Guide G82.

Galvanic corrosion testing under atmospheric exposures has been standardized and bears the titles ISO 7441-84, ASTMG 104-89 for plate tests and ASTM G116-93 for wire-on-bolt tests.[21,34,35] A form of test assembly for galvanic corrosion testing is shown in Figure 2.5.

2.1.4 Testing of Polymeric Materials

With the developments in polymeric materials and their use in corrosion control applications it is important to perform both laboratory and in-service tests for mechanical integrity, thermal integrity, fluid permeation, chemical ageing, and fluid resistance. Tests for polymeric materials consist of determination of tensile properties, fracture toughness, crack growth fatigue, stress relaxation, high-pressure gas permeation, rapid gas decompression, liquid compatibility, chemical deterioration/aging and environmental stress cracking.

Test	Methodology
Tensile properties	Mechanical properties determined by tensile testing as per ASTM D638 in service conditions (Young's modulus, tensile stress at yield, percentage elongation at yield, tensile strength at break and percent elongation at break) Tests to be done also on materials subjected to chemical ageing procedures.
Fracture toughness	Test as in European Structural Integrity Society protocol.[36] Fracture toughness is obtained by relating the total work done in displacing a compact tension test sample by a preselected amount, to the depth of the resulting crack. After the test the crack depth is measured. This test gives the fracture toughness of the material prior to crack growth

(*contd*.)

Test	Methodology
Crack-growth fatigue	The fatigue behavior of the same test piece used in fracture toughness using stress–strain cycles. Dynamic fatigue occurs under cyclic loading where crack growth appears during each load cycle. The crack-growth rate as a function of energy input is determined. The test is done as per the European Structural Integrity Society (ESIS) protocol.[36] The test is also done at different temperatures to ascertain temperature dependence
Stress relaxation	This test involves measurement of the rate of decrease in stress during a constant state of strain. A linearity between applied stress with log time is expected for viscoelastic materials, provided no chemical aging occurs during the test. When the rate of stress relaxation is high, the resulting loss of sealing force would lead to leakage or loosening of end-fittings in pipes
High-pressure gas permeation	Gas at a predetermined pressure is applied to a sealed test specimen in a cell and the gas permeation coefficient, diffusion coefficient, solubility coefficient, and the concentration are determined. The test is done at various pressures and temperatures, and a predictive model established.
Rapid gas decompression	Polymeric linings subject to prolonged exposure to gases at >500 psi are prone to internal fracturing or blistering due to rapid decompression of the gases. The test consists of exposing pipe or liner samples to the gas long enough to be saturated with the gas. Knowing the diffusion coefficient D and the concentration c, the soaking duration and the amount of gas absorbed are determined. The pressure is gradually released, say 1000 psi/min and the test repeated a few times, and the samples are inspected for damage due to rapid gas decompression[37–40]
Liquid compatibility	Testing of compatibility of the polymer liner or barrier with the liquids encountered in the service application at the intended temperatures and pressures. Measurements such as equilibrium uptake, and volume swelling of the polymer/liquid system yield data on permeation and diffusion. Tensile properties may also be obtained with samples in contact with fluids[41]
Chemical deterioration/ Aging	Chemicals such as corrosion inhibitors involving organic amines, aldehydes, thiols, mercaptans acetylinic alcohols, corrosive agents such as hydrogen sulfide in oil gas media may be deleterious and attack the polymeric material. Equilibrium uptake, volume swell for the polymer/chemical system and sometimes tensile properties may be determined after long exposure such as a year. Some changes due to aging are discoloration, changes in volume, surface fractures or total disintegration
Environmental stress cracking	Stress in combination with an aggressive environment can cause deleterious effects on the materials and cause failures. The causes could be high local swelling in solvents or chemical attack (as in cracking of white-walled tyres in very hot/sunny climates). Samples are tested in rigs at suitable strain, and immersed in the medium of interest. An appropriate test protocol has been developed[42]

2.1.5 Corrosion Testing of Refractories and Ceramic Materials

Lack of standards in testing for refractories becomes apparent when one realizes that factors such as sample size and geometry, state of stress in the lining, thermal gradient, thermal cycling and duration are difficult to scale down to a laboratory scale to simulate service conditions. Accelerated tests involving severe conditions do not always conform to realistic conditions and may lead to unrealistic results.

Crescent and Rigaud[43] classified over 100 different experimental arrangements in 12 categories as follows:

Approach		
Thermodynamic	Kinetic	Pragmatic
Pill test	Drip test	Basin test
Crucible test	Crucible test	Horizontal rotary test
Cone test	Finger test	Vertical rotary test
Immersion test	Immersion test	Spray test

The crucible test, the rotary disk test and the finger test are the commonly used nonstandard tests. Some standard ASTM tests are as follows:

ASTM Test	Application
C-768 (drip slag testing) C-874 (rotary-kiln slag testing)	Applicable to slags
C-621	Measures corrosion of refractories in molten glass under isothermal conditions
C-288	Disintegration of refractories in carbon monoxide
C-454	Disintegration of carbon refractories by alkali
C-863	Disintegration by alkali vapour of glass furnace refractories. This test determines the oxidation resistance at high temperatures

Corrosion resistance testing of ceramics is detailed in the literature.[44,45]

2.1.6 Testing of Corrosion Inhibitors

It is important to consider specific physical and chemical properties of corrosion inhibitors before testing for their performance in corrosion inhibition. Some properties of the inhibitors of relevance along with the test methods are detailed below:

Property of neat Inhibitor	Viscosity	ASTM D 2162, D88
	Pour point	ASTM D97
	Density	ASTM D1217, D1298

(*contd*.)

(*contd*.)

Effect of mixing with environment	Solubility	Bottle tests
	Water tolerance	ASTM D2550
	Formation of emulsion	ASTM D1935, bottle tests
	Foam formation	ASTM D1881
Reactivity with other components	Compatibility with bactericides scale inhibitors, dispersants	Bottle tests Effectiveness tests
Biocompatibility	Potability	Biodegradation test OECD 301D
Time of drying	Drying	Test on hot-plate
Effects of temperature	Solubility changes	Bottle tests
Toxicity (environmental friendliness)	Determination of LC_{50} and EC_{50}	

Some of the common tests methods used for testing inhibitors are given below:

Test Method	Features	References
Wheel test	Bottle containing the inhibitor and the corrosive environment, and a metal coupon is mounted on a wheel and agitated for a set period of time. An autoclave is used in place of a bottle for high pressures and temperatures. The test is useful for screening inhibitors	[1, 2]
Bubble test (stirred corrosion test/ kettle test)	Flexible laboratory test done in 1 L beaker/conical flask fitted with working electrode, counter-electrode, reference electrode, gas purge and corrosion data obtained electrochemically	[3]
Electrochemical methods		
Static test	Apparatus used is similar to that of bubble test without anyflow and corrosion rates obtained by either weight loss or electrochemical means.	
Rotating disk electrode system	The sample material forms the rotating disk working electrode.Applicable in systems with laminar flow. System can be used at high temperatures and pressures. Limiting current density is determined. Corrosion rates obtained from corrosion current density	[4]
Rotating cylinder electrode	Stable reproducible flow can be maintained. Can be operated in turbulence regime of high Reynolds numbers. Can simulate pipeline flow of fluids	[5]

(*contd*.)

(*contd*.)

Electrochemical methods		
Rotating cage	Used for evaluating inhibitors in oil and gas operations. There are four zones of flow pattern such as homogeneous zone, side-wall-affected zone, turbulent zone and top-cover-affected zone	[6,7]
Jet impingement test protocol	Can simulate high turbulence conditions at high temperatures, pressures for gas, and liquid, multiphase systems. Involves small volumes of test fluids	[8, 9]
Humidity chambers	Used in testing vapour phase inhibitors using wet–dry cycles. Tropical, marine and industrial atmospheres are simulated. Percentage of surface area rusted in the case of ferrous metals is measured. Changes in surface properties such as color in the case of nonferrous metals are assessed	[10, 11]

[1] *Wheel Test Method for Evaluation of Film Persistent Inhibitors for Oil Field Applications*, T-ID-8, NACE Publication ID 182, Houston, TX, 1982.
[2] R.H. Hausler, E.W. Stegman, R.F. Stevens, *The Methodology of Corrosion Inhibitor Development for CO_2 System*, CORROSION/88 NACE, Houston, TX, Paper NO. 88.
[3] N.D. Greene, G5-82, 1983, *Annual Book of ASTM Standards* Vol. 3, No. 2, Americian Society for Testing Materials, Philadelphia, PA, 1983, p. 122.
[4] G. Liu, D.A. Tree, M.S. High, *Corrosion*, **50**, 584 (1994).
[5] D.R. Gabe, *J. Appl., Electrochem*, **4**, 91 (1974).
[6] R.H. Hausler, E.W. Stegmann, C.J. Cruz, D. Tjandroso, *CORROSION/90*, NACE, Houston, Texas, Paper No. 6.
[7] G. Schmidt, W. Bruckoff, K. Faesler, G. Blummel, *CORROSION/90*, NACE, Houston, Texas, Paper No. 23.
[8] J.L. Dawson, C.C. Shih, *CORROSION/87*, NACE, Houston, Texas, Paper No. 453.
[9] F. Giralt, D. Trass, *J. Fluid Mech.*, **53**, 505 (1975); **54**, 148 (1976).
[10] A. Wachter, T. Skei, N. Stillman, *Corrosion*, **7**, 284 (1951).
[11] A.D. Mercer, *Br. Corrosion Journal*, **20**, 61 (1985).

The methods of measuring corrosion rates in the course of testing corrosion inhibitors are conventional weight loss, electrochemical techniques such as linear polarization resistance, potentiodynamic polarization, AC impedance, and electrochemical potential or current noise.

Conventional weight loss measurements in testing inhibitors are time-consuming since measurable weight loss is required to obtain meaningful data on corrosion rates. In general the performance of corrosion inhibitors is expressed in terms of percentage inhibition.

$$\text{Percentage inhibition} = \frac{W_0 - W_I}{W_0} \times 100$$

where W_0 and W_I are the loss in weight in the absence and in the presence of inhibitor.

The electrochemical methods of measurement of corrosion rates have been described in Chapter 1. Some features of these methods are noted below:

Linear polarization resistance	Noninvasive, rapid, suitable for screening of inhibitors
Potentiodynamic polarization	Invasive, slow
AC impedance	Noninvasive, can be rapid when three-point geometric technique is used; useful for on-line monitoring of the performance of inhibitors; useful both in laboratory and field monitoring
Electrochemical noise	Noninvasive, can be used for continuous on-line monitoring of the performance of inhibitors; can be used both in the laboratory and field monitoring

Both AC impedance and electrochemical noise have been found useful in giving useful information on general corrosion and pitting corrosion. It should be borne in mind that the degree of pitting indicated by the electrochemical noise and the depression angle obtained from the Nyquist plots of AC impedance data should be validated by measuring pit depths of the 30 deepest pits and the deepest pit among them by a profilometer. This has been well documented in the literature.[46] It is preferable that corrosion testing of inhibitors by electrochemical methods is confirmed by a conventional weight loss method.

The relative merits of corrosion testing methods are given as follows:

Service tests	Most reliable, preferred
	Most expensive, accounts for unforeseen factors
Field tests	Reliable
	Relatively expensive
	Second best
Laboratory prototype simulated test	Less reliable than field tests (does not account for unforeseen incidents)
	Moderate in cost
Rapid electrochemical methods	Needs electrochemical equipment and knowledgeable operator to take account of the limitations of the technique
	Rapid and suitable for preliminary screening of candidate materials or inhibitors

The preferred order of corrosion testing and its reliability is: service tests > field tests > laboratory tests. It is not always possible to carry out service tests and hence it is recommended that coordinated corrosion testing involving a combination of: (i) laboratory test and field test; or (ii) rapid electrochemical tests and weight loss, or any other combination that is suitable be carried out.

2.2 Corrosion Detection and Monitoring

After reliable corrosion testing, one chooses the appropriate or acceptable material or inhibitor for use in the industrial process of interest. The next step involves inspection at

periodic intervals, either to detect corrosion or to monitor corrosion rate in order to maintain acceptable levels of corrosion. Thus, inspection may be divided into periodic inspection at chosen intervals and sudden unexpected inspection when a sudden failure takes place. Periodic inspection is important since it helps to avoid accidents or to reduce the probability of their occurrence, and to decrease costs due to downtime and decreased insurance requirements.

Inspection is usually done by nondestructive techniques. This is usually known as nondestructive examination (NDE). The general term nondestructive evaluation describes the various terms used such as nondestructive inspection (NDI), nondestructive testing (NDT) and nondestructive examination (NDEx). Some of the aspects or purpose of these techniques involve detection and evaluation of flaws, leaks, dimensions, location (position), microstructures, mechanical properties and stress.

Some of the factors involved in choosing a particular nondestructive evaluation technique are the primary reason or objective, the type of flaw to be detected, the size and orientation of the flaw, the location of the flaw in the sample, the size and shape of the sample and the nature of the sample. It is also necessary to know the type of flaws that are acceptable or unacceptable in the sense that flaws may be deleterious or nondeleterious. The size, type, orientation and location of the flaws determine whether they are acceptable or unacceptable as per the code, or standard given by American Society of Mechanical Engineers Pressure Vessel Code, American Welding Society Structural Welding Code or any other applicable code or standard.

The technique used in the characterization of the flaws in the sample depends upon whether the flaw is on the surface or in the interior of the sample. Some of the common methods used in the nondestructive evaluation of the flaws are noted below:

Surface flaws		Interior flaws	
Evaluation method		Evaluation method	
Visual	Independent of sample size	Magnetic field	Sample thickness $\ll 1$ mm
Replica		Eddy current	
Liquid penetrant		Ultrasonics	Thick, dimension ≤ 10 m
Eddy current	Sample thickness $\ll 1$ mm	Accoustic emission	
Magnetic particle		Radiography	
Ultrasonics	Thick, dimension ≤ 10 m	Neutron radiography	Sample thickness ≤ 250 mm
Accoustic emission		Microwave	
		Energy dispersive X-rays	

Naturally, the nondestructive methods used in detection of defects are governed by the material properties of the samples as given below:

Liquid penetrant method	The flaw must intercept the surface
Magnetic particle method	Sample should be magnetic
Eddy current method	Sample is electrical conductor
Microwave method	Transmission of microwaves
Radiography, including neutron radiography	Changes in thickness, density and/or elemental composition

The choice of the nondestructive technique used in the examination of the sample on hand also depends upon the complexity of the shape of the sample. The following order of the methods is in progressively increasing complexity of the shape of the sample to be examined: acoustic microscopy, microwave method, eddy current, magnetic particle, X-ray radiography, ultrasonics, liquid penetrant and visual methods.

The indirect analytical nondestructive evaluation methods of interest are thermal analysis, finite element stress analysis, strain gauging, photoelasticity and brittle coatings.

2.2.1 Visual Examination

This method is the simplest of all the methods and is capable of detecting surface flaws such as corrosion, contamination, surface finish and surface discontinuities on joints.[47] The discontinuities on joints such as welds, seals, solder connections and adhesive bonds can be detected. General corrosion, qualitative pitting corrosion, stress–corrosion cracking, weld-heat-affected zone attack, erosion corrosion and other type of degradation can be observed by visual examination aided by microscopes with sufficient magnification. Degradation of plastics can also be detected by visual examination. Visual examination is also used in conjunction with other techniques, such as powerful microscopes.

In the cases where access to the sample or part of the equipment is difficult one has to resort to the use of borescopes. Borescopes of different designs are commercially available. The types of borescopes are rigid borescopes consisting of miniborescopes, hybrid, extendable and rigid chamberscopes, and flexible borescopes. Both rigid and flexible borescopes of a variety of standard and customized designs are available and the selection of a borescope for a particular application depends upon factors such as focusing, illumination, magnification, working length, direction of view and the environment. Some of the applications of borescopes are inspection of straight piping for leaks, inspection of inside walls, ducts or large tanks, equipment maintenance, checking in-service defects in turbines, automotive components and process piping, hydraulic cylinders for pitting, scoring, inspection of fit of seals, bonds, gaskets and difficult-to-reach regions in aircraft. Observation of in-service defects through a borescope designed for automotive inspection is illustrated in Figure 2.6.

It is suggested that the technical personnel in charge of detecting and monitoring corrosion in the plant periodically keep micrographs of known samples illustrative of various forms of corrosion, which can be used as references or guides in identifying the modes of attack that occur during detection and monitoring corrosion in plant operation.

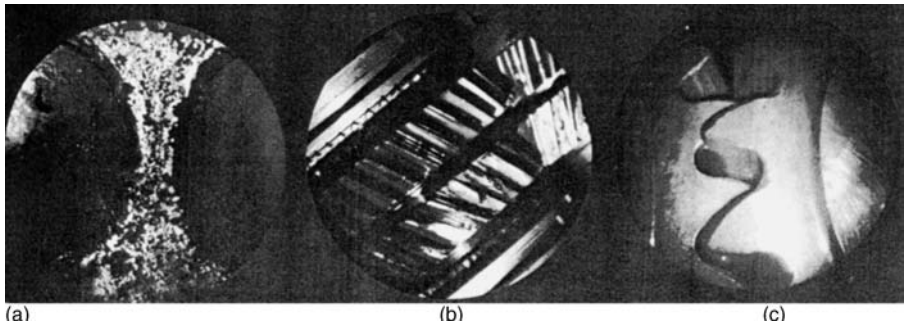

Figure 2.6 *In-service defects as seen through a borescope designed for automotive servicing. (a) Carbon on valves; (b) broken transmission gear tooth; (c) differential gear ware. Courtesy of Lenox Instrument Company. (Reprinted with permission from ASM International. All rights reserved www.asminternational.org)*

2.2.2 Laser Methods[48]

Laser inspection of the sample surface can also yield information on surface flaws such as the surface roughness and defects. The laser beam incident on the surface of the sample is scattered, and the scattered light intensity decreases when a crack is present on the surface. The experimental arrangement for scanning the surface of a sample is shown in Figure 2.7. A laser-based profilometer may also be used in the measurement of pit depths.

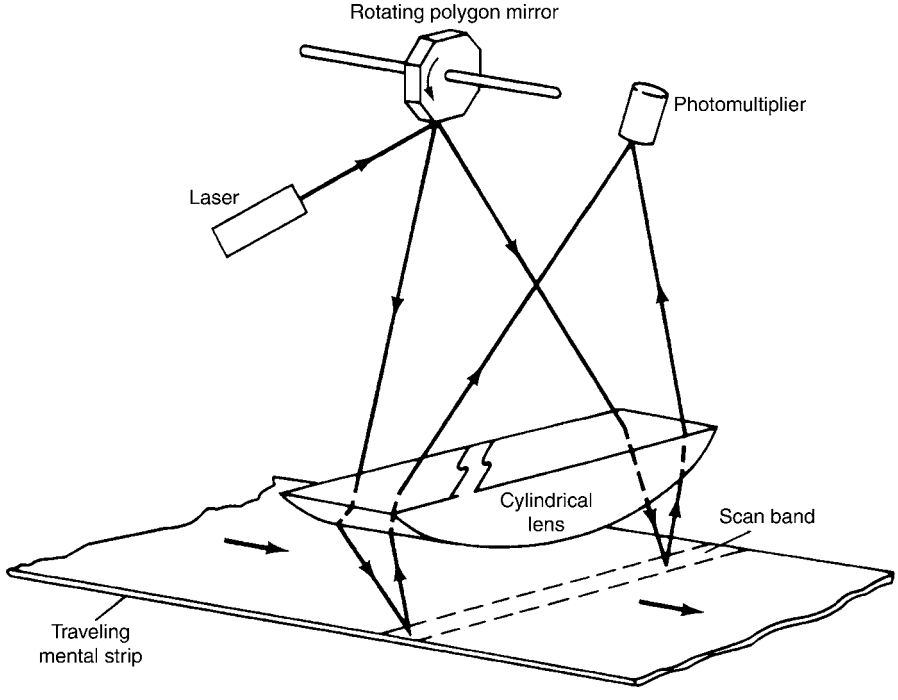

Figure 2.7 *Experimental arrangement for scanning the surface of a sample. (Reprinted with permission from ASM International. All rights reserved www.asminternational.org)*

Holographic imaging can also lead to detection of defects and has been used in detection of defects in automobile clutch plates, brake drums, gas pipelines, high-pressure tanks and turbine blades.

2.2.3 Replication Microscopy

This method can be used for *in situ* measurement of the microstructural deterioration and damage of materials exposed to environments in power plants and petrochemical industries for the purpose of determining remaining service life of components. A surface replica, using acetate, acrylic or rubber taken from a sample is examined by a microscopic technique such as electron microscopy. An extraction replica technique is used and the resulting replica of the sample surface is examined by an optical or scanning electron or transmission electron microscope, depending upon the targeted resolution. This technique is useful in microstructural analysis involving determination of cracks, creep damage and precipitate analysis which play an important role in determining the service life of a component.

Surface cracks in boiler tubes, creep damage in power plant components and precipitate analysis in components subjected to high temperature and stress have been successfully assessed by this technique and necessary further inspection scheduled, depending upon the severity of the observed defect. The following is an example of the type and severity of defects and the necessary action taken in the context of power plant operations.

Nature of defect observed*	Action
No creep defects	None
A few cavities	Schedule inspection after 20 000 h
Coalescent cavities	Inspection after 15 000 h
Microscopic creep cracks	Inspection after 10 000 h
Macroscopic cracks	Immediate remedial action

*B. Neubauer, U. Wedel, *Power Engineering*, May 1984, p. 44.

2.2.4 Radiographic Methods

The source of radiation used in the method can be either X-rays or γ-rays emitted by a radioactive element. The schematic arrangement involving the radiation source, test object and the acquisition of the resulting image of the defect is shown in Figure 2.8. The difference in intensities of radiation absorbed by the test sample due to the internal flaw and the surroundings devoid of flaws produces an image of the flaw on the sensor used, such as film. It is important to recognize the radiation hazards in using the technique and all precautions should be taken in handling the instrument.

The choice of the source and type of incident radiation used depends upon the thickness of the sample to be tested. The energy of the incident beam needs to be matched with the thickness of the sample. For example, low-voltage X-ray units and low-intensity isotope ^{169}Yb units are suitable probes for low-density samples such as aluminum. By the same token high-density materials of high thickness are examined by using high-voltage X-ray units or high-energy isotopes such as ^{60}Co and ^{192}Ir. The

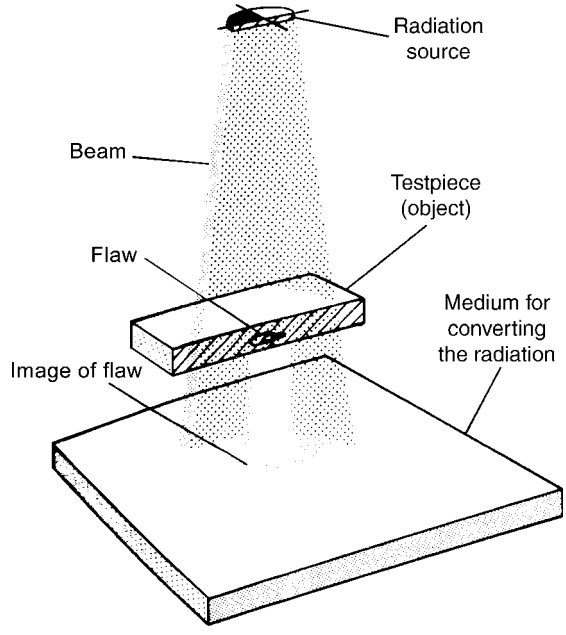

Figure 2.8 *Schematic of the basic elements of a radiographic system, showing the method of sensing the image of an internal flaw in a plate of uniform thickness. (Reprinted with permission from ASM International. All rights reserved www.asminternational.org)*

resolution of the image obtained is dependent on the distance between the defect and the film (i.e., the thickness of the sample). It is also necessary that all sides of the sample have to be exposed to the incident beam. One of the industrial applications is real-time radiography for on-line inspection of objects in assembly lines (jet engine turbine blades).

The experimental radiographic procedure for materials involving simple shapes such as flat plates, curved plates and solid cylinders are documented in the literature. Some points with respect to the direction of the incident beam in detecting flaws in the test materials are also documented. In the case of materials of complex shapes it is necessary to obtain multiple radiographs at different angles in order to determine the flaws in the samples, and their orientation. Radiography has been successfully used in determining different types of flaws in castings and weldments.

Flaws detected in castings are: microshrinkage, shrinkage porosity also known as spongy shrinkage, gas porosity, dispersed discontinuities, tears, cold cracks, cold shuts, misruns, inclusions, unfused chaplets, core shift, centerline shrinkage, shrinkage cavities, segregation and surface irregularities. In the case of welds the flaws that are determined include undercutting, incomplete fusion, cracks, porosity, slag inclusions and incomplete root penetration.

It is advisable to have many reference radiographs indicating some common flaws for use by the technical personnel. Some ASTM reference radiographs are listed in Table 2.3.

Table 2.3 *Reference radiographs in ASTM standards*

ASTM Standard	Subject of radiographs in standard
E155	Aluminum and magnesium castings
E186	Heavy-wall (50–115 mm, 2–4½ in) steel castings
E192	Investment steel castings for aerospace applications
E242	Appearance of radiographic images as certain parameters are changed
E272	High-strength copper-base and nickel-copper alloy castings
E280	Heavy-wall (115–300 mm, 4½–12 in) steel castings
E310	Tin bronze castings
E390	Steel fusion welds
E431	Semiconductors and related devices
E446	Steel castings up to 50 mm (2 in.) in thickness
E505	Aluminum and magnesium die castings
E689	Ductile cast irons
E802	Gray iron castings up to 115 mm (½–12 in) thickness

Some distinct features of flaws in castings and weldments are given below.

Flaws	Features
Castings	
Microshrinkage	Dark feathery streaks or dark irregular patches corresponding to grain boundary shrinkage often encountered in Mg alloy castings
Shrinkage porosity	Appears as a localized honeycomb or mottled pattern due to improper pouring temperature or alloy composition (e.g., Al alloys)
Gas porosity	Round or elongated smooth, dark spots located individually or in clusters distributed randomly in the casting due to release of gas during solidification or evaporation of moisture from volatiles from the mold surface
Dispersed discontinuities	Occur in Al and Mg alloy castings. Appear as tiny voids scattered in parts or throughout the castings. Gas porosity and shrinkage porosity in Al alloys are examples of this flaw
Tears	Appear as dark ragged lines of variable width without any line of continuity in groups located either on surface or interior. This is due to the contraction of the casting during or after solidification
Cold cracks	Appear as single, straight, sharp dark lines, continuous along the lengths. These cold cracks are due to internal stresses caused by temperature gradients encountered during flame cutting, grinding or quenching
Cold shuts	Appear as distinct dark lines of variable length and smooth outline. This is due to interrupted pouring or slow rate of pouring or the low temperature of pouring
Misruns	Appear as prominent dark areas of various dimensions with a definite smooth outline due to the failure of melt to completely fill the mold

(*contd*.)

(*contd*.)

Flaws	Features
Castings	
Inclusions of foreign material	Appear as light or dark areas. Sand inclusions appear as gray or light spots of uneven granular texture without distinct outlines. Some inclusions appear isolated irregular or elongated
Unfused chaplets	Appear with outline in the form of chaplet due to the lack of bond between chaplet and cast metal
Core Shift	Can be detected when the view makes it difficult to measure the deviation from a specific wall thickness. This may due to jarring of mold or insecure anchorage of cores
Contreline shrinkage	Localized along the central plane of the wall. It is a network of filamentary veinlets in the direction of the nearest riser
Shrinkage cavities	Appear as dark areas of irregular dimensions without distinct outline due to insufficient feeding of a section
Segregation	Appear as light areas of mottled type due to separation of alloy constituents into different regions of different chemical compositions as in Al alloys
Surface irregularities	Appears different from normal surface image. This is not to be mistaken for internal flaws.
Weldments	
Undercutting	Appears as a dark line of variable width along the edge of the fusion zone. A fine dark line in the dark area is indicative of a crack
Incomplete fusion	Appears as an elongated dark line. Sometimes resembles a crack or an inclusion
Cracks	Appear as fine dark lines of considerable length without much width. Cracks may be transverse or longitudinal and are located either in the fusion or heat-affected zone of the base metal
Porosity	Also known as gas holes; appear as dark spots (spherical voids). The voids may be randomly distributed in clusters or aligned along the centre line of the fusion zone. Sometimes porosity appears as tubes along the direction of solidification front
Slag inclusions	Irregular in shape with some width and located at the edge of the weld. Elongated slag deposits are generally found along the weld-joint interface while spherical inclusions can be found anywhere in weld
Incomplete root penetration	Appears as a dark straight line through the center of the weld. The width depends upon the root gap and the extent of weld penetration

Some attractive features of radiography are access to interior difficult-to-reach portion, such as valves and pipes, the objects or sample covered with insulation can be tested, reference radiographs can be accessed, the nature and severity of the attack can be assessed with ease, in principle, pit depths can be obtained although laser profilometry is the preferred method in this regard. The main drawback of the method is the whole sample needs to be exposed. Some applications of the method are determination of flaws in weldments and castings to identify sites of initiation of crevice corrosion, valve

inspection, detection of plugged lines, and detection of liquid levels in columns, core pipe location, evaluating pitting and general corrosion damage, the remaining pipe thickness in use and its serviceability.

Portability of the source is the main advantage of the γ-ray source.

Neutron Radiography.[47] A neutron beam is directed on the test sample and the resulting attenuated beam falls on a conversion screen and a radiographic image is obtained. The neutrons of different energies are classified as:

Type	Energy range (eV)	Features
Cold neutrons	<0.01	Low scattering; good detection, high absorption cross-section results in decreased transparency of samples
Thermal neutrons	0.01–0.5	Good detection and readily available sources
Epithermal neutrons	0.5–10^4	Very good discrimination of materials
Fast neutrons	10^4 to 2×10^7	Poor material discrimination; point sources are available and can be used for inspection with low-energy sources ($\sim 10^4$ eV)

The usual technique used involves thermal neutrons and the experimental arrangement is schematically shown below:

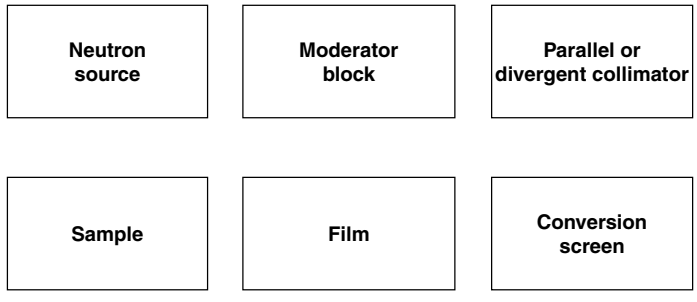

The thermal neutron sources are radioactive isotopes which emit neutrons, acclerators, and nuclear reactors. The neutrons from the sources are moderated with materials such as paraffin, graphite, water, heavy water or beryllium. Some of the radioisotopes used as sources of thermal neutrons are: antimony, polonium, americium curium and californium. The various sources have different half-lives, ranging from days to years.

Isotope	Reaction	$t_{1/2}$
^{124}Sb	(γ, n)	60 days
$^{210}P_0$	(α, n)	138 days
^{241}Am	(α, n)	458 years
^{244}Cm	(α, n)	18 years

The neutron beam impinges on the sample and the attenuated neutron beam falls on a film, together with a conversion screen. The secondary radiation exposes the film, resulting in a radiographic image of the test sample.

The method has found applications in inspection of components used in ordinance, explosives, aerospace and nuclear industries. Some example applications of the method are the indium resonance method to determine the internal characteristics of radioactive nuclear fuel elements, to check proper assembly of explosive device, corrosion defects in aircraft components, corrosion in adhesive-bonded aluminum honeycomb structures, defects in weldments such as in niobium and titanium, determining remaining core material in the interior cooling passages of air-cooled turbine blades, determining proper positioning of explosive charges, O-ring seals in explosive bolt assembles, and determination of potting levels in encapsulated electronic filters.

2.2.5 Liquid Penetrant Testing Method

This method consists of application of liquid to the surface of a sample, allowing the liquid to penetrate into the discontinuities in the sample. After some time the excess liquid on the surface is removed, leaving the liquid in the discontinuity intact. Then a developing agent is applied, which draws the liquid penetrant from the discontinuity to the surface of the sample, leaving a visible indication of the discontinuity on the sample. The liquid penetrant usually consists of a colored dye to enable ease of detection in either visible or ultraviolet light.

The method can locate discontinuities open to the surface in porous materials. It is possible to detect porosity, surface cracks and 'through' leaks, which may result from fatigue cracks, shrinkage porosity, cold shuts, grinding and heat-treat cracks, seams, forging laps and bursts as well as improper bonding between joined metals.

The method has been successfully used in detection of flaws in Al, Mg, Cu, brass, cast iron, stainless steels and titanium. This method can also be used in testing ceramics, plastics, rubber products, powdered metal products, as long as it is borne in mind that the method is limited to the detection of open discontinuities on the surface and limited to materials devoid of porous surfaces.

The true indications of the discontinuities may appear as continuous lines due to cracks, cold shuts, forging laps, scratches or die marks.

Discontinuity	Appearance
Cracks	Jagged lines
Cold shuts	Smooth, narrow straight lines
Forging laps	Smooth wavy lines
Scratches and die marks	Variable linear patterns
Flaws due to grinding Peening, machining	Intermittent lines
Porosity due to gas-holes and pinholes, deep cracks	Round indication
Pinholes, porous nature of sample, coarse grains in casting production	Small dots
Contamination of sample	Diffuse or weak indications

2.2.6 Magnetic Particle Testing

This method involves magnetization of the sample coated with a liquid dispersion of magnetic particles, and then observing the magnetic medium patterns. Discontinuities in the samples result in indications in the magnetic medium patterns different from normal patterns. The type and origin of the discontinuity along with the pattern of indication are noted below.

Type and source of discontinuity	Features
Inherent discontinuities	
Inclusions such as non-metallic like slags, sulfides and oxides	Appear as straight indications parallel to the longitudinal axis of the sample (fine lines tightly adherent) Also short and in groups
Blowholes	Appear as seems or laminations
Pipe in the centre of ingot	Located far below the surface
Segregation	Appear as thin parallel lines or bands
Processing discontinuities	
Cracks Bursts	Appear as in weldments inlines
Forging laps	Ruptures in forgings
Twist cracks	Can occur in any part of the forging
Surface tears	Located in crankshaft forgings and appear on the surface of twisted area surface rupture
Seams	Long, straight surface flaws parallel to the longitudinal axis of the bar
Laps	Occur due to improper rolling and appear similar to seams
Laminations	Thin, flat discontunities found in steel plate due to gas inclusions or pipe in the original ingot
Cracks due to grinding operations	Shallow, but sharp at roots and a source of fatigue related failure
Pickling and etching	Formation of minute cracks or small preexisting crack can be enlarged.
Heat treatment	Cracks formed are deep without any pattern. Quenching related cracks are located either at thin cross-section or at the junction of thin and thick cross-sections
Discontinuities in weldments	Surface shrinkage cracks at a crater. Cracks in parent metal adjacent to weld. Other discontinuities due to lack of fusion, penetration, overlapping and slag and gas inclusions
In-service discontinuities	
Fatigue cracks	Develop in or adjacent to location of stress concentrations. Fine cracks spread under stress and result in fatigue failure. Fatigue-related failure may be slow or immediate, depending upon stress conditions. Fatigue cracks generally run transverse to the grain flow

Is is needless to emphasize that once the selection of material is finished, the most important task is to monitor the material degradation in service so that sudden failure can be prevented.

2.2.7 Eddy Current Inspection Method[47]

This method is based on the principles of electromagnetic induction. A coil carrying an alternating current in the vicinity of the test sample produces an induced or eddy current in the sample, and the changes in the magnetic field due to the induced currents are monitored. The induced currents in the test sample are affected by electrical conductivity, permeability, the dimensions and the homogeneity of the sample.

A typical experimental arrangement for eddy current inspection of a bar or tube sample is schematically shown in Figure 2.9. The generator supplies the current to the bar or tube sample under examination and a synchronizing signal to a phase-shifter unit, which provides switching signals to the detector. The amplified output signal is recorded on a chart recorder and displayed on an oscilloscope.

The method requires the use of a reference standard sample in order to set the sensitivity level before an unknown sample is tested for discontinuities. The type of reference discontinuities used in a particular application has been specified by the American Society for Testing Materials and the American Petroleum Institute. Some reference standards are depicted in Figure 2.10. Some of the discontinuities detected are: seams, laps, cracks, slivers, scabs, pits, slugs, open welds, miswelds, improperly or misaligned welds, black or gray oxide weld penetrators, pinholes, hook cracks and surface cracks.

Some examples of the application of eddy current method are discussed in the literature,[49,50] and are given below in order to illustrate the relevance of the method in the industrial context.

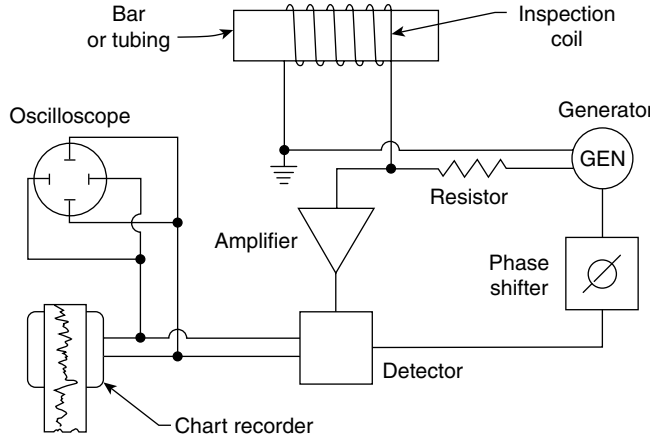

Figure 2.9 *Principal elements of a typical system for eddy current inspection of bar or tubing. See description in text. (Reprinted with permission from ASM International. All rights reserved www.asminternational.org)*

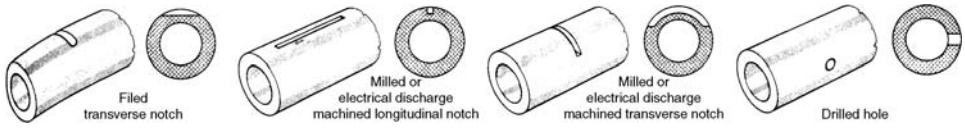

Figure 2.10 *Several fabricated discontinuities used as reference standards in eddy current inspection. (Reprinted with permission from ASM International. All rights reserved www.asminternational.org)*

i. Quality control of nonferromagnetic heat exchanger tubesheet rolled joints
ii. Inspection of ferromagnetic heat exchanger tubes
iii. Inspection of solid cylinders
iv. Inspection of round steelbars
v. Inspection of welds in welded tubing and pipes
vi. Inspection of plates, skin sections of panels and sheets (detection of shallow surface defects in zircaloy-2 plates, examination of the skin section of the first-stage booster of the Saturn rocket, detection of cracks in subsurface layers of Al–Al structures joined by Al rivets)
vii. Inspection of aircraft structural and engine components (fastener holes, jet engine blades for cracks due to low-cycle fatigue surface cracks in fasteners, cracks in nonmagnetic bushings used in clevis/lug attachments, detection of fatigue cracks in aircraft splice joints, corrosion in windowbelt panels, galvanic exfoliation corrosion of aluminum wing skins.

An instrument of the type known as Probolog is used for the inspection of tubes, detection of general corrosion, pitting corrosion, stress corrosion, fatigue based cracking and changes in microstructures of nonmagnetic materials such as tubing. The method has also been used in measuring the thickness of nonconducting surface layers such as plastics, paints or corrosion scale and the unit used is known as Turner-gauge (commercial name). The method has extensive application in oil platforms in sea especially in monitoring cracks and their growth in weld structures.)

2.2.8 Ultrasonic Inspection Method[51]

This method consists of high-frequency sound waves (0.1–25 MHz) incident upon the test sample and measuring the energy of the reflected beam. Because of the flaws in the sample there will be loss in energy of the beam, known as attenuation. Cracks, laminations, shrinkage cavities, bursts, flakes, disbonds and other discontinuities can be detected by this method.

The method consists of detecting flaws by measuring the energy of the reflected beam from the sample surface, or the time taken by the beam to traverse the sample, or attenuation of the sound waves by absorption and scattering within the sample, or the pattern in the response of either a transmitted or reflected signal.

The basic instrument consists of an electronic signal generator which produces bursts of alternating voltage, a transducer that emits ultrasonic waves on application of voltage, a couplant as an aid to transfer the ultrasonic beam energy to the test sample, a couplant to transfer the output beam energy from the sample to a transducer, an amplifer to modify

the output signal, a unit to display the output signal and an electronic timer to control the operations.

The basic ultrasonic techniques used are pulse–echo, transmission and resonance. In the pulse–echo technique the display consists of the initial pulse, the signal due to the defect and a signal due to the back echo. In the transmission technique the display consists of initial pulse and the transmitted signal. The display consists of one signal in the reasonance technique. The pulse–echo technique can be further used in the A-scan, B-scan or C-scan modes of presentation of the signal resulting in the test. In the A-scan display the three peaks corresponding to front surface reflection, reflection at the discontinuity and the back surface reflection along with the respective intensities (y-axis) and the distance along the x-axis giving the depth of penetration in the sample are obtained. The dimensions of the sample and the intensity of the reflected beam may be used to obtain relevant details about the size and the depth of the discontinuity in the sample.

In the B-scan mode the cross-section view and the distribution of discontinuities within are displayed. In the C-scan the length and width of the discontinuity is displayed. The outline or boundary of the discontinuity is also displayed. The three modes of presentation are depicted in Figures 2.11–2.13.

Some applications of ultrasonics are inspection for flaws in forgings, flat-rolled products such as strips, sheets and plates, castings, extrusion billets, rolling blooms or slabs, bar stock, pipes, welded joints, bonded joints, monitoring cracks, measurement of thickness, measurement of fluid levels, microstructural features and monitoring corrosion.

Corrosion may be monitored by measuring changes in thickness with time using ultrasonic thickness gages. An automated ultrasonic inspection system has been devised and used in monitoring corrosion in nuclear waste containers and typical variations in ultrasonic indications in corroded and uncorroded areas have been recorded successfully. Major types of equipment inspection by ultrasonic technique has been done in mill components, power equipment, jet engine parts, aircraft components, railway materials, automotive components and other machinery components.

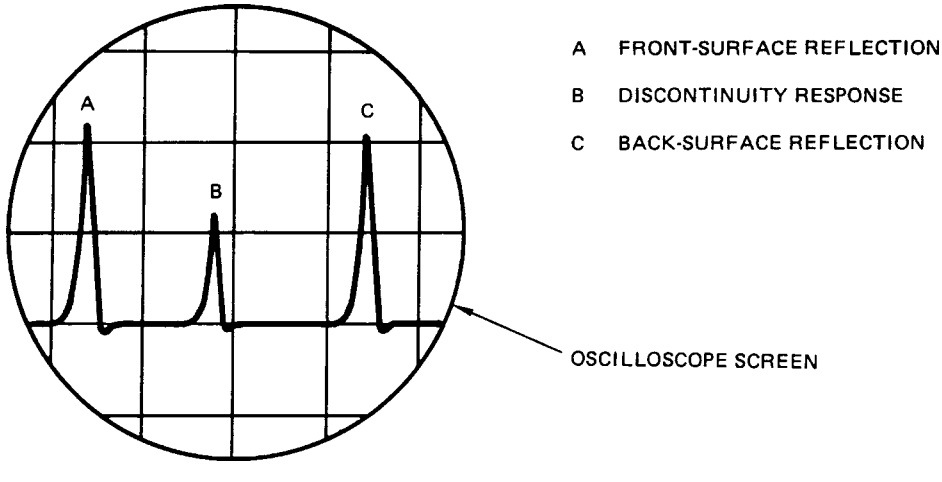

Figure 2.11 *A-scan presentation*

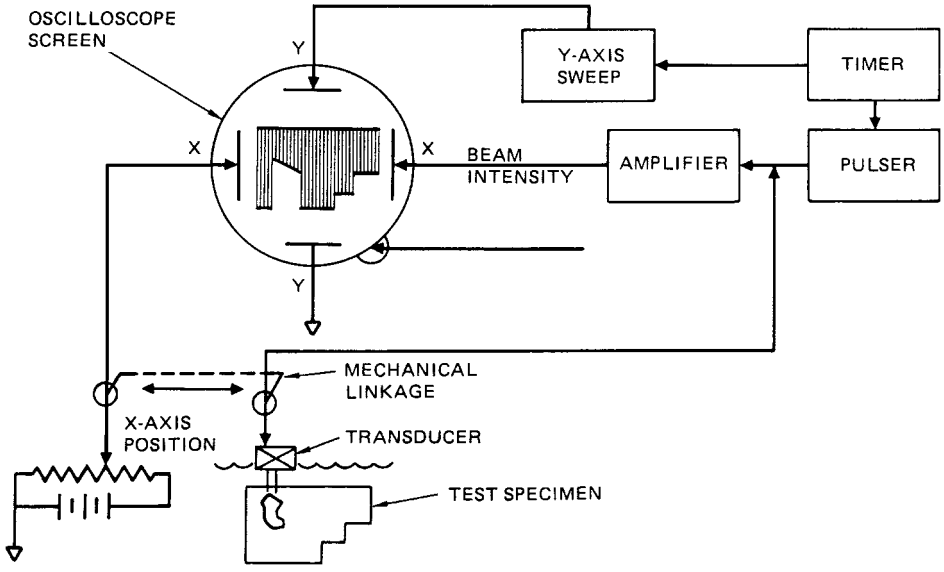

Figure 2.12 *B-scan presentation*

Some notable advantages are: (i) applicable to objects of thickness up to 6 m due to penetration power; (ii) ability to detect small defects (high sensitivity); (iii) accuracy in determination of the morphology (size, shape and orientation); (iv) needs access to only one surface of the sample; (v) rapidity; (vi) portability. Some drawbacks or limitations are: (i) standards are needed; (ii) defects in upper shallow locations may go undetected; (iii) cannot be used on samples that are rough, irregular in shape, thin or small or nonhomogeneous, and requires a highly skilled operator; (v) requires couplants for transfer of ultrasonic energy between sample and transducers.

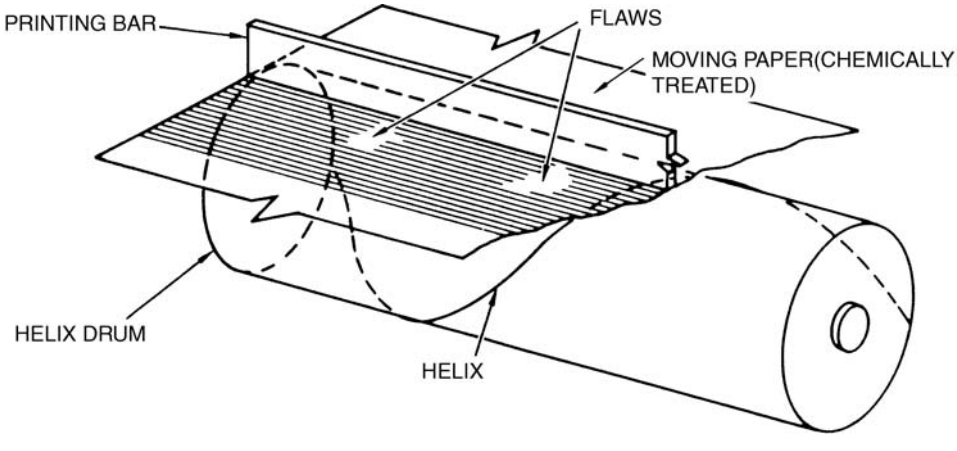

Figure 2.13 *Experimental arrangement for ultrasonic testing*

The choice of the technique used in monitoring or detection of corrosion depends upon many factors such as the size of the sample, the particular features of the defect, accessibility, sensitivity of the technique, the limitations of the techniques, knowledge and skills of the operator and the availability of the instrument. The following is a general guide for the application and suitability of the technique in the detection of discontinuity.[52]

Discontinuity	Origin	Material	Applicable method
Surface or internal bursts	Processing	Ferrous or nonferrous wrought sample	Ultrasonic method Magnetic particle method used on wrought ferrous sample
Cold shuts	Inherent	Ferrous and nonferrous cast material	Liquid penetrant method Magnetic particle method for ferrous material Radiographic method
Fillet cracks in bolts	Service	Ferrous and nonferrous wrought material	Ultrasonics, liquid penetrant method Magnetic particle method for ferrous samples
Grinding cracks	Processing	Ferrous and nonferrous samples	Liquid penetrant method Magnetic particle method for ferrous samples
Convolution cracks	Processing	Nonferrous material	Radiographic method
Heat-affected zone cracks	Processing (weldments)	Ferrous and nonferrous material	Magnetic particle method for ferrous samples Liquid penetrant method for nonferrous samples; ultrasonics in some cases
Heat-treat cracks	Processing	Ferrous and nonferrous wrought and cast material	Magnetic particle method for ferrous samples Liquid penetrant method for nonferrous samples
Surface shrink cracks	Processing (welding)	Ferrous and nonferrous material	Liquid penetrant method Magnetic particle method for ferrous samples. Eddy current method for nonferrous welded piping and tubing
Thread cracks	Service	Ferrous and nonferrous material	Fluorescent liquid penetrant method Magnetic particle method for ferrous samples
Tubing cracks (Inconel)	Inherent	Nonferrous	Eddy current method; ultrasonic method on heavy gauge tubing

(*contd*.)

(*contd*.)

Discontinuity	Origin	Material	Applicable method
Hydrogen flake	Processing	Ferrous	Ultrasonic method; magnetic particle method
Hydrogen embrittlement	Processing and service	Ferrous	Magnetic particle method Ultrasonics method may be used by adopting surface wave technique
Inclusions	Processing (weldments)	Ferrous and nonferrous	Radiographic method Eddy current method is used in thin-wall welded tubing coupled with reference standards
Inclusions	Processing	Ferrous and nonferrous wrought samples	Ultrasonics for wrought samples Magnetic particle method for machined sample surface Eddy current method for thin wall tubing and rods of small diameter
Lack of penetration	Processing	Ferrous and nonferrous weldments	Radiography, ultrasonics confined to specific cases Eddy current method used for nonferrous samples Magnetic particle and liquid penetrant methods when back surface of weld is visible
Laminations (surface and internal flaws)	Inherent	Ferrous and nonferrous wrought material	Ultrasonic method Magnetic particle method for ferrous samples Liquid penetrant method for nonferrous samples
Laps and seams (discontinuities due to dies during rolling)	Processing	Ferrous and nonferrous rolled threads	Fluorescent liquid penetrant method Magnetic particle method with care for anomalous indications
Laps and seams (discontinuities originating from blowholes, cracks elongated due to rolling)	Processing	Ferrous and nonferrous wrought material	Magnetic particle method for ferrous samples Liquid penetrant method for nonferrous samples Ultrasonics for wrought samples Eddy current testing for pipe and tubing samples
Microshrinkage	Processing	Magnesium casting	Radiography
Gas porosity	Processing	Ferrous and nonferrous weldments	Radiography, ultrasonics Eddy current method limited to weld pipe and tubing

(*contd*.)

(*contd*.)

Discontinuity	Origin	Material	Applicable method
Unfused porosity	Processing	Aluminum	Ultrasonics Liquid penetrant method
Stress corrosion	Service	Ferrous and nonferrous	Liquid penetrant method Ultrasonics method not common due to the perpendicular orientation of flaws to the surface
Hydaulic tubing	Processing and service	Aluminum 6061-T6	Eddy current method
Mandrel drag	Processing	Nonferrous thick-wall tubing	Eddy current, ultrasonics
Hot tears	Inherent	Ferrous castings	Radiography primary choice Liquid penetrant method for nonferrous samples
Intergranular corrosion	Service	Nonferrous	Liquid penetrant method is primary choice, radiography, eddy current method and ultrasonics may be used with some limitations

2.2.9 Acoustic Emission Technique

Acoustic emissions are the stress waves resulting from sudden movements in the stressed sample material. The most obvious example is the 'tin cry' due to stress in a wooden structure due to the load. It is very important that the measured acoustic emission signal be corrected for the background noise signal. Acoustic emission energy is due to the elastic stress field in the sample material. Acoustic emission is monitored by applying a controlled variable load. The principle of the method is illustrated below (Figure 2.14).

Acoustic emission can detect movement of defects in the sample due to applied load, is sensitive to the material sample, is not geometry sensitive, can be used in a plant or process without much intrusion, and is capable of testing a whole structure. The method requires that the acoustic signal be distinct from background noise. It is also useful to note that, as with

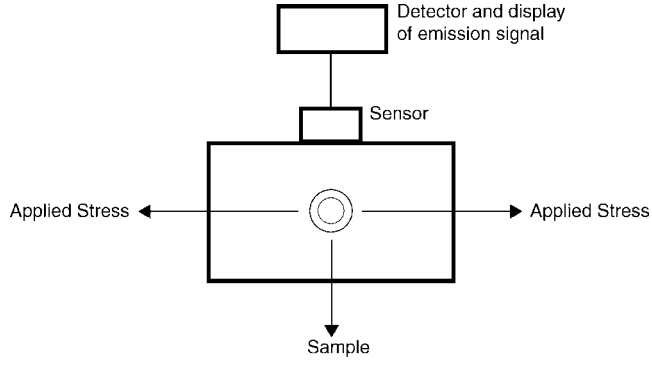

Figure 2.14 *Principle of AE method*

other methods of nondestructive testing, this method may be used in conjunction with other selected methods, known as coordinated nondestructive inspection.

Brittleness and homogeneity of a sample are indicated by a high acoustic emission pattern, while the ductile deformation mechanism due to microvoid coalescence of soft steels is characterized by low-emission signals.

The acoustic emission technique is used in the frequency range 20–1200 kHz. The technique has been useful in in-process welding monitoring, monitoring wear of tools, tribological processes,[54] detection of leaks,[53] monitoring corrosion,[53] monitoring liquid–solid transformation and solidification processes.[53]

A typical acoustic emission instrument with a 12-channel data acquisition system with computer interface for display of data, storage and analysis is commercially available (Physical Acoustics Corporation). Acoustic emission has been successfully used in materials studies, structural testing and quality control of product manufacturing. Some examples of applications are studies involving acoustic emission for optimum heat treatment of ferritic/pearlitic steels in which the features of microstructure are revealed, monitoring initiation and crack growth, application in high-temperature oxidation of metals to study the properties of oxide scale, problems in the study of metal–matrix composites such as the microcracking of the brittle reaction zones of two metal–matrix composites, product quality control is inspected by acoustic emission in processes such as welding, shaft straightening, structural inspection of aircraft, spacecraft, bridges, bucket trucks, buildings, dams, mining industrial equipment, pipelines, railroad cars, storage tanks, and pressure vessels.

A program for acoustic emission under the name Monopac was developed for external and internal corrosion, stress corrosion cracking and weld cracking.[55] This program consists of the test procedures as well as case histories.

The main advantage of this inspection technique is that the materials, such as insulation on the outside of a structure, need not be removed. A detailed account of the technique is beyond the scope of the presentation here and the reader may refer to articles in the literature.

Typical acoustic emission spectra of a steel subjected to spheriodization treatment in underannealed (80% pearlite, 20% spheroids) and optimally annealed (100% spheroids) are shown in Figure 2.15. The emission spectra show distinct features of the effect of heat treatment. Similar differences are seen in other situations such as crack growth in samples.

The utility of the acoustic emission method is also illustrated in the inspection and failure rates of FRP tank given below:

Year	Number of failures
1972	2
1973	2
1974	1
1975	2
1976	4
1977	3
1978	2
1979	3
1982	1
1984	1

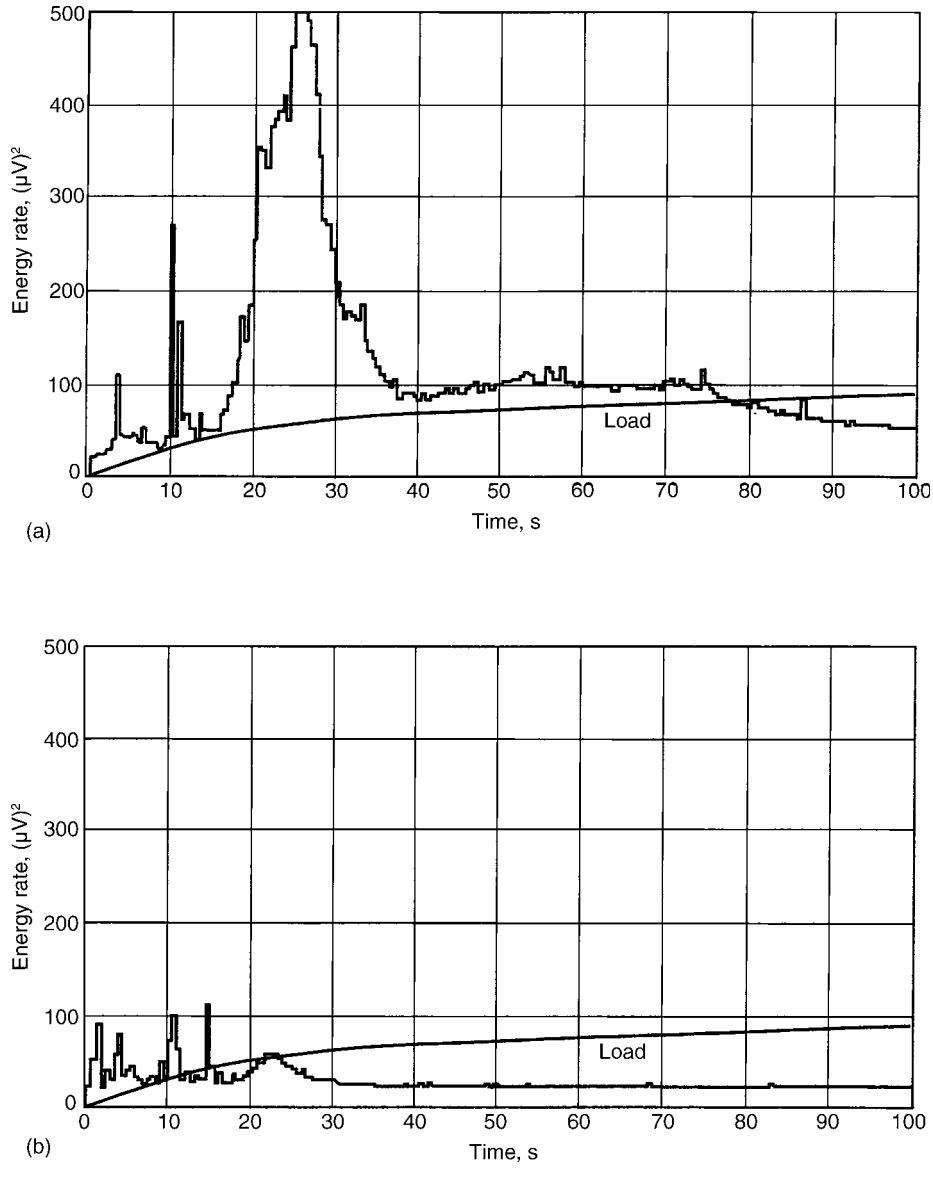

Figure 2.15 *Acoustic emission spectra of steel subjected to spheroidization heat treatment: (a) 80% pearlite, 20% spheroids (underannealed; (b) optimally annealed, 100% spheroids. (Reprinted with permission from ASM International. All rights reserved www.asminternational.org)*

The failures noted in 1982 and 1984 were predicted by the acoustic emission technique some time before the actual failure occurred. The important role played by this inspection technique in eliminating sudden failure attests to its capabilities in monitoring defects in materials.

Other methods available for nondestructive evaluations are indirect in nature, but may be useful in certain situations. These methods will only be discussed in a cursory fashion and more detailed aspects can be obtained from the literature. It is useful to note that stress in any structure plays a vital role, and that the methods involved in determining stress in an engineering component or structure in the process conditions is of vital importance. The methods used in determining stress are finite element stress analysis, strain gaging, the photoelastic method and brittle coatings.

2.2.10 Other Nondestructive Methods

The finite element method, as applied to an engineering structure, consists of dividing the structure into distinct nonoverlaping regions known as elements; the elements are connected at a discrete number of points along the periphery, known as nodal points. For each element the stiffness matrix and load vector are calculated, by assembling the calculated stiffness matrix and load vector of the elements, one obtains the overall stiffness and vector of the system or structure; the resulting simultaneous equations for the unknown displacement components of the structure (unknown nodal variables) are solved and the stress components are evaluated for the elements.

Computations involving this method are now available in the form of commercial software with many examples of engineering models.[58] Some typical problems considered are:

1. Deflection of a beam
2. Plate with a hole in tension
3. Cylinder subjected to tip load
4. Square wall-driven cavity
5. Contact between a block and a rigid cylinder
6. Analysis of a shell corner
7. Thermal stress analysis of a cylinder
8. Beam subjected to impact load
9. Beam subjected to earthquake load
10. Visualizing mesh quality
11. Pushover analysis of a frame
12. Analysis of shaft–shaft intersection
13. Analysis of a cracked body
14. Fluid flow over a flexible structure in a channel
15. Fluid flow and mass transfer in a pipe
16. Conjugate heat transfer and natural convection within an enclosed system
17. Limit load analysis of a pipe bend
18. Deformation of a pipe due to internal fluid flow
19. Heat transfer from sodifying concrete blocks
20. Analysis of a cable-stayed bridge
21. Beam subjected to harmonic and random loads
22. Unsteady fluid flow over a flexible structure in a channel
23. Analysis of a shell–shell intersection
24. Analysis of fluid structure interaction within a pipe constriction.

Finite element analysis (FEA) has advanced by leaps and bound since its introduction due to the great advances in computer software developments. Models can now be generated of the problem on hand through interactive design. The important and common applications of the method is in the determination of displacement and stress profiles in structures such as bending beams, pressure vessels, rotating disks, bridges, buildings, automobiles, aircraft, heart valves and hip joints. The procedure involves three steps: (i) preprocessing; (ii) processing; and (iii) post-processing. In the first step the conditions or parameters such as load, boundary conditions and other constraints are specified. The processing step involves solving the equations using the specified conditions or parameters. The post-processing involves the extraction of the desired information by displaying the manner in which the stress or any other parameter varies.

The applications of the method are too many to list and some typical problems[59] analyzed by the method are noted below:

Applications	Parameters
Determination of residual stress in weldments by hole drilling and FEA	Calibration of residual stress
Preform cracking in squeeze-cast magnesium-based composites	Stress and temperature
Fabrication of seam-welded aluminum tube for hydroforming	Calculation of stress and strain
Shape and process optimization for manufacture of dental burs	Optimization and temperature and stress
Pipeline infrastructure reliability	Stress, strain and temperature
Pressure tubes used in nuclear industry	FEA analysis of cooling tubes
Bearings submerged in galvanizing baths	Stress analysis
Effect of crack-tip plasticity on crack length estimation in single edge notch samples	
Estimation of fracture toughness from upper-shelf charpy energy and its use in fracture assessment	Stress
Pipe stress and pressure vessel analysis	Pressure, dead-weight, thermal expansion, vibration modal analysis of fatigue. Analysis to ensure that the piping and pressure vessels conform to the codes of ASME, API or WRC as the case may be

In any structure the entire structure responds to mechanical or thermal loads. It is also necessary to bear in mind that any structure will also experience localized stress concentrations at points of contact or separation in the structure. These points of contact or separation are sites susceptible to damage, cracking or failure initiation. Stress analysis using the finite element method in structures which are bolted, mating surfaces, vessels

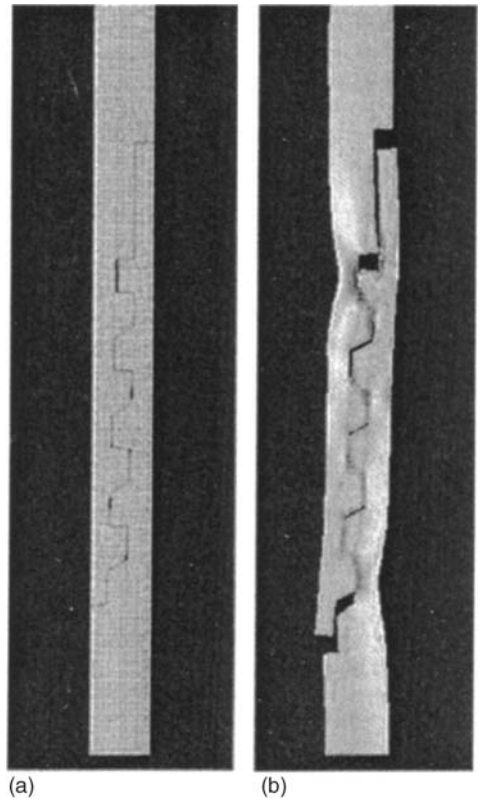

Figure 2.16 *Axisymmetric finite element model of a threaded connection showing: (a) thread contact; (b) distortion and stress state. (Reprinted with permission from ASM International. All rights reserved www.asminternational.org)*

with lids, or thermal expansion components is done by contact analysis. An example of axisymmetric finite element model of a threaded connection showing thread contact and the corresponding distorted and stress state are shown in Figure 2.16.

Elastic/plastic material behavior can be analyzed by the finite element method at the design stage or the failure analysis stage. Elastic/plastic analysis can determine both the magnitude of stress and the absorption as well as the dissipation of energy in addition to the prediction of the deformation. The elastic/plastic analysis in predicting the deformation of the shape of a transformer housing due to internal overpressurization is illustrated in Figure 2.17. The figure shows the distorted housing along with the stress state and distortion obtained from the finite element analysis.

Stress can be evaluated by using strain gages[60] located in that part of the equipment or structure which is suspected to be critical. Using the measured values of strain in the component, together with the known mechanical properties the stress of the component or structure of interest can be evaluated using the stress–strain relationships. The locations where the strains are to be measured in complex structures are obtained by techniques involving photoelasticity or brittle coating techniques. The preliminary identification of the

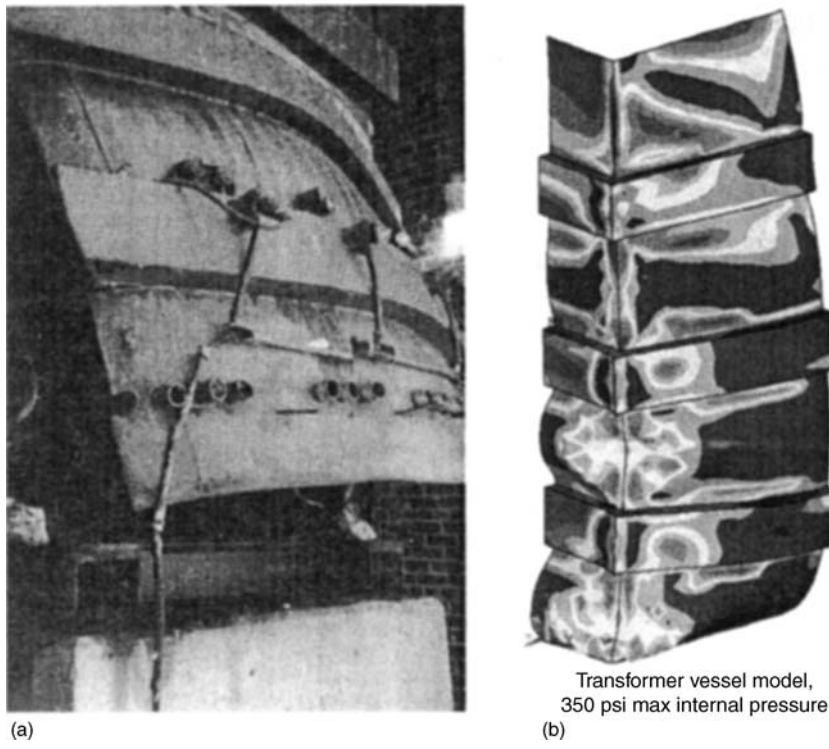

Figure 2.17 *Example of an elastic/plastic finite element analysis: (a) photograph showing distorted transformer housing from internal overpressurization; (b) finite element results showing permanently distorted shape and stress contours. (Reprinted with permission from ASM International. All rights reserved www.asminternational.org)*

location in the structure is followed by the measurement of the amount and direction of strain experimentally. It may also be necessary to determine the shear strain, depending upon factors such as load and the characteristics of the sample material.

The strain at a chosen location may be determined by either a resistance-based strain gage or photoelastic coating technique. Commercial strain gages are available with different grid geometries to measure the strain in different directions. Gages with a single grid measure normal strains in the axial direction of the grid. A three-element strain gage is used to measure in biaxial stress field. The strain gage that is used in any given context is dictated by the direction of the stress field of interest. The sensitivity of a strain gage is characterized by gage factor (GF) which is defined as the ratio of unit change in resistance $\Delta R/R$ to unit change in strain $\Delta L/L$.

$$\text{Gage factor (GF)} = \left(\frac{\Delta R}{R}\right) \Big/ \left(\frac{\Delta L}{L}\right)$$

The photoelastic coating method[61] consists of coating the sample with a thin photoelastic coating on the surface of the test sample and measurement of the transmitted strain upon the application of a known load. The strain is measured with a reflection

polariscope. Some notable attractive features of the method are that it is applicable to any size or shape of a sample, it enables measurement of strain field over the entire coated area, data on stress gradients are obtained, measurement of a large assembly of strains is possible, acquisition of dynamic data on a sample is facilitated, measurement of residual stress is possible, and it can measure the combined effect of various load conditions. The photoelastic patterns obtained are in terms of color sequence from black, yellow, red, blue-green, yellow, red, green, yellow, red and green in the order of increasing strain in the sample. The band separating red and green colors is known as a fringe and the higher fringe indicates the higher strain in the sample.

The method depends upon the optical properties of the coating material and its thickness on the sample. Reflection polariscopes are used for the measurement of the fringe patterns, and hence the strain in the static mode of measurement. It is necessary to use stroboscopic light sources for the dynamic analysis or measurement of strain on the samples by the photoelastic coating method. The brittle coating method consists of the application of strain-sensitive lacquer to the sample surface and, after drying, a load is applied and the resulting cracks appearing normal to the direction of the maximum tensile strain are noted. From the pattern of cracks the picture of the tensile strain distribution with the qualitative magnitude and direction of the strain is obtained. This method serves as a rapid indicator of the locations of critical stresses or stress concentrations in the test specimens. This qualitative and rapid method serves as a prelude to further quantitative strain gage measurements. Another useful aspect of the method is its applicability to locations in samples or test objects consisting of inaccessible areas in vehicle samples.

2.2.11 Thermal Methods of Inspection

Thermal methods of inspection can be used to detect flaws in materials of complex shape, and the methods detect subsurface flaws or voids in the samples. The limitation is that the depth of the flaw should not be large compared with its diameter. When heat flows into or out of the sample, the surface temperature is measured or continuously mapped. The resulting contours of the surface temperature indicate the morphology of the defect in the sample. Thermal inspection can be done by using either contact or noncontact sensors. The noncontact sensor consists of an infrared imaging element which may be either a portable imaging hand-held scanner or high-resolution infrared imaging system. The contact type of sensors measuring changes in temperature are material coatings and thermoelectric devices. Cholesteric liquid crystals indicate changes in temperature by changes in color in the temperature range -20 to $250^{\circ}C$. Thermally quenched phosphors or heat-sensitive paints can also used to detect changes in temperature of the test samples. It is also useful to note that reference standards are required for comparison and the thermal methods should be used in conjunction with other nondestructive methods to assure the validity of the determination of the flaws in the sample.

Some typical applications of thermal methods in the determination of flaws are hot and cold equipment such as heating ducts, steam lines[62], radiators[63], heat exchangers[64], exhaust systems, chimneys[62] and refrigeration systems, process control in processes involving temperature changes such as heat-set and heat-shaped plastics, hot-worked metal components, hot coatings, weld components, liquid or water intrusion in honeycomb

structures such as liquid levels in aircraft maintenance, detection of leaks and retained moisture in insulation, fluid levels in sealed tanks, detection of disbonds, delaminations and voids in thin laminates, honeycomb to thin face sheets and protective coatings. On-line inspection of adhesive-bonded aluminum sheets by thermal methods and the application of the cold thermal wave technique for inspection of an adhesive-bonded aluminum structure have been documented in the literature.[64]

Periodic inspection of equipment or plant for detection and monitoring corrosion should be followed by a written report, detailing all the observations and the necessary actions to be taken in future maintenance so that unexpected premature failures can be avoided. It is also necessary that all personnel involved are aware of the observations in the periodic inspection report on corrosion detection and monitoring in order to avoid future premature failures.

2.3 Failure Analysis

Failure may be defined as the inability of a component, machine or process to function properly. Failures fall into two broad categories, namely functional failure and failure to achieve the expected or specified performance of a component with respect to life or the corrosion resistance. Failures can have many consequences as detailed below:

Consequences of failure	
Serious failures	Failures resulting in environmental damage
Resulting in injury or fatalities, e.g., failure of aircraft	Pipeline carrying oil and gas
Immediate action is to remove the fleet of the particular model of aircraft from service, followed by failure analysis to rectify the situation	Immediate action is to channel efforts to minimize environmental effects followed by a detailed failure analysis to prevent future failure

Failures that are innocuous from the point of view of safety and environmental damage, like any failure, must be investigated in detail and corrective action taken to minimize losses in downtime and production. The various aspects of failure are:

1. Engineering aspects: failures related to the properties of materials or due to anomalies in design or to the improper selection of materials
2. Manufacturing aspects of materials: improper metal working, welding, heat treatment or casting results in inherent flaws
3. Failure due to fracture
4. Failure due to corrosion
5. Failure related to wear of the material
6. Failure due to improper life assessment such as overestimation of the service life of the material or equipment

7. Improper periodic inspection or errors in maintenance
8. Failure due to unforeseen factors

It is necessary in failure investigation to determine the type of damage, the cause of the damage, potential solutions to either minimize or eliminate the damage, choosing the best solution based on economics, safety and environmental considerations. The final step involves the practical implementation of the best solution in service conditions to confirm the validity and conclusion that it is indeed the best solution.

In analyzing a failure it is necessary to record the physical characteristics of the damaged component such as pitting, intergranular fracture or buckling and get an idea about the damage mode. This step is followed by the assessment of the series of events that led to the observed damage otherwise known as the damage mechanism such as high-temperature creep, hydrogen embrittlement, stress corrosion cracking, pitting, crevice corrosion, etc. The common categorization of potential damage mechanisms consists of distortion, fracture, corrosion and wear. This is a very simplified categorization since combinations of these mechanisms can also occur. Some typical combinations are given below:

Mode	Damage mechanism
Wear, stress	Spalling, rolling contact fatigue
Wear, corrosion	Fretting, velocity assisted corrosion, cavitation
Wear, temperature	Lubrication breakdown
Corrosion, temperature	Liquid metal embrittlement, hot corrosion, dealloying
Corrosion, stress	Corrosion fatigue, stress–corrosion cracking
Corrosion, stress, temperature	Sulfide stress cracking
Stress, temperature	Thermal fatigue, creep–fatigue interaction, creep, thermomechanical fatigue, thermal process cracking, impact, graphitization, hold-time fatigue
Wear	Adhesion, abrasion, erosion
Corrosion	General corrosion, crevice corrosion, pitting, hydrogen damage, caustic corrosion, intergranular corrosion, microbiological corrosion
Temperature	Melting, oxidation
Stress	Overload, buckling, bending, low-cycle and high-cycle fatigue

It is important to note that the damage mechanism such as low-cycle fatigue and high-cycle fatigue are attributed to stress. These damage mechanisms may in certain cases be enhanced by temperature. An example of this occurs in gas turbine environment where low-cycle fatigue is induced by stress from thermal cycling. Thus, in assigning damage mechanisms in any case should be done based on all the conditions that are prevalent in the particular context.

The general procedure involved in failure analysis consists of the following steps: (i) collecting all the background data on the failed component such as: location; name of item; identification numbers; owner; user; manufacturer; fabricator; function of the components; service life at the time of failure; rating, such as operating levels, normal and abnormal loads, frequency of loading and environment; materials used; manufacturing and fabrication

methods used, including specifications and codes for manufacture, fabrication, inspection and operation of the component; normal stress orientation, operating conditions such as temperatures, pressures and speeds; strength and toughness; heat treatment, stress relief; information on welding, adhesive joining, coatings, bolting and riveting procedures used in fabrication; inspection methods and quality control reports during manufacture; service and maintenance records; (ii) visual inspection or examination of the failed sample, recording the origin of failure along with the presence of stress concentrators, scale on fracture faces, direction and amount of stress, failure mode mechanism according to the best guess; direction of crack propagation and sequence of failure, presence of contributing imperfections and other relevant physical data; (iii) fractographic examination; (iv) chemical analysis of the sample for checking conformity with the specifications, analysis of corrosion products or coatings; (v) determination of mechanical properties for comparison with specifications; (vi) macroscopic examination for homogeneity and quality; (vii) determination of microstructural features by metallography; (viii) determination of microhardness to assess cold working, quality of welds and identify phases; (ix) SEM examination to study the different phases; (x) determination of the presence of inclusions and segregation by electron microprobe; (xi) determine the residual stress by X-ray diffraction; (xii) determination of relative amounts of phases such as austenite, carbides in steel; (xiii) simulation testing to evaluate the critical attributes of the material to confirm the conclusions drawn on the failure mode and mechanism such as stress corrosion cracking, or the method of heat treatment or hardenability as the case maybe; and (xiv) finite element modeling analysis to simulate the failure.

The failure analysis can be done using a judicious combination of several methods such as visual examination, metallography, microscopy, electron microprobe, energy dispersive X-ray analysis, X-ray diffraction methods for determining residual stress in the sample, surface analytical techniques to determine the nature and composition of surface deposits and finite element analysis modeling.

The visual, metallographic and scanning electron microscopic methods of examination of a failed sample can be useful in the identification of the failure mode. Some features of the fracture surfaces that are likely to be present as a result of various failure modes are noted below:

Damage mode	Visual 1–50 × fracture surface	Metallography 50–1000 × (cross-section)	Scanning electron microscopy, 20–10 000 × (fracture surface)
Ductile overload (sudden failure)	Necking or distortion in direction consistent with applied loads, dull, fibrous structure shear lips	Grain distortion and flow near fracture; Irregular, transgranular fracture	Microvoids (dimples elongated in direction of loading); single crack without branching, surface slip band emergence
Brittle overload (sudden failure)	Little or no distortion; Flat fracture; Bright or coarse structure, crystalline, grainy; Rays or chevrons point to origin	Little distortion; intergranular or transgranular; may relate to notches at surface or brittle phases internally	Cleavage or intergranular fracture; origin area may have imperfection or stress concentrator

(*contd*.)

(*contd*.)

Damage mode	Visual 1–50 × fracture surface	Metallography 50–1000 × (cross-section)	Scanning electron microscopy, 20–10 000 × (fracture surface)
Fatigue (progressive)	Flat progressive zone with beach marks overload zone consistent with applied load direction; ratchet marks where origins join	Progressive zone: usually transgranular with little apparent distortion; overload zone: may be either ductile or brittle	Progressive zone: worn appearance flat, may shown striation (>500 × overload zone; may be either ductile or brittle)
Corrosion (progressive)	General wastage, roughening, pitting or trenching, stress-corrosion and hydrogen damage may create multiple cracks that appear brittle	General or localized surface attack such as pitting, cracking; selective phase attack; thickness and morphology of corrosion scales	Path of penetration may be irregular, intergranular or a selective phase attack; corrodent may be identified by energy dispersive analysis
Wear (progressive)	Gouging, abrasion, erosion; Galling or storing in direction of motion; Roughened areas with compacted powdered debris (fretting); smooth gradual transitions in wastage	May show localized distortion at surface consistent with direction of motion; characterize embedded particles	Wear debris and/or abrasive characterized as to morphology and composition; Rolling contact fatigue appears like wear in early stages
Creep (progressive)	Multiple brittle-appearing fissures; external surface and internal fissures contain reaction scale coatings; fracture after limited dimensional change	Microstructural change typical of overheating; multiple intergranular cracks; void formed on grain boundaries or wedge shaped cracks at grain triple points; reaction scales or internal precipitation some cold flow in last stages of failures	Multiple intergranular fissures covered with reaction scale; grain faces may show porosity

Failure Mode	Causative factors
Ductile overload	Load exceeded the strength of the component; check for proper alloy and processing determining hardness and chemical analysis; loading direction may show failure to be secondary short-term, high-temperature, high-stress rupture has ductile appearance
Brittle overload	Load exceeded the dynamic strength of the sample; check for proper alloy, processing, toughness, grain size; loading direction may show failure to be secondary or impact-induced; low temperature
Fatigue	Cyclic stress exceeded the endurance limit of the sample material; check for proper strength, surface finish, assembly and operations; prior damage by mechanical or corrosion modes may have initiated cracking; alignment, vibration, balance, high cycle low stress, large fatigue zone; low cycle high stress and small fatigue zone
Corrosion	Attack morphology and type of alloy be evaluated; exposure conditions may be severe; check pH, temperature, flow-rate, dissolved oxidizing agents, electrical current, metal coupling, and aggressive species; check bulk composition and contaminants.
Wear	In case of gouging and abrasion check source of abrasives; evaluate affectiveness of lubricants; Failure of seals of filters; fretting induced by looseness in clamped joints subject to vibration; bearing or proper design may lessen or eliminate the failure; water contamination; High velocities or uneven flow, cavitation
Creep	Mild overheating and or mild overstressing at elevated temperatures; unstable microstructures and small grain size tend to increase creep rates; ruptures occur after long exposure periods; verify proper alloy

2.3.1 Visual or Macroscopic Examination

Some typical examples to illustrate the methods of examination are now considered briefly. Visual or macroscopic examination of fractured surface can reveal the presence of distortions or plastic deformation in a component indicative of the direction of applied load. Macroscopic examination has been useful in detecting bolts that have failed due to fatigue, hot spots in bearings, failure of a connecting rod bolt in a diesel engine, fracture surface in a failed crank shaft, fracture surface of steel plates in oil storage tanks, brittle failure in a steel shaft and elongated cavities due to erosion in cupro-nickel piping.

The fatigue fracture surface of a failed crankshaft and failed rod bolt in a diesel engine are shown in Figures 2.18 and 2.19, respectively.

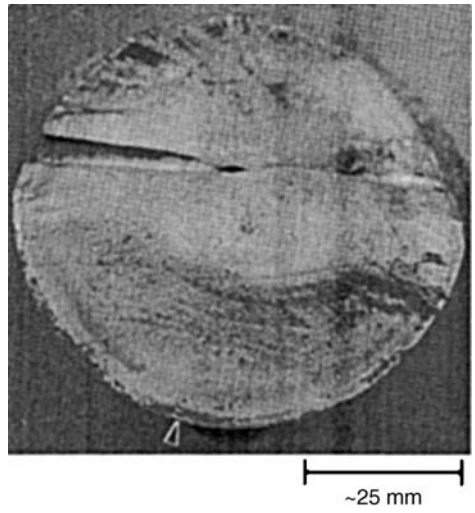

Figure 2.18 *Fatigue fracture surface appearance of a failed crankshaft, showing 'beach marks' on the lower part. The origin of the primary fracture is indicated by the arrow. (Reprinted with permission from ASM International. All rights reserved www.asminternational.org)*

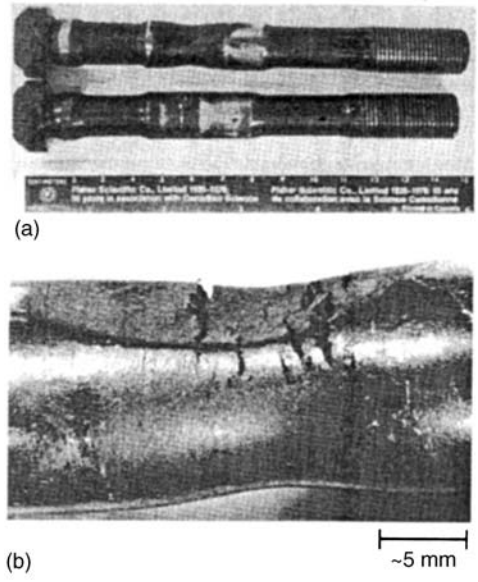

Figure 2.19 *Failure of a connecting rod bolt in a diesel engine. In (a), the failed bolt is the upper one, having necked down in a nominally larger cross-sectional area. The lower bolt is another removed from the engine in unstretched condition. In (b), the stretched region of the bolt is shown, with cracks that have opened up during bolt tensioning and subsequent operation. (Reprinted with permission from ASM International. All rights reserved www.asminternational.org)*

2.3.2 Metallography

Metallographic examination is usually done on both the failed sample and the original sample for ease of comparison and to determine the failure mode and mechanism. The samples are ground, polished and examined in the unetched condition. This method is capable of determination of the microstructure to assess if it is in accordance with the specified composition and processing of the sample, the type and extent of damage in service; evaluation of the quality of welding during fabrication; the origin, pattern of cracking and its relationship to microstructural features such as inclusions or grain boundaries; the extent of overheating in service conditions; the directionality in the microstructure with its possible relationship to failure and the distribution of phases in the sample.

Some typical examples are failure of a component that is rolled or extruded with its maximum tensile stresses along the direction of deformation when it is loaded in tension in a different direction. Cracking in steel beams with minimum specified yield strength of 300 MPa was found to have yield and tensile strengths of 180 and 288 MPa, respectively in the transverse direction. Cracking was found to occur by fatigue along banded regions containing MnS inclusions. This failure is due to faulty design in assuming the material to be isotropic. Other examples of failure examined by metallography include occurrence of decarburization or determining the depth of decarburization layer in a sample. Extensive carbide formation can lead to brittle intergranular cracking in hot-gas casing of a gas turbine, as shown in Figure 2.20.

The determination of stress–corrosion cracking (SCC) and the identification of the mechanism as to intergranular or transgranular crack propagation is made possible by metallography. An example of transgranular SCC in a 316 stainless steel orthopedic implant is shown in Figure 2.21. The cracking is an example of anodic SCC that develops from pits on the surface in the presence of chloride ions. Metallography has also been useful in

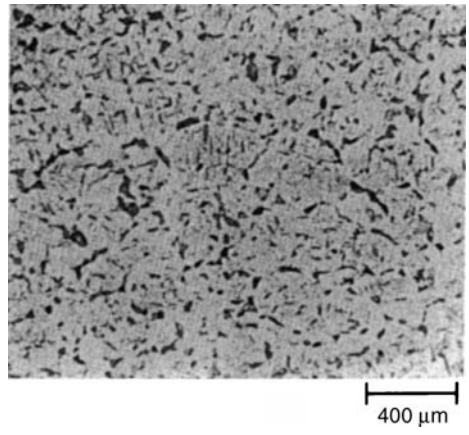

Figure 2.20 *Grain-boundary and intragranular precipitation at the hot side of the hot-gas casing of a gas turbine. Material is 321 stainless steel. Etched successively in Vilella's reagent, methanolic aqua regia, and Groesbeck's reagent to darken carbides. (Reprinted with permission from ASM International. All rights reserved www.asminternational.org)*

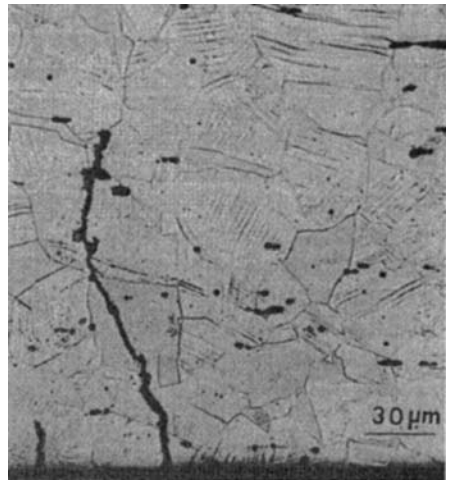

Figure 2.21 *Stress–corrosion cracking in a 316 stainless steel orthopedic implant. (Reprinted with permission from ASM International. All rights reserved www.asminternational.org)*

determining intergranular cracking in low-carbon pipeline steel, as shown in Figure 2.22. The hydrogen produced in the chemical reactions causes the cracking. The hydrogen is absorbed by the steel, leading to cracking in regions of high tensile stress.

Subsurface fatigue fractures in gears and bearings under high-contact loading are also successfully determined by metallography. An example of a crack running through the carburized surface layer on the flank of a gear tooth, fatigue crack and multiple cracks in the carburized layer of the gear tooth is shown in Figure 2.23 and 2.24.

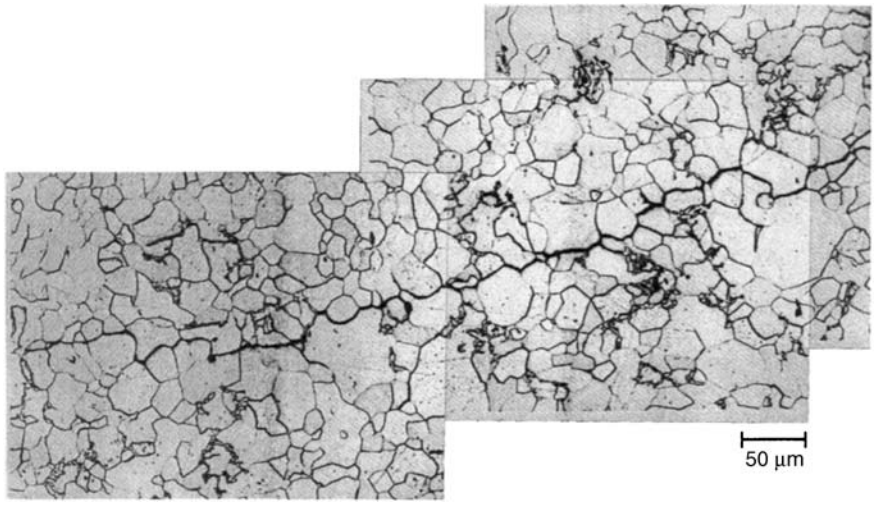

Figure 2.22 *Hydrogen-induced cracking in pipeline steel. (Reprinted with permission from ASM International. All rights reserved www.asminternational.org)*

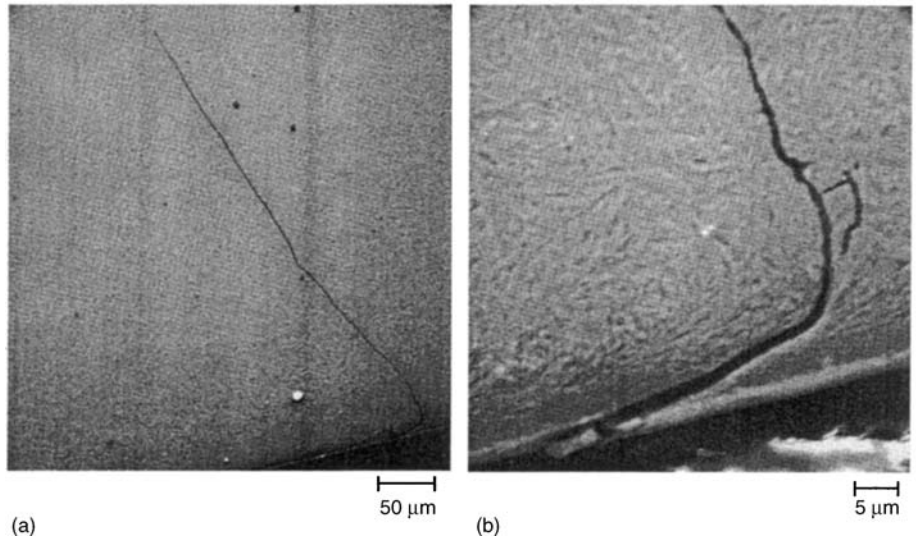

Figure 2.23 *(a) A crack running through the carburized surface layer on the flank of a gear tooth; (b) the region of the origin, shown at higher magnification. (Reprinted with permission from ASM International. All rights reserved www.asminternational.org)*

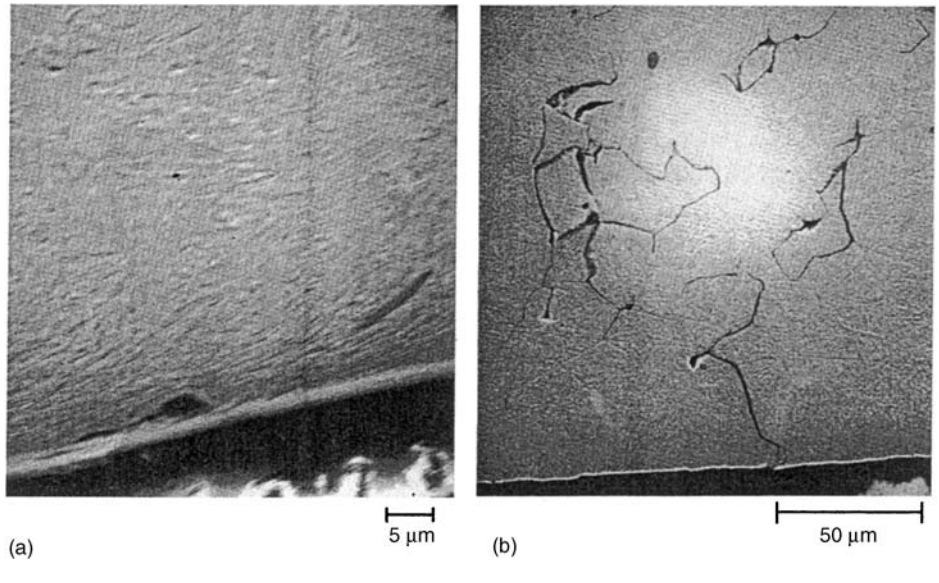

Figure 2.24 *(a) A fatigue crack initiating close to the flank surface of the gear tooth; (b) multiple cracks within the carburized surface layer of the tooth in another area. (Reprinted with permission from ASM International. All rights reserved www.asminternational.org)*

2.3.3 Microfractography

Microfractography consists of either directly using scanning electron microscopy (SEM) or examination of replicas of the sample by SEM or transmission electron microscopy (TEM). In contrast to usual light microscopes SEM has a great depth of field. The SEM view of the fracture surface of a low-carbon steel sample broken in tension is shown in Figure 2.25. It is useful to note if details such as ductile dimples, local quasicleavage and MnS inclusions are apparent.

Fracture surface replicas viewed by TEM are shown in Figure 2.26. The figure shows river patterns of brittle fracture failure of a steel fastner and fine equiaxial dimples on the surface of a tensile fracture of high-strength steel.

2.3.4 Fracture Mechanics in Failure Analysis

Structural failure may occur when the overall structural cross-section cannot support the applied load or, when the critical flaw size a_c is exceeded by preexisting discontinuity or by reaching the critical crack size through fatigue, stress corrosion cracking or creep mechanisms. Using fracture mechanics the stress at a crack tip can be calculated by a stress–intensity parameter K as,

$$K = Y\sigma\sqrt{\pi a}$$

where Y is a geometric factor (in general unity), σ is the gross stress across the fracture plane, and a is the crack length. The critical stress-intensity value K_c is given by:

$$K_c = Y\sigma_f\sqrt{\pi a_c}$$

where σ_f is the fracture stress at critical crack size a_c. The critical stress-intensity K_c is also known as fracture toughness. When the stress-intensity value reaches K_c, fracture occurs. It is useful to note that the value of K_c decreases with increasing thickness of the section until a minimum value is reached. The fracture toughness at this minimum is

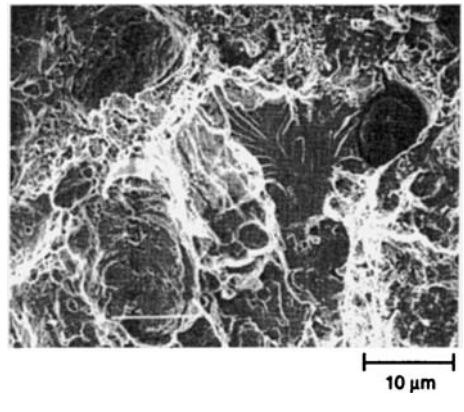

Figure 2.25 *SEM view of the fracture surface of a low-carbon steel specimen broken in tension, showing ductile dimples, local quasicleavage, and manganese sulfide inclusions. (Reprinted with permission from ASM International. All rights reserved www.asminternational.org)*

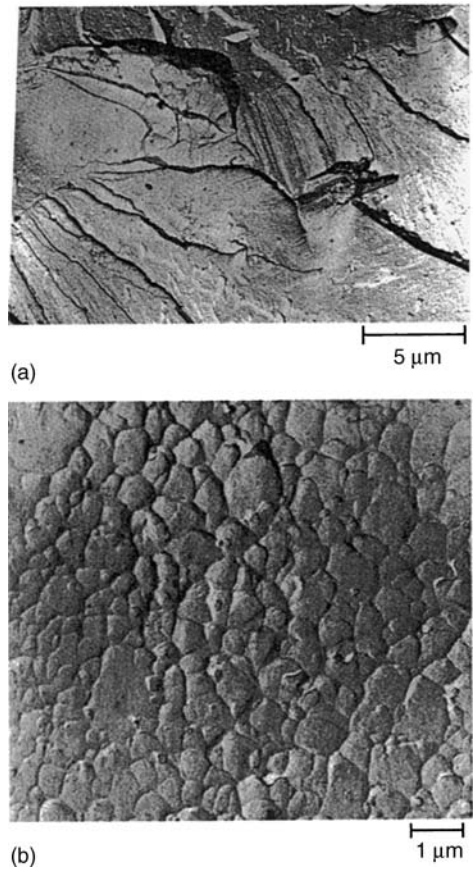

Figure 2.26 *Replicas prepared from fracture surfaces and viewed in TEM. (a) River patterns of a brittle failure of a steel fastener; (b) fine, equiaxed ductile dimples on the surface of a tensile fracture of high-strength steel. The small carbide particles where local rupture and void formation initiated are apparent. (Reprinted with permission from ASM International. All rights reserved www.asminternational.org)*

known as the plane-strain fracture toughness K_{1c} which is the inherent material property. Plane-strain fracture is a form of brittle fracture devoid of appreciable plastic deformation and falls under the regime of linear–elastic fracture mechanics. Now we can write:

$$\text{Thickness} \geq 2.5\ (K_{1c}/\sigma_y)^2$$

where σ_y is the yield strength.

Structural failures in general occur by a combination of crack initiation followed by subcritical crack growth mechanism such as stress corrosion, fatigue, and creep until a critical crack size is reached. Thus, fracture mechanics is useful in evaluating a_c that leads to failure by fracture. The application of fracture mechanics in failure analysis throws light on the progress from subcritical crack growth to fracture, the amount of load

leading to fracture, assessing material aspects such as manufacture and processing, proper design, and the effect of environment on the failure.

In the case of thin sections the measure of toughness is given by plane-stress fracture toughness, K_c and elastic–plastic fracture mechanics (EPFM) are used. It is also necessary to bear in mind that plane-stress fracture toughness K_c is higher than plane-strain fracture toughness K_{1c}.

2.3.5 Determination of Residual Stress by X-ray Diffraction

Determination of residual stress of a failed component is one of the most important steps in failure analysis. The determination of residual stress is useful when failed components experience stress concentration, overload, distortion or the formation of cracks in the absence of applied loads, subjected to corrosive environments as in stress corrosion, mechanical or thermal fatigue due to cyclic loading, or when faults in processing such as shot peening, grinding, milling and improper heat treatment such as stress relief, induction hardening, thermal strains, exposure temperature are involved.

The d-spacing changes when the material experiences stress. The method involves measurement of the shift of the X-ray diffraction peak angular position due to the residual stress in the sample. For a known X-ray wavelength λ, and n equal to unity, the diffraction angle θ is measured and the value of d-spacing calculated using Bragg's law.

$$n\lambda = 2d\sin\theta$$

The measurement of d-spacing under unstressed d_0 and stressed conditions d is used to calculate the strain, ε

$$\varepsilon = d - d_0/d_0$$

The reference axes and the direction of measurement of X-ray diffraction (XRD) residual stress are depicted in Figure 2.27.

When the plane-stress model is considered, the unstressed lattice spacing d_0 can be substituted with the measured d spacing of the sample at $\psi = 0$ (i.e., it is not necessary to

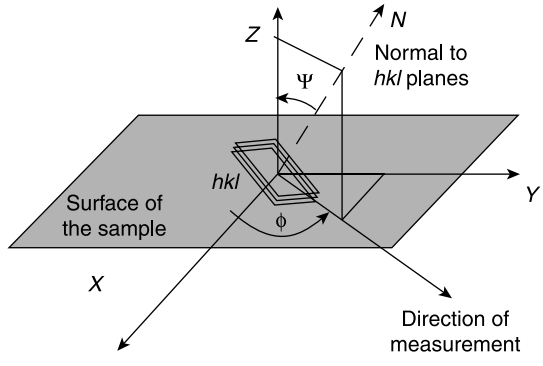

Figure 2.27 *Definition of the reference axes and the direction of measurement in XRD residual-stress analysis*

know precisely the value of d_0). In the $\sin^2\psi$ method d-spacings are measured and stresses are calculated by the equation:

$$\varepsilon_{\phi_\Psi} = ½ S_2(\sigma_{11}\cos^2\phi + \sigma_{12}\sin 2\phi + \sigma_{22}\sin^2\phi - \sigma_{33}) \times \sin^2\psi + ½ S_2\sigma_{33} - S_1(\sigma_{11} + \sigma_{22} + \sigma_{33}) + ½ S_2(\sigma_{13}\cos\phi + \sigma_{23}\sin\phi)\sin 2\psi$$

where ½ S_2 and S_1 are the X-ray elastic constants of the sample material, σ_{ij} are the stress tensor components, ϕ is the angle of direction of strain measurement, ψ is the angle subtented by the bisector of the incident and diffracted beams, with the sample normal, and $\varepsilon_{\phi\psi}$ is the strain for a given $\phi\psi$ orientation. User-friendly software is available for the measurement of stresses in sample material. Some of the applications of determination of residual stress are stress–corrosion cracking, corrosion fatigue and fatigue related failures.

Some practical cases are determination of residual stress in steel springs, the effect of mechanical loading on stress relaxation of machined and shot-peened nickel-base alloys,[65] determination of residual stress level in turbine engine disks as they accumulate engine cycles,[65,66] effect of manufacturing processes on residual stress, measurement of stress gradients in mechanical, electronic and structural components, effect of heat treatment on residual stress in steel coil springs, effect of variable heat treatment temperature on residual stress in iron alloys, measurement of stress in multiphase materials and composites and stress measurements at locations of stress concentrations.

Consider the case of cracks initiating from the tip of cloverleaf pattern in steel cargo-tie-down sockets.[67] Failure analysis[68] pointed out three mechanisms, namely overload failure, fatigue fracture and stress–corrosion cracking. In the absence of suitable evidence the latter two mechanisms were eliminated. Tests showed that overload failure mode and the transition from ductile to brittle were facilitated by a combination high brittleness of a carbon-rich transformed martensite layer introduced by flame cutting, increased hardness due to cold working and high residual stresses due to welding.

The overload mechanism of failure was confirmed by field measurement of stress on cargo ships, which showed cracking. A typical residual stress pattern obtained on the tie-down sockets installed on the ships is shown in Figure 2.28.

Finite element modeling is also useful in failure analysis. The method has been successfully applied in failure analysis. An example involving the stressed condition with maximum stress concentration in cloverleaf radius is shown in Figure 2.29. Another example of finite element modeling applied to distorted transformer housing due to internal overpressurization has been cited in Figure 2.17.

2.3.6 Mechanical Properties

Testing of failed component for its mechanical properties in order to assess its compliance with the specifications is an important step in failure analysis. The common property tested is the hardness. Hardness testing helps the analyst to assess or evaluate the heat treatment, tensile strength of the alloy, detection of work hardening or the deleterious

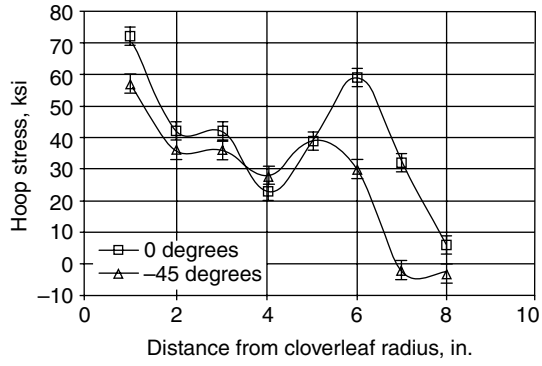

Figure 2.28 *Typical residual-stress profile as a function of distance from the maximum stress concentration in the radius of a tie-down socket. (Reprinted with permission from ASM International. All rights reserved www.asminternational.org)*

effects due to overheating, decarburization or the deleterious effects due to overheating, decarburization or absorption (pick up) of carbon or nitrogen. It is necessary to note that the proper load is used and a proper test such as the Brinell or Rockwell tests is used. For example for the case of gray cast iron sample it is appropriate to use the Brinell test protocol.

In order to confirm that the component is in compliance with specifications it is appropriate to perform tensile and impact testing of the component. Directionality is an important consideration in tensile testing of wrought metals. Care should be taken in choosing samples from the failed components for tensile testing. In some cases it is possible that quality assurance specifications indicate the manner of sampling for testing and this is typified by aircraft components. Usually tensile test samples are taken with the major axis parallel to the direction of grain flow. It is also common

Figure 2.29 *Finite element model showing maximum stress concentration in cloverleaf radius. The highest stress concentration is in the small black area surrounded by white. (Reprinted with permission from ASM International. All rights reserved www.asminternational.org)*

practice to take samples in the longitudinal and transverse directions. Samples cut transversely to the longitudinal axis of the component, such as a shaft or plate, usually give lower tensile and ductility values than those cut in the longitudinal direction.

2.3.7 Corrosion and Wear-related Failures

The various forms of corrosion, along with the characteristic features, are described in detail in Chapter 6. In the present context it will suffice to identify the particular type of corrosion failure by visual methods, metallography and analysis of the corrosion products.
Some obvious features of different forms of corrosion are:

General or uniform corrosion	Overall general attack and thinning
Galvanic corrosion	occurs when dissimilar metals are in contact through an electrolyte
Crevice corrosion	Localized attack in an area shielded from the environment
Pitting corrosion	Pits on the sample surface
Intergranular corrosion	Nondestructive testing is recommended.
Stress–corrosion cracking	Require detection by high magnification microscopy
Selectively leaching	after using suitable sample preparation technique
Erosion–corrosion	Locally elongated pits where there is rapid flow of a liquid in a pipe

Failure due to corrosion may also involve a combination of two corrosion modes. In analyzing a failure due to corrosion it is necessary to identify the corrosion mode tentatively by visual and metallographic methods, the corrosive agents, corrosion morphology, and to make a definitive identification of the corrosion product or scale.

The analysis of corrosion scale or product may be done by wet chemical methods such as spectrophotometry or atomic absorption spectrophotometry in cases where the removal of corrosion scale is permitted, or by surface analytical techniques such as X-ray photoelectron spectroscopy, Auger electron spectroscopy, electron microprobe analysis, by energy dispersive X-ray analysis in the case of samples which need to be preserved.

Energy-dispersive X-ray analysis consists of generation of X-rays characteristic of the elements when an electron beam impinges on the sample. By using this technique a rapid analysis of the elements present in the sample can be done with detection limits of the order of 0.1 wt %. A typical spectrum obtained in the analysis of deposits within a crack in pipe in a petrochemical plant is shown in Figure 2.30.

Electron probe microanalysis is also used in the analysis of corrosion scales, and the probe along with wavelength dispersive attachments can detect elements of the order of 0.01 wt %.

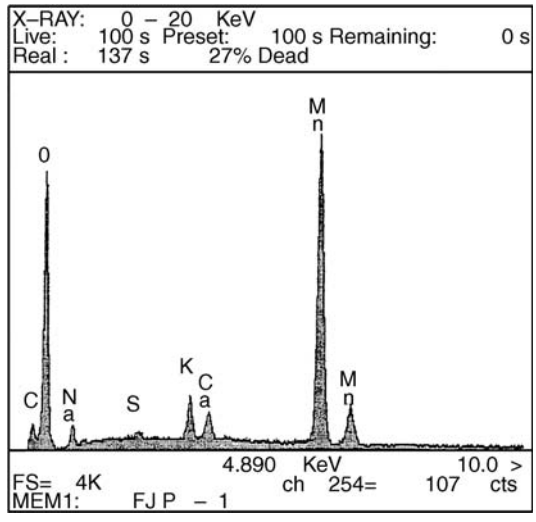

Figure 2.30 *Energy-dispersive spectroscopy analysis of deposit in a crack in a pipe from a petrochemical plant*

The corrosion deposits can be analyzed by X-ray photoelectron spectroscopy and Auger electron spectroscopy. Some characteristics of the techniques are:

	Auger electron spectroscopy	X-ray electron spectroscopy	Secondary ion mass spectrometry
Kinetic energies	50–2500 eV	100–1500 eV	
Escape depth	20 Å	20 Å	
Peak location	±1 eV	±0.1 eV	
		Oxidation state Bonding Organic structure	Mass spectrum from surface layer
Elemental sensitivity			
Elements	$Z > 2$	$Z > 2$	All elements
Specificity	Good	Very good	Good (ppm to ppb)
Quantitative analysis			
Absolute	±30%	±30%	Not possible
Relative	±5%	±5%	50%
Detection limit	0.05% monolayer	0.1% monolayer	10^{-4}% monolayer
Speed	Fast, elemental mapping in minutes	Slow, typical run in 30 min	Fast, spectra in minutes
Sample destruction	Frequent, especially organics	None	Yes

Electron probe microanalyzer and Auger electron spectroscopy have the advantage in terms of the depth of the deposit analyzed. The microprobe can have depth analyzing sensitivity of the order of 1 μm and surface analysis techniques have depth analytical range of nanometers. Further, X-ray electron spectroscopy can give data on the oxidation states of elements present in the deposits along with their mode of bonding; coordinated surface analysis is particularly useful in studies involving inhibitors and coatings.

Wear failures are difficult to analyze and the major forms are: abrasive wear, erosive wear, adhesive wear, fretting, cavitation, liquid droplet impingement, rolling-contact fatigue. About 50% of the failures are due to abrasive wear, 15% due to adhesive wear and about 8% each due to erosion and fretting. The other forms of wear account for the remaining percentages of wear failure. The different forms of wear, along with the characteristic features and remedial measures, are detailed below:

Type of wear	Appearance	Mitigation
Abrasion	Cutting, small groves (cutting tools, plows, cultivators)	Change material to high-carbon steel or 20–30% Cr white cast iron or WC or TiC composites and by increasing surface hardness using hard-chrome plate
Erosion	Similar to abrasion; cutting in ductile metal; fracture (of brittle material) very small chips or particles (e.g., impellers, propellers, fans)	Reduce fluid velocity to eliminate turbulence; select harder alloy (high chromium); hard coatings such as cement lined pipe, rubber lining
Adhesion	Occurs due to metal–metal contact; dynamic process scratches, grooves, severe tearing and deep grooving, seizure may occur	Avoid overheating of lubricant; use additives with lubricant to form film; Use grease at higher temperatures; select materials with better resistance as well as hard coatings
Fretting	Occurs between two contacting surfaces in vibratory motion; appears as discoloration and damage between two closely fitted parts such as bolts, rivets, turbine and compressor blade roots, heat exchanger tubes and may lead to fatigue cracks and fracture	Minimize relative motion by increasing the clamping force; use plastic or rubber pads or gaskets; increase hardness of material; chromium plate one of the surfaces

(*contd.*)

(*contd*.)

Type of wear	Appearance	Mitigation
Cavitation	Impact of the liquid at the surface by collapsing bubbles; pits on surface of diesel engines, wet cylinder sleeves, hydraulic turbines, nozzles, impellers	Not easy to prevent; change in design to minimize pressure drops; reduce surface roughness; increase vapor pressure of liquid
Liquid droplet impingement	Damage appearance is similar to cavitation damage; occurs in steam turbines and down stream elbows and piping	Changes in design; use hard coating; use weld overlay
Rolling-contact fatigue	Caused in rolling-element bearings, gears and rolling-mill rolls. Surface-origin pitting, subcase-origin spalling and subsurface-origin pitting are thought to be involved	Hard materials are used; rather difficult to combat the problem
Corrosive wear	This type of wear combines effects of wear and corrosion; erosion–corrosion is an example of this type of wear; an example of corrosive wear is gasoline engine wear, particularly when the engine is turned off before reaching the operating temperature	Surface coatings are beneficial. It is also possible to use lubricants containing corrosion inhibitors

As in the case of corrosion failures, the sequence of steps involved in analyzing wear failures are initial examination of the failed component including service conditions to establish the mode or combination of modes of wear failure, metallographic examination to check if the microstructure of the worn part met the specification, both in the base material and in the hardened case or applied surface coatings, existence of localized phase transformations, shear or cold worked surfaces, macroscopic and microscopic hardness testing to determine the proper heat treatment, X-ray and electron diffraction analysis to determine the composition of abrasives, wear debris, surface elements and microstructural features such as retained austenite, chemical analysis of wear debris surface films and physical properties such as viscosity and infrared spectral determination of the integrity of lubricants and abrasive characteristics of soils or minerals in the cases of wear failures of tillage tools.

The most important step in failure analysis is to identify the damage mechanism involved in the failure. In the broad sense damage mechanisms are classified as distortion, fracture, corrosion and wear. That this classification is simplistic is

Table 2.3 *Common damage mechanisms for boiler tubing*[69]

Fluidside corrosion
Underdeposit corrosion – caustic gouging
Underdeposit corrosion – hydrogen damage
Underdeposit corrosion – phosphate corrosion
Acid cleaning corrosion
Internal deposit/corrosion product buildup
Fireside wastage
Fireside oxidation
Fireside corrosion of superheater and reheater tubing
Fly ash corrosion
Sootblower corrosion
Coal particle corrosion
Steam impingement
Fireside corrosion of waterwall tubing
Low-temperature (dew point) fireside corrosion
Falling slag damage
Tube rubbing
Rupture
Short-term overheating (stress rupture)
Long-term overheating (creep rupture)
Graphitization
Cracking
Corrosion fatigue – waterside
Corrosion fatigue – fireside
Thermomechanical fatigue
Vibration fatigue
Dissmilar metal weld stress rupture
Stress–corrosion cracking
Quality control
Maintenance cleaning damage
Material imperfections/welding imperfections/discontinuities

borne out by the 28 separate damage mechanisms grouped under five categories in the case of boiler tube failure.[69] The various damage mechanisms identified are given in Table 2.3.

The detailed differentation between various failure mechanisms enables identification of the specific root causes of the failure, followed by arriving at prospective solutions. It is also necessary to point out that sometimes the general appearance of the features of different mechanisms might be similar at first glance and it is necessary to probe the features in depth to identify the different operative mechanisms. This is well illustrated by the three similar boiler waterwall mechanisms, such as caustic gouging, hydrogen damage and phosphate corrosion. The three mechanisms with their features along with the causes and suggested remedial actions are noted below:

	Caustic gouging	Hydrogen damage	Phosphate corrosion
Appearance	Rounded depressions; mottled appearance; needle Fe-rich deposits	Rounded depressions; intergranular cracking deposit may have chloride	Rounded depressions; no intergranular cracks; thick gray deposits of iron phosphate
Causes	Localized NaOH concentration; high pH	Low pH; corrosion producing hydrogen	High pressure and temperature and high phosphate concentration
Remedial action	Control water chemistry; periodic cleaning	Control water chemistry; remove from service when pH < 7.0; chemical cleaning when pH < 7	Use $Na_3\ PO_4$; reduce drum pressure

An alternate method of classification of damage mechanisms in terms of environmental conditions such as stress, temperature, corrosion, wear, radiation is known as the failure wheel. In this representation secondary mechanisms are underlined as opposed to primary damage mechanisms. The boiler tube failure discussed can be represented in terms of failure wheel, as shown in Figure 2.31. The aim in any case is to identify definitively the underlying mechanism of failure to enable one to undertake remedial action such that future failures do not occur.

2.3.8 Failure Analysis of Polymeric Materials[70]

With increasing use of polymeric materials in industry the corrosion engineer is faced with the need to have knowledge of the basic types of polymers, their characteristic features, modes of failure of polymeric components and the methods involved in characterization of polymers in failure analysis. Some characteristics of engineering polymers are as follows:

Type of polymer	Features
Polyethylene, polypropylene, polyvinyl chloride, polyamide	Flexible and crystallizable chains
Phenol–formaldehyde-cured rubber styrenated polyester	Cross-linked amorphous networks of flexible chains
Polyimide (ladder molecules)	Rigid chains
Polyethylene terephthalate	Crystalline domains in a viscous network
Terylene, cellulose acetate	
Chloroprene rubber, polyisoprene	Moderate cross-linking with some crystallinity
Heat-resistant polymers	Rigid chains, partly cross-linked

(*contd.*)

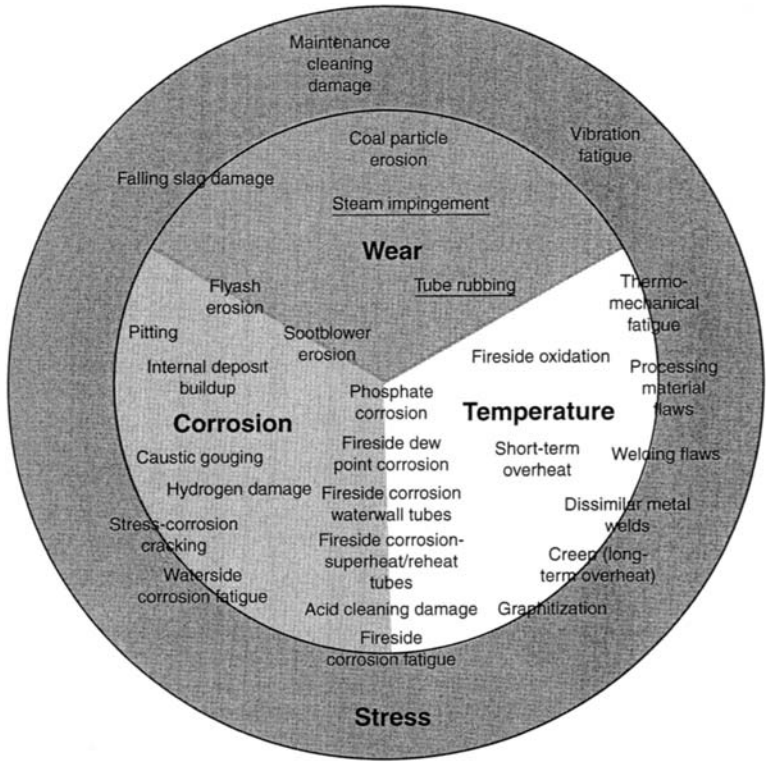

Figure 2.31 *Failure wheel for boiler tube damage mechanisms. Underlined mechanisms are always secondary in this system. (Reprinted with permission from ASM International. All rights reserved www.asminternational.org)*

(*contd*.)

Type of polymer	Features
High-strength and temperature-resistant polymers	Crystalline domains with rigid chains between them and cross-linking chains
Styrene-butadiene-styrene, triblock polymer, thermoplastic elastomer	Rigid-chain domains in a flexible-chain matrix

Some common modes of failures of polymeric materials are detailed below:

1. Plastic deformation — For amorphous polymers yield stress tends toward zero when the temperature is raised to glass transition temperature T_g. For crystalline polymers the yield stress tends toward zero when the melting temperature T_m is reached. The temperature range of usefulness of polymers is limited. At temperatures exceeding ambient value creep becomes significant and hence stresses need to be kept at such level to avoid creep

2.	Crazing	Occurs in high-impact plastics due to the combined effect of stress and aggressive environment. Crazes degenerate into microcracks which grow further, resulting in fracture
3.	Fatigue	Beachmarks appear as in the case of metals. Detailed mechanism of crack growth differs from metals and fatigue failure in polymers is not characterized by an endurance limit
4.	Thermal and residual stress	Results in change in dimensions of the material or a fixture and hence a loss in its function
5.	Physical aging	Occurs below glass transition temperature T_g and material becomes brittle
6.	Moisture effect	Lowering of T_g, increase in ductility, loss of creep resistance
7.	Photodegradation	Results in reduced strength, increased brittleness
8.	Chemical attack	Embrittlement, reduction in mechanical strength

The various methods used in failure analysis of polymeric materials are noted below:

Technique	Features
Infrared (IR) and Fourier transform infrared (FTIR) spectroscopy	Identification of functional groups in the polymer
Nuclear magnetic resonance spectroscopy (NMR)	Hydrogen in different chemical environments
Light scattering method	Molecular weight and molecular weight distribution
Differential scanning Calorimetry (DSC)	Heat of polymerization, fusion T_g, T_m
Differential thermal analysis (DTA)	Transition temperature T_g, melt/crystallization temperature T_m
Thermomechanical Analysis (TMA)	Penetration temperature, expansion coefficient
Dynamic mechanical analysis (DMA)	Elastic modulus, loss modulus
Thermogravimetric analysis (TGA)	Composition, weight loss as a function of temperature
X-ray diffraction analysis	Crystalline polymer component
Scanning electron microscopy	Surface morphology
Transmission electron microscopy	Polymer morphology
X-ray photoelectron spectroscopy	Elemental concentration; oxidation state
Auger electron spectroscopy	Elemental concentration

In the case of failure of a pipe made of polymeric material, the determination of T_g and T_m by thermochemical methods to ascertain the effects of thermal effects, determination of molecular weight and molecular weight distribution of the polymer, morphology of the sample or structure such as crystallinity and amorphous nature help to establish the cause of failure.

2.3.9 Failure Analysis of Ceramic Materials

The general principles involved in the failure analysis of ceramic materials are similar to the failure analysis of metals and alloys. Because of the brittle behavior of ceramic materials, failure may result in many pieces of the sample, which have to be reassembled in order to obtain information on the form of loading and the point of fracture initiation. The utmost care should be exercised in the reassembly of the fractured pieces so that the features of the fracture are preserved.

Crack branching is a common feature in failure of ceramic components. Cracks branch at a critical velocity, which is of the order of half the speed of sound in the specific glass under study. The acceleration of crack initiation to the critical velocity depends on the energy dissipation available from the release of stored energy. The energy source can be applied stress, prestressing or residual stress.

A crack in a ceramic material upon initiation may accelerate and interact with microstructure, stress field and the generated acoustic vibrations. These interactions may lead to some fractographic features such as fracture mirror, hackle or river patterns and Wallner lines.

Some typical features of fracture origin such as internal or surface crack are shown in Figure 2.32. The fracture mirror is a smooth surface formed when an internal crack travels radially outwards upon acceleration. Then it starts to deviate from the original plane upon reaching a critical velocity, and intersects with the microstructural features such as inclusion or precipitate. This may also occur as the direction of principal tensile

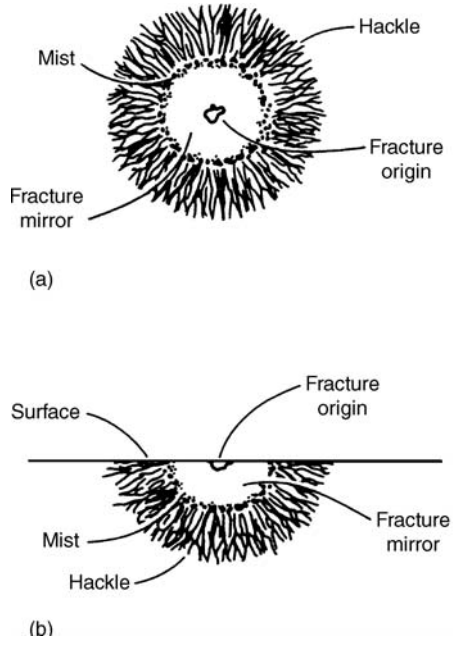

Figure 2.32 *Schematic showing typical fracture features surrounding the fracture origin in a ceramic material: (a) internal crack origin; (b) surface crack initiation. (Reprinted with permission from ASM International. All rights reserved www.asminternational.org)*

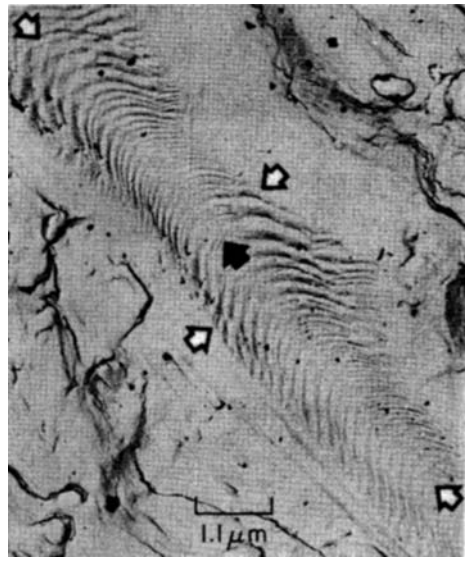

Figure 2.33 *Wallner lines (between white arrows) on the fracture surface of an aluminum alloy A356-T6 casting. The black arrow indicates the direction of crack propagation. (Reprinted with permission from ASM International. All rights reserved www.asminternational.org)*

stress changes. As a consequence small ridges are formed on the fracture plane. The ridges might look like mist on glass and later develop into hackle, comprised of ridges, which on coalescence give a smooth surface or larger steps.

Wallner lines are formed when sonic waves generated during fracture interact with principal stress driving the propagating crack front. Wallner lines appear as a series of arc shaped steps as shown in Figure 2.33.

The first and foremost step in failure analysis of ceramics consists of identifying the fracture origin and the type of cracking, which throws light on the type of failure such as failure due to impact, residual stress combined with load, thermal shock, improper machining, oxidation and corrosion. This is aided by micro- and macrofractography, examination of microstructure by SEM, chemical analysis and metallographic examination.

References

1. ISO 7539, *Corrosion of Metals and Alloys-Stress Corrosion Testing*, International Organization for Standardization, Geneva, Switzerland, 1989.
2. G49, *Standard Practice for Preparation and Use of Direct Tension Stress-Corrosion Test Specimens*, ASTM, West Conshohoken, PA, 1995.
3. TMO 177-96, *Testing of Metals for Resistance to Sulphide Stress Cracking at Ambient Temperature*, NACE International, Houston, TX, 1996.
4. G139, *Standard Test Method for Determining Stress Corrosion Resistance of Heat-Treatable Aluminum Alloy Products using Breaking Load Method*, ASTM, West Conshohoken, PA, 1996.

5. G39, *Standard Practice for Preparation and Use of Bent-Beam Stress-corrosion Test Specimens*, ASTM, West Conshohoken, PA, 1999.
6. G38, *Standard Practice for Making and using C-Ring Stress-Corrosion Test Specimens*, ASTM, West Conshohoken, PA, 1995.
7. G30, *Standard Practice for making and using U-bend Specimens for Stress-Corrosion Testing*, ASTM, West Conshohoken, PA, 1997.
8. G129, *Standard Practice for Slow-Strain Rate Testing to Evaluate the Susceptibility of Metallic Materials to Environmentally Assisted Cracking*, ASTM, West Conshohoken, PA, 1995.
9. TMO 198-98, *Slow Strain Rate Test Method for Screening Corrosion Resistant Alloys for Stress-Corrosion Cracking in Sour Oil Field Service*, NACE International, Houston, TX, 1998.
10. E399, *Standard Test Method for Plane-strain Fracture Toughness of Metallic Materials*, ASTM, West Conshohoken, PA, 1997.
11. GXXX, *Standard Practice for Making and using Precracked Double Beam Stress Corrosion Specimens*, ASTM, West Conshohoken, PA, 1999.
12. J.F. Stanners, *Corrosion and Protection of Metals*, The Institution of Metals, Iliffe Books, London, 1965, p. 88.
13. ISO 9223, *Corrosion of Metals and Alloys-corrosivity of Atmospheres-classification*, Geneva, Switzerland: ISO, 1992.
14. ISO 9225, *Corrosion of Metals and Alloys-corrosivity of Atmospheres Measurement of Pollution*, Geneva, Switzerland, 1992.
15. ISO 9226, *Corrosion of Metals and Alloys, Corrosivity of Atmospheres, Determination of Corrosion Rate of Standard Specimens for the Evaluation of Corrosivity*, Geneva, Switzerland, 1992.
16. ISO 9224, *Corrosion of Metals and Alloys-corrosivity of Atmosphere Guiding Values for the Corrosive Categories*, Geneva, Switzerland, 1992.
17. ASTM G92, *Standard Practice for Characterization of Atmospheric Test Sites*, West Conshohoken, PA, 1992.
18. ASTM G84, *Standard Practice for Measurement of Time-of-Wetness on Surfaces Exposed to Wetting Conditions as in Atmospheric Corrosion Testing*, West Conshohoken, PA, 1993.
19. ASTM G91, *Monitoring Atmospheric SO_2 using the Sulphation Plate Technique*, West Conshohoken, PA, 1992.
20. M.R. Foran, E.V. Gibbons and J.R. Wellington, *Chem. Can*, **10**, 33 (1958).
21. ASTM G116, *Standard Practice for Conducting Wire-on-Bolt Test for Atmospheric Galvanic Corrosion*, West Conshohoken, PA, 1993.
22. G.E.P. Box, W.G. Hunter and J.S. Hunter, *Statistics for Experimenters*, John Wiley & Sons, Inc., NY, 1978.
23. D.C. Montgomery, *Design and Analysis of Engineering Experiments*, 2nd edn, John Wiley & Sons, Inc., NY, 1984.
24. M.G. Natrella, Experimental Statistics, National Bureau of Standards, *Handbook 91*, Washington, DC, 1963.
25. H.H. Lawson, *Atmosphere Corrosion Test Methods*, NACE International, Houston, TX, 1995.
26. ASTM G61, *Standard Practice for Preparing, Cleaning and Evaluating Corrosion Test Specimens*, West Conshohoken, PA, 1990.
27. ASTM G50, *Standard Practice for Conducting Atmospheric Corrosion Tests on Metals*, West Conshohoken, PA, 1992.
28. ASTM G33, *Standard Practice for Recording Data from Atmospheric Corrosion Tests of Metallic-coated Steel Specimens*, West Conshohoken, PA, 1988.
29. ASTM G107, *Standard Guide for Formats for Collection and Compilation of Corrosion Data for Metals for Computerized Database Input*, West Conshohoken, PA, 1995.
30. S.W. Dean Jr., *Materials Performance*, **27**(10), 56, **27**(11), 64, **27**(12), 35 (1988); **28**(1), 52 (1989).
31. H.P. Hack, *Galvanic Corrosion Testing Methods*, NACE International, Houston, TX, 1993.
32. ASTM G71-81, *Standard Guide for Conducting and Evaluating Galvanic Corrosion Tests in Electrolytes*, Philadelphia, PA, 1981.
33. ASTM G82-83, *Standard Guide for Development and use of a Galvanic Series for Predicting Galvanic Corrosion Performance*, Philadelphia, PA, 1983.

34. ISO 7441-84, *Corrosion of Metals and Alloys Determination of Bimetallic Corrosion in Outdoor Exposure Tests*, Geneva, Switzerland, 1984.
35. ASTM G104-89, *Standard Test Method for Assessing Galvanic Corrosion caused by the Atmosphere*, Philadelphia, PA, 1989.
36. G.E. Hale, *A Testing Protocol for conducting J-crack Growth Resistance Curve Tests on Plastics*, ESIS Draft Protocol, May 1994.
37. R.P. Champion, *Cellular Polymers*, **9**, 206 (1990).
38. A.N. Gent and D.A. Tompkins, *J. Appl. Phys.*, **40**, 2520 (1969).
39. A. Stevenson and G.J. Morgan, *Rubber Chem. Tech.*, **68**, 197 (1995).
40. B.J. Briscoe, T. Savvas and C.T. Kelly, *Rubber Chem. Tech.*, **67**, 384 (1994).
41. R. Campion, *Model Test 'oils' based on Solubility Parameters for Artificial Ageing of Polymers*, Proc. of the Conference on Polymer Testing, 1996, Shawberry, Sept. 9, 1996, RAPRA, Shrewsbury, UK, 1996, pp. 1.5.
42. B. Thompson and R.P. Campion, MERL Ltd., Hertford, UK.
43. R. Crescent and M. Rigaud, *Proceedings of the International Conference on Advances in Refractories for the Metallurgical Industries*, 26th Annual Conference of Metallurgists, CIM, Montreal, Quebec, 1988, pp. 235–250.
44. *American Society for Testing and Materials*, Vol. 15, No. 1, Philadelphia, PA, USA.
45. R.A. McCauley, *Corrosion of Ceramics*, Marcel Dekker, New York, 1995.
46. V.S. Sastri, *Corrosion Inhibitors, Principles and Applications*, John Wiley & Sons, Ltd, Chichester, UK, 1998.
47. *ASM Metals Handbook*, Vol. 17, 9th edn, 1989.
48. D. Belforte, *Industrial Laser Annual Handbook*, Vol. 629, Pennwell, 1986.
49. *Nondestructive Testing: A Survey*, NASA SP-5113, National Aeronautics and Space Administration, 1973.
50. D. Hagemaier, B. Bates and A. Steinberg, *On-Aircraft Eddy Current Inspection*, Paper 7680, McDonnell Douglas Corp., 1986.
51. Y. Bar-Cohen and A.K. Mal, *ASM Metals Handbook*, Vol. 17, 9th edn, 1989.
52. Nondestructive Testing, General Dynamics, 1981.
53. Accoustic Emission Testing, Vol. 5, *Non-Destructive Testing Handbook*, R.K. Miller and P. McIntyre (eds.), American Society for Non-Destructive Testing, 1987.
54. S.L. McBride, Procedings of the World Meeting on Acoustic Emission, *ASM Handbook*, Vol. 17, 9th edn, Charlotte, NC, March 1989.
55. T.J. Fowler, Progress in Acoustic Emission, *Proceedings of 9th International, Acoustic Emission Symposium*, The Japanese Society of Non-Destructive Inspection, 1988, pp. 391–404.
56. A.A. Pollock, Acoustic Emission Inspection, *ASM Metals Handbook*, Vol. 17, 1989.
57. E. Hinton and D.R.J. Owen, *An Introduction to Finite Element Computations*, Pineridge Press Ltd., Swansea, UK, 1979.
58. ADINA User Interface Primer, Report ARD 02-6, Adina R&D Inc., Watertown, MA 02472, USA, Sept. 2002.
59. G. Shen, CANMET, Private Communications, Ottawa, Ontario, CANADA.
60. J.W. Dally and W.F. Riley, *Experimental Stress Analysis*, 2nd edn, McGraw-Hill, 1978.
61. F. Zandman, S. Redner and J.W. Dally, *Photoelastic Coatings*, The Iowa State University, Press, 1977.
62. H. Kaplan and R. Friedman, *Material Evaluation*, Vol. 39, February 1980, pp. 175–179.
63. E.P. Papadakis, H.L. Chesney and R.G. Hurley, *Material Evaluation*, Vol. 42, March 1984, pp. 333–6.
64. P. Cielo et al., *Material Evaluation*, Vol. 45, April 1987, pp. 452–460.
65. M. Belassel, M.E. Brauss and S.G. Berkley, Procurement of ICRS 6 (Oxford), 2000, pp. 144–151.
66. S.G. Berkley, *9th International Symposium on Transport Phenomena and Dynamics of Rotating Machinery*, ISROMAC-9, Honolulu, 2002.
67. M. Zoccola, Division Trio received Navy Superior Award, Wavelengths – An Employee Digest of Events and Issues, August 1999.

68. X.J. Zhang and M. Gaudet, Wavelengths – An Employee Digest of Events and Issues, Jan/Feb, 1999.
69. S.R. Paterson, T.A. Kuntz, R.S. Moser and H. Vaillancourt, Boiler Tube Failure Metallurgical Guide, TR-102433, Electric Power Research Institute, 1993.
70. A.T. Riga and E.A. Collins, Analysis of Structure, Engineering Plastics, Vol. 2, *Engineered Materials Handbook*, ASM International, 1988, pp. 824–837.

3

Regulations, Specifications and Safety

Industrial operations are generally controlled to serve the interests of the industrial organization, the working personnel and the consumers of the output product, namely the public, in a balanced manner. Industry is governed by certain regulations and specifications; industry operates in accordance with rules, known as regulations, and the contents of the rules, known as specifications. The specifications consist of series of steps or procedures to be adhered to by the operator. By following the regulations and the applicable specifications, the industrial operations can be conducted in a safe and sound manner. This implies that a code of regulations and specifications are developed with safety as the most important factor underlying the code along with the optimum function of the operation.

In every country there is an organization that has developed and specified standards under the umbrella of a national standards organization. Some standards developed by national organizations are:[1–3]

(i) American Society of Mechanical Engineers (ASME) on pressure vessels;
(ii) The UK statutory instrument 1991 No. 2749 on the simple pressure vessels (safety) regulations;
(iii) Canadian Standards Association, CAN 3-Z 299-1-85 on Quality Assurance Program, categories 1–4

In addition to these other relevant organizations are: (i) American Society of Testing and Materials (ASTM), Philadelphia; (ii) American Standards National Institute (ANSI), Washington; and (iii) International Standards Organization (ISO), Geneva, Switzerland. It is necessary to recognize the important role played by regulations and specifications, in spite of the fact they may appear uninteresting and dull.

3.1 Regulations and Specifications

As a result of serious accidents in the operation of steam boilers in an industrial environment, the need for a code of regulations and specification for the fabrication and safe

Corrosion Prevention and Protection: Practical Solutions V. S. Sastri, E. Ghali and M. Elboujdaini

operation of pressure vessels was recognized by the American Society of Mechanical Engineers (ASME), which resulted in the ASME boiler and pressure vessel code. The 1992 ASME boiler and pressure vessel code[2] consists of 11 sections, as detailed below:

1. Power boilers
2. Materials
   - Part A, Ferrous material specifications
   - Part B, Nonferrous material specifications
   - Part C, Specifications for welding rods, electrodes and filler metals
   - Part D, Properties
3. Subsection NCA – General requirements for divisions 1 and 2
   - Division 1
     - Subsection – Class 1 component
       - Class 2 components
       - Class 3 components
       - Class MC components
       - Component supports
       - Core support structures
   - Division 2 – Code for concrete reactor vessels and containments
4. Heating boilers
5. Nondestructive examination
6. Recommended rules for the care and operation of heating boilers
7. Recommended guidelines for the care of power boilers
8. Division 1. Pressure vessels
   Division 2. Alternate rules for pressure vessels
9. Welding and brazing qualifications
10. Fiber-reinforced plastic pressure vessels
11. Rules for inservice inspection of nuclear power plant components

The ASME code consists of establishing the rules of safety governing the: (i) design; (ii) fabrication; (iii) inspection during construction (materials, design, fabrication, examination, inspection, testing, certification and pressure relief) of boilers and pressure vessels. The rules were formulated to meet the needs and objectives of users, manufacturers and inspectors of pressure vessels. The formulated rules afford reasonable protection of life and property and provide a margin for deterioration in service in the useful lifetime. Any pressure boiler that is fabricated must meet the specifications and, after inspection, it is certified and provided with a stamp of approval.

The Canadian counterpart in Ontario is the Ministry of Consumers Affairs and Customer Relations, Pressure Vessels Branch. The pressure vessels acquired must meet with the requirements specified and stipulated by the ministry.

The corresponding code for simple pressure vessels in United Kingdom[3] is contained in the Statutory Instrument 1991, No. 2749. The schedule 1 consists of essential safety requirements. Some of the essential features covered by the Statutory Instrument are:

Part 1 Materials:
- Pressurized components
- Steel vessels
- Aluminum vessels
- Welding materials

	Accessories contributing to the strength of the vessels
	Non-pressurized components
Part 2	Vessel design
	Minimum and maximum working temperature
	Maximum working pressure
	Access for inspection of inside
	Ease of draining the vessels
	Optimum mechanical properties
	Resistance to corrosion in the intended environment
	Avoidance of stresses which impair safety, working pressure not to exceed the maximum pressure, circular and longitudinal seams made with penetration welds or welds of equivalent effectiveness
	Wall thickness is either calculated or experimentally determined. It is determined to enable vessels to resist five times the maximum working pressure
Part 3	Manufacturing processes
	Preparation of the components
	Welds on pressurized components be made by a qualified welder. The welds and adjacent zones must be free of surface or internal defects.
Part 4	Definitions and symbols
Definitions:	Minimum working temperature, inspection slip, maximum working temperature, maximum working pressure, yield strength at maximum working temperature are defined.
Symbols	A percentage elongation after rupture, where L is the gauge length in millimetres, S is the cross-sectional area of the sample in mm^2; A_{80mm} is the percentage elongation after rupture ($L_0 =$ 80 mm).

Quality assurance is part of the regulations specified by the national standards organizations such as the Nuclear Regulatory Commission. Quality assurance applies to any material or component or a fabricated structure in the sense that their satisfactory performance in service conditions is assured. The quality assurance and control programs in Canada are contained in Canadian Standards Association document CAN3-Z 299.1-85 consisting of four parts. The four parts of the standard are such that Part 1 covers quality assurance, Part 2 refers to quality control, Part 3 refers to quality verification, and Part 4 deals with quality inspection.

The quality assurance program consists of making sure that the products or services such as management, design and technical responsibility for quality are integrated and executed effectively. In general the program is preventive by controlling design and production processes as well as an inspection and test verifications, which assure that the products conform to specifications and readily detect and control the disposition of nonconformance and prevent recurrence.

The responsibilities of customers and suppliers of the service are clearly defined, along with the regulatory requirements of federal, provincial, territorial and municipal Acts,

Bylaws and codes that apply to the products or services. The quality assurance program elements consist of: (i) design planning, design input, preliminary design, detailed design, design output, design verification and any design changes; (ii) documentation such as quality assurance manual, quality assurance procedures, inspection and test plan; (iii) means to assure access to measuring and test equipment for verifying the product or service quality; and (iv) inspection of incoming products or services as required by the inspection and test plan including in-process and final inspection. It is also required that records of quality obtained as a result of tests and inspection are maintained with respect to the product or services.

Products or services that do not conform to the quality standards are identified and the supplier notified so that a remedial action is taken. The code gives procedures for dealing with nonconforming products, along with the necessary corrective action.

The use of statistical techniques for identifying and classifying products, process or services as a basis for quality assurance and acceptance or rejection is included in the code.

The internal and external quality audit as per the appropriate clause in the CSA standard CAN 3-Q395 may assure that the quality standards are met in the particular situation.

The foregoing discussion on quality assurance clearly shows the responsibilities of the consumer and supplier in maintaining the standards. It is needless to state that the responsibilities of both the consumer and supplier are clearly understood before embarking on implementation of a specific program. In any program of quality assurance the main factors are: (i) complexity of design; (ii) design maturity; (iii) complexity of the manufacturing process; (iv) nature of components or service; (v) safety considerations; and (vi) economics. A judicious mix of factors is to be used in the quality program that is chosen in a particular situation.

In general a quality assurance program consist of: (i) input from quality control manager; (ii) approved design specifications and calculations; (iii) control and procurement of materials in compliance with the code regulations; (iv) approved flowcharts for process control; (v) checking for nonconformity and provide necessary corrective action; (vi) checking for aspects such as weld quality and heat treatment of components in some cases; (vii) use of measuring and test equipment; (viii) maintaining all the pertinent documents of details of the procedures calculations; and (ix) periodic audits which may be necessary to assure quality control.

The single most important underlying factor of a code of regulations and specifications is safety. Most industrial organizations develop and maintain engineering standards, which are improved continuously with time. This enables the industrial organization to keep pace with progress in safe design and newer standards developed by the various standards organizations. It is also mandatory that industries have their own designated personnel such as inspection committees to oversee the operations. It is also possible in some circumstances for the industrial organizations to develop procedures of inspection and operation far more stringent than the regulated standards; an example is the use of material with greater corrosion resistance than the conventionally recommended material.

The materials delivered by the suppliers should conform to standard specifications such as corrosion resistance, chemical composition, and performance in standard tests in intended atmospheres, other properties such as mechanical properties and any other relevant properties. It is the responsibility of the suppliers to ensure that the materials supplied conform to the specified standards.

3.2 Safety Considerations

Safety and its practice are of the utmost importance for corrosion personnel, both in the corrosion laboratory and plant operations. The subject appears mundane at first glance although in realistic terms it is of paramount importance when factors such as loss of life due to accidents by nonadherence of personnel to prescribed safety procedures in laboratories and industrial operations are considered. The safety procedures used in the laboratory and field operation are intended to be preventive measures to avoid the occurrence of accidents, which may result in injury or loss of life, depending upon the nature of the accident.

The importance of safety and its practice is related to the risk and hazards involved in a particular operation. Corrosion personnel, in common with other engineers, are faced with hazards and the extent of hazards, and the severity is the decisive factor in determining the fatality rates. Thus in any industrial operation it is necessary to: (i) identify the hazard; and (ii) take necessary action to prevent the occurrence of the hazard. The identification and remedial steps taken to prevent the occurrence of the hazard is of paramount importance in loss prevention. Along with increased advances in technology, the identification of hazards has also become increasingly difficult. Loss prevention depends upon the management system. The physical hazards also may not be on the surface and thus inaccessible to a simple visual inspection.

There exists a whole battery of methods for the identification of hazards in the literature.[4] The hazard identification techniques suitable for various stages of a project are shown in Table 3.1. Among the techniques noted in Table 3.1 the most important method is safety audits, which cover the management system and specific technical features at site level and the management system at plant level.

The principal elements of audit are: (i) identification of possible hazards; (ii) assessment of the potential consequences of realization of the hazards; (iii) selection of measures to minimize frequency and consequences of realization; (iv) implementation of the measures; and (v) monitoring the changes. A typical listing of activity standards for safety audits is given in Table 3.2. The activity standards cover the organization and the activity standard, industrial hazard control, fire control and industrial hygiene and the participation, motivation and training of supervisors in the organization along with the rating, ranging from poor to excellent.

Earlier method of identifying hazards involved a procedure consisting of asking questions such as: ‘what if’? This approach consists of questioning the proper function at every stage of the process, along with consequences or the remedial features. A checklist for the simplified process hazard analysis by the ‘what if?’ method is shown in Table 3.3. Although this method is an old method of hazard analysis compared with other methods such as hazop or fault tree analysis it has proven to be quite useful.

The hazard analysis of any industrial process impacts on risk assessment. Risk assessment involves the estimation of the frequency and consequences of a range of hazard scenarios and of individual and societal risk. The risk assessment process is shown in Figure 3.1. The risk criterion used in hazard analysis is the fatal accident rate (FAR). The FAR is defined as the number of fatalities per 10^8 h exposure. The actual FAR in the U.K. was 3.5 in the chemical industry in 1975. No doubt the ideal FAR value should be zero, which is difficult to achieve in practice.

Table 3.1 *Hazard identification techniques appropriate to different project stages*

Project stage	Hazard identification technique
All stages	Management and safety system audits
	Checklists
	Feedback from workforce
Research and development	Screening and testing for:
	Chemicals (toxicity, instability, explosibility
	Reactions (explosibility)
	Impurities
	Pilot plant
Pre-design	Hazard indices
	Insurance assessments
	Hazard studies (coarse scale)
Design	Process design checks
	Unit processes
	Unit operations
	Plant equipments
	Pressure systems
	Instrument systems
	Hazard and operability studies (fine scale)
	Failure modes and effects analysis
	Fault trees and event trees
	Hazard analysis
	Reliability assessments
Commissioning	Operator task analysis and operating instructions
	Checks against design, inspection, examination and testing
	Nondestructive testing, condition monitoring
	Plant safety audits
	Emergency planning
Operation	Inspection, testing
	Nondestructive testing, condition monitoring, corrosion monitoring, malfunction detection, plant degradation audits
	Plant safety audits

The individual hazard index (IHI) is the number of fatal injuries per 10^8 h exposure. The process hazard index (PHI) is defined as the number of years per fatal injury associated with the process. One of the disadvantages with PHI is that the industrial processes do not have long enough lifetimes to give statistically useful information. Another concept that is used is the average interval between two incidents (IBI). Some major companies have accepted a value of 10^8 h for the IBI. It is useful to compare individual risks in various facets of activity[7] (Table 3.4).

The risks associated with various activities are obvious from Table 3.4. It is clear that normal activities such as aging, driving a car or flying are high-risk activities and process hazards and light industry exposure are of less severity than the first group, but more serious than natural disasters. Certainly, it is no consolation that the process hazard indices and individual hazard indices are better than aging, aviation and auto driving indices since ideally they should be comparable in values to those of natural disasters, if

Table 3.2 *Activity standards for safety audits*[5]

Activity	Poor	Fair	Good	Excellent
A. Organization and administration				
1. Statement of policy, responsibilities assigned	No statement of loss control policy, responsibility and accountability not assigned	A general understanding of loss control, responsibilities and accountability, but not written	Loss control policy and responsibilities written and distributed to supervisors	In addition to 'good', loss control policy is reviewed annually and is posted. Responsibility and accountability is emphasized in supervisory performance evaluations
2. Safe operating procedures (SOPs)	No written SOPs	Written SOPs for some, but not all hazardous operations	Written SOPs for all hazardous operations	All hazardous operations covered by a procedure, posted at the job location, with an annual documented review to determine adequacy
3. Employee selection and placement	Only pre-employment physical examination given	In addition, an aptitude test is administered to new employees	In addition to 'fair', new employees' past safety record is considered in their employment	In addition to 'good', when employees are considered for promotion, their safety attitude and record is considered
4. Emergency and disaster control plans	No plan or procedures	Verbal understanding on emergency procedures	Written plan outlining the minimum requirements	All types of emergency covered with written procedures. Responsibilities are defined with back-up personnel provisions
5. Direct management involvement	No measurable activity	Follow-up on accident problems	In addition to 'fair', management reviews all injury and property damage reports and holds supervision accountable for verifying firm corrective measures	In addition to 'good', reviews all investigation reports. Loss control problems are treated as other operational problems in staff meeting

(*contd.*)

Table 3.2 *(contd.)*

Activity	Poor	Fair	Good	Excellent
6. Plant safety rules	No written rule	Plant safety rules have been developed and posted	Plant safety rules are incorporated in the plant work rules	In addition, plant work rules are firmly enforced and updated at least annually
B. Industrial hazard control				
1. Housekeeping storage of materials, etc.	Housekeeping is generally poor. Raw materials, items being processed and finished materials are poorly stored	Housekeeping is fair. Some attempts to adequately store materials are made	Housekeeping and storage of materials are orderly. Heavy and bulky objects well stored out of aisles, etc.	Housekeeping and storage of materials are ideally controlled
2. Machine guarding	Little attempt is made to control hazardous points on machinery	Partial but inadequate or ineffective attempts at control are in evidence	There is evidence of control which meets applicable Federal and State requirements, but improvement may still be made	Machine hazards are effectively controlled to the extent that injury is unlikely. Safety of operator is given prime consideration at time of process design
3. General area guarding	Little attempt is made to control such hazards as: unprotected floor openings, slippery or defective floors, stairway surfaces, inadequate illumination, etc.	Partial, but inadequate attempts to control these hazards are evidenced	There is evidence of control, which meets applicable Federal and State requirements, but further improvement may still be made	These hazards are effectively controlled to the extent that injury is unlikely
4. Maintenance of equipment, guards, handtools, etc.	No systematic programme of maintaining guards, handtools, controls and other safety features of equipment, etc.	Partial but inadequate or ineffective maintenance	Maintenance program for equipment and safety features is adequate. Electrical handtools are tested and inspected before insurance, and on a routine basis	In addition to 'good', a preventive maintenance system is programmed for hazardous equipment and devices. Safety reports filed and safety department consulted when abnormal conditions are found

5. Material handling hand and mechanized	Little attempt is made to minimize possibility of injury from the handling of materials	Partial, but inadequate or ineffective attempts at control are in evidence	Loads are limited as to size and shape for handling by hand, and mechanization is provided for heavy or bulky loads	In addition to controls for both hand and mechanized handling, adequate measures prevail to prevent conflict between other workers and material being moved
6. Personal protective equipment for adequacy and use	Proper equipment not provided or is not adequate for specific hazards	Partial, but inadequate or ineffective provision, distribution and use of personal protective equipment	Proper equipment is provided. Equipment identified for special hazards, distribution of equipment is controlled by supervisor. Employee is required to use protective equipment	Equipment provided complies with standards. Close control maintained by supervision. Use of safety equipment recognized as an employment requirement. Injury record bears this out
C. Fire control and industrial hygiene				
1. Chemical hazard control references	No knowledge or use of reference data	Data available and used by foremen when needed	In addition to 'fair', additional standards have been requested when necessary	Data posted and followed where needed. Additional standards have been promulgated, reviewed with employees involved and posted
2. Flammable and explosive materials control	Storage facilities do not meet fire regulations. Containers do not carry name of contents. The approved dispensing equipment not used. Excessive quantities permitted in manufacturing areas	Some storage facilities meet minimum fire regulations. Most containers carry name of contents. Some approved dispensing, equipment in use.	Storage facilities meet minimum fire regulations. Most containers carry name of contents. Approved equipment generally is used. Supply at work area is limited to one-day requirement. Containers are kept in approved storage cabinets.	In addition to 'good', storage facilities exceed the minimum fire regulations and containers are always labelled. A strong policy is in evidence relative to the control of the handling, storage and use of flammable materials

(*contd.*)

Table 3.2 (*contd.*)

Activity	Poor	Fair	Good	Excellent
3. Ventilation – fumes, smoke and dust control	Ventilation rates are below industrial hygiene standards in areas where there is an industrial hy giene exposure	Ventilation rates in exposure areas meet minimum standards	In addition to 'fair', ventilation rates are periodically measured, recorded and maintained at approved levels	In addition to 'good', equipment is properly selected and maintained close to maximum efficiency
4. Skin contamination control	Little attempt at control or elimination of skin irritation exposures	Partial, but incomplete program for protecting workers. First-aid reports on skin problems are followed up on an individual basis for determination of cause	The majority of workers instructed concerning skin-irritating materials. Workers provided with approved personal protective equipment or devices. Use of this equipment is enforced	All workers informed about skin-irritating materials. Workers in all cases provided with approved personal protective equipment or devices. The use of proper equipment enforced and facilities available for maintenance. Workers are encouraged to wash skin frequently. Injury record indicates good control
5. Fire control measures	Do not meet minimum insurance or municipal requirements	Meet minimum requirements	In addition to 'fair', additional fire hoses and/or extinguishers are provided. Welding permits issued and extinguishers on all welding carts	In addition to 'good', a fire crew is organized and trained in emergency procedures and in the use of fire fighting equipment
6. Waste – trash collection and disposal, air/water pollution	Control measures are inadequate	Some controls exist for disposal of harmful wastes or trash. Controls exist but are ineffective in methods or procedures of collection and disposal. Further study is necessary	Most waste disposal problems have been identified and control programmes instituted. There is room for further improvement	Waste disposal hazards are effectively controlled. The air/water pollution potential is minimal

D. Supervisory participation, motivation and training

1.	Line supervisor safety training	Not all supervisors have received basic safety training	All shop supervisors have received some safety training	All supervisors participate in division safety training session a minimum of twice a year	In addition, specialized sessions conducted on specific problems
2.	Indoctrination of new employees	No program covering the health and safety job requirements	Verbal only	A written handout to assist in indoctrination	A formal indoctrination program to orient new employees is in effect
3.	Job hazard analysis	No written program	Job hazard analysis (JHA) program being implemented on some jobs	The JHA conducted on a majority of operations	In addition, job hazard analyses performed on a regular basis and safety procedures written and posted for all operations
4.	The training for specialized operations (fork trucks, grinding, press brakes, punch presses, solvent handling, etc.)	Inadequate training given for specialized operations	An occasional training programme given for specialized operations	The safety training is given for all specialized operations on a regular basis and retraining given periodically to review correct procedures	In addition to 'good', an evaluation is performed annually to determine training needs
5.	Internal self-inspection	No written program to identify and evaluate hazardous practices and/or conditions	The plant relies on outside sources (i.e., Insurance Safety Engineer) and assumes each supervisor inspects his area	A written programme outlining inspection guidelines, responsibilities, frequency and follow-up is in effect	The inspection programme is measured by results (i.e., reduction in accidents and costs). Inspection results are followed up by top management
6.	Safety promotion and publicity	Bulletin boards and posters are considered the primary means of safety promotion	Additional safety displays, demonstrations, films are used infrequently	Safety displays and demonstration are used on a regular basis	Special display cabinets, windows, etc., are provided. Displays are used regularly and are keyed to special themes

(*contd.*)

Table 3.2 *(contd.)*

Activity	Poor	Fair	Good	Excellent
7. Employee – supervisor safety contact and communication	Little or no attempt made by supervisor to discuss safety with employees	Infrequent safety discussions between supervisor and employees	Supervisors regularly cover safety when reviewing work practices with individual employees	In addition to items covered under 'good', supervisors make good use of the shop safety plan and regularly review job safety requirements with each worker. They contact at least one employee daily to discuss safe job performance
E. Accident investigation, statistics and reporting procedures				
1. Accident investigation by line personnel	No accident investigation made by line supervision	The line supervision makes investigation of only medical injuries	The line supervision is trained and makes complete and effective investigations of all accidents; the cause is determined; corrective measures initiated immediately with a completion date firmly established	In addition to items covered under 'good', investigation is made of every accident within 24 h of occurrence. The department manager and the plant manager review the reports
2. Accident cause and injury location analysis and statistics	No analysis of disabling and medical cases to identify prevalent causes of accidents and location where they occur	Effective analysis by both cause and location maintained on medical and first-aid cases	In addition to effective accident analysis, results are used to pinpoint accident causes so accident prevention objectives can be established	Accident causes and injuries are graphically illustrated to develop the trends and evaluate performance. Management is kept informed on status
3. Investigation of property damage	No program	Verbal requirement or general practice to inquire about property damage accidents	Written requirement that all property damage accidents of US $50 and more will be investigated	In addition, management requires a vigorous investigation effort on all property damage accidents
4. Proper reporting of accidents and contact with carrier	Accident reporting procedures are inadequate	Accidents are correctly reported on a timely basis	In addition to 'fair', accident records are maintained for analysis	In addition to 'good', there is a close liaison with the insurance carrier

Table 3.3 *'What if?' method: checklist for simplified process hazard analysis[6] (Courtesy of the American Institute of Chemical Engineers)*

Storage of raw materials, products and intermediates	
Storage tanks	Design separation, inerting, materials of construction
Dikes	Capacity and drainage
Emergency valves	Remote control hazardous materials
Inspections	Flash arresters and relief devices
Procedures	Contamination prevention, analysis
Specifications	Chemical, physical and quality stability
Limitations	Temperature, time and quantity
Material handling	
Pumps	Relief, reverse, rotation, identification of materials of construction
Ducts	Explosion relief, fire protection and support
Conveyors, mills	Stop devices, coasting and guards
Procedures	Spills, leaks and decontamination
Piping	Rating, codes, cross-connections and materials of construction
Process equipment, facilities and procedures	
Procedures	Start-up, normal, shut-down and emergency
Conformance	Job audits, shortcuts and suggestions
Loss of utilities	Electricity, heating, coolant air, inerts and agitators
Vessels	Design, materials, codes, access and materials of construction
Identification	Vessels, piping, switches and valves
Relief devices	Reactors, exchangers, glassware
Review of incidents	Plant, company and industry
Inspections, tests	Vessels, relief devices and corrosion
Hazards	Hang-fires and runaways
Electrical	Area classification, conformance and purging
Process operating ranges	Temperature, pressure, flows, ratios, concentrations, densities, levels, time and sequence
Ignition sources	Peroxides, acetylides, friction, fouling, compressors, static electricity, valves and heaters
Compability	Heating media, lubricants, flushes and packings
Safety margins	Cooling and contamination
Personnel protection	
Protection	Barricades, personal, shower and escape aids
Ventilation	General, local, air intakes and rate
Exposures	Other processes and public environment
Utilities	Isolation: air, water, inerts and steam
Hazards manual	Toxicity, flammability, reactivity, corrosion, symptoms and first aid
Environment	Sampling, vapors, dusts, noise and radiation
Control and emergency devices	
Controls	Ranges, redundancy and fail-safe
Calibration, inspection	Frequency, adequacy
Alarms	Adequacy, limits, fire and fumes
Interlocks	Tests, bypass procedures

(*contd.*)

Table 3.3 (*contd.*)

Relief devices	Adequacy, vent size, discharge, drain and support
Emergencies	Dump, drown, inhibit and dilute
Process isolation	Block valves, fire-valves and purging
Instruments	Air quality, time lag, reset wind-up and materials of construction
	Waste disposal
Hatches	Flame traps, reactions, exposures and solids
Vents	Discharge, dispersion, radiation and mists
Characteristics	Sludges, residues and fouling materials
	Sampling facilities
Sampling points	Accessibility, ventilation and valving
Procedures	Pluggage, purging
Samples	Containers, storage and disposal
Analysis	Procedures, records and feedback
	Maintenance
Decontamination	Solutions, equipment and procedures
Vessel openings	Size, obstructions and access
Procedures	Vessel entry, welding and lockout
	Fire protection
Fixed protection	Fire areas, water demands, distribution system, sprinklers, deluge, monitors, inspection, testing, procedures and adequacy
Extinguishers	Type, location and training
Fire walls	Adequacy, condition, doors and ducts
Drainage	Slope, drain rate
Emergency response	Fire brigades, staffing and training equipment

not less. It is also useful to note that corrective action is deemed necessary when PHI falls below 10 000.

The general layout of an industrial process plant involves considerations of cost and safety. Some of the factors that contribute to safety and loss prevention are: (i) segregation of different risks; (ii) minimization of vulnerable pipework; (iii) containment of accidents; (iv) limitation of exposure; (v) efficient and safe construction; (vi) efficient

Table 3.4 *Risks associated with different activities*[7]

Activity	Exposure (h)	IHI	PHI
Aging	8760	180	60
Aviation	35	2500	1500
Auto driving	350	100	3000
Accidents at home	8760	3.0	4500
Exposure to process hazards	2200	1.5	30 000
Operators in light industry	2200	0.2	230 000
Natural disasters	8760	0.04	300 000

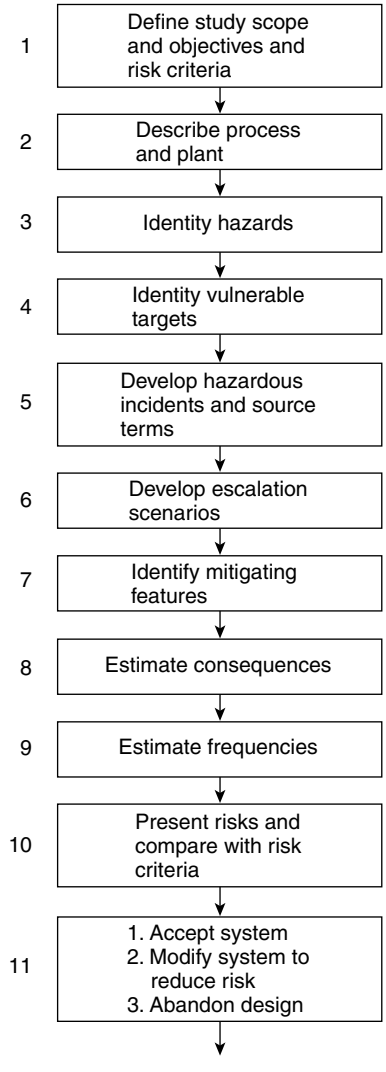

Figure 3.1 *The risk assessment process*

and safe operation; (vii) efficient and safe maintenance; (viii) safe control room design; (ix) emergency control facilities; (x) firefighting facilities; (xi) access for emergency services; and (xii) security.

The layout of the plant must be such that the PHI target minimum of 10 000 is maintained. A chemical process reactor with the possibility of failure by explosion and an IBI (interval between incidents) index of 10 000 y may be considered as an example, supposing that average number of personnel exposed is four. In such a case the process hazard index works out to 2500, which is less than the target value of 10 000. In order to achieve the target it may be necessary to decrease the number of workers

exposed to one, or to consider increasing the IBI value to much greater than 10 000. To achieve the required target PHI value of 10 000 it may also be necessary to incorporate changes in the layout.

3.2.1 Safety in the Corrosion Laboratory[9]

The laboratory must be designed with safety considerations as the guiding criterion. The normal laboratory requirements such as fume hoods should be provided. All hazardous chemical procedures such as handling of acids, gases such as hydrogen sulfide, flammable reagents, hazardous organic solvents must be done in fume hoods. It is imperative all the reagents are properly labeled with all the necessary warnings with respect to factors such as toxicity, flammability and related hazardous properties. Improperly labeled reagents, reagents of uncertain lifetime and chemical wastes must be stored in labeled waste containers and subjected to disposal method in accordance with waste disposal procedures and regulations.[8]

Hazardous wastes are characterized by their deleterious effects on human and animal life as well as on the ecosystem. The waste also may be flammable, explosive, corrosive, radioactive or irritant. It should also be recognized that the form and concentrations of the chemicals are of importance in classifying them as hazardous.

The personnel working in the corrosion laboratory are usually exposed to a variety of chemicals and gases. The monitoring of airborne contaminants is to ensure that potential employee exposures are controlled. It is also useful to monitor chemical exposure of personnel and to compare the levels with chemical exposure guidelines of National Institute for Occupational Safety and Health (NIOSH), Occupational Safety and Health Administration (OSHA) OSHA (29 CFR 910.1450, 29 CFR 1910.1048, 11910.1001-1101, Z9 CFR 1910, subpart Z and National Health Canada). It is also useful to perform a walkthrough check for hazardous chemicals and exposure of personnel to the chemicals, as shown in Figure 3.2.

Airborne contaminants can significantly impact on the work area, breathing zone and the air to which personnel are exposed. It is mandatory to carry out full-period consecutive sampling of air to obtain statistically representative results, as shown in Figure 3.3.

Some of the sources for obtaining chemical and gas monitoring equipment are noted below:

Calibration gases and equipment	Air Engineers Inc.
Carbon monoxide monitors and detectors	American Bristol Industries Inc.
Detector tubes	Ashland Chemicals
Formaldehyde monitors and detectors	Ashland Chemical Co.
	Direct Supply Co.
Hydrocarbon detectors and monitors	Andersen Samples Inc.
	CEA Instruments
	Bacharach Inc.
Infrared analyzers and sensors	Anacon
	Astro Resources International Group
	Delta Tehrmographics Inc.
Personal monitors	Air Quality Research
	Air Engineers Inc.

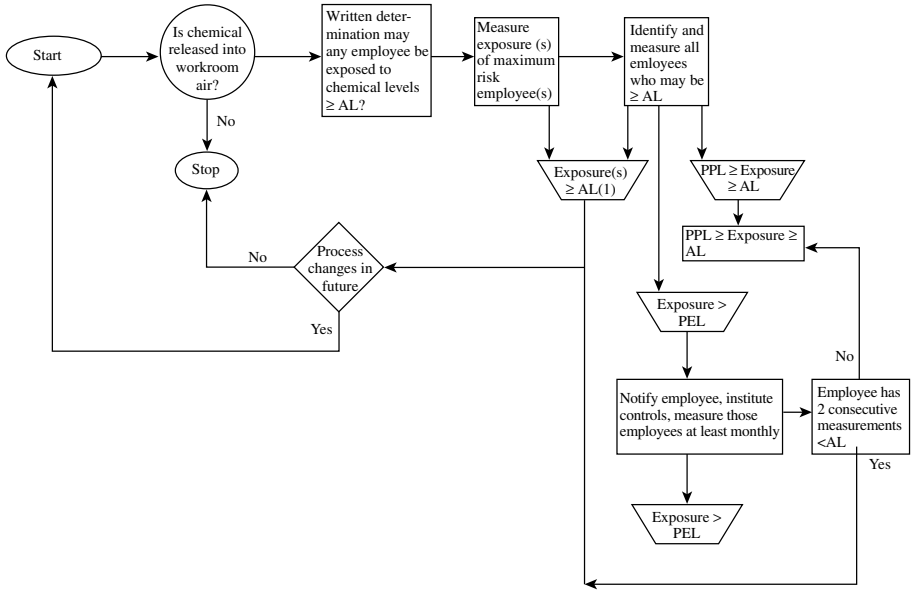

Figure 3.2 *NIOSH-recommended employee exposure determination and measurement strategy. AL = action level; PEL = permissible exposure limit. OSHA Laboratory Standard 29 CFR 1910.1450 requires employee notification of any monitoring results*

3.2.2 General Outline for a Model Chemical Hygiene Plan

The general hygiene plan involves both management and employees playing important roles. The initial step consists of policy, coverage and availability. Then, the organization, roles and responsibilities are defined in terms of: (i) chemical hygiene committee, chemical hygiene officer, laboratory management and laboratory employees; (ii) the management system policies, consisting of hazard identification, characterization and control involving chemical hygiene review committee and employee exposure determination. The employee information training and medical consultation and examinations form part of the policies; (iii) the laboratory practice policies, consisting of general chemical hygiene practices, housekeeping, inspections and glassware handling; (iv) signs, labels and keeping material safety data sheets; (v) procurement, receipt, distribution and storage of hazardous chemicals; (vi) handling and transport of hazardous chemicals; (vii) facility design, consisting of general laboratory ventilation, access and security; (viii) monitoring laboratory hoods, exhaust enclosures, inspection and maintenance of safety equipment; (ix) personal protection equipment such as eye goggles, respirators, gloves and other protection equipment should be available; (x) waste handling, storage, monitoring and disposal; (xi) emergency/contingency planning consisting of spill response, accidents, injuries and illness, emergency medical response, first aid for chemical exposures, proper recording and notification; (xii) good record keeping of medical surveillance, exposure incidents and chemical inventory.

Further to the above it is recommended that the laboratory maintain information as follows:

- Request forms for new chemicals;
- Chemical hygiene inspection checklist;

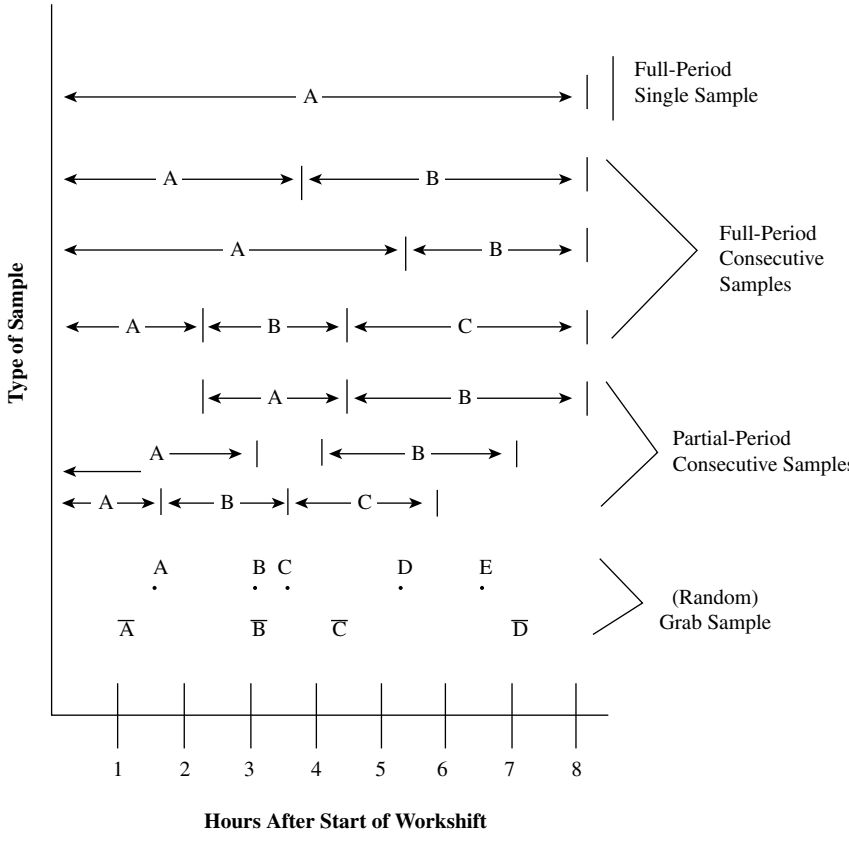

Figure 3.3 *Data analysis procedures available for sampling*

- Chemical compability chart;
- Ventilation inspection reports';
- Eye wash inspection form;
- Safety shower inspection form;
- Resistance to chemicals of glove materials;
- Glove physical properties;
- Training session attendance forms;
- Toxicity of chemicals;
- OSHA Laboratory Standard;
- Chemical inventory

3.2.3 Safety Guidelines for Radiation Sources

The different types of radiation sources used in the laboratory, such as radioactive elements emitting α-particles, β-particles and γ-rays, X-ray sources, lasers and microwave radiation are to be treated with caution. Some radiation sources can cause damage to cells in the body. The health and safety guidelines listed in the manuals of the radiation sources should be followed.

The threshold limit values for exposure to various types of radiation given must not be exceeded. For electromagnetic fields at 60 Hz, the threshold limit is 10 Gauss and the limit is ~1 Gauss for people with pacemakers.

Some general precautions are avoidance of continuous exposure, practice of electrical safety and equipping entry doors to the laboratory with electronic interlocks in order to shut off the field-generating equipment upon entry.

The Nuclear Regulatory Commission (NRC) in USA has published a code of federal regulation (CFR) 10 CFR Part 19 and 20. The latest copies of this code must be prominently displayed in the laboratory where radioactive materials are used. The code also gives the procedure for obtaining licenses, and other operating procedures, including notice of violations. Form NRC-3 gives the employees' rights and employers' responsibilities.

Part 19 of the code contains instructions for training employees in handling radioactive materials, applicable provisions of the regulations and the license granted by the commission, health effects due to the exposure to radioactive substances; equipment and procedures to minimize exposures; emergency response procedures; employee's responsibility to report unsafe conditions; procedures to request reports on individual radiation exposure. It is important to note that any violations of the code must be promptly reported to US Nuclear Regulatory Commission, Region 1, 475 Allendale Road, King of Prussia, PA 19406, USA in the United States or the relevant Nuclear Regulatory body in other countries.

Part 20 of the code consists of standards for protection against radiation such as limits for radiation exposure levels for employees and public, permissible levels for airborne contamination and effluents, monitoring procedures, posting radiation signs, pick up, receiving, opening packages containing radioactive materials, transfer and disposal of radioactive materials, and record keeping, report writing and notifications. The transportation regulations for radioactive materials such as labeling, placarding and routing of vehicles carrying radioactive materials are described in parts 172 and 177, respectively in the code Title 49 of CRF.

The implementation of safety guidelines is the responsibility of radiation safety officer and the radiation safety committee. The radiation safety officer is required to conduct periodic inspection of the locations and areas containing radioactive materials and to present a report of inspection to the safety committee for information and implementation of the recommendations.

Some general annual dose limits for exposure to radiation are as follows:

Category		Dose (rem)
Adult	Total effective dose equivalent for entire body	5
	Eye only	15
	Skin (shallow)	50
	Individual organ or tissue (deep)	50
Minors		About 10% of adult limits
Public	Total effective dose equivalent (body)	0.1 rem in 1 yr 0.002 rem in 1 h
Embryo/fetus	Occupational exposure during entire pregnancy	0.5

Radiation survey and monitoring for contamination of bench tops, hoods, floors and other laboratory surfaces should be conducted periodically. The areas of contamination should be identified and the contaminant removed by wiping. A Geiger counter or other suitable detector surveys the fixed contamination. It is a good practice to monitor daily when working with radioactive materials. Clothing and equipment should be checked for contamination at suitable intervals. Individual personnel should be monitored when necessary. The film badges worn by personnel are checked for exposure to radioactivity. It is imperative to state that the detectors must be calibrated and maintained in good working order for monitoring radioactive contamination. Records of monitoring and survey must be updated and any unsafe exposure must be reported to the radiation safety officer.

High-radiation areas must be secured carefully (i.e., level greater than 500 rad, radiation absorbed dose in 1 h at a distance of 1 m from the source) by providing proper ventilation and respiratory equipment, which monitors air contamination. It is also recommended that the radioactive material be properly stored with the required control along with posting signs such as:

Radiation area	Caution, radiation area
High-radiation area	Caution, high-radiation area Danger, high-radiation area
Very high radiation area	Grave danger, very-high radiation area
Airborne radioactive area	Caution/danger, airborne radioactive area
Labelling of containers	Radiation symbol, the isotope, caution radioactive material/danger radioactive material

Some laboratory precautions are that only authorized persons should handle radioactive materials, avoid eating, drinking and smoking, do not store food or drinks in refrigerator or laboratory drawers, no mouth pipetting, wear safety glasses, laboratory coat, safety glasses and film badge, keeping record of material used, contaminated gloves, filter paper in a radioactive disposal container, keep all the records required by the nuclear regulatory commission. It is mandatory to report loss or theft of material, accidents and individual dose exposure.

When there is an accidental spill, take steps to confine the area, monitor the people affected, use gloves to remove the spill, make and follow a careful plan to remove the spill and store the spill in a radioactive waste container. It is also mandatory that the radiation safety officer is informed and necessary measures are taken to avoid future occurrence.

3.2.4 Nonionizing Radiation Sources

Some nonionizing radiation sources and their effects on human exposure along with the precautions to be taken in their usage are summarized.

Lasers are classified as follows:

Class I	Output not more than 0.39 μW, no biological effects
Class II	Output not more than 1 mW, eye damage due to direct prolonged exposure

Class III Output not more than 500 mW, skin damage on direct exposure
Class IV Output >500 mW, can damage tissues
Class V Class II, III and IV lasers in protective housing

Microwave radiation can damage tissues and organs, and also cause birth defects, testicular degeneration, partial or total sterility, cataracts, changes in immune and endocrine functions and behaviour abnormalities. Recommended limits are:

10 mW/cm^2 for no more than 8 h in 1 day
10–25 mW/cm^2 for no more than 10 min in 1 h period
Exposure to >25 mW/cm^2 not allowed

Ultrasound

100–10 000 kHz is used in diagnosis and imaging.
Exposure to low-frequency ultrasonics causes headaches, earaches, dizziness and hypersensitivities.
Protection is achieved by insulation and isolation

Permissible exposure levels for ultrasound are given in Table 3.5. It is recommended that employees undergo audiometric and neurological examinations annually.

3.2.5 Safety at the Design Stage

The corrosion scientist or engineer must be part of the team engaged in the design of the plant. Corrosion scientists can use their knowledge and make their recommendations in the selection of materials used in fabrication. Based on the environment suitable materials are chosen, making allowance for the expected corrosion rates of the material. It is also necessary that the corrosion engineer advise on the design, and that the possibility of crevice corrosion and galvanic corrosion are avoided by suitable design and judicious choice of materials. It is needless to say that the design function is

Table 3.5 *Permissible exposure levels for ultrasound*

Mid-frequency of third-octave band (kHz)	Sound pressure levels under which nearly all workers may be repeadly exposed without adverse effect. [One third-octave band level (dB re 20 μPa)]
10.0	80
12.5	80
16.0	80
20.0	105
25.0	110
31.5	115
40.0	115
50.0	115

the most important step in the fabrication of a plant and it is advisable to make a laboratory-scale model and test for integrity and safety before embarking on the fabrication of the plant of a larger size.

3.2.6 Safety in Field Plant Inspection

Field inspection in the actual plant for corrosion involves: (i) open-space, exposed plant inspection; and (ii) closed-space plant inspection. Examples of open-space or exposed plant inspection are pipelines and bridges. The corrosion engineers face extreme hazards in field monitoring for corrosion, such as exposure to poisonous gases, e.g., hydrogen sulfide, and the need to climb tall structures (e.g., distillation towers). The corrosion inspector should be physically able and must obey safety regulations. It is necessary that the corrosion engineer be able to carry the monitoring probe used in inspection. The inspector must be physically and medically fit in addition to the technical capabilities required for inspection.

The inspection of process vessels and storage tanks represent examples of closed-space inspection. It is necessary for the management to define the closed-space inspection and provide a set of regulations for inspection. The chosen inspector must be aware of all the regulations defined by the management for inspection, along with the permission for inspection. Before entry all the technical safety requirements must be met. It is also necessary that the inspector in the closed-space process vessel must be in constant communication with other personnel outside during the entire duration of inspection. It is also possible to use mechanical robotic systems in some cases to avoid the hazards involved in closed-space entry for inspection.

The inspection of equipment in-service and in the process of failure presents a very dangerous problem to the inspector. The corrosion inspector must take the utmost care in such a situation in order to avoid both injuries and contamination of the environment. It is no exaggeration to state that this problem presents a significant challenge to the inspector. An example of this type of inspection is a leaking condensate-storage tank under pressure. In this situation it is important that the operation is shut down before beginning the safety inspection.

3.2.7 Safety in Storage and Transport

Operations dealing with hazardous materials involve storage, and transport. Space does not permit a detailed account of the topic, except to outline some aspects.[10] Some aspects of transportation of hazardous materials consist of regulatory control, classification, packaging and labelling, transport containers, hazards and hazard assessment as well as emergency planning.

All the various transport modes must conform to given codes and controls and also take into consideration the design limitations, mode of operation and possible hazard scenarios that might be encountered. Road, rail, marine, pipeline and air modes of transport are discussed in detail in the literature.[10]

References

1. Canadian Standards Association, CAN 3-Z-299.1–185, *Quality Assurance Program, Parts 1–4*, Reaffirmed 1991, CSA, Ontario, Canada.
2. American Society of Mechanical Engineers, 1992, *Boiler and Pressure Vessel Code*, New York, NY, USA.
3. The British (UK) Simple Pressure Vessels (safety) Regulations, Statutory Instrument, 1991, No. 2749.
4. F.P. Lees, *Loss Prevention in the Process Industries, Hazard Identification, Assessment and Control*, Vol. 1, 2nd edn, Butterworth Heinemann, 1996, Table 8.1, p. 8/2.
5. British Chemical Industry Safety Council, 1973.
6. A.F. Burk, *Chem. Eng. Process*, **88**(6), 90 (1992).
7. Dupont Safety and Fire Protection Guidelines, January 1981.
8. H.H. Fawcett and W.S. Wood, *Safety and Accident Prevention in Chemical Operations*, John Wiley & Sons, Ltd, 1982, p. 649.
9. R. Scott Stricoff and Douglas B. Walters, *Handbook of Laboratory Health and Safety*, John Wiley & Sons, Ltd, 1995.
10. F.P. Lees, *Loss Prevention in the Process Industries*, Hazard Identification Assessment and Control, Vol. 2, No. 23, 2nd edn, Butterworth Heinemann, 1996.

4

Materials: Metals, Alloys, Steels and Plastics

It is virtually an impossible task to list materials suitable for successful operation in every conceivable set of environmental conditions. The choice of material for use in a given environment depends upon the corrosion resistance of the material as the primary factor. The cost of the material is also an important factor in the ultimate selection of the material.

A wide range of materials is used in industry and it is important that the corrosion scientist be familiar with the corrosion resistance as well as the relevant mechanical and physical properties of the materials. Some of the mechanical properties of interest are tensile strength, yield point, elastic limit, creep strength, stress-rupture, fatigue, ductility, impact strength (toughness and brittleness), hardness and modulus of elasticity. The mechanical properties are useful in determining the production of a desired shape of part and its resistance to the anticipated mechanical forces in service conditions. Other properties of interest are density, fluidity, formability, and thermal, optical, electrical, magnetic and acoustical properties.

4.1 Cast Irons

These are classified according to ASTM A48-92 based on strength and hardness. The strength ranges between 20 000 and 65 000 psi.

(i) White cast iron is brittle and very hard. All the carbon is in the form of carbide. The rapid cooling of the melt, which in turn prevents the formation of graphite, forms the carbide. The formation of graphite requires longer cooling times. Some typical uses are in the manufacture of streetcar wheels and bulldozer tracks.

(ii) Gray cast irons are produced at slow-cooling rates and as a result most of the carbon is present as graphite flakes in a matrix of ferrite or ferrite and perlite. The fluidity of gray cast irons due to the presence of silicon enables the production of parts of

Corrosion Prevention and Protection: Practical Solutions V. S. Sastri, E. Ghali and M. Elboujdaini

intricate shapes. This form of cast iron is brittle and has useful noise and vibration damping properties as well as machinability. Some typical uses are as bases of machines and engine blocks.

(iii) Ductile irons exhibit high ductility in the as-cast form. The graphite is present as nodules or spheroids due to the nucleating agent. There irons also contain some nickel. The mechanical properties of ductile irons can be altered by heat treatment as in the case of steel.

(iv) High-silicon cast irons containing up to 14% silicon show excellent resistance to corrosion in a variety of environments. These irons are hard, brittle and not machinable and also sensitive to mechanical and thermal shocks. Silicon cast irons under the name 'Duriron' (14.5% silicon) and Durichlor (3% Molybdenum) are resistant to hydrochloric acid and chloride attack.

(v) Nickel cast irons containing up to 30% nickel have good corrosion and erosion resistance. The nickel cast irons containing Mo, Cr and Cu have been produced with improved corrosion and erosion resistance. The Ni hard white cast iron containing 4% nickel and 2% chromium is particularly used in erosion–corrosion protection in neutral and alkaline solutions and slurries.

Austenitic irons are used for valve and pump bodies; condenser water boxes in refineries, cryogenics, marine and electricity generation systems. In general austenitic irons have better corrosion resistance than unalloyed or low-alloy irons.

4.2 Carbon and Low-alloy Steels

This group of steels are used in industry extensively. The versatility and low cost are attractive features. As opposed to pure iron, alloying iron with small amounts of carbon results in improved strength and hardness without loss of ductility. These alloys are attractive from the points of view such as ease of fabrication, machinability and welding as well as good corrosion resistance.

The steels used in pressure vessels have carbon in the range 0.1–0.35%. If the carbon content exceeds this value welding problems are encountered and the formation of martensite, resulting in brittleness. The two main groups of steels are: (i) flange grade; and (ii) firebox quality. The steel supplied by manufacturer should specify both chemical analysis and mechanical properties. In the case of flange grade only the strength is specified. Both strength and chemical analysis are specified for firebox quality steels. As per the code the steels used in pressure vessels should conform to the specifications with respect to strength and chemistry.

Some important considerations in the selection of steels are detailed below:

Application	Important considerations
Steel used in thick sections	Steels with small grain size Absence of interstitial impurities
Northern pipelines Open-pit mining	Steels with low brittle to ductile Transition temperature

(*contd.*)

(*contd.*)

Application	Important considerations
Pipe	Seamless
Thick plate (2 in)	Stress relief is necessary consideration of the effect of triaxiality on fracture toughness
Use of thinner high-strength steels	Confirm mechanical stability of the structure in the design stage
All steels, particularly forgings	Assure quality control, particularly look for "banding" (i.e.) distinct parallel layers of ferrite and pearlite which might cause transverse strength problems and segregation of MnS inclusions in ferrite bands).

The four important areas of application of carbon steels are: (i) atmospheric corrosion; (ii) corrosion in fresh water; (iii) corrosion in seawater; and (iv) corrosion in soils. The atmospheric corrosion of steel is caused by major environmental factors such as: (i) time of wetness as defined by ISO 9223-1992; (ii) sulfur dioxide in the atmosphere due to the combustion of fossil fuels; and (iii) chloride carried by the wind from sea. The equations for corrosion rates of carbon steel by multiple regression analysis have been obtained.[1]

$$\text{Corrosion rate (mdd)} = 0.484\ \text{temperature}(^{\circ}\text{C}) + 0.701(\text{relative humidity}, \%) + 0.075(\text{Cl}^{-}, \text{ppm}) + 8.202(\text{SO}_2, \text{mdd}) - 0.022\left(\text{rainfall}, \frac{\text{mm}}{\text{month}}\right) - 52.67$$

Other equations of relevance obtained to fit the data are:[2]

Inland industrial atmospheres

$$\text{Corrosion rate (mdd)} = 4.15 + (\text{temperature } ^{\circ}\text{C}) - 0.073\,(\text{relative humidity}, \%) - 0.032(\text{rainfall, mm/month}) + 2.913(\text{Cl}^{-}, \text{ppm}) + 4.921(\text{SO}_2, \text{mdd})$$

Marine atmospheres

$$\text{Corrosion rate (mdd)} = 5.61 + 2.754(\text{Cl}^{-}, \text{ppm}) + 6.155\ (\text{SO}_2, \text{mdd})$$

The negative coefficients for rainfall in the equations for corrosion rates imply the beneficial effect of rainfall, which washes away the corrosive agents from the surface of the samples.

The relative severity of the atmospheres in 45 locations was evaluated in terms of weight loss. The loss in mass (g/4 × 6 in sample) ranged between 0.73 and 336 in the course of 2 yrs at Norman Wells, NWT, Canada and Galeta Point Beach, Panama, respectively.[3]

The long-term atmospheric corrosion tests conducted in Australia, Brazil, Canada, Czechoslovakia, Finland, Germany, Japan, Latin America, New Zealand, Norway, Russia, Scandinavia, Singapore, Spain, Sweden, Taiwan, UK and USA along with the number of

sites and duration are documented in the literature.[4] The resulting data for 10-yr test duration may be summarized as:

Industrial atmospheres	0.1–0.5 mm
Marine atmospheres	0.3–0.8 mm
Rural atmospheres	0.05–0.2 mm

The corrosion rate depends upon the steel composition; surface condition; and the angle of exposure. Increase in carbon, manganese and silicon content of the steel results in decrease in corrosion rate although if manganese is present as sulfide as in free-machining steels, corrosion resistance decreases. The presence of copper increases the corrosion resistance.

Rolled or pickled steels corrode faster than machined or polished steels. The mill scale on the sample must be removed before exposure to avoid the possibility of mill scale acting as cathode. The mill scale may initially give protection against atmospheric corrosion, but scale tends to crack and spall under shock conditions, resulting in bare spots on the sample exposed to the atmosphere. The vertical plates are attacked more slowly than plates at 45°.

4.2.1 Corrosion of Carbon Steels in Fresh Waters

Natural fresh waters are saturated with air and contain dissolved oxygen in the range of 8–10 ppm at room temperatures. The dissolved oxygen in the water causes corrosion by the reactions.

Anodic	$Fe \rightarrow Fe^{2+} + 2e^-$
Cathodic	$½\ O_2 + H_2O + 2e^- \rightarrow 2\,OH^-$
Overall	$Fe + ½\ O_2 + H_2O \rightarrow Fe\ (OH)_2$

It is clear from this that the dissolved oxygen in water diffuses to the surface of the metal and causes corrosion. The diffusion of oxygen to the metal surface is accentuated by an increase in turbulence of water through increase in velocity of water. The corrosion reaction proceeds as fast as the oxygen reaches the steel surface.

In the absence of a diffusion-barrier films on the steel surface the corrosion current density, i (A/cm^2) of steel in stagnant air-saturated water is given by:

$$i = (DnF/t)c \times 10^{-3}$$

where D is the diffusion coefficient of dissolved oxygen in water (cm^2/s), n is the number of electrons in the corrosion reaction, F the Faraday constant (coulombs/mol), t the thickness of diffusion layer (cm) and c is the dissolved oxygen concentration (mol/L).

Using $D = 2 \times 10^{-5}\,\text{cm}^2/\text{s}$, $n = 4$, $F = 96\,500\,\text{C/mol}$, $t = 0.05\,\text{cm}$, $c = 8/32 \times 10^{-3}\,\text{mol/L}$, a value of i of $38.6 \times 10^{-6}\,\text{A/cm}^2$, equivalent to a corrosion rate of 0.45 mm/yr or 18 mpy is obtained.

Hard waters contain high concentrations of calcium and bicarbonate and steel samples exposed to hard waters result in the deposition of calcium carbonate deposit on the steel

surface, which provides a diffusion barrier to oxygen. The corrosion rate in soft waters is higher than in hard waters. The average corrosion rate of steel in stagnant air-saturated soft waters at ordinary temperatures is roughly 0.1 mm/yr. In general increase in oxygen concentration, velocity and temperature within limits results in corrosion rate increase in soft waters.

Typically waters with hardness of less than 100 ppm are soft, 100–150 ppm are slightly hard and greater than 150 ppm hard. The corrosivity of natural fresh waters is due to pH, dissolved oxygen, hardness, chloride and sulphate. The chloride is responsible for the localized corrosion.

The corrosivity of hard waters is defined by the stability index or Ryznar index (RI) defined as:

$$\mathrm{RI} = 2\,\mathrm{pH_s} - \mathrm{pH}$$

where $\mathrm{pH_s}$ is pH at saturation.

At RI = 6.0 calcium carbonate is in equilibrium. When RI is greater than 6.0 the corrosivity increases. The corrosion rates of carbon steel have been found to obey an equation of the type:[5]

$$\text{Corrosion rate (mdd)} = -12.5(\mathrm{LSI}) + 8.99$$

where LSI is Langelier saturation index. When LSI varies from -1 to -3 the corrosion rate increases.

The corrosion of steel in soft tapwater as a function of pH showed similarity to an acid–base titration curve with three distinct regions: (i) pH 2–3 (0.24–1.0 mm/yr); (ii) pH 3–10 (0.22 mm/yr); and (iii) pH 10–13 (0.22–0.02 mm/yr).

The effect of velocity on corrosion of carbon steel shows the critical velocity above which the corrosion rate decreases due to passivation is in the range of ~0.3–0.7 m/s. At high velocities (~20 m/s) the passive film is removed and erosion–corrosion occurs. Erosion–corrosion often occurs at bends, misaligned joints of high velocity water pipe. It is also possible that cavitation–erosion might occur mechanically and is accelerated by dissolved oxygen. This type of damage occurs on rotors of pumps and the trailing side of water turbine blades made of steel and cast iron.

The most important form of corrosion in fresh waters is localized corrosion of steel and it is critical in water pipes because it might result in leaks in pipes. The major types of localized corrosion of steel in fresh water are: pitting under tubercles; groove corrosion of electric-resistance welded (ERW) pipes; and pitting at discontinuities in corrosion product films.

The tubercles or mounds of corrosion products formed in steel pipes carrying water give rise to differential aeration cells. The area under the tubercles due to limited supply of oxygen undergoes localized corrosion by the galvanic action of the surrounding cathodic areas, which have access to oxygen. The typical penetration rates of galvanized water pipes under tubercles for service periods of 5–15 yr are given in Table 4.1. The penetration rate is also a function of the resistivity of water, as shown in Figure 4.1. The increase in penetration rate with temperature is illustrated by the data given in Table 4.2.

Aerobic iron bacteria accelerate the formation of tubercles. The sulfate-reducing bacteria flourish in tubercles and can accelerate the corrosion process.

Table 4.1 *Penetration rates of galvanized tapwater pipes under tubercles*[a]

Size (in)	Wall thickness (mm)	Maximum penetration (mm)	Service period (yr)	Maximum penetration rate	
				(mm/yr)	Mils/year (mpy)
1	3.2	3	13	0.23	9
1	3.2	1	5	0.20	8
1	3.2	1.5	10	0.15	6
1¼	3.5	0.8	10	0.08	3
1	3.2	Perforated	14	0.23	9
1¼	3.5	0.8	14	0.06	2
1¼	3.5	1.2	14	0.09	3
2	3.8	0.8	14	0.06	2
1	3.2	1.4	14	0.10	4
1½	3.5	1.3	14	0.09	3
5	4.5	2	16	0.13	5
4	4.5	Perforated	15	0.30	12
1	3.2	Perforated	10	0.32	13
6	5.0	Perforated			

[a]Reproduced with permission.[5]

The grove corrosion of electric welded pipe involves local heating of the welded seam and rapid cooling by air. The local heating and cooling results in a different microstructure from the parent metal, leading to a more negative potential and corrosion on exposure to corrosive agents. The corrosion rates range between 40–120 mpy and can be as high as 400 mpy.

Corrosion of localized nature can occur at discontinuities in the corrosion product films and the data given in Table 4.2 represent this phenomenon. The corrosion products such as γ-Fe_2O_3 and Fe_3O_4 on the surface act as cathodes to the exposed discontinuities in the film and cause localized corrosion on exposure to the aqueous media.

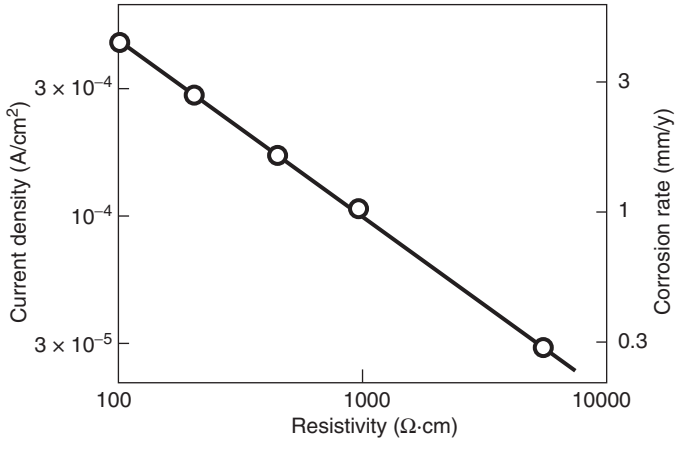

Figure 4.1 *Effect of water resistivity on theoretical penetration rate of carbon steel under tubercles*[6]

Table 4.2 *Penetration rates of steel pipes alternately exposed to hot water or steam and cold water*[7]

Item	Condition[a]	Penetration (mm)	Service period (yr)	Penetration rate (mm/yr)	Penetration rate Mils/year (mpy)
Hot water pipe	RT/90∼95°C	5.8[b]	6	0.97	38
Hot water pipe	RT/max 60°C	3.8[b]	4	0.95	37
Steam/water pipe	6 h cycle	4.2[b]	1.2	3.5	140
Boiler hot water return line near inlet of cold make-up water	48/90°C	4.5[b]	4	1.1	43

[a]Room temperature = RT
[b]Perforated

4.2.2 Corrosion of Carbon Steels in Seawater

Typical steel structures exposed to marine environments are: (i) marine piles; (ii) offshore structures; (iii) vessels; and (iv) others. The corrosive zones encountered in marine environment are: (i) atmospheric; (ii) splash; (iii) tidal; (iv) submerged; and (v) seabed-embedded zone.

The environmental factors that influence the corrosion rate vary with the depth in seawater as detailed[8] in Table 4.3. The variation of the factors in seawater at different global locations has been documented in the literature.[9]

The main factor that influences corrosion of steel in seawater is the available oxygen, which varies from 11 to 6 ppm. The solubility of oxygen in seawater varies as a function of temperature, and salinity and some data are given in Table 4.4. Some of the variables that influence the availability of oxygen for corrosion are: (i) increase in temperature increases the diffusion rate of oxygen while lowering its concentration; and (ii) it also increases the deposition rate of protective calcareous films and marine growth. Thus an increase in temperature results in opposing compensating effects on oxygen-induced corrosion of steel in seawaters.

The overall corrosion rates obtained for periods 1–40 yr range from 0.02 to 0.37 mm/yr with an average value of ∼0.1 mm/yr. The corrosion rate of steel was found to decrease with time as is evident from the data obtained by Southwell and Alexander.[10]

Duration (yr)	Corrosion rate (mm/yr)
1	0.14
2	0.11
4	0.094
8	0.084
16	0.077

Table 4.3 *Environmental factors in seawater corrosion*

Salinity	1. Open sea: variation with horizontal location is small, 32–36 ppt. 2. Near river outlets: lower. 3. Variation with depth: very small.
Dissolved oxygen concentration	1. Surface water: (1) near the equilibrium saturation concentration with atmospheric oxygen at a given temperature [6 ppm (in the tropics) 11 ppm (in the Arctic); (2) can be supersatured due to photosynthesis by microscopic plants (up to 200%) and entrainment of air bubbles (up to ~10%) 2. Variation with depth: (1) tends to be under saturated due to consumption by the biochemical oxidation of organic matter; (2) goes though a minimum at intermediate depths (400–2400 m)
Temperature	1. Surface water: in the open ocean, variations are in the range of −2 to 35°C depending on the latitude, season, currents, and so on. 2. Variation with depth: drops with depth. The difference with depth and season may be large or small, depending on the location
pH	1. Surface water: lies between 7.5 and 8.3 in the open ocean, depending on the concentration of dissolved CO_2 determined by air–sea exchange and photosynthesis activity of plants; (2) microbiological activity affects the pH value e.g., lower pHs by the formation of CO_2 through the process of biochemical oxidation, and higher pH values by the reduction of CO_2 through the process of photosynthesis; (3) affected by pollutants in coastal waters 2. Variation with depth: tends to show a profile similar to that of dissolved oxygen (the biochemical oxidation that consumes dissolved oxygen generates CO_2 reducing the pH value)
Carbonate	1. Surface water: nearly always supersaturated with respect to $CaCO_3$ (200–500%) favored by high pH values and moderate temperatures 2. Variation with depth: saturation state with respect to $CaCO_3$ decreases as the result of lower temperature and pH. Under saturated in deep waters (e.g., below 200–300 m)
Pollutants	1. H_2S may be 50 ppm or higher in polluted waters in estuaries, harbors, river mouths and fitting-out basins 2. Ammonia may be high in inshore waters and harbors
Biological organisms	1. Bacteria form bacterial films (slime) 2. Weeds grow from spores 3. Animals (e.g., barnacles, tube worms and hyroids) adhere

Discontinuities in the corrosion product film result in differential aeration cells, leading to pitting corrosion. A pitting rate of ~0.25–0.38 mm/yr on bare steel and ~0.5 mm/yr on steel with mill scale has been observed. Assuming the average corrosion rate of 0.125 mm/yr, the pitting factor works out to be 2 to 3 for

Table 4.4 *Equilibrium concentration of oxygen in seawater as a function of temperature and salinity*

Temperature (°C)	Oxygen solubility at indicated salinity (ppt)					
	0	8	16	24	31	36
0	14.6	13.9	13.1	12.4	11.8	11.4
5	12.5	11.9	11.3	10.7	10.2	9.9
10	10.9	10.4	9.8	9.4	8.9	8.7
15	9.5	9.1	8.7	8.2	7.9	7.7
20	8.5	8.1	7.7	7.3	7.0	6.8
25	7.6	7.2	6.9	6.6	6.3	6.2
30	6.8	6.5	6.2	6.0	5.7	5.

bare steel and 4 for steel with mill scale. Some data on pitting factors are given below:

Sample	Time of exposure (yr)	Pitting factor	Reference
Descaled steel	10	2.5	
Steel with mill scale	10	3.5	11
Pickled steel	15	2–2.9	12
Steel with mill scale	15	2.1–5.6	
Machined steel	1	12	
	2	17	10
	4	8	
	8	6	
	16	3 (perforated)	
Mill scaled steel	1	25	
	2	14	
	4	10	
	8	11	
	16	Perforated	

The corrosion rates of carbon steel pilings and test samples in different exposure zones with the placement of samples in vertical position show different degrees of severity of the zones.

Zone	Corrosion rate (mm/yr)
Atmospheric	0.1–0.2
Splash	0.3–0.5
Tidal	0.10
Top of submerged zone	0.5–1.0
Submerged zone	0.1
Mud zone	0.05

The corrosion rate of carbon steel increases with increase in velocity until a critical velocity is reached. This behavior is different from that of the carbon steel in fresh water where the corrosion rate decreases beyond a critical velocity due to the formation of a passive film. In seawater passive films are not formed because of the presence of high concentrations of chloride. The erosion corrosion occurs after critical velocity ~20 m/s is reached. The maximum corrosion rate of ~1.0/mm/yr is reached at velocities up to 4 m/s.

4.2.3 Corrosion of Carbon Steels in Soils

Typical steel structures used underground in contact with soils are pipelines, utility pipings and pilings. Pipelines are generally protected against corrosion with coatings and by cathodic protection. Driven pilings are commonly used in bare condition.

The factors that influence corrosion of steels in soils are the type of soil; moisture content and the position of the water table; soil resistivity and soluble ion content; soil pH; oxidation–reduction potential; and the role of microbes present in soil. The exposure of a buried pipe to the soil environment is illustrated in Figure 4.2. The steel pipe is exposed to both meteoric water passing through ground surface and the water in the ground. The meteoric water may be acidic due to the presence of carbon dioxide and sulfur dioxide in the atmosphere. The soil water may be acidic in addition to some dissolved minerals. The steel pipe is partially above the water table with the rest below the water. The pH and the dissolved ions in the ground water provide a corrosive environment.

All pipes buried in the ground are generally protected by cathodic protection or by outer protective coatings. Defects in the coating will allow water to reach the steel pipe surface. The entrapped water in the coating may differ in composition from the groundwater and cause corrosion of the pipe. Permeability depends upon the soil structure and particle size. The rate of movement of fluids or gases is in turn governed by permeability. It is obvious then that clays, consisting of small particles, have limited permeability compared with

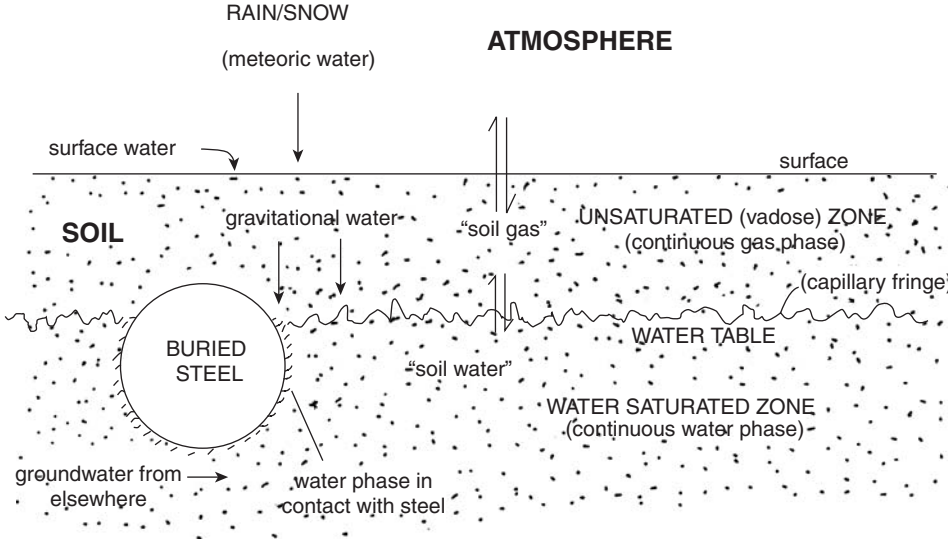

Figure 4.2 *Exposure of buried line pipe to the soil environment*

sands, of large particle size. Clays tend to adhere to the coating on the pipe and exert a physical force due to their inherent property of swelling in presence of water. This results in ingress of water into the coating and consequent tendency for corrosion. The oxidation–reduction potential is also affected by the buffering action of clays.[13] The microbiological activity in soils causing corrosion is discussed in the literature.[14]

The position of the water table determines the oxygen transport and hence the corrosion rate. The moisture content of soil greater than 20% is deemed to be corrosive (general corrosion of carbon steel) and the value of less than 20% was conducive to pitting corrosion.[15] This observation is thought to be related to the diffusion rate of oxygen.[16] The general effect of soil resistivity on the corrosivity may be denoted as:

Resistivity range (Ω cm)	Corrosivity
0–100	Very severe
1001–2000	Severe
2001–5000	Moderate
5001–10 000	Mild
10001 and above	Very mild

The pH of soil is in the range 3.5–10.0. A fair amount of corrosion of carbon steel occurs below pH of 4.0, but passivation is observed at high pH values. The nomogram involving the combined effect of pH and resistivity developed by King[18] is shown in Figure 4.3. This figure can be used to predict corrosion rates in aerobic conditions. The nomogram does not take the oxidation–reduction potential and microbial factors into account. The nomogram is useful in predicting rates in aerobic conditions.

The corrosivity of soils also depends upon the oxidation–reduction potential as classified by Booth *et al.*[15] The classification scheme of the corrosivity of soils is given in Table 4.4b. Macrogalvanic cells are formed in underground pipelines due to: foreign structure; the combination of new and old pipe; dissimilar metals (stainless steel and carbon steel); differential aeration; dissimilar soils; and stray currents. All these lead to localized corrosion of underground pipelines.

Microbially influenced corrosion occurs in soil environment. The sulfate-reducing bacteria (SRB) reduce sulfate to sulfide and as a result iron sulfide is formed due to corrosion. The iron sulfide deposit on the steel surface and the steel form a galvanic couple, which is substained by the removal of electrons in the form of cathodic hydrogen, followed by the further formation of more iron sulfide.[19,20]

The typical corrosion rates in soils range from 0.003 to 0.063 mm/yr with an average value of 0.020 mm/yr. The pitting rates range from 0.033 to >0.45 mm/yr with an average

Table 4.4b *Soil corrosivity Based on Oxidation-Reduction Potential*

ORP Range (mv)	Corrosivity
<100	Severe
100–200	Moderate
200–400	Slight
>400	Not corrosive

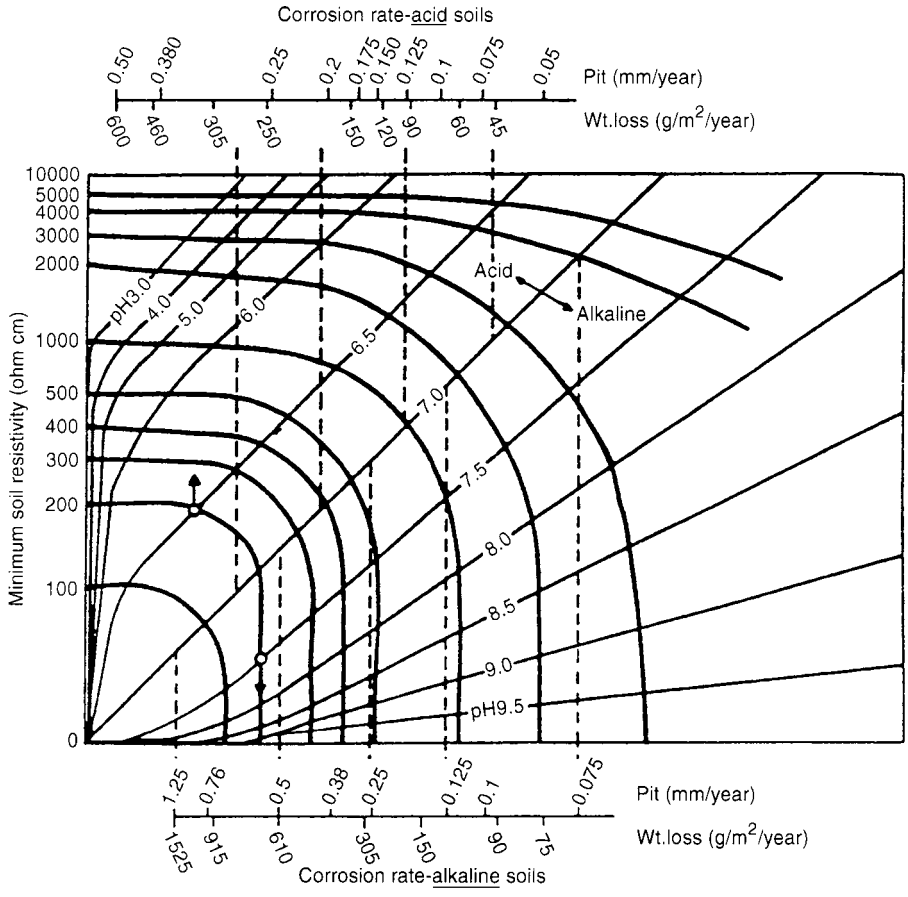

Figure 4.3 *Nomogram relating soil resistivity, pH, and corrosion rate for steel pipe in soil*

of 0.143 mm/yr. The sample with a value of >0.45 mm/yr was found to be perforated. The pitting rates given in terms of mm/yr should be viewed with caution since pitting is better expressed in terms of deepest pit depth and average of twenty deep pit depths.

Low-alloy and carbon steels, also known as weathering steels, were developed based on life cycle assessment, taking into account factors such as resources, economics, workability, reliability, reasonable life cycle cost, environmental effects and recycling possibility. These steels are thought to result in savings in energy and resources. Some steels belonging to this class are[21]: CORTEN, USS CORTEN A, USS CORTEN B, USS CORTEN B-QT, USS CORTEN C, ASTM A 242 (M), A588 A, A588 B, A588 C, A588 D, A588 K. These steels have the composition (weight percent).

C	0.06–0.20	Si	0.15–1.0	Mn	0.10–1.25	P	0.04–0.20
S	<0.05–0.035	Cu	0.20–0.55	Cr	0.30–1.50	Ni	0.25–0.65

The ASTM A588A, B, C steels have vanadium in the range of 0.01–0.10 wt %. ASTM A 588 D has 0.05–0.15 Zr, <0.04 Nb; ASTM A 588K also has ≤0.10 Mo and 0.005–0.05 wt % Nb.

As noted in the composition data, the alloying elements Cu, P, Cr, Ni and Si account for a few percent of the total. Atmospheric exposure results in the formation of a thin, adherent, and compact protective layer. Steels containing about 0.3% of copper had higher corrosion resistance than steels devoid of copper; phosphorus also showed a beneficial effect.

Copper in the range 0.2–0.3% increased corrosion resistance by a factor of ∼2. Addition of 0.5% of chromium resulted in increasing corrosion resistance by a factor of ∼2. Some corrosion data are as follows:

Alloy	Duration (yr)	Loss in weight (kg/m^2)
Low-alloy steels	8	0.3–0.4
3.2% Ni, 0.02% P	8	0.5
0.2% Cu, 0.11% P	8	∼0.80
0% Cu, 0.006% P	8	1.05

The data show the beneficial effect of phosphorus in the steel when the alloys contain 0.11% phosphorus along with 0.2% Cu.

The role of alloying elements in weathering steels consists of the effect of formation of the protective layer of corrosion products; increase in mechanical strength and toughness; and improved weldability. The protective qualities of the corrosion products on the steel depend on the continuous growth of the adherent, compact, inner layer and on low porosity within the layer. The kinetics of atmospheric corrosion were found to obey the equation,

$$C = At^B$$

Where C is corrosion loss, t is time and A and B are constants:

$$\log C = \log A + B \log t$$

Using regression analysis, the two constants A and B can be expressed in terms of alloy content or environmental parameters such as chloride and sulfate concentrations. The beneficial effects of Cu, Cr and P, and the small contributions of Si, Ni, Al and Mo in the protective layer of the corrosion products were established. The nature of corrosion product layers formed on weathering steel and plain carbon steel is shown in Figure 4.4. Typical uses of weathering steels are freight trains, trucks, agricultural equipment, bridges and other structures exposed to the atmosphere.

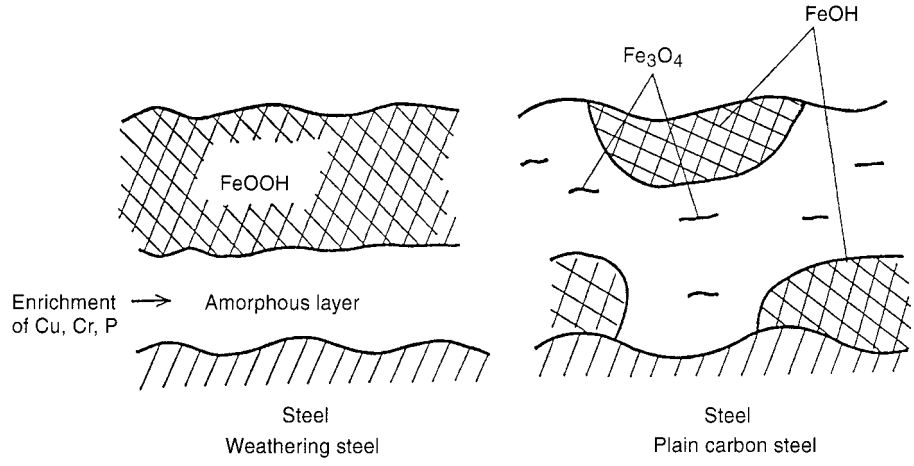

Figure 4.4 *Schematic illustration of the corrosion product layers identified on steels exposed to rural and marine atmospheres for periods of up to 5 yr*

4.3 Stainless Steels

The four stainless steel types are austenitic; ferritic; duplex and martensitic. The discovery of stainless steel (12.8% Cr, Fe alloy) is due to the work[22] of H. Brearly in 1912. The approximate composition of austenitic and ferritic stainless steels is listed in Table 4.5.

The stainless steels owe their corrosion resistance to the chromium in the iron alloy, which forms a very thin transparent film of chromium oxide on interaction with oxygen. A ready supply of oxygen with a minimum of 11% of chromium dissolved in the matrix material are necessary conditions to maintain a passive film which is self-healing in air at room temperature. The damage to the passive film results in corrosion in the environment to which the alloy is exposed. The observation that chromium in iron alloy is responsible for corrosion resistance in acid solutions led to the development of Type 430 (16–18% Cr) and Type 446 (24–27% Cr).

Some data on corrosion rates[23] in terms of weight loss/dm^2 of Fe-Cr alloys are given in Table 4.6.

It is clear from the data in Table 4.6 that the corrosion rates increase with increase in chromium in sulfuric acid solution. The presence of 10% Ni in the Fe–Cr alloy results in decreasing corrosion rate with chromium concentration. The corrosion rates of Fe–Cr alloys in ferric sulfate decrease with increasing concentration of chromium in the alloy. These observations are supported by the data on corrosion potentials of stainless steels in boiling acids and chlorides measured against a saturated calomel electrode.

Medium	Potential (V) vs SCE
65% nitric acid	+1.0 (+0.75–1.0)
Ferric sulfate – sulfuric acid (ferric chloride) (potassium permanganate – sodium chloride)	+0.60

(*contd.*)

(*contd.*)

Medium	Potential (V) vs SCE
Copper sulfate – sulfuric acid	+0.35
Copper sulfate – sulfuric acid with metallic copper	+0.1
5% sulfuric acid	−0.60

The corrosion potentials are in keeping with the experimental observations: steels attain passivity in nitric acid and ferric sulfate sulfuric acid solutions and undergo corrosion in 5% sulfuric acid solutions.

The nickel in the Fe–Cr alloy behaves in a dual manner. The corrosion rate with Fe-10 Ni 14 Cr alloy in 5% H_2SO_4 is greater than the corrosion rate of Fe-14 Cr alloy in H_2SO_4. In case of alloys with chromium content greater than 18% the corrosion rate of the nickel-based alloy is lower than the Fe–Cr alloy devoid of nickel.

Table 4.5 *Some stainless steels and their approximate compositions*

Material type (AISI No.)	Approximate percent composition (Fe remainder)					
	Cr	Ni	Mo	C	N	Other
Austenitic						
201	16–18	3.5–5.5		0.15	0.25	5.5–7.5 Mn
202	17–19	4–6		0.15	0.25	7.5–10 Mn
205	16–18	1.00–1.75	1.0–1.7	0.25	0.4	14.0–15.5 Mn
304	18–20	8.0–10.5		0.08	0.10	
304L	18–20	8–12		0.03	0.10	
304N	18–20	8–10.5		0.08	0.10–0.16	
304LN	18–20	8–12		0.03	0.10–0.16	
316	16–18	10–14	2–3	0.08	0.1	
316L	16–18	10–14	2–3	0.08	0.1	
316N	16–18	10–14	2–3	0.08	0.1	
316LN	16–18	10–14	2–3	0.03	0.1	
317	18–20	11–15	3–4	0.08		
317L	18–20	11–15	3–4	0.03		
321	17–19	9–12		0.08		<0.4 Ti
254 SMO*	20	17.5–18.5	6.0–6.5	0.02	0.18–0.22	0.5–1.0 Cu
AL-6XN	21	25	6.5	0.02	0.2	
25-6MO	19–21	24–26	6–7	0.0	0.15–0.25	<2 Mn
20 MO-6	22–26	33–37	5.0–6.7	0.03		2–4 Cu
Ferritic						
403	12–14	1		0.08		1 Mn
409	11	1		0.08		<1 Ti
430	16–18	1		0.08		
434	16–18		0.90–1.25	0.08		
440A	16–18		0.75	0.7		1 Mn
444	17.5	19.5	1.75–2.0	0.025	0.035	Ti + Nb
446	23–27			0.20	0.25	
AL 29-4-2	28–30	2.0–2.5	3.5–4.2	0.01	0.02	

*254 SMO is a registered trademark of Avesta Jernverks Aktiebolag
†Ferralium is a trademark of Langley Alloys Ltd

Table 4.6 *Corrosion rates of Fe-Cr alloys*

Alloy	Weight percent, Cr		Medium	Weightloss, g/dm
Fe–Cr	10	5%	H_2SO_4	2.0
	14		H_2SO_4	2.4
	22		H_2SO_4	4.0
	32		H_2SO_4	5.7
Fe–Cr	13		Ferric sulfate	6.0
	14		Ferric sulfate	2.7
	15		Ferric sulfate	1.2
	20		Ferric sulfate	0.1
	25		Ferric sulfate	0.0
Fe-10% Ni–Cr	13	5%	H_2SO_4	6.2
	14		H_2SO_4	5.2
	16		H_2SO_4	2.4
	18		H_2SO_4	1.4
	20		H_2SO_4	0.7
	25		H_2SO_4	0.0

The effect of the chromium content of the alloy on corrosion in boiling acids is shown in Table 4.7 along with the data for carbon steel and low-carbon and low-nitrogen 35% Cr alloys. The data show that the corrosion rates of 18 Cr-8 Ni (Type 304) is lower than Type 430 and 446 that is devoid of nickel. The nickel is the alloy probably reduces the rate of hydrogen evolution reaction. The molybdenum in Type 316 alloy was found to be useful in protection from pitting by chloride ions.

The Carpenter 20 Nb-3 alloy has good corrosion resistance in both reducing and oxidizing solutions. The high nickel content provides high resistance to chloride stress–corrosion cracking. Hastealloy provides good resistance to chloride stress cracking, pitting and crevice corrosion. The performance of the alloy in reducing solutions is fair, but poor in oxidizing solutions.

The steels are subject to intergranular corrosion; pitting and crevice corrosion; and chloride stress–corrosion cracking. When steels are exposed to temperatures of 425–875°C in operations such as welding or fabrication, chromium carbide $(Fe, Cr)_{23}\ C_6$ precipitate is formed at grain boundaries. The high chromium content in the precipitate causes depletion of chromium in the regions adjacent to the precipitate. This results in intergranular corrosion in environments in which a decrease in chromium content leads to increase in corrosion rate. An example of this phenomenon is provided by Type 446 steel (25 Cr) in ferric sulfate/sulfuric acid solutions. Similarly, the formation of chromium nitride, β-Cr_2N also leads to intergranular corrosion of the alloy. The intergranular corrosion due to the chromium carbide can be prevented by heat treatment, reduction of the carbon content, addition of stabilizer such as titanium or niobium to the alloy. The stabilizing elements combine with carbon preferentially. An example of this is the addition of Ti to Type 321 and 340 steels.

Pitting corrosion (Table 4.8) involves pit initiation (breakdown of passive film) followed by pit growth. The chloride ion induces pitting corrosion. Type 304 steel undergoes pitting more readily than Type 316 steel. The molybdenum in 316 steel is responsible for its reduced susceptibility to pitting corrosion. Type 316L steels contains

Table 4.7 *General corrosion in boiling acids*

USN No.	Alloy	Corrosion rate (mm/yr)[a,b] Nitric (65%)	50% Sulfuric acid with ferric sulfate	Formic (45%)	Oxalic (10%)	Acetic (20%)	Sodium bisulfate (10%)	Sulfuric (10%)	Hydrochloric (1%)
G10200	Carbon steel (AISI 1020)	4500		630	62	170	1000	1300	430
S4300	Type 430 (16% Cr)	0.5[c]	7.9[d]	2200	160	80	2300	6400	1500
S44600	Type 446 (25% Cr)	0.2[c]	0.9[d]	250	180	0.0[c]	1600	6900	1900
	Fe-35% Cr (high-purity)	0.2[c]	0.2[d]	0.2[d] (1100)	0.0[d] (800)	0.0[c]	0.2[d] (2700)	0.4[d] (5000)	1500
S30400	Type 304 (18 Cr-8 Ni)	0.2[c]	0.6[d]	44	15	0.1[c]	70	400	81
S31600	Type 316 (18 Cr-10 Ni-2.5 Mo)	0.3[c]	0.6[d]	13	2.4	0.1[c]	4.3	22	71
N08020	Carpenter 20 Cb-3 (20Cr-34 Ni-2.5 Mo-3.5 Cu)	0.2[c]	0.2[d]	0.2[c]	0.2	0.1[c]	0.3	1.1	0.0
N10002	Hastelloy alloy C (16Cr-54 Ni-16 Mo-4 W)	11.4[c]	6.1[d]	0.1[c]	0.2	0.0[c]	0.2	0.4	0.3
	Titanium	0.3[c]	5.9[d]	22	24	0.0[c]	6.4	160	5.6

(*contd.*)

Table 4.7 *(contd.)*

USN No.	Alloy	Corrosion rate (mm/yr)[a,b] Nitric (65%)	50% Sulfuric acid with ferric sulfate	Formic (45%)	Oxalic (10%)	Acetic (20%)	Sodium bisulfate (10%)	Sulfuric (10%)	Hydrochloric (1%)
S44400	Fe-18 Cr-2 Mo (Ti)	[5.8][d,e]	[4.1][d,e]	10	250	0.0[c]	930	2400	850
S44627	Fe-26Cr-1 Mo (high-purity)	0.1[c]	0.4[d]	0.1	0.2[d]	0.0[c]	0.0[d]	3400	0.7[d]
	Fe-26Cr-1 Mo (Ti)	0.1[c]	0.3[d]	0.1	0.2[d] (350)	0.0[c]	0.0[d] (1500)	3200	0.1[d] (1600)
	Fe-28 Cr-2 Mo-4 Ni (Nb)	0.2[c]	0.3[d]	0.1	0.1	0.0[c]	0.0	0.2	0.0
S44700	Fe-29 Cr-4 Mo	0.1[c]	0.2[d]	0.1	0.3	0.0[c]	0.2[d] (500)	1300	0.2[d] (550)
S44800	Fe-29 Cr-4 Mo-2 Ni	0.1[c]	0.2[d]	0.1	0.1	0.0[c]	0.0	0.2	0.2

[a]Acid concentrations in percent by weight. Test specimens, 25 × 25 mm (1 × 1 in); 600 mL solution. The length of testing time varied from 5 min for high rates to 10 days for low rates
[b]0.10 mm = 40 mils (thousandths of an inch) per year
[c]Cannot be activated with an iron rod
[d]Specimen is passive when immersed, but not self-repassivating when activated by contact with an iron rod while exposed to the solution. Number in parentheses is the rate in the active state. Underlined rates for self-repassivating after activation with an iron rod
[e]Severe intergranular attack

Table 4.8 *Pitting data on some alloys*

Alloy	Cr	Ni	Mo	C	N	Si	Pits/cm^2
304	18.45	8.90		0.063		0.58	7.4
316	17.93	13.50	2.47	0.031		0.31	7.3
316L	17.71	11.17	2.44	0.02	0.032		5.0
SP-2	18.79	9.24	2.40	0.039	0.23	2.5	0.0

lower carbon (0.03%) than Type 304 (0.08% C) and Type 316 (0.08% C). Further addition of ~2% silicon to Type 316 steel showed an increase in resistance to pitting corrosion. From this it can be surmised that, in steel alloys containing molybdenum, silicon, in addition to lowering the carbon content of the steel, renders it more resistant to pitting corrosion (Type 316, 316 L) than steels devoid of molybdenum (Type 304).

The chloride stress–corrosion cracking of austenitic stainless steels in chloride solutions with samples under tensile stresses has been known since 1940. There are some reports that claim the retained austenitic structure to be responsible for chloride stress–corrosion cracking.

The stress–corrosion cracking (SCC) mode of failure was later observed even in the case of ferritic stainless steels. The only clear message from this is that the exact mechanism of failure by this mode is not well established. Alloys containing >34% Ni were found to prolong the time of SCC failure. Ferritic type alloys 430 and 434 are resistant to SCC both in $MgCl_2$ and NaCl environments in the mill-annealed condition, but not in welded conditions. Also, welding impairs the ductility and their resistance to SCC.

In contrast to austenitic stainless steels solubility of carbon in ferritic steels is low and the precipitation of carbides occurs easily. Thus, lowering of carbon and nitrogen contents of ferritic steels was achieved by argon–oxygen decarburization (AOD) or vacuum–oxygen decarburization (VOD). The chromium content of ferritic steels is in the range of 18–30%. These steels contain molybdenum (1–4%) along with titanium, nickel and niobium. Typical ferritic alloys containing low amounts of carbon and nitrogen are given in Table 4.9.

The resistance to general corrosion, pitting and crevice corrosion and stress-corrosion cracking of the ferritic alloy is given in Table 4.10.

Some typical applications of austenitic stainless steels are in: (i) flue gas scrubbers in coal-fired power plants; (ii) nuclear industry; (iii) door and window frames, fittings; (iv) external claddings; (v) masonry fixings; (vi) propeller shafts; (vii) wire ropes, riggs and deck fittings; (vii) sinks, drainers, cooking utensils; (ix) surgical tools, implants; (x) chemical industry for acids production, storage and transit. The ferritic stainless steels are used in catalytic converters fitted to automobile exhaust, condensers and heat exchangers; in the food industry, chemical industry, refineries, heat exchangers, caustic evaporators in chemical and petrochemical industries and seawater cooled condensers in electric power generating stations.

4.3.1 Duplex Stainless Steels

This class of steels has an austenitic–ferritic crystal structure, with at least 25 or 30% of the lesser phase with a balance of austenite and ferrite stabilizing alloying elements to

Table 4.9 *Ferritic alloys*

Fe-18 Cr-2 Mo-Ti	C 0.025 max N 0.025 max
Fe-26 Cr-1 Mo	C 0.005 max N 0.015 max
Fe-26 Cr-1 Mo-Ti	C 0.040 max N 0.040 max 0.2-1.0 Ti
Fe-28Cr-2 Mo	$C + N \leq 0.010$
Fe-28 Cr-2 Mo-4 Ni-Nb	C 0.015 max N 0.015 max
F-29 Cr-4 Mo	C 0.010 max N 0.020 max
Fe-29 Cr-4 Mo-2 Ni	C 0.010 max N 0.020 max

achieve the mixed structure. The chemical composition of these steels is balanced to give good corrosion resistance and the correct microstructure with desirable mechanical and physical properties. Typical chemical compositions of duplex stainless steels are given in Table 4.11.

Some prominent features of these steels are relatively high room temperature strength (high proof and tensile stresses) and high fatigue strength.

The corrosion resistance of steels in acids is represented by isocorrosion diagrams. The resistance to uniform or general corrosion in various acids and sodium hydroxide was determined by weight loss measurements over a period of 96 h and the resulting data are given in Table 4.12.

The tests were performed with a temperature interval of 5°C until the critical temperature (i.e., the lowest temperature at which the corrosion rate exceeds 0.127 mm/yr (5 mpy) is obtained. The high chromium content, along with the molybdenum and nitrogen in the duplex steels contribute to the resistance of steels to pitting and crevice corrosion of the steels in halide-containing solutions. The ranking of steels to initiation of pitting is done using the pitting resistance equivalent (PRE) formula and the most commonly used form for duplex stainless steels due to Truman[25] is:

$$\text{PRE} = \%\ \text{Cr} + 3.3 \times \%\ \text{Mo} + 16 \times \%\ \text{N}$$

The values of PRE for duplex stainless steels are given in Table 4.13. It is useful to note that the PRE relationship does not take into account factors such as surface condition, internal cleanliness, heat treatment and related properties that influence

Table 4.10 *Summary of properties of ferritic alloys*

Property	Alloy[a]					
	18 Cr-2 Mo-Ti	26 Cr-1 Mo (high-purity)	26 Cr-1 Mo-Ti	28 Cr-2 Mo-4 Ni-Nb	29 Cr-4 Mo	29 Cr-4 Mo-2 Ni
Stress–corrosion cracking						
$MgC1_2$ (155°C, 310°F)	R[b,c]	R[b]	R95[b]	F	R[b]	F
NaC1 (103°C, 217°F)	R	R	R	R	R	R
Pitting and crevice corrosion						
$KMnO_4$-NaC1						
Room temperature	F	R	R	R	R	R
50°C (120°F)		R	R	R	R	R
90°C (195°F)		F	F	F	R	R
Ferric chloride						
Room temperature	F	F	F	R	R	R
50°C (120°F)						
Corrosion in boiling acids[d]						
Nitric-65%	F[e]	R	F[e]	R	R	R
Formic-45%	F	R	R	R	R	R
Oxalic-10%	F	F	F	R	R	R
Sulfuric-10%	F	F	F	R	F	R
Hydrochloric-1%	F	F	F	R	F	R
Transition temperature[f]	+25 to +75°C	−62°C	+40°C	−5°C	+16°C	−7°C
	(+75 to +75°F)	(−80°F)	(+105°F)	(+25°F)	(+60°F)	(+20°F)
Refining processes	AOD or VOD	EB or VIM	AOD	VOD or AOD	VIM or EB	VIM

[a]R = resistant; F = fails by type of corrosion shown; AOD = argon–oxygen decarburization; VOD = vacuum–oxygen decarburization; VIM = vacuum induction melting; EB = electron beam refining
[b]Copper and nickel residuals must be kept low in these alloys to resist cracking in this solution
[c]Data from Climax Molybdenum Co. publication, 18 Cr-2 Mo ferritic stainless steel
[d]R indicates passive or self-passivating with rates <0.2 mm/yr
[e]Not recommended for oxidizing solutions
[f]Full-size Charpy V-notch specimens

corrosion. A more precise approach involving the determination of critical pitting temperature (CPT) or critical crevice corrosion temperature in the environment of interest led to the data given in Table 4.14.

The duplex stainless steels have good resistance to stress corrosion cracking in contrast to austenitic steels, and hence these steels were used in a wide range of applications with minimal risk. The duplex steels have high proof and tensile stresses in addition to high fatigue strength. Thus, good corrosion resistance coupled with fatigue strength translates into good resistance to corrosion fatigue.

Table 4.11 *Typical compositions of some duplex stainless steels*

UNS No.[a]	EN No.[b]	Cr	Ni	Mo	N	Other
			Lean duplex			
S32304	1.4362	23	4.5	0.3	0.1	
S31500		18.5	5	2.7	0.07	
			Duplex			
S31803	1.4462	22	5.5	3.0	0.14	
S32205	1.4462	22.5	5.5	3.2	0.17	
S32550	1.4507	25.5	6.5	3.1	0.18	Cu 1.6
			Super duplex			
S32760	1.4501	25	6.5	3.5	0.25	Cu 0.7, W 0.7
S32750	1.4410	25	7	4.0	0.28	

[a]Unified numbering system.
[b]European Norm (European Committee for Standardization, Brussels, Belgium).

The corrosion resistance of duplex steels is comparable in corrosion resistance with austenitic steels as:

Lean duplex (S32304)	→	Type 316 (S31600)
Duplex (S31803)	→	Type 317 (S31700 and N08904)
Super duplex	→	6 MO austenitics (S31254, N08926, N08367)

Table 4.12 *Lowest temperature °C, at which the corrosion rate exceeds 0.27 mm/year (5 mpy)*

Solution	S32304	S31803/S32205	S32750	N08904	S31254
1% Hydrochloric acid (HCl)	55	85	>100	50	70
1% HCl + 0.3% $FeCl_3$	20	30–40	95	50–60	60–95
10% Sulfuric acid (H_2SO_4)	65	60	75	60	60
60% H_2SO_4 + Nitrogen (N_2)-bubbling	<15	<15	<15	85	40
96.4% H_2SO_4	15	25	30	35	20
85% Phosphoric acid (H_3PO_4)	95	90	95	120	110
83% H_3PO_4 + 2% hydrofluoric acid (HF)	35	50	60	120	90
80% Acetic acid (CH_3COOH)	>106	>106	>106	>106	>106
50% CH_3COOH + 50% acetic anhydride [$(CH_3CO)_2$]	90	100	110	>126	>126
50% Formic acid (HCOOH)	15	90	90	100	100
50% Sodium hydroxide (NaOH)	95	90	110	140	115

Table 4.13 *PRE values for some duplex steel grades*

Lean duplex grades PRE<30	
S32304	26
S31500	29
Duplex grades PRE 30–40	
S31803	34
S32205	36
S32550	39
Super duplex grades PRE >40	
S32760	41
S32750	43

The duplex stainless steels are superior to other stainless steels with respect to high resistance to chloride stress corrosion cracking, high mechanical strength, lower thermal expansion than the austenitic grade steels, and good erosion and wear resistance.

The important property of high mechanical strength of duplex stainless steels has been profitably used in the fabrication of pressure vessels, and storage tanks. The digesters in the pulp and paper industry are made of duplex stainless steels of wall thickness of 19–21 mm compared with 31 mm thickness of carbon steel. Some typical wall thickness values of steels calculated for pressure vessels are noted below:

	Wall thickness (mm) required	
Steel	ASME VIII-I	TKN-87
Carbon steel	31	30
Austenitic stainless steel (304)	**25**	**28**
Clad steel	24	22
Duplex stainless steel (S32304)	**21**	**17**
Duplex stainless steel (S31803)	19	15

Duplex steel can be used in unpressurized storage tanks of all kinds. The storage tanks are used for phosphoric acid. A storage tank of dimensions 13 m diameter, 12 m height, 1590 m^3 volume fabricated from 316 L stainless steel weighs 33 900 kg compared with

Table 4.14 *Critical temperatures in some pitting and crevice corrosion tests*

UNS No.	EN	CPT in 6% $FeCl_3$ (°C)	CPT in 6% $FeCl_3$ (°C)	CPT in 1 M NaCl (°C)
S31603	1.4436	10–25	2.5	15–35
S32304	1.4362	15–20	2.5	17.5–22.5
S31803/S32205	1.4462	35–42.5	22.5–25	50–55
S327450	1.4410	67.5–80	42.5	87.5–97.5

22 300 kg for a duplex stainless steel tank due to the use of reduced thickness of duplex grade steel.

The duplex grade stainless steels are also used in shell and tube-heat exchangers because of their high resistance to SCC and lower thermal expansion than austenitic steels. These steels are also used in high-pressure piping and also in systems requiring high-erosion resistance.

4.3.2 Martensitic Stainless Steels

The martensitic stainless steels are iron–chromium alloys with greater than 10.5% chromium which can be hardened by suitable cooling to room temperature following a high-temperature heat treatment. Because of the low chromium content and high carbon content the corrosion resistance of martensitic stainless steels is limited compared with other stainless steels. On the other hand martensitic stainless steels are hardenable and exhibit high strength and hardness. These steels are relatively low-cost alloys.

The distinction between martensitic steels and other steels is not sharp. Some ferritic stainless steels such as AISI 430 steel (UNS S4300) or the 3Cr 12 alloy (UNS S41003), can be partially martensitic. Conversely, low-carbon martensitic steels such as AISI 410S (UNS 41008) and 416 (UNS S41603) might substantially ferritic. The lower chromium alloy content steels such as AISI 500 series heat-resistant steels also have many characteristics of martensitic steels.

The general chemical composition of the martensitic steels is given in Table 4.15. The salient function of the minor elements in the martensitic stainless steels is described briefly in Table 4.16.

Most martensitic steels are hardened by heat treatment. These steels tempered below 425°C have good corrosion resistance. When the steels are tempered at about 425–540°C, resistance to SCC and hydrogen embrittlement is increased. The corrosion resistance of the steels in potable water and high-purity water at high temperature is satisfactory. These steels are highly resistant to flow erosion and erosion–corrosion. These steels are useful in applications such as boat propellers, propeller shafts and pump impellers.

Some data on corrosion rates[24] in acetic acid (5%) and phosphoric acids (5%) at 49°C and measured pitting potentials of martensitic steels and Type 409 and 430 ferritic steels are given in Tables 4.17 and 4.18, respectively. The martensitic steel samples were hardened and tempered at 204°C.

In general the corrosion rates of martensitic steels are higher than the annealed ferritic steelsAISI 409 and 430. The pitting potentials of martensitic steels are higher than AISI 409.

Some of the martensitic steels are used in oil or natural gas production and in oil refining operations. The alloys used in aqueous service environments are UNS S41000, CA-15 or CA-15 M, UNS S42400 or CA-6NM; UNS S17400, and UNS S45000 with the provision that they are properly tempered and precipitation hardened. The alloys acceptable for use in well casing or tubing in sour service are API 5CT Grade L-80, API 5 CT Grade C-90 Type 1, API 5 CT Grade T-95 Type 1 (special composition versions of Type 420 with 13% Cr) and UNS S42500 alloys.

Atmospheric exposure of materials such as Type 410 steel to marine atmosphere resulted in an average penetration rate of 0.20 μm/yr and 0.125 mm deep pits at the end of

Table 4.15 *The general compositions (percentages by weight, maximum or range) of the alloys*

UNS	Type	C	Mn	S	Si	Cr	Mo	Ni	Other
S40300	403	0.15	1.00	0.030	0.50	11.50–13.50			
S41000	410	0.15	1.00	0.030	1.00	11.50–13.50			
S41400	414	0.15	1.00	0.030	1.00	11.50–13.50		1.25–2.50	
S41500	415	0.05	0.50–1.00	0.030	0.60	11.50–14.00	0.50–1.00	3.50–5.50	
S41600	416	0.15	1.25	0.15–0.30	1.00	12.00–14.00			
S41800[a]	418	0.15–0.20	0.50	0.030	0.50	12.00–14.00		1.80–2.20	2.50–3.50 W
S42000	420	≥0.15	1.00	0.030	1.00	12.00–14.00			
S42020	420°F	≥0.15	1.25	≥0.15	1.00	12.00–14.00	0.60		
S42023	420FSe	0.30–0.40	1.25	0.06	1.00	12.00–14.00	0.60		≥0.15 Se
S42200	422	0.20–0.25	1.00	0.030	0.75	11.00–13.50	0.75–1.25	0.50–1.00	0.75–1.25 W, 0.15–0.30 V
S42400	424	0.06	0.50–1.00	0.030	0.30–0.60	12.00–14.00	0.30–0.70	3.50–4.50	
S42500	425	0.08–0.20	1.00	0.010	1.00	14.00–16.00	0.30–0.70	1.00–2.00	
	425 modified	0.50–0.55	1.00	0.030	1.00	13.00–14.00	0.80–1.20	0.50	
S43100	431	0.20	1.00	0.030	1.00	15.00–17.00		1.25–2.50	
S44002	440A	0.60–0.75	1.00	0.030	1.00	16.00–18.00	0.75		
S44003	440B	0.75–0.95	1.00	0.030	1.00	16.00–18.00	0.75		
S44004	440C	0.95–1.20	1.00	0.030	1.00	16.00–18.00	0.75		
S44020	440F	0.95–1.20	1.25	0.10–0.35	1.00	16.00–18.00	0.40–0.60	0.75	
S44023	449FSe	0.95–1.20	1.25	0.030	1.00	16.00–18.00	0.60	0.75	≥0.15 Se
J91150	CA-15	0.15	1.00	0.040	1.50	11.50–14.00	0.50	1.00	
J91151	CA-15M	0.15	1.00	0.040	0.65	11.50–14.00	0.15–1.00	1.00	
J91153	CA-40	0.20–0.40	1.00	0.040	1.50	11.50–14.00	0.50	1.00	
J91154	CA-40F	0.20–0.40	1.00	0.02–0.040	1.50	11.50–14.00	0.50	1.00	
J91650	CA-6N	0.06	0.50	0.020	1.00	10.50–12.00	0.40–1.00	6.00–8.00	
J91540	CA-6NM	0.06	1.00	0.030	1.00	11.00–12.50	0.40–1.00	3.50–4.50	
J91422	CA-28MVW	0.20–0.28	0.50–1.00	0.030	1.00	11.00–12.50	0.90–1.25	0.50–1.00	0.90–125 W, 0.20–0.30 V
J92180	CB-7Cu-1	0.07	0.70	0.030	1.00	15.50–17.70		3.60–4.60	2.50–3.20 Cu 0.15–0.35 Nb 0.05 N
J92110	CXB-7Cu-2	0.07	0.70	0.030	1.00	14.00–15.50		4.20–5.50	2.50–3.20 Cu 0.15–0.35 Nb 0.05 N

[a]S41800 is only one of the so-called super 12% Cr alloys used for elevated temperature applications. Others include S41025, S41040, S42300 and AFC-77 alloys

Table 4.16 *Function of trace elements in martensitic alloys*

AISI Grade	UNS	Description
410	S41000	The basic martensitic steel
403	S40300	Silicon reduced (~0.5%) to improve mechanical properties
414	S41400	Nickel (~2%) added to improve mechanical properties
415	S41500	Carbon decreased and nickel (~4%) added to improve corrosion resistance
416	S41600	Sulfur (0.15–0.30%) added to improve machinability
420	S42000	Higher carbon allows higher hardness for knife blades, etc.
420F	S42020	Sulfur (0.15% minimum) added to improve machinability
420FSe	S42023	Selenium (0.15% minimum) added to improve machinability
431	S43100	Higher chromium plus nickel improve corrosion resistance
440A	S44002	Higher carbon increases hardenability with increased Cr to help maintain corrosion resistance. Used for cutting blades and bearings
440B	S44003	Still higher carbon for still higher hardness
440C	S44004	The highest carbon and the highest hardness; primary carbides promote wear resistance
440F	S44020	Sulfur (0.10–0.35%) added to improve machinability
440FSe	S44023	Selenium (0.15% minimum) added to improve machinability
425	S42500	Lower carbon and higher chromium plus nickel improve corrosion resistance
425 Mod		Higher carbon allows higher hardness, molybdenum added to improve corrosion resistance
	S42400	Lower carbon and higher nickel plus some molybdenum improve corrosion resistance

Table 4.17 *Corrosion rates of some steels*

Medium	Corrosion rate, mm/yr					
	Type 409	Type 410	Type 420	Type 425 (mod)	Type 440A	Type 430
Acetic acid (5%) at 49°C	0.022	0.002	0.028	0.122	0.059	0.001
Phosphoric acid (5%) at 49°C	0.002	0.002	0.002	0.015	0.009	0.001

Table 4.18 *Pitting potentials of some steels*

Medium	Pitting potential (V vs. SCE)					
	Type 409	Type 410	Type 420	Type 425 (mod)	Type 440A	Type 430
pH 5 solution at 24°C (100 ppm of chloride)	0.439	0.502	0.581	0.619	0.598	0.590

8 yr. It has been observed that this group of steels are susceptible to SCC, and tempering the steels above 540°C improves the sensitivity of the steels to SCC. The 17-4 PH steels are more resistant to SCC because of the precipitation hardening. Martensitic steels have good oxidation resistance up to 700°C.

Typical uses of martensitic steels are: cutlery, surgical instrumentation; blades (turbine engines); bearings, aerospace equipment; petroleum production and refining; fire arms, valves and stems; and food processing equipment.

4.4 Aluminum and Aluminum Alloys

Aluminum is a commercially important metal and is abundant. It has relatively low strength and the density of alloys is about 2.7 g/mL. The recylability and available new smelting processes, low cost and high strength-to-weight ratio are attractive properties. The metal and its alloy are nonmagnetic and have high electrical and thermal conductivity and high reflectivity. The aluminum alloys fall into two categories, namely wrought alloys and cast alloys. These are further classified as heat-treatable and non-heat-treatable alloys.

The wrought alloys that are non-heat-treatable form the 1xxx, 3xxx, 4xxx and 5xxx series while the heat treatable alloys belong to the 2xxx, 6xxx and 7xxx series. The heat treatable alloys are strengthened by: (i) a solution heat treatment at 460–565°C to dissolve soluble alloying elements; (ii) quenching to retain the alloying elements in solid solution; (iii) precipitation or aging treatment either naturally at ambient temperature, or at 115–195°C to precipitate the alloying elements of an optimum size and distribution; (iv) solution heat treatment and natural aging; (v) air quenching and aging; (vi) solution heat treatment and annealed; (vii) solution heat treatment, annealed, but overaged; (viii) precipitation or accelerated aging; and (ix) precipitation or aging treatment followed by strain hardening (cold working). In the case of non-heat-treatable alloys strengthening is produced by strain hardening which can be increased by solid solution and dispersion hardening.

The terminology and nomenclature designations of the alloys are as follows:

Strengthened tempers of non-heat-treatable alloys	H (1100-H14)
Strengthened heat-treatable alloys	T (7075-T651)
Annealed heat-treatable non-heat-treatable alloys	O

The nominal chemical composition of some wrought alloys and the typical tensile properties of the alloys in tempers typical of their most common usage are given in Tables 4.19–4.21.

In general all the non-heat-treatable alloys have a high resistance to general corrosion. The 1xxx series have low strength. The 4xxx series of alloys of low strength are used for brazing, welding products and for cladding. The 5xxx series have high corrosion resistance in most of the environments, including alkaline solutions.

The 6xxx series heat-treatable alloys of moderate strength have high resistance to general corrosion. The heat-treatable 7xxx alloys devoid of copper have high corrosion

Table 4.19 *Nominal chemical compositions of representative aluminum wrought alloys*[a]

	Percentage of alloying elements								
Alloy	Si	Cu	Mn	Mg	Cr	Zn	Ti	V	Zr
				Non-heat-treatable Alloys					
1060	99.60%	min Al							
1100	99.60%	min Al							
1350	99.50%	min Al							
3003		0.12	1.20						
3004			1.20	1.0					
5052				2.5	0.25				
5454			0.80	2.7	0.12				
5456			0.80	5.1	0.12				
5083			0.70	4.4	0.15				
5086			0.45	4.0	0.15				
7072[b]						1.0			
				Heat-treatable alloys					
2014	0.8	4.400	0.80	0.5					
2219		6.30	0.30				0.06	0.10	0.18
2024		4.40	0.60	1.5					
6061	0.6	0.28		1.0	0.20				
6063	0.4			0.7					
7005			0.45	1.4	0.13	4.5	0.04		0.14
7050		2.30		2.2		6.2			
7075		1.60		2.5	0.23	5.6			

[a]Reprinted from reference 27, pp. 111–145 by courtesy of Marcel Dekker, Inc.
[b]Cladding for Alclad products

resistance. Cast aluminum alloys are of two types, namely non-heat-treatable F and heat-treatable T. The casting may involve die, permanent mold or sand-casting. As is the case with wrought alloys, the alloys containing copper have poor corrosion resistance. Alclad alloys are duplex wrought products, which have a core of an aluminum alloy and a coating on one or both sides of aluminum or an aluminum alloy.

Some nominal chemical composition of aluminum cast alloys and their tensile properties are listed in Table 4.22 and 4.23, respectively.

4.4.1 Corrosion Behavior of Aluminum and its Alloys

Aluminum is an active metal and its resistance to corrosion depends on the formation of the protective oxide film. According to the Pourbaix diagram the metal is passive in the pH range ~4–9. The protective oxide film formed in water and atmospheres at ambient temperatures is amorphous and a few nanometres in thickness. The stability of the oxide film and its disruption results in corrosion.

The dissolved oxygen in acid solution causes corrosion of aluminum; the hydrogen, nitrogen, carbon dioxide and hydrogen sulfide have no effect. Hydrogen chloride is

Table 4.20 *Typical tensile properties of representative non-heat-treatable aluminum wrought alloys in various tempers*[a,b]

Alloy and temper		Strength (MPa)		Percentage elongation	
		Ultimate	Yield	In 50 mm[c]	In 5D[d]
1060	–O	70	30	43	
	–H12	85	75	16	
	–H14	100	90	12	
	–H16	115	105	8	
	–H18	130	125	6	
1100	–O	90	35	35	42
	–H14	125	125	9	18
	–H18	165	150	5	13
3003	–O	110	40	30	37
	–H14	150	145	8	14
	–H18	200	185	4	9
3004	–O	180	70	20	22
	–H34	240	200	9	10
	–H38	285	250	5	5
5052	–O	195	90	25	27
	–H34	260	215	10	12
	–H38	290	255	7	7
5454	–O	250	115	22	
	–H32	275	205	10	
	–H34	305	240	10	
	–H111	260	180	14	
	–H112	250	125	18	
5456	–O	310	160		22
	–H111	325	230		16
	–H112	310	165		20
	H116, H321	350	255		14
5083	–O	290	145		20
	–H116, H321	315	230		14
5086	–O	260	115	22	
	–H116, H32	290	205	12	
	–H34	325	255	10	
	–H112	270	130	14	

[a]Average for various sizes, product forms and methods of manufacture, not to be specified as engineering requirements or used for design purposes
[b]Reprinted from reference 27, pp. 111–145 courtesy of Marcel Dekker, Inc.
[c]1.60-mm-thick specimen
[d]12.5-mm-diameter specimen

Table 4.21 *Typical tensile properties of representative heat-treatable aluminum wrought alloys in various tempers*[a,b]

Alloy and temper		Strength (MPa)		Percentage elongation	
		Ultimate	Yield	In 50 mm[c]	In 5D[d]
2014	–O	185	95		16
	–T4, T451	425	290		19
	–T6, T651	485	415		11
2219	–O	170	75	18	
	–T37	395	315	11	
	–T87	475	395	10	
2024	–O	185	75	20	20
	–T4, T351	470	325	20	17
	–T851	480	450	6	
	–T86	515	490	6	7
6061	–O	125	55	25	27
	–T4, T451	240	145	22	22
	–T6, T651	310	275	12	15
6063	–O	195	90	25	27
	–H34	260	215	10	12
	–H38	290	255	7	7
7005	–O	195	85		20
	–T63, T6351	370	315		10
7050	–T76, T7651	540	485		10
	–T736, T73651	510	455		10
7075	–O	230	105	17	14
	–T6, T651	570	505	11	9
	–T76, T7651	535	470		10
	–T736, T7351	500	435		11

[a]Average for various sizes, product forms and methods of manufacture, not to be specified as engineering requirements or used for design purposes
[b]Reprinted from reference 27, pp. 111–145 courtesy of Marcel Dekker, Inc.
[c]1.60-mm-thick specimen
[d]12.5-mm-diameter specimen

strongly corrosive while sulfur dioxide in solutions has an etching effect. The corrosion of the metal in aqueous solutions is severe at 70–80°C.

The relation between the corrosion rate and pH in various aqueous media is depicted in Figure 4.5 and the corrosion rate is minimal in the pH range 4–8.5. Most of the alloys are inert to concentrated nitric and acetic acids, but are attacked by dilute nitric, sulfuric and hydrochloric acids. The sodium silicate acts as an inhibitor. The sensitivity to acid attack also depends upon the alloy.

Table 4.22 *Nominal chemical composition of representative aluminum casting alloys*[a]

	Percentage of alloying elements				
Alloy	Si	Cu	Mg	Ni	Zn
Alloys not normally heat-treated					
360.0	9.5		0.5		
380.0	8.5	3.5			
443.0	5.3				
514.0			4.0		
710.0		0.5	0.7		6.5
Alloys normally heat-treated					
295.0	0.8	4.5			
336.0	12.0	1.0	1.0	2.5	
355.0	5.0	1.3	0.5		
356.0	7.0		0.3		
357.0	7.0		0.5		

[a]Reprinted from reference 27, pp. 111–145 by courtesy of Marcel Dekker Inc.

Table 4.23 *Typical tensile properties of representative aluminum casting alloys in various tempers*[a]

Alloy	and temper	Type casting	Strength (MPa) Ultimate	Strength (MPa) Yield	Percentage elongation In 50 mm[c]
295.0	T6	Sand	250	165	5
336.0	T5	Permanent mold	250	195	1
355.0	T6	Sand	240	170	3
	T6	Permanent mold	375	240	4
	T61	Sand	280	250	3
	T62	Permanent mold	400	360	1.5
356-0	T6	Sand	230	165	3.5
	T6	Permanent mold	255	185	5
	T7	Sand	235	205	2
	T7	Permanent mold	220	165	6
357.0	T6	Sand	345	295	2
	T6	Permanent mold	360	295	5
	T7	Sand	275	235	3
	T7	Permanent mold	260	205	5
360.0	F	Pressure die	325	170	3
380.0	F	Pressure die	330	165	3′
443.0	F	Pressure mold	160	60	10
514.0	F	Sand	170	85	9
710.0	F	Sand	240	170	5

[a]Reprinted from reference 27, pp. 111–145 by courtesy of Marcel Dekker, Inc.
[b]Average for separate cast test bars, not to be specified as engineering or used for design purposes
[c]1.60-mm-thick specimen

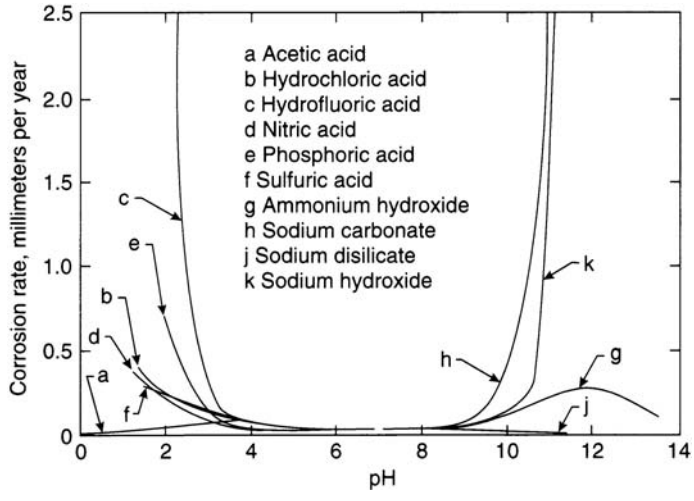

Figure 4.5 *Relation to pH of the corrosivities towards 1100-H14 alloy sheet of various chemical solutions*[27]

Fresh water. Aluminum and its alloys are not prone to corrosion on exposure to distilled water up to 180°C. Thus storage tanks, piping and fittings of the alloy can be used for handling distilled water. The composition of natural fresh water is variable. In spite of this restriction, the alloys are not attacked, even at 180°C in natural waters. It should be noted that pitting may occur when a small thickness of the sample is exposed. In this case Alclad 3003 is recommended for use to avoid failure due to pitting.

Seawater. The recommended alloys for exposure to unpolluted seawater are 5XXX wrought alloys and 356.0 and 514.0 cast alloys[27]. It is likely that some pitting corrosion may occur and rates of the order of 3–6 μm/yr during the first year and 0.8–1.5 μm/yr averaged over a 10-yr period have been observed. The depth of seawater exposure of samples appears to be of no relevance.

Atmospheric Corrosion. The aluminum-based alloys in general are corrosion resistant to outdoor exposure with the exception of copper-bearing alloys. The Alclad alloys gave the best performance. The loss in tensile strength has been used as a measure of corrosivity and the loss of 1–2% of tensile strength over a period of 1 yr and in particular a loss of 17% was observed with 2017T alloy in 1 yr of outdoor exposure.[28]

The sulfur dioxide in industrial atmospheres corrodes aluminum alloys due to the formation of sulfurous acid.

Soil Corrosion. The extent of corrosion of the alloy buried underground depends on the soil composition and climatic conditions. Some typical data[29] are given in Table 4.24. The corrosive attack of samples exposed to marshy soils was more severe than the samples exposed to well-drained soils.

Table 4.24 *Soil burial tests of 5 yr duration with aluminum alloy specimens*[a,b]

Alloy	Well-drained soil			Marshy soil		
	Maximum depth of attack[c] (in)	% change in tensile strength[d]	Remarks (in = 25.4 mm)	Maximum depth of attack (in)	% change in tensile strength	Remarks
1100-½H	0.0017	−1	Mild general etching	0.0280	−7	Pitted
5052-½H	0.0007	+1	Mild general etching	0.0140	0	Pitted
6053-T	0.0007	0	Mild general etching	0.0150	0	Pitted
6053-T, Alrok	0.0006	0	Mild general etching	0.0006	0	Mild general etching
No. 13 coated						
6053-T, aluminite	0.0003	0	Mild general etching	0.0002	+2	Mild general etching
No. 204 coated						
2017-T	0.0380	−20	Severe pitting	0.0310	−41	Severely pitted
Alclad 2024-T	0.0013	0	Mild general etching	0.0028	−1	Generally etched
Steel	0.0640	−27	Completely perforated at 3 spots	0.0190	−17	Pitted

[a]Specimens in the form of panels $3 \times 9 \times 0.064$ in thick were buried to a depth of 61 cm in soil at the Aluminum Research Laboratories, New Kensington, PA
[b]See reference 29
[c]Depth of attack determined by microscopic examination of cross-sections
[d]Change in tensile strength determined by machining tensile specimens from the panels after exposure and comparing their strength with that of unexposed tensile specimens of the same materials.

The performance of aluminum and its alloys in some environments is given below.

Exposure conditions	Remarks on degree of corrosive attack
Steam condensate	Corrosion is negligible if suitable traps are installed in the steam lines so that carry-over of water is minimized
Gases (CO_2, SO_2, H_2S)	Aluminum and its alloys are inert to dry gases. Moist SO_2 gives rise to sulfurous acid, which is corrosive Moist H_2S, is not corrosive; moist CO_2 is also not corrosive

	Al (ipy)	**Cu (ipy)**	**Steel (ipy)**
Moist CO_2	0.00004		0.00977
Moist SO_2	0.0498	0.0701	1.02
Moist H_2S	0.00028	0.0103	0.680

(*contd.*)

(*contd.*)

Exposure conditions	Remarks on degree of corrosive attack
Concentrated HNO_3 (80–99%)	Resistant to corrosion
Dilute HNO_3 and H_2SO_4	No corrosive attack of Al and its alloys corrosive attack
$HClO_4$, H_3PO_4 (intermediate concentrations)	
Alkalis	Corrosive in <0.01% solutions of NaOH and KOH. Alloys containing ~4% Mg resist corrosion
Dry phenols and CCl_4	Corrosive attack. Traces of water minimize the corrosive attack
Acetic, butyric, citric, gluconic, malic, propionic, tartaric acids	1100 and 3003 alloys immune

The various forms of corrosion encountered in the case of aluminum and its alloys are listed below:

Form of corrosion	Reference
Uniform corrosion	30, 31
Galvanic corrosion	32
Pitting corrosion	33, 34
Deposition corrosion	35
Crevice corrosion	36
Water staining	37
Filiform corrosion	37
Biological corrosion	38, 39
Erosion corrosion	37
Intergranular corrosion	37
Exfoliation corrosion	37
Stress–corrosion cracking	31, 40, 41, 42
Hydrogen embrittlement	31, 41
Fretting corrosion	43
Stray current corrosion	37

Some salient features of the aluminum alloys are given below:

Alloy	Features
1000 series	99% Al, excellent resistance to corrosion; high electrical and thermal conductivity; poor mechanical properties
2000 series	Contains copper; high strength and heat-treatable; low corrosion resistance; subject to intergranular attack and difficult to inhibit; 2024 alloy widely used in aircraft industry; subject to SCC

(*contd.*)

(*contd.*)

Alloy	Features
3000 series	Contains manganese; cannot be heat-treated; most widely used alloys; 3003 has moderate strength; good workability can be inhibited in some media
4000 series	Contains silicon; used mainly for welding because of lower melting points; used in architectures because of color effects due to applied anodic coatings; have good corrosion resistance and can be inhibited
5000 series	Contains magnesium; corrosion-resistant, can be inhibited; widely used in marine atmospheres with good performance; susceptible to SCC under certain conditions of loading
6000 series	Contains Si and Mg in a ratio required to form magnesium silicide; heat-treatable; 6061 is a major alloy; have good corrosion resistance and the alloys can be inhibited effectively
7000 series	Contains zinc, small amounts of Mg, Cu and Cr; heat-treatable, have high strength (e.g., 7075); inhibitors can be used; subject to SCC

New aluminum alloys containing 3% lithium with small amounts of zinc and magnesium may supplant 2024 and 7075 in the aircraft wings and fuselage.

The selection of an alloy for a specific application is based on the cost and the corrosion resistance of the alloy in the environment of interest. It is also possible to subject the chosen alloy to a process by which the corrosion resistance of the selected material can be improved within the acceptable limits. Some of the corrosion prevention and protection strategies with respect to the aluminum-based alloys are: (i) design; (ii) alloy selection and joint sealants; (iii) aluminum thermal spraying; anodic coatings; (iv) inhibitors; (v) conversion and organic coatings; and (vi) cathodic protection.

Galvanic corrosion of aluminum in contact with dissimilar metal such as copper or indirect galvanic effects such as aluminum in contact with solutions containing reducible heavy metal compounds should be avoided in the design stage by a judicious selection of the alloy.[28] Corrosion can also be prevented by cladding with a more corrosion-resistant alloy such as high-purity aluminum, a low-magnesium–silicon alloy or an alloy of 1% zinc. These cladding materials have been used to protect 2000 and 7000 series aluminum alloys. The cladding on each side is about 2–5% of the total thickness.

The aluminum-based alloys such as 1100, 3300, 5052, 6053, Alclad 3300, Alclad 1017-T and Alclad 20-24-T are highly resistant to most natural environments; alloys of thickness <0.076 mm should not be used. Lead and bismuth added to alloys 2021 and 6262 improve chip breakage and other machining characteristics.

Nickel is added to wrought alloys 2018, 2218 and 2618 for use in high-temperature exposures, 3XXX cast alloys for pistons, cylinder blocks and other engine parts subject to high temperatures.

Joints, depressions and similar locations accumulate moisture and dirt and are susceptible to corrosion than other areas. Plastic or semi-solid sealing compounds that adhere to

the adjacent metal surfaces are effective in preventing corrosion. Joint-sealants containing soluble inhibitors may be used.[28]

When mechanical factors such as formability or hardness are of importance aluminum alloys of 1100, 3300 or 5052 series in soft tempers might be selected and for still higher strength alloy 6061 may be chosen.

Aluminum spraying is used to coat less corrosion-resistant alloys. In the case of some composites, corrosion is due to the galvanic action between the aluminum matrix and the reinforcing material. Aluminum thermal spraying has been successfully used for the protection of the discontinous silicon carbide/aluminum composites, and continuous graphite/aluminum. Other protection procedures include sulfuric acid anodizing and iron vapor deposition on aluminum.[44]

Anodizing is an electrolytic method involving aluminum alloy as the anode, which is converted to an aluminum oxide layer of 5–30 μm thickness. Anodic coatings obtained in sulfuric acid, when properly sealed, are particularly effective against discoloration. Anodic coatings are used in the case of alloys used in architecture and as well as paint bases.

Corrosion inhibitors such as chromates, silicates, polyphosphates, nitrites, nitrates, borates and mercaptobenzothiazole have been used in corrosion inhibition of aluminum and its alloys.[45]

Conversion coatings such as chromates or phosphates may be used. Molybdates may be used in place of chromates because of the environmental toxicity of hexavalent chromium. Paint can also be applied over a conversion coating.[46]

Some measures involving cathodic protection of aluminum using zinc as the sacrificial anode,[47] and protection of aluminum ship hulls are found in the literature.[37] Overprotection may lead to alkali (cathodic corrosion) attack. Alclad alloy systems are also some form of self-contained cathodic protection systems.

4.5 Copper and Copper Alloys

Copper and its alloys are extensively used in everyday life, typical uses being copper pipes for domestic water supply, and aesthetic applications such as artwork in the form of statues. The annual production of copper water tubing is approximately 500 000 tonnes, equivalent to a length ~1.25 billion metres. The attractive features of copper and its alloys are corrosion resistance, ease of fabrication and its potential for recycling.

Copper itself is very soft and malleable and it is alloyed with Zn, Sn, Ni and Al to improve the mechanical properties and to retain its corrosion resistance. Nickel addition allows handling of increased flow rates in water systems while zinc confers greater resistance to sulfide attack. The generic classification of some copper alloys is given in Table 4.25.

Depending upon the environment to which the copper and its alloys are exposed, various forms of corrosive attack occur. The environments of interest are: (i) atmospheric; (ii) fresh water and seawater; (iii) soil; and (iv) chemical solutions, including acids and bases. The forms of corrosion of copper and its alloys in different environments

Table 4.25 *Generic classification of copper alloys*

Generic name	UNS numbers	Composition
Wrought alloys		
Copper	C10100-C15760	>99% Cu
High-copper alloys	C16200-C19600	<96% Cu
Brasses	C205-C28580	Cu-Zn
Leaded brasses	C31200-C38590	Cu-Zn-Pb
Tin brasses	C40400-C49080	Cu-Zn-Sn-Pb
Phosphor bronzes	C50100-C52400	Cu-Sn-P
Leaded phosphor bronzes	C53200-C54800	Cu-Sn-Pb-P
Copper–phosphorus and copper–silver–phosphorus alloys	C55180-C55284	Cu-P-Ag
Aluminum bronzes	C60600-C64400	Cu-Al-Ni-Fe-Si-Sn
Silicon bronzes	C64700-C66100	Cu-Si-Sn
Other copper–zinc alloys	C66400-C69900	
Copper–nickels	C70000-C79900	Cu-Ni-Fe
Nickel silvers	C73200-C79900	Cu-Ni-Zn
Cast alloys		
Coppers	C80100-C81100	>99% Cu
High-copper alloys	C81300-C82800	>94% Cu
Red and leaded red brasses	C83300-C85800	Cu-Zn-Sn-Pb (75–89% Cu)
Yellow and leaded yellow brasses	C85200-C85800	Cu-Zn-Sn-Pb (57–74% Cu)
Manganese and leaded manganese bronzes	C86100-C86800	Cu-Zn-Mn-Fe-Pb
Silicon bronzes, silicon brasses	C87300-C87900	Cu-Zn-Si
Tin bronzes and leaded tin bronzes	C90200-C94500	Cu-Sn-Zn-Pb
Nickel–tin bronzes	C94700-C94900	Cu-Ni-Sn-Zn-Pb
Aluminium bronzes	C95200-C95810	Cu-Al-Fe-Ni
Copper–nickels	C96200-C96800	Cu-Ni-Fe
Nickel silvers	C97300-C97800	Cu-Ni-Zn-Pb-Sn
Leaded coppers	C98200-C98800	Cu-Pb
Miscellaneous alloys	C99300-C99750	

are general corrosion, pitting corrosion, erosion–corrosion, dealloying (dezincification), stress–corrosion cracking and biofouling.

4.5.1 Atmospheric Corrosion

The main corrosive agents involved are oxygen, sulfur dioxide, nitrogen oxides, chlorine, hydrogen chloride, ammonia, ozone and other airborne particles present in the atmosphere. The formation of patina during atmospheric corrosion is a familiar process. The corrosion products identified are basic copper sulfate Cu_4SO_4 $(OH)_6$ H_2O (posnjakite), brochantite, $CuSO_4$ $(OH)_6$ and antlerite Cu_3SO_4 $(OH)_4$. Copper chloride and carbonate have also been identified.[48,49]

The source of chloride is seawater as well as the deicing salts used on roads. The hydrogen chloride is also present in seawater aerosols. The corrosion of copper and its alloys in marine atmospheres has been studied and a corrosion rate of 600–700 $\mu g/cm^2$ yr averaged over a period of 8 yr has been reported.[50]

Although the degree of atmospheric corrosion of copper and its alloys depends upon the corrosive agents present, the corrosion rate has been found to generally decrease with time. The copper and its alloys such as silicon bronze, tin bronze usually corrode at moderate rates, while brass, aluminum bronze, nickel silver, and copper–nickel corrode at a slower rate.[51] The most commonly used copper alloys are C11000, C22000, C38500 and C75200.

4.5.2 Soil Corrosion

Copper and its alloys can be safely buried in most soils, although high corrosion rates have been observed when cinders and acidic peat are present in the soils. When high corrosion rates are expected it is preferable to protect the samples with bituminous, plastic or paint coatings. When brasses are used dezincification problems may be encountered and hence their use should be avoided, unless high sulfide concentration is present in the soils.

4.5.3 General Corrosion in Aqueous Media

Copper, being a noble metal, has good resistance to corrosion. A thin adherent film of cuprous oxide and cupric carbonate is formed due to corrosion. Passivation is not a prominent process. The dissolved copper in solution affects the electrode potential such that the increase in velocity of the solution in contact with the metal results in increasing attack of the metal. Thus cuprous oxide is produced under dynamic flow of the solution. The thickness of the oxide film is about 500 nm.

Depending upon the composition of the water, other products may be formed. Typically the dissolved species in water such as chloride, sulfate or carbonate, present in small concentrations, give rise to the chloride, sulfate or carbonate compounds of copper.

The corrosion rates of copper in soft waters are greater than in hard waters since calcium carbonate precipitation in hard waters retards the corrosion rate of copper. Typically the corrosion rate of copper in distilled water is about 0.051–0.16 mm/yr and in rapid flowing conditions can be as high as 0.26 mm/yr.

The corrosion rate of a totally immersed copper sample in seawater is about 0.02–0.07 mm/yr and at half-tide the rate is 0.02–0.1 mm/yr. In this respect the corrosion resistance of copper is 2–5 times greater than mild steel under total immersion conditions and even greater under half-tide conditions. The copper loses its corrosion resistance in seawater of velocities greater than 1 m/s and the rate of dissolution is such that toxic copper species produced are beneficial in that they are used in marine antifouling agents.

Copper alloys C44300, C44500, C61300, C68700, C70600 and C71500 series are more corrosion resistant than copper in natural waters. In general these alloys contain corrosion-resistant metals such as nickel or metals such as iron and aluminum, which

have a tendency to readily passivate. Some typical corrosion rates in water of common copper alloys are as follows:

Alloy	Corrosion rate (mm/yr)
Brasses (natural water)	0.003–0.03
(seawater)	0.008–0.12
Copper-tin alloy (seawater)	0.013–0.034
Aluminum bronzes (seawater)	0.001–0.003
Silicon bronzes (seawater)	0.02–0.07

Aluminum bronzes, copper–nickel alloy (69 Cu-30 Ni-1 Fe and copper–nickel alloys containing added manganese are resistant to impingement and cavitation-induced damage under flowing conditions.

The composition of copper–aluminum (wrought and cast), cupronickels, copper–tin (wrought and cast) and brasses are given in Tables 4.26–4.31.

Copper alloys such as the brasses and bronzes can be cast by either the sand-casting or permanent mould cast methods. The alloys casts in permanent mould condition have greater corrosion resistance than the sand-cast alloys.[52] This difference has been attributed to the greater porosity of the alloys in sand-cast conditions.

Table 4.26 *Some common wrought copper–aluminum alloys: chemical composition*

UNS numbers	Cu	Al	Fe	Ni	Mn	Si	Sn	Others
C60800	92.5–94.8	5.0–6.5	0.10					0.02–0.35 As, 0.10 Pb
C61000	90.0–93.0	6.0–8.5	0.50			0.10		0.02 Pb
C61300	86.6–92.0	6.0–7.5	2.0–3.0	0.15	0.10	0.10	0.20–0.50	0.01 Pb
C61400	88.0–92.5	6.0–8.0	1.5–3.5					0.01 Pb
C61500	89.0–90.5	7.7–8.3		1.8–2.2				0.015 Pb
C61800	86.9–91.0	8.5–11.0	0.5–1.5			0.10		0.02 Pb
C62300	82.2–89.5	8.5–11.0	2.0–4.0	1.0	0.5	0.25	0.60	
C63000	78.0–85.0	9.0–11.0	2.0–4.0	4.0–5.5	1.5	0.25	0.20	
C63200	75.9–84.5	8.5–9.5	3.0–5.0	4.0–5.5	3.5	0.10		0.02 Pb

Table 4.27 *Some common cast copper–aluminum alloys: chemical composition*

UNS numbers	Cu	Al	Fe	Ni	Mn	Others
C95200	86.0	8.5–9.5	2.5–4.0			1.0 total
C95300	86.0	9.0–11.0	0.8–1.5			1.0 total
C95400	83.0	10.0–11.5	3.0–5.0	2.5	0.5	0.5 total
C95500	79.0	10.0–11.5	3.0–5.0	3.0–5.5	3.50	0.5 total
C95700	71.0	7.0–8.5	2.0–4.0	1.5–3.0	11.0–14.0	0.5 total
C95800	79.0	8.5–9.5	3.5–4.5	4.0–5.0	0.8–1.5	0.5 total

Table 4.28 *Some common cupronickels: chemical composition*

UNS numbers	Cu	Ni	Fe	Mn	Others
C-70600	Bal	9.0–11.0	1.0–1.8	0.0 max	Pb 0.05 max, Zn 1.0 max
C71500	Bal	29.0–33.0 29.0–33.0	0.40–0.7	1.0 max	Pb 0.05 max, Zn 1.0 max
C71900	Bal	29.0–32.0	0.25 max	0.5–1.0	Cr 2.6–3.2, Zr 0.08–0.2, Ti 0.02–0.08
C96200	Bal	9.0–11.0	1.0–1.8	1.5 max	Pb 0.03 max
C96400	Bal	28.0–32.0	0.25–1.5	1.5 max	Pb 0.03 max

Bal = balance

Table 4.29 *Some common wrought copper–tin alloys; chemical composition*

UNS numbers	Cu	Pb	Fe	Sn	Zn	P
C-51000	Rem	0.05	0.10	4.2–5.8	0.30	0.03–0.35
C-51100	Rem	0.05	0.10	3.5–4.9	0.30	0.03–0.35
C-52100	Rem	0.05	0.10	7.0–9.0	0.20	0.03–0.35
C-52400	Rem	0.05	0.10	9.0–11.0	0.20	0.03–0.35
C-54400	Rem	3.5–4.5	0.10	3.5–4.5	1.5–4.5	0.01–0.50

Rem = remaining

Table 4.30 *Some common cast copper–tin alloys, chemical composition*

UNS numbers	Cu	Sn	Pb	Zn	Fe	Sb	Ni	S	P
C-90300	86.0–89.0	7.5–9.0	0.30	2.0–5.0	0.20	0.20	1.0	0.05	0.05
C-90500	86.0–89.0	9.0–11.0	0.30	1.0–3.0	0.25	0.20	1.0	0.05	0.05
C-92200	86.0–89.0	5.5–6.5	1.0–2.0	2.0–5.0	0.25	0.25	1.0	0.05	0.05
C93700	78.0–92.0	9.0–11.0	0.8–11.0	0.8	0.15	0.55	1.0	0.08	0.15
C93800	75.0–79.0	6.3–7.5	13.0–16.0	0.8	0.15	0.8	1.0	0.08	0.05
C93900	76.5–79.5	5.0–7.0	14.0–18.0	1.5	0.4	0.50	0.8	0.08	1.5
C94700	85.0–90.0	4.5–6.0	0.10	1.0–2.5	0.25	0.15	4.5–6.5	0.05	0.05

Table 4.31 *Some common brasses, chemical composition*

UNS numbers	Cu	Pb	Fe	Zn	Sn	Others
C-27000	63.0–68.5	0.10	0.07	Rem		
C-28000	59.0–63.0	0.30	0.07	Rem		
C-44300	70.0–73.0	0.07	0.06	Rem	0.8–1.2	0.02–0.10 As
C-44400	70.0–73.0	0.07	0.06	Rem	0.8–1.2	0.02–0.10 Sb
C-44500	70.0–73.0	0.07	0.06	Rem	0.8–1.2	
C-46400	59.0–62.0	0.20	0.10	Rem	0.5–1.0	
C-46500	59.0–62.0	0.20	0.10	Rem	0.5–1.0	0.02–0.10 As
C-46600	59.0–62.0	0.20	0.10	Rem	0.5–1.0	0.02–0.10 Sb
C-46700	59.0–62.0	0.20	0.10	Rem	0.5–1.0	
C-68700	76.0–79.0	0.07	0.06	Rem		0.02–0.10 As

4.5.4 Pitting Corrosion

The pitting corrosion of copper pipes carrying water has been observed[53] as early as 1950. Not only copper, but also copper alloys such as brasses,[54] bronzes[55] and cupronickels undergo pitting corrosion in natural waters. The pitting of copper is not confined to chloride solutions since it has been observed in bicarbonate solutions.[57] Three types of pitting of copper have been observed.[58] Type 1 pitting occurs on annealed or half-hard tubes in cold tapwater, caused by a continuous carbon film formed on the inner tube surface during bright annealing. Type 2 occurs on hard-drawn tubes in hot tapwater of low pH ($<$7.4) and low bicarbonate/sulfate ratio ($<$1). Type 3 occurs on both hard and annealed tubes in cold tap water of high pH with low salt concentration.

The pitting corrosion of copper has been inhibited by injection of ferrous salt solution. Ferrous ion injection probably results in the formation of lepidrocrocite, FeO.OH, and provides protection.

4.5.5 Dealloying

Dealloying is a prominent mode of decay of copper alloys. It is possible that one of the components of the alloy is preferentially leached out. Dealloying has been observed in the case of copper alloys in the form of preferential leaching of zinc from brasses, aluminum from aluminum bronzes and nickel from cupronickels. Brasses containing $>$15% zinc are susceptible to dezincification in aqueous medium.

Dealuminification occurs in aluminum bronzes containing the γ-2 phase microstructure and the process is more severe when the γ-2 phase forms a continuous grain boundary network. Dealuminification can be averted by rapid cooling from $>$600°C, or by addition of 1–2% iron or more than 4.5% nickel. Microstructural changes can still occur during welding and lead to corrosion in the heat-affected zone.

Dezincification of brass fittings occurs when the β-phase is present. Dezincification is accelerated by high temperature, high chloride concentration, low flow-rates and differential aeration. Dezincification can be inhibited by the addition of 1% tin and $\sim$0.04% arsenic.

4.5.6 Flow-induced Corrosion

High velocities of aqueous solutions impinging on copper and brass tubes produce impingement on the metal or alloy. The aluminum brass and cupronickel alloys have great resistance to flow-induced attack up to a well-defined maximum for the flow rate, beyond which the film on the metal surface will be disrupted. Admiralty brass and aluminum brass have lower values for maximum velocity of flow than cupronickels. Admiralty brass and aluminum brass are preferred to cupronickels for use in media containing sulfide species. Coatings have been developed for cupronickel and aluminum brass condenser tubes for land-based and marine systems.

Addition of a small quantity of iron to the alloy or to the solution improves the erosion–corrosion resistance of the alloy because of the tenacity of the iron film on the metal surface. This protection function of iron has led to the successful use of iron sacrificial pieces in preference to the familiar zinc sacrificial anodes in water boxes of condensers and heat exchangers.

4.5.7 Behavior in Chemical Environments

Behavior in chemical environments can be briefly stated in terms of resistance of copper and its alloys to acids and bases. Acids such as acetic, phosphoric, dilute sulfuric and hydrochloric acids can be handled, providing there are no oxidizing agents present. Nitric and concentrated sulphuric acids dissolve copper and its alloys and cannot be tolerated. The copper and its alloys, as is the case with any system, should be tested in acid systems or any other environment of interest closely simulating the industrial plant operating conditions before finalizing the operation of the plant.

Copper and its alloys are resistant to alkalies with the exception of ammonium hydroxide and cyanides. Ammonium ions promote stress–corrosion cracking of copper and its alloys. Ferric and stannic salts are aggressive towards copper alloys. Ammonia and cyanide ions form tetramine copper and tetracyano copper complexes in ammonia and cyanide solutions, respectively.

4.5.8 Biofouling

The biological organisms are abundant in sea and coastal estuaries. These organisms attach to marine structures such as pilings, offshore platforms, boat hulls and even inside pipes and condensers. The marine organisms adhere to some metals and alloys more readily than others.[59] In this respect copper and its alloys exhibit greater resistance to the attachment of biofouling organisms than other metals. This property has been used to advantage in cladding of ship hulls with copper. In the absence of wave velocity above 0.5 m/s, slime thickens on copper alloys for up to 18 months, and organisms attach to the slime. Biofouling is by far less at higher velocities. Biofouling of copper and its alloys increases when copper is galvanically coupled and the release of cupric ions is impaired.

Sulfate-reducing bacteria (SRB) have been known to cause corrosion of copper and its alloys and various sulfides have been identified. Some of the sulfides are digenite Cu_5S_9, chalcocite Cu_2S, covellite CuS, djuerleite $Cu_{1.96}S$.

4.5.9 Stress–Corrosion Cracking

This mode of failure is possible in all the copper alloys. The principal environment involved is ammonia. The evidence also exists for other media such as citrates, tartrates, nitrites, sulfur dioxide, carbonates, nitrogen oxides and phosphates to be conducive to a stress–corrosion cracking mode of failure of copper alloys.

The most detailed studies of the phenomenon are confined to ammoniacal solutions. In the case of ammonia medium the familiar coordination complexes $Cu(NH_3)_4^{2+}$ and $Cu(NH_3)_2^{+}$ are formed, leading to selective removal of metal and causing the damage. In ammoniacal solutions traces of phosphorus (about 0.004%) increase the susceptibility to SCC. Other elements such as As and Sb have similar effects. These elements in trace amounts in the alloy produce precipitates at the grain boundaries and make the grain boundary region more anodic to the grain bodies.

Some salient features of SCC of some selected alloys with respect to susceptibility to SCC are given below:[60]

Alloy/medium	Features
Aluminum bronzes	Susceptible to SCC. Addition of 0.2–0.3% Sn or As provided immunity to intergranular cracking of α-Al bronze No effect on transgranular cracking in ammonia solutions
Copper nickels	Not susceptible; 70 Cu–30 Ni has replaced Admiralty brass in environments containing small amount of NH_3
Silicon bronzes	Susceptible to cracking in steam and mercurous nitrate solution; silicon bronzes (Cu-Si-Mn, Cu-Si-Sn, Cu-Si-Zn), susceptible to intergranular cracking in ammonia medium
Tin brasses	More resistant to SCC than Cu–Zn alloys
Tin bronzes	Crack in NH_3 and $HgNO_3$ when the alloys are cold worked; SCC susceptibility increases with Sn content
Nickel silvers	Cu–Zn–Ni alloys containing 5, 10 and 15% Ni did not crack in mercurous nitrate solution for 7 days
Aluminum brasses	Precipitation of $CuAl_2$ at grain boundaries and formation of Cu depleted zones adjacent to grain boundaries results in a potential difference of ~200 mV between the boundary and the grain and results in intergranular cracking; resistance or immunity to SCC can be achieved by quenching from solution heat-treatment temperature
Manganese bronzes	Susceptible to SCC in NH_3, but less than Cu–Zn alloys; minimum cracking time at 5–6% Mn; alloys with 4.94% Mn failed by intergranular SCC; 21.38, 24.5% Mn alloys fail by transgranular mode; mixed mode SCC observed with 10.64% Mn alloys
Brasses	Extreme sensitivity to SCC; brasses containing <15% zinc resistant to SCC; SCC increases with Zn content up to 40%
Ammonia	SCC of Cu-base alloys; 0_2 and CO_2 accelerate SCC; failure in a wide range of NH_3/air ratios of 20–80% NH_3; Alloys of 60–65% Cu resulted in both intergranular and transgranular SCC; predominantly transgranular SCC with alloys of >70% Cu
Sulfur dioxide	70 Cu–30 Zn gave rise to intergranular SCC
Citrate and tartrate	SCC of brass in citrate of pH 10.3; in tartrate intergranular; SCC at pH 13; role of Cu citrate and tartrate complexes; alloy C72000 sensitive to intergranular SCC in citrate solution containing Cu^{2+} ions in pH range 7–11
Pyridines, ethylenediamine	Intergranular SCC of brass; primary amine > secondary amine > tertiary amine; alloys C26000 and C68700 susceptible to SCC in amines
Moist HF	Monel (Ni–Cu) susceptible to SCC. Alloys with 15–30% Cu resulted in intergranular and transgranular SCC; Yellow brass susceptible to SCC in HF (petroleum industry)
Seawater, NaCl	β-brass, intergranular SCC

Table 4.32 *Nickel alloys*

Alloy systems	Some major alloys in these systems
Ni	Commercially pure nickel, alloy 200/201
Ni–Cu alloys	Alloy 400, K-500
Ni–Mo alloys	Alloy B-, B-2, B-3, B-4, B-10
Ni–Si alloys	Cast Ni-Si alloys, Lewmet, alloy D-205
Ni–Fe alloys	Invar, Pernifer, Magnifer, Hymu 80
Ni–Cr–Fe alloys	Alloys 600, 601, 800, 800H, 800HT, 690, 602CA, 45TM
Ni–Cr–Fe–Mo–Cu alloys	28, 825, 20, G, G-3, G-30, 31, 33, 6 Mo alloys
Ni–Cr–Mo alloys	625, C-276, C-4, C-22, 686, C-2000, 59, Mat 21
High-temperature alloys	602 CA, 603 GT, 2100 GT, 45 TM, 230, 625, X, 626 Si, HR 160, 718, 617, 214, Nimonic series, Udimet series and others

Miscellaneous

Cupric acetate, polluted atmosphere, sodium chlorate, sodium formate, sodium hydroxide, sodium nitrate, sodium nitrite, sodium sulfate sulphide and sodium tungstate	SCC of alloys C26000 C44300 C70600 Brass Admiralty brass

The applications and uses of copper and its alloys is very extensive such as water piping and fittings, open structures (exposed to atmosphere) such as architecture and sculpture, in fresh water and seawater cooled heat exchangers, condensers; in chemical, industrial and power-generating equipment buried in earth for water distribution systems.

4.6 Nickel and its Alloys

Nickel and its alloys, along with the commercial code names are given in Table 4.32.

The two main nickel alloys containing about 99% nickel with remaining 1% consisting of Cu, Fe, Mn, Si, C and S are known under the designation of alloys 200 and 201. The composition of these alloys is given in Table 4.33.

Some salient features of alloys 200 and 201 are: good resistance at low to moderate temperatures, to corrosion by dilute nonaerated HCl, H_2SO_4 or H_3PO_4, but corrode in

Table 4.33 *Nickel alloys*

Alloy (UNS No.)	Ni[a]	Cu	Fe	Mn	C	Si	S
200 (N02200)	99.0 min	0.25	0.40	0.35	0.15	0.35	0.01
201 (N02201)	99.0 min	0.25	0.40	0.35	0.02	0.35	0.01

[a]Ni + Co. All values maximum unless noted otherwise

Table 4.34 *Ni–Cu alloys*

Alloy (UNS No.)	Ni (+Co)	C	Mn	Fe	S	Si	Cu[a]	Other
400 (N04400)	63.0 min	0.30	2.0	2.5	0.024	0.50	31	
K-500 (N05500)	63.0 min	0.18	1.5	2.0	0.010	0.50	30	Al 2.8[a] Ti 0.60

[a]Typical; all values maximum unless noted otherwise

nonoxidizing media in the presence oxidizing species such as ferric or cupric ions, nitrates and peroxides.

Nickel's immunity to alkalies has been successfully used in caustic evaporator tubes and the corrosion rate is <0.005 mm/yr in 50% NaOH at $\sim 100^{\circ}$C. It is recommended that Alloy 201 be used at 316°C and above in order to avoid graphitization at the grain boundaries.

Nickel is resistant to chloride-induced SCC, but subject to caustic cracking in aerated solutions under high stress. Nickel is highly resistant to corrosion in natural fresh water and flowing seawater. Pitting occurs under stagnant or crevice conditions.

Nickel is resistant to organic acids; dilute ammonium hydroxide ($<2\%$); and to chlorination or fluorination. These alloys 200 and 201 are used in petrochemical, chemical industry, food industry and in the production of synthetic fibers.

The alloys consisting of nickel and copper, along with minor amounts of Fe, Mn have the composition given in Table 4.34.

Alloy 400 is known as Monel and its age-hardenable version is K-500. The corrosion resistance of alloy 400 is better than pure nickel in nonoxidizing mineral acids. The alloy shows poor corrosion resistance in HNO_3, $FeCl_3$, $CuCl_2$, moist Cl_2, chromic acid, SO_2 and NH_3; shows corrosion resistance to HF in the absence of air at all temperatures and is susceptible to SCC in moist aerated HF and H_2SiF_6. Alloy 400 is unaffected by alkaline salt solutions such as chlorides, carbonates, sulfates and acetates.

Some typical applications of the alloys are in propeller shafts, propellers, pump impeller blades, casings, condenser tubes and heat exchanger tubes. The corrosion rate in flowing seawater is <0.025 mm/yr, but can pit under stagnant water. Alloy 400 is immune to chloride SCC.

Other applications of this alloy are in roofs, gutters, architectural features, tubes of boiler water heaters, sheathing in seawaters, HF alkylination process, handling of HF, refining of uranium, distillation and condensation units, overhead condenser pipes in refineries and the petrochemical industry.

Alloy K-500 is similar to 400 in corrosion properties, but with added strength and hardness up to 600°C. Some typical applications are in pump shafts, impellers, medical blades and scrapers, oil well drill collars, electronic components, springs and valves.

Nickel alloyed with iron is known as Invar, Pernifer 36 and Magnifer and their composition is given in Table 4.35. The alloys have moderately good corrosion resistance to a variety of industrial environments. Alloy with 80% nickel, iron and molybdenum is used as inductive components in transformers, circuit breakers,

Table 4.35 *Ni–Fe alloys*

Alloy (UNS No.)	Ni	Cr	Co	Mn	Si	C	Fe	Others
36 (K93603) (Invar) Pernifer 36	36[a]	0.2	0.5	0.35	0.2	0.03	Bal	
Magnifer 7904 (Hymu 80)	80[a]			0.50[a]	0.3[a]	0.02[a]	Bal	Mo 5[a]

[a]Typical; all other values are maximum

low-frequency transducers, relay parts and screens because of its high magnetic permeability. Invar, the alloy with 36% nickel is widely used in cryogenic environments.

Nickel–silicon alloys with the chemical composition given in Table 4.36 are used in handling hot sulfuric acid, 50% nitric acid and mixtures of sulfuric and nitric acids.

Nickel–molybdenum alloys consisting of five members of the chemical composition given in Table 4.37 are known. The first member, alloy B, has been found to be susceptible to corrosion in the heat-affected zone (HAZ) in nonoxidizing acids such as acetic, formic and hydrochloric acids because of the high carbon content. The alloys B-2, B-3, B-4 were developed using argon–oxygen decarburization technology and these alloys can handle HCl in the temperature range 70–100°C as well as hot H_2SO_4. These alloys devoid of chromium cannot be used in oxidizing environments.

Alloy B2 has been used in production of acetic acid, pharmaceuticals, styrene, cumene, herbicides and a host of other organics. Alloy B4 has been used in HCl medium at 120–150°C, and in production of pesticides. This alloy is resistant to SCC,

Table 4.36 *Ni–Si system*

Alloy	Ni	Co	Mo	Cu	Cr	Si	Mn	Fe
Lewmat 66	Bal[a]	6[a]	0.2	3[a]	31[a]	3[a]	3[a]	16[a]
AlloyD-205	Bal[a]		2.5[a]	2[a]	20[a]	5[a]		6[a]

[a]Typical; all other values maximum unless noted otherwise

Table 4.37 *Ni–Mo system (B family alloys)*

Alloy (UNS No.)	Ni	Mo	Fe	Cr	C
B (N10001)	Bal	28	5	0.5	0.03
B-2 (N10665)	Bal	28	1.5	0.5	0.005
B-3 (N10675)	Bal	28	1.5	1.5	0.005
B-4 (N10629)	Bal	28	3.2	1.3	0.005
B-10 (N10624)	Bal	24	6	8	0.005

Table 4.38 *Ni–Cr–Fe alloys*

Alloy[a]	(UNS No.)	Ni	Cr	Fe	Al	Si	Others
600	(N06600)	Bal	16	9		0.3	
601	(N06601)	Bal	23	14	1.4	0.3	
800H	(N08810)	.32	21	Bal	0.4	0.5	Ti
690	(N06690)	Bal	30	10		0.3	
602CA	(N06025)	Bal	25	9.5	2.2		Y, Zr, Ti
45TM	(N06045)	Bal	27	23		2.7	RE

[a]Typical analysis

unlike B2. Alloy B10 has been successfully used in waste incinerators without any corrosive attack.

Nickel alloys containing chromium and iron of the composition given in Table 4.38 are used widely in chemical, petrochemical and other high-temperature processes.

Salient features of these alloys are as follows:

600 series
- High-temperature applications such as chlorination processing of titanium from Ilmenite or rutile, have a good oxidation and SCC resistance; have been used in furnace and heat-treatment applications; used in nuclear reactors, steam generator boiling and primary water piping systems
- Alloy 690 is superior to 600 in SCC resistance
- Alloy 601 is better than 600 alloy in that it has better high-temperature oxidation resistance and superior creep and rupture properties
- Alloy 601 is resistant to many aqueous media, chloride SCC and carburizing conditions
- Alloy 601 is used in thermal, chemical processing, pollution control and power generation
- Alloy 602 CA a modification of other 600 alloys is used in heat-treating, annealing furnaces, furnace rolls, high-temperature calcination application, catalytic support systems, and glow plugs in automobiles, vitrification of nuclear waste

800, 45 TM series
- Have high creep and rupture strength and oxidation resistance; used in petrochemical industry, coal gasification, electric range heating element sheathing and extruded tubing for steam methane reformer furnaces; Alloy 800 has corrosion resistance intermediate between Type 304 and 316 stainless steels
- Alloy 45 TM is superior to 800H in coal gasification application, incinerators, refineries and petrochemical industry

Ni–Cr–Fe–Mo–Cu alloys and their typical composition are given in Table 4.39.

Basically, the addition of Mo and Cu to Ni–Cr–Fe alloys resulted in alloys with improved corrosion resistance to sulfuric, phosphoric and hydrofluoric acids containing

Table 4.39 *Ni–Cr–Fe–Mo–Cu alloys*

Alloy[a]	(UNS No.)	Ni	Cr	Mo	Cu	Fe	Others
825	(N08825)	Bal	22	3	2	31	Ti
G	(N06007)	Bal	22	6.5	2	20	Nb + Ta
G-3	(N06985)	Bal	22	7	2	20	Nb + Ta
G-30	(N06030)	Bal	30	5	1.5	15	Nb + Ta
20	(N08020)	35	20	2.5	3.5	Bal	Nb
28	(N08028)	31	27	3.5	1.0	36	
31	(N08031)	31	27	6.5	1.2	32	N
33	(R20033)	31	33	1.6	1.2	32	N
1925hMo	(N08926)	25	21	6.3	0.9	Bal	N

[a]Typical analysis

oxidizing agents and oxidizing acids. These alloys have been extensively used in a variety of industrial atmospheres to combat corrosion. Their salient features may be summarized as follows:

825 — Good corrosion resistance in many corrosive media; resistant to chloride SCC, but fails in boiling $MgCl_2$ can be used in situations of localized corrosion and SCC in place of 300 stainless steels; resistant to H_2SO_4, H_3PO_4, boiling H_2SO_4; mixture of nitric acid and cupric and ferric sulfates; not susceptible to intergranular attack

Some typical uses are sulfuric acid pickling of steel and copper; tanks, agitators, valves, pumps in petroleum industry; pollution control equipment; nuclear fuel processing; handling radioactive waste, phosphoric acid production (evaporators, cylinders, heat exchangers)

G — Good corrosion resistance in oxidizing and reducing media as well as mixed acids, fluosilicic acid, conc. HNO_3, HF, flue gases in coal-fired power plants, resistant to chloride SSC and localized corrosion; widely used in industries similar to 825

G-3 — Similar in corrosion resistance to Alloy G, but better than G in HAZ attack resistance and weldability and localized corrosion; G-3 has replaced 825 and G in use

Alloy G-30 — Excellent corrosion resistance to H_3PO_4, nitric/hydrochloric; nitric/HF, H_2SO_4; typical uses: phosphoric acid service, mixed acid service, nuclear fuel reprocessing, components in pickling, petrochemical, agrichemical manufacture and in mining operations

1925 h Mo — Good mechanical properties and high resistance to localized corrosion; used in offshore and marine, pulp and paper, chemical process industry of both organic and inorganic compounds

Alloy 31 — Cost-effective; used in heat exchangers using seawater or brackish water for cooling; superior to Alloy 20 and C-276 in H_2SO_4 used in pulp and paper; phosphoric acid, copper smelters; H_2SO_4 production, pollution control, waste water treatment, H_2SO_4 evaporators; leaching of Cu ores, fine chemicals manufacture; viscose rayon production

Alloy 20	Resistance to H_2SO_4 and SCC; used in manufacture of synthetic rubber, high-octane gasoline, solvents, explosives, plastics, synthetic fibers, chemicals, pharmaceuticals, and food processing, not resistant to pitting and crevice corrosion in low pH chloride media
Alloy 33	Resistant to acids and alkalis, HNO_3/HF mixture; hot H_2SO_4, localized corrosion and SCC; good mechanical properties, high resistance to pitting
Alloy C-22	Has 21% Cr, 13% Mo, 3% W, 3% Fe, 60% Ni and suitable for use in oxidizing environments; corrosion resistance better than C-276, C-4 in oxidizing media, better pitting resistance; inferior to C-276, C-4 in reducing media and with respect to crevice corrosion
Alloy 59	Superior to C-22, C-276, super thermal stability attributed to the ternary system, Ni–Cr–Mo devoid of W, Cu, Ti and Ta
Alloy 686	Similar to C-276 in composition except for Cr level being 16-21%; alloy is solution annealed at 1200°C and rapidly cooled to prevent precipitation of intermetallic phases; thermal behavior not as good as Alloy 59 and its corrosion resistance was less than 59
C-2000	1.6% Cu has been added to C59; lower corrosion resistance and thermal stability than Alloy 59
Alloy MAT21	1.8% Ta added to Ni, 19% Cr, 19% Mo. Performance characteristics yet to be determined

Some corrosion rate data for the high-performance Ni–Cr–Mo alloys in boiling acids and ASTM media are given in Table 4.40 and it is apparent that Alloy 59 gives the best performance.

High-performance Ni-Cr-Mo alloy with the composition given in Table 4.41 are known as Hastealloys.

Table 4.40 *Comparison of some Ni–Cr–Mo alloys in various boiling corrosive environments*

Media	Uniform corrosion rate (mpy)[a]				
	C-276	C-22	686	C-2000	59
ASTM 28A	240	36	103	27	24
ASTM 28B	55	7	10	4	4
Green Death	26	4	8		5
10% HNO_3	19	2			2
65% HNO_3	750	52	231		40
10% H_2SO_4	23	18			8
50% H_2SO_4	240	308			176
1.5% HCl	11	14	5	1.5	3
10% HCl	239	392			179
10% $H_2SO + 1\%$ HCl	87	354			70
10% $H_2SO_4 + 1\%$ HCl[b]	41	92	67		3

[a]To convert to millimeters per year (mm/yr) multiply by 0.0254
[b]At 90°C

Table 4.41 *High-performance Ni–Cr–Mo alloys*

Alloy (UNS No.)	Ni	Cr	Mo	W	Fe	Others
C (N10002)	Bal	16	16	4	6	
625 (N06625)	Bal	22	9		2	Nb
C-276 (N10276)	Bal	16	16	4	5	
C-4 (N06455)	Bal	16	16		2	Ti
C-22/622 (N06022)	Bal	21	13	3	3	
59 (N06059)	Bal	23	16		<1	
686 (N06686)	Bal	21	16	4	2	
C-2000 (N06200)	Bal	23	16		2	Cu
MAT 21 (N06210)	Bal	19	19		<1	Ta

Their salient features are as follows:

C — Good corrosion resistance in many oxidizing and reducing media; resistant to localized corrosion and chloride SCC; subject to intergranular attack in HAZ in oxidizing, low pH and halide media; high corrosion rates in oxidizing media

625 — Immune to intergranular attack; resistant to oxidizing environments (boiling HNO_3); resistant to reducing media; resistance to corrosion and pitting in seawater, wet Cl_2, HF, HNO_3–HF, H_2SO_4–HF, H_3PO_4–HF mixtures; Hastealloy X resistant to high-temperature oxidation (1100°C); Hastealloy, alloy N developed for use in molten fluoride salts at 815°C

C-276 — Argon–oxygen decarburization was used in development of the alloy, low C and Si; similar in corrosion resistance to Alloy C without grain boundary precipitation; can be used in as-welded condition; good corrosion resistance in oxidizing and reducing media; extensively used in many industries, not stable to precipitation of carbides and intermetallic phase in some situations

C-4 — Free from precipitation of intermetallic and grain boundary precipitation; corrosion resistance similar to C-276, but better than C-276 in oxidizing media; the alloy is being gradually replaced by Alloy 59

Some data on hazardous waste incineration scrubber corrosion are given in Table 4.42 and it is obvious that alloys 59, 686, C22 and C-276 perform well.

Localized corrosion susceptibility of the alloys evaluated by ASTM G-48 test protocol and a test medium known as 'Green Death' solution is detailed in Tables 4.43 and 4.44, respectively. The superior performance of Alloy 59 and C276 is obvious from the data on localized corrosion.

Thermal stability evaluated as per ASTM G-28A after sensitization and ASTM G-28B showed Alloy 59 to be superior to other alloys with corrosion rates 40–51 mpy and 4 mpy, respectively. The comparative data are given in Tables 4.45 and 4.46, respectively.

Table 4.42 *3M Study; hazardous waste incineration scrubber corrosion data (1991 h)*[a]

Alloy	mpy[b]	Remarks
59	1.1	Clean
686	5.4	Clean
C-22	6.7	Clean
31	7.1	Clean
622	12.1	Weld attack
C-276	35.1	Clean
625	58.6	Rough
825	117	Pitting

[a]See reference 61
[b]To convert to millimeters per year (mm/yr) multiply by 0.025

Table 4.43 *Critical pitting and crevice corrosion temperature per ASTM G-48*

Alloy	Cr	Mo	PRE[a]	CPT(°C)	CCT(°C)
C-22	21	13	65	>85[b]	58
C-276	16	16	69	>85	>85
686	21	16	74	>85	>85
59	23	16	76	>85	>85

[a]PRE = % Cr + 3.3 (% Mo)
[b]Above 85°C the solution breaks down chemically

Table 4.44 *Localized corrosion resistance in Green Death solution*[a]

Alloy	PRE	CPT(°C)	CCT(°C)	Crevice depth at 105°C
C-22	65	120	105	0.35 mm
C-276	59	110	105	0.035 mm
59	76	>120[b]	110	0.025 mm
686	74	>120	110	
C-2000	76	110	100	

[a]11.5% H_2SO_4 + 1.2% HCl + 1% $FeCl_3$ + 1% $CuCl_2$
[b]Above 120°C, Green Death solution breaks down chemically

Table 4.45 *Thermal stability per ATSM G-28A after sensitization*[a]

Sensitization (h)	Corrosion rate (mpy)[b]				
	C-276	C-22	686	C-2000	59
1	>500[c]	>500[c]	>500[c]	116[c]	40[d]
3	>500[c]	>500[c]	>1000[c]	178[c]	51[d]

Table 4.46 *Thermal stability per ASTM G28B after sensitization*[a]

Sensitization (h)	Corrosion rate (mpy)[b]				
	C-276	C-22	686	C-2000	59
1	>500[c]	339	17	>500	4[d]
3	>500[c]	313	85	>500	4[d]

[a]At 870°C (1600°F)
[b]To convert to millimeters per year (mm/yr) multiply by 0.0254
[c]Alloy C-276, C-22, C-2000 and 686, heavy pitting attack with grains falling out because of deep intergranular attack
[d]Alloy 59, no pitting attack

High-temperature-resistant materials should have the desirable mechanical and corrosion resistance properties as outlined below:

Mechanical properties	Corrosion resistance properties
High-temperature strength	Oxidation
Stress rupture strength	Carburization
Creep strength	Nitriding
Fatigue strength	Sulfidation
Thermal stability	Halogenation
Thermal shock resistance	Molten salt
Toughness	Liquid metal
Other specific properties	Ash salt deposit
	Others

The role of alloying elements in nickel-based alloys may be briefly summarized as follows:

Protective scale formers	Cr as Cr_2O_3, Al as Al_2O_3 and Si as SiO_2
Solid solution strengtheners	Mo, W, Nb, Ti, Cr, Co
Age hardening strengtheners	Al + Ti, Al, Ti, Nb, Ta
Carbide strengtheners	Cr, Mo, W, Ti, Zr, Ta, Nb
Improved scale adhesion (spallation resistance)	Rare earths (La, Ce) Y, Hf, Zr, Ta

High-temperature alloys have been studied in great detail as evidenced by references in the literature.[62–64]

It is possible to summarize the general features that can be attributed to the alloying elements in the alloy with respect to aqueous corrosion resistance as given

below:

Alloying elements	Main features	Other features
Ni	Provides matrix for metallurgical compatibility to various alloying elements; improves thermal stability and fabricability	Enhances corrosion resistance in mild reducing media; alkali media improves chloride SCC
Cr	Provides resistance to oxidizing corrosive media	Enhances localized corrosion resistance
Mo	Provides resistance to reducing (nonoxidizing) corrosive media	Enhances localized corrosion resistance and chloride SCC
W	Behaves similar to Mo, but less effective. Detrimental to thermal stability in high Ni–Cr–Mo alloys	Provides solid solution strengthening
N	Austenitic stabilizer, economical substitute for nickel	Enhances localized corrosion resistance, thermal stability and mechanical properties
Cu	Improves resistance to seawater and sulfuric acid, detrimental to thermal stability in higher Ni–Cr–Mo alloys	Enhances resistance to H_2SO_4, and HF-containing acid environment
Ti, Nb, Ta	Carbon stabilizer	Improves HAZ and intergranular corrosion resistance
Si	High silicon (>4%) improves resistance to oxidizing mineral acids, sulfuric acid and nitric acid	Detrimental in certain corrosive environments
Fe	Provides matrix for metallurgical compatibility to various alloying elements	Reduces cost by replacing nickel and enhances scrap utilization

The role and significant features that are attributed to the alloying element in nickel-based alloys with respect to high-temperature corrosion resistance are given below:

Alloying elements	Main features	Other features
Cr	Improves oxidation resistance. Detrimental to nitriding and fluorination resistance	Improves sulfidation resistance; beneficial to carburization and metal dusting resistance
Si	Improves oxidation, nitriding, sulfidation and carburizing resistance. Detrimental to nonoxidizing chlorination resistance	Synergistically acts with chromium to improve high-temperature degradation

(*contd.*)

(*contd.*)

Alloying elements	Main features	Other features
Al	Independently and synergistically with Cr improves oxidation resistance; Detrimental to nitriding resistance	Helps improve sulfidation resistance; improves age-hardening effects
Mo	Improves high-temperature strength; Improves creep strength, detrimental for oxidation resistance at higher temperatures	Helps with reducing chlorination resistance
W	Behaves similarly to molybdenum	
Nb	Increases short-term creep strength; may be beneficial in carburizing; detrimental to nitriding resistance	
C	Improves strength, helps nitridation resistance, beneficial to carburization resistance, oxidation resistance adversely effected	
Ti	Improves age hardening strengthening	Detrimental to nitriding resistance
Mn	Slight positive effect on high-temperature strength and creep; detrimental to oxidation resistance; increases solubility of nitrogen	
Co	Reduces rate of sulfur diffusion; helps with sulfidation resistance; improves solid solution strength; improves solid solution resistance	
Ni	Improves carburization, nitriding, and chlorination resistance; detrimental to sulfidation resistance	
Y and RE	Improves adherence and spalling resistance of oxide layer and improves oxidation, sulfidation, carburization resistance	

Table 4.47 *Major industries using Alloy C-276/C-4/59*

I.	Petroleum
	Petroleum refining Oils/greases Natural gas processing
II.	Petrochemical
	Plastic Synthetic organic fibers Organic intermediates Organic chemicals: chlorinated/fluorinated hydrocarbons Synthetic rubber
III.	CPI (chemical process industries)
	Fine chemicals Inorganic chemicals Soaps/detergents Paints Fertilizer-agrichemicals-herbicides/pesticides Adhesives Industrial gases
IV.	Pollution control
	FGD Waste water treatment Incineration Hazardous waste Nuclear fuel reprocessing
V.	Pulp and paper
VI.	Marine/seawater
VII.	Pharmaceuticals
VIII.	Sour gas/oil and gas production
IX.	Mining/metallurgical

Some industrial applications of Alloy C-276/C-4/59 are given in Table 4.47.

4.7 Titanium and its Alloys

The commercial importance of this metal was first recognized in 1950s when its high strength/density ratios were found attractive in aerospace applications. The corrosion resistance in a variety of conditions led to its use in wet chlorine gas coolers for chlor-alkali cells, chlorine and chlorine dioxide bleaching equipment in pulp/paper mills, and reactor interiors for pressure acid leaching of metallic ores. The metal and its alloys were used in seawater power plant condensers, with over 400 million feet installed in application.[65,66] The most commonly used alloys and their composition are given in Table 4.48.

Table 4.48 *Titanium and titanium alloys commonly used in industrial applications*

Common alloy designation	UNS No.	ASTM grade	Nominal composition (%)	Minimum tensile strength	Minimum yield strength
Group I: Commercially pure titanium					
Grade I	R50250	1	0.06 O	240	170
Grade 2	R50400	2	0.12 O	345	275
Grade 3	R50550	3	0.2 O	450	380
Grade 4	R50700	4	0.3 O	550	483
Group II: Low-alloy-content titanium with Pd/Ru additions					
Grade 2, Pd	R52400	7	0.12 O, 0.15 Pd	345	275
Grade 1, Pd	R52250	11	0.06 O, 0.15 Pd	240	170
Grade 2, low Pd	R52402	16	0.12 O, 0.05 Pd	345	275
Grade 1, low Pd	R52252	17	0.06 O, 0.05 Pd	240	170
Group III: Other α and Near-α Alloys					
Ti, 5-2.5	R54520	6	5 Al, 2.5 Sn	828	793
Ti 3-2.5	R56320	9	3 Al, 2.5 V	620	483
Grade 12	R53400	12	0.3 Mo, 0.8 Ni	483	345
Ti 3-2.5, low Pd	R56322	18	3 Al, 2.5 V, 0.05 Pd	620	483
Ti 3-2.5, Ru	R56323	28	3 Al, 2.5 V, 0.1 Ru	620	483
Ti 5111	R55111	32	5 Al, 1 Sn, 1Zr, 1V, 0.8 Mo	689	586
Group IV: α-β alloys					
Ti 6-4	R56400	5	6 Al, 4V	895	828
Ti 6-4 ELI	R56407	23	6 Al, 4 V, 0.13 O max	828	759
Ti 6-4 ELI, Ru	R56404	29	6 Al, 4 V, 0.1 Ru, 0.13 O max	828	759
Group V: β alloys					
Beta C	R58640	19	3 Al, 8 V.6 Cr, 4 Zr, 4 Mo	793	759
Beta C, Pd	R58645	20	3 Al, 8 V.6 Cr, 4 Zr, 4 Mo, 0.05 Pd	793	759
Beta 21S	R58210	21	15 Mo, 3 Al, 2.7 Nb, 0.25 Si	793	759

Features of the different groups of titanium alloys are as follows:

Group I	Highly corrosion resistant
Pure Ti, variable Fe and O	Grade 1 used in applications requiring high formability; Grade 2 extensively used in non-aerospace applications
Group II	Small amounts of Pd or Ru render high corrosion resistance
Group III	α, near-α alloys of intermediate strength, good ductility, toughness, creep resistance and weldability; ideal for cryogenic applications; Mo and Ni in Grade 12, Pd in Grade 18 and Ru in Grade 28 confer corrosion resistance in reducing acid media
Group IV	Higher percentage of β-phase and strength and higher V, a β-stabilizer
Group V	The β alloys are readily cold worked in solution, heat-treated and quenched condition; high strength/density ratios allow their use in aerospace industry

4.7.1 Resistance to Waters

Titanium and its alloys resist corrosive attack in fresh water and steam at temperature in excess of 300°C, although slight tarnishing is observed in hot water and steam. The titanium is free of crevice and pitting attack on exposure to seawater, also inert in the splash zone or sulfide-containing waters. The metal and the alloys are resistant to erosion corrosion up to velocities of 35 m/s. Titanium tubes in seawater heat exchangers have given 20 yrs trouble-free service. Titanium is not resistant to marine fouling but chlorination reduces the degree of fouling.

Titanium alloys suffer crevice corrosion in hot aqueous chloride media, but the alloy containing molybdenum, 3Al-8V-6 Cr-4Zr-4 Mo has good resistance to crevice corrosion and is successfully used in hot sour well and geothermal brine applications.

4.7.2 Resistance to Chemical Environments

The most important aspect of titanium is its high resistance to oxidizability. Generally, titanium is resistant to common oxidizing solutions. The metal is attacked by dry chlorine gas and introduction of 1% of water into chlorine medium results in preventing the attack of the metal. Features relevant to particular environments are as follows:

HCl, H_2SO_4, H_3PO_4	Moderate resistance; general corrosion rate varies with the type of acid, concentration and temperature
HF	High corrosion rates, used for pickling, etching
Reducing acid environments	Pd, Ru, Mo, Ni render the titanium to be more resistant to corrosion Small amounts of oxidizing species (inhibitor) may be used; nitric acid or oxidizing ions such as Fe^{3+} (ferric); Cu^{2+} (cupric) is added to HCl or H_2SO_4 solutions; aeration of the solution may be used as in hot formic acid solution; alloying elements such as 0.2–0.5% Pd along with 0.3% Mo resist the attack; anodic impressed current protection method to stabilize the oxide film on the metal may be used and it is claimed that the corrosion rate in H_2SO_4 at 60°C is reduced by a factor of 33000 by this method
Oxidizing environments	Resistant to nitric and chromic acids; high-temperature corrosion is inhibited by Fe^{3+}, Ru^{3+}, Rh^{3+}, Ce^{4+} and Cr^{6+}; alloying with tantalum improves corrosion resistance to strong acids at high temperatures; fuming HNO_3 may result in intergranular attack; highly resistant to solutions of chlorites, hypochlorites, chlorates, perchlorates and chlorine dioxide
Alkaline solutions	Low corrosion rates in NaOH, KOH and NH_4OH solutions over wide concentration and temperature ranges; anodic dissolution in 20–40 wt % NaOH results in hydrogen absorption leading to hydrogen embrittlement; hydrogen absorption can be inhibited by adding nitrate or chlorate

Hydrogen peroxide	Corrosion of radioactive waste container at 10^{-4} M H_2O_2; medical implants (0.01–0.1 M H_2O_2; paper and pulp (0.1–0.2 M) showed that 1.0×10^{-4} M H_2O_2 increased the corrosion resistance of Ti; 0.01–0.1 M H_2O_2 produces less-protective oxide layer; small amounts of Ca, silicate and Mg are effective inhibitors; at 95°C, 2.5 M NaoH, 0.5 M H_2O_2 corrosion rate of 2300 mm/yr has been obtained.
Organic compounds	Resistant to terephthalic acid, adipic acid, alcohols, aldehydes, esters, ketones and hydrocarbons; aeration is necessary in formic acid solutions; oxygen has deleterious effect in anhydrous acetic acid and acetic anhydride medium; poor resistance to propionic acid; corrosion resistance in oxaltic acid is improved by Mo in the alloy

Environmentally induced cracking consists of: (i) stress corrosion cracking; (ii) corrosion fatigue; and (iii) hydrogen-induced cracking. The general features of these modes of failure are given below:

Stress–corrosion cracking	Majority of titanium alloys are resistant to SCC; stress–corrosion cracking has been observed in absolute methanol, red fuming nitric acid, nitrogen tetroxide, liquid, and metals of Cd and Hg and halide media[67]
Alloy composition, interstitial oxygen, nitrogen and carbon in titanium	Exposure to seawater results in decrease in critical stress intensity factor and the susceptibility to SCC[68]; 0.2% Fe improves the resistance to SCC; presence of >5 wt percent of Al increases the velocity of cracking; Sn in the alloy decreases SCC resistance; chloride; bromide and iodide induce or accelerate SCC[69]
SCC of α and α-β alloys	Occurs by trangranular cleavage of α-phase in which α-phase controls the crack propagation rate
Methanolic halide solutions	Intergranular corrosion due to formation of titanium methoxide
Hot salt SCC	May occur in jet aircraft engine components;[70] simultaneous cycling of temperature and stress may cause reduced resistance to SCC
Corrosion fatigue	Good corrosion resistance in seawater and chloride media gives rise to smooth, notched fatigue run-out stresses, which are unaffected by the environment;[71] commercially pure Ti and its weld metal showed increasing crack-growth rates with increase in stress ratio in air and seawater which may be due to crack closure effect[72]
Hydrogen-induced cracking	Stable oxide film on Ti is an effective barrier for hydrogen entry; solubility of hydrogen is ~20–150 ppm; above the solubility limit brittle titanium hydride is formed; solubility of hydrogen in β-phase (9000 ppm) is greater than in α-phase; β-phase alloy is more susceptible to hydrogen embrittlement than α-phase alloys; hydrogen embrittlement is favored when the component is cathodic and hydrogen is generated on the surface, with pH <3 or <12, abraded surface, potential more negative than −0.7 V vs SCE, >80°C and presence of high tensile stress

4.7.3 Galvanic Corrosion

Titanium is highly corrosion resistant and is often the more noble metal, the cathode, in a galvanic cell. Galvanic corrosion of the less noble metal such as Mg, Zn or Al can occur when coupled with titanium. This in turn may result in the structural failure. Galvanic corrosion can be mitigated by proper design such as reducing the cathode/anode area ratio, electrically isolating the titanium component, cathodic protection and/or corrosion inhibition of the active metal.

Titanium seawater piping alongside copper–nickel pipping systems is used on board of naval vessels and this system requires protection from galvanic attack. At the present the design uses thick-walled 'waster' pieces that have a high corrosion allowance and positioned in a manner physically separating and protecting dissimilar piping materials. The bielectrode is positioned between the cathodic and anodic pipes and generates a potential gradient opposing the galvanic potential gradient, thus eliminating the galvanic corrosion. Galvanic corrosion is also lowered by calcareous deposits and chlorine at ppm levels.

4.8 Cobalt Alloys

Chromium-containing cobalt alloys have been developed for use requiring wear resistance and high temperature corrosion resistance. The nominal composition of some wear-resistant cobalt alloys is given in Table 4.49.

The types of wear encountered in industry consists of abrasion (both low and high stress), erosion due to impingement of solid particles and liquid droplets, cavitation and slurry erosion, metal-to-metal interaction wear including galling, cyclic sliding and fretting. The description of the wear mechanisms is beyond the scope of the presentation here.[63] The net effect of the wear is gross deformation and fracture, microfatigue or wastage of metal due to the continuous disruption of the surface films. Relevant features of these alloys are:

Stellite — Contains significant amount of carbon in order to form carbides in the microstructure; the Cr and W form the respective carbides; Stellite 6 has ~13 wt % carbides; Stellite 1 has ~29 wt % carbides; carbides provide resistance to low-stress abrasion and have high hardness; lower ductility and corrosion resistance

Triballoy — High Mo and Si give rise to precipitates and provide corrosion resistance to acids

Table 4.49 *Nominal composition of wear-resistant cobalt alloys*

Alloy	Co	Cr	W	Mo	C	Ni	Fe	Si
Stellite 1	Balance	31	12		2.4	3 max	3 max	1 max
Stellite 6	Balance	29	4.5		1.1	3 max	3 max	2 max
Haynes 6B								
Stellite 12	Balance	30	8		1.4	3 max	3 max	1 max
Tribaloy T-800	Balance	17.5		28.5		3 max (Ni + Fe)	3 max (Ni + Fe)	3.4

Table 4.50 *Corrosion rates (mm/yr) for Haynes 6B in sulfuric acid*

Concentration (wt %)	24°C, 75°F	66°C, 150°F	Boiling
2			0.8
5			2.3
10	<0.1	<0.1	4
20			9.1
30	<0.1	<0.1	>10
50	<0.1	>10	>10
77	<0.1	4.5	>10

In the case of liquid droplet impingement erosion, cavitation erosion and cyclic sliding resulting in microfatigue, the ability of cobalt alloys to absorb the stress is useful. The cobalt-rich matrix is useful in wear applications. Corrosion rate data for Haynes 6B alloy in sulfuric acid, hydrochloric acid, nitric acid and phosphoric acid at different concentrations of acids and temperatures are given in Tables 4.50–4.53, respectively.

The wrought version of Haynes 6B alloy has higher corrosion resistance in aqueous media than the cast and weld overlay version (Stellite 6) because of hot forging and rolling breakdown of the interconnected carbides into discrete particles. Haynes 6B can be used in sulfuric acid in the concentration range 2–77 wt % at 24°C and in dilute solutions at higher temperatures (see Table 4.50).

The alloy can be used in 2 wt % HCl up to 66°C. The corrosion in HCl becomes significant at >2 wt % HCl at 24° and 60°C. Haynes 6B shows low and acceptable corrosion rates up to 30% HNO_3 and 70% phosphoric acid as seen from Tables 4.52 and 4.53.

Table 4.51 *Corrosion rates (mm/yr) for Haynes 6B in hydrochloric acid*

Concentration (wt %)	24°C, 75°F	66°C, 150°F
2	<0.1	<0.1
5	1.6	>10
10	2.7	>10
20	2.4	>10

Table 4.52 *Corrosion rate (mm/yr) for Haynes 6B in nitric acid*

Concentration (wt %)	24°C, 75°F
10	<0.1
30	0.2
50	>10
70	>10

Table 4.53 *Corrosion rates (mm/yr) for Haynes 6B in phosphoric acid*

Concentration (wt %)	24°C, 75°F
10	<0.1
30	0.1
50	0.5
70	0.6
85	>10

The alloy Haynes 6B is resistant to corrosion in organic acids, but subject to pitting and crevice corrosion and SCC in chloride media. The corrosion rate of 0.3 mm/yr or 12 mpy has been observed in 30 wt % of NaOH; it is likely that caustic cracking will occur at high concentrations of NaOH and temperatures in the case of all the cobalt alloys. The nominal composition of high-temperature cobalt alloys is given in Table 4.54.

Nickel present in the alloys in the range of 10–22 wt % confers thermal stability to the alloys. Tungsten present in the alloys (7–15 wt %) acts as the primary solid solution strengthening agent in preference to molybdenum. Haynes 25 and Haynes 188 alloys exhibit simple microstructures, consisting of sparse dispersion M_6C carbides. At high temperatures precipitation of $M_{23}C_6$ at grain boundaries occurs, which in turn provides increased strength.

The alloy Mar-M-509 has complicated microstructure and contains both $M_{23}C_6$ and MC carbides in the as-cast condition due to the addition of tantalum to the alloy. These carbides provide additional strength.

The high-temperature cobalt alloys used in gas turbine engines have good resistance to sulfidation (hot corrosion). Haynes 25 alloy has good resistance to oxidation up to about 1000°C. On the other hand, Haynes 188 alloy has better oxidation resistance due to the lanthanum in the alloy and can be used in oxidizing atmospheres up to 1150°C.

These cobalt alloys are not resistant to molten aluminum and bismuth, but can be used in die casting and galvanizing.

The nominal composition of two cobalt alloys designed to perform well with respect wear and aqueous corrosion is given in Table 4.55.

Table 4.54 *Nominal composition of high-temperature cobalt alloys*

	Co	Cr	W	Mo	C	Ni	Fe	Si	Others
X-40 (Stellite 31)	Balance	25.5	7.5		0.5	10.5	2		B-0.01
MAR-M 509	Balance	24	7		0.6	10			Ta-3.5 Ti-0.2 Zr-0.5
HAYNES 25 (L-605)	Balance	20	15	1 max	0.1	10	3 max	0.4 max	Mn 1.5
HAYNES 188	Balance	22	14		0.1	22	3 max	0.35	Mn 1.25 max B-0.015 max La-0.03

Table 4.55 *Nominal composition of aqueous corrosion and wear-resistant cobalt alloys*

	Co	Cr	W	Mo	C	Ni	Fe	Si	Mn	N
Vitallium	Balance	28.5		6	0.35 max	1 max	0.75 max	1 max	1 max	
Ultimet	Balance	26	2	5	0.06	9	3	0.3	0.8	0.08

The alloy vitallium is used in hip joint replacement and other biomedical applications. Ultimet alloy is widely used in chemical industry in the context of dealing with hot acids and wear, particularly in valves, pumps and nozzles. Both vitallium and ultimet have wear resistance and corrosion resistance to oxidizing media due to chromium in the alloy. The molybdenum and tungsten impart resistance to hydrochloric acid attack. Carbon is more soluble in cobalt–chromium–molybdenum alloy and improves the SCC resistance and the nitrogen enhances the strength and the resistance to pitting and crevice corrosion.

The comparative galling data in terms of degree of damage (μm) and erosion depth (ASTM G-32 test) are:

Alloy	Degree of damage (μm)	Erosion depth (mm)
Ultimet, Haynes 6B, Stellite 6/GTA	<1.0	0.012
C-276	62	0.103
625	28	
316 stainless	150	0.18
410 stainless		0.23
2205 stainless		0.15
17 - 4 pH stainless		0.11
Nitronic	120	0.02

Comparative low-stress abrasion data as per ASTM G65 test are:

Alloy	Volume loss (Cu mm)
Ultimet	90
Haynes 6B	17
Stellite 6/GTA	63
Stellite 1/GTA	30
C276	122
625	120
316 L stainless	140
410 stainless	117
2205 stainless	115
17-4 pH stainless	115
Nitronic 60	147

The corrosion resistance of Ultimet, along with other alloys such as stainless steels in H_2SO_4 and HCl of different concentrations (H_2SO_4 0–90%, HCl 0–20%) in the temperature ranges 20–250°C (H_2SO_4) and 20–100°C (HCl) was studied and the following order has been observed:

Ultimet
Ni - Cr - Mo >20 Nb - 3 } >316 L in H_2SO_4 solutions
254 SMO

C-2000 > Ultimet > 316 L in HCl solution

The resistance of the alloys tested to crevice corrosion in 6% ferric chloride is as follows:

Alloy	Critical crevice temperature °C
316 L	<0°
AL-6 XN	40°
254 SMO	40°
C-22	70°
C-276	65°
C-2000	85°
Ultimet	65°

With respect to SCC resistance in 30% $MgCl_2$ Ultimet alloy was found to be comparable to 20 Nb-3 and both alloys better than 316 L stainless steel.

4.9 Lead and Lead Alloys

The four forms of lead are pure lead, also known as corroding lead (99.94%), common lead (99.94%), chemical lead (99.99) and acid–copper lead (99.99%). The resistance of lead to sulfuric acid enables its use in batteries. It is also used as sheet and pipe in buildings. The main use is as a solder material in the electronics industry.

The corrosion of lead may be represented as:

$$Pb^{\circ} \rightarrow Pb^{2+} + 2e^{-}$$

with the potential for the reaction being 0.126 V. Some features of corrosion of lead are noted below:

Condition	Features
Coupled with steel, Al, Zn, Cd and Mg	Lead coupled with these metals acts as the cathode in most of the environments and leads to corrosion of steel or Al or Cd or Mg

(*contd.*)

(*contd.*)

Condition	Features
Coupled with Ti and passivated stainless steel or copper	Lead becomes the anode in these couples and undergoes corrosion
Nitric acid	Lead is attacked by dilute nitric acid, but not as much in concentrated nitric acid
pH range	Corrosion occurs below pH 5 and above pH 10
Sulfuric, sulfurous, chromic, phosphoric acid and hydrochloric acid	General resistance to attack by these acids
Dilute HCl, HNO_3, organic acids, or if these media contain oxidizing agents	Corrosion of lead occurs
10% caustic solutions up to 90°C	Resistance to attack
Amines	Resistant only in cold dilute amines
Water	Resistant to waters free from dissolved gases such as oxygen and carbon dioxide, and suspended solid impurities such as silicates, carbonates, sulfates, lime, silt, chloride and microorganisms; flow and agitation contribute to corrosion

The corrosion of lead in natural waters depends on the hardness of the waters, as evidenced by the data in Table 4.56. The natural waters of moderate hardness (i.e., less than 125 ppm calcium carbonate) tend to be less aggressive due to the formation of a protective film, which is also aided by the presence of silicates. On the other hand, nitrate ions disrupt the protective film and increase the corrosion rate. Corrosion of lead occurs in waters containing carbonic acid due to the conversion of carbonate in the film into

Table 4.56 *Corrosion of chemical lead in industrial and domestic waters*[a]

	Temperature			Corrosion rate		
Kind of water	°F	°C	Aeration	Agitation	mdd	mpy
Condensed steam, traces of acid	70–100	21–38	None	Slow	6.75	0.85
Mine water, pH 8.3, 110 ppm	68	20	Yes	Slow	2.08	0.26
Mine water, 160 ppm hardness	67	19	Yes	Slow	2.20	0.28
Mine water, 110 ppm hardness	72	22	Yes	Slow	1.98	0.25
Cooling tower, oxygenated Lake Erie water	60–85	16–29	Complete	None	41.7	5.3
Los Angeles aqueduct water, treated by chlorination and copper sulfate	Ambient			0.15 m/s	2.95	0.38
Spray cooling water, chromate treated	60	16	Yes		2.9	0.37

soluble bicarbonate. Sodium silicate can act as an inhibitor in the corrosion of lead, even when lead is in the solder joining copper pipes. Lead in potable water for domestic use should not exceed 15 ppb.

A linear relationship has been observed between corrosion rate in terms of loss in weight and the percentage oxygen in the atmosphere above distilled water as seen from the data given below:

Percent oxygen in atmosphere above distilled water	Loss in weight (mg/dm^2)
0.0	0.0
10.0	40.0
20.0	72.0
45.0	160.0
70.0	210.0
80.0	280.0
100.0	350.0

Lead is immune to distilled water free from CO_2 and oxygen. Air free from CO_2 in distilled water corrodes lead. In presence of CO_2 a film of basic lead carbonate in formed, which prevents further attack. The successful use of lead pipe coils for steam boiler applications depends on the use of pure water condensate, which is free from oxygen and carbon dioxide. In the event of the presence of oxygen, oxygen scavengers such as hydrazine or sodium sulfite together with cobalt nitrate may be used.

Corrosion rate data on chemical lead, Pb–Sb and Pb–Sn alloys in deionized water are presented in Table 4.57. Chemical lead gave the highest value and was observed to have waterline attack.

The corrosion rates of lead and its alloys are low in seawater, as seen from the data in Table 4.58.

Corrosion rate data of lead in phosphoric acid, HCl, HCl and $FeCl_3$, HNO_3, HNO_3–H_2SO_4 mixtures and HCl–H_2SO_4 mixtures are summarized in Tables 4.59–4.65.

Lead is rapidly corroded by dilute acetic acid or formic acid in the presence of oxygen. The tolerance of lead towards sodium or potassium hydroxide up to 30 percent alkali at 25°C or 90°C has proven useful in refining petroleum involving sulfuric acid treatment followed by alkali treatment in a lead-lined tank. Detailed data on corrosion rates of lead exposed to organic compounds are found in the literature.[74]

Table 4.57 *Corrosion of lead in demineralized water*[a]

Lead	mpy[b]	mdd[c]
Chemical lead (ASTM B29)	2.3	18
6% Antimonial lead	0.2	1.6
2% Tin–lead	0.6	4.8

[a]See reference 74
[b]mils/yr
[c]mgs/dm^2 per day

Table 4.58 *Corrosion of lead and lead alloys in seawater*[a]

Metal	Days	Depth (m)	Corrosion Rate (mpy)[b]	Corrosion Rate (mdd)[c]	Pit depth	Remarks
Chemical lead	181	1.5	1.2	9.4	0	Uniform attack
(ASTM B29)	197	713	0.3	2.4	0	Uniform attack
	123	1719	0.8	6.3	0	Uniform attack
Pb-0.04% Te	181	1.5	1.0	7.9	0	Uniform attack
	197	713	0.3	2.4	0	Uniform attack
	123	1719	1.1	8.7	0	Uniform attack
Pb-6%Sb	181	1.5	1.2	9.4	0	Uniform attack
	197	713	0.3	2.4	0	Uniform attack
	123	1719	0.8	6.3	0	Uniform attack
Pb-33%Sn	181	1.5	3.7	29.1	0	Uniform attack
	197	713	0.5	3.9	0	Uniform attack
	123	1719	0.5	3.9	0	Uniform attack

[a]See reference 75
[b]mils/yr
[c]mg/dm^2 per day

Table 4.59 *Corrosion of chemical lead in phosphoric acid at 21°C*[a]

Solution	Corrosion rate (mpy)[b]	Corrosion rate (mdd)[c]
20% H_3PO_4 (commercial)	3.4	26.8
30% H_3PO_4 (commercial)	4.9	38.6
40% H_3PO_4 (commercial)	5.7	44.9
50% H_3PO_4 (commercial)	6.4	50.4
85% H_3PO_4 (commercial)	1.6	12.6
80% H_3PO_4 (pure)	12.8	100.8

[a]See reference 74
[b]mils/yr
[c](mg/dm^2/per day)

Some combinations of lead with other metals such as iron and copper are prone to galvanic corrosion.

Acid medium	Fe–Pb couple	Iron, being the anode, is subject to corrosion
Alkaline medium	Fe–Pb couple	Lead, being the anode, is subject to corrosion
Acid solutions	Cu–Pb couple	Copper, being the anode, is subject to corrosion
Alkaline solutions	Cu–Pb couple	Lead, being the anode, is subject to corrosion

Galvanic corrosion is not considered to be of concern in the case of Pb–Sb alloys used in pumps and valves in electrical contact with pipes of Pb–Te alloys and chemical lead as well as in the context of use of caulking lead in cast iron pipe in seawater.

Table 4.60 *Corrosion of lead in hydrochloric acid at 24°C (75F)*[a]

Solution	Chemical Pb		6% Antimonial Pb	
	(mpy)[b]	(mdd)	(mpy)	(mdd)[c]
1% HCl	24	189	33	260
5% HCl	16	126	20	158
10% HCl	22	173	43	339
15% HCl	31	244	150	1181
20% HCl	74	583	160	1260
25% HCl[(d)]	190	1496	200	1575
35% HCl	350	2755	540	1452

[a]See reference 74
[b]mils/yr
[c]mg/dm^2 per day
[d]Concentrated HCl commercially available

Table 4.61 *Corrosion of lead in hydrochloric acid–ferric chloride mixtures at 24°C (75°F)*

Solution	Chemical Pb		6% Antimonial Pb	
	(mpy)	(mdd)[b]	(mpy)[c]	(mdd)
5% HCl + 5% $FeCl_3$	28	220	37	291
10% HCl + 5% $FeCl_3$	41	323	76	598
15% HCl + 5% $FeCl_3$	88	693	160	1260
20% HCl + 5% $FeCl_3$	150	1181	190	1496

[a]See reference 74
[b] mg/dm^2 per day
[c] mils/yr
[d]Concentrated HCl commercially available

Atmospheric corrosion of lead involves exposure to industrial, rural and marine environments. The mode of corrosion in the three environments is different. The rural environment consists of humidity, airflow and rainfall, which may be considered to be innocuous. The marine environment consists of chloride entrained in air and could

Table 4.62 *Corrosion of lead in nitric acid*[74]

Solution	Corrosion rate			
	24°C		50°C	
	(mpy)	(mdd)	(mpy)	(mdd)
1% HNO_3	140	1102	600	4725
5% HNO_3	1650	13000	1850	14566
10% HNO_3	3400	26800	3490	27500

Table 4.63 *Effect of nitric acid in sulfuric acid on the corrosion of lead at 118°C.*

Solution	Chemical Pb		6% Antimonial Pb	
	(mpy)	(mdd)	(mpy)	(mdd)
54% H_2SO_4 + 0% HNO_3	7.4	58.2	14	110.2
54% H_2SO_4 + 1% HNO_3	5.9	46.5	22	173.2
54% H_2SO_4 + 5% HNO_3	8.4	66.1	114	897.6

Table 4.64 *Corrosion of chemical lead with sulfuric–nitric mixed acids*[74]

Solution	Corrosion rate			
	24°C		50°C	
	(mpy)	(mdd)	(mpy)	(mdd)
78% H_2SO_4 + 0% HNO_3	1	8	2	16
78% H_2SO_4 + 1% HNO_3	3	24	12	95
78% H_2SO_4 + 3.5% HNO_3	3.6	28.3	18	142
78% H_2SO_4 + 7.5% HNO_3	4	32	35	276

Table 4.65 *Corrosion of lead in hydrochloric acid–sulfuric acid mixtures*[a]

Solution	Chemical Pb				6% Anitmonial Pb			
	(24°C)		(66°C)		(24°C)		(66°C)	
	(mpy)	(mdd)	(mpy)	(mdd)	(mpy)	(mdd)	(mpy)	(mdd)
1% HCl + 9% H_2SO_4	5	39	9	71	5	39	12	95
3% HCl + 7% H_2SO_4	14	110	32	252	21	165	41	323
5% HCl + 5% H_2SO_4	14	110	42	331	21	165	65	512
7% HCl + 3% H_2SO_4	16	126	45	355	22	173	74	583
9% HCl + 1% H_2SO_4	18	142	47	370	30	236	84	661
5% HCl + 25% H_2SO_4	10	79	22	173	22	173	34	268
10% HCl + 20% H_2SO_4	17	134	42	331	80	630	58	465
15% HCl + 15% H_2SO_4	41	323	74	529	90	709	180	1417
20% HCl + 10% H_2SO_4	86	677	120	945	110	866	180	1417
25% HCl + 5% H_2SO_4	140	110	160	1260	150	1181	210	1653
5% HCl + 45% H_2SO_4	62	488			53	417		
10% HCl + 40% H_2SO_4	65	511			84	661		
15% HCl + 35% H_2SO_4	66	520			120	945		
20% HCl + 30% H_2SO_4	84	661			130	1024		
25% HCl + 25% H_2SO_4	120	945			210	1654		

[a]See reference 74

Table 4.66 *Corrosion of lead in various natural outdoor atmospheres*[74]

Location	Type of atmosphere	Material	Duration (years)	Corrosion rate (mdd)	Corrosion rate (mpy)
Altoona, Pennsylvania	Industrial	Chem Pb	10	0.23	0.029
Altoona, Pennsylvania	Industrial	1%Sb–Pb	10	0.18	0.023
New York	Industrial	Chem Pb	20	0.12	0.015
New York	Industrial	1% Sb–Pb	20	0.10	0.013
Sandy Hook, New Jersey	Seacoast	Chem Pb	20	0.17	0.021
Sandy Hook, New Jersey	Seacoast	1%Sb–Pb	20	0.16	0.020
Key West, Florida	Seacoast	Chem Pb	10	0.18	0.023
Key West, Florida	Seacoast	1% Sb–Pb	10	0.17	0.022
La Jolla, California	Seacoast	Chem Pb	20	0.16	0.021
La Jolla, California	Seacoast	1% Sb–Pb	20	0.18	0.023
State College, Pennsylvania	Rural	Chem Pb	20	0.10	0.013
State College, Pennsylvania	Rural	1% Sb–Pb	20	0.11	0.014
Phoenix, Arizona	Semi-arid	Chem Pb	20	0.03	0.004
Phoenix, Arizona	Semi-arid	1% Sb–Pb	20	0.09	0.012
Kure Beach, North Carolina 80 ft site	East Coast marine	Chem Pb	2	0.41	0.052
Kure Beach, North Carolina 80 ft site	East Coast marine	6% Sb–Pb	2	0.32	0.041
Newark, New Jersey	Industrial	Chem Pb	2	0.46	0.058
Newark, New Jersey	Industrial	6% Sb–Pb	2	0.33	0.042
Point Reyes, California	West Coast marine	Chem Pb	2	0.28	0.036
Point Reyes, California	West Coast marine	6% Sb–Pb	2	0.20	0.026
State College, Pennsylvania	Rural	Chem Pb	2	0.43	0.055
State College Pennsylvania	Rural	6% Sb–Pb	2	0.31	0.039
Birmingham, England	Urban	99.96% Pb	7	0.29	0.037
Birmingham, England	Urban	1.6% Sb–Pb	7	0.03	0.004
Wakefield, England	Industrial	99.995% Pb	1	0.58	0.074
Southport, England	Marine	99.995% Pb	1	0.55	0.070
Bourneville, England	Suburban	99.995% Pb	1	0.61	0.077
Cardington, England	Rural	99.995% Pb	1	0.44	0.056
Cristobal CZ	Tropical marine	Chem Pb	8	0.42	0.053
Miraflores CZ	Tropical inland	Chem Pb	8	0.24	0.030

have a corrosive tendency towards the metal. Industrial environments consist of sulfur dioxide, oxides of nitrogen and carbon which are corrosive.

Corrosion rate data obtained in various outdoor atmospheres given in Table 4.66 show a range of values (0.03–0.61 mdd or 0.004–0.0077 mpy). The general trend involves decreasing corrosion rate with increasing duration.

Corrosion protection measures involve washing the metal object with reagents such as sodium sulfate or silicate, which form lead sulfate or lead silicate film. Whenever galvanic effects are envisaged use of insulation is recommended. Sodium silicate has been successfully used to inhibit release of lead from the solder in copper pipes carrying domestic water supplies.

4.9.1 Lead Alloys and their Uses

Lead alloys containing antimony in the range 1–17 % have the applications noted below:

Sb (wt %)	Application
1	Electric cable sheathing
2–4	Storage battery connectors and parts
6	Roofing and chemical industry
9	Storage battery grids
6–8	Lead pumps, valves, coatings
15 (+5Sn)	Type metal, bearing metal
15–17 (+1Sn, 1As)	Bearing metal

These alloys have the following applications:

Lead – tin	Used in solders; anodes containing 7% Sn are used in chromium plating; Pb-Sn-Sb alloys used in steam spargers in chemical reactors
Lead – calcium	Have good corrosion resistance and are superior to Pb–Sb alloys in corrosion resistance; Pb–Ca alloys with or without Sn are used for battery grids, anodes and roofing materials
Lead – tellurium	About 0.04–0.05% Te in chemical lead containing 0.04–0.08% Cu gives increased corrosion resistance in many environments
Lead – silver	About 1% Ag in Pb gives rise to very good corrosion resistance and is used in production of electrolytic Zn from sulfate solutions; addition of 1% As results in further increase in corrosion resistance and permits its use as an anode in electrowinning of Mn; Pb–Ag alloy is used in cathodic protection of ships; Pb–2.3% Ag used as a soft solder
Lead – arsenic	Arsenic is added to Pb–Sb alloy for age hardening; As helps to improve resistance to bending and creep of electric power cable sheathing alloys; most widely used alloy is Pb–0.15% As – 0.1% Sn – 0.1% Bi
Lead – copper and other alloys	In general Cu is added to lead in amounts of up to 0.08%; Alloys with addition of Ba, Ca, Co, Au, Li, Mg, Ni, Pt, Na, Ti and Zn have been tested for corrosion resistance; anodes made of Ni and Ti give good performance in sulfuric acid solutions; Ni in lead improves the weldability of steel during lead coating

4.10 Magnesium and Magnesium Alloys

The general notion that magnesium as a rapidly corroding metal is mistaken when it is known that the corrosion resistance of magnesium alloys in normal environments is comparable to that of mild steel. It is important to bear in mind that proper precautions,

such as correct design, surface contamination and metallurgical factors should be considered before the use of the alloys. The standard electrode potential, $E^0_{Mg^{2+}/Mg}$ is -2.37 V, indicating the ease of oxidation.

The corrosion resistance of magnesium and its alloys depends upon the film formation on the surface and the stability of the film.

Some typical uses of magnesium alloys are in aircraft and guided weapons and automotive industries because of its light weight and high strength/weight ratio. Magnesium is used as a canning material for uranium fuel in gas-cooled reactors. Magnesium and its alloys may also be used as sacrificial anodes. New applications are steadily appearing because of its attractive properties such as high stiffness/weight ratio and ease of machinability.

4.10.1 Magnesium Alloys

These are available as: (i) cast alloys; and (ii) wrought alloys. The two major cast alloy systems are 2–10% Al with minor amounts of Zn and Mn, and Mg alloyed with rare earths, zinc, thorium, and silver without aluminum. The alloys devoid of zirconium are satisfactory in performance in the temperature range 95–120°C. The alloys containing zirconium have better high-temperature properties. Heat-treatment of the cast alloys results in improved properties.

The code used in designating the alloys consists of identifying the alloy with the letter of the alloying element as: A for aluminum, B for bismuth, C for copper, D for cadmium, E for rare earths, F for iron, H for thorium, K for zirconium, L for lithium, M for manganese, N for nickel, P for lead, Q for silver, R for chromium, S for silicon, T for tin, W for yttrium, Y for antimony and Z for zinc. The letter corresponding to the element in larger quantity in the alloy occupies the primary position; when two elements are present in equal amounts alphabetic order is followed. The letters are followed by numbers, which represent the weight percent of the element in the alloy. For example AZ 91 represents Mg – 9 Al – 1 Zn where Al is in the range 8.3–9.0 and Zn in the range 0.4–1.0. The letter X represents experimental alloys. The designations of commonly used tempers are: T5, alloys are artificially aged after casting; T6, alloys solution-treated, quenched and artificially aged; T7, alloys solution-treated and stabilized. Typical nominal composition, tensile properties and other features of cast Mg alloys are given in Table 4.67.

Wrought materials are produced by extrusion, rolling and press forging in the temperature range of 300–500°C. Wrought alloys are of two types, namely those containing zirconium and those devoid of zirconium. The typical composition and mechanical properties are noted in Table 4.68.

4.10.2 Corrosion of Magnesium and its Alloys

The various modes of degradation encountered are: (i) general or uniform corrosion; (ii) galvanic corrosion; (iii) pitting corrosion; (iv) crevice corrosion; (v) filiform corrosion; (vi) granular corrosion; (viii) stress corrosion cracking; (viii) corrosion fatigue.

The overall corrosion reaction of magnesium in aqueous solution may be written as:

$$Mg(s) + 2H_2O_{(l)} \rightleftharpoons Mg\ (OH)_2(s) + H_2(g)$$

Table 4.67 *Nominal composition, typical tensile properties and characteristics of selected magnesium casting alloys*

Designation		Nominal composition, (wt %)												Tensile properties			
								Rare earth[b]						0.2% proof stress	Tensile strength	El_b (%)	Characteristcs
ASTM	British	Al	Zn	Mn	Si	Cu	Zr	MM	Nd	Th	Y	Ag	Condition	(MNm^{-2})	(MNm^{-2})		
AZ63		6	3	0.3									As sand-cast	75	180	4	Good room temperature strength and ductility
													T6	110	230	3	
AZ81	A8	8	0.5	0.3									As sand-cast	80	140	3	Tough, leak-tight casting with 0.0015% Be used for pressure die-casting
													T4	80	220	5	
AZ91	AZ91	9.5	0.5	0.3									As sand-cast	95	135	2	General purpose alloy used for die-casting
													T4	80	230	4	
													T6	120	200	3	
													As chill-cast	100	170	2	
													T4	80	215	5	
													T6	120	215	5	
AM50		5		0.3									As die-cast	125	200	7[c]	High-pressure die-castings
AM20		2		0.5									As die-cast	105	135	10[c]	Good ductility and impact strength
AS41		4		0.3	1								As die-cast	135	225	4.5[c]	Good creep properties up to 150°C
AS21		2		0.4	1								As die-cast	110	170	4[c]	Good creep properties up to 150°C

ZK51	Z5Z	4.5			0.7				T5	140	235	5	Sand-castings, good room temperature, strength and ductility
ZK61		6			0.7				T5	175	275	5	As for ZK51
ZE41	RZ5	4.2			0.7	1.3			T5	135	180	2	Sand-castings, good room temperature, strength and castability
ZC63	ZC63	6	0.5	3					T6	145	240	5	Pressure-tight castings, good elevated temperature strength, weldable
EZ33	ZRE1	2.7			0.7		3.2		Sand-cast T5 Chill-cast T5	95 100	140 155	3 3	Good castability, pressure-tight, weldable, creep-resistant up to 250°C
HK31	MTZ				0.7		3.2		Sand-cast T6	90	185	4	Sand-casting, good castability, weldable, creep resistant up to 350°C
HZ32	ZT1	2.2			0.7		3.2		Sand- or chill-cast (T5)	90	185	4	As for HK31
QE22	MSR				0.7		2.5	2.5	Sand- or chill-cast (T6)	185	240	2	Pressure-tight, weldable, high-proof stress up to 250°C

(*contd.*)

Table 4.67 (*contd.*)

Designation		Nominal composition, (wt %)												Tensile properties			
								Rare earth[b]									
ASTM	British	Al	Zn	Mn	Si	Cu	Zr	MM	Nd	Th	Y	Ag	Condition	0.2% proof stress (MNm^{-2})	Tensile strength (MNm^{-2})	El_b (%)	Characteristcs
QH21	QH21						0.7		1	1		2.5	As sand cast T6	185	240	2	Pressure-tight, weldable, high-proof stress up to 300°C
WE54	WE54						0.5		3.25[d]		5.1		T6	200	285	4[c]	High strength at room and elevated temperature, good corrosion resistance, weldable
WE54	WE43						0.5		3.25[d]		4		T6	190	250	7[c]	

[a]Reproduced with permission from reference 77; Institute of Materials, London, UK
[b]MM = Mischmetal; El = elongation
[c]Values quoted for tensile properties are for separately cat test bars and may not be realized in certain parts of castings
[d]Contains some heavy metal rare earth elements

Table 4.68 *Nominal composition, typical tensile properties and characteristics of selected wrought magnesium alloys*[77]

Designation		Nominal composition (wt %)								Tensile properties			
ASTM	British	Al	Zn	Mn	Zr	Th	Cu	Li	Condition	0.2% proof stress (MN m^{-2})	Tensile strength (MN m^{-2})	El (%)	Characteristics
MI	AM503			1.5					Sheet, plate/F	70	200	4	Low-to-medium-strength alloy, weldable, corrosion resistant
									Extrusions/F	130	230	4	
									Forgings/F	105	200	4	
AZ31	AZ31	3	1	0.3					Sheet, plate/O	120	240	11	Medium-strength alloy, weldable, good formability
				0.2[b]					Sheet	160	250	6	
									Plate/H24	130	230	4	
									Extrusions/F	105	200	4	
									Forgings/F				
AZ61	AZM	6.5	1	0.3					Extrusions/F	180	260	7	High-strength alloy, weldable
				0.15[b]					Forgings/F	160	275	7	
AZ80	AZ80	8.5	0.5	0.2					Forgings/T6	200	290	6	High-strength alloy
				0.12[b]									
ZM21	ZM21		2	1					Sheet plate/O	120	240	11	Medium-strength alloy, good formability, good damping capacity
									Sheet,	165	250	6	
									plate/H24	155	235	8	
									Extrusions/T6	125	200	9	
			6.5	0.75					Forgings/F				
ZMC711							1.25		Extrusions/T6	300	325	3	High-strength alloy

(*contd.*)

Table 4.68 *(contd.)*

Designation		Nominal composition (wt %)								Tensile properties			
ASTM	British	Al	Zn	Mn	Zr	Th	Cu	Li	Condition	0.2% proof stress (MN m^{-2})	Tensile strength (MN m^{-2})	El (%)	Characteristics
LA 141		1.2		0.15[b]				14	Sheet, plate/T7	95	115	10	Ultralightweight (specific gravity 1.35)
ZK31	ZW3		3		0.6				Extrusions/T5	210	295	8	High-strength alloy, some weldability
									Forgings/T5	205	290	7	
ZK61			6		0.8				Extrusions/F	210	285	6	High-strength alloy
									Extrusions/T5	240	305	4	
									Forgings/T5	160	275	7	
HK31					0.7	3.2			Sheet, plate/H24	180	255	4	High creep resistance up to 250°C, weldable
									Extrusions/T5				
HM21				0.8		2			Sheet, plate/T8	135	215	6	High creep resistance up to 350°C, short time exposure up to 425°C, weldable
									Sheet, plate/T81	180	255	4	
									Forgings/T5	175	225	3	
HZ11	ZTY		0.6		0.6	0.8			Extrusions/F	120	215	7	Creep resistance up to 350°C, weldable
									Forgings/F	130	230	6	

Table 4.69 *Results of 2.5-yr exposure tests on sheet alloys*[78]

Material	Corrosion rate (μm/yr)	Loss of tensile strength after 2–5 yr (%)
Marine atmosphere		
Aluminum alloy 2024	2.0	2.5
Magnesium alloy AZ31	18.0	7.4
Low-carbon steel (0.27% C)	150.0	75.4
Industrial atmosphere		
Aluminum alloy 2024	2.0	1.5
Magnesium alloy AZ31	27.7	11.2
Low carbon steel (0.27% C)	25.4	11.9
Rural atmosphere		
Aluminum alloy 2024	0.1	0.4
Magnesium alloy AZ31	13.0	5.9
Low carbon steel (0.27% C)	15.0	7.5

The film of magnesium hydroxide formed can give rise to passivity. This is attacked by anions such as chloride, sulfate and nitrate. The passive film formed gives reasonable protection from corrosion in rural, marine and industrial atmospheres, as evidenced by the corrosion rate data given in Table 4.69. It is obvious from the data that the corrosion performance of magnesium alloy lies between aluminum and carbon steel.

Galvanic corrosion of magnesium is to be expected since magnesium is anodic with respect to all the engineering metals. The two main causes of galvanic corrosion are: (i) poor alloy quality due to excessive levels of heavy metal or flux contamination; (ii) improper design. Some typical data obtained on the galvanic corrosion of magnesium alloys led to grouping of the alloys in terms of the severity of galvanic corrosive attack, as noted in Table 4.70.

Aluminum alloys of the series 7000 and 2000 and 380 die-cast alloy cause serious galvanic corrosion of magnesium in saline environments, especially when the iron content of the alloy exceeds 200 ppm of iron. Data on the galvanic corrosion of

Table 4.70 *Relative effects of various metals on galvanic corrosion of magnesium alloys AZ31B and AZ61A exposed at the 24.4- and 244-m (80- and 800-ft) stations, Kure Beach, NC*[a]

Group 1 (least effect)	Group 2	Group 3	Group 4	Group 5 (greatest effect)
Al alloy 5052	Al alloy 6063	AlClad alloy 2024	Zn-plated steel	Low-carbon steel
Al alloy 5056	AlClad alloy 7075	Al alloy 2017	Cd-plated steel	Stainless steel
Al alloy 6061	Al alloy 3003	Al alloy 2024		Monel, titanium
	Al alloy 7075	Zinc		Lead, copper, brass

Table 4.71 *Corrosion of Mg 6% Al-3% Zn 0.2% Mn alloy galvanically connected to other metals in various media*[2]

Dissimilar metal	Corrosion rate (mdd)					
	3% NaCl				Midland tapwater	Distilled water
	Separation					
	Close contact	0.35 cm	2.0 cm	10 cm	0.35 cm	0.35 cm
Steel	23,400	25,500	8300	3900	300	18
Aluminum alloys 2024	12,800	25,700	6800	3200	90	6
Nickel	18,800	22,400	6600		210	19
Aluminum alloys 1100	14,500	15,600	4100		40	4
Copper	8500	8200	3700		90	15
Brass	7100	4000	2500	1700	60	14
Aluminum alloys 5056		1900			10	3
Cd-plated steel	5200	2200	1000		40	14
Zinc	6200	1300	900	700	30	8
Mg–1.5% Mn		50			2	3
Mg–6% Al–3% Zn–0.2% Mn		200			7	3
Size of specimen $4 \times 1.3 \times 0.2$ cm ($1.5 \times 0.5 \times 0.079$ in.)					Temperature	Room
Relative area 1:1 (mounted face to face)					Aeration	Natural convection
Surface preparation Aloxite 150 ground. Volume of testing solution 100 mL						
Velocity quiescent						
Duration of test: 3% NaCl, 3 h; Midland tapwater, 24 h; distilled water, 4 days						

Mg 6% Al – 3% Zn – 0.2% Mn connected to other metals in various media are given in Table 4.71.

The conductivity and the composition of the medium are controlling factors in the extent of galvanic corrosion, as evidenced by the corrosion rates in 3% NaCl and tapwater (see Table 4.71). Cadmium-plated steel gives a lower corrosion rate than steel.

The zinc, cadmium or tin plating reduces the galvanic corrosion of magnesium, as seen in Figure 4.6. The compatibility of various fasteners shown in the figure leads to the order of effectiveness tin > cadmium > zinc.

In salt spray tests using cast iron disks coupled to AZ 91 die-cast plates separated by plastic spacers, the optimum separation of about 4.45 mm was needed to ensure the absence of galvanic corrosion.[79]

Aluminum can be attacked by way of cathodic corrosion in strong alkaline media generated at the cathode when magnesium corrodes sacrificially in static NaCl solutions. This mode of attack destroys compatibility in alloys containing significant iron contamination.

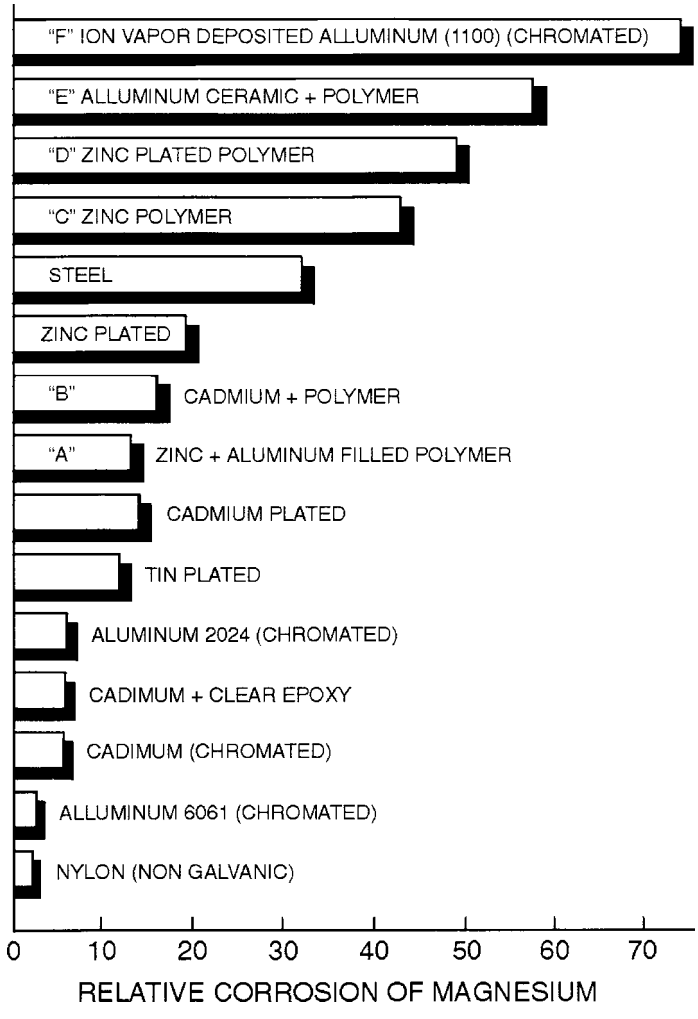

Figure 4.6 *Galvanic corrosion produced by dissimilar fasteners in AZ91D magnesium alloy*[79]

The aluminum alloys 5052 and 5056, containing significant amounts of magnesium, are resistant to this attack. Cathodic corrosion of aluminum is less severe in seawater than in NaCl solution because of the buffering effect of magnesium ions reduces the equilibrium pH from 10.5 to ~8.80. The compatibility of aluminum with magnesium is better in seawater and is less sensitive to the iron content. Cathodic damage of coatings applied to fasteners coupled to magnesium can occur due to hydrogen evolution and strong alkalinity generated at the cathode. This effect may be reduced by using alkali-resistant resins.

The usual preventive measures[79] in the galvanic corrosion are: (i) use of indoor and shelters for outdoor exposure; (ii) seal faying surfaces; (iii) proper design for joining

magnesium to dissimilar metals, (iv) use of compatible materials. Other forms of corrosion of magnesium and its alloys are detailed below:

Pitting in Mg alloys[80-83]	Pits initiate at flaws adjacent to intermetallic particles due to the breakdown of passivity; intermetallics act as cathode and Mg matrix as the anode[80]
Crevice corrosion[84]	Corrosion in crevices between Magnox A (Mg-0.18 Al) and mild steel, Magnox A and PTFE in 200 g/m^3 NaOH (pH >11.5) with chloride concentration 1 g/m^3 or more
Filiform corrosion[85]	Generally occurs on metal surface having an applied protective coating; this form of corrosion consists of a differential aeration cell driven by differences in oxygen concentration between the head and tail sections with potential of the order of 0.1–0.2 V; filiform corrosion initiates and develops into cellular or pitting corrosion; In homogeneous alloys filiform corrosion propagates transgranularly along crystallographic direction
Granular corrosion	Does not occur in Mg alloys since grain boundary constituent is cathodic to the grain body
Stress–corrosion cracking	Pure Mg is not susceptible to SCC. Mg-Al alloys are most susceptible to SCC; Mg-Zn alloys are moderately subject to SCC; failures of wrought AZ80 aircraft components due to excessive assembly and residual stresses have been reported;[86] weldments and inserts are the stress sources for SCC; SCC in Mg alloys is usually transgranular; mixed transgranular and intergranular crack propagation and occasional total intergranular cracking have been observed;[87] low incidences of SCC service failure of castings are due to low applied stresses or due to stress relaxation by yielding or creep inhibition by nitrate or carbonate of SCC in salt-chromate solutions; above pH 12 Mg alloys are SCC resistant; SCC in decreasing order of severity; NaBr, Na_2SO_4, NaCl, $NaNO_3$, Na_2CO_3, $NaC_2H_3O_2$, NaF, Na_2HPO_4; SCC has also been observed in KF, KHF_2, HF, KCl, CsCl, NaI, KI, Mg CO_3 NaOH, H_2SO_4, HNO_3 and HCl; SCC prevention methods have been reported[88,89]
Corrosion fatigue[90]	Mg 1.5% Mn, Mg – 2% Mn – 0.5% Ce alloys are more resistant than Mg–Al, Mg–Zn alloys; coatings that exclude corrosive environment give protection.

Effects of alloying elements in magnesium alloys can be summarized as follows:

(i) The corrosion rate of high-purity die-cast Mg alloys in chloride media decreases with increase in Al content up to ~4 wt %. Further increase in al up to ~9 wt % results in modest increase in corrosion resistance. With the constant Al content, AE alloys gave lower corrosion rates than AS, AM and AZ alloys.

(ii) Intermetallic compounds containing more than a few percent iron act as cathodes and hence influence the corrosion rate. Al–Mn binary phase with a low Al/Mn ratio causes an increase in corrosion rate by way of high cathodic current.

Table 4.72 *Heat-treated AZ91 corrosion rates*

Condition	Corrosion rate (mg/cm^2 day)
As-cast	10
T4	11
T6-aged at 120°C	6
T6-aged at 205°C	1

(iii) The high corrosion resistance of AE alloys may be due to the passive Al-rich zones along the grain boundaries acting as barriers against pit propagation.
(iv) Silicon in the alloy, forming Mg_2Si phase, has no effect on the corrosion since Mg_2Si is a poor cathode.
(v) The Al_4MM phase particles precipitated in AE alloys evince passive behavior and do not have significant influence on the corrosion rate. AE alloys containing large amounts of Al exhibit high resistance to localized corrosion.

The effect of heat treatment is to alter the size, amount and the distribution of the precipitated β-phase, $Mg_{17}Al_{12}$, which in turn affects the corrosion rates of AZ91 alloys, as shown in Table 4.72.

Corrosion rates of atomized, rapidly solidified alloy cast and chill cast alloys are given in Table 4.73. The data show that atomized rapidly solidified alloy is comparable in corrosion resistance to the cast AZ 1D alloys. Rapid solidification improves the corrosion resistance of the alloys since the homogeneous microstructures tend to disperse the elements and particles, which otherwise act as cathodic sites. Extended solubility of various elements may also shift the electrode potentials to more noble values.

The improved corrosion resistance of rapidly solidified Mg Al alloys due to the addition of rare earth elements is obvious from the data given in Table 4.74.

Table 4.73 *Corrosion rates of selected materials (mpy)*

Material (wt %)	Atomized	Chill cast	Cast
Mg 7.7 Al 2.9 Zn 6.6 Ce 0.35 Mn	50		
Mg 10.1 Al 2.7 Zn 1.4 Y 0.44 Mn	60		
Mg 10.2 Al 3.2 Zn 5.8 Ce 2.7 Mn		350	
Mg 11.1 Al 2.4 Zn 3.2 Y		430	
AZ 91D			28

Table 4.74 *Corrosion rates of Mg–Al alloys*

Alloy	Corrosion rate (mpy)
Mg Al Zn Si Mn	15
Mg Zn Al Y	8
Mg Zn Al Nd	11
AZ 91 HP-T6	82

4.11 Zinc and Zinc Alloys

Zinc is very widely used metal in a variety of environments. The strength and hardness of zinc are greater than those of tin or lead and are less than those of aluminum or copper. It is not possible to use pure zinc in applications involving applied stress due to its low creep resistance. Zinc recrystallizes rapidly after deformation at laboratory temperature and hence cannot be work-hardened at laboratory temperature. By alloying with other metals the temperature of recrystallization and the creep resistance can be increased to acceptable levels. The alloys of commercial importance are:

(i) Zn–Cu up to 45% Zn are brasses;
(ii) Zn–Al at 4% of Al is the basis of Zn die-casting alloys;
(iii) Zn–Fe, including the phases involved in galvanized coatings;
(iv) Zn–Pb alloys, useful in pyrometallurgical extraction processes;
(v) ternary and quaternary systems of the alloys with added Ni, Mg, Ti and Cd.

The electrochemical behavior of zinc is important in: (i) electrowinning zinc in refining; (ii) electoroplating in forming zinc coatings; (iii) zinc batteries for energy storage; (iv) zinc anodes for corrosion protection. The salient electrochemical properties of zinc that are of importance are: (i) the placement of the metal in electromotive force series; (ii) fast and reversible dissolution/deposition rates; (iii) the high overpotential for formation of hydrogen; and (iv) formation of passive films in slightly alkaline solutions.

4.11.1 Atmopheric Corrosion

As is the case with corrosion of metals the corrosion of zinc proceeds by the reaction

$$Zn \rightarrow Zn^{2+} + 2e^{-}$$

and the standard potential of the reaction is −0.763 V vs SHE, which is 0.315 V more negative than iron and 0.9 V more positive than the value for Al. The oxidation of zinc at the anode with the simultaneous reduction of hydrogen ions or the dissolved oxygen at the cathode completes the corrosion reaction scheme. Typical corrosion rates in different atmospheres are:

Rural	0.2 to 3 μm/yr
Marine (outside the splash zone)	0.5 to 8 μm/yr
Urban and industrial	2 to 16 μm/yr

The relative ranking of the degree of corrosivity of different atmospheres for zinc and steel is given in Table 4.75. The corrosivity of the atmosphere in one location or another varies as much as a factor of 100 for zinc and 500 for steel. The corrosion rates of zinc in most cases are ten times lower than those of steel. The lower corrosion rates of zinc are profitably used for the protection of steel by galvanizing steel with zinc. The plot of the corrosion rate ratio of steel to zinc as a function of corrosion rate of the steel in various atmospheres (data from Table 4.75) gives a linear plot with $R^2 = 0.495$.

The corrosion rates of various metals in industrial, marine and rural atmospheres are given in Table 4.76. Zinc has higher corrosion resistance than cadmium and iron in all the three atmospheres. Zinc has higher corrosion resistance than copper in industrial

Table 4.75 *Ranking of corrosivity in 45 locations for steel and zinc from 2 yr exposure*[91]

Ranking		Location	Weight loss (g)		Loss ratio
Steel	Zinc		Steel	Zinc	Steel/zinc
1	1	Norman Wells, NWT, Canada	0.73	0.07	10.3
2	2	Phoenix, AR	2.23	0.13	17.0
3	3	Saskatoon, SK, Canada	2.77	0.13	21.0
4	4	Esquimalt, Vancouver Island, BC, Canada	6.50	0.21	31.0
5	15	Detroit, MI	7.03	0.58	12.2
6	5	Fort Amidor Pier, Panama, C.Z.	7.10	0.28	25.2
7	11	Morenci, MI	9.53	0.53	18.0
8	7	Ottawa, Ontario, Canada	9.60	0.49	19.5
9	13	Potter County, PA	10.00	0.55	18.3
10	31	Waterbury, CT	11.00	1.12	9.8
11	10	State College, PA	11.17	0.51	22.0
12	28	Montreal, Quebec, Canada	11.44	1.05	10.9
13	6	Melbourne, Australia	12.70	0.34	37.4
14	20	Halifax (York Redoubt), Nova Scotia, Canada	12.97	0.70	18.5
15	19	Durham, NH	13.30	0.70	19.0
16	12	Middletown, OH	14.00	0.54	26.0
17	30	Pittsburgh, PA	14.90	1.14	13.1
18	27	Columbus, OH	16.00	0.95	16.8
19	21	South Bend, PA	16.20	0.78	20.8
20	18	Trail, BC, Canada	16.90	0.70	24.2
21	14	Bethlehem, PA	18.3	0.57	32.4
22	33	Cleveland, OH	19.0	1.21	15.7
23	8	Miraflores, Panama, C.Z.	20.9	0.50	41.8
24	29	London (Battersea), England	23.0	1.07	21.6
25	24	Monroeville, PA	23.8	0.84	28.4
26	35	Newark, NJ	24.7	1.63	15.1
27	16	Manila, Philippine Islands	26.2	0.66	39.8
28	32	Limon Bay, Panama, CZ	30.3	1.17	25.9
29	39	Bayonne, NJ	37.7	2.11	17.9
30	22	East Chicago, IN	41.1	0.79	52.1
31	9	Cape Kennedy, FL (½ mile from ocean)	42.0	0.50	84.0
32	23	Brazos River, TX	45.4	0.81	56.0
33	40	Pilsey Island, England	50.0	2.50	20.0
34	42	London (Stratford), England	54.3	3.06	17.8
35	43	Halifax (Federal Building), Nova Scotia, Canada	55.3	3.27	17.0
36	38	Cape Kennedy, Fl (60 yards from ocean, 60 ft elevation)	64.0	1.94	33.0
37	26	Kure Beach, NC (800 ft lot)	71.0	0.89	80.0
38	36	Cape Kennedy, FlL (60 yards from ocean, 30 ft elevation)	80.2	1.77	45.5
39	25	Daytona Beach, FL	144	0.88	164
40	44	Widness, England	174.0	4.48	39.0
41	37	Cape Kennedy, FL (60 yards from ocean, ground level)	215.0	1.83	117.0
42	34	Dungeness, England	238.0	1.60	148.0
43	17	Point Reyes, CA	244.0	0.67	364.0
44	41	Kure Beach, NC (80 ft lot)	260.0	2.80	93.0
45	45	Galeta Point Beach, Panama, CZ	336.0	6.80	49.4

[a]Specimen size 150 × 100 mm (6 × 4 in) Copyright ASTM. Reprinted with permission

Table 4.76 *Comparison of the typical rate between zinc and other common commercial metals*

Metal	Industrial	Marine	Rural
Zn	1	1	1
Cd	2	2	2.4
Sn	0.23	1.6	1.9
Al	0.13	0.3	0.09
Cu	2.4	0.72	0.38
Pb	0.07	0.3	0.28
Ni		0.6	1.1
Sb	0.06		
Mg	0.31	1.8	1.9
Fe	30	50	15

[a]See reference 92, copyright Plenum press, reproduced with permission

atmosphere. The corrosion resistance of zinc is better than tin and magnesium in marine and rural atmospheres. Atmospheric corrosion of zinc depends upon time-of-wetness (relative humidity, temperature and the amount of rain) and the level of pollutants such as sulfur dioxide. The corrosion loss of zinc as a function of time at different times of the year is depicted in Figure 4.7.

The most important pollutant in the atmosphere is sulfur dioxide, which causes a linear increase in the corrosion rate of zinc as a function of its concentration.[93,94] Other pollutants such as NO_x are not significant because of their presence in the atmosphere in trace quantities. The atmospheric corrosion rates of zinc in 1980s were found to be lower than the rates observed in 1960s and 1970s due to the decrease in the level of

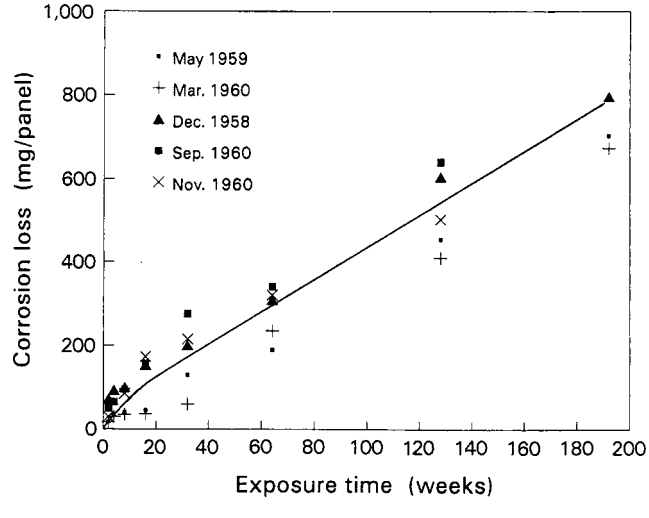

Figure 4.7 *Corrosion loss–time curve for zinc specimens exposed at different times of the year*[93]

pollutants in the atmosphere in accordance with the environmental regulations and specifications.

The corrosion rates of zinc have been found to decrease with increasing distance from the seashore and decreasing air salinity. Typical data are:

Air salinity ($g/m^3 \times 10^{-3}$)	Distance from the sea (m)	Weight loss (g/m^3)
34	1.0	40
27	5.0	19
20	10.0	5
9.0	100.0	1.0

Other factors of importance in atmospheric corrosion of zinc are: (i) the distance from the ground; (ii) orientation of the samples; (iii) wind or rain shielding; (iv) distance to the local contaminant sources; (v) wind, radiation; (vi) condensation and drying rate; (vii) amount of contaminants and nature of corrosion products; and (viii) seasonal variation of factors also should be considered. This shows the complexity of the problem of determining the atmospheric corrosion rates to a high degree of certainty. This uncertainty is exemplified by the observed corrosion rate of 0.6–3.8 μm/yr at 26 sites in rural area in Spain.[95] The corrosion rate of ~8.5 μm/yr observed on the zinc coating in an under-vehicle situation is comparable to severe marine atmospheric conditions.[96]

Corrosion products such as the oxides, hydroxides, carbonates, sulfates, basic sulfates hydroxy carbonates, hydroxy chlorides are formed in the various environments (marine, urban, rural, industrial) and the initially loosely bound products may become adherent in the course of time. Corrosion can occur in the pores of the corrosion product layers. The low corrosion rate observed in atmospheric corrosion, R has been expressed as:

$$R = ra/A$$

where r is the actual corrosion rate on the active metal surface not sealed by corrosion products, a is the area of active zinc surface and A is the total surface area. In practice the active surface area a is small and hence the value of R is small although the value of r may be high.

4.11.2 Corrosion in Aqueous Media

The corrosion rates of zinc in distilled water vary in the range 15–150 μm/yr and depend upon the dissolved oxygen and carbon dioxide, as seen in the data in Table 4.77.

The corrosion rate of zinc was found to be constant in air-saturated water between 20° and 50°C, followed by an increase with a maximum at 65°C, followed by a decrease at 100°C. The increase in the corrosion rate at 65°C has been explained in terms of transition from protective to nonprotective state of the surface.[97]

Corrosion rates of zinc in soft waters are lower than in hard waters and some data for various media are given in Table 4.78. As expected, corrosion rates in flowing waters are higher than in static waters.

Table 4.77 *Effect of oxygen on the corrosion of zinc in distilled water*[a]

Test condition[b]	Temperature (°C)	Corrosion ratec (μm/yr)
Boiled distilled water; specimens immersed in sealed flasks	Room	25.4
Boiled distilled water; specimens immersed in sealed flasks	40	48.3
Boiled distilled water; specimens immersed in sealed flasks	65	83.8
Oxygen bubbled slowly through the water	Room	218.4
Oxygen bubbled slowly through the water	40	348.0
Oxygen bubbled slowly through the water	65	315.0

[a]See reference 76
[b]High-grade zinc specimens, in duplicate, immersed for 7 days
[c]Corrosion rate calculated after removal of corrosion products

Small amounts of copper (0.1–0.3 ppm) in water increase the corrosion rate of zinc in proportion to the amount of copper due to the larger cathodic activity generated by copper.

Corrosion rates in seawater range between 20 and 70 μm/yr, depending upon factors such as location, duration of exposure and type of zinc sample with the rates decreasing over time.

The effects of different anions in solutions on the corrosion rates of zinc are seen from the data in Table 4.79. The low rates observed in the case of sodium phosphate and sodium chromate can be attributed to the passivation film formed by these reagents. The corrosion rates in neutral electrolyte solutions devoid of salts that form passivating film or

Table 4.78 *Corrosion rate of zinc and zinc coatings immersed in various types of waters*[a]

Solution	R (μm/yr)
Mine water, pH 8.3, 110 ppm hardness, aerated	31
Mine water, 160 ppm hardness, aerated	30
Mine water, 110 ppm hardness, aerated	46
Demineralized water	137
River water, moderate soft	97
River water, moderate soft	61[b]
River water, treated by chlorination and copper sulfate	81
River water, treated by chlorination and copper sulfate	64[b]
Tap water, pH 5.6, 170 ppm hardness, aerated	142
Spray cooling water, chromate-treated, aerated	15
Hard water	16
Soft water	15
Seawater in Pacific Ocean	70[c]
Seawater in Bristol Channel	64[d]
Seawater at Easport, ME	28[c]
Seawater at Kure Beach, NC	28[c]
Seawater at Panama	21[d]

[a]See reference 92
[b]Galvanized steel
[c]1 yr
[d]4 yr

Table 4.79 *Corrosion rate in different solutions in neutral pH range*

Solution	Duration	*R* (μm/year)
Distilled water	4 weeks	46
Distilled water	1 month	55
0.1 *N* benzoate	4 weeks	59
0.1 *N* NaCl	4 weeks	62
0.1 *N* Na_3PO_4	4 weeks	1.8
0.1 *N* Na_2ClO_4	4 weeks	0.4
5 g/L NaCl	2 months	90
5 g/L KCl	2 months	92
5 g/L $NaNO_3$	6 months	18
5 g/L K_2SO_4	2 months	52
8% $Na_2SO_4.10H_2O$	1 month	83
5% NaCl	3 weeks	89
3% Na_2SO_4	1 day	144

complexes are comparable to the rates in distilled water. In the absence of passivating ions the corrosion of zinc in aqueous solutions is primarily controlled by the pH of the solution. Three distinct regions may be identified as follows:

pH 0–6	Appreciable corrosion
pH 6–12	Minimum due to formation of protective corrosion product
pH 12–14	Appreciable corrosion

4.11.3 Corrosion in Soils

The factors that contribute to corrosion of zinc in soils are not well understood. The pH of soils can vary from 2.6 to 10.2 and the resistivity from 100 Ω cm to 100 KΩ cm. No correlation between corrosion rate and pH of the soil has been observed. In general low corrosion rates have been observed when the soil has high resistivity.

Some data on the corrosion rates of steel coated with zinc in soils are given in Table 4.80. The factors identified to cause corrosion in soils are: (i) poorly aerated soils; (ii) high concentrations of chlorides and sulfates causing pitting; (iii) mud, clay and peat are more corrosive than sand.

4.11.4 Corrosion of Painted Materials[99]

The most common example is automotive corrosion consisting of: (i) cosmetic corrosion; and (ii) perforation corrosion. The features of the two modes of corrosion are:

Cosmetic corrosion	Surface attack at spots where paint is damaged; related to: (i) red rust, (ii) paint creep, (iii) chipping; factors involved are (i) coating composition and thickness, (ii) surface treatment, (iii) type of paint damage, (iv) type of paint; generally evaluated by (i) measuring length of underpaint creep, (ii) extent of rust formation or paint loss

Table 4.80 *Corrosion rates of zinc coating on steel in soils of different geographic locations in the United States*[98]

Location[a,b]	Soil type	Δ(Ω cm)	pH	R(μm/yr)
1	Allis silt loam, Cleveland, OH	1215	7.0	11.8
2	Bell clay, Dallas, TX	684	7.3	1.5
3	Cecil clay, loam, Atlanta, GA	30000	5.2	1.7
4	Chester loam, Jenkintown, PA	6670	5.6	7.9
5	Dublin clay adobe, Oakland, CA	1345	7.0	7.7
6	Everett gravelly sandy loam, Seattle, WA	45100	5.9	0.5
7	Maddox silt loam, Cincinnatti, OH	2120	4.4	10.8
8	Fargo clay loam, Fargo, ND	350	7.6	3.2
9	Genesse silt loam, Sidney, OH	2820	6.8	5.2
10	Gloucester sandy loam, Middleboro, MA	7460	6.6	5.0
11	Hagerstown loam, Loch Raven, MD	11000	5.3	3.7
12	Hanford fine sandy loam, Los Angeles, CA	3190	7.1	2.2[c]
13	Hanford very fine sandy loam, Bakersfield, CA	290	9.5	3.7
14	Hempstead silt loam, St Paul, MN	3520	6.2	1.1
15	Houston black clay, San Antonio, TX	489	7.5	1.5
16	Kalmia fine sandy loam, Mobile, AL	8290	4.4	4.2
17	Keyport loam, Alexandria, VA	5980	4.5	14.8[d]
18	Lindley silt loam, Des Moines, IA	1970	4.6	2.9
19	Mahoning silt loam, Cleveland, OH	2870	7.5	4.9

[a]Average coating thickness, 121 μm
[b]Original soil identification
[c]Sheet specimens
[d]Coating corroded completely and the data included the corrosion of steel

Perforation corrosion	Initiates at the interior and spreads to cause perforation; corrosion of the coating or paint delamination, followed by corrosion of the substrate and with time shows up as perforation; delamination at the corrosion front can be physical, anodic, cathodic, and mechanical or combinations; may occur due to variations in paints, coatings, phosphates and other conditions

The possible delamination modes are: (i) loss of adhesion at paint/phosphate interface, (ii) within phosphate layer due to mechanical fracture; (iii) due to dissolution of phosphate; (iv) dissolution of coating; (v) mechanical failure at coating/steel interface.

4.11.5 Corrosion in Concrete

Galvanized steel rebar in concrete reduces the corrosion rate to acceptable levels (i.e., <0.5 μm/year in most of the cases) as shown by the data in Table 4.81.

The corrosion rates of rebar in concrete are high when the chloride content of the environment is high. Extensive laboratory test data on the corrosion of rebar in concrete are available.[92] Field test data are limited by comparison.

Corrosion in other environments such as organic media and gaseous atmospheres are discussed in the literature. Corrosion in organic media is dependant upon the viscosity and the presence of other chemical reagents. Corrosion in gaseous atmospheres is similar to atmospheric corrosion in requiring moisture and the formation of an electrolyte, which in turn can cause corrosion. The corrosion rate will vary with the type of gas such as NO_2 or SO_2 present.

Table 4.81 *Average corrosion rate of zinc coating inside concrete in marine environments*[a]

Structure	Age (yr)	Cover (cm)	Sample location	$C1^-$ (wt %) [kg/m^3]	R (μm/yr)
Longbird Bridge	23	10	Above HT[b]	0.19 [4.4]	0.2
St George Dock	12	8	Above HT	0.27 [6.4]	1.1
	10	6	Above HT	0.22 [4.6]	0.5
	7	13	Above HT	0.14 [3.0]	0.29
Hamilton Dock	10	5	Near MT	0.08 [1.9]	0.5
	10	6	Above HT	0.14 [3.6]	0.8
Bermuda Yacht Club	8	7	Below HT	0.16 [3.7]	0.0

[a]See reference 100
[b]HT = high tide; MT = mean tide

The corrosion of zinc electrode in zinc cells and batteries contributes to self-discharge, short shelf-life and hydrogen build-up.[92]

4.11.6 Forms of Corrosion

The atmospheric corrosion discussed earlier appears in the form of uniform or general corrosion. Pitting corrosion is not generally observed, except in the rare case of submerged samples in soils. Intergranular corrosion is also rare in the case of zinc and zinc products. Galvanic corrosion plays an important role in the case of zinc, particularly when zinc is used as a coating or as an anode or as zinc-based paint. The galvanic corrosion rate data when zinc is coupled to other metals in rural, urban and marine atmospheres are summarized in Table 4.82.

It is obvious from the data that galvanic corrosion of zinc in rural atmosphere can be five times the rate in corresponding atmospheric corrosion and three times that in marine atmospheres. Mild steel appears to be the most efficient cathode among the metals studied. More detailed discussions are given in the literature.[92]

As noted earlier pitting corrosion of zinc is usually not encountered, with the exception of corrosion in nonuniform soils, distilled water containing vertical samples of zinc panels, and galvanized steel in hot water tanks. In hot water tanks containing soft water,

Table 4.82 *Galvanic corrosion rate of zinc coupled to other common commercial metals in different atmospheres (μm/yr)*[95]

Coupled alloy	Rural	Urban	Marine
Zinc freely exposed	0.5	2.4	1.3
Mild steel	3.0	3.3	3.9
Stainless steel	1.1	1.8	2.0
Copper	2.2	2.0	3.2
Lead	1.6	2.4	3.4
Nickel	1.5	1.9	2.8
Aluminum	0.4	1.1	1.1
Anode aluminum	0.9	1.9	1.0
Tin	1.0	2.6	2.4
Chromium	0.7	1.4	1.9
Magnesium	0.02	0.04	1.1

Table 4.83 *Intergranular penetration rates of some zinc alloys in different environments*[92]

% Al	Zn purity (%)	Environment	Duration (days)	Rate (mm/day)
0.075	99.999	95°C water vapor	10	0.02
0.1	99.999	95°C water vapor	10	0.018
4	99.999	95°C water vapor	10	0.033
20	99.999	95°C water vapor	10	0.028
21.1		100% RH at 50°C	42	0.002
0.1	99.99	95°C tapwater		0.01

pitting corrosion can lead to penetration of coatings due to the reversed of polarity of zinc/steel couple. The presence of copper in the water has been found to accelerate the pitting corrosion of galvanized coatings in hot water.[101]

Intergranular corrosion has been observed in Zn–Al, Zn–Pb and Zn–Mg alloys and some data in the case of Zn–Al alloys are given in Table 4.83.

The intergranular corrosion of Zn–Al alloys may be attributed to the preferential attack at the Al-rich phase present in the grain boundaries.

Wet storage stain forms on galvanized steel surface during storage or transportation and appears as a voluminous, white bulky powder. This phenomenon occurs when closely packed galvanized items are stored under damp and poorly ventilated conditions. This form of staining is not harmful to the corrosion performance of the samples. Proper storage under good ventilation conditions or chromating can prevent wet storage staining during storage and transportation.

Typical applications of zinc-coated steel and products are given in Table 4.84.

Table 4.84 *Typical applications of zinc-coated steel products* [102]

Coatings	Typical applications
	Continuous electroplating and hot-dip processes
Zn and Zn–5Al	Roofing, culverts, housing, appliances, auto body panels and components, nails, guy wire, rope, utility wire and fencing
Zn–Fe	Auto body panels and structural components
Zn–Ni and Zn–Co	Auto body panels and structural components, housing, appliances and fasteners
Zn–55Al	Roofing, siding, ductwork, culverts, mufflers, tailpipes, heat shields, ovens, toasters, chimneys and silo roofs
	Hot-dip batch galvanized
Structural steel for power-generating plants, petrochemical facilities, heat exchangers, cooling coils, water-treatment facilities and electrical transmission towers and poles	
Bridge structural members, culverts, corrugated steel pipe and arches	
Reinforcing steel for concrete structures	
Highway guard rails, lighting stands and sign structures	
Marine pilings and rails	
Architectural applications of structural steel, lintels, beams, columns and related building materials	

4.12 Zirconium and its Alloys

Zirconium alloys are chiefly used as the cladding (structural) metal in nuclear reactors. The alloys are also used as grid spacers, guide tubes, pressure tubes, calandria tubes and other minor components.

The low cross-section for absorption of neutrons and high-temperature (330–350°C) aqueous corrosion resistance as well as its good mechanical properties promote the use of zirconium alloys in the nuclear reactors. In the development of zirconium alloys care must be taken that the added minor elements do not posses high cross-sections for the absorption of neutrons and contribute to greater corrosion resistance and improved mechanical properties. The good corrosion resistance of the alloys in acids and bases favors the use of zirconium alloys in chemical plants.

The zirconium alloys with the ASTM specifications are given in Table 4.85. The composition of nuclear-grade alloys is given in Table 4.86. The composition of other alloys developed for nuclear applications is given in Table 4.87.

4.12.1 Corrosion of Zirconium Alloys

The environments, along with the cracking modes of zirconium and titanium, are given in Table 4.88. It is obvious from the table that zirconium alloys are susceptible to stress–corrosion cracking in a variety of environments. It is necessary to subject the weld to heat treatment in order to lower the stress in the weld. The most serious problem encountered in the nuclear applications is delayed hydride cracking in addition to stress–corrosion cracking, particularly in Zr–2.5% Nb alloy.

Zirconium alloys are also susceptible to liquid metal embrittlement in metals such as Li, Cs, Cd, Cs/Cd, Cs/Ca, Cs/Y, Cs/Zn, Ag, Hg and Ga and the cracking of the zirconium alloys are transgranular, with the exception in Ga and Cd where the intergranular mode has been observed.[105]

Table 4.85 *ASTM chemical requirements for three commercial grades of zirconium (B 551-79)*[a]

Element	Composition (%)		
	Grade 702	Grade 704	Grade 705
Zr + Hf, min	99.2	97.5	95.5
Hafnium, max	4.5	4.5	4.5
Fe + Cr	0.20 max	0.2–0.4	0.2 max
Hydrogen, max	0.005	0.005	0.005
Nitrogen, max	0.025	0.025	0.025
Carbon, max	0.05	0.05	0.05
Niobium			2.0–3.0
Oxygen	0.16	0.18	0.18
Tin		1.0–2.0	

[a]Reprinted with permission from reference 103; copyright ASTM

Table 4.86 *Compositional ranges of nuclear grade standard alloys*[104]

ASTM reference name	R 60802 Zircaloy-2	R 60804 Zircaloy-4	R 60901 Zr-Nb	R 60904 Zr-Nb
		Alloying elements (mass %)		
Sn	1.2–1.7	1.2–1.7		
Fe	0.07–0.2	0.18–0.24		
Cr	0.05–0.15	0.070–0.13		
Ni	0.03–0.08			
Nb			2.4–2.8	2.5–2.8
O	Usually 0.1–0.14	Usually 0.1–0.14	0.09–0.13	To be specified
		Impurities (ppm)		
Al	75	75	75	75
B	0.5	0.5	0.5	0.5
Cd	0.5	0.5	0.5	0.5
C	270	270	270	150
Cr	Alloy el	Alloy el	200	100
Co	20	20	20	20
Cu	50	50	50	50
Hf	100	100	100	50
H	25	25	25	25
Fe	Alloy el	Alloy el	1500	650
Mg	20	20	20	20
Mn	50	50	50	50
Mo	50	50	50	50
Ni	Alloy el	70	70	35
N	80	80	80	65
Pb				50
Si	120	120	120	120
Sn	Alloy el	Alloy el	50	100
Ta				100
Ti	50	50	50	50
U	3.5	3.5	3.5	3.5
V				50
W	100	100	100	100

4.12.2 Corrosion of Zirconium Alloys in Acids and Alkalis

Some corrosion rate data for zirconium in HCl and mixtures of $FeCl_3$ and HCl are given in Table 4.89. The corrosion rates of zirconium in sulfuric acid, phosphoric acid, hydrochloric acid and nitric acid of various concentrations at various temperatures have been determined and the data can be summarized as follows in Table 4.90. Corrosion rates in alkali are given in Table 4.91.

4.13 Tin and Tin Plate

Tin is an extensively used metal, either alone or in combination with other metals such as copper (bronze) or carbon steel (mild steel) giving rise to tin plate. Tin is attacked when

Table 4.87 *Experimental and commercial alloys for nuclear applications*[a]

Alloy	Typical weight %								Commercial application
	Sn	Nb	Fe	Cr	Ni	V	O	Others	
Zr-1	2.5								
Zr-2	1.5		0.13	0.10	0.05		0.11		BWR clad and structures
Zr-3	0.25		0.25						
Zr-4	1.5		0.21	0.10			0.13		PWR clad and structures
ZIRLO	1.0	1.0	0.1						
NSF 0.5 (GE)	1.0	1.0	0.5				0.10		
NSF 0.2	1.0	1.0	0.20				0.10		
Valloy			0.15	1.2					
Ozhennite-0.5	0.2	0.1	0.1		0.1				
Scanuk	0.06	0.6	0.04	0.32				0.22 Mo	
Zr-3B	0.5		0.4						
Zr-3C	0.5		0.2		0.2				
Zr-3A	0.25		0.25						
Excel	3.5	0.8						0.8 Mo	
E110		1							VVER
(Zr1 Nb)									Clad
Zr2.5 Nb		2.5					0.12		CANDU
E635	1.2	1	0.4						Pressure tubes
E125		2.5							

exposed to moist air at high temperature, resulting in the formation of oxide. Tin exhibits two oxidation states as in the oxides stannous (SnO) and stannic oxide (SnO_2). These are amphoteric in behavior.

Tin is readily attacked by sulfur dioxide and hydrogen sulfide, which may be present in the atmosphere. The products of atmospheric attack are oxides and sulfides. Some data on the atmospheric corrosion of tin are as follows[107]:

Atmosphere	Corrosion rate (μm/yr)
Rural	0.05
Industrial	0.125–0.175
Marine	0.175–0.275

4.13.1 Aqueous Corrosion

Aqueous corrosion of tin results in production of oxides of tin. The oxides and hydroxides of tin are stable in the pH range 3–10. The amphoteric nature of the oxides results in attack by mineral acids to produce stannous or stannic salts, stannites and stannates in basic solutions. While borates and bicarbonate render stability to the oxide

Table 4.88 *Environments causing cracking of titanium and zirconium alloys*[a,b]

Environment	Temperature[c] (°C)	SCC in Ti	SCC in Zr alloys	
			Yes/No	Cracking mode[d]
Hydrogen				
Internal hydrogen	RT-350	Yes	Yes	TG
Hydrogen gas	RT-150	Yes	Yes	TG
Organic liquids				
Methanol and solutions with I_2, Br_2, NaC1, HC1	RT	Yes	Yes	IG initiation
Higher alcohols with similar additives	RT	Yes	Yes	TG propagation
Iodine solutions in other organic liquids	300-800	Yes	NT	
Chlorinated hydrocarbons (e.g., $CC1_4$, $CHC1_3$)				
Other halogenated hydrocarbons (e.g., freons, CH_3I)	RT	Yes	Yes	TG (DCB)
Ethylene glycol	RT	Yes	Only in I_2 solution	IG
Aqueous solutions				
HC1	25-150	Yes	Yes	IG
NaC1, KC1, etc.	25-290	Yes	Yes (needs polarization)	Mixed IG/TG
$FeC1_3$, $CuC1_2$	RT	Yes	Yes	
Hot fused halides				
NaC1, KC1, CsC1, etc.	300-450	Yes	Yes	Mixed IG/TG
$KNO_3/NaNO_3 + KBr/Cs1$	300-400	Yes	Yes	Mixed IG/Tg
$KNO_3/NaNO_3 + NaC1$	300-400	Yes	Yes	Mixed IT/TG
Halogen and halogen acid vapors	RT	NT	Yes	TG (DCB)
	200-500	Yes	Yes	Mixed IT/TG
Metals (solid, liquid, vapor)				
Hg, Cd, Cs, Zr	RT-400	Yes	Yes	TG
Mg	700	NT	Yes	IG
Oxides and oxyacids of N_2				
N_2O_4	RT	Yes	NT	
Nitric acid	RT-100	Yes	Yes	T
Sulfuric acid	RT	Yes	NT	

[a]A more detailed description of the various environments causing cracking is given in reference 10
[b]Reprinted with permission from reference 6; copyright 1990 Elsevier Science; for references see original table in reference 103
[c]RT = Room temperature
[d]DCB indicate fractures only in precracked double cantilever beam specimens

Table 4.89 *Corrosion data for zirconium and its alloys in HC1*[a]

Solution	Temperature (°C)	Duration of test (days)	Average corrosion rate (mils/yr)[b]		
			702	704	705
32% HC1	30	91	0.03	0.08	0.03
32% HC1	82	91	0.03	0.2	0.1
10% HC1, 100 ppm $FeC1_3$	30	91	0.9	1.6	0.7
32% HC1, 5 ppm $FeC1_3$	30	91	0.1	1.5	0.1
32% HC1, 50 ppm $FeC1_3$	30	91	c	c	c
32% HC1, 100 ppm $FeC1_3$	30	91	c	c	c

[a]Severe pitting and stress cracking observed
[b]1.0 mil/yr = 0.025 mm/yr

Table 4.90 *Corrosion rates in acids*[103]

Acid (wt %)	Temperature (°C)	Corrosion rate (mpy)
20–80 H_2SO_4	25–260	0–5.0 (region 1) 5–20.0 (region 2) 20–200 (region 3) >200 (region 4)
40–90% H_3PO_4	60–180	0–5 (region 1) 5–20 (region 2) 20–200 (region 3) >200 (region 4)
10–36% HCl	120–220	0–5 (region 1) 5–20 (region 2) 20–200 (region 3) >200 (region 4)
10–70% HNO_3	20–180	0–5

Table 4.91 *Corrosion rates of zirconium in alkaline solutions*[103]

Solution	Temperature (°C)	Corrosion rate (mpy)
0.6% NaOH + $NaClO_3$ + NH_3	129	0.05
5–10% NaOH	21	0.2
20% NaOH	60	13
50–73% NaOH	188	28
73% anhydrous NaOH	240–550	110
28% NH_4OH	20–100	<0.03
13% KOH + 13% KCl	29	0.09

film, chloride ion destabilizes the oxide film. Complexing agents such as citric acid, tartaric acid and malic acid destabilize the oxide film by forming soluble tin complexes in the presence of the aforementioned ligands. Lead–tin solders are attacked by soft water and lead is preferentially attacked. Detailed work on the galvanic corrosion of lead/tin solders[108] has shown that lead levels in excess of permissible values (>15 ppb) are released into drinking water supplies. Addition of inhibitors such as sodium silicate and phosphates reduced the amounts of lead released into the drinking water to within permissible levels.

Lead–tin solders have been replaced by high-tin solders such as Sn–Ag, Sn–Sb and Sn–Sb–Ag in domestic heating and water distribution systems. High-tin alloys are used in food packaging, and failure of a can through dissolution of solder is rare. Inhibitors used in automotive antifreeze have been found to attack the solder side seams in tin plate containers.[109]

4.13.2 Corrosion of Tin Plate

Tin plate consists of mild, low-carbon steel containing controlled amounts of copper, phosphorous and sulfur, and coated with tin. During the corrosion of tin the anodic and cathodic reactions are the oxidation of tin to stannous ion and the two electrons released in the reaction are taken up by oxygen and producing the hydroxyl ions. In the case of tin plate the steel with low hydrogen overvoltage accelerates the tin attack by facilitating the hydrogen formation reaction.

Atmospheric attack of tin plate in humid atmospheres results in the corrosion and production of rust. This occurs in neutral or near-neutral conditions. The presence of contaminants, which change the pH, might result in the opposite process, namely detinning.

Aqueous external corrosion results in rusting, pitting and ultimately perforation. Under certain conditions detinning may also occur. Perforation is of very serious concern because of loss of product, along with the more serious problem of contamination due to ingress of foreign material such as microbes in food cans.

The corroding agents in the cans are totally different and depend upon the material in the cans. The materials inside the cans can be foods, beverages, domestic cleaners, paints, industrial products, pharmaceuticals, aerosols and a host of others. This being the case the products in the can present many corrosion scenarios.

In food and beverage cans made of tin plate the factors that are to be considered are the pH range and the stability of oxide, the high hydrogen overvoltage and the formation and stability of complexes formed by tin with ligands such as citric acid, malic acid or tartaric acid as may be the case. The case in which tin forms complexes with the organic acids present in fruit juices results in decrease in the concentration of stannous ion in solution, which in turn accelerates tin dissolution and depresses the potential of tin. The potential may become negative enough to cause a reversal of the tin–iron couple, thus making tin active (negative).

For the formation of tin complexes it is necessary to have stannous ions in solution, and for this to happen the electrons released by the oxidation of tin may be consumed by hydrogen evolution at the iron centers in the pores of the tin plate. As tin dissolves more of the steel surface is available for the hydrogen evolution reaction and

the cycle repeats, leading to detinning. Thus, as the hydrogen gas builds up the can begins to swell. This is known as 'hydrogen swell'.

Some of the factors that contribute to the internal corrosion of tin plate cans are: (i) the ratio and concentrations of citric to malic acids which in turn depend upon the strain of fruit, the extent of ripeness; (ii) nitrate present in the fertifizers may find its way into fruits and vegetables and the nitrate may be reduced to hydroxylamine and support the detinning process; (iii) pesticides containing dithiocarbomates may find their way in and attack iron; (iv) phosphates, citrates and the low pH of cola-type beverage may dissolve iron; (iv) meats, fish and peas contain sulfur-bonded protein molecules, which can decompose to H_2S and attack the tin and iron, forming the respective sulfides. Hydrogen sulfide can react with Sn and Fe, yielding FeS and SnS, which are not poisonous, but impart some color to the canned product.

4.14 Refractories and Ceramics[110]

Corrosion of refractories and ceramics involves consideration of: (i) acid–base effects involved in the corrosion of refractory; (ii) verification of the thermal stability of each constituent; (iii) calculation of the free enthalpy of all possible reactions that might occur in the corrosion of the refractory or ceramic compound. Kinetic data are also useful in understanding the corrosion and selection of the refractory compound for a specific application.

One of the criteria in assessing the corrosion resistance of the refractory compounds is the temperature range above which the refractory compound corrodes to an unacceptable level. The durability or stability of the refractory varies in the context of particular application. The mode of degradation of the refractory can also vary, e.g., corrosion dissolution or penetration and structural spalling or both. Some data on temperature limits for slagging resistance and hot gas corrosion resistance of some refractory compounds are given in Table 4.92. The data on temperatures given in the column headed 'Slag and fluxes' represent a reaction between the slag, which can be basic ($CaO/SiO_2 > 2$) or acidic ($CaO/SiO_2 < 2$) and the refractory of a given texture. The data in the 'hot gases' column represent a reaction between the refractory and a gas with or without dusts, either oxidizing (oxygen, air) or reducing (CO, H_2). The refractories given in the table range from basic magnesia to acidic silica, including neutral ZrO_2.

Some salient features of the refractories are given below:

Basic refractories	Most commonly used are magnesia and dolomite in steel-making, copper–nickel in cement industry; magnesium bricks in combination with chrome and alumina are used; magnesia bricks made out of fused magnesia are most corrosion resistant refractories; magnesia–carbon-bonded bricks have high slag resistance
High-alumina refractories	Consist of 65% Al_2O_3 (99.3% purity) and mullite $(Al_2O_3)(SiO_2)_2$; electrofused alumina and mullite product has high corrosion resistance; increase in alumina content: (i) improves corrosion dissolution resistance, (ii) decrease slag penetration resistance as well as structural spalling resistance; improved performance due to addition of chrome or silicon carbide or carbon

Table 4.92 *A guideline for corrosion resistance based on the criterion of maximum temperature*

		Limit not reached for 'normal' durability			
		Slags and fluxes[a]		Hot gases	
		Temperature limits (°C)			
	Type of refractory	Basic	Acid	Oxidized	Reduced
1	Magnesia (M)	1700	NR	>2000	1700
	Doloma (D)	1700	NR	>1800	1700
	(M), (D) or (M + D) + Graphite	1800	1700	800	1700
	Magnesia–chrome (MK)	1700	1600	1800	NR
2	High-alumina (A)	1600	1600	1900	1900
	(A) + graphite	1700	1700	600	1700
3	Clays + (A) (65% Al_2O_3)	1300	1300	1450	NR
	Clays + (A) + C	1550	1550	600	1700
4	Super-duty fireclays (F)	1200	1250	1400	NR
	Medium–low-duty (F)	NR	1100	1200	NR
5	High silica	NR	1400	1750	1600
6	Zircon–zirconia	1450–1600	1500–1700	>2000	1800
	Silicon carbide	<1400	1500	1200	1600

NR = not recommended

High-alumina refractories with clay	45–65% alumina along with andalusite or mullite mixed with fireclays and binders; corrosion resistance varies with mineral composition.
Fireclay refractories	Super-duty 45–65%; medium-duty (30–40% alumina; low-duty (20–30%) alumina contain silica and used in kilns and furnaces since they are of low cost; limited to 1200–1250°C.
Silica refractories	Contain >93% SiO_2, <3.5% CaO, <2% Al_2O_3, <1.-5% Fe_2O_3; have high corrosion resistance to acidic slags: poor resistance to high temperatures and thermal shocks
Zircon–zirconia, silicon carbide	$ZrSiO_4$, zircon sand bricks have good wear resistance and poor wettability by molten metals up to 1450°C; zirconia bricks are stabilized by CaO or MgO in solution to avoid cracking upon heating; properly made zirconia bricks have very high corrosion resistance and are not wetted, even by steels with different oxygen content; silicon carbide refractories are used in reducing conditions; advantages of silicon carbide refractories over oxide refractories are: (i) high thermal conductivity, (ii) superior spalling and abrasion resistance, (iii) high corrosion resistance against nonoxidizing slag

4.14.1 Corrosion of Structural Ceramics

The purity and texture of structural ceramics are better than the refractories since they are produced from purified constituents rather than from naturally occurring mineral

Table 4.93 *Corrosion resistance of structural ceramics to fused salts, alkalis and low-melting oxides*

Ceramics at purity (>99.5%)	Fused salts – alkalies – low-temperatures oxides[a]							
	NaC1	NaCl + KCl	KNO_3	Na_2CO_3	Na_2SO_4	KOH	Na_2O	V_2O_5
Alumina	A1000	A800	A400	A900	A1000	B500	B500	C800
Zirconia (stabilized)		C800		C900	A1000	B500	C500	C800
SiC (reactively bonded)	B900	C800	A400	C900	C1000 (air)	C500 (air)	C600	C800
Si_3N_4 (RBSN)			A400	C750 (air)	C1000 (air)	C500	C500	C800
Si_3N_4 (HPSN)	A800	B900		C900 (air)	B1000 (air)	C500	B500	C800
BN (HP)			A400	C900 (air)	C1000 (air)	C500	C500	

[a]A, resistant to attack up to temperatures indicated (°C); B, some reaction at temperature indicated; C, appreciable attack at temperature indicated

components. The porosity is <2% for structural ceramics compared with 12% or more for refractories, sometimes up to 20% and 50–70% for insulating refractories. The porosity depends upon the grain size distribution used, along with the sintering conditions used in the synthesis of the material. The usual grain size used in production of structural ceramics is in the range 0.1–10 μm. The aim is to maximize the mechanical properties and corrosion resistance of the ceramics while in the case of refractories the objective is to maximize shock resistance, volumetric change and corrosion resistance.

The corrosion resistance of structural ceramics consisting of oxides and non-oxides is presented in Table 4.93. The data presented in the table are of limited generality. The code letters A, B and C must be used for comparison of the materials. It is obvious from the data that both oxide-based and non-oxide-based ceramic materials are attacked at low and intermediate temperatures. The relatively poor corrosion resistance of SiC and Si_3N_4 may be due to the formation of SiO_2 layers on the ceramic components. More detailed information on the corrosion resistance of structural ceramic materials may be found in the literature.[111]

Oxidation at high temperatures in air and oxygen and gaseous corrosion by gases such as carbon monoxide, hydrogen, hydrogen sulfide and steam bears some similarities to oxidation of metals with some differences: (i) ceramics have much greater oxidation resistance than metals; (ii) because of the higher temperatures, the corrosion products can be gases, liquids or solids, leading to weight loss or gain resulting in difficulties interpreting the data; and (iii) the relatively less homogeneous texture of ceramics does not permit the unambiguous characterization of the controlling mechanism of oxidation without knowledge of the processing characteristics and the intrinsic nature of the material.

Gaseous corrosion in combustion applications involving condensed phased deposits is important and sodium sulfate and vanadate deposits are most corrosive. These deposits are particularly injurious to non-oxide ceramic materials. The data on corrosion resistance of ceramic materials to hot gaseous environments are presented in Table 4.94. It is clear from the data that non-oxide ceramics show lesser corrosion resistance than oxide-based ceramics.

Table 4.94 *Corrosion resistance of structural ceramics to hot gases*[a]

Ceramics at purity (>99.5%)	Air	Steam	CO	H_2	H_2S	F(g)
Alumina	A1700	A1700	A1700	A1700		
Zirconia (stabilized)	A2400	C1800				
SiC (RB)	A1200	B300	A >1000	A >1000	A1000	A >800
Si_3N_4 (RBSN)	B1200	A220	A >800		A1000	
Si_3N_4 (HPSN)	B1250	A250	A >900	A >800	A1000	A >1000
BN (HP)	C1200	C250	A2000	A >800		

[a]A, B, C as in Table 4.93

Some important features of structural ceramics with respect to corrosion are given below:

Alumina	Versatile ceramic resistant to acids, alkalis, molten metals, molten salts, oxidizing and reducing gases at high temperatures; widely used in high-temperature laboratory and pilot-scale operations
Zirconia	Generally used in conjunction with CaO, MgO or Y_2O_3 as stabilizers; vulnerable to acid and alkali attack
Thoria	Highly stable with a melting point of about 3300°C; used in nuclear industry
Silicon carbide	Resistant to acids, including HF and molten metals; not resistant to alkalis, molten sodium sulfate; SiC produced by sintering is prone to oxidation and corrosion while single phase SiC is resistant; oxidation results in formation of SiO_2; SiC is more sensitive to hot corrosion than Si_3N_4
Silicon nitride	Oxidation produces SiO_2 and has been studied in detail;[112] exhibits high corrosion resistance at 1400°C in presence of 10^{-5}% Na, V, 0.5% S, but corrodes at 900°C in presence 0.005% Na, 0.005% V and 3% S; resistant to alkali chloride melts and alkali solutions; attacked by alkali metal sulfates and vanadium
Boron nitride	Attacked by acids and not by alkalis; oxidizes at ~700°C; can be used in reducing conditions; resistant to wetting by metals and alloys

4.15 Polymeric Materials

The best known polymeric materials are natural rubber and synthetic rubber. These materials have low modulus of elasticity. The flexibility of these materials enables their application in tubing, belting and automotive tires as encountered in everyday usage. Resistance to chemicals, abrasive attack and insulating property can be advantageous in corrosion control applications.

Naturally occurring rubber consists of a long-chain polymer with isoprene as the basic building unit. The rubber has high elasticity and a temperature limit of 160°F. Vulcanization consists of addition of elemental sulfur to rubber, followed by heating. The

resulting product becomes hard. The semi-hard and hard products are used in tires and tank liners. The general trend is increase in corrosion resistance with increase in hardness. The modulus of elasticity is in the range of 500–500 000 psi for soft and hard rubber, respectively.

Synthetic rubbers of many types are available in the market. Neoprene and nitrile rubber have resistance to oils and gasoline and are used as gasoline hoses. Neoprene–lined vessels are used for storing strong sodium hydroxide solutions. The impermeability of butyl rubber to gases has been advantageously used in innertubes and process equipment such as seals for floating-top storage tanks. Butyl rubber is resistant to oxidizing agents such as dilute nitric acid.

Compounding rubbers results in products of different hardness and mechanical properties, as for example tensile strength range of 900–4500 psi and elongation in the range of 0–1000 %. Soft rubbers can be used for applications such as in erosion conditions. Elastomers are also classified as semirigid or nonrigid plastics with modulus of 10 000–100 000 psi for semirigid and $<10\,000$ psi for the nonrigid case. Most of the common elastomers tend to be cross-linked and thermosetting. Rigid plastics have elastic modulus of $>100\,000$ psi.

Some common elastomers with salient features are as follows:[113]

Chlorosulfonated, polyethylene (Hypalon)	Close resemblance to neoprene with greater resistance to heat, ozone and some chemicals
Ethylene propylene (Nordel)	Similar to butyl rubber; good resistance to ozone, heat, water, and sunlight
Epichlorhydrin (Hydrin)	Resistance to swelling in fuels and oils, ozone, good heat-aging properties
Fluoroelastomers (Viton)	Good resistance to many corrosives and hydrocarbons, sunlight, ozone and heat-aging, useful at high temperatures
Urethane (Adiprene)	Good tensile strength, wear resistance, resistance to oxidation, oils and ozone

Physical properties such as adhesion to metals tear resistance, abrasion resistance, resistance to diffusion of gas as well as resistance to dilute and concentrated acids, aliphatic and aromatic hydrocarbons, ketones, oil and gasoline, water absorption, oxidation, ozone, sunlight, heat aging, low temperature and flame of the common elastomers are documented in the literature.[114] Rating of elastomers with respect to resistance to the factors cited above are in terms of outstanding, excellent, very good, good, fair and poor.

Plastics production and utilization in terms of various forms such as pumps, billiard balls, valves, pipes, fans, nose cones, airplane canopies, hosiery, cabinets, pot handles, heat valves and other implants make one to realize the role played by them in everyday life. Plastics are produced by casting, molding, and extrusion and calendaring; solid parts, lining, coatings, foams, fibers and films are also readily produced and available.

The definition of plastics according to the American Society of Testing Materials is: ‘A plastic is a material that contains as an essential ingredient an organic substance of large

molecular weight, is solid in its finished state, and at some stage in its manufacture or in its processing into finished articles can be shaped by flow'.

Plastics are weaker, softer, more resistant to chloride and HCl; less resistant to HNO_3 and organic solvents compared with metals and their alloys. The two types of plastics are: (i) thermoplastics; and (ii) thermosetters. The main features of the two types are:

Thermoplastics	Can be remelted and reprocessed; can be welded; soluble in some solvents; can be either amorphous or semicrystalline; contain linear-chain or branched-chain polymer; acrylics, fluoropolymers, vinyls, polystyrenes, polyphenelyneoxide, polysulfones, polypropylenes and polybutylenes are some examples of thermoplastic polymers
Thermosetters	Cannot be remelted and reprocessed; decompose on heating to high temperatures; cross-linked structure gives rise to thermosetting properties; swelling occurs in some solvents; epoxies, melamines, phenolics, polyesters and rigid urethanes are some examples of thermosetters

Some of the polymers used in corrosion control along with their trade names are:

Polyvinyl fluoride	Tedlar
Polyvinylidene difluoride	Kynar
Polyethylene	Polythene
Polypropylene	
(Poly) ethylene chlorotrifluoroethylene (ECTFE)	Halar
Polytetrafluoroethylene (PTFE)	Teflon PTEE
Polyvinyl chloride	
(Poly) ethylene tetrafluoroethylene (ETFE)	Tefzel
(Poly) Fluorinated ethylenepropylene (FEP)	Teflon FEP
Perfluoroalkoxy	Teflon PFA

Composite materials consist of a combination of two generically dissimilar materials brought together for synergy where one phase, the matrix, is continuous (thermoplastic or thermosetting), the other phase being a reinforcement which is discontinuous. Reinforcements can be particulates, fibers or cloth. A familiar example of a composite material is fiber-reinforced plastic (FRP) used in making tanks, piping, filled fluoroplymer gaskets, scrim-filled elastomers for gaskets and impoundment basin liners.

4.15.1 Application of Polymers in Corrosion Control

The polymeric materials are viscoelastic (creep) and this property is very important in corrosion applications. The temperature limit is 260°C and most of the applications are below 150°C. The tanks and piping are used below 100°C. The mechanical properties of

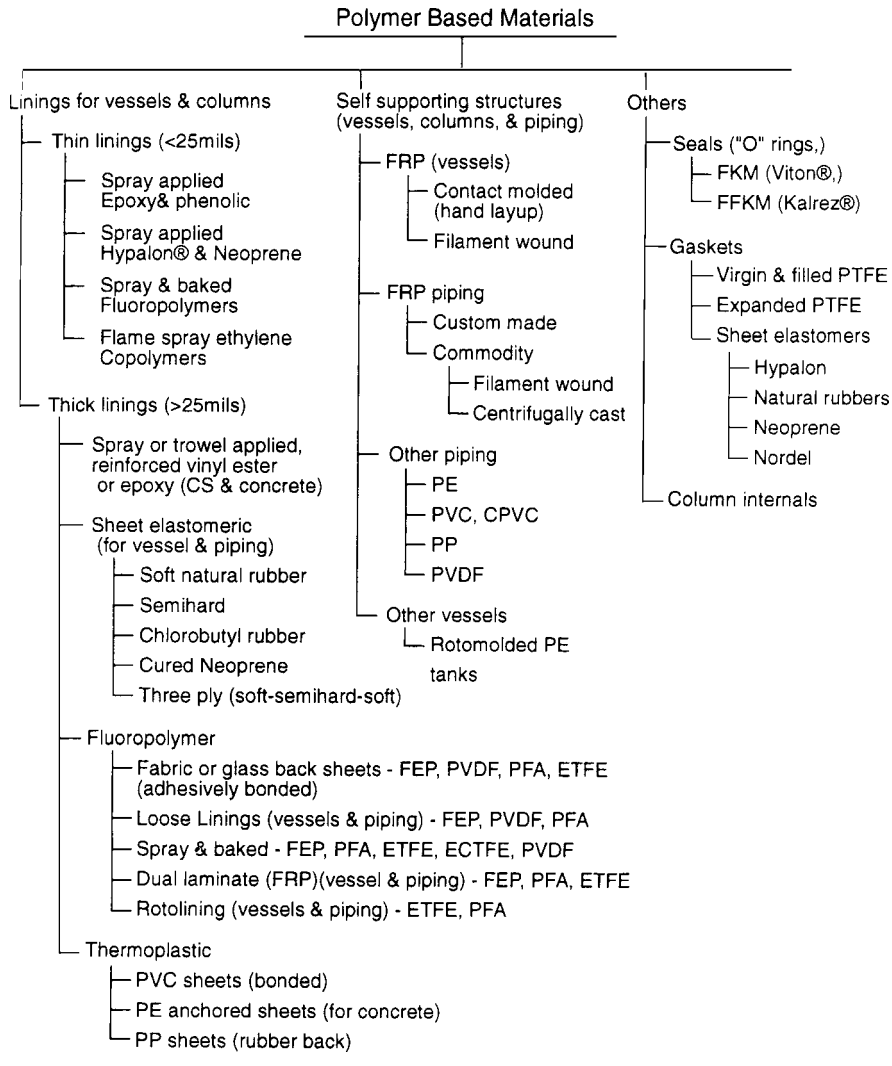

Figure 4.8 *Overview of polymer materials for corrosion control*

polymeric materials change over time since they absorb liquids and are permeable, unlike metals.

The polymeric materials are used in: (i) barrier applications; (ii) self-supporting structures (tanks, piping, valves and pumps); (ii) column internals, seals, gaskets, adhesives and caulkings. An overview of polymeric materials used in corrosion control applications is given in Figure 4.8.

The American Society for Testing and Materials (ASTM) provides standards, compatibility testing, and tests for mechanical properties, recommended practices and procedures as well as codes for polymeric materials. The various industry codes and standards are summarized in Table 4.95.

Table 4.95 *Industry codes and standards*

	Product
ASTM D2310	Standard classification of machine-made reinforced thermosetting resin pipe
ASTM D2517	Standard specification for reinforced thermosetting (epoxy) resin pipe
ASTM D2996	Standard specification for filament wound reinforced thermosetting pipe[a]
ASTM D2997	Standard specification for centrifugally cast reinforced thermosetting pipe
ASTM D4024	Standard specification for reinforced thermosetting resin flanges
ASTM D3299	Standard specification for filament-wound glass-fiber-reinforced thermoset resin chemical tanks
ASTM D4097	Standard specification for contact-molded FRP chemical-resistant tanks
ASTM F1545	Standard specification for PTFE; PFA; FEP- and ETFE-lined piping
ASTM F492	Standard specification for PE and polypropylene (PP) plastic-lined ferrous metal pipe and fittings
ASTM D1784	Rigid poly(vinyl chloride) (PVC) compounds and chlorinated poly(vinyl chloride) (CPVC) compounds
ASTM D1785	Standard specification for poly(vinyl chloride) (PVC) plastic pipe, schedules 40, 80 and 120
ASTM D3350	Standard specification for polyethylene pipe and fitting materials
ASTM D1248	Polyethylene molding and extrusion material
ASTM D4020	Ultra-high-molecular-weight polyethylene material
ASTM F1123	Nonmetallic (rubber) expansion joints
ISO 3994	Chemical transfer hose
ASTM D2564	Solvent cements for PVC (CPVC) joints
ASTM D1998	Polyethylene upright storage tanks
ASTM F118	Definition of Gasket terms
ASTM F104	Nonmetallic (rubber) expansion joints
ASTM F104	Nonmetallic gasket materials
ASTM D1330	Standard specification for rubber sheet gaskets
	Compatibility testing
ASTM D543	Test methods for determining chemical resistance of plastics
ASTM D471	Effects of liquids on rubbers, test method
ASTM C868	Test method for chemical resistance of protective linings
ASTM C581	Test method for determining chemical resistance of fiberglass-reinforced thermosetting resin
ASTM C3491	Chemical resistance test for rubber linings by Atlas blind flange test
ISO 175	Determination of effects of liquid chemicals on plastics
ISO 4599	Determination of environmental stress cracking (ESC) by the bent strip method
ISO 4600	Determination of environmental stress cracking (ESC) by the ball or pin impression method
ISO 6252	Determination of environmental stress cracking (ESC) by the constant tensile test method
ISO 8308	Liquid transmission and permeation through hose and tube
ASTM F363	Corrosion testing for gaskets
ASTM F146	Fluid resistance of gasket materials
ASTM D3615	Chemical resistance of thermoset-molded compounds used in the manufacture of molded fittings
ASTM D3681	Chemical resistance of reinforced thermosetting resin pipe in a deflected condition
(Not Standardized)	Roberts cell blind flange test for linings exposed to high temperatures and pressures

(*contd.*)

Table 4.95 (*contd.*)

Testing for mechanical properties	
ASTM D638	Standard testing for tensile properties of plastics
ASTM D412	Standard testing for tensile properties of rubbers
ASTM D1415	Test method for indentation hardness of rubbers, international hardness
ASTM D2240	Test for Durometer hardness of rubbers
ASTM D2538	Indentation hardness by Barcol hardness tester for rigid plastics
ASTM F38	Creep relaxation of gasket materials
ASTM D395	Compression set of rubbers at ambient and elevated temperatures
ASTM F152	Tension testing of gasket materials
ASTM F36	Short-term compressibility and sealability of gasket materials
ASTM F37	Sealability of gasket material
ASTM F586	Determination of Y and M values of gaskets
ASTM D2290	Apparent tensile strength of tubular (pipe) products by the split disk method
ASTM D2412	External loading characteristics of plastic pipe by parallel plate loading
ASTM D695	Compressive properties of plastics
ASTM D429	Adhesion of rubbers to metallic substrates (Procedure E1)
ASTM D1781	Climbing drum peel test
ASTM D903	Peel strength of adhesives on metals
ASTM D790	Flexural properties of reinforced and unreinforced plastics
ASTM D2584	Ignition loss of cured reinforced resin
ASTM D4541	Method of pull-off strength of coatings using portable tester
ASTM D4060	Test method for abrasion resistance of organic coatings
Recommended practices and procedures	
SSPC SP-5	Steel Structure Paint Council white metal blast surface preparation
SPI FD118	Proposed test method for pinhole detection by high-voltage spark testing by DC
MTI Project 84	Spark testing practices for linings
NACE RPO 188	Tinker Rasor wet sponge testing for thin linings
ASTM D4787	Practice for continuity testing for linings on concrete
ASTM D4417	Method for measuring surface profile of steel surfaces for coating
ASTM D4258	Cleaning of concrete
ASTM D3486	Installation of vulcanizable rubber tank linings
Codes	
RTP-1	Reinforced Thermoset Plastic Corrosion Resistant Equipment, ASME, NY
Section X	ASME Boiler and Pressure Vessel Code (for fiber-reinforced plastic pressure vessels)
ASME B31.3	Chemical Process, Petroleum Refinery Piping Code

[a]There is no industry standard for contact-molded FRP piping

References

1. K. Horikawa, S. Takiguchi, Y. Ishizu, M. Kanazashi and Boshoku Gijitu, *Corr. Eng.*, **16**, 153 (1967).
2. Rikujo Tekkotsu Kozobutsu Boshoku Kenkyu Kai, Boshoku Gijutu, *Corr. Eng.*, **22**, 106 (1973).
3. *Task Force on the Calibration of Atmospheric Corrosivity*, ASTM STP 435, ASTM, Philadelphia, PA, 1968, p. 360.

4. I. Matsushima, *Uhlig's Corrosion Handbook*, R.W. Revie (ed.), John Wiley & Sons, Inc., 2000, p. 515.
5. I. Matsushima, *Corrosion and Protection*, The Society of Materials Science, Japan, Vol. 19, 1980, p. 94.
6. K. Masamura and I. Matsushima, *23rd Annual Symposium on Corrosion and Protection*, Japan Society of Corrosion Engineering, Tokyo, Nov. 1978, p. 104.
7. I. Matsushima, Dr. Eng. Thesis, *A Study on Localized Corrosion of Steel*, University of Tokyo, 1982.
8. S.C. Dexter, *Metals Handbook*, 9th edn, American Society of Metals, Metals Park, OH, Vol. 1, 1978, p. 893.
9. S.C. Dexter and C.H. Culberson, *Mater. Performance*, **19**(9), 16 (1980).
10. C.R. Southwell and A.L. Alexander, *Mater. Prot.*, **9**(1), 179, 1970.
11. F.L. Laque, *Corrosion Handbook*, H.H. Uhlig (ed.), John Wiley & Sons, Inc., NY, 1948, p. 383.
12. ''Deterioration of Structures in Sea water'', *18th Report of the Committee of the Institution of Civil Engineers*, London, 1938.
13. W. Stum and J.J. Morgan, *Aquatic Chemistry*, 2nd edn, Wiley-Interscience, Toronto, Ontario, 1981.
14. J.E. Zajic, *Microbiological Biogeochemistry*, Elsevier, NY, 1969.
15. G.H. Booth, A.W. Copper and P.M. Cooper, *Br. Corr. J.*, **2**, 114 (1967).
16. C.L. Durr and J.A. Beavers, *Corrosion 1998*, Paper 667, NACE International, 1998.
17. J.D. Palmer, *Mat. Perf.*, **13**(1), 41–46.
18. R.A. King, TRRL Supplementary Report 316, TRRL, Crowthorne, 1977.
19. R.G. Worthingham, T.R. Jack and V. Ward, *Biologically Induced Corrosion*, NACE, 1986, p. 335.
20. R.A. King and J.D.A. Miller, *Nature*, **233**, 491–492 (1972).
21. I. Matsushima, Chijin Shokan, Tokyo, Japan, 1995, p. 21.
22. A.G. Larkin, Metallurgia, April 1966, p. 165.
23. M.A. Streicher, *Corrosion*, **29**, 337 (1993).
24. M.A. Streicher, *Uhlig's Corrosion Handbook*, R.W. Revie (ed.), John Wiley & Sons, 2000.
25. J.E. Truman, U.K, *Corrosion 1987*, Brighton, UK, October 26–28, 1987, Institution of Corrosion Science and Technology, Birmingham, UK, 1988, pp. 111–129.
26. *Allegheny Ludlum Technical Data Blue Sheet Martensitic Stainless Steel Types, 410, 420, 425 Mod and 440A*, Allegheny Ludlum Corporation, 1998.
27. E.H. Hollingsworth, H.Y. Hunsicker and P.A. Schweitzer (eds.), *Corrosion and Corrosion Protection Handbook*, Marcel Dekker, NY, 1983, pp. 111–145.
28. R.B. Mears, *Corrosion Handbook*, H.H. Uhlig (ed.), John Wiley & Sons, Inc., 1976, pp. 39–56.
29. R.B. Mears and J.R. Akers, *Proc. Amer. Soc. Brewing Chem.*, St Paul, Minnesota, Annual Meeting, 1942.
30. D.J. De Renzo, *Corrosion Resistant Materials Handbook*, Noyes Data Corporation, Park Ridge, New Jersey, USA, 1985, p. 621.
31. E.H. Hollingsworth and H.Y. Hunsicker, *Metals Handbook*, 9th edn, Vol. 13, Corrosion, ASM International, Metals Park, OH, 1987, pp. 583–609.
32. H. Reboul and R. Canon, Corrosion galvanique de l'aluminium, mesures de protection, *Revue de l'Aluminium*, **1922**, 403–406 (1984).
33. P.M. Aziz, *Corrosion*, **12**, 35 (1956).
34. M.C. Reboul, T.J. Warner, H. Maye and B. Baroux, *Materials Science Forum*, Transtech Publications, Switzerland, Vols. 217–222, 1996, pp. 1553–1558.
35. S.C. Dexter and J. Ocean, *Sci. Eng.*, **8**(1), 109 (1981).
36. I.L. Rosenfeld, *Localized Corrosion*, NACE International, Houston, TX, 1974, pp. 386–389 (localized corrosion).
37. J.E. Hatch, *Aluminum, Properties and Physical Metallurgy*, ASTM International, Metals Park, OH, 1984, pp. 248–319, 263, 307.
38. S.C. Dexter, *Localized Corrosion of Metals Handbook*, ASM International, Corrosion, Vol. 13, 1987, pp. 103–122.

39. J.J. Elpick, *Microbial Corrosion in Aircraft Fuel Systems in Microbial Aspects of Metallurgy*, J.D.A. Miller (ed.), Elsevier, NY, 1970, pp. 157–172.
40. V.A. Marichev, *Werkst Korr*, **34**, 300 (1983).
41. M.O. Spiedel, *Hydrogen in Metals*, I.M. Bernstein and A.W. Thompson (eds.), ASM International, Metals Park, OH, 1974, p. 249.
42. D.O. Sprowls and E.H. Spuhler, Greenletter, Alcoa, Avoiding SCC in High Strength Aluminum Alloy Structures, *ASM International Corrosion*, Vol. 13, Metals Park, OH, Jan. 1982.
43. L.J. Korb, Corroson in Aerospace Industry, *Metal Handbook*, 9th edn, *Corrosion*, ASM International, Vol. 13, Metals Park, OH, 1987, p. 1082.
44. D.M. Aylor and P.J. Moran, CORROSION/86, NACE International, Paper No. 202, Houston, Texas.
45. V.S. Sastri, *Corrosion Inhibitors*, John Wiley & Sons, Ltd, 1998.
46. C. Vargel, *Corrosion de l'aluminium*, Dunod, Paris, 1999, pp. 154–163.
47. H.P. Godard, *The Corrosion of Light Metals*, John Wiley & Sons, Inc., NY, 1967, pp. 46, 70–73.
48. R.E. Lobnig, R.P. Frankenthal, D.J. Siconolfi and J.D. Sinclair, *J. Electrochem. Soc.*, **140**, 1902 (1993); **141**, 2935 (1994).
49. T.E. Graedel, J.P. Franey and G.W. Kammlott, *Corrosion Science*, **23**, 1141 (1983); **27**, 639 (1987).
50. V. Kucera, D. Knotkova, J. Gullman and P. Holler, *International Congress on Metallic Corrosion*, Madras, India, Vol. 1, CERI, 1987, p. 167.
51. W.W. Kirk and H.H. Lawson (eds.), *Atmospheric Corrosion*, ASTM-STP 1239 Philadelphia, 1991.
52. M. Elboujdaini, V.S. Sastri and M. Sahoo, *American Foundrymen Society Transactions*, Chicago, 29–36, 1993, ibid: 1994.
53. H.S. Campbell, *J. Inst. Met.*, **77**, 345 (1950).
54. V.F. Lucey, *Br. Corr. J.*, **1**, 53 (1965).
55. H.S. Campbell, *Localized Corrosion*, R.W. Staehle (ed.), NACE, Houston, Texas, 1974.
56. A.M. Beccaria and J. Crousier, *Br. Corr. J.*, **26**, 215 (1991).
57. J.G.N. Thomas and A.K. Tiller, *Br. Corr. J.*, **7**, 256 (1972).
58. E. Mattson, *Br. Corr. J.*, **15**, 6 (1980).
59. H.A. Videla, *Biofouling and Biocorrosion in Industrial Water Systems*, G.G. Geesey, Z. Lewandowski and H.C. Flemming (eds.), Lewis Publishers, Boca Raton, Florida, 1994, pp. 231–241.
60. C.A.C. Sequiera, *Uhlig's Corrosion Handbook*, 2nd edn, John Wiley & Sons, Inc., NY, 2000.
61. Y. Yanish, *Proc. 2nd International Conf. on Heat Resistant Materials*, Gatlinberg, TN, Sept. 11–14, 1995, ASM, Metals Park, OH, pp. 655–656.
62. W.Z. Friend, *Corrosion of Nickel and Nickel Base Alloys*, John Wiley & Sons, NY, 1980.
63. V. Heubner, *Nickel Alloys and High Alloy Special Stainless Steels*, Krupp YDM, GmbH, P.O. Box 1820, Werdoh, Germany, 1987, 1st edn, 2nd edn.
64. G. Lai, *High Temperature Corrosion of Engineering Alloys*, ASM International, Materials Park, OH, 1990.
65. J.S. Grauman and J.J. McKetta (eds.), *Encyclopedia of Chemical Processing Design*, Marcel Dekker, NY, Vol. 58, 1998, pp. 123–147.
66. J.A. Mountford and J.S. Grauman, *Titanium for Marine Applications*, 2nd Corrosion Control Workshop, Colorado School of Mines, New Orleans, LA, February 1997.
67. M.J. Blackburn, W.H. Smyrl, J.A. Feeney and B.F. Brown (eds.), *Stress–Corrosion Cracking on High Strength Steel and in Titanium and Aluminum Alloys*, Naval Research Laboratory, Washington, DC, 1972, pp. 245–363.
68. D.J. Simbi and J. Scully, *Corr. Sci.*, **37**, 1325 (1995).
69. R.J.H. Wanhill, *Br. Corr. J.*, **10**, 69 (1975).
70. R.L. Fowler and J.A. Luzietti, *Corrosion 1980*, Paper No. 18, NACE, Houston, TX, 1980.
71. R. Boyer, G. Welsch and E.W. Collins (eds.), *Materials Properties Handbook*, Titanium Alloys, ASM, Materials Park, OH, 1994.
72. R. Murakami and W.G. Ferguson, *Fatigue Fract. Eng., Mater. Struct.*, **16**, 255 (1993).

73. P. Crook, *Mater. Perform*, **30**, 64 (1991).
74. Lead Industries Association, *Lead for Corrosion Resistant Applications – A Guide*, NY, 1974.
75. F.W. Fink and W.K. Boyd, *The Corrosion of Metals in Marine Environments*, Defence Metals Information Centre, Battelle Institute, Columbus, OH, DMIC Report 245.
76. H.H. Uhlig (ed.), *Corrosion Handbook*, John Wiley & Sons, Inc., NY, 1948.
77. I.J. Polmear, *Mater. Sci. and Technol.*, **10**, 1 (1994).
78. A. Froats, T. Kr. Aune, D. Hawke, W. Unsworth and G. Hillis, Corrosion of Magnesium and Magnesium Alloys, *Metals Handbook*, 9th edn, Vol. 13, Corrosion, ASM International, Materials Park, OH, 1987, pp. 740–754.
79. D.L. Hawke, J.E. Hillis and W. Unsworth, *Preventive Practice for Controlling the Galvanic Corrosion of Magnesium Alloys*, Technical Committee, International Magnesium Association, Mclean, VA, 1988.
80. A.I. Aspahani and W.L. Silence, Pitting Corrosion, *Corrosion*, ASM, Metals Park, OH, Vol. 13, 9th edn, 1987, p. 113.
81. W.E. Mercer and J.E. Hillis, *The Critical Contaminant Limit and Salt Water Corrosion Performance of Magnesium AE 42 Alloy*, SAE Technical Paper No. 920073, 1992.
82. O. Lunder, K. Nisancioglu and R.S. Hansen, *Corrosion of Die Cast Mg-Al Alloy*, Corrosion and Exposition, Paper No. 930 755 SAE, Detroit, MI, 26 February–2 March 1993, pp. 117–126.
83. G.L. Makar and J. Kruger, *J. Electrochem. Soc.*, **13**(2), 414 (1990).
84. C. Kirby, *Corr. Sci.*, **27**(6), 567 (1987).
85. S.C. Dexter, Localized Corrosion, *Metals Handbook*, 9th edn, Vol. 13, Corrosion, ASM International, 1987, p. 106.
86. M.O. Spiedel, *Metall. Trans A 6A*, 631 (April 1975).
87. D.K. Priest, F.H. Beck and M.G. Fontana, *ASM Trans.*, **47**, 473 (1955).
88. E. Groshart, Magnesium Part I – The Metal, *Metal Finishing*, Vol. 83, 10, October 1985.
89. M.A. Timonova, *Corrosion Cracking of Mg Alloys and Methods of Protection in Intercrystalline Corrosion and Corrosion Metals under Stress*, I.A. Levin (ed.), Translated from Russian, Consultant Bureau in New York, 1962, pp. 263–282.
90. V.A. Serdyuk and N.M. Grinberg, *Int. J. Fatigue*, **5**(2), 79 (1983).
91. *Corrosiveness of Various Atmospheric Test Sites as Measured by Specimens of Steel and Zinc*, Metal Corrosion in the Atmosphere, STP 435, ASTM, Philadelphia, PA, 1968, pp. 360–391.
92. X.G. Zhang, *Corrosion and Electrochemistry of Zinc*, Plenum, NY, 1996.
93. H. Guttman, *Effect of Atmospheric Factors on the Corrosion of Rolled Zinc*, Metal Corrosion in the Atmosphere, STP 435, ASTM, Philadelphia, PA, 1968, pp. 223–239.
94. F.H. Haynie and J.P. Upham, *Materials Protection and Performance*, **9**(8), 35–40 (1970).
95. W.H. Ailor, *Atmospheric Corrosion*, John Wiley & Sons, Inc., 1982, pp. 913–921.
96. R.J. Neville, *Automotive Corrosion by Deicing Salt*, R. Baboiam (ed.), NACE, Houston, Texas, 1981, pp. 182–218.
97. G.L. Cox, *Ind. and Eng. Chem.*, (8), 902–904 (1931).
98. M. Romanoff, *Underground Corrosion*, US National Bureau of Standards Circular 579, Washington, DC, 1957.
99. H.E. Townsend, *NACE Corrosion'91 Conference*, Cincinnati, OH, 11–15 March, 1991, Paper No. 416.
100. K.W.J. Treadway, B.L. Brown and R.N. Cox, *Corrosion of Steel in Concrete*, STP 713, ASTM, Philadelphia, PA, 1980, pp. 102–131.
101. L. Kenworthy, *J. Inst. Metals*, **69**, 67 (1943).
102. *ASTM Metals Handbook*, Vol. 5, Materials Park, OH, USA, pp. 339–348, 360–371, 349–359, 1994.
103. B.S. Frechem, J.G. Morrison and R.T. Webster, STP 728, ASTM, Philadelphia, PA, 1981, pp. 85–108.
104. IAEA-TECDOC-996 (1998), *Waterside Corrosion of Zirconium Alloys in Nuclear Power Plants*, International Atomic Energy Agency, Vienna.
105. B. Cox and Y.M. Wong, *J. Nucl. Mater.*, **245**, 34 (1997).
106. B. Cox, *J. Nucl. Mater.*, **170**, 1 (1990).

107. S.C. Britton, *Tin vs. Corrosion*, ITRI London, UK, 1975.
108. V.S. Sastri, *Water Research*, **29**, 1827 (1995).
109. H. Leidheiser, *The Corrosion of Tin, Copper and their Alloys*, John Wiley & Sons, Inc., NY, 1971.
110. M. Rigaud, *Uhlig's Corrosion Handbook*, 2nd edn, R.W. Revie (ed.), John Wiley & Sons, Ltd, 2000, p. 395.
111. R.A. McCauley, *Corrosion of Ceramics*, Marcel Dekker, NY, 1995.
112. Y.G. Gogotsi and V.A. Lavrenko, *Corrosion of High-Performance Ceramics*, Springer-Verlag, Berlin, 1992.
113. *Dupont Elastomers Notebook*, E.I. Dupont de Nemours, Wilmington, Delaware, April 1976, p. 189.
114. M.G. Fontana, *Corrosion Engineering*, McGraw-Hill, Inc., NY, 1986.

5

Corrosion Economics and Corrosion Management

Corrosion economics is important when materials for construction of plant or equipment are chosen. The corrosion costs may be significant during the lifetime of plant. Corrosion mitigation becomes important which adds to the costs of the plant operation. The other alternative is to choose corrosion-resistant materials, which may be expensive, resulting in high initial costs. It is also possible to use coatings or cathodic protection, resulting in additional costs. The economic considerations and factors such as plant life dictate the choice of materials and the corrosion prevention strategies used.

5.1 Corrosion Economics

The definitions of the terms encountered in discounted cash-flow calculations are taken from the literature.[1–3] Discounted cash flow is concerned with the analysis of the value of money as a function of time. The money available at a future date has less value at the present and should be discounted by the interest to present worth (PW). P is the notation for the present sum of money, which should be used in such a manner that it produces a future income more than other forms of investment, irrespective of whether it is used for new equipment or the corrosion mitigation process. Let F be the amount of money available in the future when an investment of P is made. The relation between P and F may be written as:

$$F = P(1 + i)^n$$

where i is the interest rate and n is the number of years. The rearrangement leads to

$$F/P = (1 + i)^n$$

Corrosion Prevention and Protection: Practical Solutions V. S. Sastri, E. Ghali and M. Elboujdaini

where *F/P* is known as the single-payment compound – amount factor. The future amount of money *F* may be discounted to the present value *P* by the reciprocal multiplication factor *P/F* known as the single-payment present-worth factor.

The annual cash flow denoted by *A* and the present value of *A* discounted by interest rate *i* is given by:

$$P = A\left[\frac{(1+i)^n - 1}{i(1+i)^n}\right]$$

The *P/A* ratio is known as the uniform-series present-worth factor. The annual cash flow may be discounted to present worth by multiplication by *P/A*. Multiplication of present value by *A/P* gives the amount of annual cash flow. The factors *P/F*, *P/A* and *A/P* for a period of 30 years at interest rates of 6, 8, 10, 12, 15 and 20% for a period of 1–30 years are given in Table 5.1. Depreciation *D* is an annual tax allowance for the

Table 5.1 *Interest factors in DCF calculations*

N	6% interest factors			10% interest factors			15% interest factors		
	P/F	*P/A*	*A/P*	*P/F*	*P/A*	*A/P*	*P/F*	*P/A*	*A/P*
1	0.9434	0.9434	1.0600	0.9091	0.9091	1.1000	0.8696	0.8696	1.1500
2	0.8900	1.8334	0.5454	0.8264	1.7355	0.5762	0.7561	1.6257	0.6151
3	0.8396	2.6730	0.3741	0.7513	2.4869	0.4021	0.6575	2.2832	0.4380
4	0.7921	3.4651	0.2886	0.6830	3.1699	0.3155	0.5718	2.8550	0.3503
5	0.7473	4.2124	0.2374	0.6209	3.7908	0.2638	0.4972	3.3522	0.2983
6	0.7050	4.9173	0.2034	0.5645	4.3553	0.2296	0.4323	3.7845	0.2642
7	0.6651	5.5824	0.1791	0.5132	4.8684	0.2054	0.3759	4.1604	0.2404
8	0.6274	6.2098	0.1610	0.4665	5.3349	0.1874	0.3269	4.4873	0.2229
9	0.5919	6.8017	0.1470	0.4241	5.7590	0.1736	0.2843	4.7716	0.2096
10	0.5584	7.3601	0.1359	0.3855	6.1446	0.1627	0.2472	5.0188	0.1993
11	0.5268	7.8869	0.1268	0.3505	6.4951	0.1540	0.2149	5.2337	0.1911
12	0.4970	8.3838	0.1193	0.3186	6.8137	0.1468	0.1869	5.4206	0.1845
13	0.4688	8.8527	0.1130	0.2897	7.1034	0.1408	0.1625	5.5831	0.1791
14	0.4423	9.2950	0.1076	0.2633	7.3667	0.1357	0.1413	5.7245	0.1747
15	0.4173	9.7122	0.1030	0.2394	7.6061	0.1315	0.1229	5.8474	0.1710
16	0.3936	10.1059	0.0990	0.2176	7.8237	0.1278	0.1069	5.9542	0.1679
17	0.3714	10.4773	0.0954	0.1978	8.0216	0.1247	0.0929	6.0472	0.1654
18	0.3503	10.8276	0.0924	0.1799	8.2014	0.1219	0.0808	6.1280	0.1632
19	0.3305	11.1581	0.0896	0.1635	8.3649	0.1195	0.0703	6.1982	0.1613
20	0.3118	11.4699	0.0872	0.1486	8.5136	0.1175	0.0611	6.2593	0.1598
21	0.2942	11.7641	0.0850	0.1351	8.6487	0.1156	0.0531	6.3125	0.1584
22	0.2775	12.0416	0.0830	0.1228	8.7715	0.1140	0.0462	6.3587	0.1573
23	0.2618	12.3034	0.0813	0.1117	8.8832	0.1126	0.0402	6.3988	0.1563
24	0.2470	12.5504	0.0797	0.1015	8.9847	0.1113	0.0349	6.4338	0.1554
25	0.2330	12.7834	0.0782	0.0923	9.0770	0.1102	0.0304	6.4641	0.1547
26	0.2198	13.0032	0.0769	0.0839	9.1609	0.1092	0.0264	6.4906	0.1541
27	0.2074	13.2105	0.0757	0.0763	9.2372	0.1083	0.0230	6.5135	0.1535
28	0.1956	13.4062	0.0746	0.0693	9.3066	0.1075	0.0200	6.5335	0.1531
29	0.1846	13.5907	0.0736	0.0630	9.3696	0.1067	0.0174	6.5509	0.1527
30	0.1741	13.7648	0.0726	0.0573	9.4269	0.1061	0.0151	6.5660	0.1528

Table 5.1 (*contd*.)

N	8% interest factors			12% interest factors			20% interest factors		
	P/F	*P/A*	*A/P*	*P/F*	*P/A*	*A/P*	*P/F*	*P/A*	*A/P*
1	0.9259	0.9259	1.0800	0.8929	0.8929	1.1200	0.8333	0.8333	1.2000
2	0.8573	1.7833	0.5608	0.7972	1.6901	0.5917	0.6944	1.5278	0.6545
3	0.7938	2.5771	0.3880	0.7118	2.4018	0.4163	0.5787	2.1065	0.4747
4	0.7350	3.3121	0.3019	0.6355	3.0373	0.3292	0.4823	2.5887	0.3863
5	0.6806	3.9927	0.2505	0.5674	3.6048	0.2774	0.4019	2.9906	0.3344
6	0.6302	4.6229	0.2163	0.5066	4.1114	0.2432	0.3349	3.3255	0.3007
7	0.5835	5.2064	0.1921	0.4523	4.5638	0.2191	0.2791	3.6046	0.2774
8	0.5403	5.7466	0.1740	0.4039	4.9676	0.2013	0.2326	3.8372	0.2606
9	0.5002	6.2469	0.1601	0.3606	5.3282	0.1877	0.1938	4.0310	0.2481
10	0.4632	6.7101	0.1490	0.3220	5.6502	0.1770	0.1615	4.1925	0.2385
11	0.4289	7.1390	0.1401	0.2875	5.9377	0.1684	0.1346	4.3271	0.2311
12	0.3971	7.5361	0.1327	0.2567	6.1944	0.1614	0.1112	4.4392	0.2253
13	0.3677	7.9038	0.1265	0.2292	6.4235	0.1557	0.0935	4.5327	0.2206
14	0.3405	8.2442	0.1213	0.2046	6.6282	0.1509	0.0779	4.6106	0.2169
15	0.3152	8.5595	0.1168	0.1827	6.8109	0.1468	0.0649	4.6755	0.2139
16	0.2919	8.8514	0.1130	0.1631	6.9740	0.1434	0.0541	4.7296	0.2114
17	0.2703	9.1216	0.1096	0.1456	7.1196	0.1405	0.0451	4.7746	0.2094
18	0.2502	9.3719	0.1067	0.1300	7.2497	0.1379	0.0376	4.8122	0.2078
19	0.2317	9.6036	0.1041	0.1161	7.3658	0.1358	0.0313	4.8435	0.2065
20	0.2145	9.8182	0.1019	0.1037	7.4694	0.1339	0.0261	4.8696	0.2054
21	0.1987	10.0168	0.0998	0.0926	7.5620	0.1322	0.0217	4.8913	0.2044
22	0.1839	10.2007	0.0980	0.0826	7.6446	0.1308	0.0181	4.9094	0.2037
23	0.1703	10.3711	0.0964	0.0738	7.7184	0.1296	0.0151	4.9245	0.2031
24	0.1577	10.5288	0.0950	0.0659	7.7843	0.1285	0.0126	4.9371	0.2025
25	0.1460	10.6748	0.0937	0.0588	7.8431	0.1275	0.0105	4.9476	0.2021
26	0.1352	10.8100	0.0925	0.0525	7.8957	0.1267	0.0087	4.9563	0.2018
27	0.1252	10.9352	0.0914	0.0469	7.9426	0.1259	0.0073	4.9636	0.2015
28	0.1159	11.0511	0.0905	0.0419	7.9844	0.1252	0.0061	4.9697	0.2012
29	0.1073	11.1584	0.0896	0.0374	8.0218	0.1247	0.0051	4.9747	0.2010
30	0.0994	11.2578	0.0888	0.0334	8.0552	0.1241	0.0042	4.9789	0.2008

From D.A. Jones, *Principles and Prevention of Corrosion*, Macmillan Publishing Co., New York, 1992. Reprinted by permission, Prentice-Hall, Upper Saddle River, NJ

deterioration of equipment, plant or property and is given by the equation:

$$D = \phi(P - S)$$

where P is the present cost, S is the salvage cost after depreciation over N yr and ϕ is the fraction allowed in a given year. When straight-line depreciation is involved, we have $\phi = 1/N$, ϕ and D are the same each year over N yr. The product P/A ϕ gives the discounted value of fractional depreciation. The depreciation is governed by tax laws, which define depreciation period and the method for various properties and equipment.

The two methods of depreciation are: (i) the sum of years digits (SOYD); and (ii) declining balance (DB). In SOYD for a period of 5 yr, we have $5 + 4 + 3 + 2 + 1 = 15$ and the ϕ values for the five years are 5/15, 4/15, 3/15 2/15 and 1/15, respectively.

In the declining-balance (DB) method, the depreciation in n yr is given by:

$$D_n = \phi(P - \Sigma D_n)$$

where n has values from 1 to N, ϕ is a given percentage, P is the initial cost and ΣD_n is the total depreciation to the nth year.

When the double declining method is considered, $\phi = 2/N$, the annual depreciation is twice that of straight-line depreciation and the amount depreciated decreases with increase in the value of n. In the case of double declining balance depreciation method, the book value $P-\Sigma D_n$ in the nth year is given by[4]:

$$P - \Sigma D_n = P[1 - 2/N]^n$$

The depreciation is allowed up to salvage value, S by US tax laws.

The various products are classified into 3-, 5-, 7-, 10-, 15- and 20-year groups in the modified accelerated cost recovery system (MACRs) in the US in 1986. The annual depreciation prescribed by the MACR system is given in Table 5.2. Some typical products belonging to various classes are noted in Table 5.3.

Verink's equation for determining the present worth (PW) for different economic design situations using straight-line depreciation were written as:

$$\text{PW} = P = t\Phi(P - S)P/A - X(1 - t)P/A + S(P/F)$$

Table 5.2 *Annual depreciation prescribed by modified accelerated cost recovery*

Recovery year	3-yr class (200% DB)	5-yr class (200% DB)	7-yr class (200% DB)	10-yr class (200% DB)	15-yr class (150% DB)	20-yr class (150% DB)
1	33.00	20.00	14.28	10.00	5.00	3.75
2	45.00	32.00	24.49	18.00	9.50	7.22
3	15.00*	19.20	17.49	14.40	8.55	6.68
4	7.00	11.52	12.49	11.52	7.69	6.18
5		11.52	8.93*	9.22	6.93	5.71
6		5.76	8.93	7.37	6.23	5.28
7			8.93	6.55*	5.90*	4.89
8			4.46	6.55	5.90	4.52
9				6.55	5.90	4.46*
10				6.55	5.90	4.46
11				3.29	5.90	4.46
12					5.90	4.46
13					5.90	4.46
14					5.90	4.46
15					5.90	4.46
16					3.00	4.46
17						4.46
18						4.46
19						4.46
20						4.46
21						2.25

*Year of switch to straight-line depreciation to maximize deduction
From DA Jones, Principles and Prevention of Corrosion, Macmillan Publishing Co., New York, 1992. Reprinted by permission, Prentice-Hall, Upper Saddle River, NJ

Table 5.3 *Typical properties belonging to different classes*

Number of years	Examples
3	Rubber products, finished plastic products, fabricated metal products
5	Computers, copiers, typewriters, trucks, trailers, cars, property used in research, cargo containers
7	Office furniture, railroad track, agricultural equipment
10	Vessels, assets used in petroleum refining or tobacco products and food products
15	Sewage-treatment plants, telephone distribution plants

where P is the present value of the money, t is the tax rate, S is the salvage value, and X is the sum of the expenses excluding depreciation. The values of P/A and P/F given in Table 5.1 are functions of the interest rate.

P is the present value of the money and is negative since it is expenditure. The second term represents tax savings or incomes and has a positive sign. X and Xt, are negative and positive respectively because they represent expenditure and tax savings. The final term represents salvage value and is positive.

The relationship for the present worth (PW) can be converted to annual cost at interest rate i over n yr and is written as:

$$A = (\mathrm{PW})(A/P)$$

The relationship of present worth as applied in the context of modified accelerated cost recovery method of depreciation may be written as:

$$\mathrm{PW} = -P + t(P)\Sigma[\Phi_n(P/F)n] - X(1-t)(P/A)$$

where the term containing S is omitted.

The Canadian Income Tax Act IT-285R2 dated March 31, 1994 gives some general definitions and remarks on depreciation of property and capital cost allowance. Schedule II lists the types of property divided into classes, percentage depreciation and description of the property. Some examples are given in Table 5.4.

Some examples illustrative of discounted cash-flow calculations taken from the literature are as follows:

Example 1: A new heat exchanger is required and the lifetime of a carbon steel exchanger is 5 yr with a cost of \$9500. The 316 stainless steel heat exchanger with a lifetime of 15 yr costs \$26500, which can be written off in 11 yr. Assuming the minimum acceptable rate of 10%, tax rate of 48% and a straight-line depreciation, determine which unit is more economical based on annual costs. Using the equations

$$\mathrm{PW} = -P + \phi t P(P/A)_{10\%} n$$

$$A = \mathrm{PW}(A/P)_{10\%}, n$$

and the given data, the annual costs of the carbon steel and stainless steel heat exchangers are \$1594 and \$2497, respectively. In the case of the carbon steel heat

Table 5.4 *Depreciation of property*

Class	Depreciation (%)	Property or material
1	4	Bridge, culvert, dam, road, parking area, storage area, railway track, railway traffic control equipment, subway or tunnel, electrical generating equipment, pipeline other than gas and oil building
2	6	Electrical generating equipment, generating or distributing equipment and plant, manufacturing plant, water distribution equipment, property for producing gas
3	5	Building or structure, including heating equipment, elevators, dock, windmill, wharf and jetty
4	6	Railway system, tramway or trolley bus system
5	10	Chemical pulp mill, wood pulp mill including building and machinery
6	10	Building of frame, log, stucco, galvanized iron not included in another class, fence, greenhouse, oil or water storage tank, railway locomotive
7	15	Canoe or rowboat, scow, vessel, furniture, spare engine, marine railway
8	20	Manufacturing or processing machinery not included in class 2, 7, 9, 11 or 12, building such as kiln, tank or vat; building for storing fresh fruit or vegetables, gas well, mine, oil well, tramway track, rapid transit car and greenhouse.
9	25	Electrical generating equipment, radar equipment, radio transmission and receiving equipment and aircraft
10	30	Automotive equipment, sleigh or wagon, trailers, electronic data processing equipment including software, telecommunication spacecraft, refinery, contractor's movable equipment, including buildings, gas or oil well equipment, airport, dam, dock, fire hall, hospital, natural gas pipeline, sewage disposal plant, water pipeline, equipment for cutting timber and logging, crude oil processing and passenger vehicle
11	35	Property not included in any other class and which is used for rental purpose
12	100	Property not included in any other class, books, china, cutlery, kitchenware, die, jip, pattern, mould, medical and dental equipment, mine shaft, linen, cutting or shaping part of a machine, video tapes, movies, computer, software and videotape cassette

exchanger when the maintenance cost is $300 per year, the annual cost works out to be $3012 which is higher than the value of $2497 obtained for the stainless steel exchanger.

Example 2: A paint system costing $0.38 per sq. ft failed after 4 yr. (a) If the paint system is renewed at the same cost for a total life of 12 yrs. Calculate the annual cost, assuming the first application is capitalized and those in the 4th and 8th years are expenses, interest rate of 10%, tax rate of 48% and straight-line depreciation.
Using the equations for PW and A, the annual cost of $0.068 sq. ft is obtained.

(b) The maximum that can be spent on preventive maintenance such as biennial touch-up may be calculated using the relationship.

$$X' = X[(P/F)_{10\%,\,2y} + (P/F)_{10\%,\,4Y} + (P/F)_{10\%,\,6y} + (P/F)_{10\%,\,8y} + (P/F)_{10\%\,(10\text{ yr})}](A/P)_{10\%\,(12\text{ yr})}$$

The value of $X = \$0.1492$ sq. ft is obtained.

Example 3: A plant storage tank requires either: (i) replacement to last 25 yr with no maintenance at a cost of \$690 000; or (ii) a coating system with maintenance cost of 10% of installation costs, tax rate of 48%, interest rate of 10% and straight-line depreciation.

Using the relationship

$$\text{PW} = -P + tP(1/n)(P/A)_{10\%,\,25\text{ y}}$$

a value of \$569 700 for replacement is obtained. For coating system the value of \$513 700 is obtained for *P*. Thus coating system is preferred to the replacement of the tank.

5.2 Corrosion Management

According to Trethewey and Chamberlain[5] corrosion management is defined to include people along with corrosion control which concerns with the materials used in a particular environment. The corrosion related failure may be due to: (i) primary corrosion mechanism; and/or (ii) secondary corrosion mechanism as shown below:

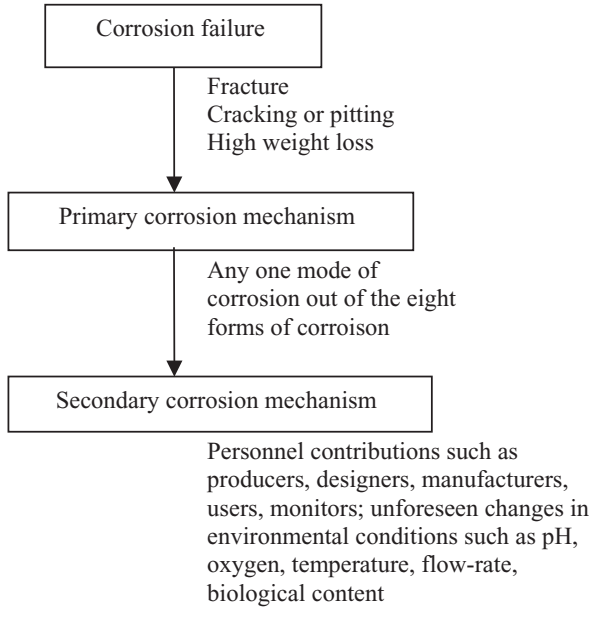

The secondary corrosion mechanism involves the contributions of people in different ways and the people factor should be rated as high in corrosion management. The various

functions of personnel in different stages of a corrosion performance of systems may be identified as follows:

Procurer	Designer	Manufacturer and supplier
Specifications of the system Intersystem compatibility, control of budget	Shape and structure, choice of materials operational conditions; use of coatings	Correct production of design; use of specified materials Correct heat treatment Correct fabrication methods Correct application of coatings

User/monitor
Correct operation Use correct replacement parts Monitoring environment Checking protective coatings for integrity

In the analysis of failures, it is possible to identify the failure when the failure occurs due to a simple corrosion mechanism such as galvanic corrosion, localized corrosion such as pitting or crevice corrosion, stress–corrosion cracking, erosion–corrosion or severe general corrosion. In all these cases the factors involved are materials; environment and flow rate of the medium. These types of failure are avoidable when proper choice of materials, design and the environment are considered. In spite of good available knowledge of various factors contributing to corrosion failures, we do encounter corrosion-related failures at remarkable frequency. In quite a few instances of corrosion-related failures such as galvanic corrosion-related failure, squarely the culprit is the improper choice of materials selected and designed by the engineer. This clearly shows the people factor involved in improper choice of materials and its use in the particular environment.

Proper corrosion management ensures that simple mistakes such as improper selection of materials, or errors in design or improper selection of inhibitors are avoided by the corrosion personnel. In some cases unusual factors may be involved in the case of a corrosion failure. An example is a failure due to stray current corrosion. The identification of such a failure by a conventional approach might be time consuming, in the worst-case scenario it may be impossible to identify the root cause of the failure. The conventional approach can be time consuming as well as leading to the wrong conclusions. On the other hand, an expert systems approach with the focus on the system as a whole can lead one, with a series of questions, in a logical stepwise manner. The answers to the questions lead one to a logical cause of the failure with great reliability in a very short time compared with the conventional, less reliable non-expert approach with singular focus on materials.

As seen from the foregoing discussion the contribution of people to the failure of system is important and can be introduced into the total probability of corrosion failure as:

$$\begin{aligned}\text{Probability of corrosion failure} = {} & \text{Probability factor due to materials} \\ & \times \text{probability factor due to environment} \\ & \times \text{probability factor due to personnel.}\end{aligned}$$

Corrosion failure incorporating the people factor may also be analyzed in terms of fault-tree analysis as given below:

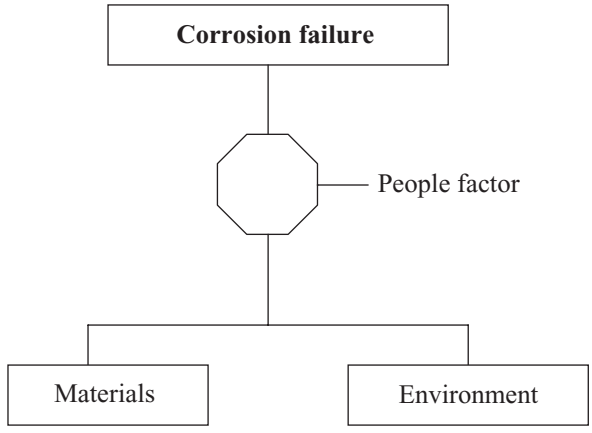

The people factor is difficult to quantify in any case of failure. It is needless to emphasize that extensive multidisciplinary knowledge in a variety of subjects such as chemistry, electrochemistry, physics, statistics, mechanical engineering, metallurgy and management is desirable in order to reduce the people contribution factor to a minimum ($0 <$ people factor < 1). An example where reliability and safety has been very high is provided by the aerospace industry. The fault-tree structure for corrosion failure can be programmed into a computer and used to analyze the risk of system failure. This methodology has been successfully used by Nova Oil Corp. to analyze pipeline failures caused by stress corrosion cracking.[6] The accounting of decisions made by people is based upon a host of disciplines such as fuzzy logic[7,8], Bayesian logic[9], influence diagrams[10,11] and approximate reasoning principle[12] in the course of research in artificial intelligence.

5.3 Computer Applications

Knowledge–based systems, also known as expert systems, have been developed to reduce erratic human influence. The computer simulation of human knowledge can be classified as: (i) skill-based knowledge and action which lends itself to automation and replaces human operators by microprocessor devices and human knowledge by software; (ii) rule-based knowledge and action is goal-driven and applicable to predefined situations; and (iii) formal reason-based knowledge and action applicable to unfamiliar situations in which human experts often invoke heuristic and other high-level intelligent responses.

The computer-based corrosion problem-solving systems have been categorized as: (i) systems for modeling corrosion/cracking processes; (ii) material selection and equipment specification programs; (iii) computer-based corrosion monitoring systems; (iv) computer-based systems for control of corrosion testing equipment; (v) databases and hypertext systems; and (vi) internet-based databases and software programs.

Table 5.5 *Early sofware (expert) systems in corrosion*

Name	Application	Country of development	Shell used
Achilles	Diagnosis and prediction of localized corrosion	UK	Spices
Aurora	Prediction of localized corrosion in austenitic steels	Finland	Level 5
Auscor	Prediction of corrosion of austenitic stainless steels	UK	Savior
ChemCor	Materials selection for hazardous chemical service	USA	KES/Level 5
DIASCC	Evaluation of cracking in stainless steels	Japan	OPS83
KISS	Materials selection	Germany	Nexpert Object
Prime	Materials selection for chemical process industry	Belgium	KEE
Socrates	Selection of CRAs for oil field service	USA	PCPLUS
Suscept	Evaluation of SSC in steels	USA	PCPLUS

Many of the early computer programs are known as expert systems since the programs were based on human expertise in corrosion[13] and these programs were based on research-based development efforts and lacking rigorous software engineering foundations necessary for commercial distribution. Most of these programs used software platforms known as shells that allowed implementation of rules of thumb and common reasoning concepts. Some of the programs developed in late 1980s and early 1990s[14–19] are given in Table 5.5.

The most popular application of computers involves programs developed for modeling corrosion and cracking as well as programs for diagnosis, failure analysis and prediction/analysis. The systems developed are:

Lipucorr[21]	
Cormed[22]	Prediction of general corrosion
Predict[23]	
Coris[24]	Expert system database that integrates corrosion problem-solving expertise with a comprehensive database in corrosion, materials and thermodynamic properties of corrosive media
Socrates[25]	Automated basis for materials selection for oil and gas production
Selmatel[26]	Selection of materials exposed to high temperatures in refinery furnace tubes
Chem Corr[13]	Evaluation of materials applicable to different segments in chemical processing industries
CORSUR[27]	Large database application on corrosion behavior of metals and nonmetals in over 700 chemical environments

The types of computer programs which have been applied in corrosion engineering and science fall into categories such as: (i) conventional software systems; (ii) artificial intelligence and expert systems applications; (iii) object-oriented software systems;

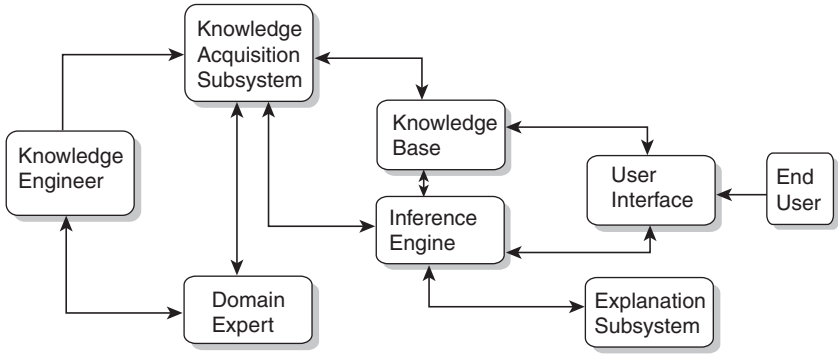

Figure 5.1 *Structural components in an expert system*

(iv) neural networks; and (v) hybrid systems that utilize one or more previously mentioned methods.

Early computer programs developed during 1970s and 1980s used Basic, Fortran, Pascal languages which provided front end for data modeling and analysis. Expert systems or knowledge-based systems differ from the early computer programs in the sense that the knowledge is usually separated from the reasoning process, also known as the inference engine. The typical structural components in an export system are shown in Figure 5.1. The knowledge base obviously contains the expertise and the inference engine controls the logical path used by the expert system to access the information in the knowledge base to make decisions. Some applications of expert systems are in different aspects of corrosion,[6] cathodic protection,[28] assessment of cracking in light water nuclear reactors[29] and prediction of localized corrosion of stainless steels.[30]

Object-oriented systems use the concept of reusable entities that contain both the data and procedures relevant to the object, and thus eliminating the separation of knowledge and reasoning found in expert systems. In object-oriented systems computation is behavior simulation of real-life systems. Once certain classes of objects are created, they can be reused to create other objects and properties with interface and behavior. The self-contained character of objects is known as encapsulation. Inheritance allows derivation of new objects from existent ones, and encapsulation defines the limits of services an object can provide to other objects. An example of this system is provided by GENERA,[31] and a schematic representation is given in Figure 5.2.

The materials and corrosion are represented as objects whose states are defined in terms of critical parameters along with inerrelationships between the parameters.

The neural networks evolving from neurobiological concepts have been used in corrosion data modeling and prediction,[32] corrosion data reduction[33] and analysis of electrochemical impedance data.[34] The neural networks are built from a large number of very simple processing elements that deal individually with pieces of a big problem. A processing element (PE) multiplies the input by a set of weights and the result is transformed by a nonlinear function into an output value. The strength of neural computation depends upon the massive interconnection among the processing elements which carry tasks of overall processing and the adaption of the parameters (weights) that interconnect the processing elements.

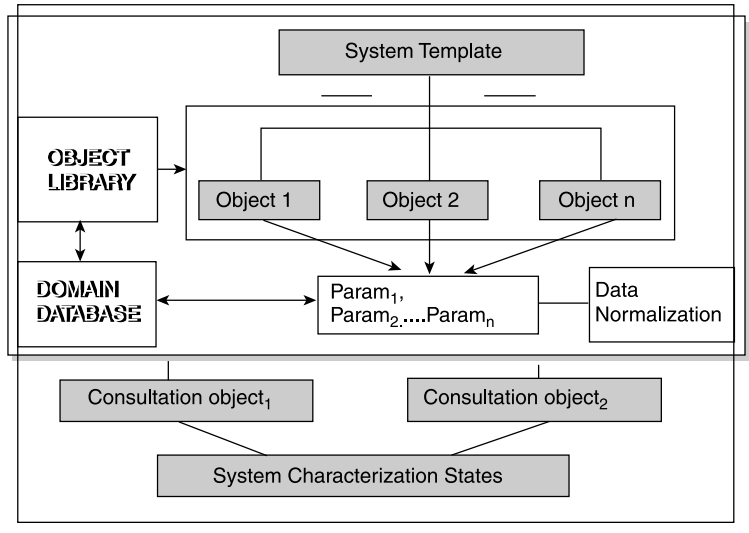

Figure 5.2 *Structural framework of the generic development system*

A neural network consists of several layers of processing elements. The most basic and common neural network is the multilayered perceptron (MLP). A typical MLP consists of an input layer, a middle or hidden layer and the output layer of elements and connecting lines represent a scaling factor or weighted connections between processing elements. The MLP calculation is based on the desired output (signal) and error criterion. The output is compared with the desired response to produce an error. The calculation is repeated with different weights until the error of the desired signal is minimized. A simple form of an MLP is depicted in Figure 5.3.

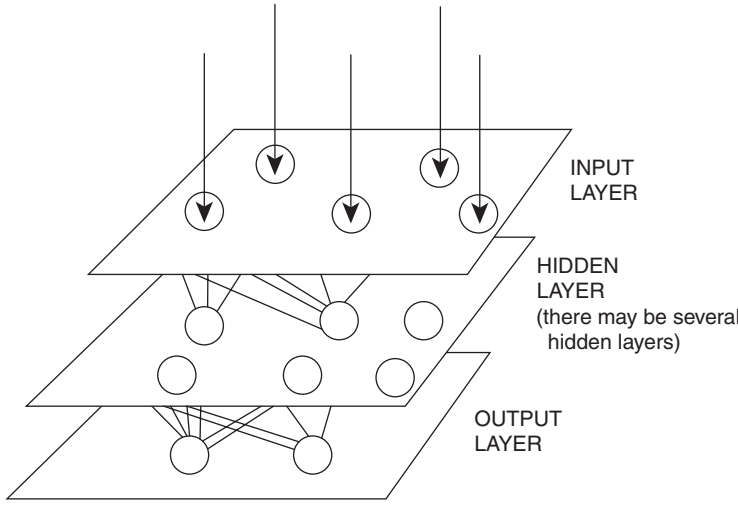

Figure 5.3 *Simple multilayered perceptron of an artificial neural network*

Currently, computer programs for corrosion assessment and control use a combination of expert systems and an object-oriented program such as evaluation of hydrogen-induced cracking of steels,[35] or a combination of expert systems and neural networks in corrosion data modeling and prediction.[32]

The developments in computer tools for corrosion assessment and control have been quite extensive, as evidenced by 57 expert systems and many hundreds of computer programs, including databases. A representative sample of current software programs for corrosion and their control is shown in Table 5.6.

Some specific examples of computer systems for different applications are:

(i) Programs for selection of materials for oil and gas application;
(ii) Programs for online corrosion monitoring and control;
(iii) Database systems for evaluation of metals and non-metals;
(iv) Use of neural networks in corrosion data reduction;
(v) Computer-aided packages for teaching corrosion

Table 5.6 *Representative sample of current day software programs for corrosion*

Application	Type of system
CORSUR, corrosion data for metals and nonmetals in over 700 chemical environments	Relational database with a user friendly front-end
CP Diagnosic, trouble-shooting and diagnosis of sacrificial anode and impressed current cathodic protection systems	Shell-based expert system with a database on CP data
Damage predictor, evaluation of material performance for stress–corrosion cracking in boiling water reactors and determination of crack growth rates	FORTRAN program modules that calculate radiolytic species concentration and assess crack growth rates
ECORR, computer-aided learning package designed to assist in training students in corrosion concepts	Uses an authoring package to provide multimedia information
EIS data extrapolation, uses neural networks to train on electrochemical impedance spectroscopy data for extrapolation	Artificial neural network (ANN) application
Filter debris analysis (FDA) expert system, condition monitoring of aircrafts	Visual basic-based interface and knowledge base
GENERA, generic problem-solving framework for characterizing corrosion and materials problems	Object oriented system implemented in C++
LipuCor, prediction of corrosion in oil and gas systems	Implemented as a conventional structured program
Predict, prediction of corrosion in oil and gas production and transmission environments	Object-oriented program using lab data and numerical relationships
Socrates, selection of materials for oil and gas production service	Object-oriented expert system implemented in C++ interfacing with a database on materials and compositions
Strategy, programs for evaluation of cracking in steels used in pipelines and refineries	Implemented in C++ and integrated with databases in Paradox
USL Corrosion Model, program for prediction of corrosion in gas condensate wells	Implemented as an expert system in visual basic

The CORMED program predicts the probability of corrosion in oil wells using detailed analysis of field experience on CO_2 corrosion, and other data in the literature, involving factors such as CO_2, *in situ* pH and bicarbonate in the wells.[22] The corrosion damage is also predicted by computer models such as Predict[23], Lipucorr[21] and USL, based on a larger number of factors.[36]

The object-oriented Socrates system is concerned with material selection such as corrosion-resistant alloys (CRA) in a chosen environment. The system uses published data in the literature involving both laboratory and field data in the oil and gas environments.

The flow diagram depicted in Figure 5.4 shows an example of the sequential steps. Since the system is object-oriented it is not necessary to use the data in a sequential manner. The initial set of applicable materials can be obtained by the chosen application.

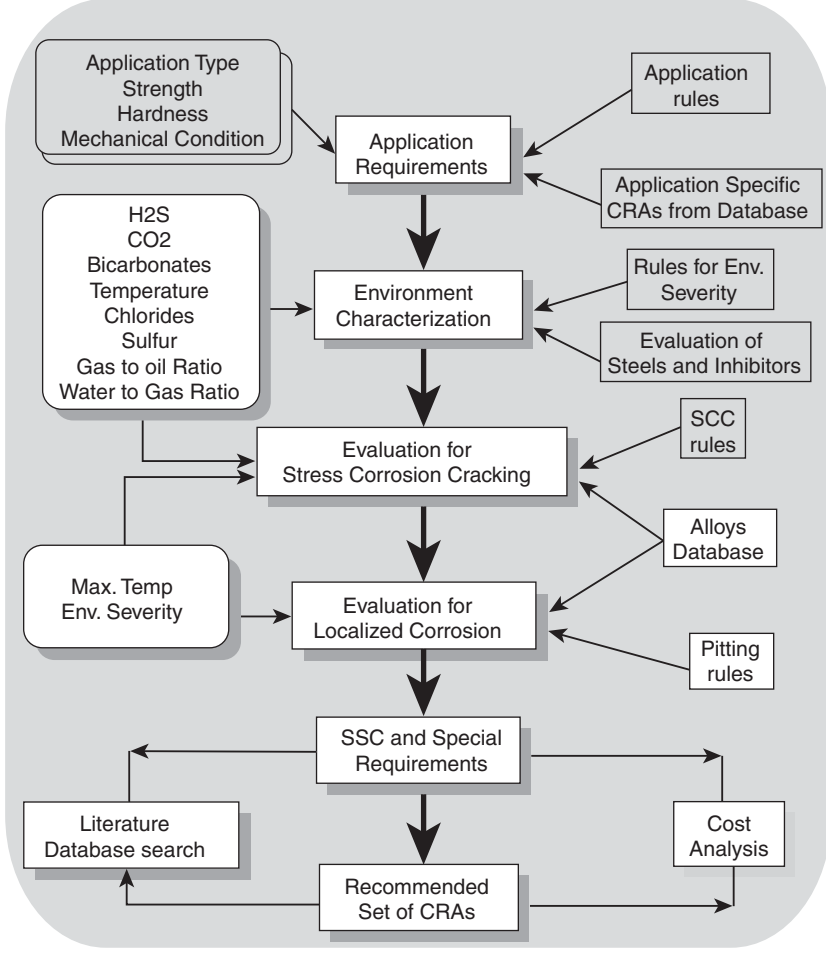

Figure 5.4 *Flow of data in the Socrates system*

The system defines the severity of the environment with respect to various forms of corrosion, using the environmental conditions and the metallurgical parameters.

One of the most important applications of neural network methodology is in the extrapolation of electrochemical impedance data obtained in corrosion studies.[34] Electrochemical impedance spectroscopy (EIS) can be used to obtain instantaneous corrosion rates. The validation of extension of EIS data frequency range, which is conventionally difficult, can be done using a neural network system. In addition to extension of impedance data frequency range, the neural network identifies problems such as the inherent variability of corrosion data and provides solutions to the problems. Furthermore, noisy or poor-quality data are dealt with by neural works through the output of the parameters variance and confidence.[33]

ECORR or engineering corrosion[37] is a computer-aided learning (CAL) system, representing application of computing to corrosion education. This program is very valuable to students in learning about corrosion. The student is presented with a series of problems to be solved by reference to supporting information. The system consists of objects such as text, photographs, video or sound objects. The system contains a theory base, case studies, a glossary, and a control center to coordinate navigation and information flow between the student and different modules. The basic corrosion information provided can be used in studying the particular case study. There are twelve case study modules at basic/Level 1 and Advanced/Level 2 in the program.

Computers and programs are also important in corrosion monitoring systems, such as an automated constant rate extension system (A Cert) shown schematically in Figure 5.5. This system may be used for conducting corrosion and cracking evaluation tests. The system is capable of initiation and conducting tests as well as data acquisition and analysis. There is very little human intervention and the system is capable of corrosion evaluation in environments which are difficult to simulate. This system is a

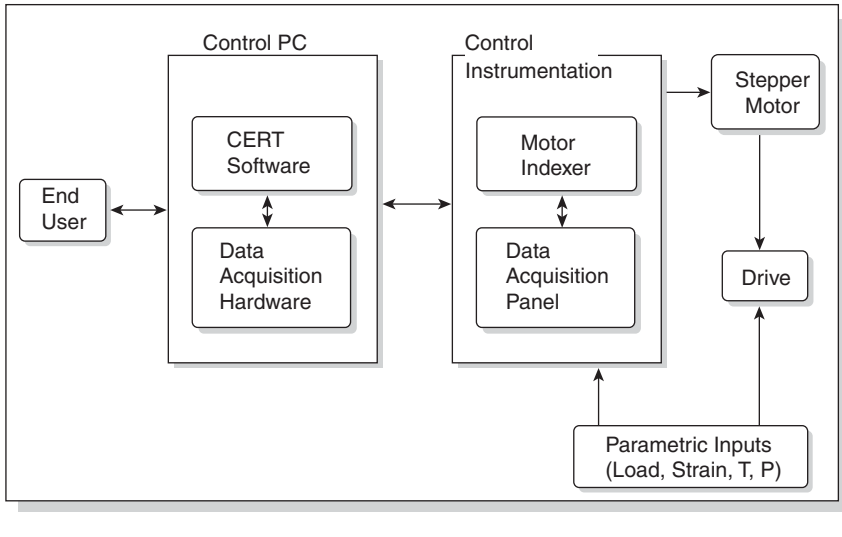

Figure 5.5 *Schematic representation of an automated constant extension rate tester*

computer-controlled, closed-loop feedback system, capable of operation over a wide range of speeds. This automated system can be programmed to conduct constant extension rate tests, cyclic slow-strain-rate tests, and crack growth rate tests and fracture mechanics tests.

The role of internet in corrosion science and engineering, as in any other field, has been increasingly useful in the past decade. The internet is playing a significant role in sharing and exchanging information. The resources available to the corrosion engineer/scientist are: (i) e-mail-based; (ii) newsgroups and discussion threads; and (iii) technical resource websites. Electronic mail is a convenient mechanism for exchanging information of interest among scientists. This may also involve a mailing list of people interested in the technical topic and an example of this is the CORROS-L list[38] operated by the corrosion and Protection Centre at the University of Manchester, email: corros-L@istserv.rl.ac.uk.

Newsgroups are analogous to worldwide bulletin boards where questions, messages, comments, discussions and answers are given. Currently there exist over 6000 Usenet newsgroups covering a wide range of corrosion related topics, such as metallurgy, materials, electrochemistry, chemistry, engineering and nondestructive testing.

Discussion threads are conceptually similar to newsgroups, but can be accessed on the web. The two most popular threads relevant to corrosion and materials are www.intercorr.com/discuss/x where x can be coatings, inhibitor, cathodic protection, multi-phase flow, fracture mechanics, etc.

The web-based resources for corrosion may be classified as: (i) resources for solving corrosion problems; (ii) resources for sharing information with the aid of virtual libraries and online databases; and (iii) resources for sharing information within the organization (intranets). Some of the relevant websites for corrosion and materials are:

www.Metalogic.be	Overview of corrosive environments
www.intercorr.com	A number of important papers, data and software on corrosion and materials
www.nist.gov/srd/material.htm	NIST materials databases
www.oilonline.com	Online news, rig counts, product and literature on oil industry
http://www.xs4all.nl/-edewaard/	Overview of corrosion processes

Websites are also available dealing with electrochemistry, corrosion mechanisms, industrial corrosion and materials. The internet also provides significant technical resources online and some examples are: (i) different types of technical databases such as data on general corrosion, localized corrosion, galvanic, intergranular, erosion-corrosion, SCC, SSC, HEC: materials data on steels, plastics and composites; (ii) corrosion and materials problem-solving software; (iii) archival laboratory testing data and reports with respect to oil and gas, power generation and nuclear industries; (iv) conference proceedings and journals available online; and (v) virtual conferences such as the first global internet corrosion conference, Intercorr/96.

It is conceivable that most of the tasks performed by humans may be replaced by computers in the future, but the role of people in corrosion management will not be diminished in spite of the technical advances being made.

References

1. E.D. Verink, *Metals Handbook*, Vol. 13, Corrosion, 9th edn, Metals Park, OH, ASM International, p. 389.
2. E.D. Verink, *Corrosion/86*, Paper No. 383, NACE, Houston, Texas.
3. *Engineering Economy*, Z94-5, American National Standards Institute, Institute of Industrial Engineers.
4. D.G. Newman, *Engineering Economic Analysis*, San Jose, CA, Engineering Press, 1975, p. 195.
5. K.R. Trethewey and J. Chamberlain, *Corrosion for Science and Engineering*, Longman, 1995.
6. P. Roberge, *Modelling Aqueous Corrosion*, K.R. Trethewey and P.R. Roberge, ed. Kluwer Academic Academic, Dordrecht, The Netherlands, 1994, pp. 319–416.
7. B. Kosko, *Neural Networks and Fuzzy Systems*, Prentice Hall, Englewood Cliffs, NY, 1992.
8. J. Durkin, *Fuzzy Logic*, MacMillan, NY, 1994, pp. 363–403.
9. J. Durkin, Bayesian Logic, MacMillan, NY, 1994, pp. 305–331.
10. R.A. Howard, J.E. Matheson, Influence Diagrams in the Principles and Applications of Decision Analysis, Editors R.A. Howard, J.E. Matheson, Strategic Decisions Group, Menlo Park, CA, Vol. II, pp. 720–762.
11. R.D. Schacter, Probabilistic Influence and Influence Diagrams, Operations Research, Vol. 36, 1988, pp. 589–604.
12. R.K. Bhatnagar, L.N. Kanal, Handling Uncertain Information: A Review of Numeric and Non-Numeric Information, in Uncertainty in Artificial Intelligence, Editors L.N. Kanal, J.F. Lemmer, North Holland, Amsterdam, Vol. 4, 1986, pp. 3–26.
13. P.R. Roberge, CORROSION/94, Paper No. 368, NACE, Houston, Texas, 1994.
14. The Achilles Club Project, Expert System on Corrosion and Corrosion Control, NPL, Teddington, Middlesex, UK, 1986.
15. J.G. Hines, A. Basden, *British Corrosion Journal*, **26**(3), 151 (1986).
16. A. Jadot, L. Lancus, *'Escort', Expert Software for Corrosion Technology*, PhD Thesis, K.V. Leuven University, Belgium, 1985.
17. G.M. Ugiansky, A.C. Vanorden, D.E. Clausen, ''The NACE-NES Corrosion Data Program in Computers Corrosion Control'', J. Fu, R. Heidersbach and R. Erbar, Editors, NACE, Houston, Texas, 1986, pp. 15–20.
18. C.S. Fang, J.D. Garber, P. Perkins, J.R. Reinhardt, ''Computer Model of a Gas Condensate Well Containing Carbon Dioxide'', CORROSION/89'', Paper No. 465, NACE, Houston, Texas, 1989.
19. S. Srinivasan, R.D. Kane, ''Expert Systems for Material Selection in Corrosive Environments'', Paper No. 564, CORROSION/90, NACE, Houston, TX, 1990.
20. C.P. Sturrock, W.F. Bogaerts, A.S. Krisher, Paper No. 375, CORROSION/94, NACE, Houston, TX, 1994.
21. Y.M. Gunaltan, Paper No. 27, CORROSION/96, NACE, Houston, TX, 1996.
22. J.L. Crolet, M.R. Bonis, ''Prediction of the Risks of CO_2 Corrosion in Oil and Gas Wells'', *SPE Production Engineering*, **6**(4), 449 1991.
23. S. Srinivasan, V.R. Jangama, R.D. Kane, ''Prediction of Corrosivity of CO_2/H_2S Systems'', EuroCorr/97, The European Corrosion Congress, Trondheim, Norway, Sept. 22–25, 1997, Publ. by Norwegian University of Science and Technology, Trondheim, Norway, Vol. 1, 1997, pp. 33–40.
24. A. Hatzinosios, ''CORIS'', CORROSION/94, Paper No. 373, NACE, Houston, TX, 1994.
25. S. Srinivasan, ''Role of Expert System in Technology Transfer of Materials for Petroleum Applications'', *Proceedings of the 12th International Corrosion Congress*, 19–24, September 1993, NACE International, Houston, TX, 1993.
26. A. Valdes, A. Gonzalez, R. Techorrewski, B. Hopkinson, ''An Expert System for the Selection of Materials Exposed to Elevated Temperatures'', Paper No. 275, CORROSION/92, NACE, Houston, TX, 1992.
27. B. Mashayekhi, C.P. Sturrock, D. Flanigan, ''Corrosion Data Survey, The Next Generation'', Paper No. 604, CORROSION/97, NACE International, Houston, TX, 1997.

28. V.L. Van Blaricum, A. Kumar, Y.T. Park, Paper No. 384, CORROSION/94, NACE, Houston, TX, 1994.
29. M. Urqidi-McDonald, Paper No. 340, CORROSION/90, NACE, 1990.
30. T.J. Hakkarainen, CORROSION/96, Paper No. 363, NACE, Houston, TX, 1996.
31. S. Srinivasan, CORROSION/96, Paper No. 368, NACE, Houston, TX, 1996.
32. D.C. Silverman, E.M. Rosen, CORROSION/92, Paper No. 264, NACE, Houston, TX, 1996.
33. R.A. Cotis, I. Helliwell, M. Turega, CORROSION/96, Paper No. 379, NACE, Houston, TX, 1992.
34. M. Urquidi-MacDonald, P.C. Egan, Corrosion Reviews: Special Issue on Application of Computers in Corrosion, P.R. Roberge, ed., **15**(1–2), 1997.
35. R.D. Kane and S. Srinivasan, Serviceability of Petroleum, Process and power Equipment, D. Bagnoli, M. Prager, D.M. Schlader, Editors, PVP Vol. 239, ASME, NY, 1992.
36. P.R. Roberge, Corrosion Reviews: Special Issue on Applications of Computers in Corrosion, P.R. Roberge, Editor, **15**(1–2), 1997.
37. R.A. Cotis, M. Fay, S. Faidi, CORROSION/96, Paper No. 377, NACE, Houston, TX, 1996.
38. R.A. Cotis, S.B. Lyon, CORROSION/96, Paper No. 376, NACE, Houston, TX, 1996.
39. S. Srinivasan, R.D. Kane, *Materials and Corrosion Resources on the Internet, 2nd NACE Latin American Corrosion Congress*, Rio de Janeiro, Brazil, September 1996.

Part II

6

The Forms of Corrosion

Note: Some reference citations in this chapter refer to Handbooks containing several individual references. These are indicated in the text as (ASTM G 52004)[4], for example, and the addition of RO4 in the reference list stands for revised 2004.

6.1 Corrosion Reactions

Corrosion of materials is a direct chemical reaction of a metal with its environment or a flow of electricity in an electrochemical reaction in an aggressive medium such as natural media (atmospheric, water or underground) or process media. Local cells (short-circuited) electrochemical cells of the same active metal or between an active metallic surface and that of another more noble conducting material can give rise to corrosion. The following general reaction may be written as:

$$aA + bB \rightarrow cC + dD$$

where a moles of solid substance A (metal for example react with b moles of substance B (environment) to form c moles of substance C (oxidized metal or material) and d moles of D (reduced environment). A 'wet' reaction of iron in an oxygenated aqueous medium can be represented by the equation:

$$Fe + 0.5\,H_2O + 0.75\,O_2 \rightarrow 0.5\,Fe_2O_3 \bullet H_2O$$

A 'dry' reaction of corrosion of iron can be written as:

$$Fe + 0.75\,O_2 \rightarrow 0.5\,Fe_2O_3$$

Oxidation of metals includes all reactions in which the charge is transported through a film of reaction product on the metal surface. Parabolic, logarithmic, asymptotic, rates involve the presence of a rate-determining film, while linear growth rates correspond to the absence of such films. These reactions are generally considered as dry reactions.

Corrosion Prevention and Protection: Practical Solutions V. S. Sastri, E. Ghali and M. Elboujdaini

Exceptions can exist since the corrosion in a wet solution of the interior boiler drum (steel) with dilute caustic soda at high temperature and high pressure and the reaction of high temperature water with aluminum and zirconium have been found to be best interpreted in terms of a dry corrosion mechanism.[1]

Corrosion can also occur by a direct chemical reaction of a metal with its environment such as the formation of a volatile oxide or compounds, the dissolution of metals in fused metal halides. The reaction of molybdenum with oxygen and the reaction of iron or aluminum with chlorine are typical examples of metal/gas chemical reactions. In these reactions, the metal surface stays film-free and there is no transport of electrical charge.[1] Fontana and Staehle[2] have stated that corrosion should include the reaction of metals, glasses, ionic solids, polymeric solids and composites with environments that embrace liquid metals, gases, aqueous and other nonaqueous solutions.

6.2 Corrosion Media

The majority of corrosion reactions fall into three categories: (1) aqueous corrosion; (2) nonaqueous corrosion; and (3) high-temperature corrosion. The corrosion media consist of four types:

6.2.1 Atmospheric Exposure

The natural environments—rural, marine and industrial—and some combination of these are of primary concern. Some contaminated atmospheres, such as those containing hydrogen sulfide, ammonia, sulfur dioxide, etc., should be considered rigorously. Relative humidity and its cycling are of major importance for corrosion kinetics and a material's resistance to corrosion. Temperature and pressure are major factors to consider, together with the chemical composition of the medium.

6.2.2 Aqueous Environments

These include natural or industrial waters, as well as extremely dilute inorganic or organic chemical media.

6.2.3 Underground Media

This category includes the underground installations of piping and vessels and the underside of structures such as tank bottoms.

6.2.4 Process Media

This includes organic and inorganic syntheses and other processing environments such as liquids or gases that affect materials.[3]

The nature of the *corrosion product* plays an important part in deciding if the reaction occurs through a film or film-free reaction. This can distinguish electrochemical from chemical reactions. If a film is formed due to the oxidation of the metal, the properties of this film, such as coverage and protection capacity, partial pressure, resistivity, porosity,

toughness, hardness as well as resistance to different chemicals and gases, are important. This is true for almost all electrochemical reactions in aqueous solutions as well as for high-temperature oxidation.

Rust of iron (the most abundant corrosion product), and white rust of zinc are examples of nonprotective oxides. Aluminum and magnesium oxides are more protective than iron and zinc oxides. Patina on copper is protective in certain atmospheres. Stainless steels are passivated and protected, especially in chloride-free aqueous environments due to a very thin passive film of Cr_2O_3 on the surface of the steel. Most films having low porosities can control the corrosion rate by diffusion of reactants through the film. In certain cases of uniform general corrosion of metals in acids (e.g., aluminum in hydrochloric acid or iron in reducible acids or alkalis), a thin film of oxide is present on the metal surface. These reactions cannot be considered film-free although the film is not a rate-determining one.[1]

6.3 Active and Active–Passive Corrosion Behavior

The active state of a metal corresponds to the dissolution or the attack of the metal in a certain environment since this metal is not stable naturally or thermodynamically in its new material/media conditions. There is a marked tendency of the metal to go back to its thermodynamic stable state or to another stable one. This electrochemical active state can be described by electrochemical polarization tests. In these tests, using a potentiostat, the applied potential is varied over a wide range, covering the cathodic and anodic regions of the metal/solution system, and the corresponding current at every potential is recorded. Similarly, an infrequently changing current can be imposed on the metal, recording the corresponding potential. (ASTM G5)[4] Plots of E_{appl} versus $\log I$ are called Tafel plots (Figure 6.1). The corrosion current density i_{corr}, can be determined using two equations by extrapolation of the Tafel lines:

$$E_{\text{appl}} = E_{\text{corr}} + \beta_{\text{a}} \log(i/i_{\text{corr}})$$
$$E_{\text{appl}} = E_{\text{corr}} - \beta_{\text{c}} \log(i/i_{\text{corr}})$$

where β_{a} and β_{c} are positive constants. From i_{corr} the corrosion rate can be calculated using Faraday's law. (ASTM G102)[4]

In measurement of the polarization resistance, a small electrochemical signal of the order of 10 mV is applied to ensure that the system under consideration stays linear. This requirement does not perturb the system and can be used for monitoring. The polarization resistance R_{p} is defined as $R_{\text{p}} = (\text{d}E/\text{d}i)_{E\text{corr}}$ and is determined as the slope of the polarization curve when $I = 0$ or $i_{\text{a}} = i_{\text{c}}$ in absolute values. (ASTM G59)[4] The $i_{\text{corr}} = B/R_{\text{p}}$ and $B = \beta_{\text{a}}\beta_{\text{c}}/2.3(\beta_{\text{a}} + \beta_{\text{c}})$, where R_{p} is a constituent of the total resistance in the circuit (R_{p} and R_{s}). Elimination of R_{s} is highly recommended, as discussed before. Also, if the accurate values of β_{a} and β_{c} are determined from Tafel slopes, this method reflects corrosion rates because of minimum perturbation of the state of equilibrium. Figure 6.2 gives a standard polarization curve for type 430 stainless steel in 1.0 NH_2SO_4, purged with hydrogen, nitrogen or argon at 30°C. Experimental curves should lie between curves 1 and 3, otherwise experimental errors occur.[4,5]

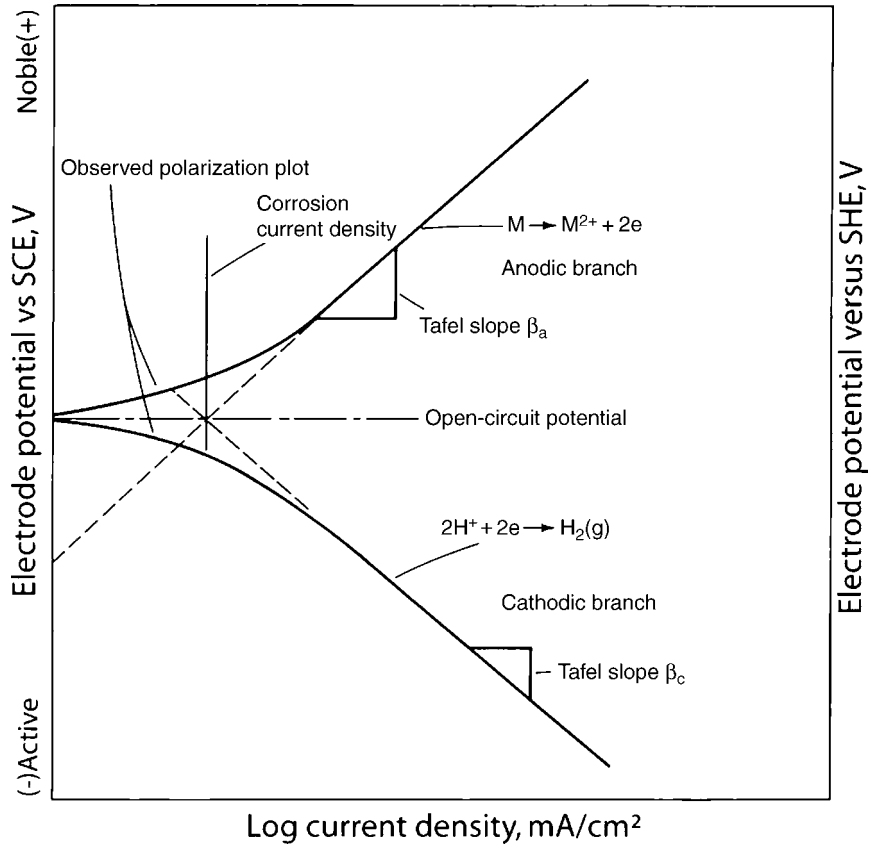

Figure 6.1 *Theoretical Tafel plots describing the tafel slopes and illustrating a graphical method of i_{corr} determination[5,18], (Mansfeld)[5]*

Chemical passivity corresponds to the state where the metal surface is stable or substantially unchanged in a solution with which it has a thermodynamic tendency to react. The surface of a metal or alloy in aqueous or organic solvent is protected from corrosion by a thin film (1–4 nm), compact, and adherent oxide or oxyhydroxide. The metallic surface is characterized by a low corrosion rate and a more noble potential. Aluminum, magnesium, chromium and stainless steels passivate on exposure to natural or certain corrosive media and are used because of their active–passive behavior. Stainless steels are excellent examples and are widely used because of their stable passive films in numerous natural and industrial media.[6]

Some inhibitors produce films on the anode and hence stifle the corrosion reaction (iron in chromate or nitrite solutions). Several authors consider the presence of a thick barrier of corrosion products, relatively protective, on the metallic surface as passivation. Inhibitors may enhance the formation of passive films on top of the substrate, such as benzotriazole on copper or benzoate on iron, or they may form monomolecular

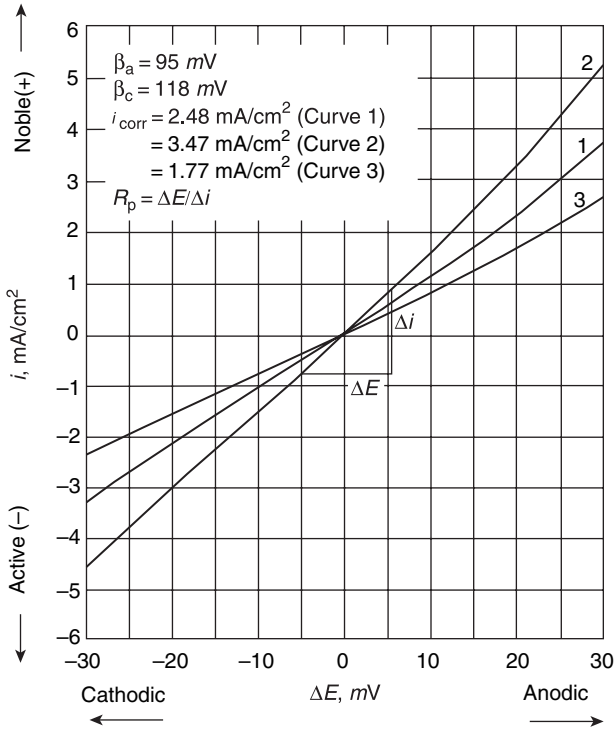

Figure 6.2 *Standard potentiodynamic polarization curves in the vicinity of E_{corr} for type 430 stainless steel; in 1 N H_2SO_4 at 30°C (Mansfeld)*[5]

adsorption layers and prevent the dissolution of the substrate and the reduction of oxygen by changing the potential drop across the interface and/or the reaction mechanism.[7–9]

Starting with an oxide-free surface of iron for example, the current increases with increase in potential, reaches a maximum and then decreases again. There is a region of over a volt where iron does not dissolve or more precisely corrodes at a very slow rate, corresponding to the passive current for every potential, and then the current rises again, due to oxygen evolution and/or transpassive metal dissolution. In the passive region, iron is covered by a thin film of cubic oxide ($\gamma Fe_2O_3/Fe_3O_4$) formed. The film thickness increases with anodic potential until a limiting value approaches 5 nm (Figure 6.3). This is the same type of film that is formed by the reaction of clean iron with oxygen or dry air. The dissolution occurs because of the imperfections of the film since there is always some existing porosity. Also, the rate of dissolution can increase due to a film breakdown and the kinetics depends in this case on film breakdown and repair.[10,11]

It is now well accepted that the passive film is not a single layer, but rather has a stratified structure. The inner layer plays the role of a barrier layer against corrosion and the outer layer plays the role of an exchange layer. The chemical composition is a

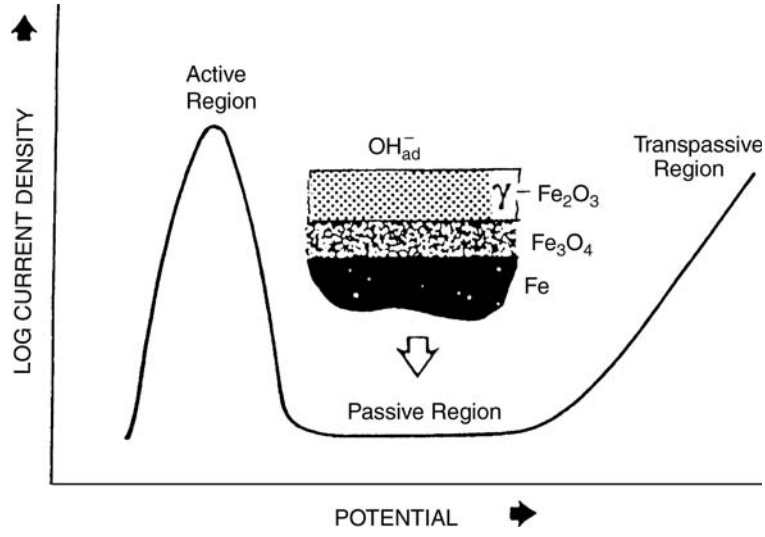

Figure 6.3 *Schematic of anodic polarization curve of iron,[10] showing active–passive behavior of iron in sodium borate–boric acid buffer solution at pH 8.4*

function of the microstructure of the metal, the pH of the electrolyte and the level of the anodic potential. Film growth is generally a direct growth due to the reaction between the metal and the aqueous solution. However, it could be also the result of a dissolution/precipitation (dissolution of metal ions and subsequent precipitation of an oxide, oxyhydroxide, or hydroxide) and anodic deposition process that consists of anodic oxidation of metal ions in the solution and deposition on the surface. Aluminum and other metals (titanium, zirconium, hafnium, tantalum, and niobium), show that thicker anodic oxide films can be grown because these oxides are insulators. Thick films of $\sim$100 μm are generally porous whereas the barrier film is $<\sim$1 μm. These oxide films formed on valve metals exhibit dielectric breakdown at high voltages.[12–13]

6.4 Forms of Corrosion

Bruce Craig and Steven L. Pohlman[14] presented five forms of corrosion that have been considered by Covino and Cramer,[5] and added the microbiologically influenced corrosion as a separate corrosion form. This approach is based on the mechanism of attack involved rather than the proposed eight forms of corrosion by Fontana.[15] Uniform corrosion, localized corrosion, metallurgically influenced corrosion and microbiologically influenced corrosion fit under the classification of corrosion that is not influenced by an external influence while mechanically assisted degradation and environmentally induced cracking involve corrosion that is influenced by another process.

Six forms of corrosion can be identified based on the apparent morphology of corrosion, the basic factor influencing the mechanism of corrosion in every form. The six forms are given in Table 6.1.

Table 6.1 *The six forms of corrosion including some types or categories of every form (Craig and Pohlman)[14], (Covino and Cramer)[5]*

1	General Corrosion	Uniform, quasi uniform and non uniform corrosion; galvanic corrosion
2	Localized Corrosion	Pitting corrosion; crevice corrosion; filiform corrosion
3	Metallurgically influenced corrosion	Intergranular corrosion; sensitization; exfoliation; dealloying
4	Microbiologically influenced corrosion	
5	Mechanically assited corrosion	Wear corrosion; erosion–corrosion; corrosion fatigue, etc.
6	Environmentally induced cracking	Stress–corrosion cracking; hydrogen damage; embrittlement; hydrogen-induced blistering; high-temperature hydrogen attack; hot cracking; hybride formation; liquid metal embrittlement; solid metal-induced embrittlement

The following observations explain the significance of these forms of corrosion:

1. In many cases, one form of corrosion can lead to another or may mitigate another, and a single case of corrosion may provide more than one form of corrosion.
2. Galvanic corrosion can cause general or localized corrosion, depending on the relative surface areas of anode to cathode, the geometry of the corrosion cell, agitation, the nature of the material, the conductivity and the composition of the corrosive media. Natural corrosion media such as atmospheric, marine, underground corrosion, etc., may give general and localized corrosion.
3. Stray-current corrosion leads to general corrosion, but creates localized corrosion areas in many circumstances, such as that on a pipe tube at the departure of the vagabond current from the pipeline, however it is treated as general corrosion form. Parting is treated as a type of metallurgically influenced corrosion, and it can give general or localized corrosion.
4. High-temperature corrosion frequently shows general corrosion, as in oxidation, sulfidation, carburization, hot corrosion and hydrogen effects, etc. It should be noted that subsurface corrosion or internal corrosion at high-temperature corrosion is a highly localized corrosion phenomenon.
5. There is an overlap between the different forms of corrosion, for example between general and/or localized corrosion and stress–corrosion cracking. Dealloying or selective leaching may be a precursor to stress–corrosion cracking. The transition from uniform corrosion to highly localized attack is not clearly understood. In certain circumstances pitting or crevice corrosion is observed while in other conditions environmentally induced cracking can occur.[3,14]

These six forms are explained in more detail in Sections 6.7.1–6.7.6.

6.5 Types and Modes of Corrosion

Types of Corrosion. It is suggested that a corrosion case should be described at least by its form, the corrosion reactions and corrosion products. This can also include their

occurrence, mechanism, kinetics and the description of galvanic cells that intervene. When well described, this could be considered as a type or subtype of corrosion. A type of corrosion is expected to characterize, and describe more profoundly the circumstances leading to a corrosion or a failure of a certain material and complement the more vast divisions of the six forms of corrosion.

Modes of Corrosion. Fontana defined eight forms of corrosion, as general corrosion, pitting corrosion, intergranular corrosion, parting, galvanic corrosion, crevice corrosion, stress–corrosion cracking and erosion–corrosion.[15,16] In refining these eight forms, there are really two broad categories of modes of corrosion: Intrinsic and extrinsic. The intrinsic modes of corrosion which occur independent of design are:

- General corrosion
- Pitting
- Intergranular corrosion
- Parting
- Stress–corrosion cracking

The extrinsic modes affected by the design include:

- Crevice or under-deposit corrosion
- Galvanic corrosion
- Erosion–corrosion
- Fretting corrosion
- Corrosion fatigue

To further define the differences: within a crevice it is possible for any of the intrinsic modes to occur. For example, within a crevice it is possible to have general corrosion, pitting, intergranular corrosion while none of these is occurring on the free surface. Thus, there is no unique crevice corrosion; rather the intrinsic modes may occur within a crevice. From the point of view of design, the designer may elect to remove or minimize the crevice and thereby prevent these modes from occurring. The option to prevent the various intrinsic modes by reconsidering the extrinsic or design-dominated modes is the responsibility of the designer.[17,18]

6.6 The Morphology of Corroded Materials

In reality, the identification of one or more forms of corrosion requires visual observation, nondestructive inspection methods, optical microscopic examination, and sometimes electron scanning microscopy, etc. The first study of the corrosion appearance of a case should divide corrosion into uniform and localized corrosion. Localized corrosion can be further identified as macroscopic or microscopic local corrosion. Microscopic attack refers to a minute amount of dissolved metal, accompanied by considerable damage, before the phenomenon becomes visible to the naked eye.

Macroscopic forms of corrosion affect greater areas of corroded metal and are generally observable with the naked eye or can be viewed with the aid of a low-power magnifying device. Macroscopic examination can identify the following forms: galvanic, erosion–corrosion, crevice or pitting, exfoliation, and dealloying. Microscopic

examination can identify: intergranular corrosion, stress–corrosion cracking, corrosion fatigue, and subsurface corrosion (frequently observed at high temperature).[19]

Microscopy, in conjunction with other techniques, may be used to study different types of corrosion. For example, a scanning electron microscope is a valuable tool to differentiate intergranular stress corrosion cracking from hot-short cracking, and transgranular stress corrosion cracking from corrosion fatigue. Identification of the influence of the media needs more care. The effects of particulate matter in a stream may require microscopy to assess its influence combined with the flow pattern of water in erosion–corrosion. A biochemical analysis is required to identify the organism in bacterial corrosion. Subsurface corrosion in case of high-temperature corrosion needs special attention since observation by the naked eye of the surface could lead to faulty conclusion.[3]

6.7 Published Corrosion Data

The most desirable data are those obtained for the material of interest in the intended conditions of exposure. Such data are not readily available in the literature. Published data on atmospheric corrosion should be used with caution since atmospheric conditions are changing with time, as for example acid rain as a variable factor. Accelerated testing, including electrochemical tests, should have a good link with the natural and practical conditions. Published data should be consulted because they are generally useful. Some published data are mentioned here as examples since they are useful in selecting materials or discussion of case histories:

However, the performance data of alloys can vary from the reported or published data based on accelerated testing, for some reasons such as:

a. Impurities in the alloys
b. Impurities in the environment (natural or industrial); e.g., small amounts of copper in solution can deposit as metallic copper on aluminum or steel surfaces and accelerate corrosion
c. Suspended solids can give rise to erosion–corrosion, or corrosion–erosion, i.e., the intervention of other phenomenon associated with corrosion
d. Aeration and oxidants such as ferric and cupric ions; however, the most frequent cell is the oxygen differential aeration cell
e. Agitation and interfacial properties as solution pH at the interface and concentration in electrochemical and nonactive ions
f. Microorganisms in action which is frequently an important factor that has been overlooked by investigators or designers.

Examples of corrosion resistance of many metals and alloys in a variety of media and conditions that are available in the literature and given in the following books mentioned in the Bibliography: [NACE Graver ed., 1985; ASM International, 1995; Schweitzer, 1986; De Renzo, 1985*; McNaughton, 1980; ASM International, 1990; Climax Molybdenum Company, 1961].

*De Renzo (ed). Corrosion Resistant Materials (1985)

6.7.1 General Corrosion

Uniform and Quasi-Uniform Corrosion. Definition and Characteristics. The first and most common form of corrosion is general corrosion. This can be uniform (even) or quasi-uniform (near-uniform corrosion) or uneven general corrosion. General corrosion accounts for the greatest loss of metal or material. However, it is predictable and the designer can avoid catastrophic accidental corrosion problems. Generally, the galvanic abundant cell in corrosion is complex and corresponds to the dissolution of the active metal and oxygen reduction or hydrogen evolution on the cathode surface. Electrochemical general corrosion in aqueous media can include galvanic or bimetallic corrosion, atmospheric corrosion, stray-current dissolution, and biological corrosion.

Dissolution of steel or zinc in sulfuric or hydrochloric acid is a typical example of uniform electrochemical attack. Steel and copper alloys are more vulnerable to general corrosion than other alloys. Uniform corrosion often results from atmospheric exposure (polluted industrial environments); exposure in fresh, brackish, and salt waters; or exposure in soils and chemicals. The rusting of steel, the green patina on copper, tarnishing silver and white rust on zinc on atmospheric exposure are due to uniform corrosion.[14]

In such reactions as the tarnishing of silver in air, the oxidation of aluminum in air, or attack of lead in sulfate-containing environments, thin, tightly adherent protective films are formed, and the metal surface remains smooth. It should be mentioned that underground corrosion is frequently observed as localized corrosion. Oxidation, sulfidation, carburization, hydrogen effects, and hot corrosion can be considered as types of general corrosion.[20]

Liquid metals and molten salts at high temperature lead very frequently to general corrosion.[1] Micro-electrochemical cells result in uniform general corrosion. Dissolution of metals in acids is due to the presence of indistinguishable anodic and cathodic sites. Uniform general corrosion can be observed during chemical, electrochemical polishing, and passivity where anodic and cathodic sites are physically inseparable. A polished surface of a pure active metal immersed in a natural medium (atmosphere) can suffer from galvanic cells. Most of the time, the asperities act as anodes and the cavities as cathodes. If these anodic and cathodic sites are mobile and change in a continuous dynamic way, uniform or quasi-uniform corrosion is observed. If some anodic sites persist and are not covered by protective corrosion products or do not passivate, localized corrosion is observed.[1]

Some macro-electrochemical cells can cause a uniform or near-uniform general attack of certain regions. General uneven corrosion or quasi-uniform corrosion is observed in natural environments and is much more common. For some metals or alloys, uniform corrosion produces a somewhat rough surface by removal of a substantial amount of metal, which either dissolves in the environment or reacts with it to produce a loosely adherent, porous coating of corrosion products. As an example, following a careful removal of the rust after general atmospheric corrosion of steel, the surface reveals an undulated surface, indicating nonuniform attack of different areas (Figure 6.4.).[1] In natural atmospheres, the general corrosion of metals can be localized. The conductivity, ionic species, temperature of the electrolyte, alloy composition, phases and homogeneity in microstructure of the alloy, differential oxygenation cell, etc. can influence the

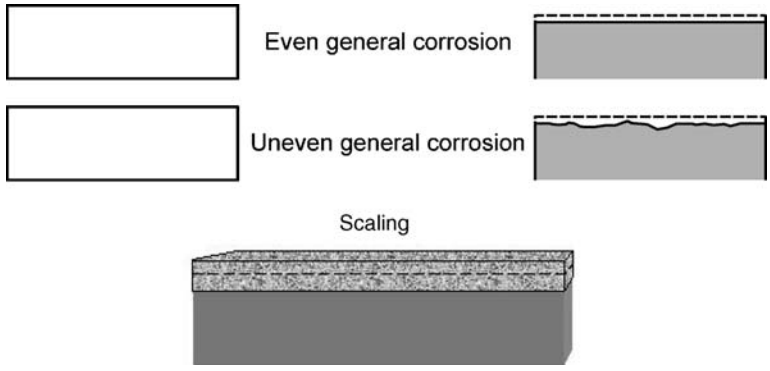

Figure 6.4 *Even and uneven general corrosion, and high-temperature attack (scaling)*[1,3]

corrosion morphology. Figure 6.4 also shows high-temperature attack, normally uniform. However, subsurface corrosion films within the matrix of the alloy can be observed by microscopic examination due to film formation at the interface of certain microstrucrures in several alloys at high temperature.[3]

Key Factors

1. The agitation of the medium or the level of agitation of the electrolyte has a great influence on the corrosion performance of most of the metallic alloys since agitation causes acceleration of diffusion of aggressive species or destruction of the passive layer mechanically.
2. Acid pH accelerates corrosion for most of the alloys, since, for an active metal such as iron or zinc, the cathodic reaction controls the rate of the reaction according to $E = E^0 - 0.0592$ pH. Figure 6.5 shows the Evans diagrams that can be obtained by extrapolation of the Tafel slopes for the cathodic and anodic polarisation curves (shown in Figure 6.1). In general, cathodic Tafel slopes are more reproducible and more reliable to evaluate corrosion rates since they represent the almost noncorroded or original state of the surface. It can be observed from Figure 6.5a that there is a marked increase in corrosion current for a more acidic solution. It should be noted that the influence of pH depends also on the composition of the alloy as shown in Figure 6.5b. In the case of zinc curve B, amalgamation with a more noble metal such as mercury decreases the corrosion rate in addition to the slower hydrogen evolution reaction which requires high overpotentials (curve A). Platinum gives high corrosion rates because it provides effective cathodic sites for hydrogen evolution (curve C). Another factor is the stability of the passive film of the system metal/solution in acid, neutral or alkaline pH. Magnesium fluoride is for example protective for magnesium in alkaline medium. Aluminum oxide is amphoteric and is stable[1] at pH ($\sim$4–8).
3. A difference in temperature in the case of copper tube at different temperatures can create a corrosion cell. Generally, the increase in temperature accelerates corrosion. For temperatures between 15 and 70°C, the rate of corrosion of steel in dilute acidic solutions can be doubled for every increase of 10°C. Above this range of

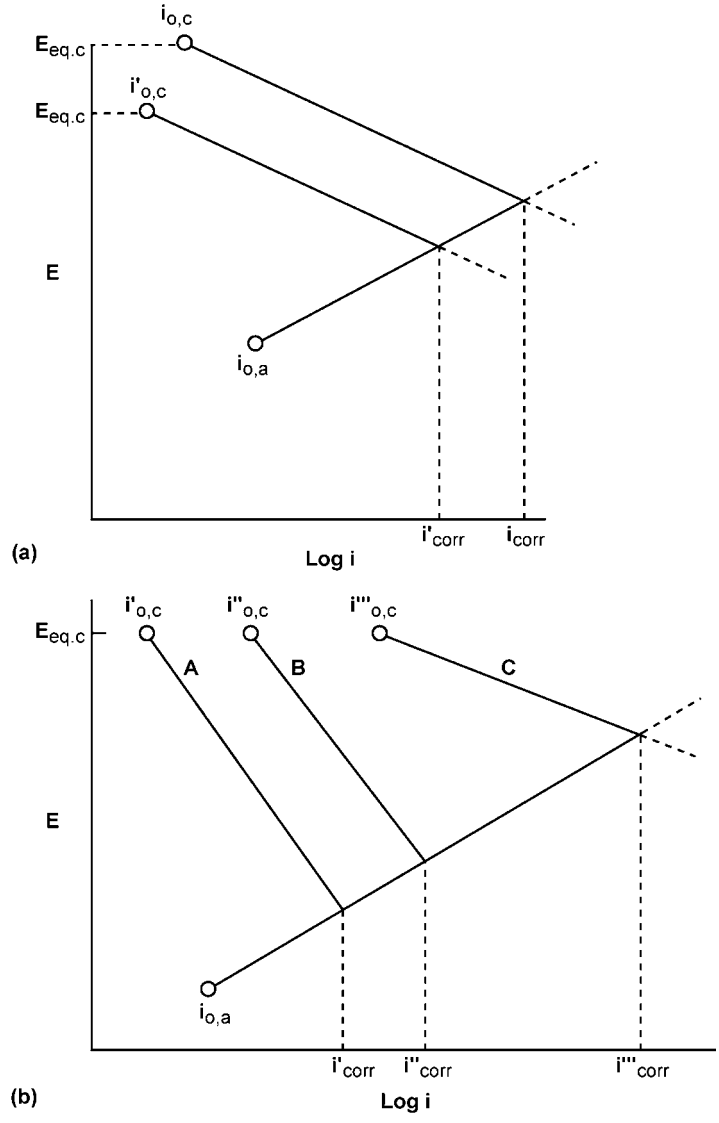

Figure 6.5 *Schematics of corrosion of zinc in deoxygenated solution as a function of: (a) pH and (b) composition of the alloy where A, B, and C correspond to the alloys Zn–Hg, Zn and Zn–Pt respectively*[25]

temperatures, the solubility of oxygen in water is low and the rate of corrosion cannot be doubled as before since oxygen has an accelerating effect on the cathodic reaction.

4. Protective passive films similar to that of stainless steel, for example, result in uniform corrosion because of the mobility of active sites that passivate readily. Corrosion products and/or passive films are characteristic of numerous electrochemical corrosion of alloys. A film is protective depending on coverage capacity, conductivity,

partial pressure, porosity, toughness, hardness and resistance to chemicals and gases. Rust (Fe) and white rust (Zn) are generally not protective, while patina (Cu), Al_2O_3, MgO and Cr_2O_3 are protective in certain environments. Corrosion is generally controlled by diffusion of active species through the film. The film free reaction is generally considered a chemical reaction. (Craig and Pohlman)[14]

Prevention of General Corrosion. Proper selection of materials. In design, a metal or alloy that forms a stable passive film should be recommended. A surface pretreatment in oxidized solutions has been adopted for stainless steels and is recommended in many circumstances. The most popular process 'a 300 min immersion in a 20 vol% nitric acid at 50°C' is recommended for some types of stainless steels.[21] The environment can be modified in the bulk and should be effective at the interface in adding oxidizing agents, such as nitrite or strong nitric acid, that maintain the passive state on some metals and alloys.[8]

Proper design and thickness considerations. Proper design is based on knowledge (Figure 6.6).

Landrum[22] suggested the following thickness of a tank wall (steel) based on 10-yr useful life based on the predicted general corrosion rate:

1. Specify wall thickness for mechanical considerations	5 mm
2. Expected life (10 yr) and uniform corrosion rate 0.4 mm/yr	4 mm
3. Safety considerations (100% of the total corrosion rate)	4 mm
Recommended thickness	$\Rightarrow$ 13 mm

Corrosion control. Generally corrosion inhibitors, cathodic protection, anodic protection, and coatings are used for this purpose or combination of them. However, cathodic protection is the only method that avoids corrosion completely if the system is not sensitive to hydrogen embrittlement or alkaline medium. Anodic protection is a recent approach when the metal can be passivated in the corrosive solution. In this technique, a current can be applied using a potentiostat, which can set and control the potential at a value greater than the passive potential E_p or below the pitting potential E_{pit} for environments containing corrosive species such as chlorides, bromides, etc.

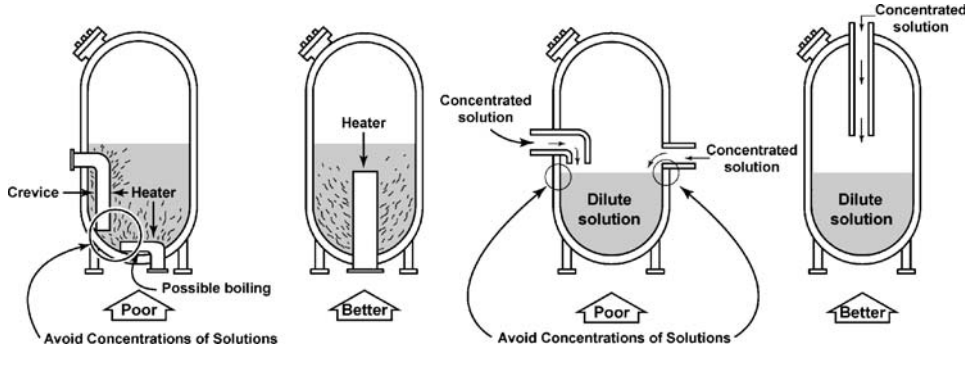

Figure 6.6 *Comparison between a good and bad design of a boiler tank*[173]

6.7.2 Galvanic Corrosion

Formation of a Galvanic Cell. When a metal or alloy is electrically coupled to another metal or conducting nonmetal in the same electrolyte, a galvanic cell is created. The electromotive force and current of the galvanic cell depend on the properties of the electrolyte and polarization characteristics of anodic and cathodic reactions. The term galvanic corrosion has been employed to identify the corrosion caused by the contact between two metals or conductors with different potentials. It is also called dissimilar metallic corrosion or bimetallic corrosion where metal is the conductor material.

Galvanic corrosion can lead to general corrosion, localized corrosion and sometimes both. Although the dissolution of active metals in acids is due to the presence of numerous galvanic cells on the same metallic surface, it is generally referred to as general corrosion. However, in less aggressive media, such as some natural media (dissimilar electrode cells), galvanic corrosion can start as a general corrosion that can be lead to localized corrosion because of different microstructures or impurities in several cases. Local galvanic attack depends on the distribution and morphology of metallic phases, solution properties, agitation, temperature etc. Localized galvanic corrosion case generally results in perforation or failure of the structure. The following are some factors that lead to general or localized corrosion:

Dissimilar metals. Galvanic corrosion occurs when two metals with different electrochemical potentials are in contact in the same solution [Figures 6.7 and 6.8]. In both cases, the corrosion of iron (steel) is exothermic and the cathodic reaction is controlling the corrosion rate. The more noble metal, copper increases the corrosion through cathodic reaction of hydrogen ion reduction and hydrogen evolution A passive oxide film on stainless steel for example can accelerate hydrogen reduction reaction.

In engineering design, a junction of two different metals is seldom recommended. Sometimes, alloys with close values of potentials in a certain medium can be used. However, mechanical shaping, bending, or lamination of a part of the metal, thermal treatment of a part of a metallic structure, welding, cooling coils in vessels, and heat exchangers can create galvanic cells in the same metal. Sometimes, these electrochemical cells are called macrogalvanic cells to distinguish them from the microgalvanic cells which are present on even pure metals in a corrosive medium.[22] (Baboian)[5]

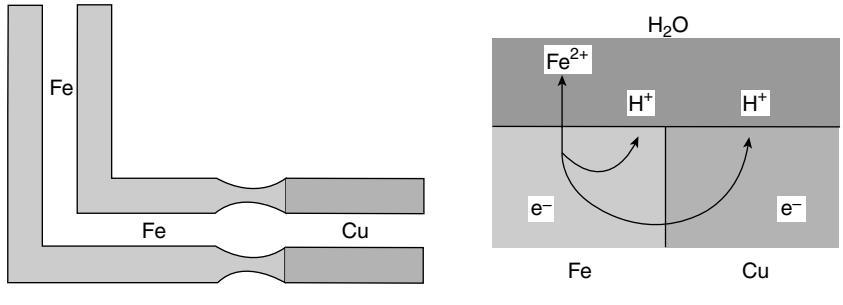

Figure 6.7 *A schematic presentation of galvanic corrosion of a mild steel elbow fixed to a copper pipe*[22]

Figure 6.8 *Glavanic corrosion of painted steel auto body panel in contact with stainless steel wheel opening molding (Baboian)*[5]

Generally, the galvanic cell is influenced by: (i) the difference of potential between the two materials; (ii) the nature of the environment; (iii) the polarization of every metal; and (iv) the geometry of the anodic and cathodic sites (shape, relative surface areas, distance, etc.). For example, it is not desirable to have a structure containing a small anode connected to a large cathode since the anodic dissolution will be localized and enormously accelerated. Figure 6.9a shows rivets of copper on a steel plate (on the left) and steel rivets on a copper plate (on the right). After 15 months immersion in sea water, the steel plate was covered by corrosion products while the rivets in Figure 6.9b

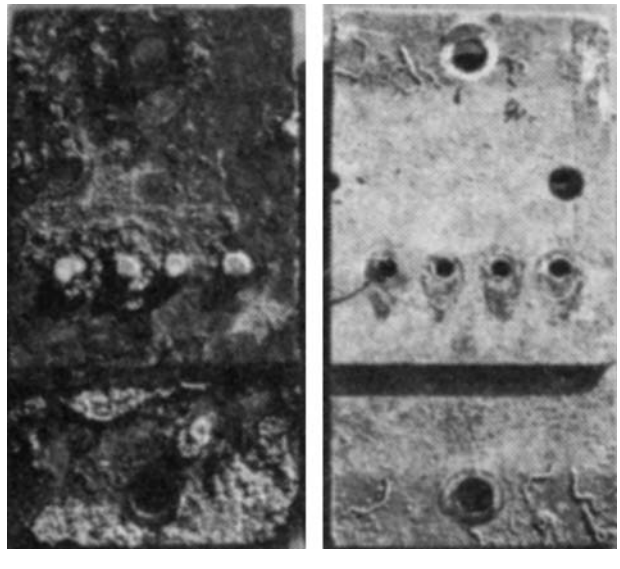

Figure 6.9 *Area effect of the galvanic corrosion cell on (a) steel and (b) copper plates*[16]

corroded and disappeared completely. The copper is more noble and accelerated the hydrogen reduction reaction for the oxidation of the steel plate. In the case of copper plate, severe corrosion of the steel rivets was observed because of the relative important cathodic surface of copper. The same reasoning is valid for the corrosion of the limited noncoated parts in the auto body panel in contact with the important large surface of stainless steel in Figure 6.8.

Nonmetallic conductors and corrosion products. Carbon brick in vessels is strongly cathodic to the common structural alloys. Impervious graphite, especially in heat-exchangers, is cathodic to structural steel. Carbon-filled polymers can act as active cathodes. Some oxides or sulfates are conductors, such as mill scale (magnetite Fe_3O_4), iron sulfides on steel, lead sulfate on lead can act as effective cathodes with an important area to that of the anodes. Very frequently, the pores of the conductive film are the preferable anodic sites that leads to localized corrosion (pitting).[5]

Metallic coatings and sacrificial anodes. Sacrificial metal coatings provide cathodic protection for base metal, such as galvanized steel or Alclad aluminum. If the metal coating is more noble than a base metal, such as nickel on steel, pitting of the base metal can occur at pores, damage sites, and edges (Figure 6.10). Care should be taken to keep the coat free of pores, scratches or any penetrating chemical attack or deterioration of the coat (a paint for example). Sacrificial anodes, such as magnesium, zinc, and aluminum are used extensively for cathodic protection, especially in some urban locations where impressed-current systems are forbidden because of stray currents.

Polarity inversion. The properties of the electrolyte (pH, potential, temperature, fluid flow, concentration of different ions, dissolved gases and conductivity) can change with time and influence polarization, the properties of the interface and the galvanic potential of every component. For example the change of the ion activity of one metal can reverse the polarity of Fe–Sn couple for iron-plated tin in food media. (Hack)[5]. This shows the importance of the medium in galvanic corrosion where the canned food boxes are made of iron and coated inside with a protective layer of tin. The tin sometimes reacts with some constituents of food and forms a soluble complex. The concentration of tin could correspond then to some ppm and, applying the Nernst equation, the tin potential becomes more active or anodic to that of iron and corrodes intensively. Also, iron is protected by a zinc coating as a sacrificial anode (galvanization) because of the formation of loose flocculent $Zn(OH)_2$ (white rust), however at temperatures above $>60°C$ a hard compact ZnO layer is formed, which is cathodic to

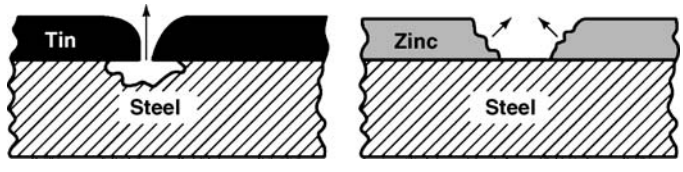

Figure 6.10 *Perforation in the coating gives rise to localized attack of steel (left) or consumption of the sacrificial Zn (right)*[16]

iron and this layer is able to reverse the polarity sign of the couple Fe–Zn. This is observed for other couples such as copper on aluminum or silver on copper.[7,16,20]

Deposition corrosion. Dissimilar metallic corrosion can occur due to the cementation of a more noble metal. If soft acid water (containing carbonic acid) flows through copper pipes and into a galvanized tank, any dissolved copper ions can be deposited in the tank according to the equation $Cu^{2+} + Zn \rightarrow Cu + Zn^{2+}$ and this causes additional galvanic corrosion of zinc.[20] Severe corrosion may occur for active aluminum or magnesium alloys, for example in neutral solutions of salts of heavy metals, such as copper, iron, and nickel. Such corrosion occurs when the heavy metal, the heavy metal basic salts, or both, plate out to form active cathodes on the anodic magnesium surface. This is a type of galvanic corrosion that leads typically to localized pitting corrosion.

Hydrogen cracking or damage. Self-tapping of martensitic stainless steel screws has been observed due to a spontaneous quick cracking of the screws after being attached to an aluminum roof in a seacoast atmosphere (anodic surface). Similarly, hardened martensitic stainless steel propellers coupled to the steel hull of a ship have failed by cracking soon after being placed in service. Tantalum is readily embrittled by hydrogen at room temperature when the metal is cathodically polarized, or when coupled in an electrolyte to a more active metal in the galvanic series.[7]

High-temperature galvanic corrosion. Galvanic coupling at high temperature affects the corrosion rate. The reaction of silver with gaseous iodine at 174°C in 1 atm oxygen, for example, is accelerated by contact of silver with tantalum, platinum, or graphite.[7]

Factors Involved in Galvanic Corrosion. Emf series and 'practical nobility' of metals and metalloids. The emf. series is a list of half-cell potentials proportional to the free energy changes of the corresponding reversible half-cell reactions for standard state of unit activity with respect to the standard hydrogen electrode (SHE). This is also known as Nernst scale of 'solution potentials' since it allows to classification of the metals in order of 'nobility' according to the value of the equilibrium potential of their reaction of dissolution in the standard state (1 g ion/l). This 'thermodynamic nobility' can differ from 'practical nobility' due to the formation of a passive layer and electrochemical kinetics.

Ignoring the kinetic factors and assuming as a first approximation that the passivating films are perfectly protective, practical nobility depends on the immunity and passivation domains and the stability domain of water. In the case of identical surfaces for some metals, it is accepted that this 'practical nobility' is greater the more the immunity and passivation domains extend below and above the stability domain of water, and the more these domains overlap the section of the diagrams corresponding to pH values between 4 and 10, which are most common in practice. Table 6.2 shows the classification of 43 elements on one hand according to 'thermodynamic nobility' and on the other, according to 'practical nobility'. This table shows the ennobling effect which passivation has on niobium, tantalum, titanium, gallium, zirconium, hafnium, beryllium, aluminium, indium and chromium. This must be regarded as guide since the electrochemical equilibrium diagrams are themselves approximations and in some cases necessitate drastic alteration (e.g., those for nickel and cobalt, and because corrosion and/or passivation reactions are sometimes strongly irreversible).[23]

Table 6.2 *Emf series of some elements and classification of metals and metalloids in order of nobility*[23]

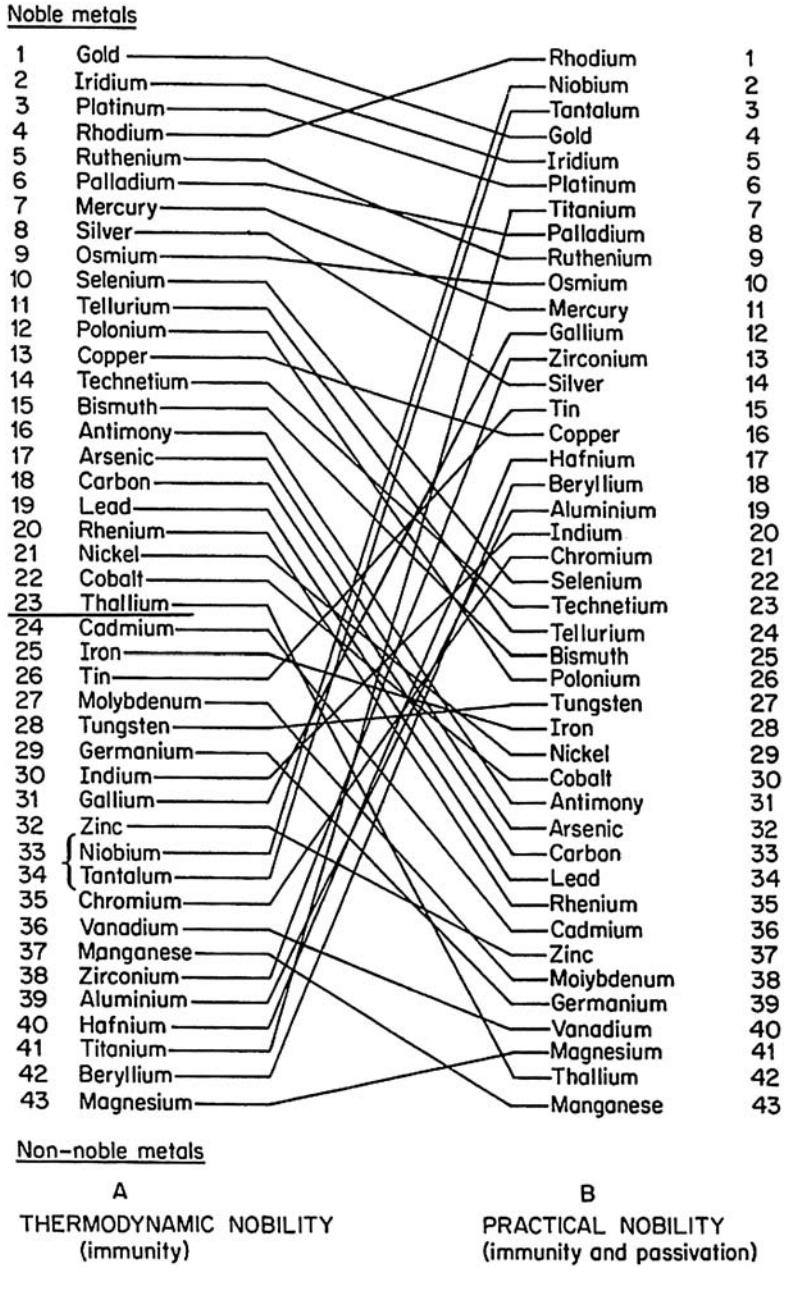

The galvanic series and corrosion. The practical change of the potential of every component of a galvanic couple as a function of time is of major importance. If the potential difference between the two metals is sufficient to create a sustained galvanic cell, the potential of every material or electrode can be subjected to certain changes because of the active–passive behavior, the properties of the passive or corrosion barriers and the change in the ion concentrations etc. The galvanic series is a list of corrosion potentials, each of which is formed by polarization of two or more half-cell reactions to a common mixed potential E_{corr}, measured with respect to a reference electrode such as calomel electrode. Figure 6.11 shows the galvanic series of some metals and alloys in seawater. The material with the most negative potential has a tendency to corrode when connected to a material with a more positive or noble potential. Some alloys in this medium can have active and passive potentials and sometimes a potential between these two extremes. (Hack)[5] The galvanic series thus gives qualitative indications of the likelihood of galvanic corrosion in a given medium under certain environmental conditions.

The properties of the interface metal/solution. Cast iron corrodes because of exposure of its graphite to the surface (graphitic corrosion), which is cathodic to both low-alloy and mild steels. The trim of a valve must always maintain dimensional accuracy and be free of pitting and hence it should stay cathodic to the valve body. Hence, in aggressive media, valve bodies are frequently chosen of steel rather than cast iron. Because of increased anodic polarization, low-alloy steel (Cr and Ni as noble components) is cathodic to normal steel in most natural media. Accordingly, steel bolts and nuts coupled to underground mild steel pipes, or a weld rod used for steel plates on the hull of a ship, should always be of a low-nickel, low chromium steel or from a similar composition to that of the steel pipe.[7]

The potential difference developed between aluminium and stainless steel is about the same as that developed between aluminium and copper. The cathodic reaction is easier on copper oxide than that on the highly protective passive oxide of stainless steels. Then, it is not the difference of potential between anode and cathode which counts, but the facility and rate of every reaction. A bare metal is generally a much better cathode than one covered with an oxide. Aluminium is more active than zinc in the electrochemical series. Practically, zinc protects aluminium which becomes covered with an oxide film.[20] All more noble metals accelerate corrosion similarly, except when a surface film (e.g., on lead) acts as a barrier to diffusion of oxygen or when the metal is a poor catalyst for reduction of oxygen.

Polarization of the galvanic cell. The different phenomena of polarization of the anodic and cathodic reactions (activation, diffusion, convection, etc.), should be well known as a function of the evolution and change of the properties of the interface as a function of time. The polarization behavior of the cathodic and anodic reactions on the two electrodes should be examined (see Figure 6.5). In natural atmospheres, the cathodic reaction controls frequently the attack rate. The diffusion of oxygen is an important parameter to avoid control and polarization of the corrosion by the rate of the cathodic reaction (Figure 6.12).[7]

The resistance overpotential of the cell IR is mainly a function of the solution conductivity of the electrolyte and the distance between the electrodes since the electrolytic resistivity is far more important than the electric resistance of metals.

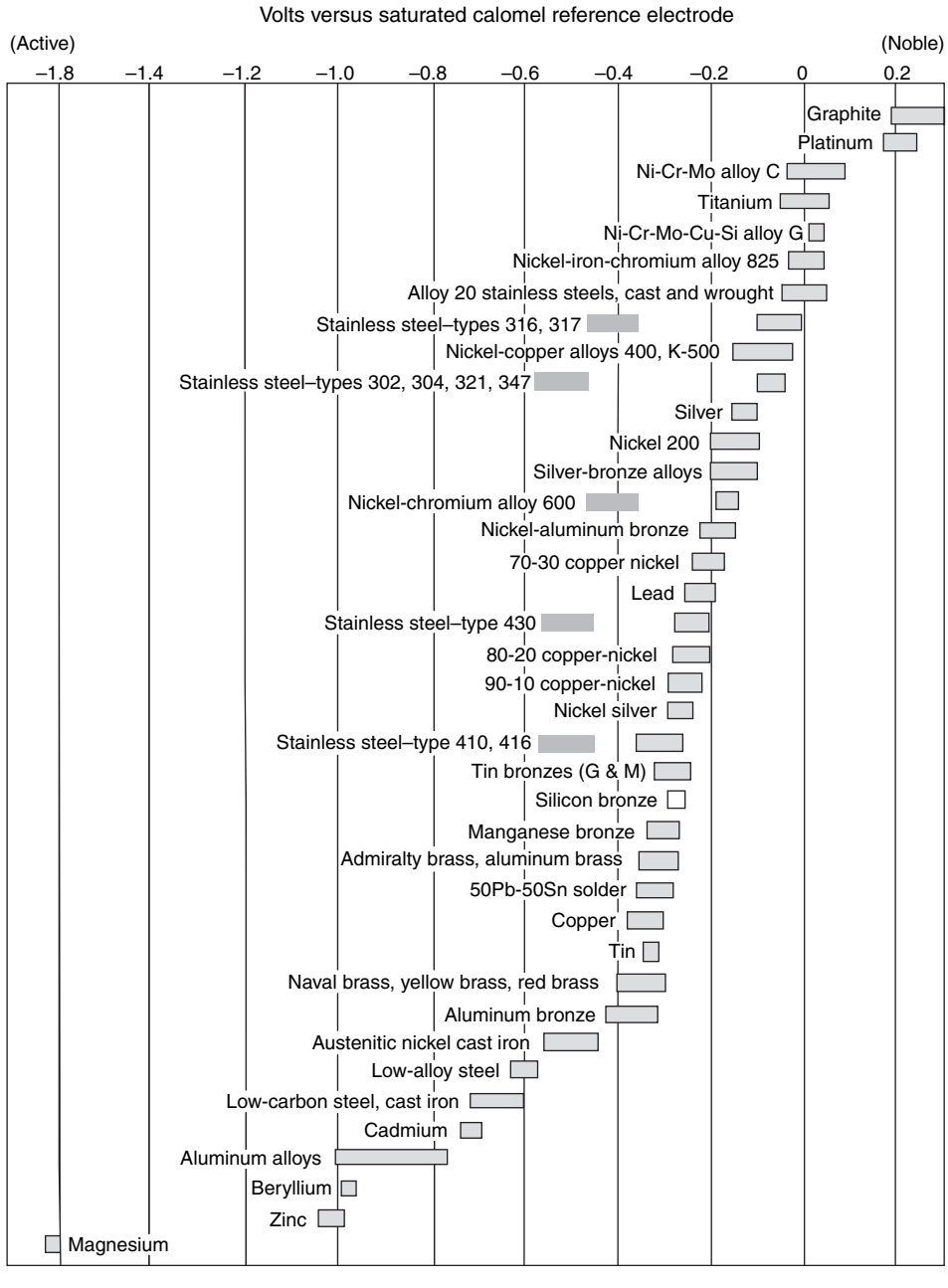

Figure 6.11 *Galvanic series for some metals in seawater (Hack)*[5]

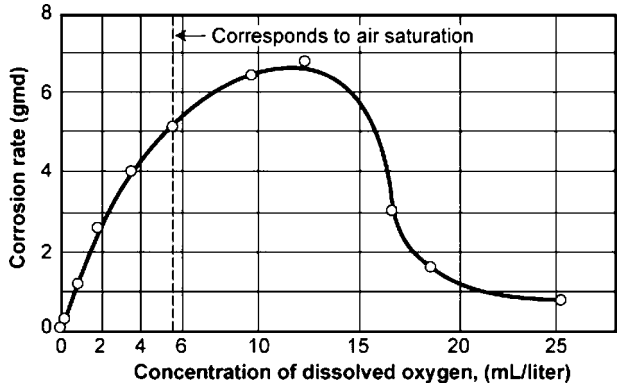

Figure 6.12 *Effect of oxygen concentration on corrosion of mild steel[7] in slowly moving distilled water, 48 h test, 25°C*

Thus, if dissimilar pipes are butt-welded with the electrolyte flowing through them, the most severe corrosion will occur adjacent to the weld on the active metal. The current of the galvanic cell takes the path of least resistance and this affects corrosion in that current does not readily flow around corners. In soft water, the critical distance between copper and iron may be 5 mm; in seawater it may be several decimeters. The critical distance is greater the larger the potential difference between anode and cathode. Then, the geometry of the circuit affects galvanic corrosion and this is observed in the case of stray current corrosion.[7] (Baboian)[5]

The relative area of the anodic to cathodic sites is critical for general and/or localized attack. This parameter, together with the conductivity of the electrolyte can control the corrosion rate. If the surface area of the anode is relatively small compared with that of the cathode, and the electrolyte has a low conductivity, uniform corrosion can be change to quasi-uniform corrosion, to severe pitting or to other types of localized corrosion of the alloy. Since the diffusion of oxygen is frequently the rate-determining factor in aqueous corrosion, large cathode/anode area ratios will frequently result in intense galvanic attack.[20]

For the case where diffusion of the corrosive ions is the rate controlling reaction, it has been found that $P = p_0\ (1 + A_c/A_a)$ where p is the penetration that is proportional to the corrosion rate and p_0 is the corrosion rate of the less noble uncoupled metal A_c and A_a are the areas of the more noble and active metal respectively (Uhlig and Revie, pp. 101–103).[7] If a galvanic cell is not avoidable, a large anode and a limited size of cathode are recommended. Stagnant conditions and weak electrolytes may lead to pitting in spite of the large area of the exposed active metal.

The following example illustrates the effect of the relative areas of anodic to cathodic surfaces. Reservoirs made of steel covered with a phenolic paint and the bottom clad with stainless steel were intended to handle mild corrosive solutions for steel. A few months later, perforation of the steel wall started at approximately 5 cm away from the weld of steel wall close to the stainless steel bottom (Figure 6.13).[16] Large cathodes and small anodic surfaces should be avoided since there is no perfect coating, and the paint on steel

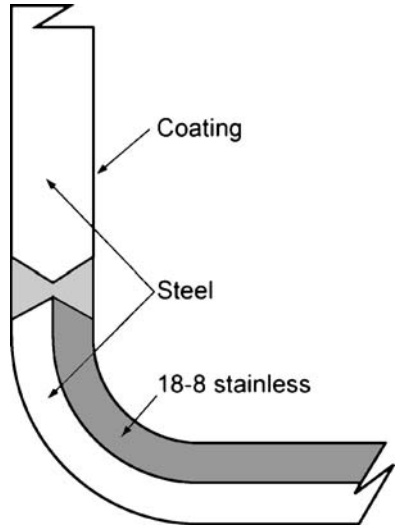

Figure 6.13 *Perforation of coated steel due to pores and large cathodic surface at the bottom clad steel*[16]

has always some defects and the pores act as small anodic surfaces close to the stainless steel bottom (big cathode). The corrosion current (microampere/cm^2) can be multiplied by a factor of 10–20, leading to a quick penetration of the anodic sites. In other words, the cathodic control which limits the corrosion current in several aqueous solutions is not operational. This failure also shows the effect of the distance since the perforation was observed near the welding junction, especially in low-conducting solutions.

Prevention of Galvanic Corrosion. Galvanic corrosion can be prevented or reduced by:

1. Avoid contact between metals with different potentials. Complete isolation of one from the other should be made and inspected periodically. To predict or avoid galvanic corrosion, the potential of every metal or conductor should be evaluated as a function of time in the intended medium. The variation of the properties at the interface should be carefully evaluated as a function of time.
2. Protection by metallic, nonmetallic, nonorganic, organic (paints, lacquer, etc.) coatings is recommended. If the metal coating is more noble than the base metal, care should be taken to have a coating free of pores. Applying a sacrificial coating such as Al, Zn, Mg or Cd to an active metal is recommended. Also, adding a paint layer to sacrificial zinc coating, for example, can extend the life by a factor of ten. Applying nonmetallic coatings as anodic films should be accompanied by sealing to avoid the small bare surfaces.
3. Large cathodes and small anodic surfaces should be avoided. The current practice considers coating of the more noble surface first, and preferably both cathodic and anodic surfaces. Such effects of large cathodes and small anodes are most likely to occur at joints of structures joined together by a different metal. They can be avoided by plating, e.g., with zinc or any other metal, provided that the new couple is safer.[20]

4. Electrochemical testing and determination of polarization characteristics of every component are recommended. If one of the metals has active–passive behavior, the state of the contact material should be considered for the expected active and passive states. Both Pourbaix pH diagrams and the potential of the passive metal or alloy can be helpful for this purpose. Bacterial corrosion in case of intended media and conditions should be investigated.
5. The use of corrosion inhibitors in appropriate concentrations could improve the corrosion resistance through different mechanisms of adsorption, barrier film, etc.
6. Prediction of the anodic and cathodic components of the galvanic cell and inversion of polarity of the cell should be considered.
7. Cathodic protection offers the only complete protection of the metallic surface, however, the metal should not be sensitive to fragility or attack in alkaline medium.

Testing of Galvanic Corrosion. Corrosion testing for galvanic corrosion can be predicted specifically by ASTM standards in the form of potential measurements. In general, the corrosion potential difference between anode and cathode becomes the driving force for galvanic corrosion. Galvanic corrosion tests between different metals or microstructures can be accomplished in acid or neutral chloride solutions containing hundreds of ppm Cl^- up to 5% Cl^- ion at ambient laboratory temperature or at the desired temperature to examine the galvanic effect of different materials. The galvanic currents are measured between two dissimilar metals using a zero resistance ammeter (ZRA) for an appropriate duration. The ratio of the anode to the cathode areas of the specimen is generally 1:1 or adjusted to the projected use. Agitation or circulation of the electrolyte should be as in the conditions of the projected use.

Stray-current Corrosion. Stray currents in the past have resulted from DC-powered trolled systems, which have become obsolete. An electric welding machine on board a ship with a grounded DC line located on shore will cause accelerated attack of the ship's hull as the stray currents generated at the welding electrodes pass out of the ship's hull through the water back to the shore. Houses in close proximity can dramatically corrode at the waterline. The pipes in one house can be completely corroded, while those in the neighboring house may be intact.

The major stray-current corrosion problems now result in cathodic protection systems. Current from an impressed-current cathodic protection system will pass through the metal of a neighboring pipeline at some distance before it returns to the protected surface. Increased anodic corrosion is frequently localized on the pipe at the zone where the current leaves the pipe back to the protected steel tank.

Stray current flowing along a pipeline very frequently will not cause damage inside the pipe, because of the high conductivity of the electric path compared with the electrolytic one. The damage occurs when the current re-enters the electrolyte and will be localized on the outside surface of the metal. If the pipe has insulated joints and the stray current enters the internal fluid, the corrosion will be localized on the internal side of the pipe. The best solution is the electrical bonding of nearby structure and adding as required additional anodes and possibly increasing rectifier capacity.[24] (Craig)[5]

Stray currents follow paths other than their intended circuit. They leave their principal path because of poor electrical connections or poor insulation around the intended conductive material. The escaped current then will pass through the soil, water or any

other suitable electrolyte to find a low buried path such as a metallic pipe. Stray currents cause accelerated corrosion when they leave the metal structure and enter the surrounding electrolyte. These sites can be hundreds of meters away or more.

At points where the current enters the structure, the site will become cathodic in nature because of changes in potential, while the area where the current leaves the metal will become anodic. Electric railways, cathodic protection, electrical welding machines, and grounded DC electrical sources are subject to stray current corrosion. (Craig)[5]

Although the damage of stray current is always localized in a part of the system, stray current may lead to uniform corrosion of this part of the system, and so this is considered as a general form of corrosion although, the attack by stray current is generally more localized, causing in certain circumstances a concentration of pits. Stray-current corrosion can show penetration along the grain boundaries or a selective attack of the ferrite within the matrix of gray cast iron. Aluminum and zinc (amphoteric metals) can show signs of corrosion at the cathodic portion of the metal because of the localized alkalinity. Buried power lines can give rise to AC stray currents. Basically, alternating current causes less damage than DC, the stray current corrosion decreasing with increase in the frequency. However, damage to passive alloys such as stainless steel and aluminum alloys is important because of the alternating reduction and oxidation of the passive or barrier layer on the surface and which may lead to porous and non protective passive layers. (Craig)[5]

Prevention of stray-current corrosion. Measurement of the current before it enters the soil as around the electrolyte can monitor escaping current. The current leakage from the metallic structure to the ground should be stopped by good electrical connections and insulation. Bonding consists of connecting the stray-current conductor with the source ground via a separate conductor and thus eliminating the need for the current to leave the metal and enter the soil. Sacrificial anodes can be used to prevent stray-current corrosion. Insulation should be applied with care and should be sufficient to make the current sufficiently small. Coatings are not suitable since cracks, pinholes or pores will accelerate localized corrosion. However coatings on cathodically protected structures are beneficial and usually make the problems of stray current less severe and more easily controlled. Figure 6.14 illustrates two close underground structures designed to avoid stray-current corrosion. (Hanson)[5]

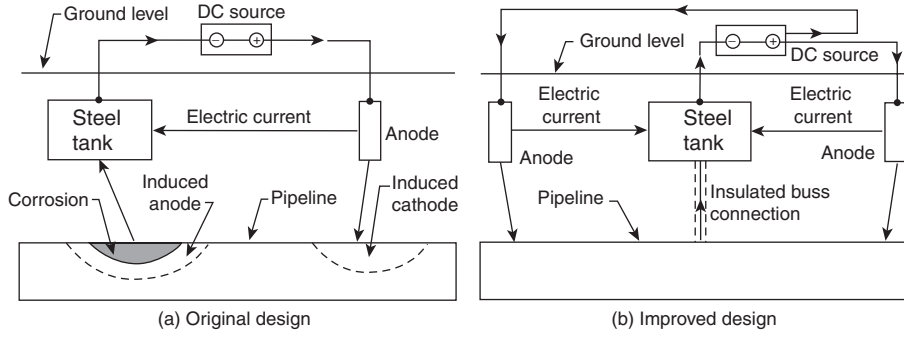

Figure 6.14 *Localized corrosion of (a) unprotected buried pipeline and (b) an improved design including cathodic protection of both tank and pipeline(Hanson)[5]*

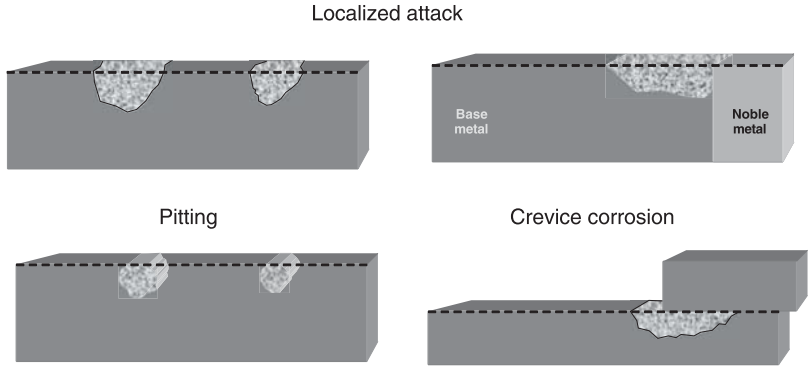

Figure 6.15 *Some morphologies and types of localized corrosion*[3]

6.7.3 Localized Corrosion

This is the most insidious corrosion because it is by far less predictable than general corrosion and can have serious consequences such as total failure. All forms of general corrosion that result in a nonuniform surface can be considered as localized corrosion. Figure 6.15 shows the various types of localized corrosion.

The two major types of localized corrosion discussed are pitting corrosion, and crevice corrosion including filiform corrosion. In spite of the different morphological appearance of these two types of corrosion (Figure 6.15), the electrochemical basis of these two types are almost the same. The difference may rise from different causes in the initiation step of pitting or crevice corrosion.[25]

Pitting Corrosion. Pitting corrosion may be caused by a number of factors such as mill scale, which is a very common form of pitting corrosion of steel. Areas where a brass valve is incorporated into steel or galvanized pipeline serve as good examples. The junction between the two areas is often pitted, and if the pipe is threaded, the thread in close contact with the brass valve rapidly pits, causing a leak. This occurs frequently in industry, as well as in homes and farms. The deep pitting of tankers on the horizontal surfaces of cargo ballast tanks is a particularly aggravated type of pitting (i.e., pits are deep and frequent). In this case, pits are caused by frequent changes of cargo and salt water which perpetrate the oxidation reduction corrosion cycle.[26]

Pitting can also occur under atmospheric conditions. The corrosion starts at the break and continues to undercut the coating, forming a rather heavy tubercle of hard rust or scale with the pit underneath the original metal. The corrosion products help to isolate the aggressive medium inside the pit. These are common in marine environments as well as various industries where strong corrosive conditions exist.[26] Also, pits with their mouth open (uncovered) exist and are responsible for loss of thickness and can act as stress raisers.

Pitting is often a concern in applications involving passivating metals and alloys in aggressive environments. It can also occur in nonpassive alloys with protective coatings or in certain heterogeneous corrosive media. (Sprowls)[14] Although in appearance pitting corrosion may seem unimportant, the depth of the pit and pit propagation rate are extremely dangerous and one of most serious types of corrosion. When the active state

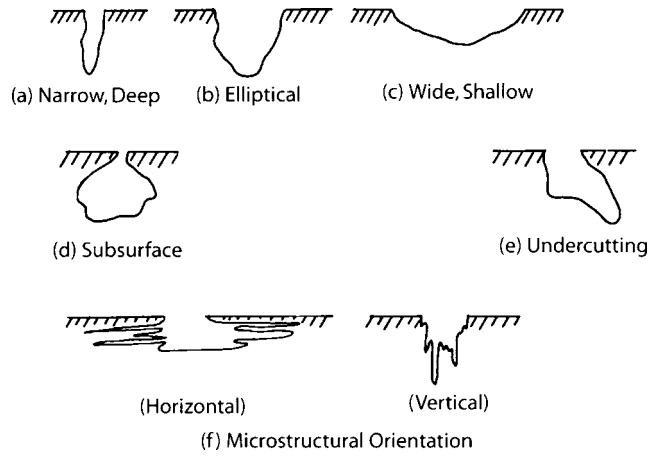

Figure 6.16 *Frequent variations of the cross-sectional shape of the pits (ASTM G46-94)*[4]

within pits and crevices is maintained over an extended period of time, rapid metal dissolution usually occurs. The resulting pit and crevice geometries as well as the surface state within the pits vary markedly from open and polished hemispherical pits on free surfaces to etched crack-like shapes within crevices, depending largely on the type of rate-controlling reactions during the growth stage.[27] Stress–corrosion cracking, and fatigue corrosion may result from pitting. Figure 6.16 shows the influence of three shapes of pits and the extent of undercutting or subsurface corrosion as well as the influence of the microstructure on the orientation of the grain attack. (ASTM G46)[4]

Mechanism of formation. The initiation of pitting starts at the defects in the passive film such as thinning, rupture, scratch, pore, etc. These sites are anodic in relation to the remainder of the surface that leads to the dissolution of metal. Once the process of dissolution starts, the dissolution does not need to be stimulated anymore because the process is generally autocatalytic. Although, in certain cases the propagation can be mitigated, in a temporary or permanent way, if some impervious products precipitate on the active sites or due to some other factors such as the rates of pit growth compared with that of repassivation, or a difference in the microstructure of the alloy, etc. The anodic zone limits itself to a specific area, on a point and leads to deep perforation. Pits usually grow gravitationally.

The mechanism of pitting is depicted in Fig. 6.17. It is self-initiating and self-propagating. The initiation of the pit can be caused by a discontinuity in the film, an impurity, different phase or a scratch, etc. For example, active metal, immersed in an oxygenated solution of NaCl, dissolves itself in the pit and the oxygen goes close to the pit. The positive charge of dissolved cations attracts chloride ions from the solution inside the pit. There is metal chloride formation and hydrolysis of these chlorides that leads to form H^+ and Cl^-, accelerating the metal dissolution:

$$M^+ + Cl^- \rightarrow MCl$$

$$MCl + H_2O \rightarrow MOH + HCl$$

$$HCl \rightarrow H^+ + Cl^-$$

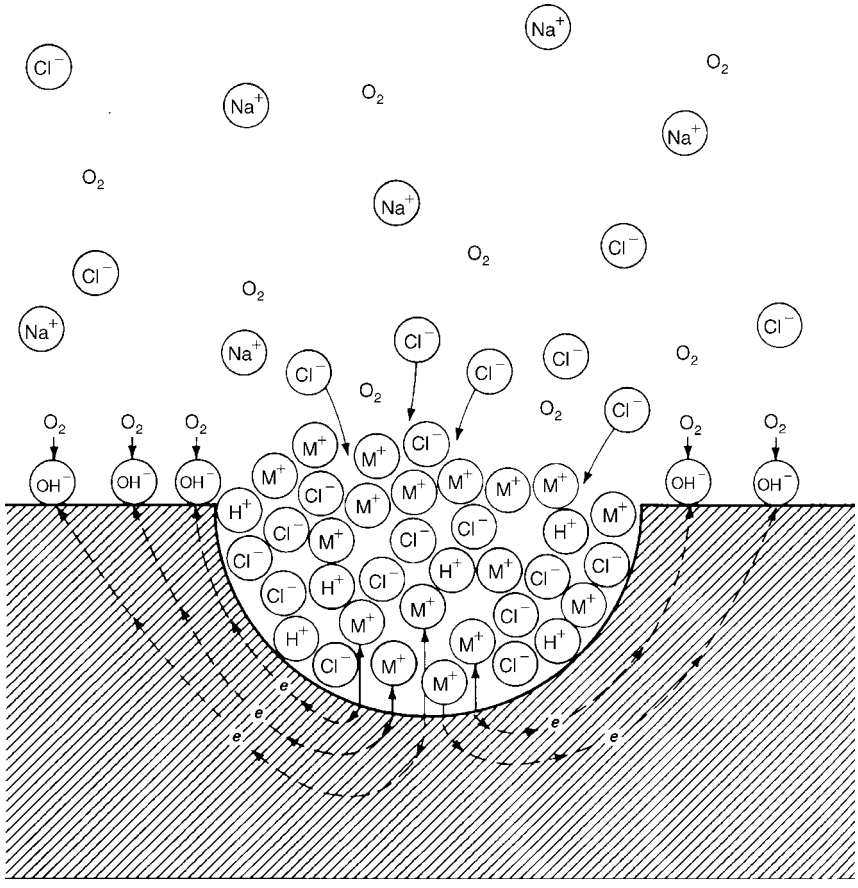

Figure 6.17 *Mechanism of pitting corrosion (Frankel)*[5]

The pH changes during pitting corrosion can arise from two different reduction reactions; reduction of dissolved oxygen and that of hydrogen ions. If the metal hydroxide precipitates at the mouth or the sides of the pit, this can help the autocatalytic nature of penetration of the pit. The rust tubercules on cast iron indicate that pitting is in progress, and the environment inside the rust bubble has been found lower in pH and higher in chlorides than outside the bubble.

Figure 6.18 shows the corrosion of iron. It represents a section of the pit and a growing pit inside the metal. The pitting factor $= P/d$ considers the deepest pit compared with the uniform corrosion loss (Figure 6.19). However to characterise the pitting phenomenon statistically, it is recommended to take the average of the deepest 10 pits as recommended in ASTM G48.[4]

There are two distinct processes before stable pit formation occurs: pit nucleation and growth of the metastable pit; and the pit precursors or metastable pits cannot grow until a pitting potential is reached.[28] There are many examples of pitting in practice as follows:

Underground structures and pitting. The bottom of a metallic pipe or hose buried in the earth, with a relatively limited surface of metal poorly aerated, has the tendency to

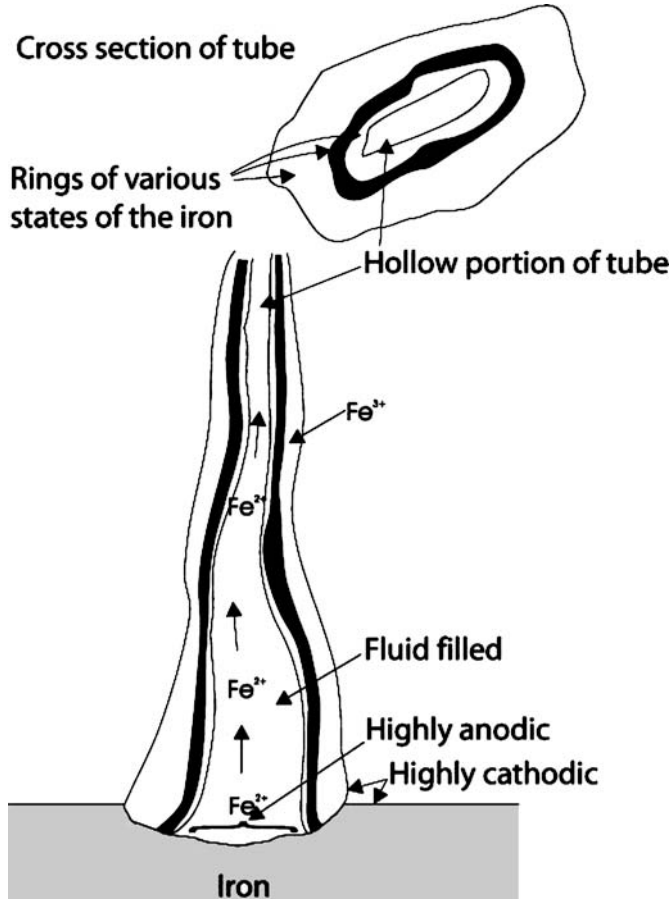

Figure 6.18 *Mechanism of iron corrosion*[16]

become anodic in relation to the large aerated surface of the rest of the metal. During the periodic verification of underground tanks or pipes, etc., the bottom of the buried metallic pipe in soil should be checked since it is vulnerable to the oxygen differential cell in its outermost performance.

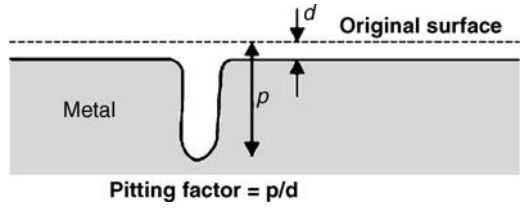

Figure 6.19 *The deepest pit in relation with the penetration in metal and the pitting factor*[7]

Mill scale (rust) and pitting. The three layers of iron oxide scale formed on steel during rolling vary with the operation performed and the rolling temperature. When mill scale is placed in an electrolyte, any defect in the mill scale surface becomes the anode; the remainder of the mill scale, which is usually many times larger than the defect, becomes a very strong cathode. An electric current can easily be produced between the steel and the mill scale. This electrochemical action will corrode the steel without affecting the mill scale.

The thickness of the mill scale depends upon the final rolling conditions and can be ~0.051–0.51 mm. The main composition is FeO and Fe_2O_3 having Fe_3O_4 as intermediate (magnetic). FeO can be mixed with the surface crystalline structure, unstable and oxidizes to ferric accompanied by increase in volume. Also, the black magnetite Fe_3O_4 can be converted to Fe_2O_3 (rust). This becomes loose and creates a galvanic cell having an electromotive force of 200–300 mV, similar to copper/steel couple.[29] The initial stages of pitting and the e.m.f. can be slightly different, but during the propagation state, reactions are comparable:

$$\text{Anodic reaction} \qquad Fe \rightarrow Fe^{2+} + 2\,e^-$$

at 25°C with traces of ferrous iron. Application of the Nernst equation to calculate the e.m.f. of the cell, considering that the activity of Fe^{2+} is equal to 10^{-6} M give

$$E = E^0 - \frac{RT}{zF}\ln\frac{a_{\text{products}}}{a_{\text{reactants}}} = E^0_{Fe/Fe^{2+}} - \frac{0.0592}{2}\log 10^{-6} + \eta_a$$

$$\text{Cathodic reaction} \qquad 2\,H^+ + \tfrac{1}{2}O_2 + 2\,e \rightarrow H_2O \quad \text{at } 25\,^\circ C$$

$$E = 1.23 - 0.0592\,pH - \eta_c$$

where η_a and η_c are the respective anodic and cathodic overpotentials.

Oxygen comes from the mill scale or diffuses from the air to the steel surface. The coating breakdown occurs because of movement of the electrolyte, gases (oxygen) and moisture through the film to the pinholes and micropores. Water and gases passing through the mill scale film dissolve ionic material and cause osmotic pressure. Water diffusion and visual blistering can be observed. Permeation is at its best at (65–96°C) accelerated by osmotic pressure, electroendosmotic pressure, thermal agitation and vibration of the coating film molecules. The electroendosmotic gradient is created between the corroding area and the protected areas in electrical contact.

Poultice Corrosion. Poultice corrosion is a special case of localized corrosion due to differential aeration, which usually takes the form of pitting. It occurs when an absorptive material such as paper, wood, asbestos, sacking, cloth, etc., is in contact with a metallic surface that becomes wetted periodically. During the drying periods adjacent wet and drying regions develop. Near the edges of wet zones and because of limited quantities of dissolved oxygen, differential aeration cell develops and this leads to pitting. As example is the extensive damage observed for the aluminum surface of fuel tanks in aircraft because of the accumulation of organic materials inside tanks due to bacterial and fungal growths in jet aviation fuel. Poultice corrosion can be avoided by avoiding the contact of absorptive materials with a metallic surface, by design or by painting for example.[30]

Crevice Corrosion. This type of corrosion is due to the presence of a corrosive solution that is stagnant in the neighborhood of a hole, under a deposit, or any geometric shape that can form a crevice. It is also called cavernous corrosion or corrosion under deposit. It results from a concentration cell formed between the electrolyte within the crevice, which is generally oxygen starved, and the electrolyte outside the crevice, where oxygen is more plentiful. The material within the crevice acts as the anode, and the exterior material becomes the cathode. This difference in aeration produces a different equilibrium potential, given by the Nernst equation applied to the equation: $\frac{1}{2}O_2 + 2H^+ + 2e^- \rightarrow H_2O$. Using the activities of the dissolved species in water and considering the activity of water equal to 1, we get:

$$E = E^0 + 0.0592/2 \log(O_2)^{1/2}(H^+)^2/H_2O = 1.23 - 0.0592\,pH$$

in volts at 25°C.

The difference in this potential due to oxygen concentration leads to a cell sufficient for localized corrosion. The more aerated surfaces act as the cathode because of their more noble potential. In other situations difference in metal ion concentration can cause localized corrosion where the crevice rich in ions can play the role of the cathode (Figure 6.20).

Crevices may be produced by design or accident. Crevices caused by design occur at gaskets, flanges, rubber O-rings, washers, bolt holes, rolled tube ends, threaded joints, riveted seams, overlapping screen wires, lap joints, beneath coatings (filiform corrosion) or insulation (poultice corrosion described in pitting), and anywhere close-fitting surfaces are present.[31]

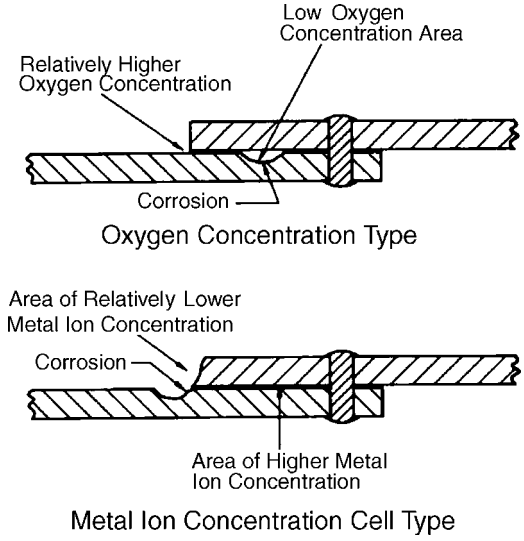

Figure 6.20 *Two types of crevice corrosion; oxygen concentration cell and metal ion concentration cell*[174]

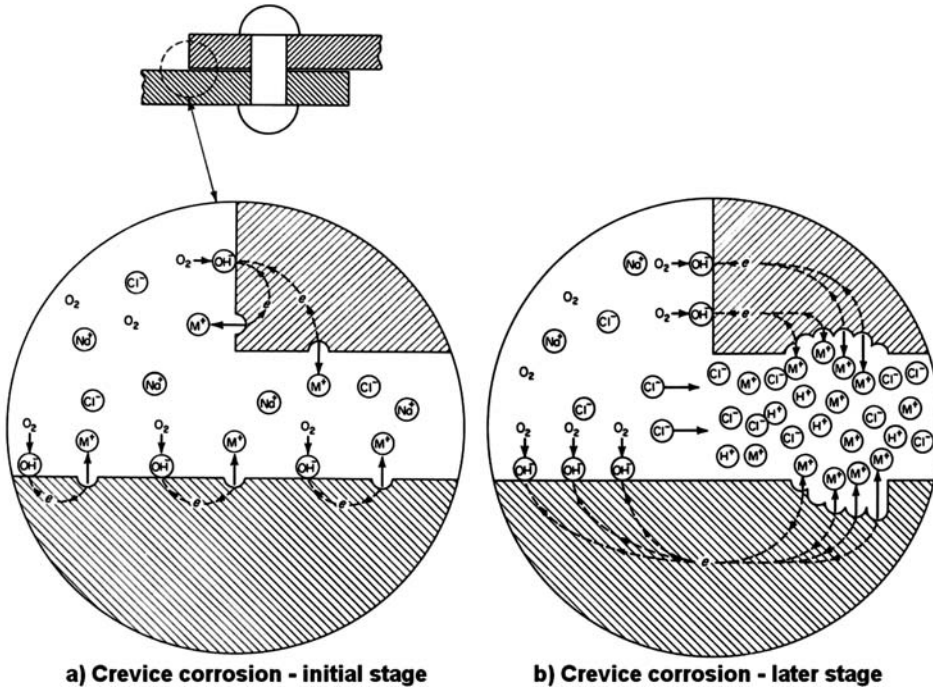

Figure 6.21 *Crevice corrosion*[16]

Oxygen differential cells could be established between the oxygenated seawater outside or at the opening of the crevice surfaces, for example, and inside crevice anodic areas. This crevice must be sufficiently large to permit the entry of the corrosive solution, but narrow enough to form a stagnant state and hold a solution with the desired characteristics. The opening is generally of the order of 50–200 μm. The narrow space present between two metals or between a metal and a nonmetal is favorable site for crevice corrosion (Figure 6.21). Hydrolysis reactions within crevices could produce changes in pH and chloride concentration in the crevice environment. The space between the two materials is less aired, has a weak surface and contains a solution often rich in salt. (Kain)[14] It is very probable that crevice corrosion can be initiated in special cases such as in magnesium and magnesium alloys due to the hydrolysis reaction and acid formation only, in certain conditions where it is believed that oxygen does not play a major role in corrosion mechanism.[5]

The crevice corrosion mechanism is very similar to that of pitting with respect to the autocatalytic propagation. However, the causes of initiation, the morphology and the penetration of pitting are quite different from that of crevice corrosion (Figure 6.21).[16]

Filiform Corrosion. This consists of the filamentary corrosion occuring on metallic surfaces and is a special type of crevice corrosion, sometimes called underfilm corrosion. It is frequently observed under the painted body of some used cars. It appears as a blister

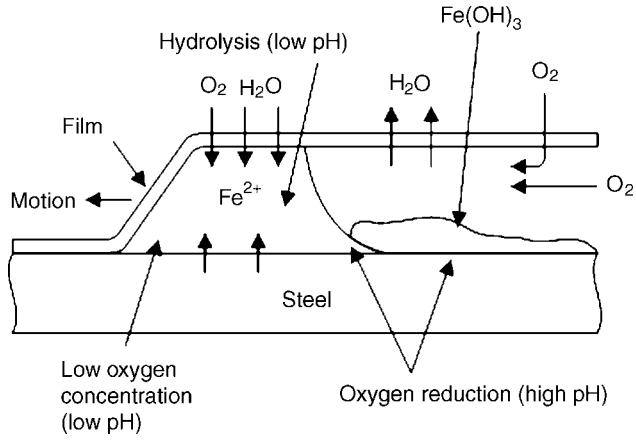

Figure 6.22 *Cross-section of a filament on painted steel*[16]

under the paint. The filament propagation underfilm can appear, split or can join together, since, they propagate in direct lines, some of them reflecting because of obstacles such as adhesive parts of the organic film to the substrate and become trapped in a very narrow place (final stage).[16] Figure 6.22 gives a schematic view of a filament on painted iron, and illustrates the role of the oxygen differential cell.

The filament occurs on metals covered by an organic film and because of a certain discontinuity in the film, air and water penetrate through the coating and reach the underlying metal. This adjacent humid layer becomes saturated or rich in corrosive ions from soluble salts, and forms the zone called the active head of the filament. The dissolution of metal decreases as the solubility of the oxygen increases. The metallic ions oxidize and form compounds or corrosion products. These zones are called tails. Figure 6.22 illustrates a section and explains the mechanism of initiation and propagation of the filament.

Filiform corrosion of AZ 91 magnesium alloy has been studied in detail and the mechanism different from the conventional mechanism has been postulated. In this case dissolved oxygen is not necessary and the filiform propagation is fueled by hydrogen evolution at the filament head and is controlled by mass transfer due to the salt film on the tip of the filament.[32,33]

Breakdown of Passivation. Pitting and crevice corrosion are usually associated with the breakdown of passivity. During pitting corrosion of passive metals and alloys, local metal dissolution leads to the formation of cavities within a passivated surface area. In practice, pitting corrosion of passive metals is commonly observed in the presence of chlorides or other halides. However, pitting may also occur in pure water as in the case of carbon steel in high-purity water at elevated temperature or aluminum in nitrate solutions at high potentials. In all these forms of localized corrosion, active and passive surface states are simultaneously stable on the same metal surface over an extended period of time, so that local pits can grow to macroscopic size.[27] (Sprowls)[14]

According to Hoar,[6] it is necessary to exceed the critical anodic potential E_{bd} for the electrochemical breakdown of passivation by pitting and consisting of the following general steps:

1. Presence of damaging species such as chlorides or higher atomic weight halides at the interface
2. Induction time for initiation of the breakdown process and ending with localized conditions that could raise the localized corrosion current density
3. The local sites became immobile and localized at certain sites resulting in favourable environmental conditions inside the pit for propagation

Electrochemical breakdown of oxides of some metals is possible since they are readily reduced cathodically to the metal in many solutions such as copper, tin and lead while ferric oxide is readily reduced to ferrous ions in aqueous solutions. Other metal oxides, such as those of zinc and aluminum are not cathodically reducible at the potentials obtainable in aqueous media; hydrogen is reduced instead. However, the vigorous evolution of hydrogen gas assisted by the electron-conducting zinc oxide can accelerate the breakdown of passivity. In the case of aluminum, the very feebly electron-conducting aluminum oxide can produce hydrogen gas that can push the film and followed by protons entering the film without discharge and render it conducting. Under high-field conditions, aluminum ions may even transfer from film to metal since the metal/film interface is nonaqueous.[1,25]

Among metals, there are differences in the composition and stoichiometry of these films that influence the stability and growth of these oxides. In aqueous solutions, anions such as halide and non halide types, can play a major role in passive film growth and breakdown. Borates, for example, appear to have a beneficial effect. It is necessary to consider the nature of the oxide film, the solution in which the film is formed, and the electrochemical conditions of formation of the film to evaluate the characteristics of the passive layer. Halide ions such as Cl^- can give rise to severe localized corrosion (e.g., pitting) Pitting is associated with particular combination of film thickness and halide concentration. Chloride is more aggressive than Br^-. It is agreed that well-developed pits have high chloride concentration and low pH. Pitting can be random and amenable to stochastic (statistical) theory, and can be considered as deterministic, but very sensitive to experimental parameters such as induction time and electrochemical properties which are difficult to reproduce. Electrochemical noise may clarify the initial conditions for pit initiation.[34]

The potency of halides to complex with metal cations is very important in understanding the stabilization of a corrosion pit by prevention of the repassivation of a defect site within the passive layer. Enhancement of the transfer of metal cations from the oxide to the electrolyte by halides, especially the strongly complexing fluoride, is valid for many metals. The slow dissolution kinetics of the Cr (III) salts can explain the resistance of chromium to localized corrosion (Strehblow, pp. 201–237).[13] Detrimental effects of sulfur species has been encountered in a large number of service conditions. However, the effects of chloride ions on passivity have been studied extensively. Recently the connection between the effects of atomic-scale surface reactions of sulfur and passivity has been studied in detail.[12,35] Chemical dissolution of passivating oxide films is in general an exothermic reaction. Higher-valent oxides are usually the best passivating

films because of their slow rate of dissolution. Increase in temperature accelerates dissolution rate of oxides such as Fe_2O_3, Cr_2O_3 and Al_2O_3.[25]

Breakdown of passivity is the first stage in pitting corrosion. Pit growth and repassivation phenomena are characteristic of every corrosion passivation system. Metals show different patterns of passivation. Al and Cu are not passive in strongly acidic electrolytes, while Fe, Ni, and steels are passive, even in strongly acidic electrolytes, in disagreement with the predictions of Pourbaix diagrams. Localized acidification by the hydrolysis of corrosion products may serve as a stabilizing factor for pitting in certain metals.[13] Alloying additions such as chromium and molybdenum to steel can substantially change the structure and composition of the passive oxide film and improve the process of passivation. For austenitic stainless steels, the barrier oxide layers, the salt deposit layers, and the alloy surface layers play an important role in the process of passivity and breakdown of passivity. Modeling passivation processes can provide new insights into alloy performance, and new alloy design concepts.[36,37]

There are two forms of pitting that follow breakdown of a passive metal or alloy surface, and they can be distinguished as pitting at low and high potentials. Pitting at low potential is influenced by cathodic or self activation and leads to merging etch pits that can eventually lead to general corrosion with etching. High-potential pitting takes the form of hemispherical pits corresponding to anodic dissolution in the electrobrightening mode. This requires a random dissolution due to the presence of film-breakdown factors and is independent of the crystal structure of the metal. This takes place through a random defective solid film that is none the less a very good ion conductor. Pits of either kind lead to occluded corrosion.[1,25] This is also in agreement with the definition of two types of passivation depending on the level of potential of the passive metal (noble or active potential.[8])

Recently, statistical and stochastic approaches involving Gaussian and Poisson distributions to localized corrosion have been reviewed by.[38] The Poisson distribution was found to be a better approach for pit generation. The results indicate that different pit generation rates can be observed as a function of time. The models consider either pit generation events alone or pit generation and subsequent repassivation processes. Theoretical models that describe the initiation process leading to passive film breakdown may be grouped into three classes: (1) adsorption and adsorption-induced mechanisms, where the adsorption of aggressive ions such as Cl^- is of major importance; (2) ion migration and penetration models; and (3) mechanical film breakdown model.[27]

Coatings and localized corrosion. This type of corrosion can occur where protective coatings are applied over metal and where there is a break in the coating so that the large coated area acts as a cathode, and the small defective area as the anode.[26]

Electrochemical Studies of Localized Corrosion. There are several electrochemical methods to determine the electrochemical conditions of pitting and crevice corrosion. However, emphasis is placed here on pitting as an example:

Cyclic potentiodynamic polarization method. Electrochemical studies of pitting corrosion usually indicate that pitting occurs only within or above a critical potential or potential range. Therefore the susceptibility of passive metals to pitting corrosion is often investigated by electrochemical methods such as potentiodynamic or potentiostatic

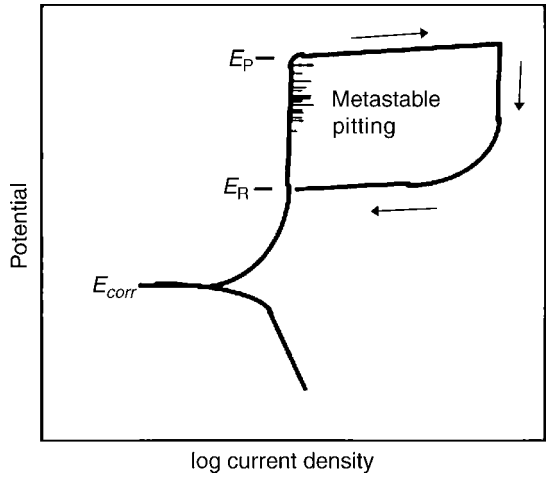

Figure 6.23 *Schematic of a polarization curve showing E_p (pitting potential) E_R (repassivation potential) relative to E_{corr}, critical potentials and metastable region (Frankel)*[5]

methods. The parameters are: (1) the critical current density i_{crit} characterizing the active–passive transition; (2) the pitting potential where stable pits start to grow; and (3) the repassivation or protection potential (after reversal of the potential sweep direction) below which the already growing pits are repassivated and the growth stops.[27,28]

Cyclic potentiodynamic polarization, the conventional method to determine pitting potential consists of scanning the potential to more anodic and protection potentials during the forward scan and return scan and compare the behavior of different alloys in the same conditions of scan rate, solution and experimental conditions [Figure 6.23]. The polarization curve of an alloy (with or without coating) showing active-passive behavior can be then obtained in a certain medium as a function of increasing chloride concentration E_b, E_{bd}, E_{pit}, or E_p (pitting potential) are symbols used frequently for the breakdown potential while E_{prot}, $E_{protection}$ (protection), E_R (repassivation) or E_{rep} or E_{pp} are used frequently for the potential at which the reverse scan curve re-crosses the passive current measured on the forward scan. Scan rates of 0.05–0.2 mV/s can be used to obtain the standard active–passive curve and argon or nitrogen should be bubbled to deaerate the solution. The breakdown potential corresponding to the considerable increase of the anodic current at a certain scan rate gives the susceptible condition for the initation of localized attack. The more noble is this breakdown potential, the more resistant will be the alloy to pitting and crevice corrosion. The potential at which the hysteresis loop is completed upon reverse polarization scan determines the potential below which there is no localized attack for this scan rate. (ASTM G5)[4] (ASTM G61)[4] However, the absolute values of pitting or breakdown potential and the protection potential are dependent on the scan rate and do not reflect the induction time required for pitting. Also, allowing too much pitting propagation to occur along with the accompanying chemistry changes can influence the reversal in the scan rate. (Scully)[14]

Recent experimental work suggests that E_{pit} and E_{prot} would converge to a unique pitting potential.[39] Thompson and Syrett[40] introduced a unique pitting potential which corresponds to both the most active value of E_p determined after a long incubation time and the most noble value of E_r measured following only minimal pit growth. Some authors suggest that the stationary pitting potential corresponds to a value between that of the pitting and protection potentials. A critical pitting temperature (CPT) has been defined, below which a steel in an aggressive Cl^--containing solution, usually a $FeCl_3$ solution, would not pit, regardless of potential and exposure time.[27] Also, a good measure of pitting susceptibility is the difference between protection and pitting potentials. Alloys that are susceptible to pitting corrosion exhibit a large hysteresis. This range of potentials can correspond to metastable pitting, a term used to express the region where pits initiate and grow for a limited time before repassivation. Large pits can stop growing for different reasons, but metastable pits are typically considered to be those of micrometer size, at most, with a lifetime of the order of seconds or less but under certain conditions, they continue to grow to form large pits.[39,41] (Frankel)[5]

Increasing temperature usually also increases the pitting tendency of metals and alloys. At low temperature, high pitting potentials are observed. Temperature dependence of pitting susceptibility of stainless steels has been used in ranking of these steels with respect to their pitting resistance.

Galvanostatic methods for localized corrosion. At constant chosen currents, the evolution of potential as a function of time is recorded until the rate of change in potential with time approaches zero. This technique is under development for aluminum alloys in ASTM G1[4] as a test method for application to aluminum alloys. (Scully)[14]

Potentiostatic methods. Once the breakdown potential is determined by cyclic potentiodynamic polarization methods, polarizing individual samples at potentials above and below this value will indicate the validity of the chosen scan rate and give some kinetic data on the initiation and propagation of pits at different levels. Another possibility is to initiate pits above the pitting or breakdown potential and then shift to lower values above or below the protection potential. It is assumed that at imposed values below the protection potential, one should observe current decrease until complete repassivation.

The critical pitting potential E_{cpr} lies between the breakdown potential and the protection potential and can be determined by the scratch repassivation method. In the scratch repassivation method for localized corrosion, the alloy surface is scratched and exposed to a constant potential. The current change is monitored as a function of time and this will show the influence of potential on the induction time and the repassivation time. A careful choice of the level of potential between the breakdown potential and the critical pitting potential can give the critical pitting potential for a chosen material in given conditions.[42] (Scully)[14]

Prevention of Localized Corrosion. Available data on the various physical and chemical aspects of passivity, including the composition, thickness, structure, growth, and properties of passive layers should be used in the studies of localized corrosion. A good understanding of the surface reactions involved in the formation and composition of passive films, passivation/repassivation, is necessary for the development of highly

corrosion-resistant alloys. A Good level of understanding of the metallurgical factors and the rational use of alloyed elements can help to control general and localized corrosion such as pitting. The mechanism of failure or passivity breakdown of passive films in pitting corrosion is essential for safety purposes.[25]

Design-to-prevent is the best approach to avoid pitting and crevice corrosion. Some examples of surface treatments and coatings are:

- sacrificial coatings such as zinc (galvanization or plating) for steel
- Anodizing and sealing are effective methods for natural media, accompanied by appropriate painting for more aggressive environments
- steel phosphating before painting, or using corrosion inhibitors as a pigment in paintings (chromate, phosphate or molybdate etc.) or zinc-rich primers (70–75 μm thick)
- light barrier protective paint coating ~ 100 μm, or heavy 6–13-mm thick to acid proof brick lining
- a thin organic coating for sacrificial zinc can extend useful life of zinc by a factor of 10. A compatible organic coating with an accompanying cathodic protection is the best solution
- It is recommended to examine the strained portions of metal including the welded areas that tend to be anodic with respect to unstrained portions (cathodic areas) and the bottom of underground structures such as steel tanks in aggressive environments, etc.

Testing and Evaluating of Localized Corrosion. Basic electrochemical testing. The susceptibility of alloys to localized corrosion can be evaluated, such as that of an alloy having active–passive behavior in certain media by cyclic voltammetric, potentiodynamic, galvanostatic, scratch potentiostatic, triboellipsometric methods, pit-propagation rate curves, impedance spectroscopic studies and electrochemical noise measurements. Time-to-perforation data can be obtained by designing a specimen that is pressurized with air. This pressure is monitored over a period of time until failure is indicated by a decrease in pressure. (Scully)[14]

Some selected procedures or standards. Measurement of mass loss, along with visual comparison of pitted surfaces, may be sufficient to rank the relative resistance of alloys in laboratory tests. Visual examination of pits should determine the size, shape, density of pits as far as possible. Metallographic examination is very important to show the correlation with the microstructure and to distinguish pits between pitting, intergranular corrosion or dealloying[4]. ASTM G46[4] gives the standard rating chart for pits and the different methods of examination of pits and also describes nondestructive inspection of pitting that include radiographic, electromagnetic, ultrasonic, and dye penetration inspection. The statistical approach is briefly described in ASTM G46[4] but is covered in detail in ASTM G16.[4]

It is useful to compare the resistance to pitting as a function of the critical concentration of chloride which causes pit initiation on different alloys. The appearance, morphology, distribution and depth of pits (average penetration of the 10 deepest pits and the deepest one) should be determined in parallel with pitting potential determinations. The statistical distribution of pits and morphology of the pit should be examined by different microscopic techniques. The pit depth can be

measured by several methods, including metallographic examination, machining, use of a micrometer or a depth gage, and the microscope. The metal penetration can be expressed as a pitting factor, which is the ratio of the deepest metal penetration to the average metal penetration. Determining the pitting and crevice corrosion resistance of stainless steel and related alloys in 6% ferric chloride solution at 22 or 50°C is described in ASTM G48.[4] This can be applied to other alloys. ASTM G78[4] is an important guide for crevice corrosion testing of iron and nickel base alloys in seawater and shows the importance of the crevice geometry and specimen preparation on the corrosion results.

The Materials Technology Institute of the Chemical Process Industry (MTI); has identified five corrosion tests for iron- and nickel-based alloys, out of which two concern the resistance to crevice corrosion. The method MTI-2, originating from ASTM G48, involves the use of 6% ferric chloride solution for determining the relative resistance of alloys to crevice corrosion in oxidizing chloride environment. The method MTI-4 uses an increase in neutral bulk Cl^- concentration at eight levels, ranging from 0.1 to 3% NaCl, to establish the minimum critical Cl^- concentration that produces crevice corrosion at room temperature (20–24°C).[43,44]

The test method ASTM F746[4] covers the determination of the resistance to either pitting or crevice corrosion of passive metals and alloys from which surgical implants are produced. The resistance of surgical implants to localized corrosion is carried out in dilute sodium chloride solution under specific conditions of potentiodynamic test method. Typical transient decay curves under potentiostatic polarization should monitor susceptibility to localized corrosion. Alloys are ranked in terms of the critical potential for pitting, the higher (more noble) this potential, the more resistant is to passive film breakdown and to localized corrosion. (Sprowls)[14]

The corrosion potential of the working electrode (specimen) is generally recorded for one hour in the 9 g/L NaCl solution. The initial and final potentials E_1 as well as pH should be noted. The current is recorded at +0.8 vs SCE for a period that depends upon the reaction. If localized corrosion is not simulated in the initial 20 s, the polarizing currents will remain very small or decrease rapidly with time. If localized corrosion is not stimulated in 15 min, the test is terminated and the material is considered to have a very high resistance to localized corrosion. Stimulation of localized corrosion is indicated by increasing polarization current with time or by current densities that exceed 500 $\mu A/cm^2$. In these two cases, the potential is then returned quickly to the final corrosion potential E_1 (after 1 h immersion), to determine if the specimen will repassivate or if localized corrosion will continue to propagate. If the pitted or local regions do not repassivate then the critical voltage is this value. The test consists of alternating between stimulation at 0.8 vs SCE and returning to a preselected potential (E_1+ a jump of +50 mV in the noble direction) until continuous increases or large fluctuations in current during the 15-min observation period are observed. Evidence of pitting and crevice corrosion should be noted in ASTM F746.[4]

Loss in mechanical properties. The change of mechanical property can be used to identify or quantify the degree of pitting in the case of relatively intensive pitting corrosion. However, replicates for exposed and reference samples are recommended. Consideration should be given to such factors as edge effects, direction of rolling, and surface conditions [ASM Sprowls, 1987].[14]

Some Electrochemical Techniques of Evaluation. Electrochemical noise technologies. New and accurate technologies are required to investigate the rather fast kinetics of localized corrosion. Electrochemical noise is an interesting tool to monitor metastable pitting by recording the galvanic current between nominally identical electrodes at the corrosion potential of a single electrode.[28,45]

The spatial separation of the anodic processes in the pit and the cathodic processes on the surrounding surfaces necessitates the passage of current that gives rise to the measured noise signals. Since localized corrosion sites are typically very small, of the order of 100 μm in diameter or less, the current densities inside these cavities can be of the order of 1 A/cm^2. Electrochemical noise studies can be performed under open-circuit potential, and close to the natural conditions of pitting. Also, electrochemical noise fluctuations in an anodic current below the pitting potential, under potentiostatic control or fluctuation of the potential under applied anodic current have been carried out by several researchers in chloride environments. It has been suggested that current transients below the pitting potential may be attributed to the formation of pit embryos.[28]

Noise measurements are extensively used in the studies of metastable pits. Pistorius[37] discussed several factors that can influence the proper interpretation of electrochemical noise measurements (ENM). These factors can be: probe size, sampling rate, and system noise. The current measurements seem to give clearer information on the corroding system than that of the potential.[28,46]

Noise electrochemistry (NE) gives instantaneous data that can show the relative corrosion resistance of different alloys in the same medium over long periods. However, agitation or convection can mask the noise signals, making it difficult to simulate operational conditions in certain situations. The zero resistance ammeter (ZRA) is an electronic instrument designed to measure the current flowing in a circuit without introducing the additional voltage drop associated with standard ammeter. As with the potentiostat, the main functional component is an operational electronic amplifier that supplies current necessary at its output to maintain zero potential difference between the two input potentials so that no current flows into or out of its input terminals.[39]

Noise analysis obtained from microelectrochemical investigations of stainless steels under potentiostatic conditions revealed that the current noise, expressed as standard deviation σ_i of the passive current, increases linearly with the size of the exposed area, whereas the pitting potential decreases.[47] However, to complete the electrochemical studies and distinguish between repassivating superficial pits and penetrating ones, microscopic studies are highly desirable. The scanning reference electrode technique (SRET) should be an appropriate complementary tool.[28]

EIS and localized corrosion. Electrochemical impedance spectroscopy for localised corrosion is still in progress for localized corrosion studies involving pitting. The statistical variation of pit nucleation and the absence of steady states prevent long-time measurements in the low-frequency region. In addition, in the pitting region a complicated Nyquist plot is obtained and difficult to interpret. However, Mansfeld *et al.*[48] demonstrated that characteristic changes have been discovered in the low-frequency region. It should be noted that the impedance spectra for pits in stainless steels and magnesium are different from those of aluminum.[27,28]

The scanning reference electrode technique (SRET). The SRET has enabled the measurement of localized corrosion current densities in the vicinity of pits in stainless

steel in natural water. Novel potentiodynamic pitting scans have been obtained for localized areas immediately adjacent to accurately defined regions of the electrode surface. Isaacs has designed the scanning reference electrode technique to study the pitting and intergranular corrosion in stainless steels. He is also associated with the scanning vibrating electrode technique (SVET), in which the probe is mounted on a biomorph piezoelectric reed which vibrates the tip normal to the electrode at a characteristic frequency.[49] Another variation of the technique has been used in localized measurement of electrochemical impedance spectra (LEIS).[50] The description of the electrochemistry of the method is provided by Eden.[45]

Recently, a new microelectrochemical technique applying microcapillaries as electrochemical cells has been developed. Only small surface areas, a few micrometers or even nanometers in diameter, are exposed to the electrolyte. This leads to current resolution, down to picoamperes. Microelectrochemical techniques, combined with statistical evaluation of the experimental results may give greater insight into the mechanism of these processes.[27]

6.7.4 Metallurgically Influenced Corrosion

Very pure single crystals have defects that can effect corrosion, but impurities and alloying elements, grain boundaries, second phases, and inclusions often have serious effects. Welded structures invariably corrode first at the welds because of metallurgical heterogeneities that exist in and near welds. The most susceptible site or defect in a metal will be the first to be attacked on exposure to a corrosive environment. Sometimes such attack simply results in innocuous removal of the susceptible material, leaving a surface with improved corrosion resistance. (Frankel)[5]

Metallurgically influenced corrosion is mainly composed of the corrosion due to chemical composition (alloying elements, metalloids and impurities), metallurgical properties (metallic phases, grain joints) and fabrication procedures (thermal treatments, lamination and welding). Figure 6.24 shows weld zone, dealloying, exfoliation and internal modes of attack.

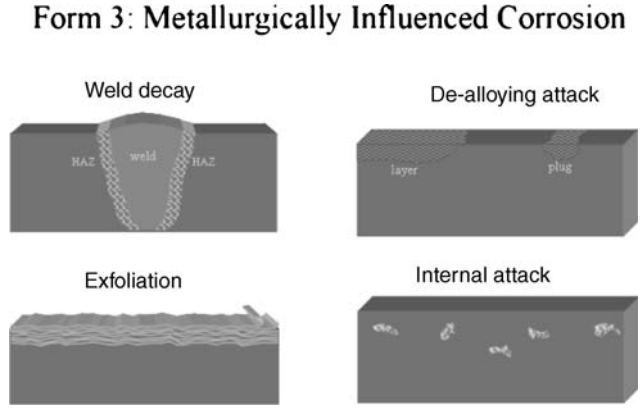

Figure 6.24 *Heat-affected zone and some morphlogies of metallurgically influenced corrosion*[3]

The selective corrosion of cast iron (graphitization), the preferential corrosion of the steel welding (grooving corrosion), sensitization and knife line attack of welded stainless steels are typical examples of corrosion influenced by metallurgical parameters.

Influence of Metallurgical Properties in Aqueous Media. Chemical composition and microstructure. When an alloy composed of various elements corrodes, usually one or more elements dissolve preferentially, leaving a surface enriched with other elements. This dealloying depends strongly on factors such as environment and potential. However, the dealloyed microstructure is vastly altered, often resulting in a reduction of strength and other properties. (Frankel)[5] The corrosion resistance of stainless steels and nickel-based alloys varies markedly, depending on the alloying elements and processing conditions. When a solutionized low-sulfur stainless steel is exposed to boiling nitric acid, the attack is not localized, but rather is dominated by the orientation of the grains so that a stepped structure develops with the most susceptible orientations corroding faster. (Frankel)[5]

In amorphous form, glassy metals have been formed by very rapid cooling, of the order of $\sim 10^6$ K/s during the solidification of a melt. This 'freezes' the atoms almost instantly in nearly the same positions they occupied in the liquid state. The resultant material is thus chemically and structurally homogeneous and free form one- and two-dimensional defects, secondary phases, and grain boundaries. As a result of the extensive disorder, glassy metals often have physical, chemical, and mechanical properties that differ greatly from those of crystalline alloys of the same elemental compositions. They can be much more corrosion resistant than the compositionally equivalent crystalline alloys, in large part due to the absence of multiple phases, grain boundaries, and other defects. (Noël)[5]

The various classes of metallic phases that may be encountered in crystalline alloys include substantially pure elements, solid solutions of one element in another and intermetallic compounds. In crystalline form, alloys are subject to the same type of defects as pure metals. Crystalline alloys may consist of a solid solution of one or more elements (solutes) in the major (base) component, or they may contain more than one phase. That is, adjacent grains may have slightly or extremely different compositions and be of identical or disparate crystallographic types. Often, there is one predominant phase, known as the matrix, and other secondary phases, called precipitates. The presence of these kinds of inhomogeneities often results in the alloy having radically different mechanical properties and chemical reactivities from the pure constituent elements. (Noël)[5]

Grain boundaries. Usually, the spatial orientations of different grains (as defined by their intrinsic crystallographic planes) are random with respect to each other. This means that there must be a zone of transition over which the crystallographic orientation changes from that found in one grain to that found in its neighbors. This transitional zone is known as a grain boundary. This disorder makes grain boundaries energetically favorable sites of residence for impurities and other imperfections. Impurities tend to find the grain boundary regions to be energetically more favorable sites of residence than sites within the crystal lattice, especially if the impurities are present in concentrations beyond their solubility limits. The grain boundaries in alloys and impure metals are preferred sites for accumulation (segregation) of solute atoms. Likewise, solute atoms and impurities tend to congregate at defects within the grains as well. Grain boundaries

are also the favored precipitation sites for secondary phases formed during solid-state transformations. Consequently, the grain boundaries are often more resistant to mechanical deformation and have different chemical reactivities from the grains themselves.[51,] (Noël)[5]

Defects and inclusions. Point defects (zero-dimensional) include interstitial atoms, which are atoms present in the spaces between the lattice positions, vacancies (the absence of one or more atoms from the crystal lattice), and foreign atoms in lattice positions. Line defects (one-dimensional) are of two types: edge dislocations and screw dislocations. An edge dislocation is the region of imperfection that lies along the internal edge of an incomplete plane of atoms within a crystal. In a screw dislocation, a portion of the crystal is displaced, comprised of a single, continuous ribbon-like structure. Plane defects – stacking faults (two-dimensional) are imperfect regions of a crystal, resulting from errors in the positioning of entire atomic layers. Stacking faults arise during crystal growth or as a consequence of plastic deformation, but can occur only along the close-packed planes within a crystal. (Noël)[5]

Inclusions are three-dimensional defects consisting of soluble particles of foreign material in the metal and may be either intentionally or accidentally incorporated. Voids (another type of three-dimensional defect) are empty or gas-filled spaces within the metal. Particles composed of various oxides, sulfides, and silicates are common inclusions in metals and alloys; for example, manganese sulfide in stainless steels, well known as sites for pitting initiation. For example, cold working of a metal, introduces defects amounting to 100kJ/kg of stored energy that can create only about 3 mV of potential difference. This potential shift corresponds to a corrosion rate change of about 10%.[51,] (Noël)[5]

Passivation. For a passivating metal, the corrosion rate is less dependent on potential, and hence intergranular corrosion driven by free energy differences arising from disorder in the metal are even less likely. However, on surfaces protected by a passive film, grain boundaries and defects can sometimes promote preferential attack by disrupting the formation of a continuous protective layer. (Noël)[5] Passivation and repassivation tend to be enhanced on densely packed crystallographic planes because there are fewer steps and kinks. Hence texture can have an impact on the passivation characteristics. The susceptibility to stress–corrosion cracking can also be impacted by material texture, because the bias in grain orientation will favor alignment of stacking faults in different grains along preferred directions, with consequent effects on slip processes and, ultimately, stress-corrosion cracking, depending on the direction of tensile stresses. (Noël)[5]

Breakdown of passivation and pitting. The local breakdown of passivity of metals, such as stainless steels, nickel, or aluminum, occurs preferentially at sites of local heterogeneities, such as inclusions, second-phase precipitates, or even dislocations. The size, shape, distribution, as well as the chemical or electrochemical dissolution behavior (active or inactive) of these heterogeneities in a given environment, determine to a large extent whether pit initiation is followed either by repassivation (metastable pitting) or stable pit growth.[27]

Localized corrosion of passivating metals initiates at local heterogeneities, such as inclusions and second-phase precipitates as well as grain boundaries, dislocations, flaws, or sites of mechanical damage. In the case of stainless steel surfaces, pit initiation occurs at sites of MnS inclusions. Exclusion of inclusions and precipitates, nonequilibrium

single-phase conditions can be attained by techniques, such as rapidly quenching or physical vapor deposition. The resulting microstructure is either nanocrystalline or amorphous. Sputter-deposited aluminum alloys containing only a few atom percent of metal solute such as Cr, Ta, Nb, W, Mo, or Ti, exhibit an increase of E_p of 0.2–1 V. The increase in pitting resistance was explained by the reduced pit initiation tendency as well as by a more protective passive film, favoring rapid repassivation.[47]

Pitting potential increased with increase in chromium contents $\geq$20 wt%, and molybdenum of 2–6 wt%. Recent results, applying microelectrochemical techniques, confirmed that even in the superaustenitic stainless steels molybdenum strongly improves the repassivation behavior but has no influence on pit initiation.[27] The corrosion resistance of aluminum alloys is totally dependent on metallurgical factors.[52,] (Frankel)[5]

Internal or subsurface attack (oxidation). High-temperature corrosion can be identified by simple visual observation of the surface. However, subsurface phenomena within the matrix of the alloy, as well as obscured relations at the interface of the alloy with the surface films formed in many high temperature exposures can be seen in Figure 6.24. Electrochemical corrosion at high temperature at the interface also involves the diffusion of the aggressive gas phase to the vulnerable phase in the subsurface, leading to corrosion most of the time.

Dealloying or Selective Dissolution. Dealloying is a corrosion process involving selective dissolution of one or more elements, leaving behind a porous residue of the remaining element(s). Dealloying, also referred to as selective leaching or parting corrosion, is a corrosion process in which the more active metal is selectively removed from an alloy, leaving behind a porous weak deposit of the more noble metal. For example, the preferential leaching of zinc from brass is called dezincification. In the case of gray iron, dealloying is called graphitic corrosion.[31] Dealloying can occur in nearly any system in which a large difference in equilibrium potential between the alloying components and the fraction of the less noble constituent (s) exits and is significantly high. (Corcoran)[5]

Dezincification. Copper–Zinc alloys containing more than 15% zinc are susceptible to dezincification. In the dezincification of brass, selective removal of zinc leaves a relatively porous and weak layer of copper and copper oxide. Corrosion of a similar nature continues beneath the primary corrosion layer, resulting in gradual replacement of sound brass by weak, porous copper. Uniform dealloying in admiralty brass is shown in Figure 6.25.[5,7,53,54]

Brass is only one strong phase of the copper and zinc dissolved. In certain circumstances one notes a preferential dissolution of brass however. This dezincification (Figure 6.24) can be localized (plug dezincification) or more uniformly distributed (layer dezincification).[7] Figure 6.26 shows the selective attack of the rich phase of the alloy.

Dezincification of α-brass can be minimized by adding 1% Sn, as in admiralty brass (71 Cu–28Zn–1Sn, and further inhibited by adding less than 0.1% of arsenic),[55] antimony, or phosphorus. Where dezincification is a problem, red brass, commercial bronze, inhibited admiralty metal, and inhibited brass can be successfully used.

Graphitic corrosion has been observed on buried pipelines after many years of service. Gray cast iron has a continuous graphite network in its microstructure that is cathodic to iron and remains behind as a weak, porous network as the iron is selectively removed

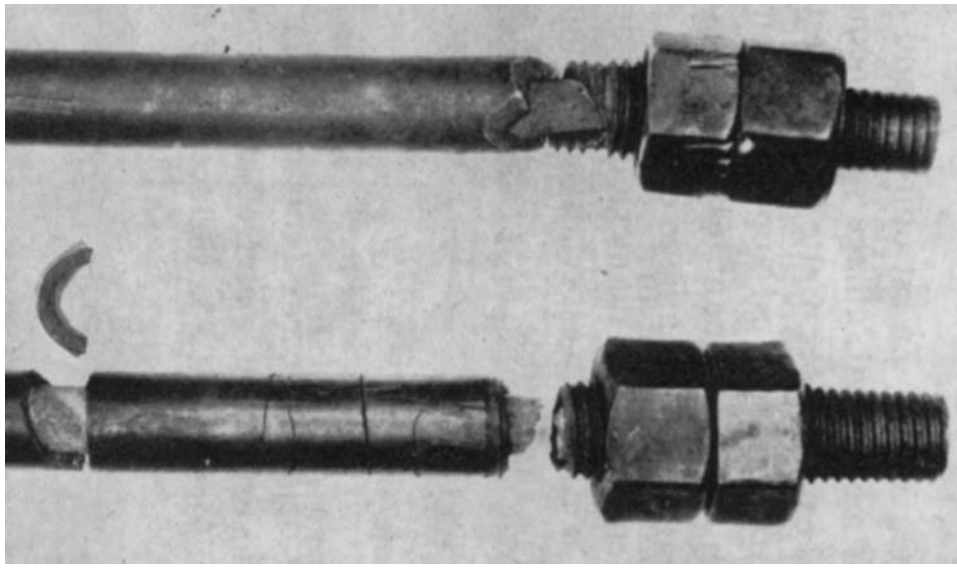

Figure 6.25 *Selective corrosion by layer type (dezincification) of a bolt in brass*[7]

from the alloy. (Corcoran)[5] Attack by graphitic corrosion is reduced by alloy substitution (e.g., use of a ductile or alloyed iron rather than gray iron), altering the environment (raising the water pH to neutral or slightly alkaline levels), the use of inhibitors, and avoiding stagnant conditions and/or cathodic protection can be used to prevent graphitization.[31]

Dealuminification. Recent investigations have shown the importance of the dealloying of S-phase (Al_2CuMg) particles on the corrosion of aluminum aircraft alloys, specifically aluminum alloy 2024-T3. In 2024-T3, the S-phase particles represent approximately 60% of the particle population. These particles are of the order of 1 μm diameter, with a separation of the order of 5 μm representing an surface area fraction of 3%.[56] The selective removal of aluminum and magnesium from these particles leaves behind a porous copper particle that becomes the preferential site for oxygen reduction.[57,] (Corcoran)[5]

Dealloying has also been observed with Ag–Au, Cu–Au, Cu–Pt, Al–Pt, Al–Cu, Cu–Zn–Al, Cu–Ni and Mn–Cu alloys. (Corcoran)[5]

Other Systems. Evidence for dealloying has been reported in austenitic stainless steel and iron–nickel alloys in acidified chloride-containing solutions, reduction of titanium dioxide in molten calcium chloride, and copper-zinc-aluminum alloy pellets in NaOH solutions to produce Raney metal particles. (Corcoran)[5]

Mechanisms and Models of dealloying. In the dealloying process, typically one of two mechanisms occurs: alloy dissolution and replating of the cathodic element or selective dissolution of an anodic alloy constituent. In either case, the metal is left spongy and porous and loses much of its strength, hardness, and ductility.[31] For brass, for example, it is generally accepted that the alloy attack occurs, giving rise to both dissolution of copper and zinc ions and the subsequent redeposition of copper during the corrosion of

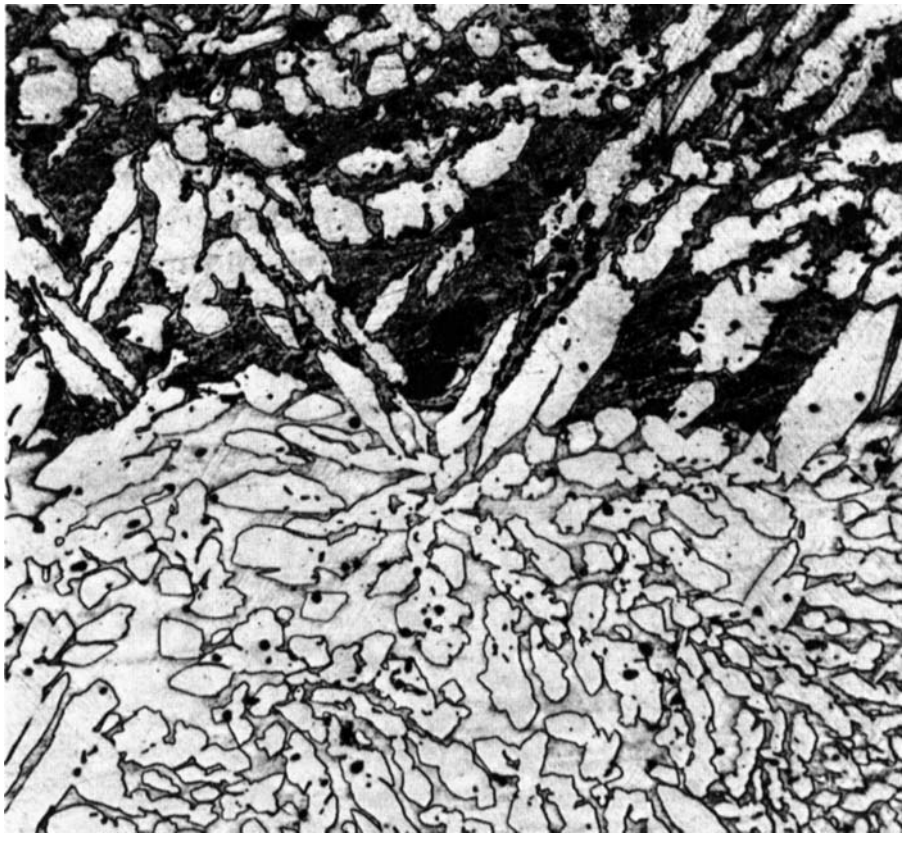

Figure 6.26 *Dezincification of a brass of two phases[175] (preferential attack of the phase β(top) rich in zinc as compared to the phase α(bottom) × 133*

copper–zinc alloys in many electrolytic solutions. However, this is not the only mechanism for dezincification to occur, although it enhances the rate. In case of the gold–silver system, only selective removal of silver occurs in 0.1 *M* $HClO_4$. (Corcoran)[5] The dissolution process is maintained beyond the first few monolayers by volume diffusion of both elements in the solid phase. The inherent problem with this mechanism is that, at room temperature, the rate of transport of the less noble element to the surface is not sufficient to support the dealloying current densities greater than 10 mA/cm^2 observed experimentally. (Corcoran)[5]

Two suggested ways to explain the continuous rapid supply of the more active or less noble metal give rise to two models of dissolution. One of them proposes that the less noble element is preferentially dissolved. The remaining more noble element is now in a highly disordered state and begins to reorder by surface diffusion and nucleation of islands of almost pure noble metal. The coalescence of these islands continues to expose fresh alloy surface where further dissolution will occur, leading to the formation of tunnels and pits. (Corcoran)[5]

The second model extends the surface diffusion model to include the importance of the atomic placement of atoms in the randomly packed alloy. The model considers that a continuous connected cluster of the less noble atoms must exist to maintain the selective dissolution process for more than just the few monolayers of the alloy. This percolating cluster of atoms provides a continuous active pathway for the corrosion process as well as a pathway for the electrolyte to penetrate the solid. This is expected to depend on a sharp critical composition of the less noble element, below which dealloying does not occur.[54,] (Corcoran)[5]

Intergranular Corrosion and Exfoliation. Intergranular corrosion (IGC) is preferential attack of either grain boundaries or areas immediately adjacent to grain boundaries in a material exposed to a corrosive environment, but with little corrosion of the grains themselves. (Phull)[5] This dissolution is caused by potential differences between the grain boundary region and any precipitates, intermetallic phases, or impurities that form at the grain boundaries. Susceptibility to intergranular attack depends on the corrosive solution and on the extent of intergranular precipitation, which is a function of alloy composition, fabrication, and heat-treatment factors. (Phull)[5]

Steel phases have an influence on the rate of corrosion. Ferrite has a weak resistance to pitting. The presence of martensite can increase the hydrogen fragilization of steel. Intermetallic phases as Fe_2Mo in high Ni content alloys can influence the corrosion resistance. The precipitate $CuAl_2$ in aluminum alloys the series 2000 is more noble than the matrix, with corrosion around the precipitate. The majority of case histories reported in the literature have involved austenitic stainless steels, aluminum alloys, and to a lesser degree, some ferritic stainless steels and nickel-based alloys.[31]

Impurities that segregate at grain boundaries may promote galvanic action in a corrosive environment by acting either as anodic or cathodic sites. For example, in 2000-series (2xxx) aluminum alloys, the copper-depleted (anodic) band on either side of the grain boundary is dissolved while the grain boundary is cathodic due to the $CuAl_2$ precipitates. Conversely, in the 5000-series (5xxx) aluminum alloys, intermetallic precipitates such as Mg_2Al_3 (anodic) are attacked when they form a continuous phase in the grain boundary. During exposures to chloride solutions, the galvanic couples formed between these precipitates and the alloy matrix can lead to severe intergranular attack. Actual susceptibility to intergranular attack and degree of corrosion depends on the corrosive environment and on the extent of intergranular precipitation, which is a function of alloy composition, fabrication, and heat-treatment parameters.[31,] (Phull)[5]

Precipitates that form as a result of the exposure of metals at elevated temperatures (for example, during production, fabrication, and welding) often nucleate and grow preferentially at grain boundaries. If these precipitates are rich in alloying elements that are essential for corrosion resistance, the regions adjacent to the grain boundary are depleted of these elements. The metal is thus sensitized and is susceptible to intergranular attack in a corrosive environment. An example is in austenitic stainless steels such as AISI type 304; the cause of intergranular attack is the precipitation of chromium (Davis) p. 25.[31] Another example of grain boundary segregation is σ-phase formation in Cr-Mo alloys; σ-phase is usually more difficult to resolve visually in the microstructure than Cr-carbides. (Phull)[5]

At temperatures above approximately 1035°C, chromium carbides are completely dissolved in austenitic stainless steels. However, when these steels are slowly cooled from these high temperatures or reheated into the range of 425–815°C, chromium carbides are precipitated at the grain boundaries. These carbides contain more chromium than the matrix. The precipitation of the carbides depletes the matrix of chromium adjacent to the grain boundary. This sensitization occurs because the depleted zones have higher corrosion rates than the matrix in many environments. (Fritz)[5]

Most serious cases of intergranular attack arise from compositional dissimilarities rather than structural defects. One form of corrosion in which structural defects do seem to play a role is stress–corrosion cracking. The presence of a large number of stacking faults makes it easier for grains to slip (i.e., facilitates shear displacement of one part of the grain with respect to another). The material then has a greater tendency to creep rather than crack to relieve tensile stresses. In some materials, decreasing the free energy stored in stacking faults can change the nature of stress–corrosion cracking from intergranular to transgranular. (Noël)[5,] (Phull)[5]

Intergranular corrosion at elevated temperatures is a serious problem in sulfidation of nickel alloys. Deep penetration can occur rapidly, until it becomes complete through the thickness of the alloy. The techniques for evaluating this type of IGC include: (a) X-ray mapping during examination in a scanning electron microscope (equipped with an energy-dispersive X-ray detector); and (b) transmission electron microscopy. (Phull)[5]

Intergranular corrosion in aluminum alloys is controlled by material selection and by proper selection of thermal (tempering) treatments that can affect the amount, size, and distribution of second-phase intermetallic precipitates. Resistance to intergranular corrosion is obtained by the use of heat treatments that cause precipitation to be more general throughout the grain structure. Guidelines for selecting proper heat treatments for these alloys are available.[57]

Exfoliation is a form of macroscopic intergranular corrosion that primarily affects aluminum alloys in industrial or marine environments. Corrosion proceeds laterally from initiation sites on the surface and generally proceeds intergranularly along planes parallel to the surface. The corrosion products that form in the grain boundaries force metal away from the underlying base material, resulting in a layered or flake-like appearance.[31] In certain materials, corrosion progressing laterally along planes parallel to rolled surfaces is known as exfoliation, and it generally occurs along grain boundaries – hence, intergranular corrosion. A layered appearance is a common manifestation of exfoliation (also referred to *as layer corrosion*), resulting from voluminous corrosion products prying open the material, for example, in aluminum alloys. (Phull)[5]

The most susceptible alloys are the high-strength heat-treatable 2xxx and 7xxx alloys. Exfoliation corrosion of Al 6xxx in salt medium has been observed. Exfoliation corrosion in these alloys is usually confined to relatively thin sections of highly worked products.[57] Exfoliation corrosion is observed in unalloyed magnesium above a critical chloride concentration, but this morphology was not seen in magnesium alloys, in which individual grains were preferentially attacked along certain crystallographic planes. The early stages of this form of attack caused swelling at points on the surface due to apparent delamination of the magnesium crystals with interspersed corrosion products, but, as attack proceeded, whole grains or parts of grains disintegrated and dropped out, leaving the equivalent of large irregularly shaped pits.[58]

Testing of intergranular attack necessitates metallographic examination. The standard practice ASTM G110,[4] 1992 evaluates intergranular corrosion resistance of heat-treatable aluminum alloys by immersion in sodium chloride and hydrogen peroxide solution. For example, ASTM A262[4] contains six practices for detecting susceptibility to IGC in austenitic stainless steels using different oxidizing reagents at different temperatures, and kinetics is examined by microscopic examination of the etched microstructure for $Cr_{23}C_6$ sensitization and weight loss measurements. (Phull)[5] Similarly, tests for detecting susceptibility to IGC in ferritic stainless steels have been incorporated into ASTM A763[4] and for wrought Ni-rich, Cr-bearing alloys, into ASTM G28.[4,] (Phull)[5]

ASTM G108[4] describes a laboratory procedure for conducting a nondestructive electrochemical reactivation (EPR) test on Types 304 and 304L stainless steel to quantify the degree of sensitization. The metallographically mounted and highly polished test specimen is potentiodynamically polarized from the normally passive condition, in 0.5 *M* $H_2SO_4 + 0.01$ *M* KSCN solution at $30 \pm 1°C$, to active potentials–a process known as reactivation. The amount of charge passed is related to the degree of IGC associated with $Cr_{23}C_6$ precipitation, which occurs predominately at the grain boundaries. After the single-loop EPR test, the microstructure is examined. (Phull)[5] Certain media have been commonly used for evaluating the susceptibility to IGC of magnesium, copper, lead, and zinc alloys. (Phull)[5]

Weldment Corrosion. The factors that can initiate or propagate different forms of corrosion of welded regions are numerous, interrelated and hard to define, however a systematic approach should consider: weldment design, fabrication technique, welding practice, welding sequence, moisture contamination, organic or inorganic chemical species, oxide film and scale, weld slag and spatter, incomplete weld penetration or fusion, porosity, Cracks (crevices), high residual stresses improper choice of filler metal, and final surface finish. Consequently, the corrosion resistance of welds may be inferior to that of the properly annealed base metal because of: microsegregation, precipitation of secondary phases, formation of unmixed zones, recrystallization and grain growth in the weld heat-affected zone (HAZ), volatilization of alloying elements from the molten weld pool, contamination of the solidifying weld pool.[5] [ASM, Frankel, 2003]

Welded microstructures can be extremely complex and often change drastically over a very short distance. The fusion zone or weld metal is a dendritic structure that has solidified from a molten state. Bordering the fusion zone are transition, unmixed and partially melted zones, and the heat-affected zone (HAZ). These zones can be reheated and altered by subsequent weld passes, in multipass welding. For alloys with structures that depend strongly on thermal history, such as steels, the final microstructure can be extremely complex. Since welded structures are often quite susceptible to corrosion, overalloyed filler metals are often used to enhance the weld corrosion resistance. For stainless steels with sufficiently high carbon content, sensitization in the HAZ is another major problem. (Frankel)[5]

Carbon steels. The corrosion behavior of carbon steel weldments produced by fusion welding can be due to metallurgical effects, such as preferential corrosion of the heat-affected zone (HAZ) or weld metal, or it can be associated with geometric aspects, such as stress concentration at the weld toe, or creation of crevices due to joint design.

Additionally, specific environmental conditions can induce localized corrosion such as temperature, conductivity of the corrosive fluid, or thickness of the liquid corrosive film in contact with the metal. In some cases, both metallurgical and geometric factors will influence behavior, such as in stress–corrosion cracking. Preferential weldment corrosion of carbon steels has been investigated since the 1950s, commencing with the problems on icebreakers, but the problem continues today in different applications. (Bond)[5]

There is clearly a microstructural dependence, and studies on HAZs show corrosion to be appreciably more severe when the material composition and welding parameters are such that hardened structures are formed. It has been known for many years that hardened steel may corrode more rapidly in acid conditions than fully tempered material, apparently because local microcathodes on the hardened surface stimulate the cathodic hydrogen evolution reaction. (Bond)[5]

Grooving corrosion. There is a particular case of preferential weldment corrosion worth highlighting in respect to electric-resistance-welded/high-frequency-induction-welded (ERW/HFI) pipe, where attack of the seam weld HAZ/fusion line can occur in aqueous environments or when exposed to the water phase in a mixed-phase system due to flow conditions or water dropout at low points. This grooving corrosion has been attributed to inclusions within the pipe material being exposed at the pipe surface and modified by the weld thermal cycle.[59] This type of corrosion is probably caused by the redistribution of sulfide inclusions along the welding. It has been suggested that MnS is concentrated by the movement of the liquid metal during welding. The elevated temperature can dissociate the sulfide of manganese to sulfur and can form iron sulfide.[60] A normalizing heat treatment can reduce or prevent the occurrence. The remedial action is the selection of a cleaner alloyed steel.

Corrosion is due to electrochemical potential differences (galvanic corrosion) between the HAZ/fusion line and the parent material, attributed to the unstable MnS inclusions produced during the welding cycle. It was observed that enhanced corrosion of the weld metal was due to electrochemical potential differences between the weld metal and the base metal, such that the weld metal is anodic in the galvanic couple. The potential difference may only be of the order of perhaps 30–70 mV, but the low surface area ratio of anode to cathode results in high corrosion rates (1–10 mm). (Bond)[5]

Stress-corrosion cracking. This failure may occur by both active path and hydrogen embrittlement mechanisms, and, in the latter case, failure maybe especially likely at low-heat-input welds because of the enhanced susceptibility of the hardened structures inevitably formed. Most SCC studies of welds in carbon and carbon–manganese steels have evaluated resistance to hydrogen-induced SCC, especially under sour (H_2S) conditions prevalent in the oil and gas industry, which is commonly referred to as sulfide stress cracking (SSC). Although full definition of the effect of specific microstructural types has not been obtained, an overriding influence of hardness is evident. On this basis, it is probable that soft, transformed microstructures around welds are preferable. In order that hard spots in the HAZ are not overlooked in weld procedure qualification, many standards now require the use of the Vickers hardness testing for welds. SCC in Oil Refineries. (Bond)[5]

Failures in refineries have shown cracks parallel or normal to welds, depending upon the orientation of principal stresses. Both transgranular and intergranular cracks have been observed.

Equipment found to suffer from cracking included tanks, absorbers, carbon treater drums, skimming drums, and piping. All welds of deaerator vessels in carbon steel should be post-weld stress relieved to minimize cracking and pitting. (Bond)[5]

Stainless steels are iron-based alloys that contain a minimum of approximately 11% Cr, the amount needed to prevent rusting. Few stainless steels contain more than 30% Cr or less than 50% Fe. They achieve their stainless characteristics through the formation of an invisible and adherent chromium-rich oxide surface film. This oxide forms and heals itself in the presence of oxygen. (Krysiak)[14]

The conditions created by arc-welding operations produce a scale composed of elements that have been selectively oxidized from the base metal. The region near the surface of an oxidized stainless steel is depleted in one or more of the elements that have reacted with the surrounding atmosphere to form the scale. (Wahid)[61] Backing rings are sometimes used when welding pipe. In corrosion applications, it is important that the backing ring insert be consumed during the welding process to avoid a crevice. (Krysiak)[14,] (Wahid)[61]

The welding filler metal must at least match the contents of the base metal in terms of specific alloying elements, such as chromium, nickel, and molybdenum. The cycle of heating and cooling that occurs during the welding process affects the microstructure and surface composition of welds and adjacent base metal. Consequently, the corrosion resistance of autogenous welds (welds made without the use of filler metals) and welds made with matching filler metal may be inferior to that of properly annealed base metal because of: microsegregation, precipitation of secondary phases, formation of unmixed zones, recrystallization and grain growth in the weld heat-affected zone (HAZ), and volatilization of alloying elements from the molten weld pool, contamination of the solidifying weld pool. (Krysiak)[14,] (Wahid)[61]

Unmixed zones. All methods of welding stainless steel with a filler metal produce a weld fusion boundary consisting of base metal that has been melted, but not mechanically mixed with filler metal and a partially melted zone in the base metal. An unmixed zone has the composition of base metal, but the microstructure of an autogenous weld. The microsegregation and precipitation phenomena characteristic of autogenous weldments decrease the corrosion resistance of an unmixed zone relative to the parent metal. Unmixed zones bordering welds made from overalloyed filler metals can be preferentially attacked when exposed on the weldment surface.[14,61]

Sensitization. Welding is the common cause of the sensitization of stainless steels to intergranular corrosion. In austenitic stainless steels, the principal weld metal precipitates are δ-ferrite, σ-phase, and $M_{23}C_6$ carbides. Small amounts of M_6C carbide may also be present. Although the cooling rates in the weld itself and the base metal immediately adjacent to it are sufficiently high to avoid carbide precipitation, the weld thermal cycle brings part of the heat-affected zone (HAZ) into the precipitation temperature range. Carbides can precipitate, and a zone somewhat removed from the weld becomes susceptible to intergranular corrosion (Figure 6.27). Once the precipitation has occurred, it can be removed by reheating the alloy to above 1035°C and cooling it rapidly. This practice is commonly termed solution anneal.[5]

The best-known weld-related corrosion problem in stainless steels is weld decay (sensitization) caused by carbide precipitation in the weld HAZ. This sensitized

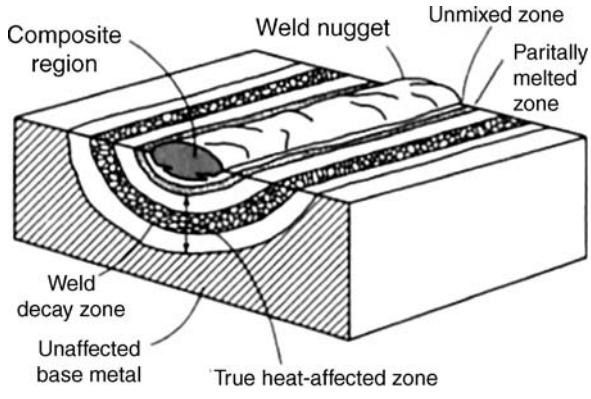

Figure 6.27 *Schematic diagram of different microstructures (sensitization) in an austenitic stainless steel weldment (Fritz)*[5]

microstructure is much less corrosion resistant, because the chromium-depleted layer and the precipitate can be subject to preferential attack (Figure 6.28).

Pitting and stress–corrosion cracking. Under moderately oxidizing conditions, such as in pulp and paper bleach plants, weld metal austenite may suffer preferential pitting in alloy-depleted regions. This attack is independent of any weld metal precipitation and is a consequence of microsegregation or coring in weld metal dendrites. (Wahid)[61], (Krysiak)[14] In the case of austenitic steels (18-8), ruptures of SCC are intergranular when steel is subjected to non suitable thermal treatment such as in the zone of carbide precipitation, between 400 and 800°C. With a steel subjected to 'hyperquenching' ruptures are almost always transgranular.

Austenitic stainless steels that are susceptible to intergranular corrosion are also subject to intergranular SCC. The problem of the intergranular SCC of sensitized austenitic

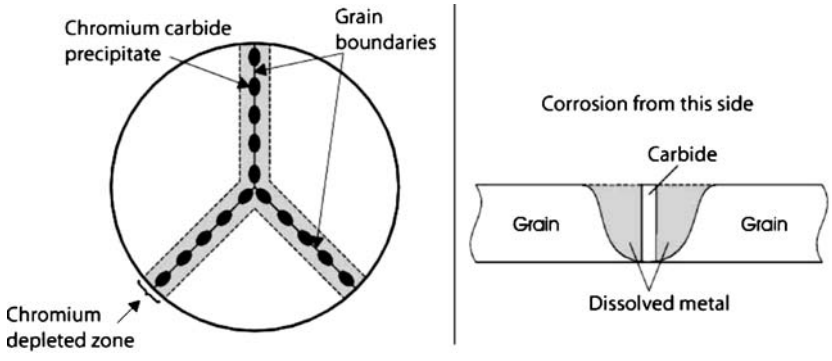

Figure 6.28 *Schema of a grain boundary (on the left), and a concentration profile near the grain boundary (on the right) of a sensitized stainless steel type 304*[16]

stainless steels in boiling high-purity water containing oxygen has been well studied. Cracking of sensitized stainless steels in many boiling water nuclear reactors has been observed. Sensitized stainless alloys of all types crack very rapidly in the polythionic acid that forms during the shutdown of desulfurization units in petroleum refineries. (Fritz)[5] Intergranular corrosion of 430, 434 and 446 steels during welding has been observed. (Wahid)[61,] (Krysiak)[14] Figure 6.27 shows a schematic diagram of weld decay (sensitization) in an austenitic stainless steel weldment. (Fritz)[5] The grain joints become impoverished in chromium because of the formation of carbides of chromium (Figure 6.28).

Knife-line attack. Stabilized austenitic stainless steels may become susceptible to a localized form of intergranular corrosion known as knife-line attack or knife-line corrosion. During welding, the base metal immediately adjacent to the fusion line is heated to temperatures high enough to dissolve the stabilizing carbides, but the cooling rate is rapid enough to prevent carbide precipitation. If weldments in stabilized grades are then heated into the sensitizing temperature range of 425–815°C, for example, during stress-relieving treatments, high-temperature service, or subsequent weld passes, chromium carbide can precipitate. The precipitation of chromium carbide leaves the narrow band adjacent to the fusion line susceptible to intergranular corrosion. Knife-line attack can be avoided by the proper choice of welding variables and by the use of stabilizing heat treatments.[5]

Localized biological corrosion of stainless steels. There are three general sets of conditions under which localized biological corrosion of austenitic stainless steel occurs (Figure 6.29). These conditions should be examined for metals that show active–passive corrosion behavior. Microbiological corrosion in austenitic steel weldments has been documented. (Wahid)[61,] (Krysiak)[14]

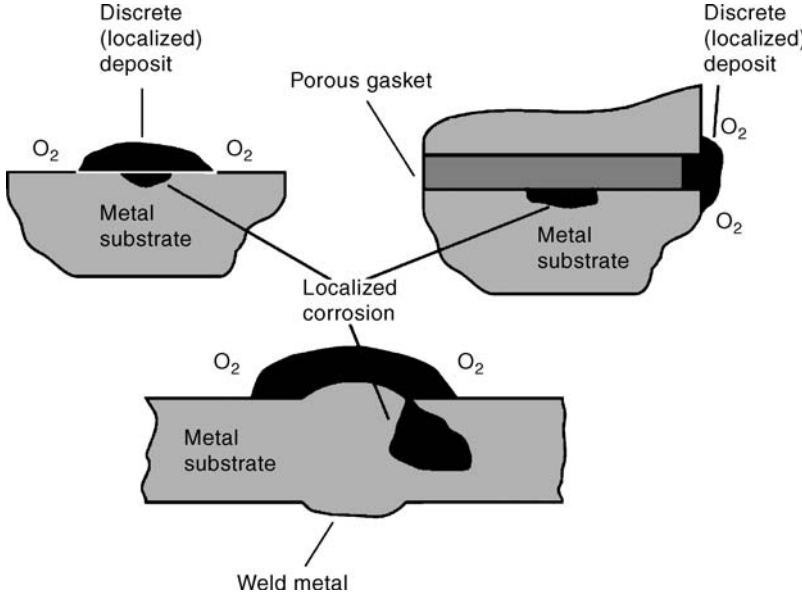

Figure 6.29 *Three favorable conditions of penetration of bacteria through a pinhole, causing a corroded subsurface cavity in stainless austenitic steels*[31]

Prevention. In North America, susceptibility to intergranular corrosion and sensitization can be avoided generally by the use of low-carbon grades such as type 316L (0.03% C maximum) in place of sensitization-susceptible type 316 (0.08% C maximum). In Europe, it is more common to use 0.05% C (maximum) steels, which are still reasonably resistant to sensitization, particularly if they contain molybdenum and nitrogen; these elements appear to raise the tolerable level of carbon and/or heat input. (Wahid)[61,] (Krysiak)[14] However, this method is not effective for eliminating sensitization that would result from long-term service exposure at 425–815°C.

At temperatures above 815°C, titanium and niobium form more stable carbides than chromium and are added to stainless steels to form these stable carbides, which remove carbon from solid solution and prevent precipitation of chromium carbides. (Fritz)[5]

In the wrought condition, duplex stainless steels have microstructures consisting of a fairly even balance of austenite and ferrite. The new generations of duplex alloys, which have a composition centered around Fe-26Cr-6.5Ni-3.0Mo, are now being produced with low carbon and a nitrogen addition. These alloys are useful because of their good resistance to chloride SCC, pitting corrosion, and intergranular corrosion in the as-welded condition. (Wahid)[61,] (Krysiak)[14]

Choosing the proper welding parameters, balancing alloy compositions to inhibit certain precipitation reactions, shielding molten and hot metal surfaces from reactive gases in the weld environment, removing chromium-enriched oxides, and chromium-depleted base metal from thermally discolored (heat tinted) surfaces. (Wahid)[61,] (Krysiak)[14]

Corrosion resistance of aluminum alloys. Researchers have shown that aluminum alloys, both welded and unwelded, have good resistance to uninhibited HNO_3 (both red and white) up to 50°C. Above this temperature, most aluminum alloys exhibit knife-line attack (a very thin region of corrosion) adjacent to the welds. In inhibited fuming HNO_3 containing at least 0.1% hydrofluoric acid (HF), no knife-line attack was observed for any commercial aluminum alloy or weldment even at 70°C (160°F).

Weldments of non-heat-treatable alloys have good resistance to corrosion. In the case of heat-treatable alloys, corrosion is selective in the weld or in the heat-affected zone. Welding can crack because of mercury–zinc amalgam and residual stresses, e.g., welded crack of Al 7xxx alloys by Hg–Zn amalgam. Stress–corrosion cracking cases in weldments due to residual stresses introduced during welding are rare. Brazed joints in aluminum alloys have good resistance to corrosion, but excessive flux should be removed. Soldered joints are good in milder environment, but not in more aggressive ones.[62]

Corrosion Resistance of Nickel-based Alloys. Nickel-based alloys are solid solutions based on nickel. Nickel-based alloys used for low-temperature aqueous or condensed systems are generally known as corrosion-resistant alloys (CRA), and nickel alloys used for high-temperature applications are known as heat-resistant alloys (HRA), high-temperature alloys (HTA), or superalloys. The corrosion performance could change due to the presence of second phase or a weld seam. (Rebak)[5]

The most common failures are associated with oxidation, carburization and metal dusting, sulfidation, chlorination, and nitridation. The most common high-temperature degradation mode is oxidation, and the protection against oxidation, in general, is given by the formation of a chromium oxide scale. The presence of a small amount of aluminum or silicon in the alloy may improve the resistance against oxidation of a

chromia-forming alloy. Attack by other elements, such as chlorine and sulfur, depends strongly on the partial pressure of oxygen in the environment. (Rebak)[5]

In general, industrial environments can be divided into two broad categories: *reducing* and *oxidizing*. These terms refer to the range of electrode potential that the alloy experiences, and it is controlled by the cathodic reaction in the system. Uniform corrosion can occur under reducing conditions in the active region of potentials and also under oxidizing conditions in the form of a slow, passive corrosion. Localized corrosion, such as pitting and crevice corrosion, generally occurs under oxidizing conditions. Stress–corrosion cracking (SCC) or environmentally assisted cracking (EAC) can occur at any electrochemical potential range. (Rebak)[5]

Based on the chemical composition, corrosion-resistant nickel-based alloys consist of commercially pure nickel. Ni–Cu alloys, Ni–Mo alloys, Ni–Cr–Mo alloys, and Ni–Cr–Fe alloys.[63] The cast versions of the nickel-based alloys do not have the same corrosion resistance as the corresponding wrought products, mainly due to the higher carbon and silicon contents and the anisotropic microstructure of the cast products. (Rebak)[5]

The performance of a cast nickel-based alloy is generally based on the microstructural quality, such as the amount of interdendritic segregation, secondary carbides, and intermetallic phases. With the same overall chemical composition, the corrosion rate of the same alloy can vary by several orders of magnitude, depending on its particular microstructure. The most important metallurgical factors that need to be considered are second-phase precipitation by thermal instability and the presence of cold work. The latter is especially important in cases where SCC may be expected. (Rebak)[5]

6.7.5 Microbiologically Influenced Corrosion

Growth and Metabolism. The most important requirement for microbial growth is the existence and availability of water. Microorganisms take up substances that are dissolved in water (nutrients) and produce cell material.[64] Under favorable conditions, some bacteria can double in number every 20 min or less. Thus, a single bacterium can produce a mass of over one million microorganisms in less than 7 h The bacteria as a group can survive from -10 to $>100^{\circ}$C, pH $\sim$0–10.5, dissolved oxygen (0 to saturation), pressure (vacuum to >31 MPa) and salinity (parts par billion to about 30%). Most bacteria that have been implicated in corrosion grow best at temperatures 15–45°C and pH 6–8. (Dexter)[14]

A large percentage of these microorganisms can form extracellular polymeric materials termed simply polymer, or slime. The slime helps glue the organisms to the surface, helps trap, concentrate nutrients as food for microbes and shields the organisms from biocides. This slime can change the concentrations of different elements and pH at the electrochemical interface by acting as a diffusion barrier. (Dexter)[14]

Environments. A great variety of microscopic organisms (microorganisms) are present in virtually all natural aqueous environments, such as bays, estuaries, harbors, coastal and open ocean seawaters, as well as rivers, streams, lakes, ponds, aqueous industrial fluids and waste waters. Larger, macroscopic organisms, such as the well-known barnacles and mussels, are also present in many environments. In natural conditions, sulfate reducing bacteria (SRB) grow in association with other microorganisms and use a range of

carboxylic acids and fatty acids, which are common by-products of other micro-organisms. Biological slimes are commonly found in the water phases of industrial process plants. A wide range of common bacteria (e.g., *Pseudomonas* and *Flavobacterium*) can secrete large amounts of organic material under both aerobic and oxygen-free (anaerobic) conditions. (Dexter)[14]

Biological corrosion in freshwater environments. In fresh water environments, there are bacteria and algae (yeasts and moulds). The organisms attach themselves to and grow on the surface of structural materials, resulting in the formation of a biofilm. The film itself can range from a microbiological slime film on fresh water heat-transfer surfaces to a heavy encrustation of hard-shelled fouling organisms on structures in coastal seawater. It is important to note, that the presence of a biofilm does not necessarily mean that there will always be a significant effect on corrosion. (Dexter)[14]

Microbial films will affect the general corrosion rate only when the film is continuous. However, this is not frequently the case since micro-organisms form in discrete deposits or colonies, and the resulting corrosion is likely to be localized. A uniform slime film formation on the piping of potable water-handling systems and on the heat-transfer surfaces of low-temperature heat exchangers is inconsequential unless it leads to obstruction of the flow, leading to a health hazard by growth of the organisms or localized corrosion. (Dexter)[14]

Biological corrosion in marine environments. A heavy fouling of macro-organisms (barnacles, mussels, etc.) decreases the amount of dissolved oxygen at the interface and acts as a barrier on structural steel in the splash zone and shields the metal from the damaging effect of wave action. Also, a continuous film of bacteria, algae, and slime (microorganisms) can have the same beneficial effect as that of the macro-organisms. However, in most cases, these films are not continuous and an oxygen preferential cell is created. Microbial films are suspected of being capable of inducing pit initiation on stainless steels and copper alloys in marine environments. Natural seawater is more corrosive than artificial solutions because of the living organisms. (Dexter)[14]

Figure 6.30 shows an incomplete coverage by barnacles that is more likely to initiate pitting and crevice corrosion. Effectively, barnacles were attached to the periphery of a high-strength steel rudder, which had originally been coated with an antifouling paint. During use, the paint around the edges had been removed by mechanical action, thus allowing the attachment of barnacles. On the other hand, a continuous film of bacteria, algae, and slime can occur, sometimes providing a barrier film and limiting corrosion; however, it is rare that a film of microorganisms in the marine environment is continuous over larger areas of exposed surface. (Dexter)[14]

Industries affected. The various industries that have been affected by microbiological corrosion problems are numerous and problems in every industry depend on the material and the characteristics of the medium. Industries affected by microbiologically influenced corrosion include: Chemical processing, energy generation systems, pulp and paper, hydraulic systems, fire protection, water treatment, sewage handling and treatment, highway maintenance, buildings and stoneworks, aviation, underground pipeline and onshore and offshore oil and gas equipment. (Dexter)[5]

Influence of Some Microbiological Species on Corrosion.[64] Some bacteria are involved directly in the oxidation or reduction of metal ions, particularly iron and manganese.

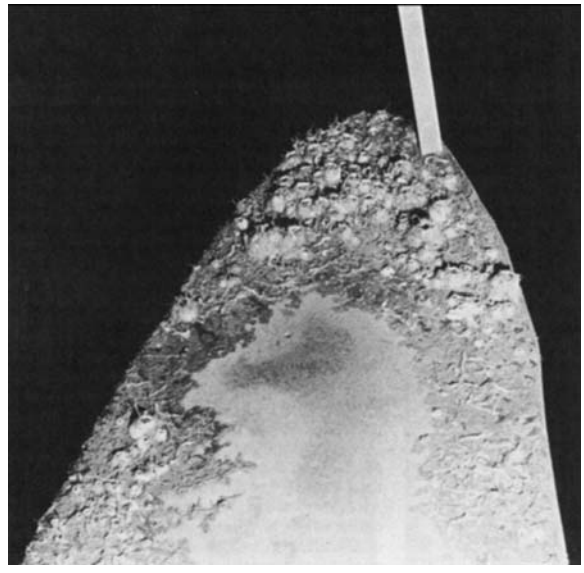

Figure 6.30 *An incomplete recovery of high-strength steel rudder by barnacles in ocean water (Dexter)*[14]

Some microbes can produce organic acids, such as formic and succinic, or mineral acids such as sulfuric acid. Some bacteria can oxidize sulfur or sulfide to sulfate or reduce sulfates, very often to hydrogen sulfide as end product. (Dexter)[14]

Sulfate-reducing bacteria are anaerobic (oxygen-free) bacteria that obtain their required carbon from organic nutrients and their energy from the reduction of sulfate ions to sulfide. Sulfate is abundant in fresh waters, seawater, and soils. Sulfide appears as H_2S (dissolved or gaseous), HS^- ions, S^{2-} ions, metal sulfides, or a combination of these, according to the conditions. Sulfides are highly corrosive. (Stott)[5] SRB are anaerobic bacteria and facilitate the cathodic reaction which controls the corrosion rate in these media. Considering a buried steel in a soil containing a near-neutral pH solution, the presence of sulfate-reducing bacteria accelerates the electrochemical reaction of corrosion according to the following equations. (Dexter)[14]

$$4\,Fe \rightarrow 4\,Fe^{2+} + 8\,e^- \qquad \text{(anodic)}$$

$$8\,H^+ + 8\,e^- \rightarrow 8\,H \qquad \text{(cathodic)}$$

$$SO_4^{2-} + 8\,H^+ \xrightarrow{SRB} S^{2-} + 4\,H_2O$$

$$Fe^{2+} + S^{2-} \rightarrow FeS \qquad \text{(corrosion product)}$$

$$Fe^{2+} + 2\,(OH)^- \rightarrow Fe(OH)_2 \qquad \text{(corrosion product)}$$

$$2\,H^+ + S^{2-} \rightarrow H_2S \qquad \text{(possible gas product)}$$

The ferrous sulfide film is not continuous and the base iron can corrode. Hydrogen sulfide can also be produced. The SRB have been identified to contribute to the corrosion of stainless steels, copper and aluminum alloys. (Dexter)[14]

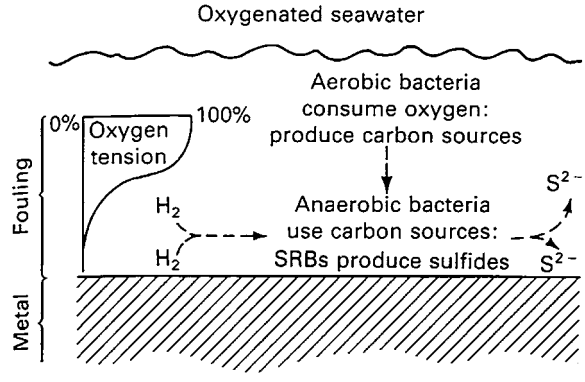

Figure 6.31 *Association of anaerobic and aerobic bacteria*[65]

Most sulfate-reducing bacteria are obligate anaerobes, yet they are known to accelerate corrosion in aerated environments. This is possible when aerobic organisms form a film or colony and then, through their metabolism, create a microenvironment favorable for anaerobic bacteria. Aerobic organisms near the outer surface of the film consume oxygen and create a suitable habitat for the sulfate-reducing bacteria (SRB) at the metal surface (Figure 6.31) The accompanying flora delivers the nutrients SRB needs, e.g., acetic acid, butyric acid, etc., and consumes the oxygen which is toxic for the SRB.[64,65,] (Dexter)[5,] (Dexter)[14]

Anaerobic corrosion. Desulfovibrio, Desulfotomaculum, and *Desulfomonas* in anaerobic microenvironments can exist under biodeposits of aerobic organisms, in crevices built into the structure, and at flaws in various types of coating systems. The most commonly encountered SRB type is known as *Desulfovibrio*. The most corrosive environments are often those in which alternate aerobic–anaerobic conditions exist because of the action of variable-flow hydrodynamics or periodic mechanical action. Conditions at the base of even thin slimes (biofilms) can be ideal for the growth of SRB, with high organic nutrient status, without oxygen, low redox potential, and protection from biocidal agents. (Stott)[5] Figure 6.32 explains the corrosion of iron and steel showing the action of sulfate-reducing bacteria (SRB) in removing hydrogen from the surface to form FeS and H_2S. (Dexter)[5] SRB-induced corrosion is encountered in oil and gas industry.[64]

Attack by organisms other than SRB. Ammonia and amines are produced by microbial decomposition of organic matter under both aerobic and anaerobic conditions (ammonification). (Stott)[5] These compounds are oxidized to nitrite by aerobic bacteria such as *Nitrosomonas* or *Nitrobacter* species. *Nitrobacter* is very efficient at destroying the corrosion-inhibition properties, of nitrate-based corrosion inhibitors by oxidation, unless a biocidal agent is included in the formulation. The release of ammonia at the surfaces of heat-exchanger tubes has a detrimental effect. (Stott)[5]

Bacteria of the genus *Thiobacillus*, obtain energy not by oxidation of organic compounds, but by oxidation of inorganic sulfur compounds (including sulfides) to sulfuric acid. The following reactions are performed by mixed cultures of *Thiobacilli*

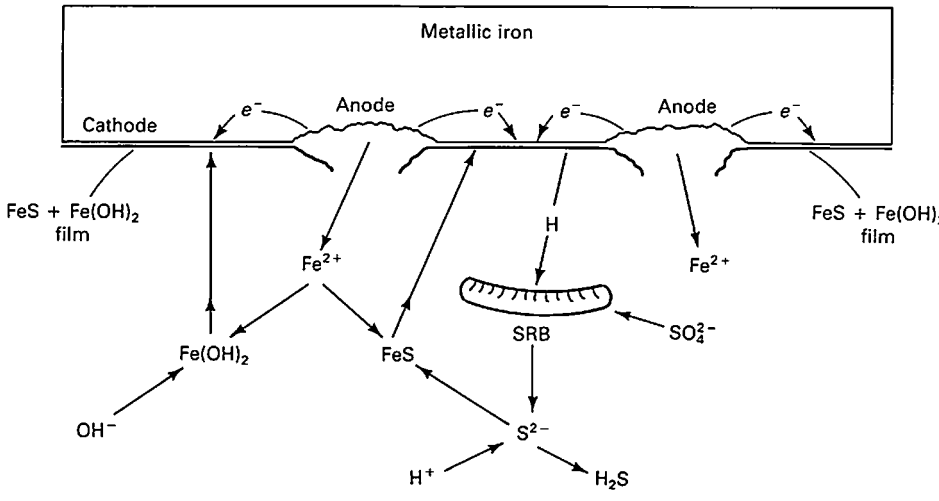

Figure 6.32 *Schematic of the corrosion of iron and steel in presence of anaerobic reducing bacteria (SRB) (Dexter)*[14]

acting on elemental sulfur or sulfides. Certain of the *Thiobacilli* will also leach metal sulfide ores according to the following reaction.

$$4\,FeS_2 + 15\,O_2 + 2\,H_2O \rightarrow 2\,Fe_2(SO_4)_3 + 2\,H_2SO_4$$

The important point to note is that these bacteria require oxygen and a source of reduced sulfur. The end product is sulfuric acid. The problem of septic sewage systems in hot climates starts with growth of anaerobic SRB in the sewage, producing H_2S. This gas migrates to the air space at the top of the line, where it is oxidized into sulfuric acid in the water droplets at the crown of the pipe by *Thiobacillus*. The corrosion problem is due to the combination of the bacterial action that results in dissolution of the alkaline mortar by the acid, followed by corrosion of the ductile iron. (Stott)[5]

Corrosion Mechanisms. The influence of microbiological organisms can be the initiation of either general or localized corrosion. This influence derives from the ability of the organisms to change variables such as pH, oxidizing power, velocity of flow, and concentration of chemical species at the metal/solution interface. (Dexter)[5] Corrosion can be influenced by microorganisms in the following ways:

Production of differential aeration cell: A scatter of individual barnacles on a stainless steel surface creates oxygen concentration cells. The formation of biofilm generates several critical conditions for corrosion initiation. Uncovered areas will have free access to oxygen and act as cathodes, while the covered zones act as anodes. Underdeposit corrosion (crevice corrosion) or pitting can occur. Depending on the oxidizing capacity of the bacteria and the chloride ion concentration, the corrosion rate can be accelerated. However, the presence of a biofilm does not necessarily mean that there will always be a significant effect on corrosion. (Dexter)[5]

Considering pit formation on the surface of iron, the anodic and cathodic reactions are:

$$2\,Fe \rightarrow 2\,Fe^{2+} + 4\,e^{-} \qquad \text{(anodic)}$$

$$O_2 + 2\,H_2O + 4\,e^{-} \rightarrow 4\,OH^{-} \qquad \text{(cathodic)}$$

The insoluble corrosion product $Fe(OH)_2$ can help bacterial film to control the diffusion of oxygen to the anodic sites in the pit. This forms a typical tubercle. If chlorides are present in the aqueous solution, the pH of the solution trapped in the tubercle can become very acid due to the autocatalytic propagation mechanism of localized corrosion due to deposit formation and generation of hydrochloric acid.

$$FeCl_2 + 2\,H_2O \rightarrow Fe(OH)_2 + 2\,HCl$$

Production of biofilms. The bacteria implicated in corrosion may begin their lives on a metal surface as a scatter of individual cells. As the biofilm matures, however, the organisms are usually found as individuals or in colonies embedded in the matrix of a semicontinuous and highly heterogeneous biofilm (Figure 6.33). (Dexter)[5] Microorganisms start on the surface from scattered individual bacteria to thick, semicontinuous films or colonies (slime or polymer) which can influence corrosion.

Depending on the velocity of fluid flow, the thickness varies from 10 to 100 μm, and it may cover from less than 20% to more than 90% of the metal surface. Biofilms or macrofouling in seawater can cause redox reactions that initiate or accelerate corrosion. Biofilms accumulate ions, manganese and iron, in concentrations far above those in the surrounding bulk water. They can also act as a diffusion barrier. Finally, some bacteria are capable of being directly involved in the oxidation or reduction of metal ions, particularly iron and manganese. Such bacteria can shift the chemical equilibrium between Fe, Fe^{2+}, and Fe^{3+}, which often influences the corrosion rate. (Dexter)[5]

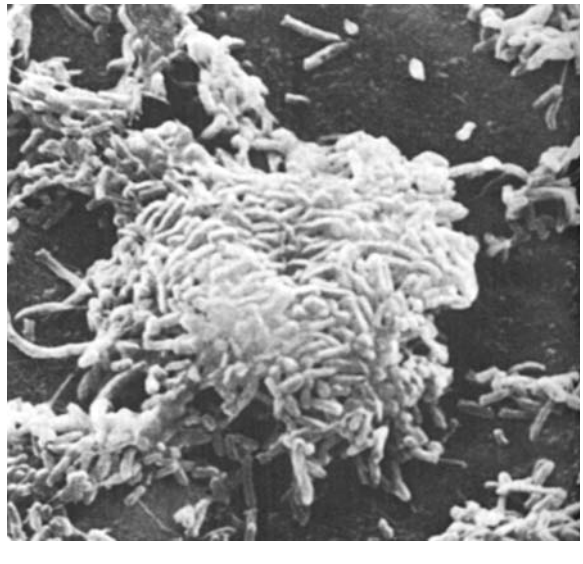

Figure 6.33 *Bacteria cells in a colony × 2700 (Dexter)*[14]

Production of sulfides. This may involve the production of FeS, Fe $(OH)_2$ etc. and an aggressive chemical agent such as hydrogen sulfide (H_2S) or acidity. Micro-organisms may also consume chemical species that are important in corrosion reactions (e.g., oxygen or nitrite inhibitors). Alternatively, their physical presence may form a slime or poultice, which leads to differential aeration cell attack or crevice corrosion. They may also break down the desirable physical properties of lubricating oils or protective coatings. (Stott)[5]

Production of organic and inorganic acids. The sulfur oxidizing bacteria can produce up to about 10% H_2SO_4. This low pH is highly corrosive to many metals, coatings, ceramics and concrete. Other bacteria can produce organic acids such as formic and succinic acids which are also harmful, and especially to some organic coatings. (Dexter)[5]

Gases and corrosion processes. Organisms that have a fermentative type of metabolism produce carbon dioxide (CO_2) and hydrogen (H_2) while others can utilize these gases. Other microbes can use CO_2 and H_2 as sources of carbon and energy, respectively. Numerous species of bacteria and algae either produce or use oxygen. One series of bacteria can reduce nitrates to nitrogen gas, others can convert nitrates to nitrogen dioxide, or vice versa, or they can break it to ammonia. Some of these gases can cause corrosion. (Dexter)[5]

MIC of Materials. Many cases have been documented of the biodeterioration by bacteria and/or fungi of architectural building materials, stonework, fiber-reinforced composites, polymeric coatings, and concrete.[66] Biodeterioration then proceeds by the processes of staining, patina formation, pitting, etching, disaggregation, and exfoliation. (Dexter)[5]

Wood and, polymers. Natural materials as well as materials manufactured from plant or animal origin, such as wood, cotton, paper products, wool, and leather, etc., are fully biodegradable under aerobic conditions. (Dexter)[5] Plastics are materials that consist mainly of highly polymeric, organic compounds. Also, nondegradable polymer may become degradable by a combined chemical, physical, and biological attack.[64,67]

Hydrocarbons. This generic term includes crude oils, distillation and cracking products (coal tar), as well as emulsions of these substances. Principally, all these substances are microbially degradable. Since hydrocarbons offer microorganisms good living conditions, microbial growth often causes damage to surrounding materials, e.g., fuel tanks or pipelines.[64]

Concrete can be damaged by the acids, sulfates, ammona, and other species produced by micro-organisms. Steel reinforcing bars in concrete corrode readily in such environments. Even in the absence of acid attack on the concrete, it has been shown that H_2S production by SRB can cause corrosion of the rebar in reinforced-concrete structures. (Dexter)[5] Concrete deterioration is caused by bacteria of the genus *Thiobacillus*. These are bacteria that transform sulfur and/or reduced sulfur compounds by producing and excreting sulfuric acid. The acid reacts with the [Ca $(OH)_2$, $CaCO_3$] to form gypsum ($CaSO_4$), which can be washed out. In this way, sewage pipelines made of concrete are destroyed.[64]

Forms of corrosion of metals and alloys. It should be noted that organisms are more likely to cause localized than general corrosion because of the differential oxygen cell. In each case, the localized attack was found beneath macrofouling layers. Corrosion of copper, steel, and aluminum anodes was significantly higher when connected to cathodes on which the biofilm was allowed to grow naturally Unexpectedly rapid localized

corrosion of steel bulkheads in marine harbor environments and of ship hull plating of several tankers has been documented. (Dexter)[14]

The increase in cathodic kinetics due to the action of biofilms on passive alloy surfaces can also increase the propagation rate of galvanic corrosion. Potentiodynamic polarization studies show that cathodic kinetics are increased during biofilm formation on passive alloy surfaces. Tests on crevice corrosion samples of passive alloys S30400 and S31600 revealed that crevice initiation times were reduced when natural marine biofilms were allowed to form on the exposed external cathode surface. (Dexter)[5]

Pitting corrosion of integral wing aluminum fuel tanks in aircraft that use kerosene-based fuels has been a problem since the 1950s.The fuel becomes contaminated with water by vapor condensation during variable-temperature flight conditions. Attack occurs under microbial deposits in the water phase and at the fuel–water interface. *Cladosporium resinae* is usually the principal organism involved: it produces a variety of organic acids (pH 3–4 or lower) and metabolizes certain fuel constituents. These organisms may also act in concert with the slime-forming *Pseudomonas* to produce oxygen concentration cells under the deposit. Active SRB have sometimes been identified at the base of such deposits.[68,] (Dexter)[5]

Hormoconis resinae is a continuing problem in fuel storage tanks and in aluminum integral fuel tanks of aircraft. Brown, slimy mats of *Hormoconis resinae* may cover large areas of aluminum alloy, causing pitting, exfoliation, and intergranular attack due to organic acids produced by the microbes and the differential aeration cells. The problem of fungal growth in the fuel tanks of jet aircraft has generally diminished as the design of fuel tanks has improved to facilitate better drainage of condensed water and as biocides such as organoboranes have gained acceptance as fuel additives.[5]

Only those organisms having a high tolerance for copper are likely to have a substantial effect. *Thiobacillus thiooxidans*, for example, can withstand copper concentrations as high as 2%. Localized corrosion of copper alloys by SRB in estuarine environments has been observed. (Dexter)[5] Copper–nickel tubes from the fan coolers in a nuclear power plant were found to show pitting corrosion under bacterial deposits. Slime-forming bacteria acting in concert with iron- and manganese-oxidizing bacteria were responsible for the deposits.[5] Monel 400 (66.5% Ni, 31.5% Cu, and 1.25% Fe) tubing was severely pitted after exposure to marine and estuarine waters containing SRB. (Dexter)[5]

It has been shown that welds provide unique environments for the colonization of SRB with the subsequent production of sulfides that affect the weld seam surface of the heat-affected zone. Exposure of sulfide-derived surfaces to fresh, aerated seawater resulted in rapid spalling on the downstream side of weld seams. The bared surfaces became anodic to the sulfide-coated weld root, initiating and accelerating localized corrosion. (Dexter)[5]

Microbiological Impacts and Testing. Evidence of harmful impact. Microorganisms, including the corrosion-inducing microorganisms, are present in soils, fresh water, seawater, and air. In most cases, the organisms influence corrosion. However, in a few cases the organisms can reproduce the attack when introduced into a sterile system. (Stott)[5] Hydrotesting of fabricated stainless steel structures has often been done with untreated fresh well waters. Such waters may contain micro-organisms, such as *gallionella*, which cause corrosion.

Four types of evidence – metallurgical, microbiological, chemical, and electrochemical – are generally used to determine if the influence of the organisms is important enough to invoke a corrosion control program. (Dexter)[5]

Metallographic evidence. Some types of MIC are recognizable, in part, by the pattern of corrosion products on the surface.

Microbiological evidence. The data must be gathered while the corrosion site is still wet. It is important to photograph the initial appearance of the corrosion site soon, while the organisms are still alive. Analysis of biological materials and corrosion products must be done.

Chemical evidence. Detailed chemical analysis should be done for the corrosion products and any biological mounds present at or near the corrosion site. Evaluation of the chemistry of the liquid phase and its variability, both spatially and with time in relation to the observed corrosive attack is necessary. Details should include the color, texture, odor, and distribution of the materials as well as their organic and inorganic chemistries. (Dexter)[5] The color change of corrosion deposits from black to brown is, in itself, a good indication of sulfide corrosion product. (Stott)[5] Tests for sulfate, total organic carbon (TOC), pH, sulfide and oxygen concentration are also useful indicators of the potential for SRB growth. (Stott)[5]

Electrochemical evidence. Conventional techniques such as variation of corrosion potential and corrosion rates at different periods. Noise electrochemical techniques should be very fruitful for monitoring corrosion evolution. (Little)[5]

Monitoring schemes. An effective monitoring scheme for controlling both biofouling and biocorrosion should include the generation of as many of the following types of data as possible.[69,70,] (Dexter)[5]

- Sessile bacterial counts of the organisms in the biofilm on the metal surface done by either conventional biological techniques or optical microscopy.[71,] (Stott)[5]
- Direct observation of the community structure of the biofilm. This can be done on metal coupons made from the same alloy used for the system
- Electrochemical corrosion measurements using electrical resistance or polarization-resistance-types probes. Electrochemical noise measurements should give an interesting dimension, but this is not a routine technique.
- Water quality and oxidation–reduction potential measurements.
- Identification of the microorganisms found in both the process water and on the metal surface. Tests for nitrite-utilizing bacteria or sulfur oxidizers are more complex. (Stott)[5]
- Identification and analysis of corrosion products and biofilms.
- Evaluation of the morphology, form and type of corrosion after removal of biological and corrosion product deposits.

A group of researchers at Shell Petroleum Company have developed an approach to risk assessment of carbon steel pipelines, based on the details of water chemistry and operation parameters.[72,] (Stott)[5]

Prevention. The general approaches to maintaining a system free of biocorrosion problems vary with the materials of construction, environment, economics, and duty cycle of the equipment. The most common approaches involve the use of sterilization,

coatings, cathodic protection and appropriate selection of materials. The most important step in prevention is to start with a clean system and to keep it clean.

Sterilization by physical methods such as irradiation (gamma or UV) for disinfection of materials and environments.[64]

Sterilization by chemical methods. Biocidal action has been widely used for many years to control biofilm formation in closed systems, such as heat exchangers, cooling towers, and storage tanks.[64,] (Dexter)[5]

6.7.6 Mechanically Assisted Corrosion

Mechanically assisted degradation can consist of the following types of corrosion: erosion–corrosion, water drop impingement erosion, cavitation erosion, erosive and corrosive wear, fretting corrosion, and corrosion fatigue (Figure 6.34). Erosion–corrosion phenomena are generally corrosion processes enhanced by erosion or wear. Erosive and corrosive wear are strong combinations of these phenomena of degradation because of suspended solid particles in the flow. Fretting corrosion is a wear process enhanced by corrosion. Corrosion fatigue appears in the presence of combined actions of a fluctuating or cyclic stress and a corrosive environment.

Corrosion and Wear. The progressive deterioration, due to corrosion and wear, of metallic surfaces in use in major industrial plants ultimately leads to loss of plant efficiency and in the worst case to shutdown. For example, corrosion and wear damage to materials, both directly and indirectly, cost the United States economy almost $300 billion per year at current prices. Similar studies on wear failure have shown that the wear of materials costs the U.S. economy about $20 billion per year

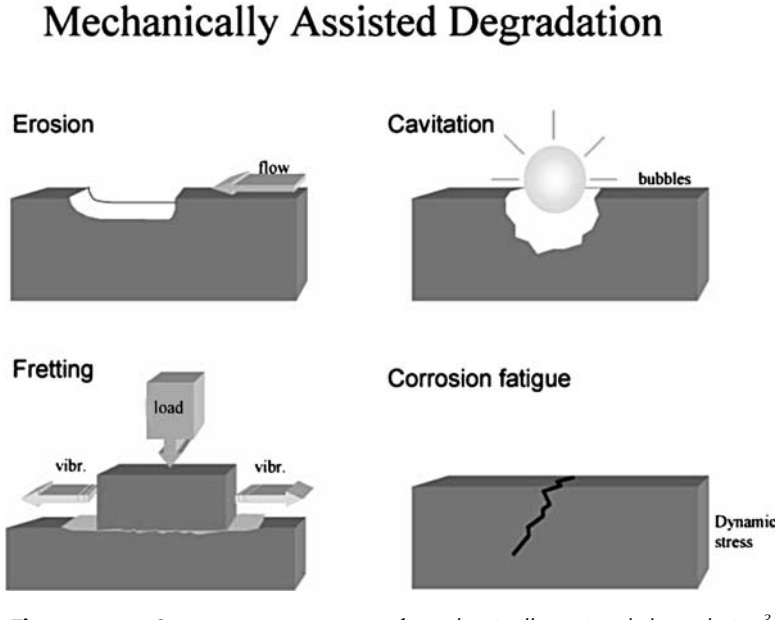

Figure 6.34 *Some corrosion types of mechanically assisted degradation*[3]

(in 1978 dollars) compared with about $80 billion annually for corrosion during the same period.[31,73]

The combination of wear or abrasion and corrosion results in more severe attack than with either mechanical or chemical corrosive action alone. Metal is removed from the surface as dissolved ions, as particles of solid corrosion products, or as elemental metal. The spectrum of erosion corrosion ranges from primarily erosive attack, such as sandblasting, filing, or grinding of a metal surface, to primarily corrosion failures, devoid of mechanical action.

Although corrosion can often occur in the absence of mechanical wear, the opposite is rarely true. Corrosion accompanies the wear process to some extent in all environments, except in vacuum and inert atmospheres. Corrosion and wear often combine to cause extensive damage in a number of industries, such as mining, mineral processing, chemical processing, pulp and paper production, and energy production. Wear debris and corrosion products that are formed during crushing and grinding of mineral ores (comminution) affect product quality and can adversely affect subsequent beneficiation by altering the chemical and electrochemical properties of the mineral.[31]

Exposure to the environment (gases and humidity) affects mechanical properties, friction, and wear of polymers. Most of the time, synergistic effects between abrasion, wear and corrosion are created and that amplifies the damage.[74,75] Dunn[76] has summarized the dominant and synergistic influence of every factor as follows.

Abrasion: removes protective oxidized metal and polarized coatings to expose unoxidized metal, in addition to removing metal particles. Forms microscopic grooves and dents for concentration cell corrosion. Increases microscopic surface area exposed to corrosion. Removes strain-hardened surface layers. Cracks brittle metal constituents, forming sites for impact hydraulic splitting. Plastic deformation by high-stress metal-mineral contact causes strain hardening and susceptibility to chemical attack.

Wear impact: plastic deformation makes some constituents more susceptible to corrosion. Cracks brittle constituents, tears apart ductile constituents to form sites for crevice corrosion, hydraulic splitting. Supplies kinetic energy to drive abrasion mechanism. Pressurizes mill water to cause splitting, cavitation, and jet erosion of metal and protective oxidized material. Pressurizes mill water and gases to produce unknown temperatures, phases changes, and decomposition or reaction products from ore and water constituents. Heats ball metal, ore, fluids to increase corrosive effects.

Corrosion influence: produces pits that induce microcracking. Microcracks at pits invite hydraulic splitting during impact. Roughens surface, reducing energy needed to abrade metal. May produce hydrogen with subsequent absorption and cracking in steel. Selectively attacks grain boundaries and less noble phases of multiphase microstructures, weakening adjacent metal.

Wear damage mechanisms. Wear is the surface damage or removal of material from one or both of two solid surfaces in a sliding, rolling or impact motion relative to one another. Wear damage precedes actual loss of material, and it may also occur independently. Strictly, wear, as in the case of friction, is not an inherent material property; it depends on the operating conditions and surface conditions. Wear rate does not necessarily relate to friction. Wear occurs by mechanical and/or chemical means and is generally accelerated by frictional heating. Various regimes of mechanical (plastically

dominated) and chemical (oxidation) wear for a particular sliding material pair are observed on a single-wear-regime mode.[75,77,78]

Principal wear mechanisms include: (1) adhesive, (2) abrasive, (3) fatigue, (4) impact by erosion and percussion, (5) chemical, and (6) electrical-arc-induced wear. Other, not distinct, mechanisms are fretting, fretting corrosion and fretting corrosion fatigue, a combination of adhesive, corrosive, and abrasive forms of wear. Wear by all mechanisms, except by the fatigue mechanism, occurs by gradual removal of material. Of the aforementioned wear mechanisms, one or more may be operating in any particular machine. In many cases, wear is initiated by one mechanism and it may proceed by other wear mechanisms, thereby complicating failure analysis.[75]

Adhesive wear. Adhesive wear occurs because of adhesion at asperity contacts at the interface. These contacts are sheared by sliding which may result in detachment of a fragment from one surface to another surface. Some are fractured by a fatigue process during repeated loading and unloading, resulting in formation of loose particles.

During sliding, surface asperities undergo plastic deformation and/or fracture. The subsurface, up to several micrometers in thickness, also undergoes plastic deformation and strain hardening with microhardness, by as much as a factor of two or higher, than the bulk hardness.[75]

Abrasive wear occurs when asperities of a rough, hard surface or hard particles slide on a softer surface, and damage the interface by plastic deformation or fracture in the case of ductile and brittle materials, respectively. In many cases, the wear mechanism at the start is adhesive, which generates wear particles that get trapped at the interface, resulting in three-body abrasive wear. In most abrasive wear situations, scratching is observed with a series of grooves parallel to the direction of sliding.[75]

Fatigue wear. Subsurface and surface fatigue are observed during repeated rolling (negligible friction) and sliding (coefficient of friction ≥ 0.3), respectively. The repeated loading and unloading cycles to which the materials are exposed may induce the formation of subsurface and surface cracks, which eventually, after a critical number of cycles, result in the breakup of the surface with the formation of large fragments, leaving large pits on the surface. In this mode, negligible wear takes place, since wear does not require direct physical contact between two surfaces. Mating surfaces experience large stresses, transmitted through the lubricating film during the rolling motion, such as in well-designed rolling element bearings. The failure time in wear fatigue is statistical in nature. Chemically induced crack growth (most common in ceramics) is commonly referred to as static fatigue. In the presence of tensile stresses and water vapor at the crack tip in many ceramics, a chemically induced rupture of the crack-tip bonds occurs rapidly, which increases the crack velocity. Chemically enhanced deformation and fracture results in an increased wear of surface layers in static and dynamic (rolling and sliding) conditions.[75]

Prevention of wear fatigue corrosion involves inherent physical properties of the alloy, for example, a gear must be tough and fatigue resistant yet have a surface that resists wear. For applications requiring only a moderate degree of impact strength, fatigue resistance and wear resistance, higher-carbon through-hardening steel may be sufficient. For more severe conditions, however, surface-hardened steel may be used.[31]

Impact wear includes erosive and percussive wear. *Erosion* can occur by jets, liquid droplets, and implosion of bubbles formed in the fluid and streams of solid particle. Solid

particle erosion occurs by impingement when discrete solid particles strike a surface, and the contact stress arises from the kinetic energy of particles flowing in an air or liquid stream as it encounters a surface. Wear debris formed in erosion occurs as a result of repeated impacts.[75] Neighboring particles may exert contact forces, and a flowing fluid, if present, will cause drag. Under some conditions, gravity may be important.

As in the case of abrasion, erosive wear mechanisms can involve both plastic deformation and brittle fracture. The particle velocity and impact angle combined with the size of the abrasive particle gives a measure of the kinetic energy of the impinging particles, that is proportional to the square of the velocity. Ductile materials will undergo wear by a process of plastic deformation in which the material is removed by the displacing or cutting action of the eroded particle. Some brittle materials undergo wear predominantly either by flow or by fracture, depending on the impact conditions. Wear-rate dependence on the impact angle for ductile and brittle materials is different.[75,79]

Slug flow is the dominant flow regime in multiphase systems. Flow visualization has shown that bubbles distort and elongate in the vicinity of the pipe wall in a manner similar to collapsing bubbles. The corrosion rate increases due to a thinning of the mass transfer and corrosion product layers, as well as due to localized damage of the corrosion product film. Multiphase environments can also occur in several industries. Change in pressure and temperature in process equipment and the mixing of various streams can force the mixture into two- or three-phase situation. The associated corrosion is of concern in nuclear and thermal power plants, chemical process industries, and in waste management. Slug flow can occur sooner in smaller diameter pipe, where the coalescence of bubbles can cause a transition from bubble flow to slug flow. Slug flow effects corrosion in two ways. First, a dramatic increase in the turbulent intensity that can increase the mass transport of corrosive species by 1000 times. In addition, extensive damage to the corrosion product layer occurs and exposes the surface to more attack.[80]

Percussion is a repetitive solid body impact, such as experienced by print hammers in high-speed electromechanical applications and high asperities of the surfaces in a gas bearing. Repeated impacts result in progressive loss of solid material. Percussive wear occurs by hybrid wear mechanisms, which combine several of the following mechanisms: adhesive, abrasive, surface fatigue, fracture, and tribochemical wear.[75]

Chemical or corrosive wear. Corrosive wear occurs when sliding takes place in a corrosive environment. In air, the most dominant corrosive medium is oxygen. Therefore, chemical wear in air is generally called oxidative wear. In the absence of sliding, the chemical products of the corrosion (e.g., oxides) would form a film typically less than a micrometer thick on the surfaces, which would tend to slow down or even arrest the corrosion, but the sliding action wears the chemical film away, so that the chemical attack can continue. Thus, chemical wear requires both chemical reaction (corrosion) and rubbing. Corrosion occurs in a highly corrosive environment and in high-temperature and high-humidity environments. Corrosive fluids may provide a conductive medium necessary for electrochemical corrosion to occur on the rubbing surfaces. The most common liquid environments are aqueous, and here small amounts of dissolved gases, commonly oxygen or carbon dioxide, influence corrosion.[75]

Chemical wear is important in a number of industries, such as mining mineral processing, chemical processing, and slurry handling. A typical example of a corroded roller subsequent to running in a bearing is shown in Figure 6.35. The corrosion left a

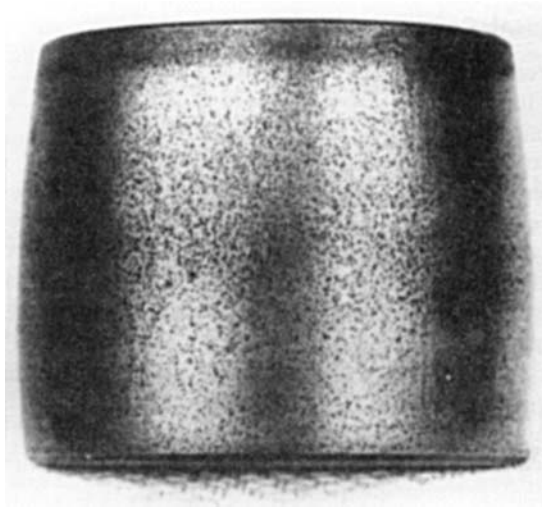

Figure 6.35 *SEM micrograph of 52 100 quenched and tempered roller bearing after corrosive wear*[75]

multitude of dark-bottomed pits, the surroundings of which are polished by running. The condition subsequently creates extensive, surface-originated spallings from a multitude of initiated points.[75]

Friction modifies the kinetics of chemical reactions of sliding bodies with each other, and with the gaseous or liquid environment, to the extent that reactions which occur at high temperatures occur at moderate, even ambient, temperatures during sliding. Chemistry dealing with modification of chemical reaction by friction or mechanical energy is referred to as tribochemistry, and the wear controlled by this reaction is referred to as tribochemical wear.[81] The mechanisms by which friction increases the rate of chemical reaction (tribochemistry) are frictional heat, removal of product scale resulting in fresh surfaces, accelerated diffusion and direct mechanochemical excitation of surface bonds. The tribochemical reactions result in oxidative wear of metals and tribochemical wear of ceramics.[75]

Oxidative wear. Interface temperatures produced at asperity contacts during sliding of metallic pairs under nominally unlubricated conditions result in thermal oxidation, which produces oxide films several micrometers thick. The oxidation is generally a beneficial form of corrosion. A thick oxide film reduces the shear strength of the interface, which suppresses the wear as a result of plastic deformation.[81] In many cases, tribological oxidation can reduce the wear rate of metallic pairs by as much as two orders of magnitude, compared with that of the same pair under an inert atmosphere. Tribological oxidation can also occur under conditions of boundary lubrication when the oil film thickness is less than the combined surface roughness of the interface. The oxidation can prevent severe wear. In oxidation wear, debris is generated from the oxide film.[75]

At low ambient temperatures, oxidation occurs at asperity contacts due to frictional heating. At higher ambient temperatures, general oxidation of the entire surface occurs and affects wear. In the case of steels, the predominant oxide present in the debris

depends on the sliding conditions. At low speeds and ambient temperatures, the predominant oxide is α-Fe_2O_3, at intermediate conditions it is Fe_3O_4, and at high speeds and temperatures it is FeO.[81] Oxygen and other molecules are adsorbed on clean metals and ceramic surfaces, and form strong chemical bonds with them. Since this reaction is controlled by the diffusion of the reacting species through the layers of corrosion product, oxidation of iron and many metals follows a parabolic law, with the oxide film thickness increasing with the square root of time.[75]

$$h = Ct^{1/2} \tag{6.1}$$

where h is the oxide film thickness, t is the average growth time, and C is the parabolic rate constant at elevated temperatures.

Since diffusion is thermally activated, the growth rate in oxide film thickness during sliding as a function of temperature, similar to thermal oxidation under static conditions, follows an Arrhenius type of relationship

$$K = Ae^{(-Q/RT)} \tag{6.2}$$

where K is the parabolic rate constant for the growth of the oxide film, A is the parabolic Arrhenius constant (kg^2/m^4s) for the reaction, Q is the parabolic activation energy associated with oxide (kJ/mol), R is the universal gas constant and T is the absolute temperature of the surface.

It has been reported that the Arrhenius constant for sliding is several orders of magnitude larger than that for static conditions. The oxidation rate during sliding may result from increased diffusion rates of ions through a growing oxide film, which generally involves a high defect density due to mechanical perturbations.[75]

Electric-arc-induced wear. When a high potential is present over a thin air film in a sliding process, a dielectric breakdown results, leading to arcing. During arcing, a relatively high-power density occurs over a very short period. The heat-affected zone is usually very shallow (of the order of 50 μm) and the heating results in considerable melting and subsequent resolidification, corrosion, hardness changes, and other phase changes, and even in the direct ablation of material. Arcing causes large craters, and any sliding or oscillation after an arc either shears or fractures the lips, leading to three-body abrasion, corrosion, surface fatigue and fretting.[75,82,83]

Erosion–corrosion. Generally, all types of corrosive media can cause erosion–corrosion, including aqueous solutions, organic media, gases, and liquid metals. The corrodent can be a bulk fluid, a film, droplets or a substance adsorbed on or absorbed on another substance. For example, hot gases may oxidize a metal at high velocity and blow off an otherwise protective scale. Solid suspensions in liquids (slurries) are particularly destructive from the standpoint of erosion corrosion.[16,31]

All types of equipment, exposed to fluids in motion, are subject to the erosion–corrosion phenomena. This can include pipeline networks (particularly curves, elbows and T-squares), floodgates, pumps, centrifugal fans, helixes, wheels of turbine, tubes of intersections of heat exchangers and measuring devices. In many cases, failures due to erosion–corrosion occur in a relatively short time.[16] Most metals are susceptible to erosion–corrosion in the liquid phase under specific conditions. Resistance of metals depends on the physical and chemical properties of the corrosion product and/or the

Figure 6.36 *Erosion corrosion of a pump propeller in Cu–10Sn–2Zn alloy*[1]

passive layers and their adhesion to the metallic surface. Passivating metals such as stainless steels and titanium are relatively immune to erosion–corrosion in many oxidizing environments.

A stainless steel pump impeller with an expected lifetime of two years failed in three weeks in a reducing solution. Metals that are soft are readily damaged or worn mechanically; examples are copper and lead. Even the noble or precious metals, such as silver, gold, platinum, are subject to erosion–corrosion.[16,31]

Impingement is a type of erosion–corrosion in which the liquid is in turbulent flow, containing bubbles of air and suspended particles that can hit the metallic surface strongly and destroy its protective film. The shock of bubbles of water or air against metal provokes wear of the surface. It takes the shape of a directional progress of the attack. The bottom portion becomes anodic in relation to the adjacent outer surfaces. The attack can also occur in this way when the solution does not contain bubbles of air or particles in suspension. Figure 6.36 shows a typical attack by impingement.[1,25] Erosion–corrosion is characterized by the appearance of grooves, gullies, waves, rounded holes, and valleys and usually exhibits a directional pattern. The Figure 6.37 gives a section of

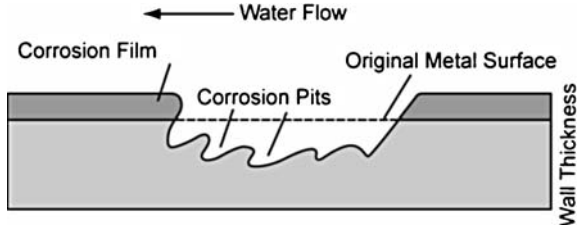

Figure 6.37 *Schematic of erosion–corrosion of a condenser tube wall*[31]

the metallic surface, showing the resulting attack where the protective film on the tube was disrupted.[31]

Agitation or circulation of the electrolyte leads to an increase in corrosion because of:

- Destruction or prevention of the formation of a protective film. (Froats)[14]
- Increase in the rate of diffusion of aggressive ions due to the speed of the fluid decreases the cathodic polarization and increases the corrosion current density as in the case of steels in the presence of oxygen, carbon dioxide or bisulphate.

However, the speed of the fluid can decrease the attack in some systems through:

- Improving the efficiency of inhibitors, while bringing them more quickly to the metal–solution interface.
- Forming the passive layer for an active metal and that can reduce corrosion rate. An increase in the flow speed permits to supply oxygen at the interface and attain the critical passive current for alloy in a given medium.
- Sweeping away corrosive ionic species. The attack of stainless steel decreases as the solution flow speed increases. Stainless steel in nitric acid without agitation, is attacked autocatalytically because of the formation of nitrous acid, as a cathodic reaction product.
- Agitation and circulation at certain speeds of the medium can avoid pitting and crevice corrosion.[16]

Turbulence. When the rate of the flow of a fluid becomes very large, another form of attack occurs by the combined action of erosion and corrosion. In general, the greater the speed, the greater the abrasive action of the flow. The speed strongly influences mechanisms intervening in corrosion. In the majority of cases, erosion–corrosion is due to the turbulence of the flow and this influences the chemical and mechanical stability of surface films. The type of flow (laminar or turbulent) depends on the rate and the quantity of transported fluid and also on the geometry or design of the equipment. Flow in a straight line is less damaging. Turbulence results in a more intimate contact between the environment and metal. Other factors such as edges, cracks, deposits, abrupt changes of section, and other obstacles disrupting the laminar flow contribute to the turbulence and the attack by impingement.[16] Figure 6.38 describes schematically how turbulent eddies probably thin the protective film locally to account for downstream undercutting.[84]

Elevated speeds have a marked effect on wear, and this is more pronounced if the solution contains some solid particles in suspension. Aluminum forms films of aluminum nitrate or oxide in fuming nitric acid. At low flow rates there is no attack whereas for speeds greater than 1.22 m s^{-1}, the protective layer is removed and erosion–corrosion occurs more readily.[16]

Galvanic effect. The galvanic cell between two different metals can have serious effects in a flowing system. For example, the galvanic cell was not present between stainless steel type 316 and lead in 10% sulfuric acid under static conditions, but when the flow rate increased to 11.89 m s^{-1}, the rate of erosion–corrosion increased enormously

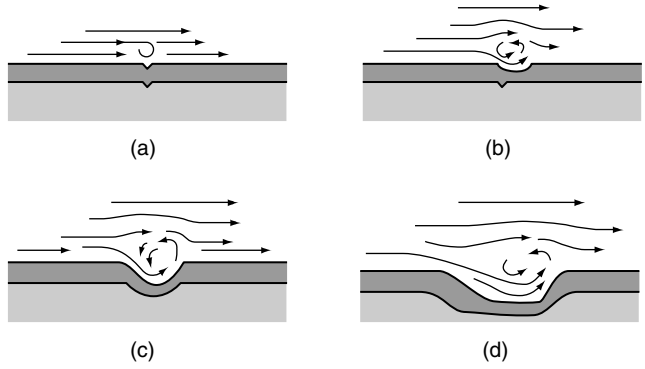

Figure 6.38 *Erosive and corrosive wear by turbulent eddy mechanism for downstream undercutting pits*[84]

because of the destruction of the passive film by the combined effect of galvanic corrosion and erosion corrosion.[16]

Water droplet impingement erosion. In liquid impingement erosion, with small drops of liquid striking the surface of a solid at high speeds (as low as 300 m s^{-1}), very high pressures are experienced, exceeding the yield strength of most materials. Thus, plastic deformation or fracture can result from a single impact, and repeated impact leads to pitting and erosive wear.[75] Water droplet impingement causes pitting and may cause cavitation damage. Damage may appear to be somewhat different from cavitation damage in ductile materials. The cavities in the surface show a directionality that is related to the angle of the attack of the drop, as in erosion–corrosion. Two areas most vulnerable for this type of corrosion are steam turbines and water rotor blades. In turbines, condensation of steam produces droplets that are carried into the rotor blades and causes surface damage. Rain drop erosion on helicopter blades can generate tensile stresses just below the surface and leads to cracking. (Glaeser and Wright)[14]

Prevention. The following measures can be taken to reduce or prevent erosion–corrosion:

1. A proper geometric design of the system in order to get a laminar flow with minimum turbulence, as in pipelines of large diameters and avoid abrupt changes or streamline bends.
2. The composition of a metal largely determines its resistance to corrosion. A noble metal or alloy has an inherent high resistance to corrosion, while for a more reactive material its resistance to corrosion depends mainly on its ability to form and to maintain a protective film.[16] The protective nature and properties of the film on some metals and alloys are very important for the resistance to erosion–corrosion. The chemical composition has a great influence on the metal properties. The addition of a third element to the alloy often increases the resistance to erosion–corrosion through the formation of a strong passive or protective film. For example, an addition of 2% Al to brass to form a brass–aluminum alloy and an addition of 1.2% Fe to cupronickels: in the two cases, the addition of an element to the alloy produces a marked increase of the resistance to impingement. It has been shown that the high performance of

condensation tubes in brass–aluminum against the impingement due to the presence of iron in the protective film, coming from products of the corrosion in water.[1] Also, the addition of Mo to 18-8 stainless steel to form steel type 316 is widely known for its resistance.

3. Toughness can influence the performance of materials under conditions of erosion–corrosion. The soft metals are often more susceptible to erosion corrosion because they are more susceptible to mechanical wear. The toughness is a good criterion for the resistance to the mechanical erosion or abrasion, but this is not necessarily a good criterion to predict the resistance to the erosion–corrosion. Stellite (Co–Cr–W–Fe–C alloy), which has better toughness than 18-8 stainless steel, showed better resistance to cavitation erosion on a water brake.[25]
4. There are several ways to harden alloys. A certain procedure to increase the resistance to the erosion corrosion is the hardening by solid solution. One adds an element to another to produce a solid solution that is resistant to the corrosion by hardening the metal. The thermal treatment is also a method to harden a metal or alloy, but it changes the microstructure and can induce a greater susceptibility to corrosion. Hardening by cold work is also an important procedure and it is the reason for using stainless steel to resist cavitation erosion. This material, initially hard, attains an even harder surface by cold work and becomes more resistant to attack and erosion.
5. Modification of the environment. Deoxygenation and the addition of inhibitors are useful methods to decrease the aggressiveness of a flowing liquid environment; they are not economical, even though they minimize erosion corrosion. One can also filter out the particles in suspension. The temperature should be lowered when possible.
6. Applying hard, tough protective coatings with resilient materials such as rubber and some plastics is recommended.[31]
7. Cathodic protection is efficient in order to reduce the electrochemical attack.

Cavitation is a form of corrosion that is caused by the repeated nucleation, growth, and violent collapse of vapor bubbles in a liquid against a metal surface. Cavitation erosion arises when a solid and fluid are in relative motion, and bubbles formed in the fluid become unstable and implode against the surface of the solid. Cavitation erosion is similar to surface wear fatigue.[75] A metal having undergone a cavitation erosion has an appearance similar to a pitted metal.[31]

Figure 6.39 shows an example of damage caused by cavitation erosion on a cylinder of diesel motor. The appearance of cavitation is similar to pitting, except that surfaces in the pits are usually much rougher. The affected region, if observed immediately, is free of deposits and accumulated corrosion products. One uses the term cavitation corrosion when the mechanical effect of the cavitation is limited to destruction of the oxide layer formed by corrosion. On the other hand, if the mechanical effect damages metal appreciably, it is rather cavitation erosion. Damage by these processes is found in components such as ship propellers, runners of hydraulic turbines, centrifugal pumps, pump impellers, and on many surfaces in contact with high-velocity liquids subject to changes in pressure.

Cavitation erosion. In certain conditions, a thin layer of liquid, nearly static at the metal–liquid interface can prevent impingement of the surface by the turbulent flow of the liquid. However, due to the turbulence of water, bubbles of air or gas of size larger

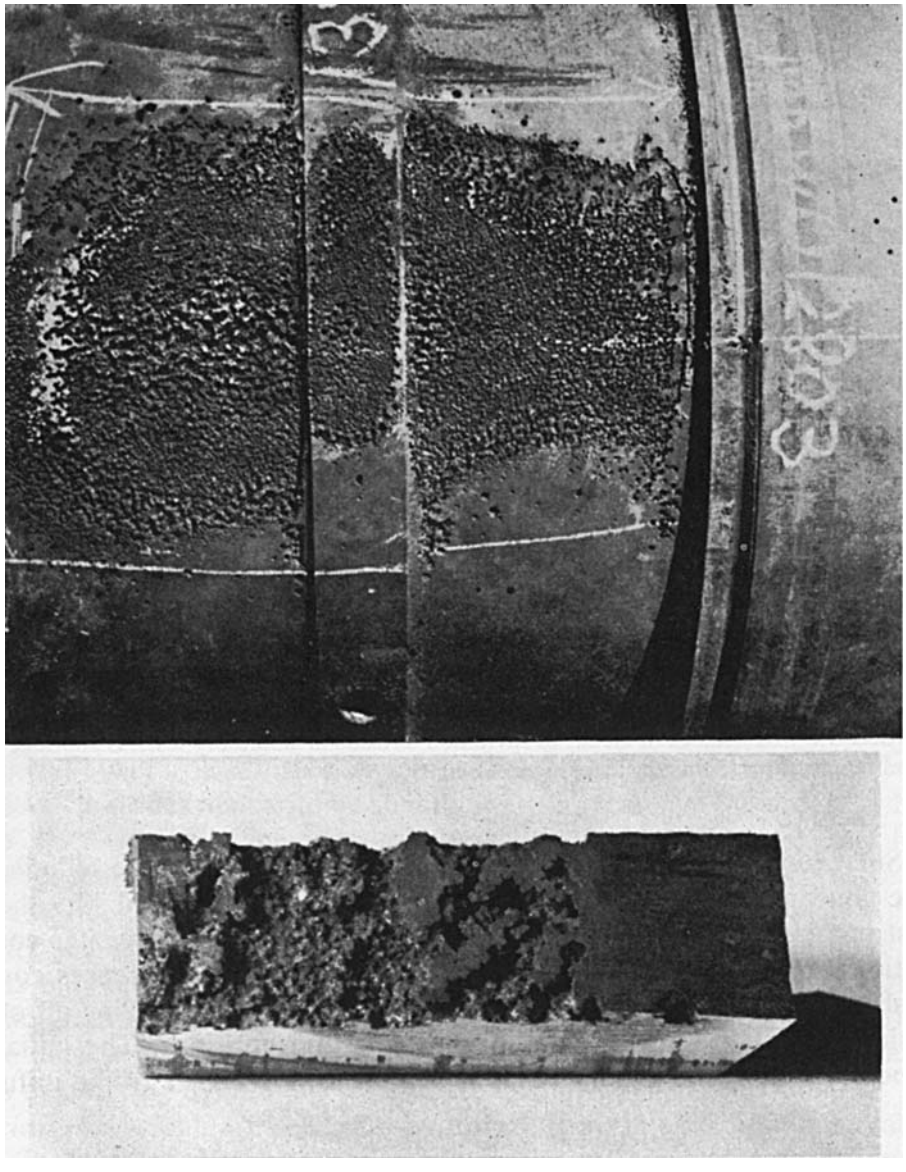

Figure 6.39 *Cavitation erosion damage of a cylinder liner of a diesel engine*[7]

than the thickness of the layer can interrupt, break the border layer and cause a continuous rupture of the protective film. A film of semiconductor oxide on the surface as Cu_2O, surrounding the damaged areas, produces a big cathode for reduction of the dissolved oxygen on the surface and causes pitting.

Impacting bubbles. When bubbles collapse that are in contact with or very close to a solid surface, they collapse asymmetrically. Consider a spherical bubble impacting a

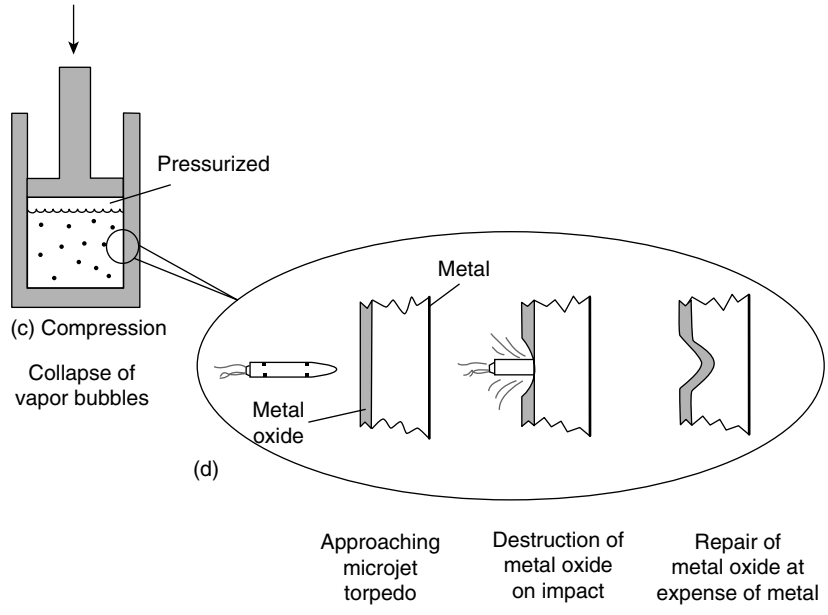

Figure 6.40 *Schematic representation of the disintegration of protective corrosion product by impacting microjet (torpedo)*[31]

plane solid surface. The bubble becomes elongated with a tail, and then collapses. The jet from the bubbles is believed to cause cavitation erosion on a solid wall.[85] As shown in Figure 6.40, implosion of a vapor bubble creates a microjet of liquid or microscopic 'torpedo' of water that is ejected from the collapsing bubble at velocities that may range from 100 to 500 m s^{-1}. When the torpedo impacts on the metal surface, it dislodges protective surface films and/or locally deforms the metal itself.

The solid material will absorb the impact energy, resulting in elastic or plastic deformation or even fracture. The latter two processes may cause localized deformation and/or erosion of the solid surface. Douglas *et al.*[86] suggest that the bubble grows and collapses, giving rise to high pressure for a few milliseconds. The local pressures observed during those few milliseconds may be up to 4000 atmospheres, with a temperature increase up to 800°C. This accelerates the corrosion rate. Fresh surfaces are exposed to corrosion, followed by reformation of protective films, which is followed by more cavitation. This cycle repeats itself.[31,75]

Single-phase flow may have a definite pattern, whereas several flow patterns exist for multiphase flows. Multiphase flow involves the simultaneous flow of more than one phase within a pipe as for example: oil/water or three-phase oil/water/gas flows in carbon steel pipelines have an important influence on the form and kinetics of corrosion. Slug flow is the dominant flow regime in multiphase systems. It involves unique flow mechanisms with pulses of gas bubbles being released into a turbulent mixing zone due to a mixing vortex behind the slug front. These bubbles impact and collapse on the pipe wall, causing severe localized, cavitation type corrosion, which can be up to 1000 times the values normally seen in other flow regimes.[80,85,86]

Prevention. The following preventive measures can be used in addition to the measures given under erosion–corrosion:

1. Cavitation can be minimized by a proper design to minimize hydrodynamic pressure differences and specifying a smooth finish on all critical metal surfaces. One can use higher pressure or lower temperature to reduce the formation of the damaging steam bubbles causing cavitation. Proper operation of pumps and equipment is necessary, for example, a pump should not be operated on plugged or impaired flow lines.[84]
2. Cathodic protection is sometimes beneficial to avoid cavitation, not because of the reduced rate of corrosion but because of the cushioning effect of hydrogen evolved on the surface. Removal of dissolved air is often beneficial because dissolved gases more easily nucleate cavitating bubbles at low pressures.
3. The hard, tough metals or elastomeric polymers may be used to resist the cavitation erosion. The physical property intervening here is the resilience, which is the capacity to dispose the energy of an impact without absorbing some. Another property of the rubber that can also have an influence on the resistance to cavitation erosion is its resistance to abrasion.[25]

Fretting corrosion is a combined wear and corrosion process in which material is removed from contacting surfaces when motion between the surfaces is restricted to very small amplitude oscillations (often, the relative movement is barely discernible ranging from a few tens of nanometers to a few tens of micrometers). Fretting occurs where low-amplitude oscillatory motion in the tangential direction takes place between contacting surfaces, which are nominally at rest.[87,89,] (Waterhouse)[88] It is necessary that the load be sufficient to produce a distortion of surfaces. This is a common occurrence, since most machinery is subjected to vibration, both in transit and in operation. Figure 6.41 shows a typical example. Pressed-on wheels can often fret at the shaft/wheel hole interface.[31]

Oxidation is the most common factor in the fretting process. In oxidizing systems, fine metal particles removed by adhesive wear are oxidized and trapped between the fretting surfaces. The oxides act like an abrasive (such as lapping red) and increase the rate of

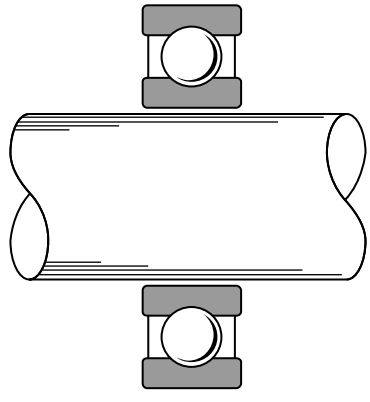

Figure 6.41 *Example of typical fretting corrosion location*[16]

material removal. The red material, easily lost from between the contacting surfaces, is an example of this type of fretting in ferrous alloys.

Examples of vulnerable components are shrink-fits, bolted parts, and splines. The contacts between hubs, shrink- and press-fits, and bearing housings on loaded rotating shafts or axles and many parts of vibrating machinery are particularly prone to fretting damage. Flexible couplings and splines, particularly where they form a connection between two shafts and are designed to accommodate some misalignment, can suffer fretting wear.[75] Fretting corrosion is frequently observed between the crown of a ball bearing and its axle, or the head of a screw and the metallic surface, and in jewel bearings, elements of machines in movement, suspension springs, electric relay contacts, king pins of auto steering mechanisms.[7,90]

Fretting corrosion is characterized by discoloration and takes the form of local surface dislocations and deep pits. It is at such pits that fatigue cracks eventually nucleate. These occur in regions where slight relative movements have occurred between mating, highly loaded surfaces.[31] With time, fretting corrosion can cause a tarnished appearance of the metallic surface and a variation of piece sizes. Products of corrosion can also cause blockages in machines in movement. As examples, these products are (NiO + a little Ni) for Ni, (Cu_2O + lesser amounts of CuO and Cu) for Cu; and (brown Fe_2O_3 + a small quantity of iron powder) for steel, (particles of black alumina with a core of metallic aluminium) for Al.[7,90] Figure 6.42 shows the scanning electron micrograph of a 303 stainless steel shaft after it underwent fretting corrosion.

Mechanism. Basically, fretting is a form of adhesive or abrasive wear, where the normal load causes adhesion between asperities and oscillatory movement causes ruptures, resulting in wear debris. Most commonly, fretting is combined with corrosion, in which case the wear mode is known as fretting corrosion. For example, in the case of steel particles, the freshly worn nascent surfaces oxidize (corrode) to Fe_2O_3, and the

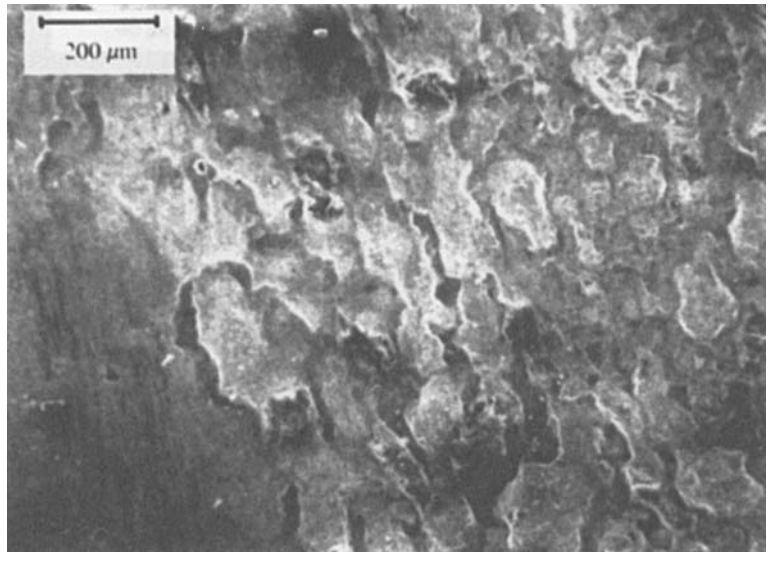

Figure 6.42 *Scanning electron micrograph of 303 stainless steel shaft surface after fretting corrosion*[75]

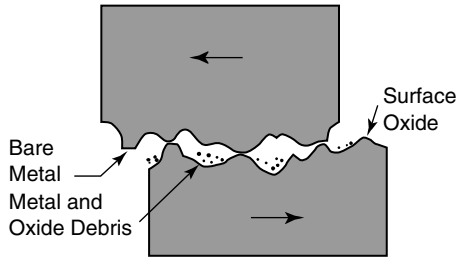

Figure 6.43 *Schematic of the fretting process showing the final effects of wear and oxidation*[19]

characteristic fine reddish-brown powder is produced, known as 'cocoa'. These oxide particles are abrasive. Because of the close fit of the surfaces and the oscillatory small-amplitude motion (of the order of a few tens of micrometers), the surfaces are never brought out of contact, and therefore there is little opportunity for the products of the action to escape. Further oscillatory motion causes abrasive wear and oxidation, and so on. Therefore, the amount of wear per unit sliding distance due to fretting may be larger than that from adhesive and abrasive wear.[75]

Two approaches are considered, depending on what phenomenon initiates and propagates the damage: wear-oxidation and oxidation-wear.[91] In wear-oxidation two surfaces are in contact; and they are never perfectly smooth. They are in contact through their asperities and the relative displacement of the two surfaces entails the wear of their crests.[92] It occurs as a type of cold welding or fusion at the interface of metal surfaces under pressure. During displacements, these points of contact break and fragments of metal are produced. These fragments are very small and immediately oxidize because of the heat generated due to friction. This phenomenon repeats itself and residues accumulate (Figure 6.43). Subsequent oxidation of the damaged material has a secondary effect. Wear by fretting without debris of oxides has been observed for noble metals, mica, glass, etc.[16]

In oxidation-wear, most the metallic active surfaces are first protected from atmospheric oxidation by a thin layer of adherent oxide. When metals are in contact (under load) and subjected to repeated weak movements, the layer of oxide is broken at the level of asperities and it removes some oxide particles. The fresh exposed surfaces oxidize all over again and the process repeats itself. The basis of this approach is that the accelerated oxidation is considered to be due to the effects of friction.[90]

A more plausible theory could be a combination of the two previous approaches with the relative importance of one or the other depending on the particular system, and is therefore a function of the medium, surface finishing and the nature of materials in contact. However, in both approaches the presence of oxygen accelerates the corrosion by fretting, especially for the ferrous alloys.[16]

Evidently, fretting is worse in air than in an inert atmosphere.[25] There is less damage in a humid atmosphere than in dry air since humidity can have a lubricant action, and the hydrated oxides are less hard than the dry oxides.[25,90,93] Surfaces subjected to fretting wear have a characteristic appearance with red-brown patches on ferrous metals and adjacent areas that are highly polished because of the lapping quality of the hard iron oxide debris.

There appears to be no critical measurable amplitude below which fretting does not occur. However, if the deflection caused is only elastic, it is not likely that fretting

damage can occur. A rapid increase in wear rate occurs with slip amplitude over a certain amplitude range. For a given slip amplitude, the amount of wear per unit sliding distance per unit applied normal load increases linearly with a number of oscillating cycles up to an amplitude of about 100 μm. Above this amplitude, wear rate per unit sliding distance becomes constant.[75]

The fretting wear rate is directly proportional to the normal load for a given slip amplitude. However, in the total-slip situation, the frequency has little effect. (Waterhouse)[88] In a partial-slip situation, the frequency of oscillation has little effect on wear rate per unit distance in the low-frequency range, whereas the increase in the strain rate at high frequencies leads to increased fatigue damage and increased corrosion due to a rise in temperature.[75]

However, the effect of temperature on fretting depends on the oxidation characteristics of the metals. If increased temperature results in the growth of a protective, tough oxide layer that prevents metal-to-metal contact, the fretting rate is lower. An incubation period is observed when fretting wear is negligible, followed by a steady rate. (Glaeser and Wright)[5]

A rapid increase in wear rate with slip amplitude occurs over a range of amplitude. Wear debris is generally classified as plate-shaped, ribbon-shaped, spherical and irregularly shaped, based on morphology.

Wear of a material is dependent on the mating material (or material pair), surface preparation and operating conditions. Clean metals and alloys exhibit high adhesion, and consequently high friction and wear. Any contamination mitigates contact, and chemically produced films, which reduce adhesion, result in reduction in friction and wear. In dry sliding, identical metals, particularly iron on iron, are metallurgically compatible and exhibit high friction and wear and they must be avoided. Soft and ductile metals such as In, Pb, and Sn exhibit high friction and wear. Hexagonal metals such as Co and Mg as well as some nonhexagonal metals such as Mo and Cr exhibit low friction and wear. Lead-based white metals (babbitts), brass, bronze, and gray cast iron generally exhibit relatively low friction and wear, and are commonly used in dry and lubricated bearing and sea applications. For high-temperature applications, cobalt-based alloys are used which exhibit good galling resistance. Galling or welding resistance is a measure of normal stress at which two materials loaded against each other. Nickel-based alloys are poor in unlubricated sliding because of generally catastrophic galling.[75]

Modeling fretting corrosion. An equation has been used for steel to evaluate the loss of weight W caused by fretting corrosion based on a model that combines the chemical and mechanical effect of the corrosion by fretting. The chemical factor concerns the oxidation that occurs at the time of wear, corresponding to adsorption of oxygen to form the oxide. The mechanical factor concerns the loss of particles, at the asperities on the opposite surface.

$$W = \underbrace{(K_0 L^{1/2} - K_1 L)\frac{C}{f}}_{\text{chemical factor}} + \underbrace{K_2 lLC}_{\text{mechanical factor}} \tag{6.3}$$

where $L =$ charge between surfaces, $C =$ number of cycles, $f =$ frequency of movements, $l =$ slip and K_0, K_1, K_2 are constants.

The chemical factor decreases with increase in frequency of movement because there is less available time for the chemical reaction. The mechanical factor is a function of the slip

and the load. In an atmosphere of nitrogen only the mechanical factor is important for the wear of steel debris on the metallic iron powder, and W is independent of the frequency.[7]

Fretting corrosion fatigue. Fatigue failures traceable to fretting corrosion are found in many aircraft engine parts, such as connecting rods, knuckle pins, splined shafts, clamped and bolted flanges, couplings, and many others. Such failures also occur in railway axle shafts at the wheel seats and in automobile axle shafts, suspension springs, steering knuckles, etc.[25,90,91] The oscillatory movement is usually the result of external vibration, but in many cases it is the consequence of one of the members of the contact being subjected to a cyclic stress (i.e., fatigue), which results in early initiation of fatigue cracks and usually results in a more damaging aspect of fretting, known as fretting fatigue.[75] Fretting also causes the rupture of adhesive ties because of the strengths of oscillations, and this action can generate the fine cracks that in certain conditions propagate to form a major fracture of the sample.

It is found in some systems that the quantity of metal lost by fretting is directly related to the reduction of the resistance to fatigue. The frequent oscillations cause the formation of pits that initiate cracks of fatigue and increase the susceptibility to fatigue fractures. Fretting corrosion causes loss of material in highly loaded bolted assemblies. This loosens bolts and studs, increasing their liability to fatigue failure. This is very serious when the bolt or stud is very short as in aircraft engine cylinder hold-down studs.[91] It has been shown that the initiation of the fretting fatigue crack is located at the boundary of the fretting scar at the fretted zone. The fatigue crack then propagates into the surface at an angle to the surface, as shown in Figure 6.44. (Glaeser and Wright)[5]

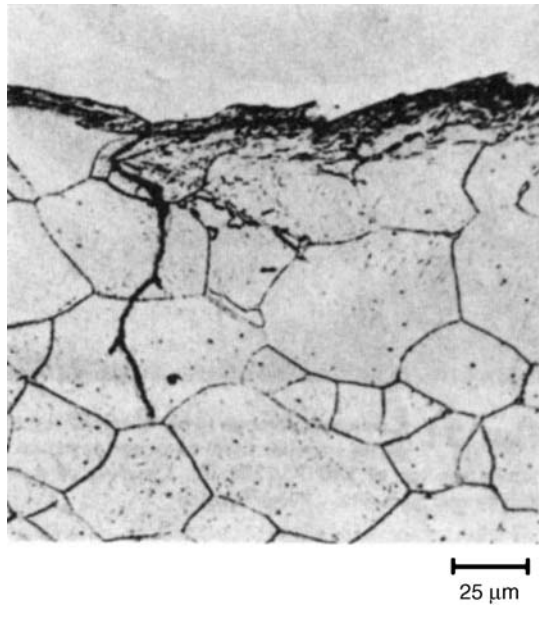

Figure 6.44 *Section showing fretting damage and fatigue crack initiation in 0.2% C steel (Waterhouse)*[5]

Prevention. Various design changes can minimize fretting wear. The machinery should be designed to reduce oscillatory movement, reduce stresses or eliminate two-piece design altogether.[75] Some examples of possible approaches to consider are:

1. Lubrication of the faying surfaces with low-viscosity, high-tenacity oils and greases to exclude direct contact with air. This is an adequate but not complete remedy. Phosphate conversion coatings of steels, for example, are used in conjunction with lubricants since they are porous and provide oil reservoirs.[16]
2. Use of gaskets to absorb vibration and limit oxygen at bearing surfaces.
3. Restricting the degree of the movement; shot peening offers the double advantage of inducing residual surface compression stress to retard corrosion and roughening the surface to increase friction.[91]
4. Increase the hardness of one or both of the contacting surfaces. Surface hardening such as carburizing and nitriding or applying suitable protective coatings by electrodeposition, plasma spraying, or vapor deposition, anodizing of aluminum alloys. Hard materials are more resistant than soft materials. At sufficiently large loads, soft metals serve to exclude air at the interface; furthermore, a soft surface can yield by shearing instead of sliding at the interface.[7]
5. Increase load to reduce slip between mating surfaces.[16,31,] (Waterhouse)[88]
6. Considerable improvement in wear resistance can be achieved when dissimilar metals are coupled, and this is especially true for steels coupled with silicon bronze and Stellite alloys. The wear data further suggest that improvement in wear resistance can be achieved by altering the surface characteristics, such as by surface treatment or by adding a coating.[75]

Testing. The measurement of corrosion, wear, and corrosion–wear interactions as well as erosion–corrosion interactions is a multistep process. Each component of the interaction must be measured separately. The results may then be combined to identify the synergistic effects and create a complete picture of the damage process. Measurement of the interaction between corrosion and wear modes or damage is more difficult. The standard (ASTM, G119)[4] applies to systems in liquid solutions or slurries and some aspects of it can be adapted to dry corrosion and wear interactions as well. (Tylczak and Adler)[5]

Measurement of wear and corrosion. Jet and whirling arm tests are currently used in the field of erosion.[4] In case of the whirling-arm test, the impact velocity is well known, and an entire face of the specimen can be eroded, producing a more uniform surface. The machining test is the most commonly used in high-temperature abrasive tests, because the process of machining produces an elevated temperature. For slow abrasive elevated-temperature tests one of the most commonly used is a high-temperature ring-on-disk test. (Tylczak and Adler)[5] (Madsen)[88]

Galling stress. Wear galling is a good measure of wear resistance of a given material pair. Galling appears as a groove, or score mark, terminating in a mound of metal. Galling data are indicative and show for example that identical metal couples usually do poorly in terms of galling compared with dissimilar metal couples. When stainless steels are coupled with each other, with the exception of some Nitronic steels, they exhibit worse galling resistance than all other steels by a factor of 2 or more.[75]

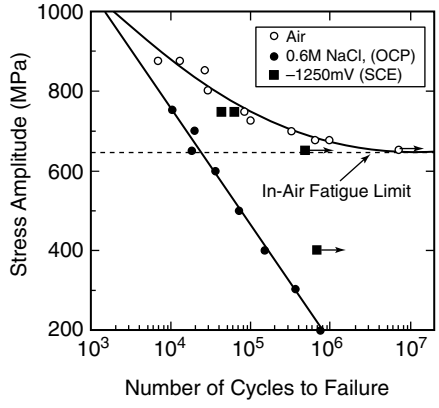

Figure 6.45 *Fatigue life data, S–N curves, for a high-strength steel under different environmental conditions. Stress ratio R = −1. Loading frequency 1 Hz for tests in 0.6 M NaCl solution. Horizontal arrows indicate failure condition not attained. OCP = open-circuit potential*[102]

Corrosion Fatigue. Corrosion fatigue (CF) is a term that is used to describe the phenomenon of cracking in materials under the combined actions of a fluctuating or cyclic stress and a corrosive environment. The damage due to corrosion fatigue is usually greater than the sum of the damage by corrosion and fatigue acting separately. Figure 6.45 shows an example of the reduction of fatigue life and the elimination of the fatigue limit of high-strength steel in a sodium chloride solution.[94] It also shows that cathodic polarization restores the fatigue properties of the steel.

As an example, the shaft of a ship propeller, slightly above the waterline, can normally function until a leak occurs, allowing the water to impinge on the shaft in the area of maximum alternating stress. Another example is failure of the shaft in a period of days. Tubes of pumping made of steel for oil well have a limited life span because of the corrosion fatigue that results from exposures to oil well brines. Also, pipes carrying steam or hot liquids of variable temperature may fail because of periodic expansion and contraction (thermal cycling).[7]

Morphology of CF ruptures. Corrosion fatigue produces fine-to-broad cracks with little or no branching and this is different from SCC, which often exhibits considerable branching. The cracks may occur singly, but commonly appear as families or parallel cracks. It rarely appears as a single important crack. They are typically filled with dense corrosion product. They are frequently associated with pits, grooves, or some other forms of stress concentrator. Transgranular fracture paths, frequently ramified or branched, are more common than intergranular fractures, except for lead and zinc (Figures 6.46 and 6.47, respectively). Some systems show the combination of both paths.[7,31]

When the surface of a ruptured material by fatigue is examined, two zones of variable importance can be distinguished: a smooth, silken aspect, not having undergone any plastic distortion, and resulting from the propagation of the fatigue crack through the metal. The cyclic constraint has the tendency to smooth the surface of the rupture by wearing. A final rupture zone, rough and damaged due to plastic deformation, is noted. The crack propagates until the area of the transverse section of metal is reduced,

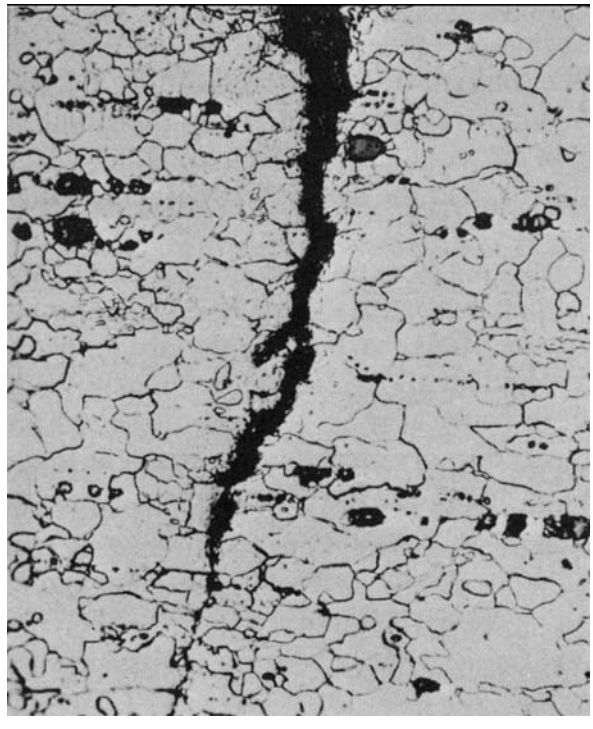

Figure 6.46 *Corrosion fatigue crack through mild steel sheet, resulting from fluttering of the sheet in a flue gas condensate*[7]

sufficient so that the ultimate stress limit is reached and then a fragile and brutal rupture occurs.

Key factors of corrosion fatigue. Corrosion fatigue is not specific since most materials suffer degradation due to their fatigue properties in aqueous media. Steel for example undergoes corrosion fatigue in fresh waters, seawater, products of combustion condensates, general chemical environments, etc.[7] For a given material, the fatigue strength (or fatigue life at a given maximum stress value) generally decreases in the presence of an aggressive environment. The effect varies widely, depending primarily on the particular metal–environment combination. The environment may affect the probability of fatigue crack initiation, the fatigue crack growth rate, or both.[95]

Corrosion fatigue depends strongly on the combined interactions of the mechanical (loading), metallurgical, and environmental variables.[31]

Stresses. The main mechanical properties to consider are: maximum stress or stress intensity factor, σ_{max} or K_{max}, cyclic stress or stress-intensity range, $\Delta\sigma$ or ΔK, stress ratio R, cyclic loading frequency, cyclic load waveform (constant-amplitude loading), load interactions in variable-amplitude loading, state of stress, residual stress, and crack size and shape, and their relation to component size geometry.[31]

The greater the applied stress at each cycle, the shorter the time to failure. Mechanical damage is more important when load and frequency are high, while corrosion damage

Figure 6.47 *Example of an intergranular corrosion fatigue failure in a Ti-6Al-4V alloy (Glaeser and Wright)*[5]

becomes dominant at an intermediate load and/or frequency. In such conditions, cracking may be transgranular or intergranular, and the morphology may become very similar to SCC crack morphology. Cyclic stress has a negligible influence on the resistance to fatigue while the resistance to corrosion fatigue is influenced distinctly by the frequency of the cyclic stress. The corrosion influence in fatigue corrosion is more pronounced at low frequencies because contact between the corrosive species and metal is longer.

Materials that are extremely sensitive to the environment, such as ultra-high-strength steel in distilled water, are characterized by high growth rates that depend on stress intensity range ΔK to a reduced power. Time-dependent corrosion fatigue crack growth occurs mainly above the threshold stress intensity for static load cracking and is modeled through linear superposition of SCC and inert environment fatigue rates. (Glaeser and Wright)[5] The description of corrosion fatigue behavior should consider the level of mechanical loading, the frequency and the shape of the cycles. It is then recommended to express corrosion fatigue as a function of crack growth rate da/dt, rather than the most frequently used cycle-dependent crack growth rate.[95]

Cyclic load frequency is the most important factor that influences corrosion fatigue for most material environment and stress intensity conditions. The dominance of frequency is related directly to the time dependence of the mass transport and chemical reaction steps involved for brittle cracking.

Stress ratio. Rates of corrosion fatigue crack propagation generally are enhanced by increased stress ratio R, which is the ratio of the minimum stress to the maximum stress.

Some *other factors*, including the metallurgical condition of the material (such as composition and heat treatment) and the loading mode (such as uniaxial), affect corrosion fatigue crack propagation. (Glaeser and Wright)[5]

Environmental factors. In general, environmental properties to consider are: types of environments (gaseous, liquid, liquid metal, etc.), temperature, partial pressure of damaging species in gaseous environments, concentration of damaging species in aqueous or other liquid media, corrosion potential, pH, conductivity, halogen or sulfide ion content, viscosity of the environment, oxygen concentration, solution composition, inhibitors, coatings, etc.[31] Corrosion products are identified on or within fracture surfaces. Corrosion fatigue cracking of high-strength steel exposed to a hydrogen-producing gas, such as water vapor, may be difficult to differentiate from some other forms of hydrogen damage. At sufficiently high frequencies, the fracture surface features produced by corrosion fatigue crack initiation and propagation do not differ significantly from those produced by fatigue in nonaggressive environments. (Glaeser and Wright)[5]

The usual test of fatigue of metals in air is influenced by oxygen or humidity and always represents a measure of corrosion fatigue. Early tests showed that the endurance limit for copper in a partial vacuum was found to be 14% higher than that in air. The main effect has been assigned to oxygen, which has little influence on initiation, but has a considerable influence on crack propagation.[7] The natural waters and particularly brackish waters have a greater effect on corrosion fatigue of steel than of copper. Controlled changes in the potential of a specimen can result in either the complete elimination or the dramatic increase in brittle fatigue cracking. (Glaeser and Wright)[5]

Material factors. The main metallurgical properties of importance are: alloy composition, distribution of alloying elements and impurities, microstructure and crystal structure, heat treatment, mechanical working, preferred orientation of grains and grain boundaries (texture), mechanical properties (strength, fracture toughness, etc.).[31]

Tests for fatigue consist in subjecting a metal to alternate cyclic stresses, compression–tension of different values, and measuring the time (number of cycles N) before rupture. A short characteristic of the fatigue test is called the C–N curve, giving the number of cycles N to rupture. The value of the maximal stress for which an infinite number of cycles can be supported without rupture is called the endurance limit or fatigue limit. This exists for steels, but not necessarily for other metals, and is roughly equal to half the tensile strength. Nonferrous metals, such as the aluminum and magnesium, alloys of copper, do not possess a fatigue limit. In these cases, one refers to fatigue strength or resistance to a certain arbitrary number of cycles, e.g., 10^8 cycles.[90]

Growth rates of cracks are influenced by metallurgical variables, including impurities in composition, microstructure, and the cyclic deformation mode. In carbon steel, cracks often originate at hemispherical corrosion pits and often contain significant amounts of corrosion products. The cracks are often transgranular and may exhibit a slight amount of branching. Surface pitting is not a prerequisite for corrosion fatigue cracking of carbon steels nor is the transgranular fracture path; corrosion fatigue cracks sometimes occur in the absence of pits and follow boundaries or prior-austenite grain boundaries. (Glaeser and Wright)[5]

In aluminum alloys exposed to aqueous chloride solutions, corrosion fatigue cracks frequently originate at sites of pitting or intergranular corrosion. Initial crack propagation

is normal to the axis of principal stress. This is contrary to the behavior of fatigue cracks initiated in dry air, where initial growth follows crystallographic planes. Initial corrosion fatigue cracking normal to the axis of principal stress also occurs in aluminum alloys exposed to humid air, but pitting is not a requisite for crack initiation. (Glaeser and Wright)[5]

Corrosion fatigue cracks in copper and various copper alloys initiate and propagate intergranularly. Copper–zinc and copper–aluminum alloys, however, exhibit a marked reduction in fatigue resistance, particularly in aqueous chloride solutions. This type of failure is difficult to distinguish from stress–corrosion cracking (SCC), except that it may occur in environments that normally do not cause failures under static stress, such as sodium chloride or sodium sulfate solutions. (Glaeser and Wright)[5]

The corrosion fatigue of low alloy steels in water at high temperature is an example where modification of the crack tip chemistry has been identified as the main cause of an environmentally assisted cracking (EAC) phenomenon. In some instances, hot water may cause a drastic increase of the fatigue crack propagation rate in low-alloy steels.[96] However, this effect occurs only if the sulfur content of the wrought steel exceeds a critical value of 100–150 ppm.[96,97] The cause of EAC has been identified as the accumulation of sulfide ions in the crack tip environment, originating from the dissolution of MnS inclusions bared by the crack advance.[98,99] In aerated environments, the potential gradient inside the crack tends to inhibit outward diffusion of the sulfide and this leads to EAC over a larger range of loading conditions, particularly at lower frequencies.[100,101]

Mechanisms of corrosion fatigue. The mechanism of the fatigue in air proceeds by localized slip within grains of the metal caused by stress. Adsorption of air on the fresh surface exposed at slip steps prevents rewelding on the reverse stress cycle. Continued slip produces displaced clusters of slip bands, which protrude above the metal surface (extrusions); corresponding incipient cracks form elsewhere (intrusions). The corrosion process may remove barriers to plastic deformation (e.g., dislocations), induce plastic deformation by reducing surface energy and favors slip step formation, or by injecting dislocations along slip planes (Figure 6.48).[7] After or during the initiation of microcracks, it is likely that the propagation results, in part, due to the adsorption of oxygen or water or different ionic species along partitions of the crack. This adsorption reduces the energy of surface and prevents the welding of the metallic surface during the inverse constraint cycle. The formation of differential aeration cells due to different concentrations of oxygen in the localized sites can play a role on the dissolution of metal at the bottom of the crack (anode) and contribute to the propagation of the crack. A corrosive environment eliminates the fatigue limit or shortens the life above the fatigue limit.

Wang[102] classified fatigue damage into four stages:

1. Precrack cyclic deformation that includes the formation of persistent slip bands, formation of extrusions and intrusions.
2. Crack initiation and stage one growth that deepens the intrusions within the plane of high shear stress.
3. Stage two crack propagation of well-defined cracks on the planes of high tensile stress in the direction normal to the maximum tensile stress.
4. Ductile fracture propagation.

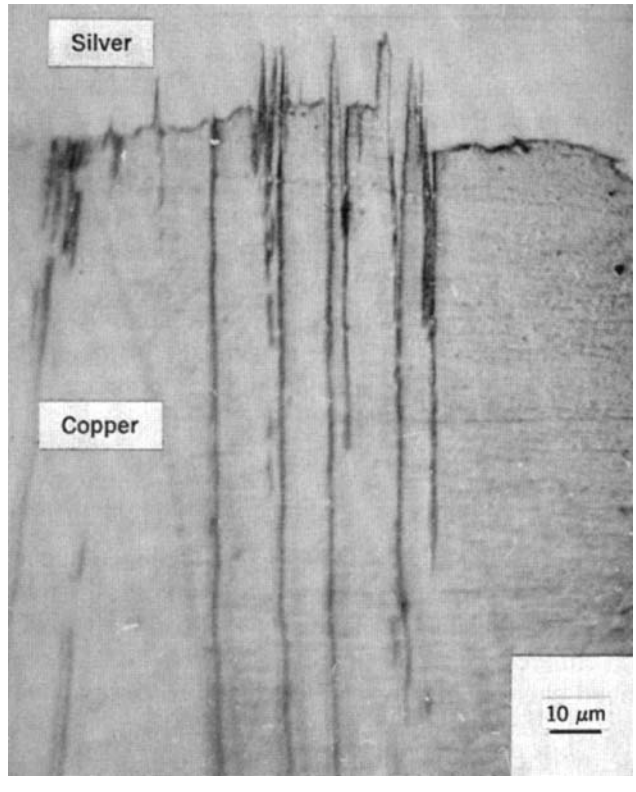

Figure 6.48 *Extrusions and intrusions in the copper[7] after 6×10^5 cycles in air. Sample covered with silver and mounted at an angle to magnify surface protuberances ×20*

Crack initiation. Corrosion fatigue cracks are always initiated at the surface, unless there are near-surface defects that act as stress concentration sites and facilitate subsurface crack initiation. (Glaeser and Wright)[5] Crack initiation takes place independently of the fatigue limit in air since it can be decreased or eliminated through the increase of dissolution rates at anodic sites. Localized corrosion such as pitting strongly favors fatigue crack initiation through stress concentration and a local acidic environment. The two main mechanisms of corrosion fatigue are anodic slip dissolution and hydrogen embrittlement, as schematically shown in Figure 6.49.[103]

As shown in Figure 6.49a, the cracks grow by slip dissolution due to diffusion of active water molecules, halide ions, etc., to the crack tip, followed by a rupture of the protective oxide film by strain concentration, fretting contact between the crack faces. This is followed by dissolution of the fresh exposed surface and growth of the oxide on the bare surface. For the alternative mechanism of hydrogen embrittlement in aqueous media, the critical steps involve: diffusion of water molecules or hydrogen ions to the crack tip; reduction to hydrogen atoms at the crack tip; surface diffusion of adsorbed atoms to preferential surface locations; absorption and diffusion to critical locations in the

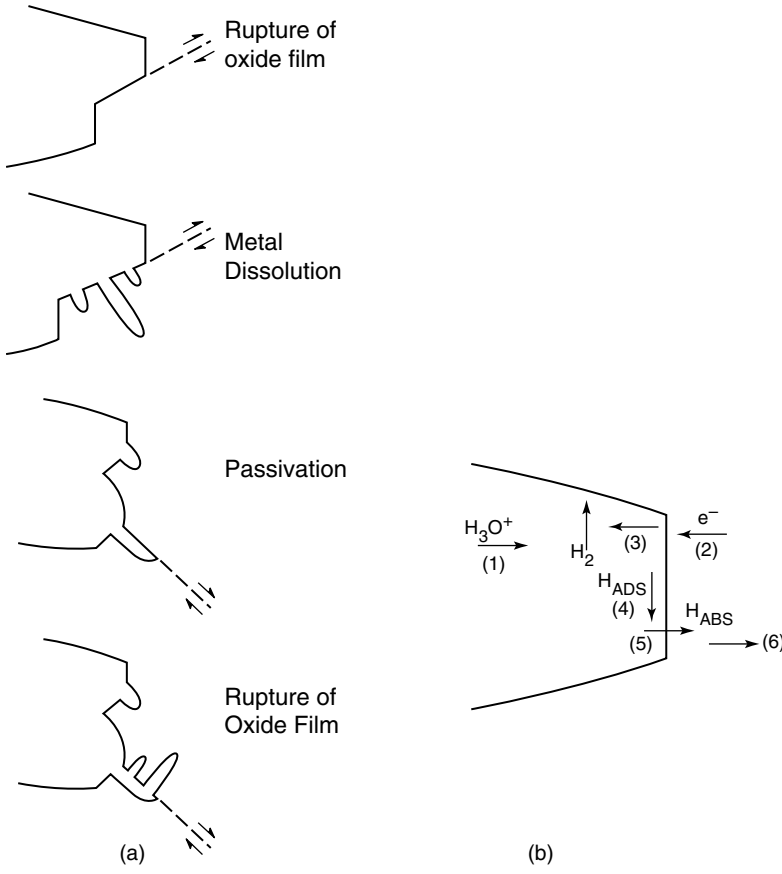

Figure 6.49 *Schematic presentation of (a) the slip dissolution and (b) the hydrogen embrittlement models*[102]

microstructure (e.g., grain boundaries, the regions of high triaxiality ahead of a crack tip, or void). Under cyclic loading, fretting contact between the mating crack faces, pumping of the aqueous environments to the crack tip by the crack walls, and continual blunting and resharpening of the crack tip by the reversing load influencing the rate of dissolution.[102]

Fatigue crack initiation in commercial alloys occurs on the surface or the subsurface and is usually associated with surface defects or discontinuities such as nonmetallic inclusions, notches and pits. For low-stress, high-cycle fatigue, crack initiation spans a large portion of the total lifetime. For high-strength steel exposed to sodium chloride, it was found that sulfide inclusions contribute sites for corrosion pits and subsequent fatigue crack initiation. Corrosion pits were developed by selective dissolution of MnS inclusions. Cathodic polarization suppresses the dissolution rate and prevents pit formation, but hydrogen effects can increase crack growth rates of well-defined

cracks.[102] Duquette[104] classified materials and corrosive environments into three groups on the basis of surface corrosion conditions:[102]

1. Active dissolution conditions
2. Electrochemically passive conditions
3. Bulk surface films, such as three-dimensional oxides

In the first group, emerging persistent slip bands (PSBs) are preferentially attacked by dissolution. This preferential attack leads to mechanical instability of the free surface and the generation of new and larger PSBs, followed by localized corrosion attack, resulting in crack initiation. Under passive conditions, the relative rates of periodic rupture and reformation of the passive film control the extent to which corrosion reduces fatigue resistance. When bulk oxide films are present on a surface, rupture of the films by PSBs leads to preferential dissolution of the fresh metal that is produced.[102]

Crack propagation. The effect of the environment on crack propagation in corrosion fatigue can lead to increase in the crack growth rate. Three types of behavior have been reported.[95,105]

Figure 6.50a schematically illustrates the sigmoidal variation of fatigue crack growth as a function of stress intensity factor range on a log–log scale under purely mechanical loading conditions. The typical variation in crack velocity da/dt as a function of the applied stress factor K is plotted on a log–log scale in Figure 6.50b for growth of cracks in metallic materials under sustained loading in the presence of an environment. It can be seen that the environment has no effect on fracture behavior below a static intensity factor K_{ISCC}, the threshold intensity stress factor for the growth of stress corrosion cracks in tensile opening mode. Above K_{ISCC} the crack velocity increases precipitously with increasing stress intensity factor K (region I). This region is followed by a region II in which da/dt is independent of K. There is then a steep increase in crack velocity as the maximum intensity factor approaches the fracture toughness of the material (K_{IC} region III).

Figure 6.50c illustrates type A true corrosion fatigue growth behavior, in which the synergistic interaction between cyclic plastic deformation and environment produces cycle- and time-dependent crack growth rates. True corrosion fatigue influences cyclic fracture, even at maximum stress intensity factor K_{max} in fatigue less than K_{ISCC}. The cyclic load form is important.[102] The crack growth rate increases and the fatigue threshold decreases compared with that in air. The crack growth rate obeys a Paris law with an increase crack growth rate and a decreased fatigue threshold compared with the behavior in air.[95]

Figure 6.50d shows the stress–corrosion fatigue process, type B, purely time-dependent corrosion fatigue crack propagation that is a simple superposition of mechanical fatigue, (Figure 6.50a) and SCC (Figure 6.50b). Stress–corrosion fatigue occurs only when $K_{max} > K_{ISCC}$. In this model, the cyclic character of loading is not important. The combination of true corrosion fatigue and stress–corrosion fatigue results in type C, the most general form of corrosion fatigue crack propagation behavior.[102]

This behavior is characterized by a plateau region, which prevails above a definite threshold K_{th}. It is often referred to as stress–corrosion fatigue because SCC systems usually exhibit this behavior, and the most common theory assumes that the crack growth rate results from the addition of SCC, and pure fatigue crack advance. This is a type of

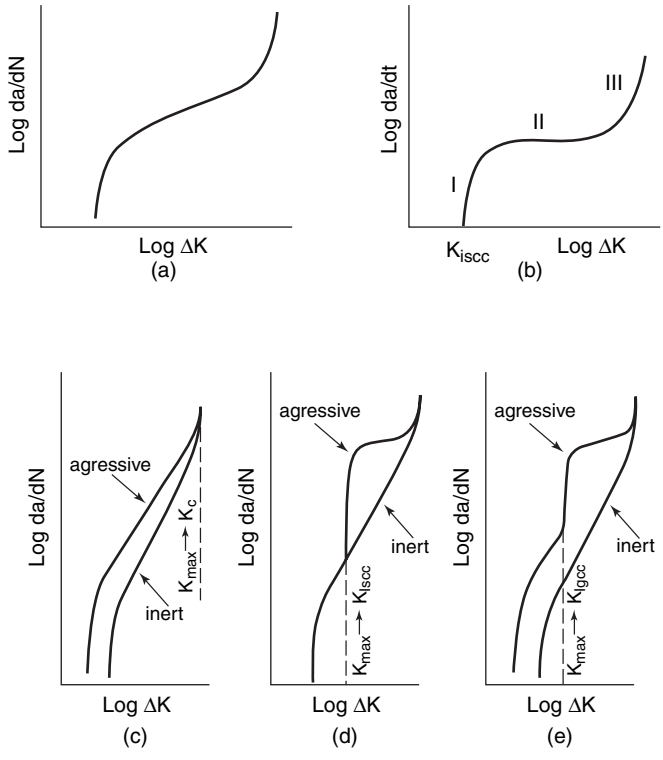

Figure 6.50 *Schematic representations of the combinations of the mechanical fatigue and environmentally assisted crack growth. (a) Fatigue crack growth behavior in inert environments; (b) stress corrosion crack growth under sustained loads; (c) type A corrosion fatigue crack growth, true corrosion fatigue, arising from synergistic effects of cyclic loads and aggressive environment; (d) stress-corrosion fatigue behavior obtained from a superposition of mechanical fatigue (a) and stress corrosion cracking (b); (e) mixed corrosion fatigue behavior obtained from a combination of (c) and (d)*[102]

synergistic effect that can be observed in systems that are not sensitive to SCC, for example, ferritic stainless steels in seawater under cathodic polarization.[106] It is often associated with hydrogen embrittlement. It is likely that the plateau behavior corresponds to control of the crack growth rate by nonmechanical processes, as for example, transport processes.[95]

Figure 6.50e shows cyclic time-dependent acceleration in da/dN below K_{ISCC}, combined with time-dependent cracking (SCC) above the threshold.[102] This combines the environment effects of behaviors c and d. Examples of types A and C corrosion fatigue has been observed in similar steels under different potential conditions, type C behavior being clearly associated with the cathodic potential and thus with hydrogen embrittlement.[95] This is a mix of true fatigue and stress–corrosion fatigue where one can dominate the other in its influence on crack growth, depending on the properties of the interface.[107]

Prevention of corrosion fatigue. One or a combination of the following procedures is recommended to prevent corrosion fatigue:

1. Redesigning to reduce or eliminate both temporary and permanent cyclic stresses. Compared with reducing the maximum stress level, it is often more beneficial and more cost effective to reduce the magnitude of the stress fluctuation.[102]
2. Selecting a material or heat treatment with higher corrosion fatigue strengths.
3. Use of corrosion inhibitors, reduction of oxidizers or pH increase, depending on the system and the environment, can delay the initiation of corrosion fatigue cracks. For example, in the case of mild steel, the deoxygenation of a saline solution brings back the limit of corrosion fatigue to that measured in air;[108] an addition of 200 ppm of $Na_2Cr_2O_7$ to the city water supply reduces the corrosion fatigue of normalized 0.35% C steel to a lower level than that measured in the air.
4. Cathodic protection, provided that the material is not susceptible to embrittlement. Sacrificial zinc (galvanized) coatings.
5. Application of surface treatments such as shot peening, nitriding of steels and sandblasting of the surface of metal or others producing constraints of compression are beneficial.[1]
6. Organic coatings can successfully impede corrosion fatigue. Organic coatings can be applied if they contain some inhibitory pigments in the primary layer. The relatively low corrosion fatigue strength of carbon steel is reduced still further when local breaks in a coating occur.[31,84]
7. Noble metal coatings (e.g., nickel) can be effective, but only if they remain unbroken and are of sufficient density and thickness. Electrolytic deposits of tin, lead, copper or silver on steel are also considered as protectors and probably do not modify the normal features of fatigue because they suppress contact with the surrounding environment. Observations made on the use of deposits of nickel or chromium are contradictory.[7]

Testing of corrosion fatigue. The following factors must be considered in corrosion fatigue testing:

- Stresses: stress intensity range, load frequency and stress ratio
- Environmental: electrode potential in aqueous environment and intended environment composition.
- Metallurgical: alloy composition, microstructure, and yield strength. (Phull)[5]

The scientific basis for reliable estimate of fatigue life for all conceivable load and environmental combinations remains elusive, despite the estimated billions of dollars spent combating fatigue. Tests of fatigue consist in submitting the material to a certain frequency of alternate cyclic stresses (compression–tension) of different values and plotting the C–N curve. The parameters mentioned earlier should be considered. The presence of rust or other products of corrosion does not necessarily mean that the fatigue has decreased. It is necessary to carry out fatigue tests and show that the fatigue resistance has decreased.[16]

Types of tests. Laboratory corrosion fatigue tests can be classified as either cycles-to-failure (complete fracture) or crack propagation (crack growth) test. In cycles-to-failure testing, specimens or parts are subjected to a sufficient number of stress cycles to initiate and propagate cracks until complete fracture occurs. Such data are usually obtained by

testing smooth or notched specimens. However, it is difficult to distinguish between CFC initiation and CFC propagation life with this type of testing.

In crack propagation testing, preexisting cracks or sharp defects in a material reduce or eliminate the crack initiation portion of the fatigue life of the component. Both types of testing are important.[109] In the United States, the ASTM International issues voluntary standards and recommended practices. F 1801 concerns the Corrosion Fatigue testing of metallic implant materials. (ASTM F1160)[4], (Phull)[5]

A typical fatigue test specimen has three areas: the test section and the two grip ends. The design and type of specimen depend on the fatigue testing machine and the objective of the fatigue study. The test section in the specimen is reduced in cross-section to prevent failure in the grips ends. Round specimens for axial fatigue machines may be threaded, buttonhead, or constant-diameter types for clamping in V-wedge pressure grips. For rotating-beam machines, short, tapered grip ends with internal threads are used, and the specimen is pulled into the grip by a draw bar. Torsional fatigue specimens are generally cylindrical. Flat specimens for either axial or bending fatigue tests are generally reduced in width in the rest of the section, but may also have thickness reductions. (Phull)[5]

Fracture mechanics approach. Fracture mechanics provides the basis for many modern fatigue crack-growth studies. ΔK is the stress intensity range ($K_{\max}-K_{\min}$) where K is the magnitude of the mathematically ideal crack-tip stress field in a homogeneous linear-elastic body and is a function of applied load and crack geometry.

$$\Delta K = \alpha\sqrt{\pi\alpha(\sigma_{\max} - \sigma_{\min})} \tag{6.4}$$

In Equation (6.4) α is a function of the geometry of the rupture and the test sample, and σ is the stress.

The growth or extension of a fatigue crack under cyclic loading is principally controlled by the maximum load and stress ratio (minimum/maximum stress). However, as in crack initiation, there are a number of additional factors that may exert a strong influence, especially in the presence of an aggressive environment.

Most CFC growth-rate investigations attempt to follow the general provisions of standard test method ASTM E647.[4] In this constant-load-amplitude method, crack length is measured visually or by an equivalent method as a function of elapsed cycles, and these data are subjected to numerical analysis to establish the rate of crack growth. Crack growth rates are then expressed as a function of crack tip intensity range ΔK, which is calculated from expressions based on linear-elastic stress analysis. (Phull)[5]

Expressing the crack growth rate da/dN (where a is crack length and N is number of cycles) as a function of ΔK provides results that are independent of specimen geometry, and this enables the comparison of data obtained from a variety of specimen configurations and loading conditions. (Phull)[5]

Results of fatigue crack growth rate tests for many metallic structural materials have shown that complete da/dN versus ΔK curves have three distinct regions of behavior, Figure 6.51. In an inert (or benign) environment, the rate of crack growth depends strongly on K at K levels approaching K_{Ic} (plane-strain fracture toughness) at the high end (region III) and at levels approaching an apparent threshold ΔK_{th}, at the lower end (region I), with an intermediate region II that depends[105] on some power of

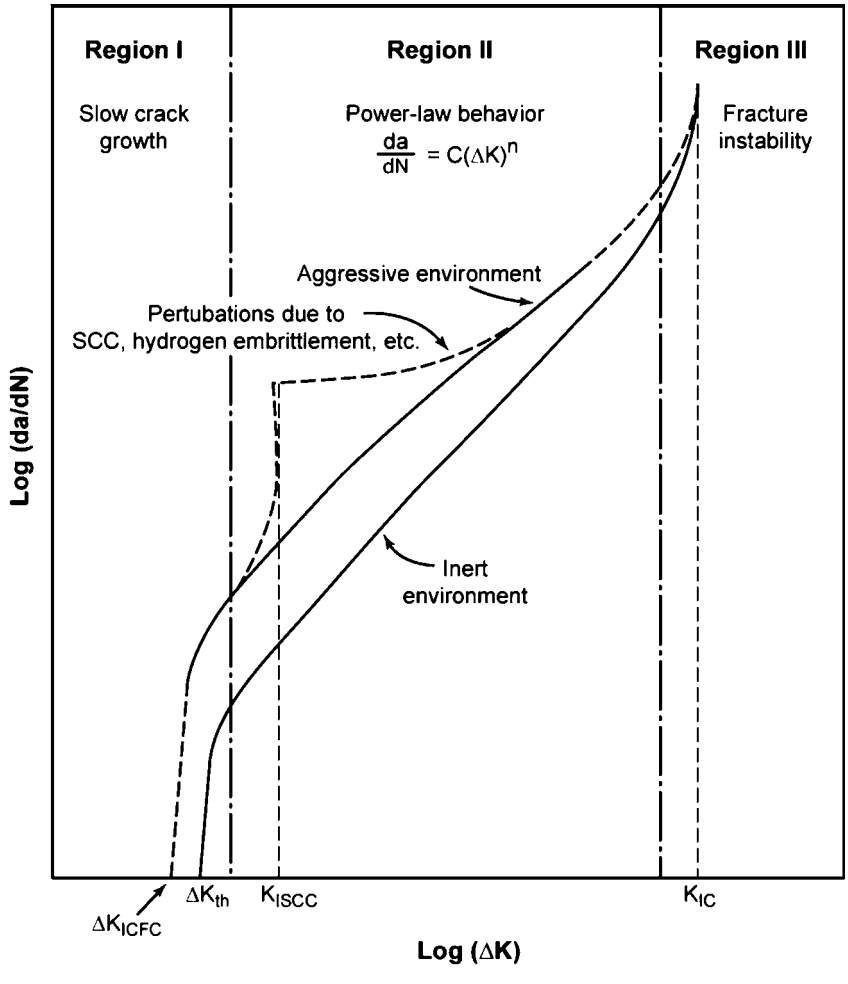

Figure 6.51 *Corrosion fatigue crack propagation rate* (da/d*N*) *as a function of the cyclic crack tip stress intensity range* (ΔK) *(Phull)*[5]

K or ΔK of the order of 2–10. This is described by the power-law relationship. (Phull)[5]

$$\frac{da}{dN} = C(\Delta K)^n \tag{6.5}$$

where C and n are constants for a given material and stress ratio. In an aggressive environment, the CFC growth curve can be quite different from the pure fatigue curve, depending on the sensitivity of the material to the given environment and the occurrence of various static stress fracture mechanisms. The environmental effects are quite strong above some threshold for SCC (K_{ISCC}) and may be negligible below this level (K_{ISCC} is the stress intensity threshold for plane-strain environment-assisted cracking). In addition,

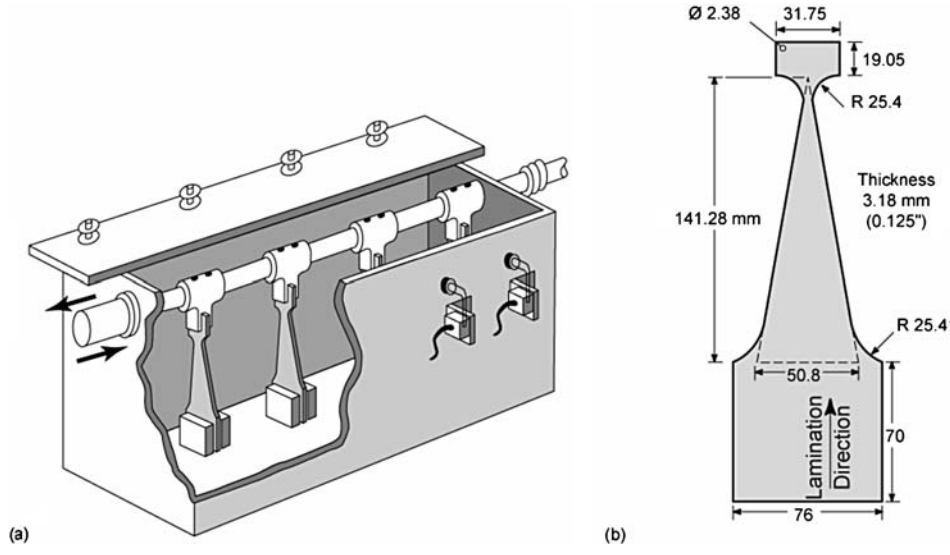

Figure 6.52 *Schema of CF test sample and test apparatus*[110,112]

certain loading factors, such as frequency, stress ratio, and stress waveform, can have marked effects on the crack growth curves in aggressive environments. (Phull)[5]

Apparatus for electrochemical measurements during corrosion fatigue. CF tests can be done using an apparatus designed by the Continental Oil Company, as shown in Figure 6.52.[110,111] The polarization potential and current can be controlled for the four samples tests at the same time. The apparatus consists of a Monel tank in which four specimens are subjected to cyclic bending. The preliminary step in the experiment is to determine the displacement caused by the desired applied load. The exact stresses are then determined with the use of strain gages.

The frequency of the applied cyclic bending is equal to 60 cycles/min and the stress amplitude $R = -1$. The electrolyte is generally an aqueous solution of 3% sodium chloride utilized at ambient temperature and deoxygenated by the bubbling of argon for 1 h before and during the test. Samples can be polished, sandblasted, shot peened, etc. The behavior of the alloy in CF can be studied at the free corrosion potential under different percentages of stress amplitude of the elastic limit. From potentiokinetic curves $I = f(E)$, the protection or the pitting potential can be applied and maintained for the entire duration of the stress tests. Each test can include up to four samples for each material at the same time. The average difference between the results obtained for similar tests depends on the particular system, but generally does not exceed 15%.[112]

6.7.7 Environmentally Induced Cracking

In some environments and under certain conditions, a microscopically brittle fracture of materials can occur at levels of mechanical stress that may be far below those required for general yielding or those that could lead to significant damage in the absence of an environment. This susceptibility also depends on the chemical composition and

microstructure of the alloy. This form of corrosion necessitates an interaction between the electrochemical dissolution of the metal, hydrogen absorption, and the mechanical loading conditions (stress, strain, and strain rate).[95] The nature of these fracture modes varies from one class of material to another. However, all given fracture modes are largely similar to each other. Environmentally assisted cracking (EAC) is not limited to metals, and it also occurs in glasses (plexiglass), ceramics, and polymers. Structural failures due to EAC are often sudden and unpredictable, occurring after a few hours of exposure, or after months or even years of satisfactory service.[113,114] Environmentally assisted cracking can be divided to mechanically assisted cracking (MAC) and environmentally induced cracking (EIC) which is the main topic of this section.

The total cost of material fracture amounts to 4% of gross domestic product in the USA as well as in Europe.[115,116] Fracture modes included in these studies were stress-induced failures (tension, compression, flexure, and shear), overload, deformation, delamination, and time-dependent modes, such as fatigue, creep, SCC, and embrittlement. The EAC problem is directly related to maintenance of the safety and reliability of potentially dangerous engineering systems, such as nuclear power plants, fossil fuel power plants, oil and gas pipelines, oil production platforms, aircraft and aerospace technologies, chemical plants, etc. Losses resulting from the EAC of materials annually exceed many billions of dollars and are increasing throughout the world.[114]

Stress–Corrosion Cracking. The conditions for SCC to occur are: (i) a crack-promoting environment; (ii) the susceptibility of material to SCC; (iii) tensile stresses must exceed the threshold value. SCC is distinguished by the fact that the stress corrosion faces suffer very low corrosion, even in solutions that cause some damage to the free surfaces. As an example is the SCC of stainless steel at 200°C in a caustic solution or in aerated chloride solution where almost no traces of dissolution are visible on the crack faces (Figure 6.53).[84,95] For example, SCC of metals has been by far the most prevalent

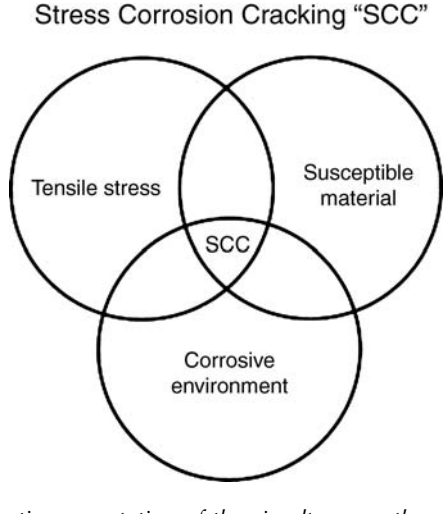

Figure 6.53 *Schematic presentation of the simultaneous three conditions of SCC*[84]

cause of the failure of steam generator components in pressurized water reactors (PWRs) (69% of all cases), piping in boiling water reactors (59.7%) and PWRs (23.7%). More than 60% of inspected steam turbines in nuclear power plants have stress corrosion cracked disks.[117]

Two classic examples of the SCC are seasonal cracking of brass and the caustic embrittlement of steel. Seasonal cracking refers to SCC of brass cartridge cases. Cracks were observed during the period of heavy rainfall during hot weather in the tropics. This intergranular SCC was attributed to the effect of internal stresses, in ammonia solution that resulted from the decomposition of organic matter in presence of O_2 and humidity. Many explosions of riveted boilers occurred in the early steam-driven boilers at the tubes of riveted furnaces due to the fact that some areas were cold worked during riveting operations. A carbon steel subjected to a stress close to the elastic limit and exposed to the hot concentrated alkali solutions, or nitrate solutions is susceptible to SCC. SCC was observed in rivets used in water boilers although the furnace water was treated normally with alkalies to minimize corrosion. Crevices between rivets and the boiler plate of the furnace allowed boiler water to concentrate until the content of alkali in the crevice is sufficient to attend the required pH to induce cracking.[16]

Morphology. Failed specimens appear macroscopically brittle and exhibit highly branched cracks that propagate transgranularly and/or intergranularly, depending on the metal–environment combination. Transgranular stress corrosion crack propagation is often discontinuous on the microscopic scale and occurs by periodic jumps of the order of a micrometer (Figure 6.54) while intergranular cracks are believed to propagate continuously or discontinuously, depending on the system (Figure 6.55).[16,95]

Intergranular and transgranular cracking often occur simultaneously in the same alloy. Such transitions in crack modes are observed in alloys with high amounts of nickel, iron chromium and brasses. In corrosion under tension, ruptures are fragile and are sometimes characterized by the presence of cleavages, notably in the case of hydrogen embrittlement.[16]

Cleavage is a brittle fracture that occurs along specific crystallographic planes. Cleavage has a well-defined crystallographic orientation and it is easy to recognize its occurrence by optical microscopy as it exhibits brilliant and flat fracture facets that are related to the dimension of the grain size of the material under study. Under the scanning electron microscope, flat fracture facets exhibit cleavage steps and river patterns that are caused by the crack moving through the crystal along a number of parallel planes which form a series plateaus and connecting ledges.

Key factors of SCC. The *stress* applied on a metal is nominally static or slowly increasing tensile stress. The stresses can be applied externally, but residual stresses often cause SCC failures. Internal stresses in a metal can be due to cold work or a heat treatment. In fact, all manufacturing processes create some internal stresses. Stresses introduced by cold work arise from processes such as lamination, bending, machining, rectification, drawing, drift, and riveting. Stresses introduced by thermal treatments are due to the dilation and contraction of metal or indirectly by the modification of the microstructure of the material. Welded steels contain residual stresses near the yield point. Corrosion products have been shown to be another source of stress and can cause a wedging action.

Figure 6.54 *Transgranular SCC of stainless steel grade 304(× 500)*[16]

Stage 1 corresponds to a rapid increase of the crack propagation with the stress intensity factor (Figure 6.56). No crack is observed below some threshold stress intensity. The stress corrosion cracks initiate when the stress exceeds a threshold value σ_1 and propagate when the stress intensity factor is in excess of a threshold K_{ISCC}. This threshold stress-intensity level, K_{ISCC} is determined by the alloy composition, microstructure, and the environment (composition and temperature). The values lie typically between 10 and 25 MPa m^{-2} and σ_1 is usually of the order of 60–100% of the yield stress, but much lower values can be observed, such as for 304 stainless steel exposed to boiling magnesium chloride at 154°C. In certain cases, stresses as low as 10% of the elastic limit have been observed. It is necessary to use this level with prudence since the environmental conditions of a system can change at the metal/solution interface during service and accidental presence of a slash or a corrosion pit can increase stresses locally and reach the necessary level of K_{ISCC}.[16]

At intermediate stress intensity levels (stage 2) the crack propagation rate shows a plateau velocity $V_{plateau}$ that is virtually independent of the mechanical stress, but depends on the alloy/environment interface and the the rate-limiting environmental processes such as mass transport of the aggressive species to the crack tip. The plateau in a quenched and tempered low-alloy steel of 1700 MPa yield strength in deaerated water at 100°C

Figure 6.55 *Intergranular SCC of brass*[16]

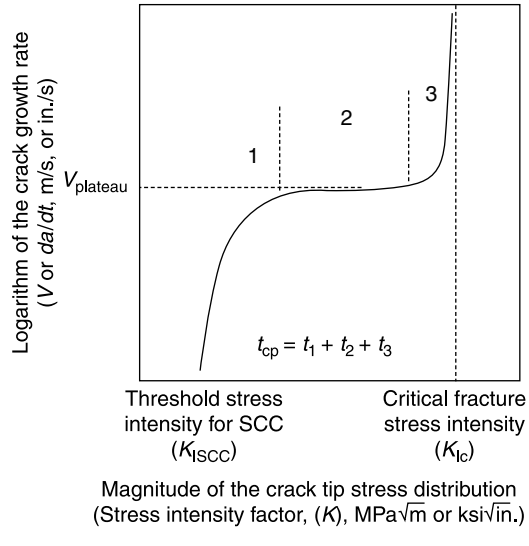

Figure 6.56 *Schematic of the regions of crack propagation as a function of the crack tip stress-intensity magnitude factor K expressed in MPa $\sqrt{m}$ (Jones)*[5]

(e.g., 10^{-4} m/s at stress intensity of 30–80 MPa$\sqrt{}$m) can be higher than that in a similar steel of 760 MPa yield strength ($\sim 10^{-11}$ m/s) by 7 orders of magnitude.[114,117,118] Stage 3 corresponds to the critical stress intensity level for mechanical fracture in an inert environment.

The crack growth rate depends on the strength of the metal, in almost all aggressive environments. Doubling the yield strength σ_{YS} of martensitic steel (from 800 to 1600 MPa) is accompanied by a tenfold (from 70 to 7 MPa$\sqrt{}$m) decrease of the threshold stress intensity K_{ISCC}, corresponding to the onset stress corrosion crack growth in alloys in chloride solutions at ambient temperature.[113,119] Stress sources likely to promote cracking are weldments and inserts. Welded structures of these alloys require stress-relief annealing.

In some media, stress–corrosion cracking can occur above a certain temperature. Also, increasing the temperature generally lowers the threshold for cracking (σ_1 and K_{ISCC}) and increases the growth rate of propagation. An example consists of SCC of stainless steel near neutral solutions above 40 and 80°C as opposed to SCC at pH–1 and room temperature.[95] Hydrogen absorption can favor local plasticity, very near the crack tip region, due to enhanced dislocation velocities with hydrogen. Hydrogen penetration can be accelerated very near the crack tip region by stress-assisted diffusion and dislocation transport.[120]

Material parameters in SCC. The susceptibility to SCC is affected by the chemical composition, the preferential orientation of grains, the composition and the distribution of the precipitates (particularly intergranular), the interaction of dislocations, the progression of the phase transformations and cold work.[16]

The carbon content and its distribution in the steel matrix are the main metallurgical factors controlling the SCC. The threshold stress for cracking was found to be a function of carbon content of the steel.[1] The effect of carbon on the mechanical properties of steel can play a favorable role, but the influence of carbon particles on the microstructure is important, and depends on the distribution of the different phases. For example, identification of carbon particles at the ferrite grain boundaries has been observed in the case of intergranular cracking for carbon steels with >0.1% C.[1] The other alloy elements have a role beneficial or harmful to SCC resistance, depending on whether they favor the segregation of the carbon particles (cementite) at grain joints. These elements sometimes tend to segregate at the grain joints, but their influence is much weaker than that of C because of the low concentrations.

Increasing the zinc content in brasses increases the sensitivity to cracking in ammonia-containing solutions while low amounts of tin, lead, or arsenic improve their resistance.[121] The addition of molybdenum to austenitic steels improves their resistance to cracking in chloride environments and decreases it in caustic media. This susceptibility also depends also on the nature of the environment. For example, the presence of a semicontinuous network of intergranular, coherent, chromium-rich carbide precipitates increases the resistance to intergranular cracking in hot caustic solutions, but the related chromium depletion of grain boundaries (sensitization) promotes intergranular cracking in hot, aerated 'pure' water or in polythionates.[95]

Potential–pH diagram and SCC. Critical potentials for SCC of a system metal/solution can be related to its *E*–pH diagram, because these diagrams describe the conditions at

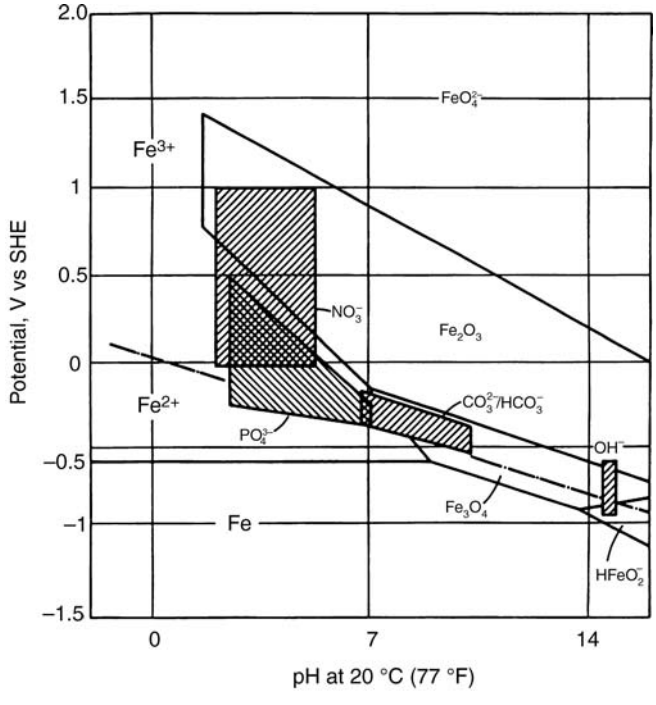

Figure 6.57 *E–pH diagram showing the zones of severe susceptibility of carbon steel in various environments and the stability regions for solid and dissolved species (Jones and Ricker)*[24]

which film formation and metal oxidation occur. An example of an *E*–pH diagram of Fe/H_2O in relation to carbon steel is given in Figure 6.57. SCC is associated with potentials and pHs at which phosphate, carbonate, or magnetite films are stable while the species Fe^{2+}, $HFeO_2^-$ are metastable. A comparable diagram exists for a 70Cu–30Zn brass in a variety of solutions. (Jones and Ricker)[24]

The effect of factors such as pH, oxygen concentration, and temperature can be related to their effect on the *E*–pH diagram. Considering the iron *E*–pH diagram, it can be seen that a shift of pH and/or potential from a region of stability due to the formation of an oxide film, to a region of active general corrosion or a zone of severe cracking susceptibility for a specific ion. Increasing oxygen concentration for example shifts the potential to more noble or positive potentials and temperature variation has an influence on the regions of stability. Hydrogen evolution or reduction of iron in water at 25°C is shown by the dashed line a in Figure 6.57 and this indicates that hydrogen evolution becomes less endothermic with a shift of pH to more acidic values and this is important in SCC–hydrogen-induced subcritical crack growth mechanisms.

The *E*–pH diagram of the cracking metal/solution interface is a basic tool to evaluate and understand the mechanism of the SCC, however there are certain difficulties for a

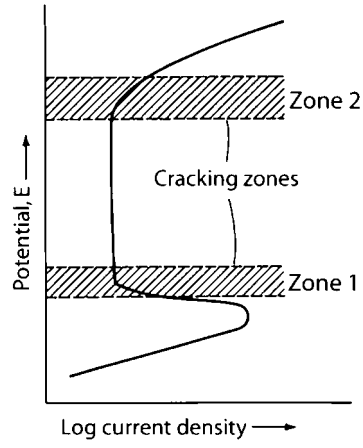

Figure 6.58 *Potentiodynamic polarization curve and electrode potential values at which stress–corrosion cracking appears (Jones)*[5]

precise evaluation. The *E*–pH of the crack tip–solution interface is substantially different from that of the bulk solution.[122–124,] (Jones and Ricker)[24]

Active–passive behavior and susceptible zone of potentials. An example of active–passive behavior of a metal/environment interface such as stainless steel in 1 *M* sulfuric acid solution is shown in Figure 6.58. (Jones)[5] It is interesting to define two ranges of potentials that can show transgranular SCC. Intergranular SCC can occur in a wider ranges of potentials. Zones 1 and 2 correspond to the active–passive and passive–active state transitions. The active state describes that of the crack tip and the passive state or film formation corresponds to that of the crack walls. Zone 2 is frequently above the pitting potential of the system indicating the possibility of pit initiation and propagation which is important in SCC.

Identification of critical zones of potentials susceptible to SCC can be achieved by determining the potential–current curves at different speed rates. An example for carbon steel is given in Figure 6.59. Potentiodynamic polarization curves consist of scanning a suitable region of potentials with a fast sweep rate ($1\,\mathrm{V\,min^{-1}}$) for a film-free surface and recording the corresponding current. This simulates the state of the crack tip where there is very thin film or no film at all. In order to simulate the state of the walls of the crack, one makes a slow sweep rate of the order of $10\,\mathrm{mV\,min^{-1}}$ so that the allocated time permits the formation of the oxide or passive film. The intermediate anodic region between these two curves is the region where SCC is expected to occur. This technique correctly anticipates the SCC of carbon steel in a number of different media. These measurements are applicable to the systems where the formation of air-formed oxide films can be reductively dissolved so that a film-free surface can be prepared before the sweeps, otherwise, straining or scraping electrodes are used to study the bare surface. The polarization curve also shows the active zone of pitting and the stable passive zone before and after the expected zone of SCC susceptibility, respectively.

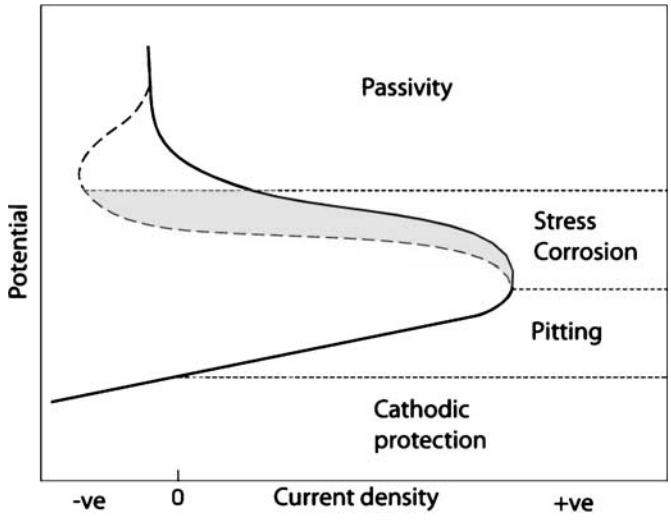

Figure 6.59 *Potentiodynamic polarization curves showing especially the domain of susceptiblity to SCC*[1]

Electrode Potential and crack growth. In SCC systems, slight variations of material composition or microstructure, or slight modification of the environmental composition or redox potential, may drastically change the sensitivity to cracking. The crack growth rate is determined frequently by the electrode potential, whereby an insignificant change, with all other conditions (specimen, solution, pH, temperature, frequency, stress ratio, etc.) being constant, can lead to the acceleration of fatigue crack growth by a dozen times. This can cause the rapid growth of the crack that was 'static' at open-circuit potential (when $K < K_{ISCC}$), retard, or stop the crack growth at $K > K_{ISCC}$.[113,125,126]

Inhibitors. The SCC of an alloy/solution system is generally associated with the presence of a specific corrosive environment that, most of the time, would attack the alloy only very superficially in the absence of mechanical stress. It is necessary to note that nitrates and hydroxides, that generally act as anodic inhibitors for the corrosion of carbon steels, also cause the cracking of mild steels. Similarly, the failure of storage steel reservoirs containing anhydrous NH_3 generally occurs only in the presence of air containing CO_2 that forms the well-known anodic inhibitor $(NH_4)_2CO_3$ which causes cracking. Figure 6.59 illustrates the current density differences slow in polarization curves at various potentials between fast and slow sweep rates for mild steel immersed in hydroxide, carbonate–bicarbonate and nitrate solutions. Figure 6.60 shows the results from controlled potential slow-strain-rate tests involving the same species, and it is interesting to note that the potential ranges in which cracking occurred are those predicted for each of the three solutions.

Differential aeration galvanic cell. Distilled water is an important medium since it is commonly used. Evans' differential aeration cell (a galvanic cell created by a difference in oxygen concentration) for pitting has been shown to be important or essential for cracking in distilled water. (Miller)[24]

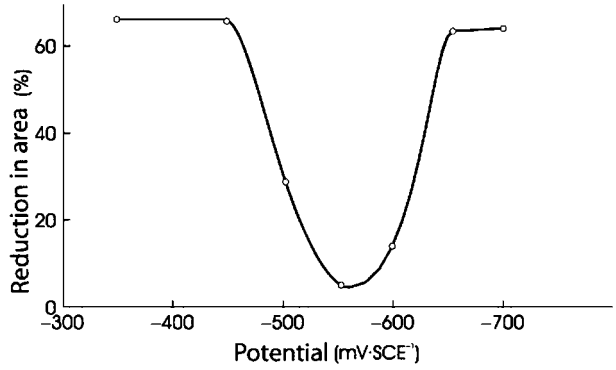

Figure 6.60 *Effects of applied potential upon cracking of mild steel in 2 N $(NH_4)_2CO_3$ at 75°C*[1]

Alloy/liquid interface. Table 6.3 lists some of the alloy–environment combinations that result in SCC. This table, as well as others published in the literature, should be used only as a guide for screening candidate materials prior to further in-depth investigation, testing, and evaluation.[31]

SCC often occurs in *hot gaseous atmospheres* on materials under creep or fatigue conditions. A few cases of susceptibility have been reported for certain titanium alloys in gases, including moist chlorine, dry HCl, and dry hydrogen. In moist chlorine gas at 288°C Ti–8Al–1Mo–1V alloy exhibits cracking, for example. Various binary titanium alloys are also known to experience cracking in this gas at 427°C. (Schutz)[24]

Table 6.3 *Some environment–alloy combinations known to result in SCC*[31]

Alloy	Environment
Aluminum alloys	Aqueous chloride; cyanide; high-purity hot water
Carbon steels	Aqueous amines; anhydrous ammonia; aqueous carbonate; CO_2; aqueous hydroxides; nitrates
Copper alloys	Aqueous amines; aqueous ammonia; hydrofluoric acid; aqueous nitrates; aqueous nitrites; steam
Nickel alloys	Aqueous chlorides; concentrated chlorides; boiling chlorides; aqueous fluorides; concentrated hydroxides; polythionic acids; high-purity hot water
Austenitic stainless steels	Aqueous chlorides; concentrated chlorides; aqueous hydroxides; concentrated hydroxides; polythionic acids; sulfides plus chlorides; sulfurous acid
Duplex stainless steels	Aqueous chlorides; concentrated chlorides; aqueous hydroxides; concentrated hydroxides; sulfides plus chlorides
Martensitic stainless steels	Aqueous hydroxides; concentrated hydroxides; aqueous nitrates; sulfides plus chlorides
Titanium alloys	Dry hot chlorides; hydrochloric acid; methanol plus halides fuming nitric acid; nitrogen tetroxide
Zirconium alloys	Aqueous bromine; aqueous chloride; chlorinated solvents; methanol plus halides; concentrated nitric acid

Hot salt SCC and hot gaseous SCC of titanium alloys have been reported. (Schutz)[24] Irradiation-assisted SCC has also been reported in nuclear reactors. (Andersen)[24]

Hydrogen embrittlement and hydrogen stress cracking. The interaction between hydrogen and metals can result in the formation of solid solutions of hydrogen in metals, molecular hydrogen, gaseous products that are formed by reactions between hydrogen and elements constituting the alloy, and hydrides. Depending on the type of hydrogen/metal interaction, hydrogen damage of metal manifests itself in one of the following several ways.[31,117]

Hydrogen embrittlement (HE) is a loss of ductility of materials containing hydrogen and occurs most often in high-strength steels, primarily quenched-and-tempered and precipitation-hardened steels, with tensile strengths greater than about 1034 MPa. (Craig)[5] There are two types of hydrogen embrittlement.

Hydrogen environment embrittlement occurs during the plastic deformation of alloys in contact with hydrogen-bearing gases or a corrosion reaction and is therefore strain rate dependent. Explicit examples are the degradation of the mechanical properties of ferritic steels, nickel-based alloys, titanium alloys, and metastable austenitic stainless steel when the strain rate is low and the hydrogen pressure and the purity are high.

Hydrogen stress cracking or hydrogen-induced cracking (HIC) is characterized by a brittle fracture under sustained load in the presence of hydrogen. This cracking mechanism depends on the hydrogen fugacity, strength of the material, heat treatment/microstructure, applied stress, and temperature. For many, steels, a threshold stress exists below which hydrogen stress cracking does not occur, but this cannot be considered as a material property since it depends on the strength of the steel and the specific hydrogen-bearing environment. This is sometimes called stepwise cracking (SWC).

All modes of cracking have been observed in most commercial alloy systems; however, hydrogen stress cracking usually produces sharp, singular cracks in contrast to the extensive branching observed for SCC. Experimental evidence supporting a hydrogen embrittlement mechanism is that immersion in a cracking solution before stress application produces a fracture similar to a SCC fracture. The effect of pre-immersion in a cracking solution is reversed by vacuum annealing. Testing in gaseous hydrogen results in the same crack characteristics produced in aqueous solution tests. SCC occurs at crack velocities at which only when adsorbed hydrogen is present at the crack tip.

A critical minimum stress exists, below which delayed cracking will not take place. The critical stress decreases with increase in hydrogen concentration. These effects are shown in Figure 6.61 for SAE 4340 steel (0.4% C) charged with hydrogen by cathodic polarization in sulfuric acid, then cadmium plated to help retain hydrogen, and finally subjected to a static stress.[7,] (Craig)[5]

Formation of metallic Hydrides. The precipitation of a brittle metal hydride at the crack tip results in significant loss in strength and large loss in ductility and toughness of some metals, such as magnesium, tantalum, niobium, vanadaium, thorium, uranium, zirconium, titanium, and their alloys in hydrogen environments.[31] Alloy systems that form hydrides fracture by ductile fracture. Nickel and aluminum alloys may also form a highly unstable hydride that contributes to hydrogen damage of these alloys. However some of these alloys are susceptible to failure in hydrogen by other mechanisms. (Craig)[5]

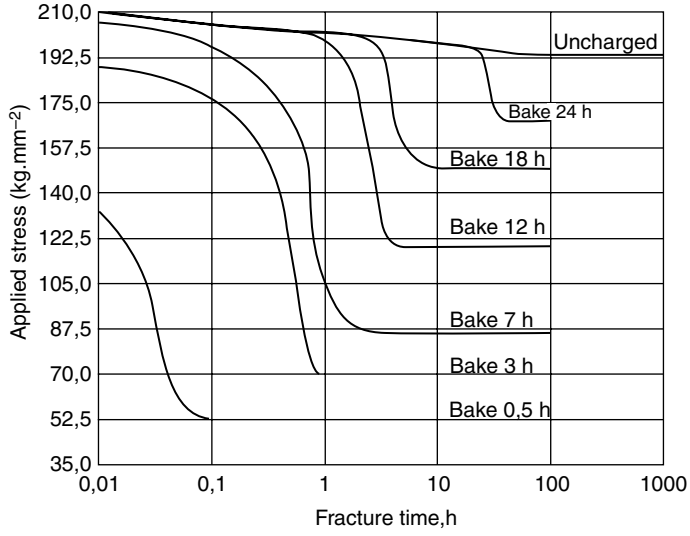

Figure 6.61 *Delayed fracture times and minimum stress for cracking of 0.4% C steel for various hydrogen concentrations obtained by different baking times at 150°C of cathodically charged specimens (Craig)*[5]

Accelerating ions. Chemical species that have been reported to accelerate hydrogen damage include hydrogen sulfide (H_2S), carbon dioxide (CO_2), chloride (Cl^-), cyanide (CN^-), and ammonium ion (NH_4^+). Some of these ions help to produce severe hydrogen charging of steel equipment and may lead to HIC and stress-oriented hydrogen-induced cracking (SOHIC), either of which can cause failure. It is essential to characterize the cracking severity of environments, so that either aggressive environment can be modified and/or materials can be selected with adequate resistance to cracking. Cracking requires the production of nascent hydrogen atoms at the steel surface for example, usually by a corrosion reaction in an H_2S-containing, aqueous solution.

$$H_2S + Fe^{2+} \xrightarrow{H_2O} FeS + 2H$$

The hydrogen atoms produced at the steel surface may combine to form innocuous hydrogen gas molecules (H_2); however, in the presence of sulfide or cyanide, the hydrogen recombination reaction is poisoned, so that the nascent hydrogen atoms diffuse into the steel rather than recombining on the metal surface to form hydrogen gas. Hydrogen atoms that enter the metallic lattice and permeate through the metal can cause embrittlement and failure of structures in service environments. It is generally observed that, if large amounts of hydrogen are absorbed, there may be a general loss in ductility.

Internal blisters may occur if large amounts of hydrogen collect in localized areas.[127,128] Small amounts of dissolved hydrogen may also react with microstructural features of alloys to produce failures at applied stress far below the yield strength. All these phenomena are referred to as hydrogen embrittlement.

Hydrogen-induced cracking may propagate in a straight or stepwise manner. Straight growth occurs in steels having ferrite pearlite structures if there are high levels of Mn and

P segregation or if there are martensitic or bainitic transformation structures. The Mn level around linear cracks may be twice that in the matrix, whereas the P level may be elevated by a factor of 10.[129]

Sulfide stress cracking (SSC) is an important cracking process in the embrittling environments containing hydrogen sulfide and is considered as a special case of hydrogen-induced cracking (HIC). Natural environments (rainwater, seawater, and atmospheric moisture) contaminated with hydrogen sulphide is particularly serious. The presence of H_2S in high concentrations in salt water associated with certain deep oil wells (sour wells) places an upper limit of 620 MPa on the yield strength that can be tolerated in stressed steel in such environments. (Phull)[5]

Sulfide stress cracking is a form of hydrogen embrittlement that occurs in high-strength steels[130] and in localized hard zones in weldments[131] of susceptible materials. In the heat-affected zones adjacent to welds, there are often very narrow hard zones combined with regions of high residual tensile stress that may become embrittled to such an extent by dissolved atomic hydrogen that they crack. Sulfide stress cracking is directly related to the amount of atomic hydrogen dissolved in the metal lattice and usually occurs at temperatures below 90°C (194°F).[132] Sulfide stress cracking also depends on the composition, microstructure, strength, and the total stress (residual stress plus applied stress) levels of the steel.[133] Sulfide stress cracking was first recognized in oil industry failures of tubular steels and well head equipment[134] constructed from steels with hardness values greater than HRC 22. Heat treatment of steels to hardness levels less than HRC 22 eliminates this damage. Although the base metal of steel pipe normally has hardness levels well below this value, service failures have occurred in regions of high hardness in the weld heat-affected zone. It is, therefore, common to apply the HRC 22 limit (equivalent to Vickers hardness HV 248) to the weld/HAZ areas in pipeline steels. There are, however, a number of well-established test procedures for SSC, of which the most widely used is the NACE test.[130,135]

The important features of HIC and SSC are given in Table 6.4.

Hydrogen-induced blistering, and precipitation of internal hydrogen. Hydrogen-induced blistering is a cracking process due to absorbed hydrogen atoms. Also commonly referred to as hydrogen-induced cracking (HIC), it occurs in lower-strength (unhardened) steels, typically with tensile strengths less than about 550 MPa (80 ksi). Pipeline steels used in sour gas environments are susceptible to HIC.[19,31]

Table 6.4 *Comparison of features of HIC and SSC*[135]

	Hydrogen-induced cracking	Sulfide stress cracking
Crack direction	Parallel to applied stress	Perpendicular to stress
Applied stress	No effect	Affects critically
Material strength	Primarily in low-strength steel	Primarily in high strength steel
Location	Ingot core	Anywhere
Microstructure	Trivial effect	Critical effect, Q and T treatment enhances SSC resistance
Environment	Highly corrosive conditions, appreciable hydrogen uptake	Can occur even in mildly corrosive media

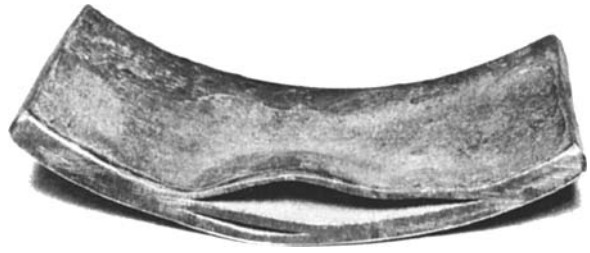

Figure 6.62 *Cross-section of carbon steel plate showing a large hydrogen blister removed after 2 yr exposure from a petroleum process stream*[16]

Another damage also caused by the penetration of hydrogen into metal is the formation of blisters. This phenomenon also entails a mechanical property deterioration. An example is illustrated in Figure 6.62 and the mechanism of blister formation is illustrated Figure 6.63. The inside of the reservoir contains an acidic electrolyte and the outside is exposed to the atmosphere. There is evolution of hydrogen on the internal surface, resulting from corrosion reaction or cathodic protection. A part of atomic hydrogen diffuses through the steel and most of it evolves on the exterior surface, but if some atoms of hydrogen diffuses into a void, they combine into molecular hydrogen. Molecules of hydrogen do not diffuse and the pressure of the hydrogen gas within the void increases. The pressure of the molecular hydrogen in contact with the atomic hydrogen is several hundred thousand atmospheres, sufficient to cause the rupture of any known engineering material.[16] Filiform corrosion can form blisters and hydrogen evolution under paint can show a swelling, but the mechanisms of formation of these similar defects in appearance are completely different from that of hydrogen blistering.

Hydrogen blistering occurs as a result of nascent hydrogen atoms diffusing through the steel and accumulating at hydrogen traps, typically voids around inclusions. When hydrogen atoms meet in a trap and combine, they form hydrogen gas (H_2) molecules in the trap. As more gas molecules form, the pressure increases, causing HIC and blister

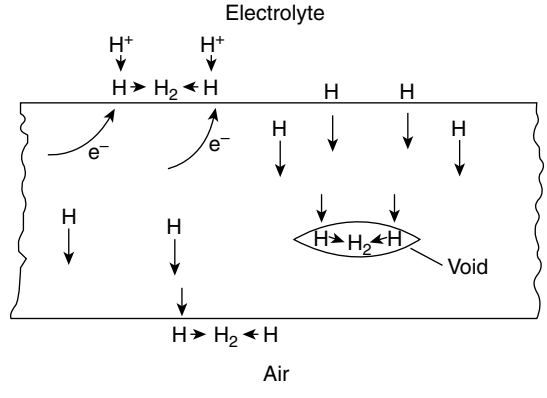

Figure 6.63 *Schematic showing the mechanisn of hydrogen blistering*[16]

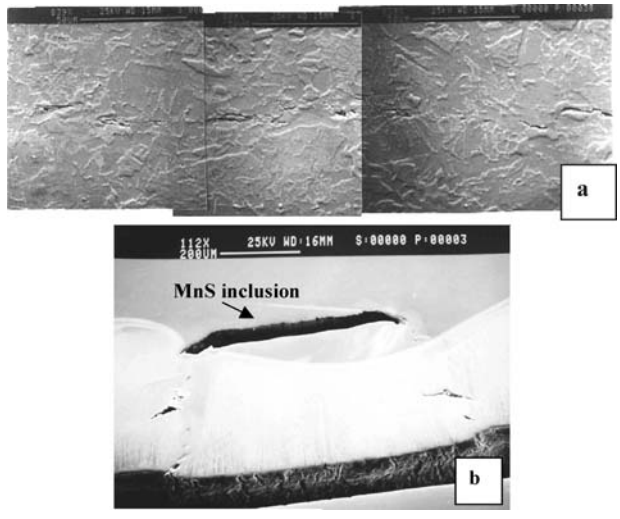

Figure 6.64 *Hydrogen-induced cracking: (a) centreline cracks; and (b) blister crack*[111]

formation. Blisters occur primarily in low-strength steels (<80 ksi or 535 MPa yield strength) and are formed preferentially along elongated nonmetallic inclusions or laminations in the steels used for linepipe.[136,137]

Two types of HIC cracks are shown in Figure 6.64; typical center-line cracks are shown in (a) and blister cracks form near the surface in (b), where hydrogen pressure forms blisters. The formation of blister cracks is related to the type and distribution of nonmetallic inclusions in the steel. MnS inclusions as well as planar arrays of other inclusions are the predominant initiation sites for cracking. Since inclusions are elongated and/or aligned in the longitudinal (rolling) direction, the cracks propagate in the longitudinal direction.

The steels most susceptible to this form of attack are those with high concentrations of sulfur and manganese, which combine during melting to form MnS inclusions. Rolling tends to elongate these inclusions, increasing the surface area of hydrogen traps. Nevertheless, low-S steels are not necessarily HIC resistant, since alloying for inclusion shape control, reduced centerline segregation, and reduction of nitrides and oxides are also necessary. In addition, high-S steels are not necessarily susceptible to HIC. Microsegregation and inclusion shape are more important than bulk sulfur content.[138]

Hydrogen sulfide damage. One of the most studied failures in practice is that of pipeline steel for the petroleum industry. Figure 6.65 shows a typical cracking failure of this category.

Stress-oriented hydrogen-induced cracking (SOHIC) is caused by atomic hydrogen dissolved in steel combining irreversibly to form molecular hydrogen. The molecular hydrogen collects at defects in the metal lattice, as in HIC. However, due to either applied or residual stresses, the trapped molecular hydrogen produces microfissures that align and interconnect in the through wall direction. Although SOHIC can propagate from blisters caused by HIC and SSC, and from prior weld defects, neither HIC nor SSC are

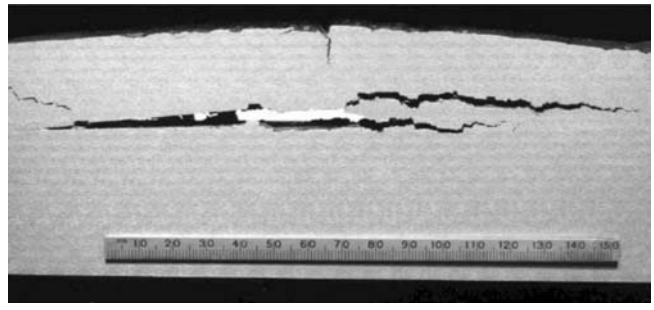

Figure 6.65 *HIC in plate steel exposed to sour gas*[176]

preconditions for SOHIC.[132,133] As with HIC, the primary cause of SOHIC is probably atomic hydrogen produced at the steel surface by wet acid gas corrosion.[139]

Stress-oriented hydrogen-induced cracking tends to occur in the base metal adjacent to hard weldments in pipe and plate steels where cracks may initiate by SSC. SOHIC is characterized by interlinking microscopic cracks oriented both in the direction perpendicular to the stress and in the plane defined by nonmetallic inclusions, as shown in Figure 6.66. SOHIC is a process by which SSC can propagate in relatively low-strength steels (hardness <22 HRC) which would otherwise be considered resistant to SSC.[135]

It is important to underline that there may be more than one cracking phenomenon that can cause a failure. The following four main environmental cracking phenomena of concern can be observed when steels are exposed to wet H_2S environments.[139,140]

1. Hydrogen blistering: blister formation, originating at nonmetallic inclusions.
2. Hydrogen-induced cracking (HIC): also known as stepwise cracking (SWC).
3. Stress-oriented hydrogen-induced cracking (SOHIC).
4. Sulfide stress cracking (SSC): cracking in steels of high strength or high hardness.[135]

Precipitation of internal hydrogen. During cooling of the melt, hydrogen diffuses and precipitates in voids and discontinuities. Cracking from precipitation of internal hydrogen can be considered as a special case of blistering and occurs when excess hydrogen is picked up during melting or welding. Examples include shatter cracks, flakes, and fisheyes found in steel forgings, weldments, and castings.

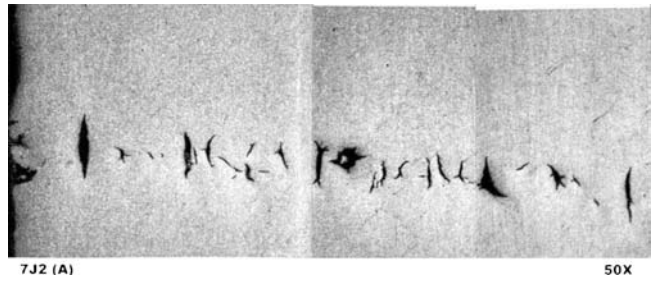

Figure 6.66 *SOHIC in linepipe laboratory test; SOHIC in plate steel exposed to sour gas*[176]

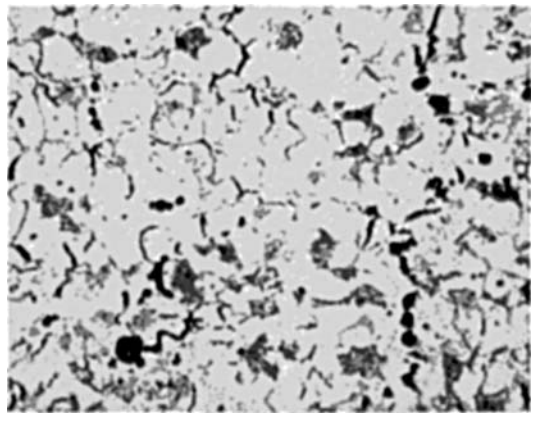

Figure 6.67 *Microstructure of hydrogen-attacked pipe near the midwall of ASTM steel A 106 carbon steel pipe*[19]

High-temperature high-pressure exposure to hydrogen is commonly experienced by steels used in petrochemical plant equipment that often handles hydrogen and hydrogen–hydrocarbon streams at pressures as high 21 MPa (3ksi) and temperatures up to 540°C. It is important to note that this type of hydrogen damage causes irreversible damage while hydrogen embrittlement is often reversible and occurs below 200°C. Absorbed hydrogen reacts internally with carbides present in steel and produces methane bubbles along grain boundaries. These bubbles grow and cause fissures. Figure 6.67 shows that fissuring is at grain boundaries and this was accompanied by decarburization. The pipe failed after 15 months of service in hydrogen-rich gas at 34.5 MPa and 320°C in petrochemical plant equipment. Another alloy susceptible to hydrogen attack is copper containing small amounts of cuprous oxide. This oxide reacts to form steam within the alloy, resulting in significant void formation. (Kane)[5]

Hydrogen gas exposures may also result in titanium embrittlement, depending on gas temperature, pressure, and purity. (Schutz)[24]

Other types of hydrogen attack. Hydrogen trapping, microperforation and degradation in flow properties have been documented. (Craig)[5] Liquid-metal-induced embrittlement (LMIE) is the catastrophic brittle failure of a normally ductile metal when coated with a thin film of a liquid metal and subsequently stressed in tension.[141,] (Kolman)[5,] (Kamdar)[14] Solid-metal-induced embrittlement (SMIE) occurs below the melting temperature of the solid in certain liquid metal environments (LMIE couples). The severity of embrittlement increases with temperature, with a sharp and significant increase in severity at the melting point T_m of the embrittler. (Kolman)[5,] (Kamdar)[14]

Mechanisms of Environmentally Induced Cracking (EIC). Environmentally assisted cracking spans a wide range from brittle fracture to electrochemical process and the underlying mechanisms are complex.

The overlapping of cracking phenomena. There are a number of corrosion-related causes of the premature fracture of structural components. The most common of these

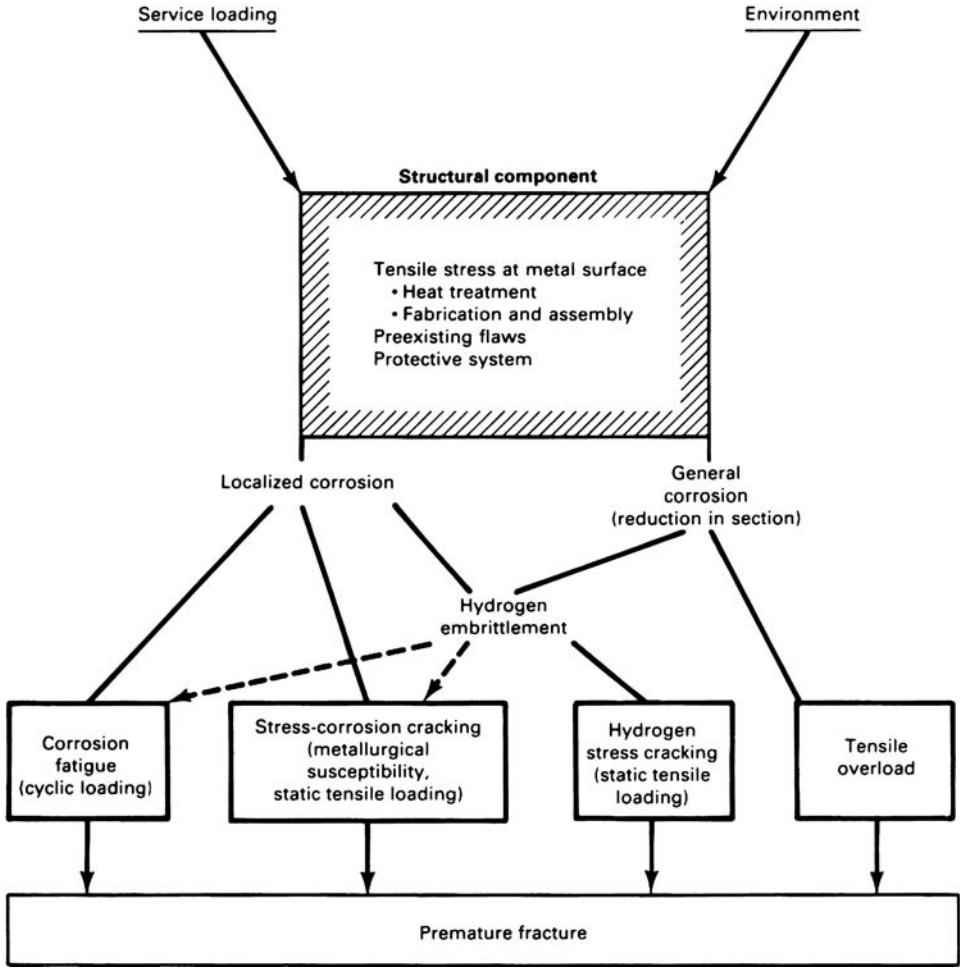

Figure 6.68 *Causes of premature fracture influenced by the corrosion of a structural component (Phull)*[5]

are compared in Figure 6.68. Corrosion fatigue cracking occurs only under cyclic or fluctuating operating loads, while SCC and HE occur under static or slowly rising loads.

It is admitted that CF, SCC and HE could simultaneously occur in metallic alloys/media systems. The simultaneous and the overlapping of SCC and HE is obvious in many circumstances and service conditions. Figure 6.69 illustrates a conceptual interrelationship of corrosion fatigue, stress corrosion, and hydrogen embrittlement. The most serious practical situations involving ductile alloy/environment systems are in the cross-hatched regions. These regions indicate the combination of any two failure mechanisms. In the center, all three phenomena interact, which is probably representative of many practical situations involving ductile alloy/aqueous environment systems. (Phull)[5]

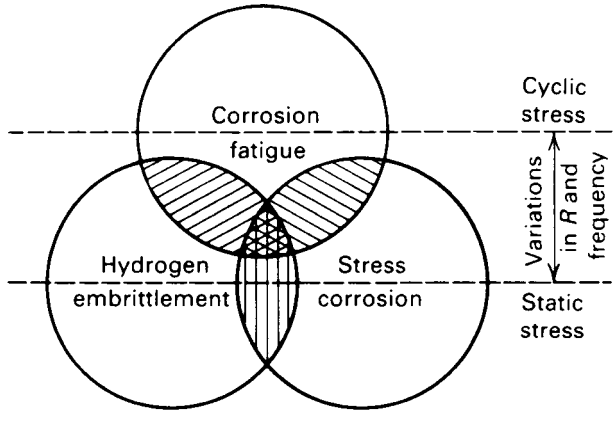

Figure 6.69 *Venn diagram illustrating the interrelationship among stress corrosion, corrosion fatigue, and hydrogen embrittlement; R = ratio of minimum stress to maximum stress (Phull)*[5]

For example, in CF and SCC, a surface pit constitutes a stress raiser, especially in the initiation process. CF can help initiation of the fracture while SCC and/or HE could assist more or less intensively the crack propagation. In certain conditions, one or the other can dominate the morphology and mechanism of fracture propagation. Under fatigue loading, modification of the number of persistent slip bands (PSBs) in fatigue and of the slip offset height in PSBs has been observed, in comparison with air for nickel single crystals in 0.5 N H_2SO_4 and copper crystals according to the applied potential. Moreover, cyclic softening effects under anodic dissolution can occur in austenitic and ferritic stainless steels in NaCl solutions.[95,104]

Both the decrease of K_{ISCC} and the acceleration of crack growth rates due to the increase of the metal strength become more apparent under cyclic loading. K_{ISCC} is always much higher than ΔK_{th}, the threshold stress intensity range at the corrosion fatigue crack growth rate $\leq 10^{-10}$ m/cycle. The rate da/dN in aqueous solutions is much higher (by a dozens times) than that in ambient air. However, by suitable choice of solution composition, the corrosion fatigue crack growth rate can be somewhat decreased (e.g., in titanium alloys and magnesium alloys) comparable to that in air.[113,126]

For materials that exhibit classical active–passive behavior, passivation is more conducive under static rather than dynamic conditions. For the latter, the frequency of cyclic loading is often one of the critical factors that influences CF in corrosive environments. Cathodic protection generally mitigates CF and SCC, but increases the probability of HEC of susceptible materials.

Electrode potential and pH at an active crack tip may be significantly different from those on boldly exposed surfaces of a material. Low-pH conditions can lead to local dissolution of metal and crack-tip blunting, which reduces stress concentration effects. In contrast, low-pH conditions favor hydrogen generation and, consequently increased risk of HEC. Reduction in local ductility associated with HEC is more likely to produce sharp crack tips, which, in turn, can exacerbate stress concentration effects for any synergistic SCC or CF. (Phull)[5]

In many systems, but certainly not all systems, SCC occurs in a limited range of electrochemical conditions, as has been shown for the potential/pH domains for cracking of mild steel in different environments. Three main types of SCC as a function of the level of potential have been identified by Ford:[142]

- Low-potential regions where water reduction produces significant amounts of hydrogen that can be absorbed by the material (hydrogen embrittlement).
- Passive regions close to active–passive transitions as for nickel–chromium–iron alloy 600 or steel in caustic solutions (Figure 6.58).[143,144]
- Regions close to critical potential for localized corrosion. This is observed for austenitic stainless steel in near-neutral solutions.[95,145]

Thus, it is apparent from the foregoing that complex relationships can exist between CFC, SCC, and HEC. (Phull)[5] and the distinction between HE and SCC or CF is often very difficult or even meaningless in certain circumstances, because it is likely that hydrogen–metal interaction near the crack tip is the controlling process of SCC or CF crack propagation.[95]

Mechanisms of SCC. Crack initiation of EAC is complex and not well understood till now. Most of the SCC systems exhibit short initiation times ranging from minutes to weeks and cracking often occurs due to the change in the environment rather than to a very long initiation time. Stress–corrosion crack growth rates are usually 10^{-11} and 10^{-6} m s^{-1}. In systems such as stainless steels in chloride solutions, localized corrosion may create the local conditions prone to crack development, but it is still difficult to explain the initiation of the crack in the absence of localized corrosion in environmental conditions different from that of the crack propagation.[95] It should be mentioned that dealloyed surface layers such as certain copper alloys in ammonia-containing solutions are believed to cause SCC.[54]

Surface films appear to play a major role in the initiation of SCC and may also contribute to hydrogen embrittlement effects. It is assumed that the main role of the surface film is to localize the damage inflicted on the material by the environment. This can be caused by mechanical breakdown of the protective film by slip step or electromechanical breakdown of the passive film.[95] SCC may be related to the nature of the surface film. It has been observed that the SCC of C-Steels is related to the presence of magnetite in several 'low'-temperature environments (around 90°C), except when pitting is involved in the crack initiation process, as in nitrates or in high-temperature water.[124,146]

Mechanisms of hydrogen embrittlement. If the environment provides hydrogen species that are adsorbed at the crack tip to reduce the effective bond strength, then the surface energy is effectively lowered, alternatively the hydrogen atoms may diffuse into the metal (Figure 6.70a and b). With decohesion of atoms by hydrogen influx to the dilated lattice (Figure 6.70c), certain interactions may occur in advance of the crack tip where the stress and/or the strain conditions are particularly appropriate for the nucleation of a crack. This can be followed by the formation of a brittle phase (metal hydride, Figure 6.70d). On the other hand, the recombination of two atoms of hydrogen can form the molecular hydrogen that exercises a pressure inside the metallic network and can cause inflation, and this is a mechanism for the formation of a blister.

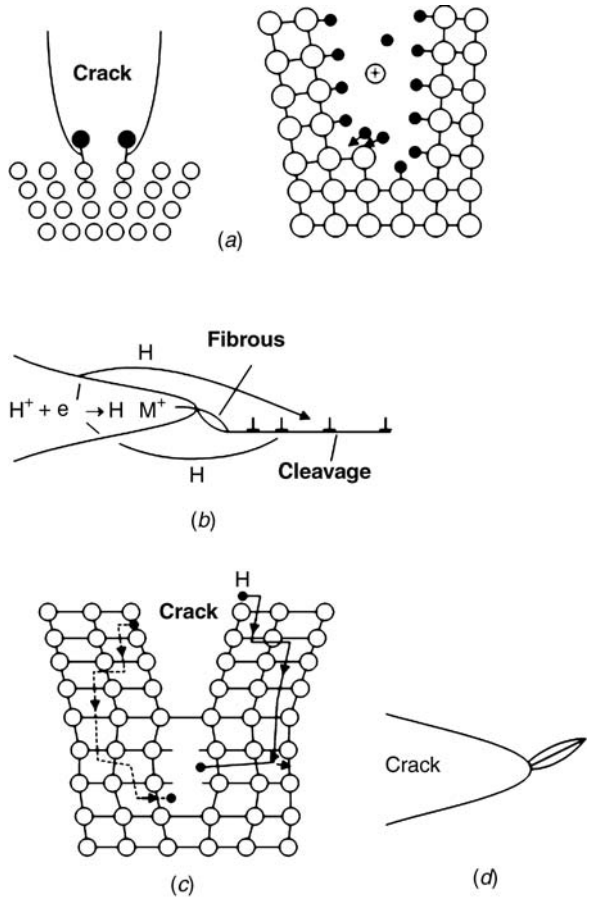

Figure 6.70 *Possible mechanisms of hydrogen embrittlement: (a) chemical adsorption of hydrogen; (b) absorption of atomic hydrogen; (c) decohesion of atoms; (d) possible brittle hydride particle at the tip*[1]

Hydrogen-induced crack growth as the dominant SCC mechanism has been suggested for ferritic steels, nickel-based alloys, titanium alloys, and aluminum alloys, although ferritic steels show the predominant evidence of this mechanism. The effects of factors such as yield strength, impurity segregation, and temperature on the crack growth behavior of ferritic materials in aqueous solutions follow the trends of hydrogen embrittlement. It has also been shown that tin and antimony, known as hydrogen recombinant poisons, segregated to the grain boundaries of nickel alloy, and enhanced the atomic hydrogen uptake (Figure 6.71).[147,] (Jones)[5]

Temperature plays an important role in the hydrogen embrittlement of ferrous alloys. Embrittlement is most severe near room temperature and becomes less severe or

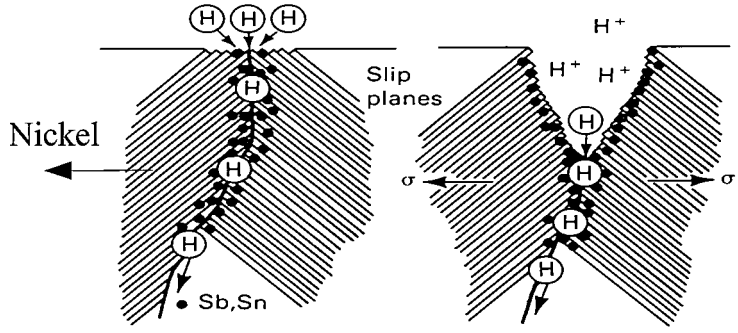

Figure 6.71 *Schematic showing the relation between the presence of some impurities and the grain boundary embrittlement processes that can lead to intergranular SCC of nickel (Jones)*[5]

nonexistent at higher or low temperatures. At lower temperatures, the diffusivity of hydrogen is low to fill sufficient traps, but at high temperatures, hydrogen mobility is enhanced. At high strain rate fracture proceeds without the assistance of hydrogen. (Craig)[5] For example, the crack growth rate of a 3% Ni steel as a function of the temperature and that of 4340 steel in gaseous hydrogen have been studied. The maximum crack growth rate occurs at about 20°C for steel (Figure 6.72), with similar decreases at both higher and lower temperatures for nickel. However, anodic stress corrosion processes become active at temperatures above 100°C for the nickel tested in water, suggesting that an SCC mechanism has assumed control. (Jones)[5]

Threshold stress intensity for crack growth in iron-based alloys generally decreases with increasing yield strength, regardless of environment and very-high-strength steels cannot be used in hydrogen environments. In this regard, hydrogen sulfide is one of the most severe environments. At lower yield strengths, the mechanisms for hydrogen-assisted failure apparently changes, and blistering becomes the more common feature of failure. The threshold stress intensities for high–strength steels subjected to hydrogen environments are significantly less than those measured under benign conditions (K_{ISCC} or K_{HI}).

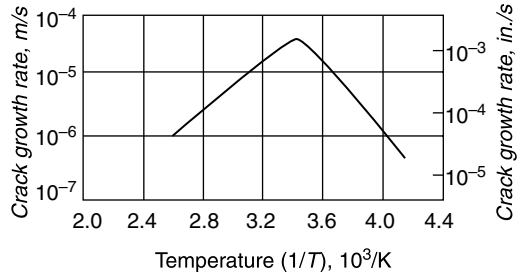

Figure 6.72 *Schematic of crack growth rate vesus temperature for 4340 steel in gaseous hydrogen (Jones)*[5]

In low-strength steels (700 MPa or 100 ksi yield strength or less), hydrogen damage occurs by loss in tensile ductility or blistering. For loss in tensile ductility, hydrogen promotes the formation and/or growth of voids by enhancing the decohesion of the matrix at carbide particles and inclusion interfaces. At higher hydrogen fugacities and often in the absence of stress, blistering or a form of cracking also associated with inclusions called stepwise cracking, blister cracking or hydrogen-induced cracking (HIC) is observed (Figure 6.65). This type of cracking is not a function of steel strength, but depends strictly on steel composition, processing, and hydrogen environment. In H_2S environments, a cracking morphology has been observed in low-strength steels that combines the features of hydrogen stress cracking and HIC, and has been designated as stress-oriented hydrogen-induced cracking (SOHIC). (Craig)[5]

Localized corrosion and stress–corrosion cracking may often be observed. Stress–corrosion cracks invariably initiate at pits in numerous systems. The role of pitting is to disrupt films that otherwise prevent the ingress of hydrogen, and the stress factor due to pits is not significant.[148,149] Use of electrochemical polarization to distinguish between SCC and hydrogen embrittlement mechanisms in a high-strength steel immersed in sodium chloride solution has been studied.[150,] (Phull)[5]

Propagation Models. Usually, stress–corrosion cracking is considered to be brittle, i.e., when it occurs at stresses below general yield and propagates as an essentially elastic body, even though local plasticity may be necessary for the cracking process. Thus, linear elastic fracture mechanics (LEFM) is used for studying SCC. Propagation of the crack is very frequently due to periodic microruptures although the anodic dissolution is an important or controlling process. Local attack gives rise to a localized hydrogen absorption and that can cause local or bulk embrittlement and even plasticity, and so anodic dissolution and hydrogen could play a role in the same system. The local environment leading to crack propagation is not well defined, particularly in SCC phenomena. The transport of water to the crack tip can be an important and controlling process. Except for the slip dissolution model, EAC models are not able to provide quantitative prediction of the crack propagation rate.[95]

The following schema describes the models of stress corrosion cracking mechanisms.

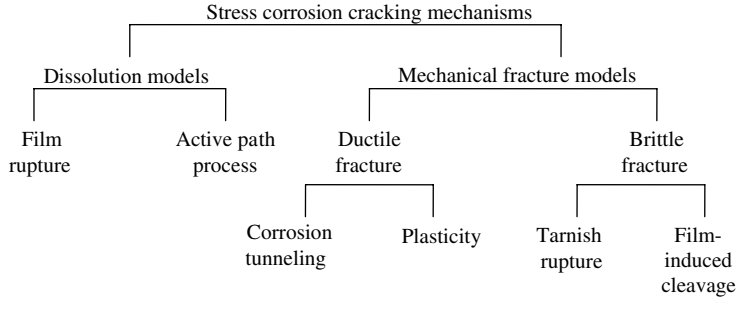

Dissolution models. The dissolution models consider that the crack propagates because of preferential dissolution at the crack tip. The preferential dissolution can give rise to the formation of active paths in the material, stresses at the crack tip, and

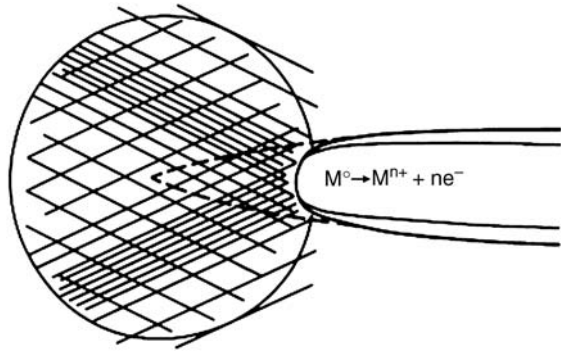

Figure 6.73 *Schematic representation of crack propagation by the film rupture model (Jones)*[5]

chemical–mechanical interactions. Recently, the debate has been centered on the following model.

Film rupture or slip dissolution model. The model assumes the presence of an active protective film and that the stress acts to open the crack and rupture the protective film. Localized plastic deformation at the crack tip ruptures the passivating film, exposing bare metal at the crack tip, and the freshly exposed surface dissolves rapidly as shown in Figure 6.73. However, it is also suggested that the crack tip remains bare since the rate of repassivation is slower than that of film rupture during propagation. Intergranular corrosion may be considered the low-stress limiting case of this mechanism and so this model is viable for intergranular SCC and generally not accepted as a mechanism for transgranular SCC. (Jones)[5]

The limiting velocity for the crack growth according to the dissolution model may be written as

$$da/dt = i_a M/zF\rho$$

where i_a is the anodic current, M is the atomic weight, z is the valence, F is Faraday's constant, and ρ is the density of material. In general, the crack-growth rate depends on the rate at which the film is ruptured and reformed. (Jones and Ricker)[24]

Ductile mechanical models. Stress concentrations at the base of corrosion slots or pits increase to the point of ductile formation or fracture.

In the corrosion tunneling model, it is assumed that a fine array of small corrosion tunnels form at emerging slip steps. These tunnels grow in diameter and length until the stress in the remaining ligaments causes ductile deformation and fracture. It was suggested that the application of a tensile stress results in a change in the morphology of the corrosion damage from tunnels to thin slots, as shown in Figure 6.74. (Jones)[5]

Adsorption-enhanced plasticity models. Fractographic studies showed that cleavage fracture is not an atomically brittle process, but occurs instead by alternate slip at the crack tip in conjunction with formation of very small voids ahead of the crack. It was also proposed that chemisorption of environmental species facilitated the nucleation of dislocations at the crack tip, promoting the shear process responsible for brittle-like fracture. (Jones)[5]

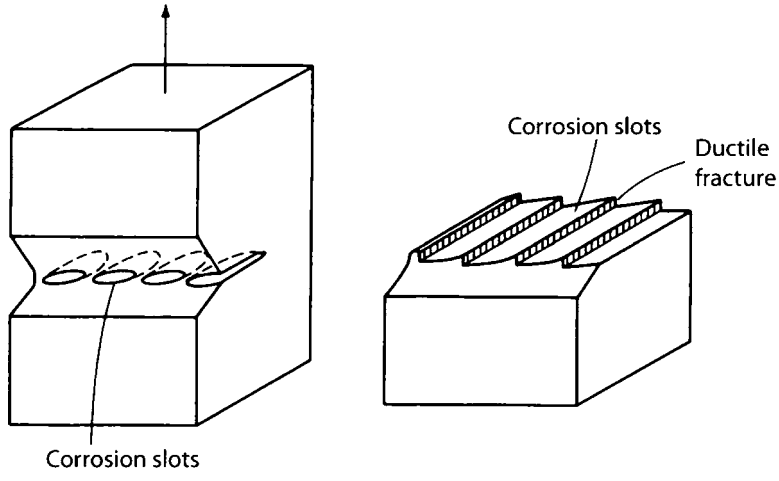

Figure 6.74 *Schematic diagram of the tunnel mechanism of SCC and flat slot formation (Jones)*[5]

Corrosion enhanced plasticity models. These are based on a localized softening effect at the very crack tip, due to corrosion. Fracture occurs because of the enhancement plasticity along one slip system, inducing the formation of a pile-up and a local decrease of the cohesion energy due to the presence of hydrogen. The role of dissolution is to create vacancies that can enhance the plasticity at the crack tip and create defects in the passivated metals at the slip band emergence required for hydrogen absorption. Vacancies may also act as hydrogen trapping sites, thus increasing its crack tip concentration.[151] This model has been extended to intergranular SCC through the same corrosion–deformation interactions in the vicinity of grain boundaries.[152]

The enhancement of creep by anodic dissolution is well known, for copper in acetic acid[153] and austenitic stainless steels and nickel-based alloys in pressurized water reactor (PWR) environments. The initial vacancy injection from the surface is followed by vacancy attraction to the inside dislocations, which promotes easier glide, climb, and crossing of microstructural barriers. This mechanism illustrates the corrosion-enhanced plasticity approach.[95]

The tarnish rupture model. In this model, fracture of the film exposes the bare surface, which rapidly reacts with the environment to re-form the surface film. The crack propagates by alternating film growth and fracture, as shown in Figure 6.75.[154] This model was first proposed to explain transgranular SCC and then modified to explain intergranular SCC by assuming that the oxide film penetrates along the grain boundary ahead of the crack tip, which may not be the case for all systems.[155,] (Jones)[5]

Film-induced cleavage models. It has been suggested that dealloying and/or vacancy injection could induce brittle fracture. The model assumes that a brittle crack initiates in a surface film or layer and this crosses the film/matrix without loss of speed. The brittle crack will continue in the ductile matrix until it eventually blunts and arrests. Verification of this model needs better understanding of the surface films and brittle fracture. (Jones)[5]

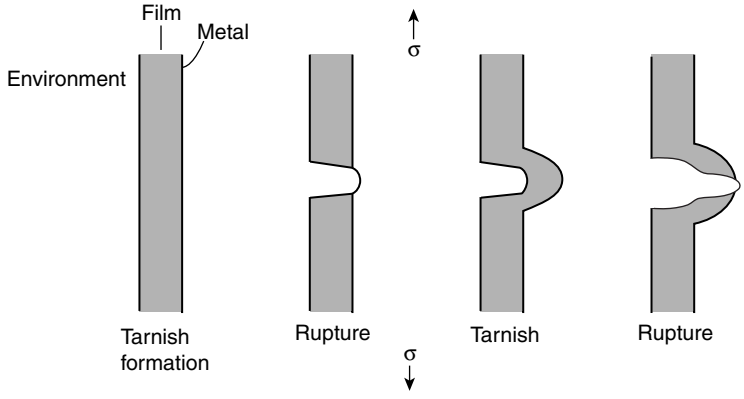

Figure 6.75 *Tarnish rupture model for SCC (Jones)*[5]

Adsorption-induced brittle fracture. This model is based on the hypothesis that adsorption of environmental species lowers the interatomic bond strength and the stress required for cleavage. This model of chemical adsorption can explain the fact that a certain alloy is susceptible to specific ions. An important factor in support of this mechanism is the existence of a critical potential below which the SCC does not occur in some systems, and this model underlines the relation between the potential value and the capacity of adsorption of the aggressive ion. It also explains the preventive action of SCC for some systems by cathodic protection. This model may interpret the rupture of plastic materials or glass. It is referred to as the stress–sorption model, and similar mechanisms have been proposed for HE and LME. In this model, the crack should propagate in a continuous way at a rate determined by the arrival of the embrittling species at the crack tip. The model does not explain how the crack maintains a sharp tip in a normally ductile material.[156]

Decohesion models. Interactions between a localized dislocation array and the crack tip under an applied stress produce a maximum stress ahead of the crack tip to which hydrogen is driven under the stress fields from behind the tip. When the hydrogen concentration reaches a critical value, a microcrack is nucleated because either the local cohesive strength is reduced, dislocation motion is blocked in the hydrogen-enriched zone, or both. The microcrack arrests about 1 μm ahead of the original location of the tip and these processes then repeat, leading to discontinuous microcracking.[95] This is sometimes called hydrogen-enhanced decohesion (HEDE).

Hydrogen-induced plasticity. Another approach is related to the fact that hydrogen increases local plasticity. Two models have been proposed based on the adsorption and absorption of hydrogen.

- The adsorbed hydrogen-induced model is based on the fact that adsorbed hydrogen atoms weaken interatomic bonds at crack tips and thereby facilitate the injection of dislocations (alternate slip) at crack tips. Crack growth occurs by alternate slip at the

crack tips, which promotes the coalescence of cracks with small voids nucleated ahead of the cracks.
- The second is the absorbed hydrogen-enhanced local plasticity mechanism (HELP). This is based on the fact that the local decrease of the flow stress by hydrogen leads to highly localized failure by ductile processes, while the local macroscopic deformation remains small. Shear localization results from local hydrogen absorption, giving a macroscopically 'brittle' fracture related to microscopic localized deformation.[95]

Prevention. Prevention of SCC. Although the cause of the SCC is a combination of several factors, the measures to prevent or reduce the risk of SCC can be arbitrarily divided as a function of the stresses, environmental considerations, metallurgical properties, and surface treatments.[31,146]

Stresses:

- The sum of stresses in service and residual stresses, including those due to fabrication, should be below the threshold level which, in the absence of reliable data, should be evaluated by testing as a percentage of the tensile yield strength. This can be achieved by a design that avoids initial concentration of stresses, reducing operating stresses, relieving fabrication stresses by a heat treatment and by choosing appropriate dimensions of the loaded alloy.
- During use, avoid stress concentrators by increasing susceptibility to different forms of degradation in service, especially localized corrosion, galvanic corrosion, and erosion–corrosion. Accidental or nondesigned cyclic loading should be avoided.
- Bolted or riveted joints can produce high local stresses that can cause SCC, so that attention should be given to proper joint design and construction. Examples include the use of preformed parts, avoid over-torquing of bolts, and provide adequate spacing and edge margins for rivets.

Environmental considerations:

- Eliminate potential aggressive ions that induce SCC, dissolved gases, heavy metals and impurities by chemical or physical methods such as degasification, demineralization, distillation, etc.
- Add efficient inhibitors for certain systems since it is believed to assist the formation of a stronger, more stable or more readily repaired passive film. (Miller)[24] Phosphates and other inorganic or organic corrosion inhibitors, used in fairly corrosive surroundings, decrease the effects of the SCC. A minimal critical concentration of some oxidizing inhibitors such as nitrites is absolutely necessary to avoid pitting.
- The application of a mixture of inhibitors for the corrosion control may be useful. Capillary condensation can cause the formation of a liquid in the crevices at lower values of relative humidity. It would be prudent to fill crevices with corrosion-inhibited putty.
- Cathodic polarization may reduce, or even prevent SCC of some materials in certain aqueous solutions, but this should be used with great care for the alloys that resist all types of critical hydrogen damage.

- Avoid if possible the temperature level or range that causes SCC, e.g., SCC of steel in caustic medium at >105°C.

Metallurgical considerations:

- Select a resistant alloy with a suitable chemical composition and microstructure for the given environment.
- Shot peening and other mechanical processes that create compressive residual stresses at the surface are recommended.
- Stress-relief at low appropriate temperatures is commonly used to lower susceptibility. Tensile residual stresses from welding can be particularly dangerous and a low-temperature thermal stress-relief treatment is recommended for welded assemblies.[157]
- Change the alloy composition and/or the alloy microstructure, for example, the nickel base superalloy Inconel can replace the stainless steel grade 304 in certain media.

Surface treatments:

- Surface conversion by oxidation, phosphating, anodizing are helpful for certain alloys if they are followed by sealing with appropriate application of inhibitors or coatings.
- Coatings have been shown to extend life, but do not totally prevent SCC, since defects in the coating lower protection.[1]
- Cladding a susceptible alloy with a nonsusceptible one.
- Perform nondestructive testing, inspection and maintenance programs to avoid SCC precursors, such as a concentration of stresses by localized corrosion. In case of protective coatings, routine maintenance is essential since scratches could create favorable sites for initiation of SCC.

Prevention of Hydrogen Damage involves the following metallurgical considerations:

- Modifying the design to lower stresses as well as choice of materials resistant to HIC such as nickel-containing and nickel–based alloys because of their low hydrogen diffusion rates.[16] Hydrogen damage can often be prevented by using more resistant material, for example, alloying high-strength steels with nickel or molybdenum reduces susceptibility to hydrogen embrittlement.
- Since susceptibility of pipeline steels to HIC depends on nonmetallic inclusions and anomalous structures due to P and Mn segregation in steel, HIC can be reduced, either by reducing the proportion of nonmetallic inclusions by lowering the S content, or by modifying the morphology of segregation by adding Ca. Tempering is effective in eliminating the low-temperature anomalous structure. Addition of Cu ($>0.2\%$) is also effective. It is claimed that Ca and rare earth metals inhibit HIC susceptibility by modifying the morphology of inclusions.[158] Calcium and rare earth metals, such as La and Ce, spheroidize nonmetallic inclusions, raising C_{th}, (i.e., the resistance); these additions are often used in making steels for severe environments.[159] Also, Co, Ccopper and cobalt, copper and tungsten, and Ni are stated to be effective. Hot strip mill products are more susceptible than plate mill products. If S is reduced from 0.002 to 0.005%, the number of nonmetallic inclusions in steel, such as MnS, may be reduced and HIC inhibited.
- One can prevent the formation of hydrogen blisters by using a 'clean' steel without voids such as killed steels instead of rimmed ones. Manufacturing processes and

treatments affect the MnS morphology and influence sensitivity; for example, rimmed and Si-killed steels have relatively low susceptibility.[160,161] If the MnS inclusion content is sufficiently low, even the adverse effects of low-temperature controlled rolling are reduced.[162] Both quenching and tempering treatments can reduce the susceptibility substantially.[163] Tempering is also effective in eliminating localized Mn and P segregation if the Mn level is more than 1%; tempering reduces hardness around inclusions, and thus, the HIC susceptibility.[135]

- Reduce hydrogen embrittlement during welding by using dry conditions, without humidity since water and the steam are the major sources of hydrogen. Low-hydrogen welding rods should be used.[16]
- One can add inhibitors to reduce the corrosion reaction rate which is a source of hydrogen. Post-processing bake-out treatments can also be used. Baking of electroplated high-strength steel parts reduces the possibility of hydrogen embrittlement. Careful inhibitor additions during pickling can avoid vigorous hydrogen evolution and cause a subsequent decrease in hydrogen pickup. Proper choice of plating baths can reduce the hydrogen pickup during plating. A common way of removing hydrogen from steels for example is by baking at 93–148°C and this is highly recommended for electroplated galvanized steels. The pH can be raised to reduce HIC.[164]
- Changing the environment can be very efficient. For example, blistering rarely occurs in pure acid corrosives without hydrogen–evolution poisons such as sulfides, arsenic compounds, cyanides, and phosphorus-containing ions.[31]
- Coatings are recommended for hydrogen damage as for SCC, but they should be impervious to hydrogen penetration as well as resistant to the corrosive medium. Metallic, inorganic and organic coatings are often used to prevent the formation of HIC and blisters of hydrogen.[135,165–167]

Corrosion Testing. Typical objectives of SCC testing programs include:

- Determination of the risk of SCC for a given application and comparison of alloys and mill products
- Examination of the influence of chemical composition, metallurgical processing, and fabrication practices for structural components
- Evaluation of protective systems and prediction of service life
- Development of new alloys that can be less expensive, and offer longer, safes and more efficient service for certain environments
- Evaluation of claims for SCC performance of improved mill products

Predictions of the corrosion performance should be obtained from published data and through testing.The essential requirements of accelerated testing are that the acceleration should produce the same mode of failure and reflect at least a known order of resistance of some alloys in service media.[168] The most common approaches employed to achieve testing objectives in SCC are the use of high stresses, slow continuous straining, precracked specimens, higher concentration of species in the test environment than in the service environment, increased temperature, and electrochemical stimulation.[169] For electrochemical corrosion, the properties of the medium at the interface should be considered in accelerated tests.

Media considerations. SCC tests can be divided into those conducted in natural environments, such as atmospheric exposure tests and seawater immersion tests, and those which are conducted under laboratory conditions or other fabricating operations. The principal disadvantage of atmospheric exposure tests is the comparatively long time required for their completion; however, they are reliable since they can reflect the projected use. There is a standard practice for evaluating stress–corrosion cracking resistance of metals and alloys by alternate immersion in a solution of NaCl 3.5%, pH 6.5. For spray testing, ASTM B-117, 2003 states the relevant conditions for conducting the test. (ASTM G44)[4]

Test specimens. The specimens commonly used for tests under elastic-range stress are bend-beam specimens, C-ring specimens, O-ring specimens, tension specimens and tuning fork specimens. Plastic strain specimens and residual stress specimens are also used for certain conditions. Static loading of precracked specimens as well as slow-strain-rate testing should be considered. Stressed O-rings have also been used to evaluate protective treatmens for SCC prevention. The specimens can be subjected to various loading conditions involving constant load, constant strain, or monotonically increasing strain to total failure in some of the slow-strain-rate tests. Other tests include cyclic loading as well as slow straining over a limited stress range.[170,] (Sprowls)[24]

Stressors. Corrosion acceleration for testing alloys is achieved through the use of various 'stressors' such as cold work of the material, higher concentration of the aggressive ion, lower pH, higher temperature, higher stress, etc. Externally applied loads are easier to evaluate and to control, but residual stresses are those which normally are responsible for stress–corrosion failures under service conditions. It is a good practice to employ both methods of stressing. Although laboratory tests are useful in encouraging conservative design of the alloy structures, results of long-term atmospheric tests of tensile-loaded specimens are considered to be more reliable.

Constant-load SCC tests have been shown to be more severe than constant-deflection tests. Under a constant load, stress increases as the cross-section is reduced by cracking or corrosion. However, this condition produces decreasing stress when deflection is fixed. It has been suggested that SCC threshold stress is associated with the onset of plastic deformation, that is, the elastic limit of the alloy. The elastic limit is difficult to measure unambiguously, however, the stress at which 0.2% plastic deformation occurs is generally used.

Slow strain test. The strain rate chosen frequently for the tests, based on several studies, indicates important susceptibility to cracking at about 2×10^{-6} s^{-1} for steels, aluminum and magnesium alloys. However, the tests refer to open-circuit conditions and the strain rate sensitivity of cracking is dependent upon potential as well as solution composition. Where necessary the potential of the specimens can be controlled using a potentiostat during slow-strain-rate tensile testing.[171] The reduction of area is a simple and appropriate way to quantify the susceptibility to SCC.

Both AC and DC potential-drop methods are well-established techniques for monitoring subcritical crack growth. A combined AC/DC potential-drop measuring technique can, in some cases, help in obtaining more information from a single test, in particular for the onset of stable crack growth.[172]

References

1. Shreir, L.L., Jarman, R.A., Burnstein, G.T., (eds.), "Corrosion", Vol. 1, Butterworth Heinemann, *Principles of Corrosion and Oxydation*, pp. 1:1–303; Environments, pp. 2:120–142, Effect of Mechanical Factors on Corrosion, pp. 8: 1–244, 1994.
2. Fontana, M.G., Staehle, R.W., *Advances in Corrosion Science and Technology*, Plenum Press, NY, preface to volume 1, p. 2, 1990.
3. Dillon, C.P., Introduction, in *Forms of Corrosion - Recognition and Prevention*, NACE Handbook, Vol. 1, C.P. Dillon (ed.), NACE International, Houston, TX, USA, pp. 1–4; Verink, E.D., pp. 5–18, 1982.
4. Annual Book of ASTM Standards, **Vol. 01.03**, A 262-02, A 763-93 (2004); **Vol. 03.01**, E 647-00; **Vol. 03.02**, B 117-03; G 1-90; G 5-94 R04; G 16-95; G 28-02; G 44-99 R05; G 46-94; G 48-92; G 59-97 R03; G 61-86; G 76-04; G 78-95; G 102-89 R04; G 108-94 R04; G 110-92 R03; G 119-04; **Vol. 13.01**, F 746-04, and F 1160-05, 2005.
5. ASM, *Corrosion*, Vol. 13A, ASM Committee: 301–321, S.D. Cramer, B.S. Covino (eds.), ASM International, Ohio, USA, Mansfeld: pp. 446–462; Baboian: 210–213, 83–87; Baloun: 207–211; Bond: 294–300; Corcoran: 287–293; Craig: 367–380; Dexter: 398–416; Frankel: 236–241, 257; Fritz: 266–274; Glaeser and Wright: 322–330; Hack: 562–567; Hanson: 214–215; Jones: 346–366; Kane: 228–235; Kolman: 381–397; Little: 478–486; Noël: 258–265; Phull: 568–616, 625–638; Rebak: 279–286; Stott: 644–649; Tylczak and Adler: 338–344; Waterhouse R.B., Fig. 17, p. 237, 2003.
6. Hoar, T.P., *Corrosion Science*, **7**, 355 (1967).
7. Uhlig, H.H., Revie, R.W., *Corrosion and Corrosion Control*, 3rd edn, John Wiley & Sons, NY, pp. 327–340; 28–30; 90–164; 198–199; 320; 386; 6-15; 123–164; 60–89; 405–414, 1985.
8. Kruger, J., Passivity, in *Uhlig's Corrosion Handbook*, R.W. Revie (ed.), John Wiley & Sons, Inc., NY, pp. 165–170, 2000.
9. Sastri, V.S., An Overview of Corrosion Inhibition, in *Corrosion Inhibitors*, Principles and Applications, John Wiley & Sons, Ltd, pp. 33–49, 1998.
10. Macdougall, B., Graham, M.J., Growth and stability of passive films, in *Corrosion mechanisms in theory and practice*, P. Marcus and J. Oudar (eds.), Marcel Dekker, Inc., pp. 143–173, 1995.
11. Nagayama, M., Cohen, M., *Journal Electrochemical Society*, **109**, 781, **110**, 670 (1962 and 1963).
12. Marcus, P., Maurice, V., Passivity of Metals and Alloys, *Corrosion and Environmental Degradation*, M. Schütze (ed.), Wiley-VCH, Weinheim, Germany, pp. 131–169, 2000.
13. Strehblow, H.H., Mechanisms of Pitting Corrosion, in *Corrosion Mechanisms in Theory and Practice*, P. Marcus, J. Oudar (eds.), Marcel Dekker, NY, pp. 201–237, 1995.
14. ASM Metals Handbook, *Corrosion*, Vol. 13, 9th edn, L.J. Korb, D.L. Olson (eds.), ASM International, Ohio, USA, Craig and Pohlman: pp. 77–189; Dexter: 87–88; Froats: 745; Glaeser and Wright: 136–144; Kain: 303–310; Kamdar: 171–189; Scully: 212–220; Sprowls: 231–233; Krysiak (ASM Committee chairman): 344–368, 1987.
15. Fontana, M.G., *The Eight Forms of Corrosion, Process Industries Corrosion*, NACE International, Houston, TX, USA, pp. 1–39, 1975.
16. Fontana, M.G., Greene, N.D., The Eight Forms of Corrosion, *Corrosion Engineering*, McGraw-Hill, New York, pp. 1–115; Fig. 3-24, 1978.
17. Staehle, R.W., Environmental Definition, *30th Annual Conference of Metallurgists of CIM*, Proc. of the Inter. Symp. on Materials Performance Maintenance, Ottawa, Ontario, Canada, August 18–21, Pergamon Press, NY, pp. 3–46, 1991.
18. Staehle, R.W., Lifetime Prediction of Materials in Environments, in *Uhlig's Corrosion Handbook*, R.W. Revie (ed.), pp. 27–84, 2000.
19. ASM, Forms of Corrosion: Recognition and Prevention, in *Corrosion: Understanding, the Basics*, J.R. Davis (ed.), ASM International, Ohio, USA, pp. 99–192; 10–15, 2000.
20. Scully, J.C., *The Fundamentals of Corrosion*, Pergamon Press, pp. 90–92, 1966.
21. Peckner, D., Bernstein, I.M., *Handbook of Stainless Steels*, McGraw-Hill, NY, p. 24, 1977.

22. (a) Landrum, R.J., *Fundamentals of Designing for Corrosion Control*, NACE International, Houston, TX, USA, pp. 1–24, 1992.
(b) Piron, D.L., Corrosion Failures of Metals, in *The Electrochemistry of Corrosion*, NACE International, Houston, TX, pp. 164–174; 151–181, 1991.
23. Pourbaix, M., Corrosion, in *Atlas of Electrochemical Equilibrium in Aqueous Solutions*, NACE International, CEbelcor, pp. 70–85, 1974.
24. ASM, in *Stress-Corrosion Cracking*, R.H. Jones, R.E. Ricker (eds.), ASM International, Metals Park, Ohio, USA, Jones and Ricker: pp. 1–40; Andersen: 181–210; Miller: 251–263; Schutz: 256–297; Sprowls: 336–415, 1992.
25. Shreir, L.L., Corrosion, *Metal/Environment Reactions*, Vol. 1, L.L. Shreir (ed.), Newnes-Butterworths, London, 2nd edn, pp. 1:169–174; 8:1–129, 1976.
26. Bogaerts, W.F., Agena, K.S., *Active Library on Corrosion*, Elsevier, Amsterdam, The Netherlands in conjunction with NACE, Houston, TX, USA, 1996.
27. Böhni, H., Localized corrosion of passive metals, in *Uhlig's Corrosion Handbook*, 2nd edn, R.W. Revie (ed.), John Wiley & Sons, Inc., NY, pp. 173–190, 2000.
28. Szklarska-Smialowska, Z., *Pitting and Crevice corrosion*, NACE International, Houston, TX, USA, pp. 5–43, 2005.
29. Berger, D.M., Electrochemical and galvanic corrosion of coated steel surfaces, in *Corrosion Source Book*, NACE, Houston, TX, USA, pp. 11–14, 1984.
30. Godard, H.P., Localized Corrosion, in *NACE basic corrosion course*, NACE, Houston, TX, pp. 8:1–15, 1970.
31. ASM, *Surface Engineering for Corrosion and Wear Resistance*, J.R. Davis (ed.), ASM International, Ohio, USA, pp. 16–27; 1–81, 2001.
32. Lunder, O., Lein, J.E., Hesjevik, S.M., Aune, T.K., Nisancioglu, K., *Werkstoffe und Korrosion*, **45**, 331–340 (1994).
33. Yamamoto, A., Watanabe, A., Sugahara, K., Fukumoto, S., Tsubakino, H., ESCCD, Applying a Vapor Deposition Technique to Improve Corrosion Resistance in Magnesium Alloys, *Proc. of the 2nd Int. Conf. on Environment Sensitive Cracking and Corrosion Damage*, M. Matsumura, H. Nagano, K. Nakasa, Y. Isomoto (eds.), Nishiki Printing, Hiroshima, Japan, pp. 160–167, 2001.
34. Macdougall, B., Graham, M.J., Growth and Stability of Passive Films, in *Corrosion Mechanisms in Theory and Practice*, P. Marcus, J. Oudar (eds.), Marcel Dekker, NY, pp. 143–173, 1995.
35. Marcus, P., Sulfur Assisted Corrosion Mechanisms and the Role of Alloyed Elements, *Corrosion Mechanisms in Theory and Practice*, P. Marcus, J. Oudar (eds.), Marcel Dekker, NY, pp. 239–263, 1995.
36. Clayton, C.R., Olefjord, I., in *Corrosion Mechanisms in Theory and Practice*, P. Marcus, J. Oudar (eds.), Marcel Dekker, New York, pp. 175–199, 1995.
37. Pistorius, P.C., *Corrosion*, **53**, 273 (1997).
38. Shibata, T., *Corrosion*, **52**, 813 (1996).
39. Thompson, N.G., Payer, J.H., DC Electrochemical Test Methods, in *Corrosion Testing Made Easy*, B.C. Syrett (ed.), NACE International, Houston, TX, USA, pp. 72–77, 1998.
40. Thompson, N.G., Syrett, B.C., *Corrosion*, **48**, 649 (1992).
41. Frankel, G.S., *J. Electrochemical Society*, **145**(6), 2186–2198 (1998).
42. Sato, N., Okamoto, G., Electrochemical Passivation of Metals, in *Comprehensive Treatise of Electrochemistry*, J.O.M. Bockris, B.E. Conway, E. Yeager, R.E. White (eds.), Plenum Press, NY and London, pp. 193–245, 1981.
43. Kain, R.M., *Corrosion*, **40**(6), 313–321 (1984).
44. Treseder, R.S., Kachick, E.A., MTI Corrosion Tests for Iron and Nickel–Base Corrosion Resistant Alloys, in *Laboratory Corrosion Tests and Standards*, STP 866, ASTM, pp. 373–399, 1985.
45. Eden, D.A., Electrochemical Noise, in *Uhlig's Corrosion Handbook*, R.W. Revie (ed.), pp. 1227–1238, 2000.
46. Pistorius, P.C., Burstein, G.T., *Phil. Trans. R. Soc. Lond.*, **A 341**, 531 (1992).
47. Suter, T., Bohni, H., *Electrochim. Acta*, **43**, 2843 (1998).

48. Mansfeld, F., Wang, Y., Shih, H., in *Critical Factors in Localized Corrosion*, G.S. Frankel, R.C. Newman (eds.), Electrochemical Society, Proceedings, Pennington, NJ, USA, p. 497, 1999.
49. Jaffe, L.F., Nuticelli, R., *The Journal of Cell Biology*, **63**, 614–628 (1974).
50. Isaacs, H.S., Kendig, M.W., *Corrosion*, **36**, 269 (1980).
51. Samuels, L.E., *Metals Engineering: A Technical Guide*, ASM International, pp. 5; 6; 238, 1988.
52. Muller, L., Galvele, J.R., *Corrosion Science*, **17**, 1201 (1977).
53. Moore, H., Beckinsale, S., Mallinson, C.E., *Journal of Institute of Metals*, **25**, 35–153 (1921).
54. Sieradzki, K., Kim, J.S., Cole, A.T., Newman, R.C., *J. Electrochemical Society*, **134**, 1635–1639 (1987).
55. Pryor, M.J., Kar-Kheng, G., *J. Electrochemical Society*, **129**, 2157–2163 (1982).
56. Buchheit, R.G., Grant, P.P., Hlava, P.F., McKenzie, B., Zender, G.L., *Journal of the Electrochemical Society*, **144**, 2621–2628 (1997).
57. (a) Dimitrov, N., Mann, J.A., Vukmirovic, M., Sieradzki, K., *Journal of the Electrochemical Society*, **147**, 3282–3285 (2000).
    (b) ASM, *Corrosion of Aluminum and Aluminum Alloys*, J.R. Davis (ed.), ASM International, Materials Park, Ohio, USA, p. 25, 1999.
58. Mitrovic-Scepanovic, V., Brigham, R.J., *Corrosion*, **48**(9), 780–784 (1992).
59. Robinson, J.L., Preferential Corrosion of Welds, *The Welding Institute Research Bulletin*, Vol. 20, Jan. and Feb. 1979.
60. Matsushima, I., Carbon Steel-Corrosion in Fresh Water, *Uhlig's Corrosion Handbook*, 2nd edn, R.W. Revie (ed.), John Wiley & Sons, Inc., NY, pp. 529–544, 2000.
61. Wahid, A., Olson, D.L., Matlock, D.K., Cross, C.E., "Corrosion of Weldments", in *Welding, Brazing, and Soldering, ASM Metals Handbook*, Vol. 6, ASM International, Ohio, USA, pp. 1065–1069, 1993.
62. Ghali, E., Aluminum and Aluminum Alloys, in *Uhlig's Corrosion Handbook*, 2nd edn, R.W. Revie (ed.), John Wiley & Sons, Inc., NY, pp. 677–716, 2000.
63. Rebak, R.B., Corrosion of Non-Ferrous Alloys, Part I: Nickel-, Cobalt-, Copper-, Zirconium- and Titanium-Base Alloys, *Corrosion and Environmental Degradation*, Vol. II, Wiley-VCH, Weinheim, p. 69, 2000.
64. Sand, W., Microbial Corrosion, in *Corrosion and Environmental Degradation*, M. Schutze (ed.), Wiley-VCH, Weinheim, pp. 172–202, 2000.
65. Hamilton, W.A., Maxwell, S., Biological and Corrosion Activity of SRB in Natural Biofilms, *Proceedings of Biologically Induced Corrosion*, NACE International, pp. 131–136, 1986.
66. Perry, T.D., Breuker, M., Mitchell, R., Biodeterioration of Concrete and Stone, *Proceedings of the Corrosion 2002 Research Topical Symposium: Microbiologically Influenced Corrosion*, NACE International, pp. 113–121, 2002.
67. Holmes, P.E., *Journal of Applied Environmental Microbiology*, **52**, 1391 (1986).
68. Elpjick, J.J., Microbial Corrosion in Aircraft Fuel Systems, *Microbial Aspects of Metallurgy*, J.D.A. Miller (ed.), American Elsevier, pp. 157–172, 1970.
69. Videla, H.A., *Manual of Biocorrosion*, CRC Press, pp. 13–45, 121–133, 160–173, 179–185, 228–237, 232, 1996.
70. Zintel, T.P., Licina, G.J., Jack, T.R., Techniques for MIC Monitoring, *A Practical Manual on Microbiologically Influenced Corrosion*, Vol. 2, J.G. Stoecker (ed.), NACE International, p. 10.1, 2001.
71. NACE Standard TMO-194-94, *Field Monitoring of Bacterial Growth in Oilfield Systems*, NACE International, Houston, TX, 1994.
72. John, R.C., Rippon, I.J., Maarten, J.J., Thomas, S., Kapusta, S.D., Girgis, M.M., Whitham, T., *B.F.M. Pots*, Paper 02235, NACE International, Houston, TX, USA, 2002.
73. Battelle Columbus Laboratories and the National Institute of Standards and Technology Economic, *Effects of Metallic Corrosion in the United States*, 1978 and 1995.
74. Schubert, R., *ASME J. Lub. Tech.*, **93**, 216–223 (1971).
75. Bhushan, B., *Introduction to Tribology*, John Wiley & Sons, Inc., NY, pp. 331–420, 2002.
76. Dunn, D.J., Metal Removal Mechanisms Comprising Wear in Mineral Processing, *Wear of Materials*, K.C. Ludema (ed.), American Society of Mechanical Engineers, pp. 501–508, 1985.
77. Lim, S.C., Ashby, M.F., Brunton, J.H., *Acta Metallurgica*, **35**, 1343–1348 (1987b).
78. Lim, S.C., Ashby, M.F., *Acta Metallurgica*, **35**, 1–24 (1987a).

79. Hutchings, I.M., *Tribology: Friction and Wear of Engineering Materials*, CRC Press, Boca Raton, Florida, pp. 171–197, 1992.
80. Gopal, M., Jepson, W.P., Effect of Multiphase Flow on Corrosion, in *Corrosion and Environmental Degradation*, Wiley-VCH, Vol. 1, M. Schütze (ed.), pp. 265–284, 2000.
81. (a) Fischer, T.E., Anderson, M.P., Jahanmir, S., Salher, R., *Wear*, **124**, 133–148 (1988).
    (b) Quinn, T.F.J., Review of Oxidational Wear-Part I and II, *Tribol. Inter.*, **16**, 257–271; 305–315 (1983).
82. Guile, A.E., Juttner, B., Basic Erosion Process of Oxidized and Clean Metal Cathodes by Electric Arcs, *IEEE Trans. Components, Hybrids, Manuf. Technol.*, PS-8, pp. 259–269, 1980.
83. Bhushan, B., Davis, R.E., *Thin Solid Film*, **108**(2), 135–156 (1983).
84. Jones, D.A., *Principles and Prevention of Corrosion*, Prentice-Hall, Upper Saddle River, N.J., USA, 2nd edn, pp. 235–291; 343–356, 1996.
85. Van Dyke, M., *An Album of Fluid Motion*, The Parabolic Press, p. 107, 1982.
86. Douglas, J.F., Gasiorek, J.M., Swaffield, J.A., *Fluid Mechanics*, Pitman, p. 648, 1979.
87. Hurricks, P.L., The Mechanism of Fretting-A Review, *Wear*, **15**, 389–409 (1970).
88. ASM b, in *Friction, Lubrication and Wear Technology*, Vol. 18, P.J. Blau (ed.), ASM International, Ohio, USA, Waterhouse: pp. 242–256; Madsen: pp. 271–279, 1992.
89. Waterhouse, R.B., Fretting Wear, *Proc. Int. Conf. on Wear of Materials*, ASME, NY, pp. 17–22, 1981.
90. Uhlig, H.H., *Corrosion et protection*, Dunod, Paris, France, pp. 98–108, 136–143; CF pp. 148–157, 1970.
91. Almen, J.O., Fretting Corrosion, in *The Corrosion Handbook*, The Electrochemical Society, H.H. Uhlig (ed.), John Wiley & Sons, Inc., NY, pp. 590–597, 1948.
92. Dorlot, J.M., Baïllon, J.P., *Des Matériaux*, 2^{e} édition, École Polytechnique de Montréal, pp. 201–239, 1986.
93. Wranglen, G., *An Introduction to Corrosion and Protection of Metals*, Chapman and Hall, London, England, pp. 118–119, 1984.
94. Wang, Y.Z., Akid, R., Miller, K.J., *Fatigue Fracture Eng. Mater. Structures*, 18, 293, Publ. Blackwell Science Ltd., Oxford, UK, Fig. 1, p. 295, 1995.
95. Magnin, T., Combrade, P., Environment Sensitive Fracture, in *Materials Science and Technology, Corrosion and Environmental Degradation*, Vol. 1, M. Schutze (ed.), Wiley-VCH, pp. 207–263; 216–318, 2000.
96. Bamford, W., *Ins. Mech. Eng. Conf. Publ.*, **4**, 51 (1977).
97. Amzallag, C., Bernard, J.L., Slama, G., On Environmental Degradation of Materials in Nuclear Power Systems – Water Reactors, *Proc. Int. Symp.* Myrtle Beach, South CA, NACE, p. 727, 1984.
98. Atkinson, J., Tice, D., Scott, P.M., in *Proc. 2nd IAEA Specialist's Meeting on Subcritical Crack Growth*, Sendaï, W.H. Cullen (ed.), NUREG/CP-0067, Vol. 1, p. 251, 1985.
99. Combrade, P., Foucault, M., Slama, G., in *Proc. 2nd IAEA Specialist's Meeting on Subcritical Crack Growth*, Sendaï, W.H. Cullen (ed.), NUREG/CP-0067, Vol. 2, p. 201, 1985.
100. Van Der Sluys, W.A., in *Proc. 4th Int. Symp. On Environmental Degradation of Materials in Nuclear Power Systems – Water Reactors*, Traverse City, MI, p. 277, 1988.
101. Young, L.M., Andresen, P.L., in: *Proc. 7th Int. Symp. On Environmental Degradation of Materials in Nuclear Power Systems – Water Reactors*, NACE, Vol. 2, p. 1193, 1995.
102. Wang, Y.Z., Corrosion Fatigue, in *Uhlig Handbook*, R.W. Revie (ed.), pp. 221–232, 2000.
103. Suresh, S., Fatigue of Materials, *Cambridge Solid State Science Series*, Cambridge University Press, Cambridge, UK, pp. 363–368, 1991.
104. Duquette, D.J., Corrosion Fatigue Crack Initiation Processes: A State-of-The-Art Review, in *Environment-Induced Cracking of Metals*, R.P. Gangloff, M.B. Yves (eds.), NACE-10, Houston, TX, p. 45, 1990.
105. McEvily, A.J., Wei, R.P., *Fracture Mechanics and Corrosion Fatigue: Chemistry, Mechanics and Microstructure*, O. Devereux, A.J. McEvily, R.W. Staehle (eds.), NACE, Houston, TX, pp. 381–395, 1973.
106. Amzallag, C., Mayonobe, C., Rabbe, P., in *Electrochemical Corrosion Testing*, ASTM STP 727, F. Mansfeld and U. Bertocci (eds.), ASTM, Philadelphia, USA, p. 69, 1981.
107. Vosikovski, O., *Trans. ASME*, **97**(4), 298 (1975).

108. Duquette, D., Uhlig, H.H., *Trans. Am. Soc. Metals*, **61**, 449 (1968).
109. Westwood, H.J., Lee, W.K., Corrosion-Fatigue Cracking in Fossil-Fueled Boilers, Corrosion Cracking, *Proc. in the International Conf. on Fatigue, Corrosion Cracking, Fracture Mechanics and Failure Analysis*, ASM, Salt Lake City, UT, pp. 23–34, 1986.
110. Mehdizadeh, P., Mcglasson, R.L., Landers, J.E., *Corrosion*, **22**(12), 325–335 (1966).
111. Elboujdaini, M., Shehata, M.T., A Review on the Initiation of Environmentally Assisted Cracking in Line Pipe Steel, *Proceedings of the Egyptian Corrosion Society*, pp. 1–13, December 2004.
112. Elboujdaini, M., Shehata, M.T., Ghali, E., Stress Corrosion Cracking and Corrosion Fatigue of 5083 and 6061 Aluminum Alloys, *Microstructural Science*, D.E. Alman, J.A. Hawk, J.W. Simmons (eds.), IMS and ASM International, Ohio, USA, Vol. 25, pp. 41–49, 1997.
113. Shipilov, S.A., *Technology, Law & Insurance*, **1**(3), 131–142 (1996a).
114. Shipilov, S.A., Fundamentals of Physico-Chemical Mechanics of Fracture: Purposes and Contents of the New Education Course, *Teaching and Education in Fracture and Fatigue*, H.P. Rossmanith (ed.), E & FN Spon, London, pp. 293–299, 1996b.
115. Reed, R.P., Smith, J.H., Christ, B.W., *The Economic Effects of Fracture in the United States: Final Report*, NBS Special Publication, pp. 647–1; 19, 1983.
116. Faria, L., *The Economic Effects of Fracture in Europe: Final Report*, Study Contract No. 320105, Commission of the European Communities, pp. 1–57, 1991.
117. Shipilov, S.A., Catastrophic Failures Due to Environment-Assisted Cracking of Metals: Case Histories, in *Proceedings of the International Symposium on Environmental Degradation of Materials and Corrosion Control in Metals*, M. Elboujdaini, E. Ghali (eds.), The Conference of Metallurgists, COM, METSOC, pp. 225–242, 1999.
118. Speidel, M.O., Stress Corrosion Cracking and Corrosion Fatigue - Fracture Mechanics, in *Corrosion in Power Generating Equipment*, M.O. Speidel, A. Atrens (eds.), Plenum Press, NY, pp. 85–132, 1984.
119. Peterson, M.H., Brown, B.F., Newbegin, R.L., Groover, R.E., *Corrosion*, **23**(5), 142–148 (1967).
120. Van Leeuwen, H.P., *Engineering Fracture Mechanical*, **6**, 141 (1974).
121. Mazille, E.H., Uhlig, H.H., *Corrosion*, **28**, 427 (1972).
122. Turnbull, A., Progress in the Understanding of the Electrochemistry in Cracks, in *Embrittlement By the Local Crack Environment*, R.P. Gangloff (ed.), The Metallurgical Society, p. 3, 1984.
123. Danielson, M.J., Oster, C., Jones, R.H., *Journal of Corrosion Science*, **32**(1), 1 (1991).
124. Parkins, R.N., Prevention of Environment Sensitive Fracture by Inhibition, in *Embrittlement by the Local Crack Environment*, R.P. Gangloff (ed.), The Metallurgical Society, p. 385, 1984.
125. Vosikovsky, O., *Journal of Engineering Materials and Technology*, **97H**(4), 298–304 (1975).
126. Tsai, W.T., MoccariI, A., Szklarska-Smialovska, Z., Macdonald, D.D., *Corrosion*, **40**(11), 573–583 (1984).
127. McHenry, I., Read, D.T., Shives, T.R., *Mater. Perform.*, **26**, 18 (1987).
128. Birnbaum, H.K., *Environment Sensitive Fracture of Engineering Materials*, Z.A. Foroulis (ed.), American Institute of Mining, Metallurgical, and Petroleum Engineers, Warrendale, PA, pp. 326–357, 1979.
129. Taira, T., Kobayachi, Y., Seki, N., Tsukada, K., Tanimura, M., Inagaki, H., *Technol. Rep. NKK (Nipon Kokan)* (67), 421 (1980).
130. NACE Standard MR175-90, *Standard Materials Requirements-Sulfide Stress Cracking Resistant Metallic Materials for Oilfield Equipment*, NACE International, Houston, TX, 1990.
131. Kane, R.D., Greer, J.B., *Journal of Petrochemical Technology*, 1483 (1977).
132. Gutzeit, J., *Mat. Perform.*, **29**, 54 (1990).
133. Buchheim, G.M., *Oil and Gas Journal*, 92 (1990).
134. Parades, F., Mize, W.W., *Oil Gas Journal*, **52**, 99 (1954).
135. Elboujdaini, M., *Hydrogen Induced Cracking and Sulfide Stress Cracking*, CANMET Materials Technology Laboratory, Ottawa, Canada, pp. 1–13, 2005.
136. Elboujdaini, M., Shehata, M.T., Revie, W., Ramsingh, R.R., *Corrosion 98*, Proceedings of the 53rd annual conference at San Diego California, National Association of Corrosion Engineers, ed., Houston, Texas, Paper No. 748, 1998.
137. Bartz, M.H., Rawlings, C.E., *Corrosion*, **4**, 187 (1948).

138. Moore, E.M., McIntyre, D.R., *Materials Performance*, **37**, 77 (1998).
139. Merrick, R.D., *Corrosion 87*, Proceedings of the annual conference at San Francisco California, National Association of Corrosion Engineers, ed., Houston, Texas, Paper No. 190, 1987.
140. Merrick, R.D., Bullen, M.L., *Corrosion 89*, Proceedings of the annual conference at New Orleans Louisiane, National Association of Corrosion Engineers, ed., Houston, Texas, Paper No. 269, 1989.
141. Lynch, S.P., Trevena, P., *Corrosion*, **44**(2), 113–124 (1988).
142. Ford, F.P., in *Corrosion Processes*, R.N. Parkins (ed.), London: Applied Science, p. 271, 1982.
143. Pessall, N., *Corrosion Science*, **20**, 225 (1980).
144. Le, H.H., Ghali, E., *Applied Electrochemistry*, **19**, 368–376 (1989).
145. Cragnolino, G., Lin, L.F., Szlarska-Smialowska, Z., *Corrosion*, **37**(6), 312–320 (1981).
146. Parkins, R.N., *An Overview- Prevention and Control of Stress Corrosion Cracking, Materials Performance*, **24**, 9–20 (1995).
147. Latanision, R.M., *Metallurgical Transactions, Scientific and Technical Book Service*, Vol. 5, p. 483, 1974.
148. Szlarska-Smialowska, Z., Gust, J., *Corrosion Science*, **19**, 753 (1979).
149. Szklarska-Smialowska, Z., *Hydrogen Embrittlement and Stress Corrosion Cracking*, R. Gibala, R.F. Hehemann (eds.), ASM International, pp. 99; 207–230, 1995.
150. Bhatt, H.J., Phelps, E.H., *Corrosion*, **17**, 430t–434t (1961).
151. Magnin, T., Chieragatti, R., Oltra, R., *Acta Metallurgica*, **38**, 1313 (1990).
152. Magnin, T., Chambreuil, A., Bayle, B., *Acta Metallurgica*, **44**(4), 1457 (1996).
153. Revie, R.H., Uhlig, H.H., *Acta Metallurgica*, **22**, 619 (1974).
154. Forty, A.J., Humble, P., *Philos. Mag.*, **8**, 247 (1963).
155. Beavers, J.A., Rosenberg, I.C., Pugh, E.N., in *Proceedings of the 1972 Tri-Service Conference on Corrosion*, MCIC-73-19, Metals and Ceramics Information Center, p. 57, 1972.
156. Uhlig, H.H., *Physical Metallurgy of Stress Corrosion Fracture*, T.N. Rhodin (ed.), Interscience, p. 1, 1959.
157. Scully, J.C., in *SCC of Magnesium*, L.L. Shreir, R.A. Jarman, G.T. Burstein (eds.), 3rd edn, Butterworth Heinemann, pp. 8; 127–129, 1994.
158. Pérez, T.E., Quintanilla, H., Rey, E., *Corrosion 98*, Proceedings of the annual conference at San Diego California, National Association of Corrosion Engineers, ed., Houston, Texas, Paper No. 121, 1998.
159. Kane, R.D., Cayard, M.S., Roles of H_2 and H_2S in Behaviour of Engineering Alloys in Petroleum Applications, *Proceedings Materials for Resource Recovery and Transport*, L. Collins (ed.), The Metallurgical Society of CIM, Calgary, pp. 3–49, August 1998.
160. Moore, E.M., Warga, J.J., *Materials Performance*, **15**, 17 (1976).
161. Schuyler, R.L., *Materials Performance*, **18**, 9 (1979).
162. Miyoshi, E., Tanaka, T., Terazaki, F., Ikeda, A., *J. Eng. Ind.*, **98**, 221 (1976).
163. Taira, T., *Wet H_2S Cracking of Carbon Steels and Weldments*, R.D. Kane, R.J. Horvarth, M.C. Cayard (eds.), NACE International, pp. 471–478, 1996.
164. Perumareddi, J.R., Elboujdaini, M., Sastri, V.S., Inhibition of Hydrogen Entry Into Steel, *Proceedings Materials for Resource Recovery and Transport*, L. Collins (ed.), The Metallurgical Society of CIM, Calgary, Canada, pp. 117–187, August 1998.
165. Miyasaka, A., Yamaguchi, Y., Miyagawa, T., Nakamura, A., *Corrosion 94*, Proceedings of the annual conference at Baltimore Maryland, National Association of Corrosion Engineers, ed., Houston, Texas, Paper No. 83, 1994.
166. Masamura, K., Takeuchi, Y., Tamaki, K., Miyagawa, T., Nakamura, A., *Corrosion 94*, Proceedings of the annual conference at Baltimore Maryland, ed., Houston, Texas, Paper No. 84, 1994.
167. Tamaki, K., Nakamura, A., Miyagawa, T., Ogasawara, M., *Corrosion 94*, Proceedings of the annual conference at Baltimore Maryland, National Association of Corrosion Engineers, ed., Houston, Texas, Paper No. 85, 1994.
168. Lifka, B.W., Aluminum (and Alloys), *Corrosion Testing and Standards*, R. Baboian (ed.), ASTM, West Conshohocken, PA, pp. 447–457, 1995.

169. Hillis, J.E., Magnesium, in *Corrosion Testing and Standards: Application and Interpretation*, R. Baboian (ed.), ASTM, Philadelphia, PA, USA, pp. 438–446, 1995.
170. Parkins, R.N., Suzuki, Y., *Corrosion Science*, **23**, 577 (1983).
171. Ebtehaj, K., Hardie, D., Parkins, R.N., *Corrosion Science*, **28**(8), 811–829 (1988).
172. Dietzel, W., Schwalbe, K.H., *Monitoring Stable Crack Growth Using a Combined AC/DC Potential Drop Technique*, *Material Prufing*, Band 28, pp. 368–372, 1986.
173. Coburn, S.K., *Corrosion Source Book*, ASM, Metals Park, Ohio NACE International, pp. 95–101, pp. 99, 100, 1984.
174. Landrum, R.J., *Fundamentals of Designing for Corrosion Control- A Corrosion Aid for the Designer*, NACE International, Houston, TX, pp. 49–67; 51, 1989.
175. Gilbert, P.T., Copper and Copper Alloys, *Corrosion*, L.L. Shreir, pp. 4:33–67, 1976.
176. Hay, M., COM', Shell Canada, *Short Courses at the 42nd Annual Conference of Metallurgists of CIM*, August 24–27, Vancouver, B.C., Canada, 2003.

Bibliography

ASM, 1990, *Atlas of Stress-Corrosion Cracking and corrosion fatigue curves*, A.J. McEvily (ed.), ASM International, Ohio, USA.
ASM, 1995, *Handbook of Corrosion DATA*, B.D. Craig, D.S. Anderson (eds.), 2nd edn, ASM International, Ohio, USA.
Climax Molybdenum Company, a division of American Metal Climax, Inc., A guide to corrosion resistance 304, 316, 317, 20 and NI-O-NEL, N.Y., U.S.A., 1961.
Corrosion and environmental degradation, VCH Germany, Vols. 1 and 2, M. Shutze (ed.), Wiley, VCH, Weinheim, Germany, 2000.
Corrosion mechanisms in theory and practice, P. Marcus and J. Oudar (eds.), Marcel Dekker, Inc., New York, 1995.
Corrosion Resistant Materials Handbook, De Renzo (ed.), 4th edn, Noyes Data Corporation, N.J., U.S.A., 1985.
Corrosion, Metal/environment reactions, 3rd edn, Vols. 1 and 2, L.L. Shreir, R.A. Jarman and G.T. Burstein, Butterworth Heinemann, London, 1995.
Evans, U.R., *The Corrosion and Oxidation of Metals*, Edward Arnold LTD., London, 1960.
Fontana, M.G. and Greene, N.D., *Corrosion Engineering*, McGraw-Hill Book Co., N.Y., U.S.A., 1978.
Landrum, R.J., *Fundamentals of Designing for Corrosion Control*, NACE International, Houston, Texas, U.S.A., 1989.
Metals Handbook, Vols. 13A and 13B, *Corrosion: Fundamentals, Testing, and Protection*, and *Corrosion: Materials*, S.D. Cramer and B.S. Covino (eds.), ASM International, Metals Park, Ohio, U.S.A., 2003.
McNaughton, K.J., *Materials Engineering 1, Selecting Materials For Process Equipment*, Chemical Engineering Magazine, McGraw-Hill Publications Co., NY, USA, 1980.
NACE, *Corrosion Data Survey*, 6th edn, D.L. Graver (ed.), TX, USA, 1985.
National Association of Corrosion Engineers, *Corrosion Testing made easy* series, Houston, Texas, U.S.A., 1985.
Pourbaix, M., *Atlas of electrochemical equilibrium in aqueous solutions*, NACE International, CEBELCOR, Houston, Texas, USA, 1974.
Piron, D.L., Corrosion failures of metals in *The electrochemistry of corrosion*, 1991.
Roberge, P.R., *Handbook of Corrosion Engineering*, Mc-Graw-Hill, N.Y., U.S.A., 1999.
Sastri, V.S., *Corrosion inhibitors, Principles and applications*, John Wiley, London, 1998.
Schweitzer, A.S., *Corrosion Resistant tables, metals, plastics, nonmetallics, and rubbers*, 2nd edn, Marcel Dekker, 1986.
Uhlig, H.H. and Revie, R.W., *Corrosion and Corrosion Control*, 3rd edn, John Wiley & Sons, Inc., NY, 1985.
Uhlig's Corrosion Handbook, 2nd edn, R.W. Revie (ed.), John Wiley & Sons, Inc., NY, U.S.A., 2000.

7

Practical Solutions

7.1 Cathodic Protection of Water Mains

Two examples of cathodic protection are discussed: protection of a ductile iron main; protection of a cast-iron-lined main.

7.1.1 Ductile Iron Main

In this example, the valve, buried in 1995, was in soil area of approximate resistivity 800–900 Ω cm, thus providing active conditions. The 8-inch valve was epoxy-coated with an anode (zinc) attached to the top body by an exothermic weld. This type of valve is a two-part casting and is fabricated with a sealing ring and 5/8-inch diameter bolts around the flange. The larger bolts create a continuous electrical circuit. This valve failed as a result of a combination of ½-inch diameter bolts holding the top body instead of 5/8-inch bolts and corrosion affecting the undersized ½-inch bolts until they failed. The corrosion took place on the lower section of the valve. As the valve was epoxy-coated, the corrosion occurred mainly on the 12-inch coupling bolts and on the undersized ½-inch bolts that held the valve together. These bolts were carbon steel and not coated. The undersized ½-inch bolts did not provide electrical continuity between the top body and the valve as with the larger bolts, resulting on the lower part of the valve being unprotected (Figure 7.1).

In the valve system, bolts are generally the first to be affected by corrosion. In chambers, it is sometimes very clear as to the cause of the corrosion, and in the early stages corrective action can be taken. These chambers are generally filled with water and soil that run into the chambers from the road runoff. In addition water from the ditches and along the water main enters in openings where the main enters the manhole. Leaks can be reduced, but with the loading of traffic and shifting of the chamber in the frost

Corrosion Prevention and Protection: Practical Solutions V. S. Sastri, E. Ghali and M. Elboujdaini

Figure 7.1 *12-inch bolt from coupling. (Reprinted with permission of Dave Raymond, City of Ottawa, Public Works and Services)*

cycles, it becomes very difficult to completely eliminate the inflow of water. Chambers in these areas are found with bolt heads completely corroded. Bolts are also found with the stem reduced to pencil lead thickness. Rungs of aluminum ladders for access to these chambers have completely disappeared. These are some of the problems encountered during rehabilitation of these valve chambers that, in some cases, were installed in the mid 1980s.

Corrective action consists of replacing mild steel bolts with 304 stainless steel bolts. The bolts were coated with a wax-based primer to reduce the corrosion of the bolts in flooded chambers.

In the chambers crevice corrosion and galvanic corrosion along with general corrosion of the aluminum ladder were observed (Figure 7.2). Crevice corrosion was also observed on couplings and bolts with valves. The aluminum steps in some valve chambers were attacked by chlorides/phosphates.

7.1.2 Cast-iron-lined Main

A chamber in service for a 10-yr period in which rebuilt valves were present was found to be saturated with chlorides and phosphates. The chloride caused the corrosion of bolts to such an extent that the chamber was leaking. The chamber housed 24-inch and 16-inch valves along with air drain-out. All the bolts on the valves required replacement. Furthermore, the aluminum ladder rungs were completely corroded.

The corrosion prevention strategy consisted of wrapping the valve with wax tape, along with use of magnesium anodes. The chamber was thoroughly cleaned and valves wrapped in wax tape, as shown in Figure 7.3. Since the chamber was entered for limited number of times the corroded ladder was left intact and enter with the restraining device and/or portable ladder.

Figure 7.2 *Aluminum ladder rungs. (Reprinted with permission of Dave Raymond, City of Ottawa, Public Works and Services)*

The use of wax taping and magnesium anodes resulted in very little corrosion, requiring only normal operating maintenance and inspection of the chamber for valve integrity.

Corrosion of bolts in areas other than valves was observed, as shown in Figures 7.4 and 7.5. The economics of cathodic protection compared with replacement of the water main are illustrated in Table 7.1.

Figure 7.3 *Tape-wrapped air valve. (Reprinted with permission of Dave Raymond, City of Ottawa, Public Works and Services)*

Figure 7.4 *4 inch T-bolt from 8-inch valve. (Reprinted with permission of Dave Raymond, City of Ottawa, Public Works and Services)*

Figure 7.5 *Hydrant bolt from base flange. (Reprinted with permission of Dave Raymond, City of Ottawa, Public Works and Services)*

Table 7.1 *Cost of replacement and of cathodic protection, showing savings obtainable*

1 Km	Replacement ($)	Cathodic protection ($)	Savings ($)	% cost
6-inch water main	$800,000.00	$20 000.00 × 3 cycles	$740 000.00	7.5
12-inch water main	$1100 000.00	$37 500.00 × 3 cycles	$987 500.00	10.25

Bibliography

ASTM B 843, Type M1-C for chemical composition
ASTM G 97, Standard Current Efficiency Test for Magnesium
RPO169-96, *NACE Book of Standards*, Standard Recommended Practices
J.T.N. Atkinson and H. Van Droffelaar, *Corrosion and Its Control, An introduction to the Subject*, 2nd Edition, NACE International Houston, 1995, pp. 270, 280, 281.

7.2 Internal Corrosion of Aluminum Compressed Air Cylinders

Aluminum compressed air cylinder safety has been an important issue in recent years. Safety procedures regarding the use, care and maintenance of compressed air cylinders have been in placed to ensure the public safety. Many attentions have been paid especially so-called sustained-load cracking (SLC) failures. SLC is a metallurgical anomaly that occasionally develops in high-pressure cylinders made generally from aluminum alloys.

The objective of investigation is to clarify the mechanisms of corrosion-induced pitting and cracking of the aluminum compressed air cylinder for the purpose of determining key factors.

7.2.1 Destructive Visual Inspection

The aluminum cylinder was made of 6161 aluminum alloy in 1989. It was taken out of service after 5 yr because it failed a safety test due to high moisture content (>200 ppm). An optical probe inspection (with mirror and a light source) revealed internal corrosion. Figure 7.6 is a photo of the aluminum cylinder before it was opened.

The cylinder was cut open (Figure 7.7). The internal surface of cylinder was completely corroded. A corrosion pattern that appeared to be caused by condensation was observed.

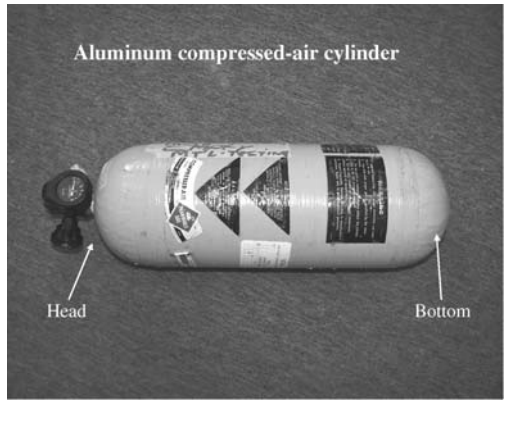

Figure 7.6 *Out-of-service compressed air cylinder. (Copyright of Her Majesty the Queen in Right of Canada, as represented by the Minister of Natural Resources, 2004, 2006)*

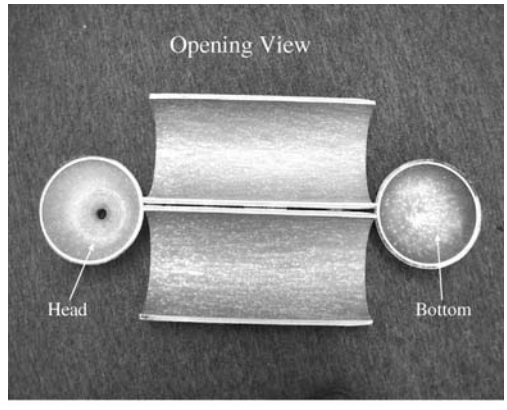

Figure 7.7 *Overall view of internal surface. (Copyright of Her Majesty the Queen in Right of Canada, as represented by the Minister of Natural Resources, 2004, 2006)*

Figure 7.8 is a view of the bottom of the cylinder. It appears that corrosion pattern is uniformly distributed inside the cylinder. Figure 7.9 is a close-up of the corrosion surface. The white spots appear to be corrosion pits.

7.2.2 Corrosion-induced Cracking

In the visual inspection, the white spot is some kind of corrosion pit. A cross-section sample was subjected to SEM investigation. The pitting corrosion is more like corrosion-induced cracking. As shown in Figure 7.10, the pitting grows intergranularly, e.g., the pit deepens along the boundary of the aluminum grains. Figure 7.11 provides a closer look at the corrosion and cracking pattern.

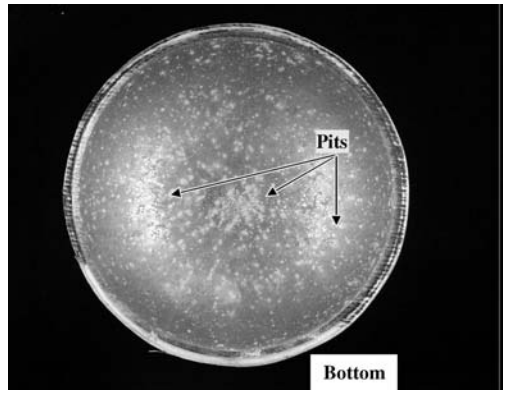

Figure 7.8 *Close-up of the internal surface of the bottom of the cylinder. (Copyright of Her Majesty the Queen in Right of Canada, as represented by the Minister of Natural Resources, 2004, 2006)*

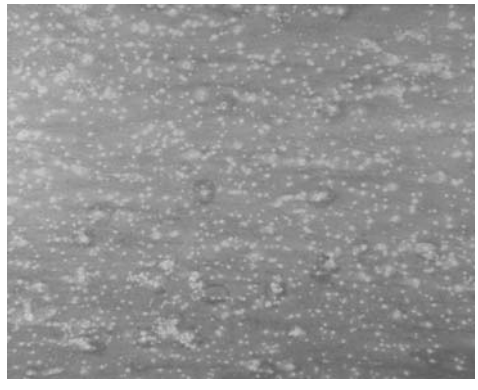

Figure 7.9 *Close-up of the internal surface of the opened cylinder. (Copyright of Her Majesty the Queen in Right of Canada, as represented by the Minister of Natural Resources, 2004, 2006)*

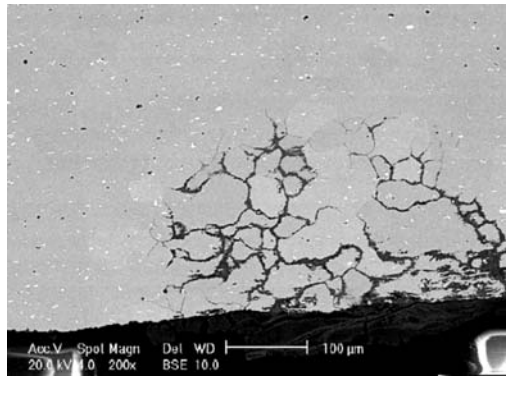

Figure 7.10 *SEM photo of the cross-section of a corrosion 'pit'. The intergranular cracks shown penetrate about 12% of the cylinder wall thickness (~2.72 mm thick). (Copyright of Her Majesty the Queen in Right of Canada, as represented by the Minister of Natural Resources, 2004, 2006)*

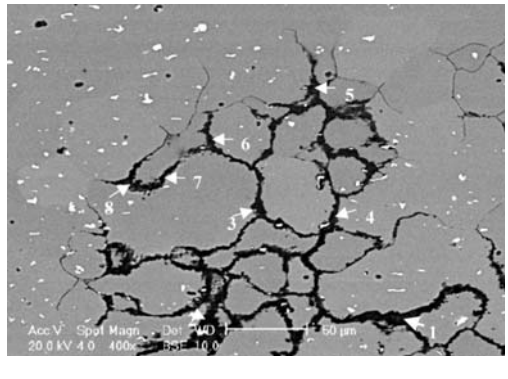

Figure 7.11 *SEM photo of an enlarged cross-section of a corrosion 'pit'*

Table 7.2 *O/Al ratios determined at various locations in the cracks*

Location	O (atom %)	Al (atom %)	O/Al ratio
1	57.9	42.1	1.375
2	59.2	40.8	1.45
3	66.4	33.6	1.97
4	65.1	34.9	1.865
5	66.9	33.1	2.021
6	68	32	2.125
7	59.9	40.1	1.494
8	63.6	36.4	1.747

Oxygen/aluminum ratios were also determined at various locations in the cracks as indicated in Figure 7.11 and results are given in Table 7.2. The oxygen/aluminum ratio increases from ~1.5 to 2.0 as the crack location moves towards the crack tip. The ratios of 1.5 and 2.0 likely represent Al_2O_3 and AlO_2^-, respectively. This observation tends to indicate that corrosion induced cracking took place.

7.2.3 Corrosion Mechanism

High-purity aluminum has excellent corrosion resistance. Information collected over the years from manufacturers and users has shown that aluminum structures will provide reliable service for periods in excess of 30 yr. The factor that assures the long life of aluminum is a self-forming microscopically thin surface layer of aluminum oxide. The air-formed film on new aluminum surfaces is about 2.5 nm thick, while the film on aluminum that is several years old may be 10 nm thick or more. The film is composed of two parts:

- a thin, inner barrier layer;
- a much thicker bulk outer layer, which is more permeable than the inner barrier layer.

Chemically, the film is a hydrated form of aluminum oxide. The corrosion resistance of aluminum depends upon this protective oxide film, which is stable in aqueous media when the pH is between about 4.0 and 8.5. The oxide film is naturally self-renewing and accidental abrasion or other mechanical damage of the surface film is rapidly repaired. The conditions that promote corrosion of aluminum and its alloys, therefore, must be those that continuously abrade the film mechanically or promote conditions that locally degrade the protective oxide film and minimize the availability of oxygen to rebuild it. The acidity or alkalinity of the environment significantly affects the corrosion behavior of aluminum alloys. At lower and higher pH, aluminum is more likely to corrode.

In the case of compressed air cylinder corrosion, there are additional factors that should be taken into account:

- sustained pressure (normally at 2200 psi);
- moisture content and condensation;
- carbon dioxide content.

The fact that the aluminum cylinder is constantly under pressure is believed to be a contributing factor for stress corrosion. The moisture content is very critical since condensation occurs when pressure changes rapidly. Therefore, moisture content and slow refilling procedure are strictly regulated. Carbon dioxide content is also critical since it increases its dissolubility as pressure increases. As a result, it could bring the pH value of condensed water below the level where aluminum oxide is no longer stable.

7.2.4 Summary

The internal surface of the cylinder has been entirely covered by white spots appear to be corrosion pits.

All cross-sections of a corrosion pit exhibits intergranular corrosion caused by selective attack of grain boundaries.

The metallographic cross-section of a pit area shows that penetration is about 10–15% of the cylinder wall thickness.

The aluminum cylinder is constantly under pressure and this is believed to be a contributing factor for stress corrosion cracking (SCC).

The moisture content is very critical since condensation occurs when pressure changes rapidly. Carbon dioxide content is also critical since it increases its dissolubility as pressure increases.

If the oxide film of aluminum is broken by chemical action, and in the presence of moisture, corrosion proceeds rapidly. The effect can be severe when stress (pressure) is present.

Bibliography

J. Steinbachs, Protective gear fails firefighters, *Ottawa Sun*, 28 April 2003.
H. Lake, Firefighter fix cost $400 000, *Ottawa Sun*, 28 April 2003.
C. Barriere, Respirateurs contamines, *Le Droit*, 29 April 2003.
W.L. High, 6351 Alloy tanks go bust – Analysis of cracking and rupture of SCBA and SCUBA aluminum cylinders, http://www.cdnn.info/article/high/high.html
B. High, Cracking and ruptures of SCBA and SCUBA aluminum cylinders, http://www.psicylinders.com/library/cracking.htm

7.3 Some Common Failure Modes in Aircraft Structures

It is a well-known fact that failure of an aircraft component can have catastrophic consequences such as loss of precious life and aircraft. It is obvious from Table 7.3 that failures due to fatigue are predominant in aircraft components. When the component is no longer able to withstand the imposed stress, failure will occur. Thus failures are associated with stress concentrations which can occur due to:

(i) design defects presence of holes, notches, tight fillet radii;
(ii) presence of voids, inclusions in microstructure;
(iii) corrosion such as pitting can cause a local stress concentration.

Table 7.3 *Failure mode (in 2002)*[1]

	Failures (%)	
	Engineering components	Aircraft components
Corrosion	29	16
Fatigue	25	55
Overload	11	14
High temp. corrosion	7	2
SCC/Corrosion Fatigue/Hydrogen Embrittlement	6	7
Wear/abrasion/erosion	3	6
Brittle Fracture	16	
Creep	3	

7.3.1 Example 1

A nose undercarriage turning tube failed on landing after only 1300 flight cycles, well below the expected service life. Scanning electron microscopy (SEM) examination of the sample tube showed the fracture surface to have ductile appearance consistent with a ductile overload. Figure 7.12 shows fatigue striations indicating the fracture mode to be fatigue resulting in a fast fracture (overload) upon reaching a critical crack length. The striations on the fracture surface consisted of distinct bands of repetitive units of striation spacing as seen in the figure. Measurement of striation spacing and band spacing at various points along the crack from the origin to the end enabled the determination of the crack growth rate graphically. Since the striations and bands are related to load cycles, a comparison of the load cycles with the anticipated load spectrum makes it possible to determine the load cycles required to propagate the fatigue crack to the point of failure. The number of cycles that caused the failure was in the range that the component was in service which indicated that the fatigue crack initiated very close to the beginning of the component's service life.

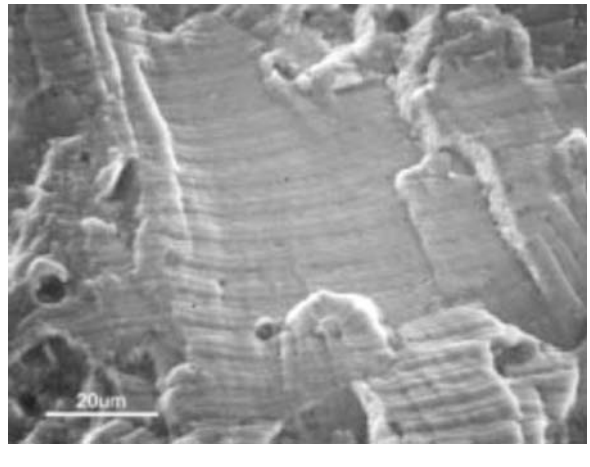

Figure 7.12 *Fatigue striations observed on the fracture surface*

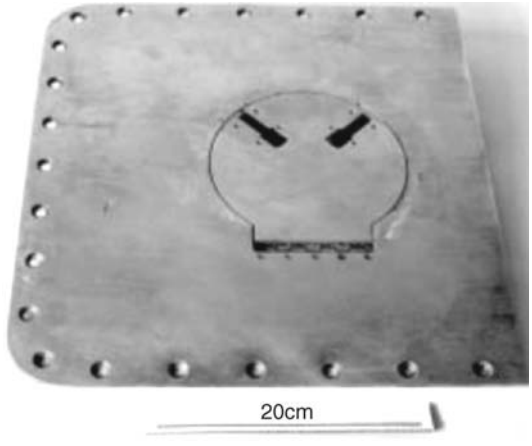

Figure 7.13 *Outer surface of wing panel and door after paint stripping and removal of catches*[1]

The origin of the crack was located at a notch on the surface of the tube. In all likelihood the notch produced the required stress concentration in the surface of the tube, thereby reducing the initiation time of the crack. In all probability the notch in the surface of the tube occurred during manufacture.

7.3.2 Example 2

During service inspection corrosion of an upper surface wing panel containing an access door was observed. The panel and door were made from an alloy plate to which aluminum catches were attached for securing the door in the closed position. Stainless shims were fitted between the catches and the aluminum plate.

The outer surface of the panel and door after stripping point and removing the catches is shown in Figure 7.13. There appears to be no damage to the plate and the door. The examination of the inner surface showed extensive exfoliation corrosion on the panel and the door in the catch positions (Figure 7.14). Cracking originating from the catch position

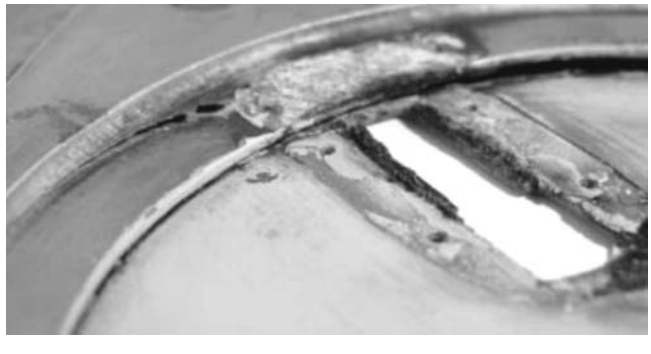

Figure 7.14 *Exfoliation corrosion on the inner surface of the panel and door around a catch location*[1]

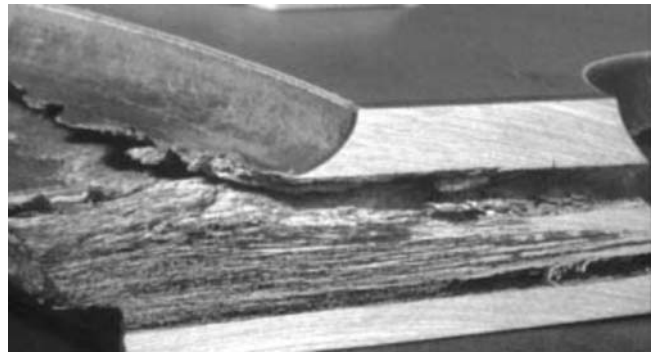

Figure 7.15 *Cross-section through the panel, showing the exfoliation corrosion*[1]

was observed in the stiffening ribs. A cross-section of plate containing extensively corroded area is shown in Figure 7.15.

Exfoliation corrosion occurs when the attack occurs along grain boundaries, particularly when they are elongated and form thin platelets. The voluminous corrosion product causes splitting of layers uncorroded material.

The material conformed to the specification and the aluminum alloy is known to be subject to exfoliation corrosion. The corrosion was extensive at the catch positions and attributed to the stainless steel shims fitted below the catches. The paint between aluminum and stainless steel shims deteriorated, resulting in galvanic corrosion with the stainless steel acting as the noble metal.

7.3.3 Example 3

A bolt from an aircraft flap control unit fractured in the threaded region of the shank near the shoulder with the head upon installation after a major service. The bolt was made from cadmium-plated high-strength steel. The bolt conformed to the specifications and had ultimate tensile strength of $\sim$1400 MPa.

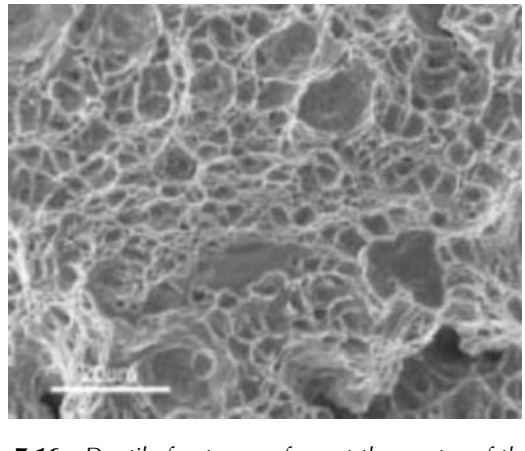

Figure 7.16 *Ductile fracture surface at the center of the bolt*[1]

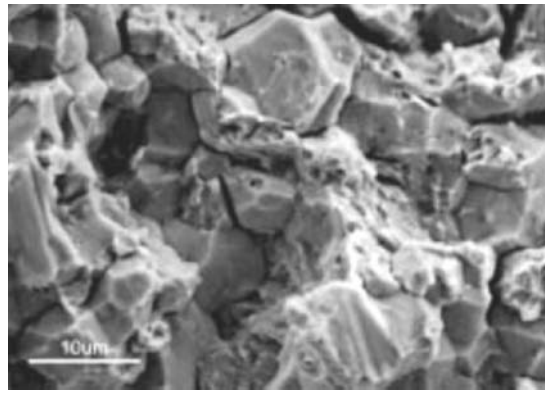

Figure 7.17 *Intergranular region of the fracture surface around the outer circumference of the bolt*[1]

SEM examination showed ductile features (Figure 7.16) on the center of the bolt and intergranular features on the outer circumference (Figure 7.17) both modes of cracking were caused by static overload failure with the ductile features at the center present throughout. The intergranular appearance around the edge is suggestive of embrittlement leading to premature failure at loads below those expected.

The embrittlement is attributed to cadmium plating on the bolts applied to protect them from corrosion. During plating with cadmium hydrogen is absorbed by steel and cadmium acts as a barrier for the escape of hydrogen. In high-strength steels ($>$1100 MPa) hydrogen embrittlement (HE) occurs, but can be minimized by baking at 175°C for 24 h or by treatment with 1:1:1 mixture of nitric, acetic and phosphoric acids.

Reference

1. S.J. Findlay and N.D. Harrison – "**Why aircraft fail**", Materialstoday, November 2002, pp. 18–25.

7.4 Premature Failure of Tie Rods of a Suspension Bridge

Tie rods of a newly built suspension bridge in service for only six winter months at temperatures of -20°C failed due to the cleavage and lack of low-temperature toughness of the steel. Fatigue crack propagation due to cyclic and uneven loading was also a contributing factor. The use of steels of higher toughness with intrinsic weathering resistance has been advanced as a remedial measure.

The bridge is 150 m in length with three sections. The middle section is 70 m in length sandwiched between four columns that support tie rods. The other two sections are 40 m in length. There are 32 tie bars which are 90 mm in diameter. The bars attached to several columns, 4 overhead columns that rise above and 8 columns that drop below to the base of the bridge. Figure 7.18 shows a view of the column with a missing tie rode. Figure 7.19 shows a close-up view of the exposed tie rods and corrosion of the threaded

Figure 7.18 *General view of the bridge*[1]

portions is evident. Figure 7.20 is another view of the tie rods and corroded threads are obvious. Figure 7.21 shows the fractured surface of the failed tie rod.

Metallographic examination showed that the cracks initiated at the first thread, immediately adjacent to the nut. Beach marks were present which indicate the presence of fatigue. The final area of the fracture showed the presence of shiny granular appearance, indicating a sudden brittle (cleavage) fracture and this is also confirmed by the SEM photographs showing cleavage steps and river pattern.

Fractured tie rods were sectioned and examined with an optical microscope and no evidence was found for microcracks at the root of the threaded notch and along the fracture path.

Figure 7.19 *Close-up view of the exposed tie rods; corrosion of the unpainted exposed areas may be noted*[1]

Figure 7.20 *Close-up view of the upright column with a missing tie rod*[1]

Figure 7.21 *Close-up view of tie rods showing corroded threads, nuts and washer*[1]

7.4.1 Conclusions

1. The presence of beach marks shows that fatigue is a major factor in the failure. Relatively small areas of crack propagation zone indicate short service life.
2. Steel 350 W is unable to withstand −20°C temperature.
3. Fatigue cracks initiated next to nut on the washer side due to stress concentration when the nut is tightened.
4. Lack of microcracks shows the absence of machining defects.
5. Use of steels (350 WT, 350 AT, A710) is recommended.

Reference

1. Edward Ghali and Madhavarao Krishnadev,"Physical and mechanical metallurgy of premature failure of tie rods of a cable stayed bridge", Engineering failure analysis, Volume 13, Issue 1, January 2006, pages 117–126.

7.5 Corrosion and Lead Leaching of Domestic Hot and Cold Water Loops in a Building

7.5.1 Hot Water System Corrosion

A schematic diagram of the domestic hot water system is given in Figure 7.22. During the visual inspection, the following observations were made:

(i) Different metals such as copper, galvanized steel and cast iron pipes, and brass joints, etc., are used in the hot water distribution line.
(ii) A noticeable temperature difference is observed in the heat exchanger loop where the water in the hot water tank is circulated to a heater. No mechanical pump is used in this loop, the water flow is by convection. Slow water circulation results in a larger temperature difference between the upper and lower pipe sections. A temperature difference is also seen in the heat circulation loop where circulated hot water is mixed with incoming cold water. Severe corrosion was observed in these areas.
(iii) In some sections of the pipe, a large copper pipe area in contact with a relatively small area of galvanized iron and steel pipe was observed.

Water samples taken from various locations (denoted in the *National Printing Bureau Domestic* Water Systems Preliminary Investigation Report),[1] indicated the high iron content in samples taken from locations where the cold and hot water are mixed, e.g., the heat exchange loop and hot water recirculation pump (Figure 7.22).

Visual inspection and the results of metal ion content in water samples, shows internal pipe corrosion in various locations in the hot water distribution system that compromises the quality of hot water. The cause of the internal pipe corrosion can be attributed to the following factors or a combination of the factors.

Galvanic Cell Formation. When dissimilar metals are in contact and with the presence of electrolyte, a so-called galvanic cell will be established due to the electrochemical potential difference.[2] The result of the galvanic cell is corrosion of the metal that is less noble. For instance, when copper is in contact with iron in the presence of electrolyte

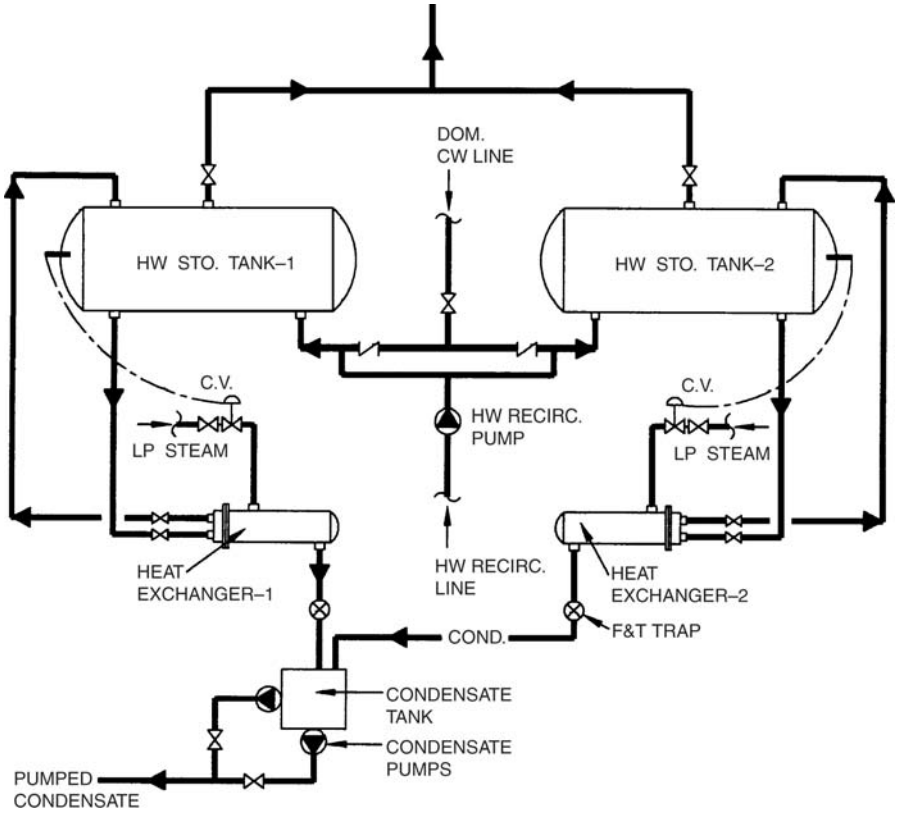

Figure 7.22 *Schematic of the hot water system*

(water); iron (the anode) will corrode to generate Fe^{2+} ions, which further react with oxygen to form iron oxide, a brown product, while oxygen reduction reaction takes place on the copper (the cathode). The reactions are as follows.

Anodic reaction:

$$Fe - 2e^- = Fe^{2+}$$

$$Fe^{2+} + 2H_2O = Fe(OH)_2 + 2H^+$$

$$2Fe(OH)_2 + \frac{1}{2}O_2 = Fe_2O_3 + 2H_2O$$

Cathodic reaction:

$$\frac{1}{2}O_2 + H_2O + 2e^- = 2OH^-$$

It should be noted that there is a reduction of pH in the anode area, which further accelerates the iron dissolution (corrosion).

Temperature Difference. The severe corrosion that takes place in the heat exchange and heat circulation pump locations is explained by the temperature effect. Thermodynamically, a potential difference can result in a temperature difference, even within the same

material. For example, if there is a pipe with hot water at one end and with cold water at the other end, such a temperature difference can result in a potential difference. A simple estimation of 60°C difference could contribute to >20 mV electrochemical potential difference, which may be enough to accelerate iron pipe corrosion in the area of lower temperature. As there is no mechanical pumping in the heat exchange system, the circulation of water depends solely on convection, which creates a relatively slow flow and causes a larger temperature difference. All this will contribute to the severe corrosion of iron components nearby.

Large Cathode and Small Anode. Such a situation is known to lead to an acceleration of corrosion of the anode. If a small section of iron or steel pipe is in contact with a large piece of copper pipe, the area effect will accelerate the corrosion of the iron pipe that acts as an anode of a galvanic cell.

7.5.2 Conclusions

The cause of corrosion in the domestic hot water system in the building is attributed to the improper use of dissimilar metal pipes and associated components. The temperature difference in the heat exchanger and heat circulation locations makes the corrosion more severe. An area effect is also a contributor to the corrosion. The remedial measures should be aimed at reducing the existing galvanic cell, to minimize the temperature and area effects.

The high contents of Al and Zn reported may possibly explained by the use of galvanized pipes and a sacrificial anode cathodic protection system in the hot water tank.

References

1. *National Printing Bureau Domestic Water Systems Preliminary Investigation report*, Mansour Keenan and Associates Limited, January 2003.
2. *Corrosion Engineering*, M. G. Fontana, 1986, p. 43.

7.6 Cathodic Protection of Steel in Concrete

More than 5 billion dollars are spent every year in repairs to concrete structures such as bridges, buildings, parking garages and other structures. Carbon dioxide enters the concrete and reacts with the lime, lowering the pH by forming carbonic acid. Further, the chloride in deicing salts, along with oxygen and water, creates an aggressive corrosive environment. An electrochemical corrosion cell is formed and delamination occurs. The rebar corrodes and the resulting rust is voluminous, leading to cracking, spalling and delamination of the concrete. Figure 7.23 illustrates the corrosion process.

Cathodic protection is one of the methods to mitigate the corrosion of steel in concrete Figure 7.24. Some factors to be considered in this connection are: remaining service life of the structure should be more than 10 yr; delamination and spalls should be less than 50% by weight of concrete; half-cell potential should be less than −200 mV (indicating breakdown of passive film); the structure should be sound; the reinforcing bars should be electrically continuous; AC power should be available.

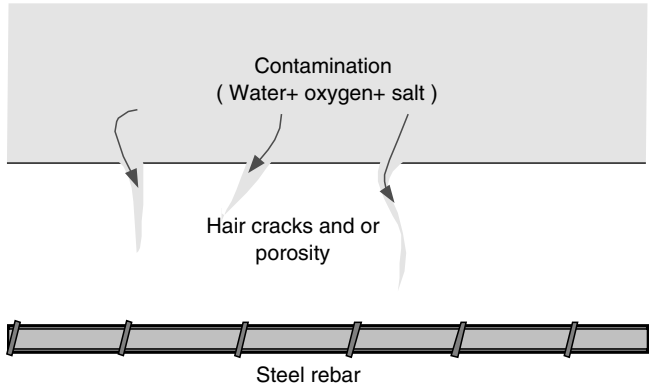

Figure 7.23 *Atmospheric Contamination*

The two types of cathodic protection are: (i) sacrificial anode; and (ii) impressed current systems.

The sacrificial anode system typically uses magnesium, zinc or aluminum and their alloys Figure 7.25. These metals or alloys act as anodes when coupled with steel and its

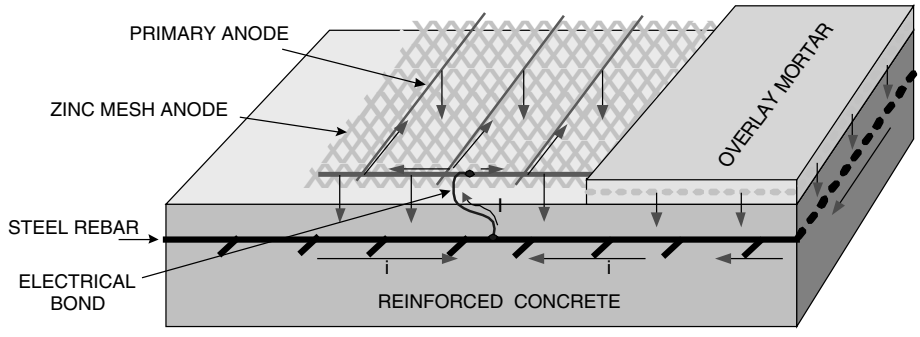

Figure 7.24 *Galvanic anode cathodic protection*

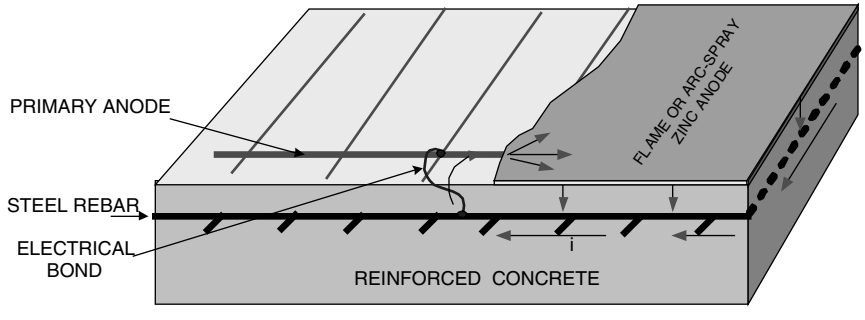

Figure 7.25 *Arc-sprayed galvanic layer anode*

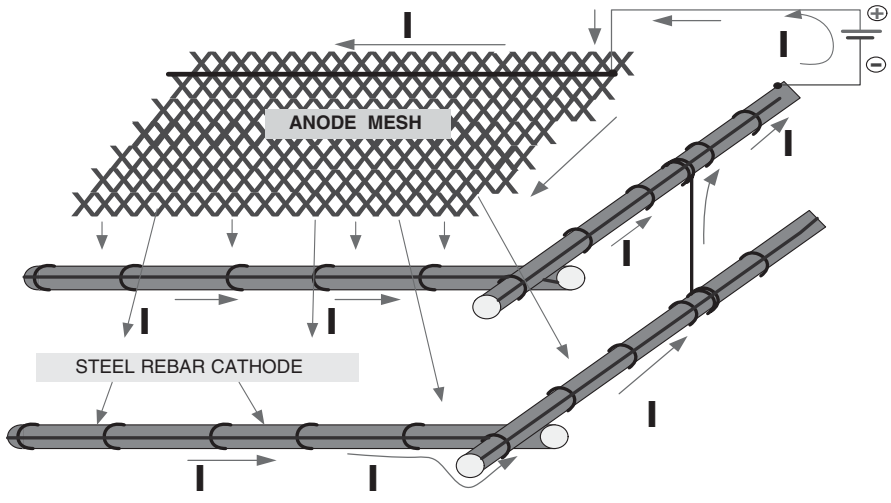

Figure 7.26 *Impressed current system line diagram*

alloys. These metals or alloys act as anodes when coupled with steel and preferentially corrode. Magnesium is often used in fresh water media while zinc and aluminum are used in seawater and brackish water media.

Impressed current cathodic protection requires:

(i) DC power supply (rectifier);
(ii) an inert anode such as catalyzed titanium anode mesh;
(iii) a Wiring conduit;
(iv) an embedded silver/silver chloride reference electrode.

A schematic of an impressed current cathodic system is depicted in Figure 7.26. By an impressed current the potential of the steel is shifted to greater than −850 mV, thus making the steel bar cathodic and prevent the corrosion.

Bibliography

M.Y. El-Shazly, Cathodic Protection of Steel in Concrete, *24th Annual Conference on Corrosion Problems in Industry*, Egyptian Corrosion Society, 5–8 December 2005, Les Rois Hotel, Egypt.

7.7 Corrosion of Aluminum Components in the Glass Curtain Wall of a Building

Corrosion was observed on the aluminum pressure plates and dress-caps that hold the glazing in place on a curtain-walled building. The dress-caps (which have L-shaped cross-sections) were externally clad with thin copper sheet.

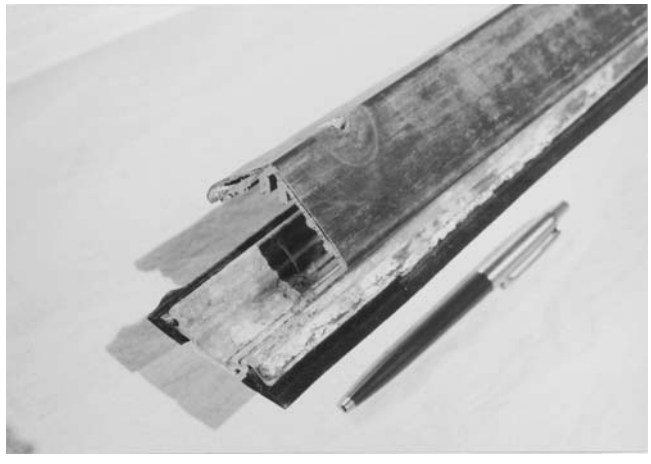

Figure 7.27 *A pressure plate (bottom) and a dress-cap (top). The dress cap is clad with copper sheet. The pressure plate is fitted with two rubber inserts. (Reproduced from COM'1999 and 2005 with permission from the Metallurgy Society of CIM)*

7.7.1 Introduction

In order to hide the aluminum extrusions, rubber strips and screws (dress-caps) were fitted over the top of the pressure plates. They were also aluminum extrusions with L-shaped cross-sections. For aesthetic reasons, the original building design required the dress-caps to be externally clad with thin copper sheet. The copper sheet was mechanically attached by rolling over the two longitudinal edges onto the internal surfaces of the dress-cap. Figure 7.27 shows a pressure plate and one of the dress-caps.

Several years after the building was constructed, it was noticed that some of the copper cladding was separating from the dress caps, particularly near the base of the building.

7.7.2 Observations

Pressure Plates. The aluminum extrusions were partially covered with loose, white-grey corrosion products. Water washing and scrubbing removed these products and revealed general corrosion and pitting of the aluminum surfaces.

Dress-caps. The aluminum extrusions showed extensive general corrosion and pitting on their inner (non-clad) surfaces (Figure 7.28). The copper cladding sheet was bulged at a few locations along the dress-cap edges. Cross-sectional cuts were made through some of these bulges. A typical cross-section is shown in Figure 7.29.

It can be seen that the bulge was caused by the formation of a white corrosion product on the outer surface of the aluminum extrusion. This voluminous material, trapped between the copper and the aluminum, exerted pressure on the relatively soft copper sheet, causing it to deform.

The cross-section shown in Figure 7.29 reveals that the aluminum has been badly corroded at one edge and has cracked away. This has resulted in the copper sheet

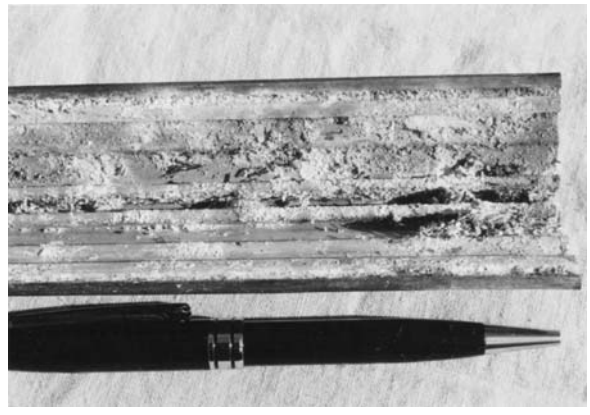

Figure 7.28 *Aluminum corrosion products on the interior surface of a dress-cap. (Reproduced from COM'1999 and 2005 with permission from the Metallurgy Society of CIM)*

becoming partially detached at this location. All of the copper cladding, which was a commercially pure architectural grade, was found to be in excellent condition with no significant metal loss.

The major damage suffered by the dress-caps was clearly caused by galvanic corrosion between the copper cladding and the aluminum extrusion. In addition, if a copper-containing solution runs over aluminum, electrochemical reactions will cause the aluminum to corrode and metallic copper to be deposited. These reactions establish local galvanic cells that can cause rapid deterioration of the aluminum. Copper has a very low corrosion rate in most atmospheric environments, thus enabling it to perform well for decades in architectural applications. The fact that copper is very slowly corroding can be judged by the blue-green run-off that is seen coming from the copper roofs of many public buildings.

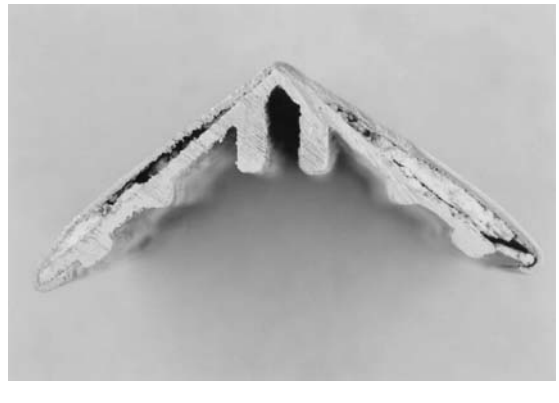

Figure 7.29 *Cross-section through a bulge in the copper cladding on a dress-cap; note the white aluminum corrosion product and the thinned and cracked edge (lower right). (Reproduced from COM'1999 and 2005 with permission from the Metallurgy Society of CIM)*

7.7.3 Recommendations

The new dress-cap substrate material should be either fiber-reinforced plastic (FRP) or Type 316 stainless steel. Being a nonmetallic insulator, FRP would eliminate any possibility of galvanic corrosion. Type 316 stainless steel demonstrates good passivity in urban atmospheres and has been successfully used in contact with copper.[1]

Contact between aluminum and metallic copper and/or copper-containing solutions must be avoided irrespective of the corrosivity of the environment.

Although corrosion engineers are well aware of the mechanism and the detrimental effects of galvanic (dissimilar metal) corrosion, it would seem necessary to make some designers, architects and engineers in other disciplines aware of this very damaging form of corrosion.

References

1. H.P. Godard, W.B. Jepson, M.R. Bothwell and R.L. Kane, *The Corrosion of Light Metals*, Chap. 3, John Wiley & Sons Inc., New York 1967.
2. W. Seale, Copper Development Association, private communication, 28 October 2004.

7.8 Corrosion in a Cooling Water System

Cooling water tubes are used in extensively industry. Corrosion of cooling water tubes or pipes is a common phenomenon. The heat exchanger is opened to examine the extent of corrosion. Heavy deposits are revealed inside the tubes (Figure 7.30). The outer surface of the carbon steel tubes are in good condition and free from pitting attack (Figure 7.31).

Some tubes were split open and subsequent examination showed the presence of very hard deposits on the surface (Figure 7.32). Isolated, but deep pits were present under the hard deposits (Figure 7.33). The measured thickness of the tube, mechanical tests, chemical analysis and etching showed the tubes to conform to the properties specified for SA 179 tubes.

Examination of cooling water side tubing showed mild pitting and a hard, sticky, uniform deposit inside the tube (Figure 7.34). At some points the deposit was in the form

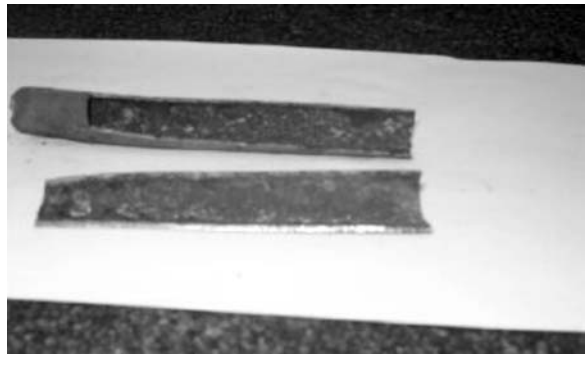

Figure 7.30 *Hard deposits inside GE3B tubes*[1]

Figure 7.31 *GE3B tube outside surface shows no corrosion or pitting*[1]

Figure 7.32 *GE3B tube filled with deposits*[1]

Figure 7.33 *Deep pitting inside GE3B tube*[1]

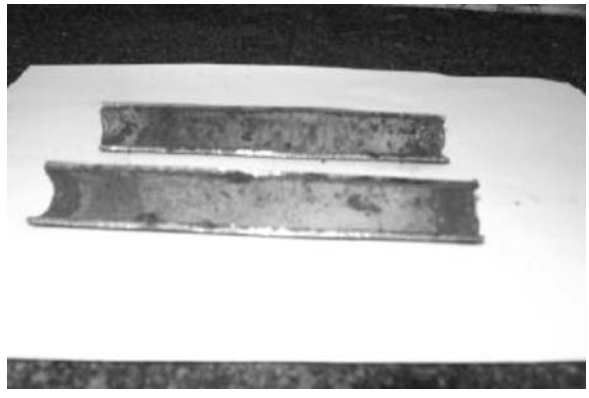

Figure 7.34 *Hard deposit inside GE16 tube*[1]

of lumps. Deep pits were also observed below the solid deposits, and perforation below the deposit in one case (Figure 7.35). Measurement of the thickness of the tubes showed no general thinning.

Flow measurements showed flow rates lower than expected and backwashing was observed. The backwash contained brownish siliceous matter and other solid impurities. All three heat exchangers had silt and dirt deposits and partially plugged tubes. The tube ends were corroded and thinned down. Perforation of the tubes originated from inside (cooling water side). Pitting shows it to be underdeposit corrosion.

A commercial cooling water program during start-up and stabilization of the cooling tower after major repairs is likely to avoid the adverse results. The water quality should be maintained.

Reference

1. R.J. Sampathkumar and A.N. Screeram – International Congress, Gloccorr 2002, National Corrosion Council of India.

Figure 7.35 *Perforated GE 16 tube*[1]

7.9 Pitting Corrosion of 90/10 Cupronickel Chiller Tubes

The in-service 90/10 cupro-nickel tubes in a water-chiller system suffered from severe corrosion damage during their relatively short service life causing unexpected down time. Figure 7.36 shows the top section of the condenser in question where large numbers of tubes are undergoing internal corrosion. Several tube sections were opened and subjected to SEM and energy dispersive X-ray (EDS) to investigate the corrosion morphology and to identify the chemical composition and elements involved in the corrosion process.

7.9.1 Optical Examination

Various sections of the opened tubes were examined by optical techniques. Figure 7.37a shows one of many pits where there are several pinhole-sized pits surrounding a large pit that appears to have burst open, and most of its corrosion products were washed away, although areas of different colors are clearly seen. The light-blue product consists of copper salts, including $CuO/Cu(OH)_2$,$CuCl_2$, etc.; the red is a layer of redeposited Cu/Cu_2O, and the golden color is the brass substrate.

7.9.2 SEM and EDS Studies

Microscopic examination revealed the pit initiation. Figure 7.37b shows a typical small pit (the size of a pinhole) observed on the inside surface of the tube. It is clear that a layer of deposit can be seen. EDS analysis was carried out in three of the representative locations as shown in Figure 7.37b: (i) on the surface of the deposit layer, (ii) inside a pit, and (iii) immediately outside the pit. Higher magnification SEM images revealing details of the bottom the pit are shown in Figure 7.37c and d, respectively. EDS study of location A showed O, Al, Si, Fe and Cl peaks. It is suspected that the deposit layer consists of iron

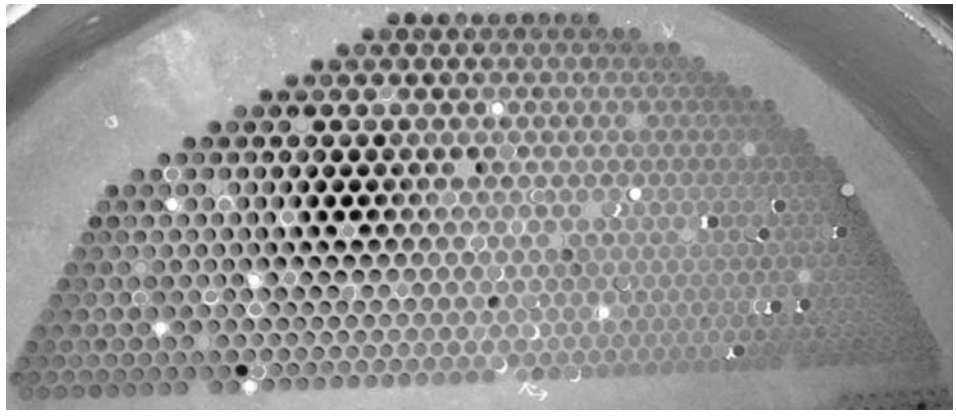

Figure 7.36 (Plate 1) *Top section of a condenser. White indicates tubes plugged with extensive internal corrosion; blue indicates tubes identified with internal corrosion to be monitored; and orange indicates tubes previously replaced. (Reproduced from COM'1999 and 2005 with permission from the Metallurgy Society of CIM)*

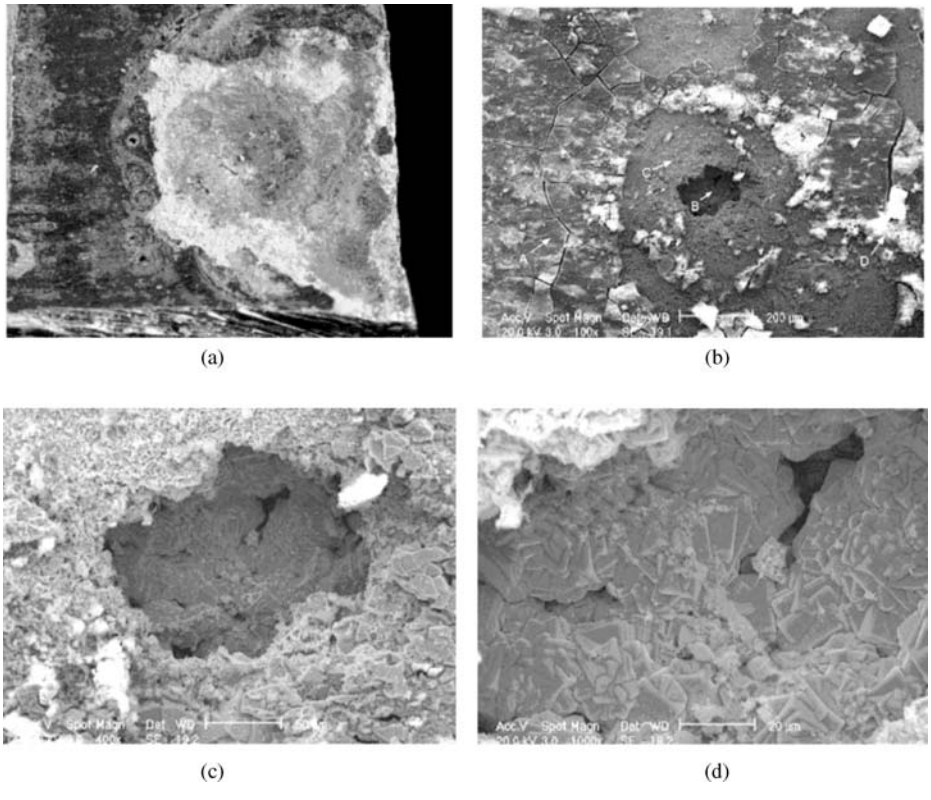

Figure 7.37 *(a) A large pit that was opened and washed (Reproduced from COM'1999 and 2005 with permission from the Metallurgy Society of CIM); (b) SEM photo of a tiny pit outside the large pit; (c) a close-up of a pit; (d) a close-up of the inside of as it*

oxide and fine sand deposit. The Cl peak appears strong. Many other locations were also examined with similar results. Sulfur peaks were seen.

EDS study at location B, at the bottom of a pit showed that location was mainly composed of Cu and Ni with a small amount of Fe, which could be attributed to contamination since Fe was not detected in some other pits. The EDS result indicates no 'denickelification' inside the pit since both Ni and Cu were found, and the crystals appear to be compact with no evidence of any copper crystal deposit or selective nickel dissolution leaving a porous structure. It should also be noted that there was no corrosion product at the bottom of the pit, and there was clear evidence of copper redeposit at the edge of the pit, as indicated in EDS of the copper and oxygen peaks.

7.9.3 Pitting Initiation and Propagation Mechanism

The main mode of attack is pitting of Cu-Ni 90/10 tubes. Pit-like attack in condenser tubes is often caused by impingement that occurs at sites where large air bubbles impinge on the tube surface and break into small bubbles on impact, causing local destruction of

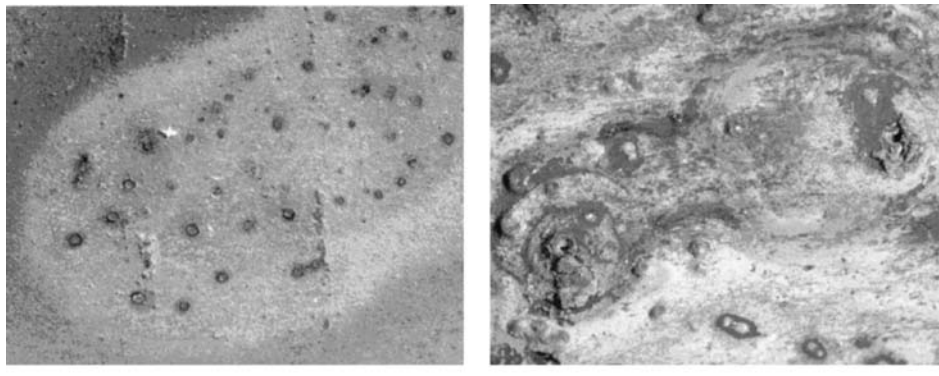

Figure 7.38 *(a) Copper oxide ringlets observed around newly initial pits; (b) copper oxide ringlets observed around larger pits. (Reproduced from COM'1999 and 2005 with permission from the Metallurgy Society of CIM)*

the protective film. However, pits produced in this way have a characteristic shape; they are elongated in the direction of the flow and are usually clean and free of corrosion products. The pitting corrosion observed in this study did not show any of these characteristics. In contrast, copper oxide ringlets were observed around the pits, indicating that the corrosion occurred in an environment with appropriate concentrations of corrosive ions, moisture and oxygen, as indicated in Figure 7.38. This observation suggests that the condenser might not have been kept full (with water) for a period of time.

Pitting probably occurs due to the reactions:

Low pH (anodic):

$$\mathrm{Cu} - 2\mathrm{e}^- == \mathrm{Cu}^{2+} \qquad 1(\mathrm{a})$$

$$\mathrm{Ni} - 2\mathrm{e}^- == \mathrm{Ni}^{2+} \qquad 1(\mathrm{b})$$

Neutral solution (pH close to 7) (anodic):

$$\mathrm{Cu} - 2\mathrm{e}^- + \mathrm{H_2O} == \mathrm{Cu(OH)_2} + 2\mathrm{H}^+ \qquad 2(\mathrm{a})$$

$$\mathrm{Ni} - 2\mathrm{e}^- + \mathrm{H_2O} == \mathrm{Ni(OH)_2} + 2\mathrm{H}^+ \qquad 2(\mathrm{b})$$

Cathodic reactions:

$$½\,\mathrm{O_2} + \mathrm{H_2O} + 2\mathrm{e}^- == 2^-\mathrm{OH}^- \qquad 3(\mathrm{a})$$

$$\mathrm{Cu}^{2+} + 2\mathrm{e}^- == \mathrm{Cu}\ (\text{redeposit}) \qquad 3(\mathrm{b})$$

Anodic reactions Equation (1a,b) lead to dissolution of metal (copper–nickel 90/10). At the beginning of pit initiation, the reactions of Equation (2a,b) might take place,

resulting in a local pH decrease. Cathodic reaction (Equation 3a) also likely occurred during pit initiation due to the abundance of available oxygen. However, pit propagation can take place without oxygen as the copper ions redeposit (Equation 3b). This reaction is thermodynamically driven by the low pH and high copper ion concentration inside a pit and supported by observation of copper redeposit around a pit. It appears that the denickelification is a result of pit propagation. It is possible that the copper redeposit reaction accelerates the pit propagation, thus reducing the lifetime of the condenser tubes.

7.9.4 Conclusion

The results of this study indicate that pit initiation takes place in areas where the oxide film is broken or damaged under a stagnant environment in the presence of sufficient moisture and oxygen. It is possible that pit propagation could occur without oxygen, and that it is accelerated by the copper redeposit reaction. In such a case, preventing pit initiation becomes very important.

Bibliography

1. W.S. Janssen, Corrosion Control in a Refinery Sea Water Cooling System, *Materials Protection*, **1**(10), 42–53 (1962).
2. W. Matthewman and G.J. Evans, Power Station Condensers, *Corrosion Technology*, 1964, 15–17.
3. I.G. Slater, L.Kenworth and R.May, Corrosion and Related Problems in Sea-water Cooling and Pipe Systems in H.M. Ships, *Corrosion*, **8**(12), 417–429 (1952).
4. H.A.Todhunter, Material Selection for Condenser Tubes, *Corrosion*, **11**, 39–44 (1955).
5. *CTL Report*, Forensic Analysis of Condenser Tubes from York Chiller in Ottawa, April 2003.
6. Rt Worthington, Copper–Nickel Tubes, their Advantages for Steam Condensers, *Metal Progress*, **24**(1), 20–24 (1933).
7. V.D. Baan, Experience with Condenser Tubes at a Major Oil Refinery, *Corrosion*, **6**(1), 14–18 (1950).
8. N.V. Nowlan, Influence of Water Movement on Corrosion, *Corrosion Technology*, 397–399 (1960).
9. R.C. Mifflin and D.B. Bird, Performance of tube Alloys Cooled by Brackish Delaware River Water, *Materials Protection*, **8**(9), 72–76 (1969).

7.10 Weld Metal Overlay: a Cost-effective Solution to High-temperature Corrosion and Wear Problems

High-temperature corrosion and wear is encountered in various industries such as waste incineration, fossil energy, pulp and paper, petroleum refining, chemical and petrochemical, mining and smelting operations. One of the methods to combat corrosion and wear and its control is to select suitable material, i.e., an alloy, for the plant design and maintenance. The selection of proper material for plant design and fabrication is followed

Table 7.4 *Applications of overlay technology*

Application	Corrosives	Number of Boilers using the overlay
Waste-to-energy boilers	Municipal waste containing chloride, sulfur, alkali metals, zinc and lead	59 (alloy 625 overlay weld metal used)
Coal-fired Boilers	Sulfidation attack; boiler tube wastage (50–60 mpy)	8 (alloy 625 and 309 SS)
Pulp and paper digesters	Thiosulfate and polysulfides	21 (overlaid with 309 SS)
Kraft recovery boilers	Sulfate, thiosulfate Chloride	11 (309 L on lower furnace sidewalls; 625 on floor tubes and smelt opening)

by a weld metal overlay of the plant equipment so that failures due to corrosion and wear may be avoided.

Welding Services Inc. has developed Unifuse overlay technology based on pulse spray gas metal arc welding (PSGMAW). The technology has made significant improvements in welding metallurgy to achieve low heat input, fast deposition rates covering large areas, sound metallurgical bonds with minimal lack of fusion and other defects, low dilution for the overlay chemistry and minimal distortion for the part being overlaid.

Some of the industrial applications of uniform overlay technology are noted in Table 7.4.

Failed tube 310 stainless steel in a waste-to-energy boiler is depicted in Figure 7.39. Figure 7.40 shows the appearance of uniform composite tubes with alloy 625 overlay on Cr, Mo steel. Figure 7.41 shows the 309 overlay on Cr, Mo boiler tube in service in a coal-fired boiler devoid of corrosion and cracking for 7 yr.

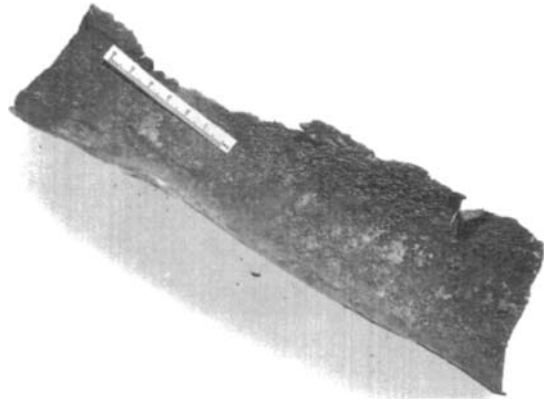

Figure 7.39 *A Type 310 SS tube failed after less than 2 yr service in a waste-to-energy boiler (Reproduced from COM' 1997 with permission from the metallurgy Society of CIM)*

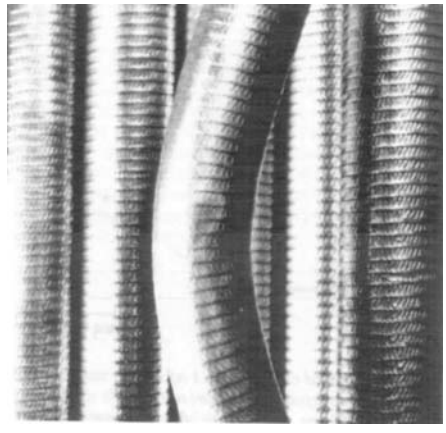

Figure 7.40 *Surface appearance of the Unifuse composite tubes with alloy 625 weld overlay (Reproduced from COM' 1997 with permission from the metallurgy Society of CIM)*

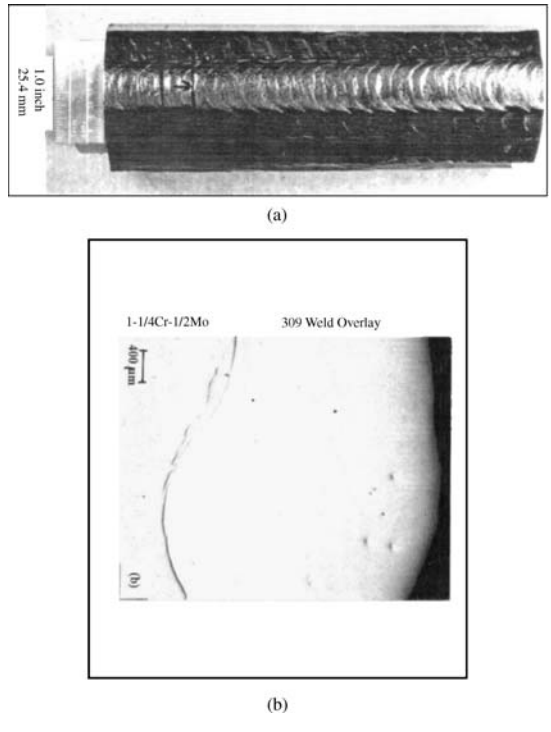

Figure 7.41 *309 Unifuse overlay on 1-1/4Cr-1/2Mo boiler tube in the wall blower region after service for about 7 yr in a supercritical unit of the coal-fired boiler: (a) surface appearance of the weld overlay, weld beads are still clearly visible; (b) cross-section of the weld overlay showing no corrosion and no cracking on the weld overlay at the fusion line (Reproduced from COM' 1997 with permission from the metallurgy Society of CIM)*

Bibliography

G. Lai, M. Jirinec, P. Hulsizer and F. Novac, *Proceedings of International Symposium on Corrosion and wear of Metals: Metallurgical Society of Canadian Institute of Mining, 36th Annual Conference*, Sudbury, Ontario, Canada, August 1997.

7.11 Equipment Cracking Failure Case Studies

One factor, which should always be considered when performing materials failure investigations, is the influence of human error. This section provides three examples of equipment failures due to cracking for which the root cause of failure was found to be associated with human error.

1. The first involves the misapplication of chromium electroplating to an engine crankshaft during a rebuild procedure, which resulted in a fatigue failure shortly after the unit was put back into service.
2. The second failure involves an error made during the weld repair of an electric motor drive shaft, which again resulted in a fatigue failure.
3. The third example describes mistakes made during the design, procurement and construction of a high-pressure steam piping system, resulting in a catastrophic failure of a pipe connector, due to chloride stress corrosion cracking.

Material failures can be caused by a number of factors, either individually, or in combination, including: substandard materials, inappropriate materials selection, poor design, equipment abuse, unexpected stresses or environmental conditions, and poor maintenance practices and/or neglect. Many failures, in one way or another, involve human error to some extent.

The failure investigations described in this paper illustrate two situations where human error during common maintenance and repair activities ultimately played a role in the failure of industrial machinery. The third failure investigation revealed how, even when the potential for failure is known (i.e., SCC of 304 SS), human error during the procurement and/or installation phase of the piping clamps resulted in an SCC-susceptible material being installed and ultimately failing in a catastrophic manner.

7.11.1 Industrial Engine Crankshaft Failure

This failure involved the crankshaft from an eight cylinder 2400 horsepower natural-gas-fired engine, operating at a speed of approximately 900 rpm, and used to drive a gas compressor. The engine had operated virtually trouble-free for approximately 50 000 h ($\simeq 5\frac{1}{2}$ yr), having been subjected to the normal oil changes and other regular maintenance practices. After 50 000 h, the engine was torn down for a major overhaul, as is common practice for industrial engines of this type. The crankshaft was removed for inspection and polishing of the bearing journal surfaces at an experienced engine maintenance shop. No cracking or abnormal wear was observed during this overhaul; however, measurements of the critical crankshaft dimensions after polishing revealed that the journals had been over-polished, resulting in the journal diameters being approximately 0.03 mm under tolerance. At this time, it was agreed between the

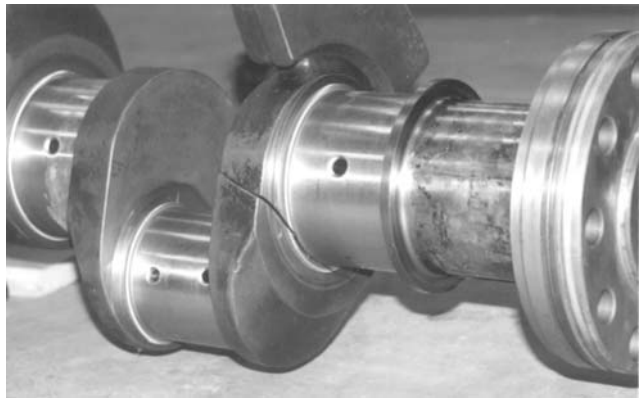

Figure 7.42 *Appearance of large crankshaft crack. (Reproduced from COM'1999 and 2005 with permission from the Metallurgy Society of CIM)*

maintenance shop and the engine owner that the journals would be lightly machined and then built back up with the application of a chromium electroplating layer.

The crankshaft journal dimensions were back within tolerance after the machining, electroplating and honing procedures. The engine was reassembled, including all new crankshaft bearings and piston liners. After recommissioning, the engine operated for approximately 2000 h ($\simeq$83 days), at which time the crankshaft failure was discovered. It was noted by the operating staff that the engine exhibited abnormal operating characteristics in the days leading up to the discovery of the failure. The crankshaft was removed from the engine and was found to be cracked through the web between the last rod journal and the last main journal, next to the flywheel, as shown in Figure 7.42.

Failure Investigation. The crack shown in Figure 7.42 had propagated through almost the entire cross-sectional area of the crankshaft web. The remaining ligament was broken open to expose the crack faces where, as is shown in Figure 7.43, it became readily

Figure 7.43 *Fatigue fracture face, showing crack growth direction. (Reproduced from COM'1999 and 2005 with permission from the Metallurgy Society of CIM)*

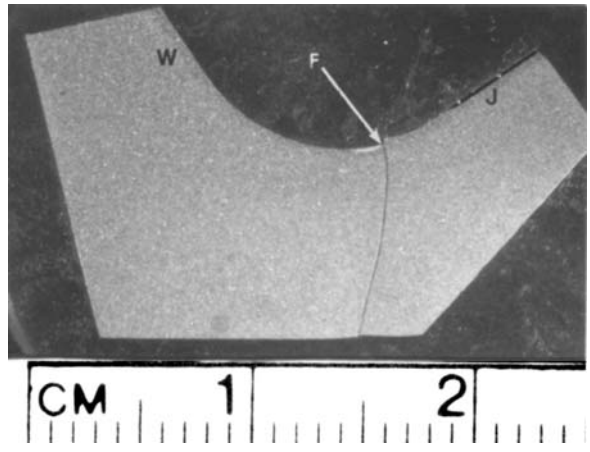

Figure 7.44 *Prepared metallographic specimen: F = fatigue fracture; W = web; J = journal. (Reproduced from COM'1999 and 2005 with permission from the Metallurgy Society of CIM)*

apparent that the failure was associated with a high-cycle, low-stress fatigue crack, which initiated in the machined fillet at the edge of the main journal and had propagated through the web until it reached the fillet of the adjacent rod journal. The fracture faces exhibited the characteristic ratchet marks, beach marks and smooth texture, typically associated with high-cycle fatigue.

Wet fluorescent magnetic particle inspection of the remaining journal fillets on this crankshaft revealed the presence of a number of secondary cracks in the same orientation and position as the failure initiation site. A metallographic specimen, including the matching halves of the fracture from the initiation site in the fillet of main journal, was cut, mounted, polished and etched in 2% nital, in preparation for examination with an optical microscope. The polished and etched specimen is shown in Figure 7.44.

Metallographic examination of the prepared specimen revealed the presence of a very thin chromium layer on the journal side of the fracture. As can be seen in the photomicrograph in Figure 7.45, the fracture initiated at the tip of this tapered chromium layer. The underlying crankshaft microstructure was a relatively coarse (ASTM E112 grain size $\simeq 7:\mathrm{m}$) mixture of ferrite and pearlite, with a measured Rockwell hardness of 90–95 HRB. There was no evidence of prior shot peening in this fillet region. The fracture profile was nonbranching and transgranular, consistent with high-cycle fatigue. A secondary crack, exhibiting a mixed intergranular/transgranular morphology, is also evident on the left side of the photomicrograph.

Due to the observed presence of the chromium layer adjacent to the fatigue initiation, Canspec performed a macroetching procedure, using 15% nital, on several of the other journals in the fillet regions. Since the nitric acid etch will darken a machined steel surface, but will not affect chromium, this etching technique was capable of delineating the edges of the chromium electroplated layer on the journals. From this etching examination, a number of journal fillets were found to have chromium electroplating present.

Conclusions. This case study reveals how a common and normally acceptable engine overhaul procedure can lead to premature failure. There are a number of industry

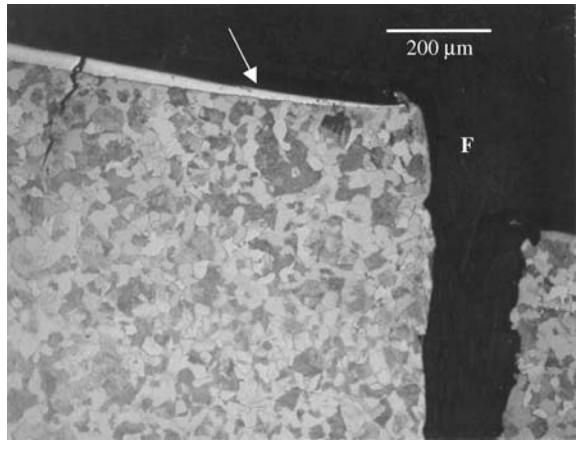

Figure 7.45 *Chromium layer (arrow) at fatigue initiation site (F). (Reproduced from COM'1999 and 2005 with permission from the Metallurgy Society of CIM)*

specifications, including ASTM, Military (MIL) and U.S. Federal Specifications (QQ), that warn of the dangers of fatigue cracking when using chromium electroplated steels in dynamically loaded service environments. These specifications go on to describe the recommended cleaning, shot peening, electroplating, heat treating and quality control procedures that should be employed for the use of industrial hard chromium coatings. In particular, for dynamically loaded steel components, there are guidelines for shot peening of steel surfaces to be coated, as well as advice with respect to masking high-stress areas (e.g., journal fillets) from the electroplating process. It is apparent that, for the crankshaft in this case, the fillet regions were not shot peened and the chromium electroplating was inadvertently applied to many of the journal fillets, where masking should have been used.

7.11.2 Electric Motor Drive Shaft Failure

A 350 horsepower electric motor drive shaft broke adjacent to the coupling, which was connected to a three-stage compressor. The motor operated at a speed of 1200 rpm and had run for a period of approximately 5 yr. Approximately 3.5 yr after the initial start-up, the motor shaft had been severely damaged by wear, due to a lack of lubrication on the bearings, as a result of poor maintenance practices. A repair was made by machining the shaft down to sound metal and building up the shaft surface to its original diameter with a weld overlay. After approximately 1.5 yr of service, the shaft broke in the region of this weld repair. The original shaft material was reported to be a medium-carbon, low-alloy Ni–Cr–Mo steel.

Failure Investigation. The shaft broke at a 45° angle and the macroscopic fracture morphology was consistent with high-cycle fatigue (i.e., macroscopically smooth, ratchet marks at the origin and concentric beach marks radiating from the origin). The 45° fracture orientation was consistent with torsional fatigue. The fatigue crack had propagated through almost the entire 4-inch diameter shaft, indicating that the nominal stresses on the shaft were relatively low, in comparison to the shaft strength. As shown in Figure 7.46, a foreign material was embedded in the shaft just below the surface and

Figure 7.46 *Drive shaft fatigue fracture face, showing initiation point (arrow) and foreign keyway material (K)*

coincident with the fatigue initiation point. It was subsequently determined that it is common practice to insert a 'dummy' material into an old shaft keyway when applying a weld overlay to repair a worn shaft. The use of a 'dummy' key saves machining and welding time, thus minimizing the repair cost.

Metallographic examinations of a cross-section through the 'dummy' key at the fatigue origin revealed evidence of slag and nonfusion associated with the half-inch-thick weld overlay. There was also a distinct difference observed in the microstructural appearance between the overlay and the original underlying shaft material. A photograph of the polished and etched cross section is shown in Figure 7.47.

The weld overlay was analyzed and found to be a plain carbon steel, with a hardness of Rockwell 80 HRB, consistent with a low-strength welding consumable (e.g., E7018). The

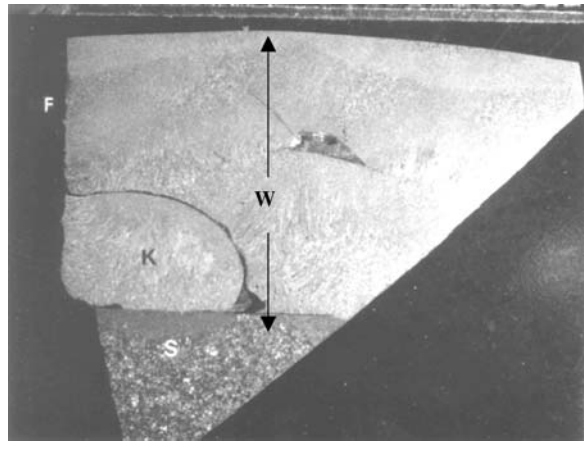

Figure 7.47 *Polished and etched section, showing fracture profile (F), weld overlay (W), foreign key material (K) and original shaft material (S)*

original shaft material was found to be a normalized plain carbon steel (AISI 1040), with a hardness of 90 HRB. It was noted that the shaft material did not comply with the specified Ni–Cr–Mo low alloy steel composition, and was significantly softer than this specified shaft alloy.

Conclusions. Most of the information associated with the cause of the failure could be acquired from the visual examination of the fracture face. The fracture morphology and orientation indicated that this was a torsional fatigue failure. The presence of a foreign (nonfused) material embedded in the former keyway and coincident with the fatigue initiation point suggests that this subsurface anomaly acted as the stress raiser responsible for the fatigue initiation. The fact that the fatigue crack had propagated through almost the entire shaft thickness without the shaft breaking indicated that the applied stresses on this shaft were relatively low.

In addition to the nonfusion defects and other flaws in the weld overlay repair, the relatively low strength of the weld overlay material (80 HRB) undoubtedly exacerbated the problem. This low-strength weld deposit would be expected to have relatively low fatigue resistance. In addition, it was determined that the original shaft material did not comply with the compositional and hardness requirements specified by the manufacturer. Again, the lower than expected strength of the shaft core material would also have a detrimental effect on the fatigue strength of the shaft.

7.11.3 Pipe Clamp Joint Connector Failure

A clamp-type pipe joint connector failed a short time after it was put into service. This clamp, shown in Figure 7.48, had been used to join two ends of NPS 8 carbon steel steam piping, operating at a pressure of approximately 11 MPa (1600 psi). The boiler feedwater used in this process had been softened by cation exchange ($Ca \leftrightarrow Na$) and was fully deaerated. The feedwater was recycled water from an oilfield operation and contained several thousand ppm dissolved chlorides. The steam was 80% quality and at a temperature of approximately 330°C.

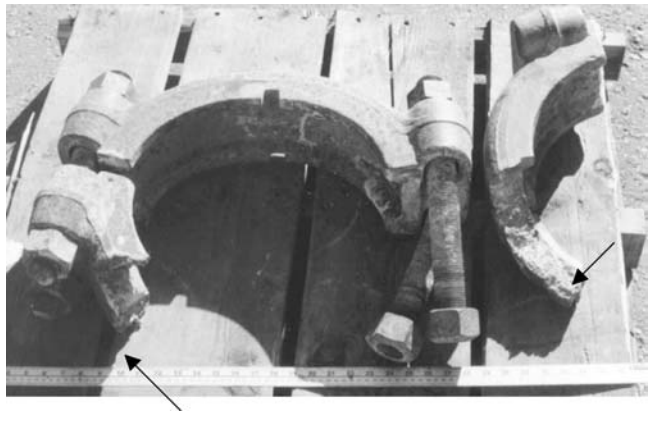

Figure 7.48 *Fractured pipe clamp (arrows) and fasteners. (Reproduced from COM'1999 and 2005 with permission from the Metallurgy Society of CIM)*

As can be seen in Figure 7.48, the pipe clamp consisted of two U-shaped half-shells, with two 1 ½-inch threaded studs at each end, used to tighten the two half-shells together around the nubbin ends of the pipe. The failure involved the complete fracture of the bottom half-shell, as it was positioned on the pipe. All four of the threaded fasteners were still intact, with no evidence of cracking, although the studs had been bent as a result of the failure.

The failure was preceded by a noticeable steam leak at this piping joint. Attempts were made to tighten to clamp, but this failed to stop the leak. The ensuing clamp fracture and pipe rupture caused an extensive amount of damage within the process building. Fortunately, no one was present in the building at the time of the failure and there were no injuries.

Failure Investigation. The clamp was nonmagnetic and the stamped identification on the side of the U-shaped shells indicated that they were fabricated from forged 304 austenitic stainless steel. Visual examination of the fracture surfaces revealed they were entirely brittle and exhibited a very coarse fracture morphology. Liquid penetrant inspection revealed the presence of additional cracks in the fractured half of the clamp. There was no cracking present in the high-strength steel fasteners.

Chemical analysis of scale deposits present on the surface of the failed clamp by X-ray diffraction revealed the presence of predominantly sodium iron oxide, sodium carbonate sodium chloride (∼10%), iron oxide and iron sulfide. The scale composition was consistent with the evaporated residue from the 80% quality steam, which had been leaking from the joint prior to the failure. The high sodium concentration in the scale was attributed to the zeolite ion exchange system used to soften the boiler feedwater, while the chlorides and sulfides were naturally present in the feedwater.

Metallographic examinations of a cross-section through the failed clamp material confirmed it was an austenitic stainless steel and that extensive branched transgranular cracks were present throughout the material, as illustrated in Figure 7.49.

Conclusions. Examination of the failed pipe clamp revealed the presence of brittle fracture surfaces as well as an extensive array of branched transgranular cracks. The identification of the clamp material indicated it was a forged 304 stainless steel component

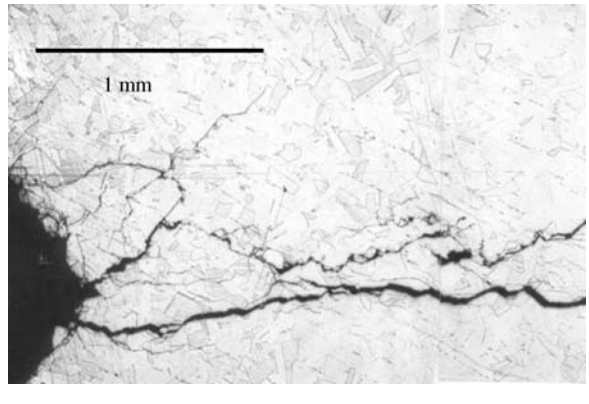

Figure 7.49 *Photomicrograph of transgranular cracking*

and metallographic examination confirmed this. The high-pressure 80% quality steam being handled by the piping was produced from treated recycled water from oil production fluids and contained several thousand parts per million of dissolved chlorides.

The pipe joint had been leaking steam and water prior to the failure, and chemical analysis of the scale deposits on the clamp surface after the failure confirmed the presence of a number of sodium-based mineral compounds from the leaking steam, including approximately 10% sodium chloride. The presence of high concentrations of moist, hot chloride salts on the highly stressed austenitic stainless steel surface, particularly with concurrent exposure to atmospheric oxygen, created an ideal chloride stress–corrosion cracking (SCC) environment.

It could also be argued that this failure would not have occurred if the steam piping had been joined by welding, instead of using high-pressure clamps. However, these types of pipe joint connectors are reportedly commonly used in many process piping installations, including drilling rigs, power plants and petrochemical plants, without incident.

The root cause of this failure was the human error associated with the installation of stainless steel in this service. It was reported that the engineering personnel involved in the design and construction of this steam plant were aware of the potential for SCC of stainless steels in this hot saline process. For this reason, all of the piping and clamp materials were specified to be carbon steel during the design phase. A review of the remaining pipe clamps in the process after the failure revealed the presence of one additional stainless steel clamp, while the rest were forged carbon steel, as specified. It was then determined that, due to a shortage of carbon steel clamps of the appropriate pressure rating for NPS 8 piping, these two stainless steel clamps were substituted as an 'upgraded' replacement material. Unfortunately, the potential catastrophic consequences of this materials 'upgrade' were not appreciated by those involved in the procurement and installation of these clamps who were aware of the material substitution.

7.12 Failure of a Conveyor Drive Shaft

A steel coal-conveyor drive shaft failed in service due to the occurrence of a transverse crack that passed through the right keyway near the centre of the keyway as shown in Figure 7.50. The shaft was cut so that the crack could be opened to expose the corroded mating fracture surfaces. After cleaning with hydrochloric acid, examination of the fracture surfaces showed them to be relatively smooth textured, flat and perpendicular to the axis of the shaft and the keyway. Two sets of crack arrest marks was concentric to

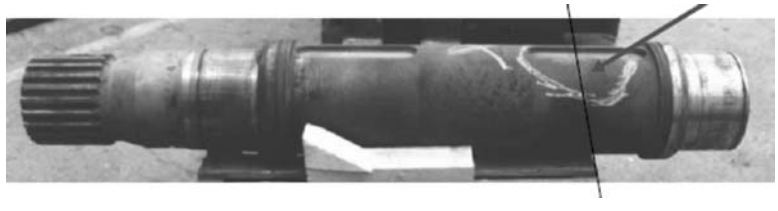

Figure 7.50 *Coal-conveyor drive shaft that cracked in service. (Reprinted with the permission of M. Zamanzadeh, ATCO Associates, Pittsburgh, USA)*

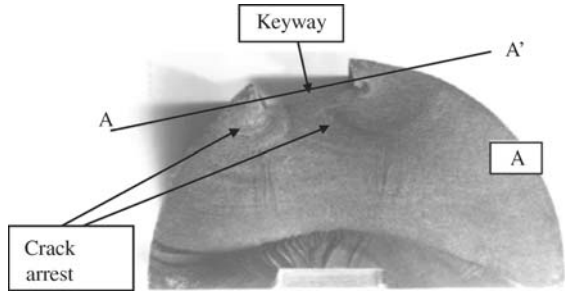

Figure 7.51 *The fracture surfaces were relatively smooth-textured and flat; two sets of concentric crack arrest marks were visible on the fracture surface. (Reprinted with the permission of M. Zamanzadeh, ATCO Associates, Pittsburgh, USA)*

each corner of the keyway, as shown in Figure 7.51. Transverse cross-sections were found to have secondary cracks (Figure 7.52).

The chemical analysis, mechanical properties, hardness and impact properties were determined and found to conform to the specifications of the German Grade 30 NiMoCr8 alloy steel suitable for use as a shaft.

7.12.1 Conclusions

The conveyor drive shaft failed as a results of corrosion fatigue in bending. Failure was initiated at both corners of the keyway. Numerous secondary fatigue cracks were observed, indicating the presence of a large number of stress concentrator sites that caused by presence of corrosion pitting on the surface. Fatigue cracks initiate at locations of maximum local stress and/or minimum local strength.

It is concluded that the conveyor drive shaft failed as a result of corrosion fatigue in bending. The use of protective coatings or some other means of shielding the shaft from the corrosive medium could prolong the life of the drive shaft.

Figure 7.52 *Secondary cracks. (Reprinted with the permission of M. Zamanzadeh, ATCO Associates, Pittsburgh, USA)*

7.13 Failure Analysis of Copper Pipe in a Sprinkler System

Two type of copper piping, namely straight sections and T-sections, were examined for the forms of corrosion present in the samples. The water samples and the corrosion products were tested for microbiological activity.

7.13.1 Observations

The straight section of the pipe showed dark red and greenish spots on the outer surface, (Figure 7.53); through-wall pits were present in the red spots.

The T-sections did not have reddish spots on the external surface (Figure 7.54), but one sample had a crack (Figure 7.55). This crack may be due to poor fabrication technique. The appearance of the joint is suggestive of lack of shielding and overheating which might allow penetration of oxygen, leading to cracking.

Internal examination of pipe sections showed thick black adherent scale, (Figure 7.56). Green deposits were also present (Figure 7.57). Some areas in the pipe showed the

Figure 7.53 (Plate 2) *Dark red and greenish spots on the outside surface*

Figure 7.54 (Plate 3) *Sample did not display the reddish spots on the exterior surface*

Figure 7.55 (Plate 4) *Sample did not display the reddish spots on the exterior surface, even though the surface contained a visible crack*

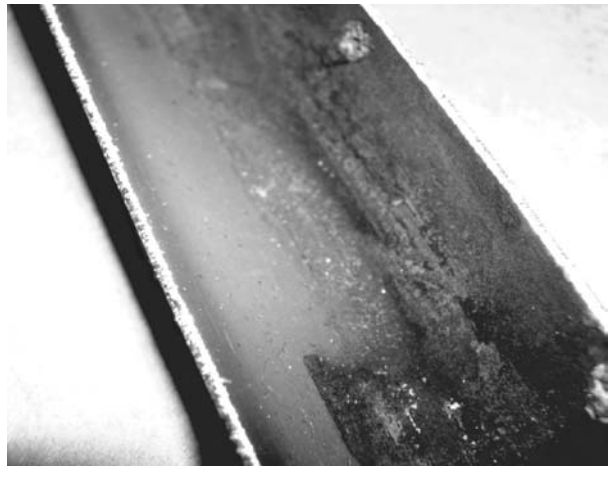

Figure 7.56 (Plate 5) *Internal surface of pipe is coated with a thick, black, tightly adherent scale*

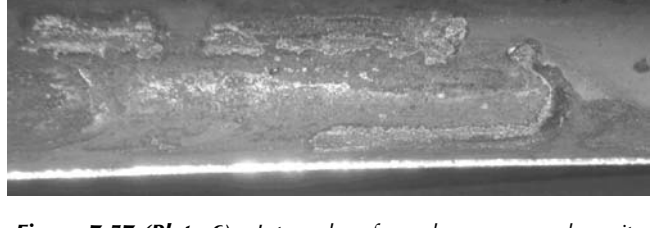

Figure 7.57 (Plate 6) *Internal surface shows green deposits*

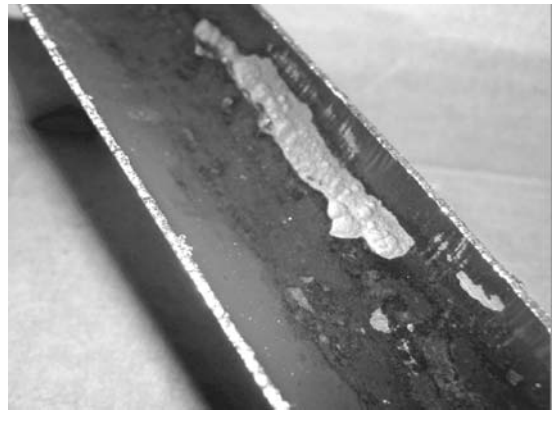

Figure 7.58 (Plate 7) *Bright shiny copper can be seen with greenish deposits*

presence of both green deposits and shiny copper (Figure 7.58). Pits were present in areas where copper is surrounded by green deposits (Figure 7.59). The green deposits indicate significant corrosion.

The black scale was carefully removed to identify the morphology of pits (Figure 7.60). The pits were located at the bottom of a hole (Figure 7.61). The morphology of the pits is characteristic of microbiologically influenced corrosion (MIC).

Figure 7.59 *Well-developed pits, with pits impinging upon one another*

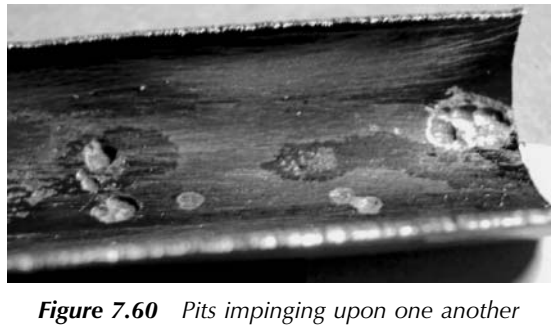

Figure 7.60 *Pits impinging upon one another*

Figure 7.61 *Many pits were elongated, but retained a smooth, scooped-out appearance characteristic of MIC*

The T-sections were free from pitting and the inside surface was clean. The water samples and the corrosion products were analyzed for microbiological activity. The water contained significant amount of iron-reducing biological activity.

7.13.2 Conclusions

Significant microbiologically induced corrosion due to the presence of bacteria in the water is evidenced by saucer-shaped pits, smooth sided pits, bright shiny copper to matte red clean areas. The black deposits, corrosion products from carbon steel, may cause underdeposit corrosion and may cause the failure. Treatment of the water with biocide may minimize microbiologically induced corrosion.

7.14 Failure of Rock Bolts

The properties and design of rock bolts are available in the literature.[1] A Swellex rock bolt is shown in Figure 7.62. The modes of support for rock bolts can be:

(i) beam building;
(ii) suspension;
(iii) pressure arch;
(iv) support of discrete bolts.

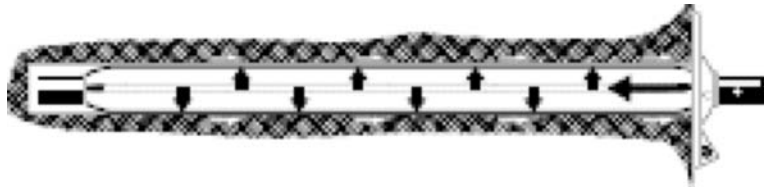

Figure 7.62 *Swellex bolt, after Atlas Copco*[2]

7.14.1 Corrosion Modes of Rock Bolts

The corrosion modes are:

(i) uniform corrosion;
(ii) localized corrosion pitting or crevice corrosion;
(iii) galvanic corrosion.

Factors involved in corrosion are: low-pH acid mine water due to oxidation of iron sulfides or bacterial oxidation such as SRB; carbon dioxide; chloride and sulfate (10 ppm Cl^-, 25 ppm sulfate; 1080 ppm Cl^-; 300 ppm sulfate). Mine air contains SO_2 and NO_2.

7.14.2 Fracture and Failure

A bolt fails when it can no longer provide the support it is designed for. Fracture is the separation of a solid body into two or more parts under the action of stress. It consists of crack initiation and propagation.

Ductile fracture is characterized by considerable plastic deformation prior to and during propagation of the crack. An important amount of gross deformation is usually present at the fracture surfaces. Figure 7.63 is an example of a ductile fracture of a Swellex bolt. Note the failure plane at 45° and localized reduction of the surface.

Brittle fracture in metals is characterized by a rapid rate of crack propagation, with no gross deformation and very little microdeformation. This is demonstrated by cleavage. Brittle fracture can occur without warning. Cleavage fracture exhibits little or no plastic deformation and occurs along well-defined crystallographic planes.

A 'dimple' is a concave depression on the fracture surface resulting from microvoid growth in coalescence. As a result of the state of stress during fracture, the dimple may be elongated, oval or equiaxed.

The average composition of Swellex bolts is given in Table 7.5.

Visual appearance of a fracture is shown in Figure 7.63.

Figure 7.63 *Visual examination of a fracture*

Table 7.5 *Swellex bolt composition, SAE J403 grade 1010*

C	Mn	Ni	P	S	Mo	Si	Al	Cr	Cu
0.099	0.377	0.017	0.005	0.010	0.003	0.041	0.038	0.022	0.034

Figure 7.64 shows a failed bolt where the failure surface is investigated by SEM at 1000 magnification. The observed dimples are relatively shallow with respect to the surface and oblique. The presence of inclusions as in (A), characteristic of this type of steel that initiate dimples. The shape and orientation of dimples can be used to indicate the direction and application of load as well as the degree of ductility of the samples. In this case, as the dimples are parallel to the direction of fracture, this was classified as a shear fracture.

Figures 7.64 and 7.65 provide a view of the fracture surface of a bolt recovered following a fall of ground from a hardrock mine. This is at magnification $\times$ 10. A close-up of dimpled areas is presented in Figure 7.66, at a magnification $\times$ 1500. The dimples are shallow and inclined characteristic of ductile fracture. No sign of cleavage or quasi-cleavage, is observed (absence of 'river' pattern that would be associated with brittle fracture). In the upper right part of the photo dimpled areas are masked by oxidation.

Metallographic analysis allows the determination of the surface reduction along the fracture and defines the fragile or ductile nature of the fracture. By employing a longitudinal section, it was possible to evaluate the magnitude of corrosion close to the surface of the fracture.

Figure 7.67 shows an extremely irregular attack of the external surface of a longitudinal section of rock bolt. The presence of the oxide layer in Figure 7.67 and the dispersion of a metallic piece in Figure 7.68 support the analysis that, for this particular rock bolt, corrosion attack was rigorous and probably contributed in the failure of the rock bolt.

It is useful to conduct metallographic analysis of the transverse sections, far away from the fracture surface as a reference. Figure 7.69 is a micrograph which shows typical equiaxed grains, free from plastic deformation. However, oblique section metallography through the fracture surface shows the presence of elongated grains developed during shearing at failure (Figure 6.70).

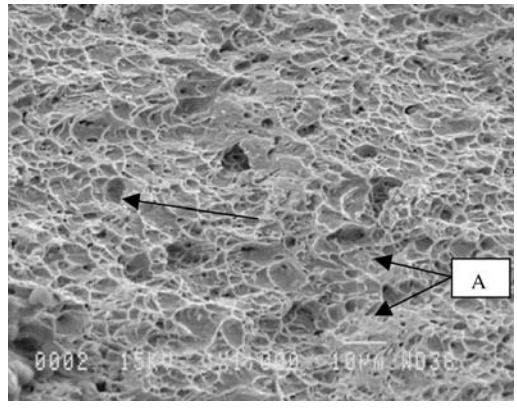

Figure 7.64 *Fractography of a Swellex bolt*

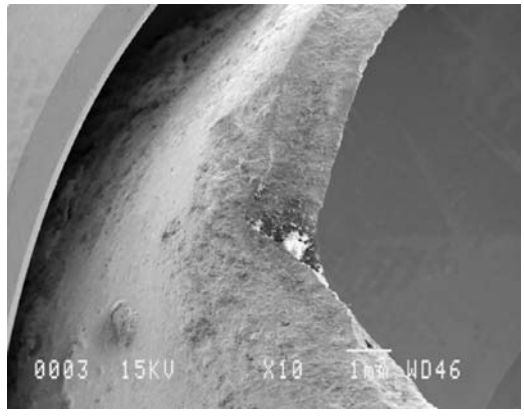

Figure 7.65 *Fractography of failure surface, × 10*

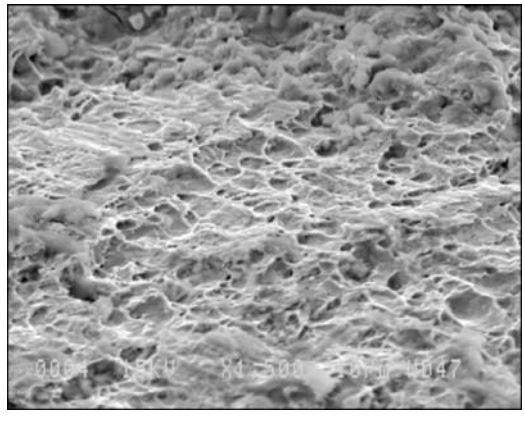

Figure 7.66 *Close-up of the failure surface of Figure 7.64, × 1500*

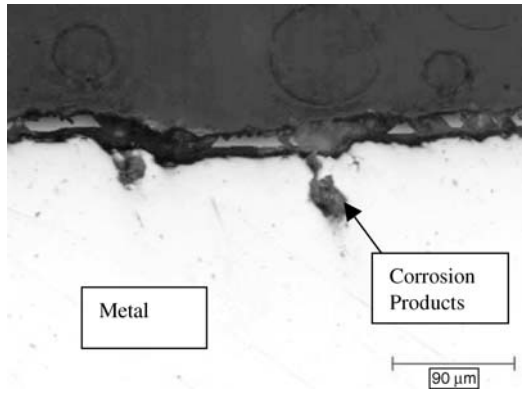

Figure 7.67 *Longitudinal section showing extreme localized attack and fragmentation of the metallic surface*

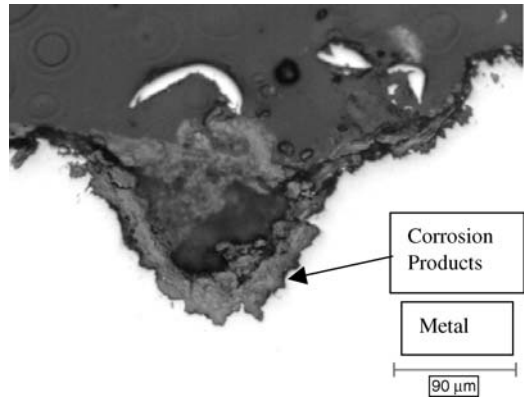

Figure 7.68 *Longitudinal section displaying extreme localized attack and fragmentation of the metallic surface*

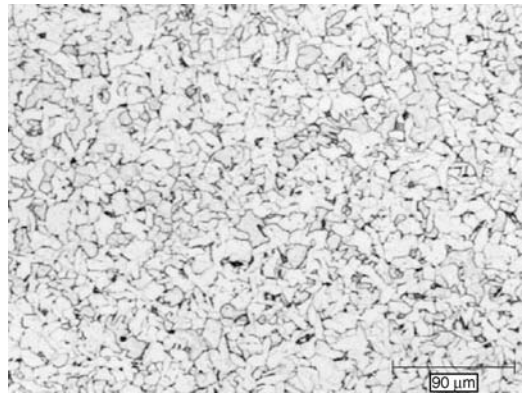

Figure 7.69 *Micrograph away from the fracture surface, showing equiaxed grains*

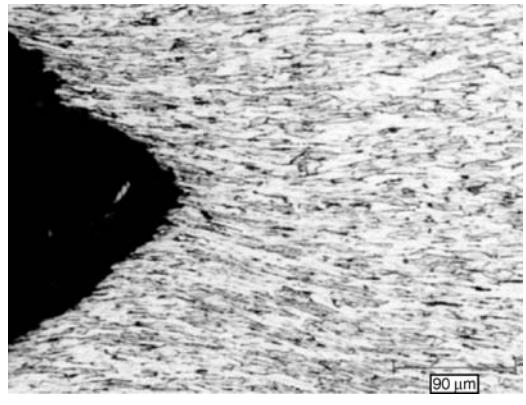

Figure 7.70 *Oblique section metallograph showing elongated grains*

References

1. J. Hadjigeorgiou and F. Charette, Rock Bolting for underground Excavations, Chap. 63 of *Underground Mining*, Society of Mining Engineers, Hustrulid & Bullock, eds, pp 547–554, 2001.
2. V.S. Sastri, G.R. Hoey and R.W. Revie, CIM Bulletin, p. 87–99, 1994.

7.15 Failure Analysis of 316L Stainless Steel Tubing of a High-pressure Still Condenser

7.15.1 Problem

Corrosion problems were observed with stainless steel tubing of a high-pressure still condenser employed for ammonia recovery. The feed solution in the high-pressure still is typically 135 g/L ammonia and 4.7 g/L CO_2. Figure 7.71 shows a simplified view of the high-pressure still (HPS) and condenser.

The HPS condenser is made of 316L seamless tubes with a nominal outer diameter of 25 mm, a nominal wall thickness of 2.2 mm and a length of 6.4 m. The tube ends are joined to the tube sheet (100 mm thick) to form a bundle 1.1 m in diameter that is welded to the shell to make up the shell-and-tube condenser. The tubes are weld sealed at the top of the tube sheet as shown in Figure 7.72. The condenser is installed vertically with severe operating conditions[1] at the inlet of the top tube sheet as the temperature reaches 150°C and pressure 250 psi.

Corrosion has resulted in leak failures of many tubes and led to several shutdowns. The corrosion attack was evident in the top 100 mm where the tube was expanded (rolled) to

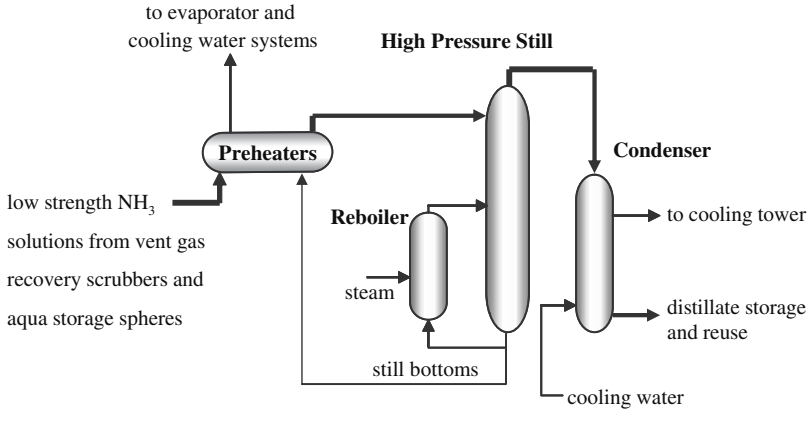

Figure 7.71 *A simplified view of the high-pressure still (HPS) and condenser. (Reproduced from COM'1999 and 2005 with permission from the Metallurgy Society of CIM)*

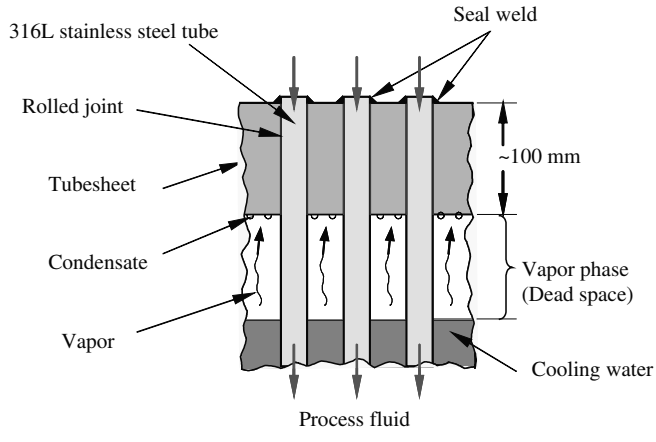

Figure 7.72 *Schematic, showing a section of the top portion of the HPS condenser (corrosion end). (Reproduced from COM'1999 and 2005 with permission from the Metallurgy Society of CIM)*

join the top tube sheet, but the rest of the tube was still intact and in its original condition. The rolled end of the tube is referred to as the corrosion end.

Repairing the condenser by plugging the leaking tubes was unsuccessful, as evidenced by severe corrosion of the plugs, top tube sheet and seal welds. Plugging the tubes affected flow and caused turbulence which eroded the passive film on the steel plugs and the top plate severe corrosion of the plugs, top tube sheet and seal welds was evident.[2]

7.15.2 Material

Table 7.6 shows the chemical composition of SA213 316L stainless steel. The microstructure was determined to be an equiaxed structure with average grain size of ~50 μm, measured by the mean intercept method.

7.15.3 Results

A portion of the tube about 3 cm long containing the cracks was cut and examined by SEM. The inner surfaces of the three tubes were covered with a mixed black/brown scale that extended for about 100 mm over the length of the tube-to-tubesheet joint. The

Table 7.6 *Nominal chemical composition (wt %) of the 316L stainless steel*

Cr	Ni	C	Mn	P	Cu	Co	Mo	Fe
16.2	12.1	0.02	1.6	0.0293	0.39	0.2	1.6	Bal

Figure 7.73 (Plate 8) *Section of tube showing the inner surface covered with a mixed black/brown scale that extended over the rolled portion of the tube for ~100 mm. (Reproduced from COM'1999 and 2005 with permission from the Metallurgy Society of CIM)*

remaining part of the tubes' inner surfaces appears to be unaffected, and the original protective oxide layer was still intact. A section of tube A is shown in Figure 7.73 where the inner surface was covered with a mixed black/brown scale that extended over the whole length of the tube joint.

7.15.4 SEM Examination

SEM examination revealed several major circumferential cracks, ranging from 3 to 4 mm long. Table 7.7 lists the number of major cracks seen on each tube. Figure 7.74 is an example of a circumferential crack seen in tube B. Circumferential cracks appeared to grow in a zigzag fashion with their tips close together. Figure 7.75 is an optical photo of a typical chloride SCC propagated in the axial direction. Some smaller cracks showed a combination of axial and circumferential growth. Microcracks were also observed as well as signs of crevice corrosion in the rough area adjacent to the cracks shown in Figure 7.74. Because oxygen diffusion into the crevice is restricted, a differential aeration cell is formed between the crevice and the bulk environment. Differential cells can lead to the creation of highly corrosive conditions, even in a benign bulk environment.

Longitudinal sectioning of the tube wall revealed multiple crack initiation that took place on the outer surface of tube B as shown in Figure 7.76. Note the direction of the crack growth shown in Figure 7.76 is from top (outer surface) to bottom (inner surface).

Table 7.7 *Number of major cracks and their orientations observed for each tube*

	Longitudinal cracks	Circumferential cracks	Mixed orientation
Tube A	0	0	0
Tube B	0	4	1
Tube C	1	6	1

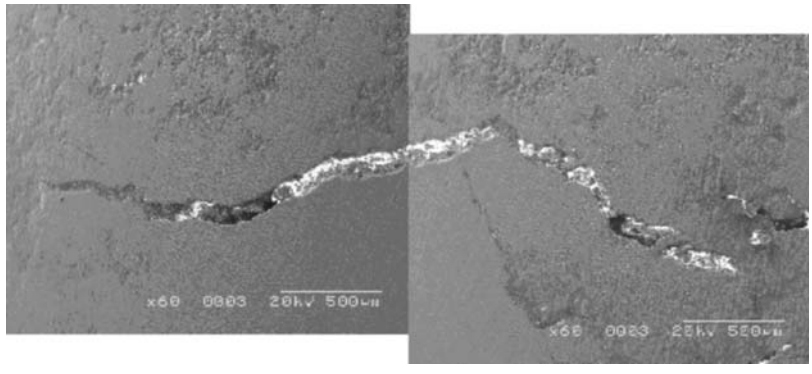

Figure 7.74 *SEM photo of one of the major circumferential cracks observed in tube B. (Reproduced from COM'1999 and 2005 with permission from the Metallurgy Society of CIM)*

The cracks showed significant branching. In the case of tube B, none of the cracks penetrated the wall thickness; they appeared to extend through only about one third of the wall thickness. Cracks propagated in both axial and circumferential directions to form semi-elliptical cracks. The cracks were fine in the early stages of growth, and they widened by secondary corrosion at a later stage due to the aggressive crevice conditions. More cracks were evident in tube C with significant secondary corrosion leading to wider cracks. In some cases, wide cracks appeared to develop into deep pits. Figure 7.77 shows one of the cracks that penetrated the whole wall thickness and resulted in a leak failure accompanied with significant plastic deformation. Tube A was the least attacked, and it showed much smaller cracks.

7.15.5 Conclusions

Failure analysis revealed that the tubes had suffered both internal and external corrosion attack; the corrosion attack was confined to the region within the joint between the tube

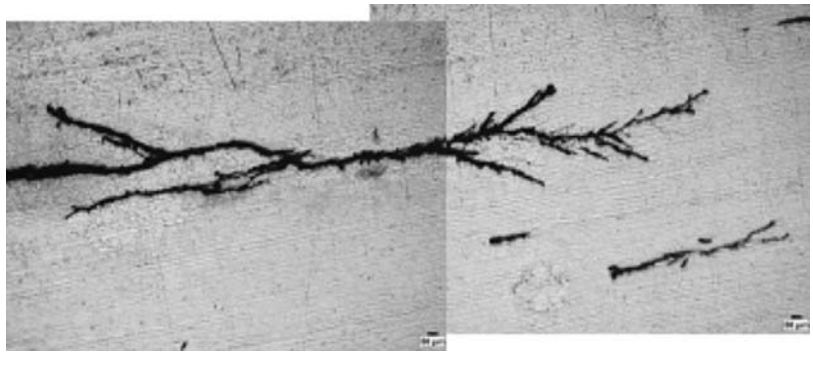

Figure 7.75 *Optical photo of typical chloride SCC of austenitic stainless steel observed in the longitudinal direction in tube C. (Reproduced from COM'1999 and 2005 with permission from the Metallurgy Society of CIM)*

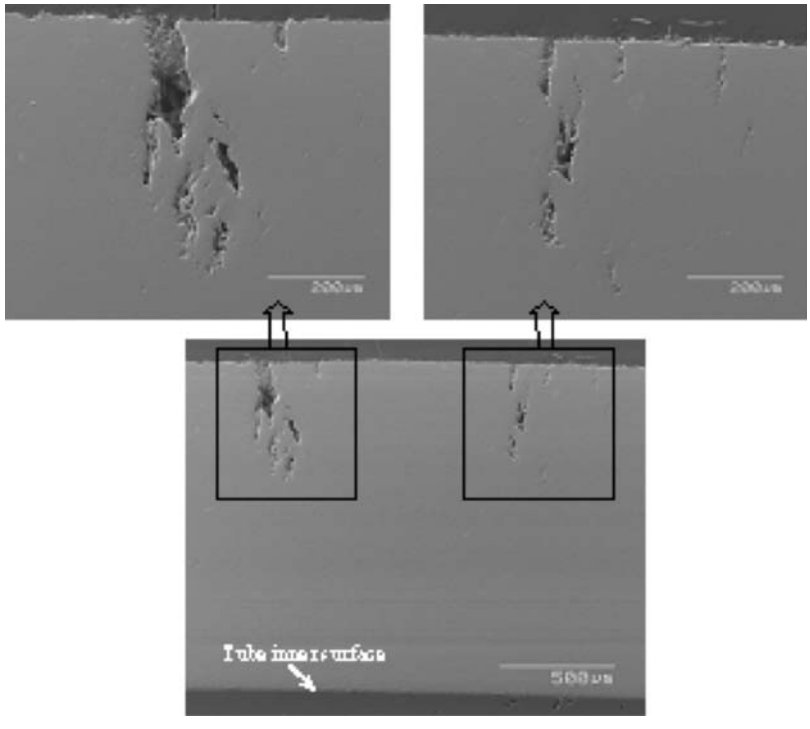

Figure 7.76 *Longitudinal section of tube B wall, showing branching and multiple initiation of SCC at the external surface of the tube. (Reproduced from COM'1999 and 2005 with permission from the Metallurgy Society of CIM)*

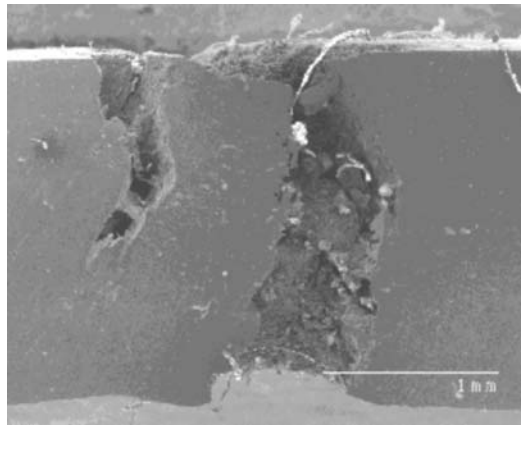

Figure 7.77 *A circumferential crack that penetrated the whole thickness of tube C, resulting in a leak failure*

and tubesheet. Inlet erosion corrosion was observed inside the tube throughout the length of the joint due to the process fluid that contained ammonia, CO_2 and ammonium carbonate solution. Stress–corrosion cracking and crevice corrosion was evident on the external surface of the tube at the rolled end. It was concluded that SCC occurred due to the chloride buildup in the shielded area at the joint in the absence of proper venting. Some of the cracks grew throughout the whole thickness and ultimately led to leakage failure. Most of the SCC attacks were oriented in the circumferential direction, suggesting that the primary source of stress was the tensile residual stress in the axial direction that was created due to tube rolling of the joint. Results suggest that poor venting and tube end over-rolling appear to play a major a role in the degradation of the tube in such a short time.

7.15.6 Prevention

1. Greater care should be taken and proper procedures followed by the condenser manufacturer when rolling the tube ends to avoid excessive wall reduction and tube extrusion. To prevent crevice corrosion in the tube-to-tubesheet joint, the tube end should be rolled for the full thickness of the tube sheet.[12]
2. Proper venting of the condenser to eliminate the dead space below the top tubesheet is extremely important. This is to ensure that there is no vapor space and that the tubes will be wet all the time, thus avoiding wetting and drying cycles.[10] About one-third of SCC failures were caused by the existence of a vapor phase.[12,13] The proper method of venting vertical water-cooled condensers, is given in the MTI Manual.[4]
3. Development of an effective cooling water treatment that minimize chloride and oxygen contents[14] would be beneficial.
4. Stress-relief by heat treatment or shot peening is recommended subsequent to rolling of the tube ends to reduce residual stress to a level at which SCC is less likely to occur.
5. Using thin-walled metallic tube shields over the inlet end to combat erosion/corrosion of tube inner surface[5], is recommended.

References

1. T.M. Ahmed and A. Alfantazi, *High Temperature High Pressure Corrosion in Ammonia Carbamate Environments: Literature Review*, Report submitted to Sherritt International Corporation, November 2004.
2. S. Yakemchuk and D. Roth, *Equipment Inspection Report*, Sherritt Final Report, S.O. 343371, November 23, 2003.
3. C.P. Dillon & Associates, *Guidelines for Control of Stress Corrosion Cracking of Nickel-bearing Stainless Steels and Nickel Alloys*, MTI Manual No. 1, The Materials Technology Institute of the Chemical Process Industries Inc., 1979.
4. P.M. Tallman, Restore Corroded Heat Exchanger Tubes, *Chemical Engineering Progress*, **96**(8), 47–50 (2000).
5. M. Allam, A. Chaaban and A. Bazergui, Estimation of Residual Stresses in Hydraulically Expanded Tube-to-Tubesheet Joints, *Journal of Pressure Vessel Technology*, **120**, 129–137 (1998).
6. D.R. McIntyre, Evaluation of the Cost of Corrosion-Control Methods, *Chemical Engineering*, April 1982, 127–132.

7. X. Hu, X. Renb, X. Chen, W. Han and F. Zou, A Study on the Corrosion of 316L Stainless Steel in the Media of High-Pressure Carbamate Condenser, *Proceedings of the Asian-Pacific Corrosion Control Conference*, Bangkok, December 6–11 1993, 237–244.
8. S. Yokell, Expanded and Welded-and-Expanded Tube-to-Tubesheet Joints, *Journal of Pressure Vessel Technology*, **114**, 157–165 (1992).
9. S. Haruyama, Stress Corrosion Cracking by Cooling Water of Stainless-Steel Shell and Tube Heat Exchangers, *Materials Performance*, March 1982, 14–19.
10. C.R. Ascolese, D.I. Bain, Take Advantage of Effective Cooling Water Treatment Programs, *Chemical Engineering Progress*, **94**(3), 49–54 (1998).

7.16 Failure of a Landing Gear Steel Pin

The landing gear pin is shown in Figure 7.78 and the arrow indicates the location of the failure. The failure occurred in 1.23 inch diameter cylindrical part of the pin which was corroded on the outer surface. The fractured surface is shown in Figure 7.79. Convergent chevron patterns are seen at the initiation site. The fracture surface is covered by the dark corrosion product. A set of coarse low-cycle fatigue crack arrest marks were present at the ends of two discolored crack propagation fronts. The exterior surface of the cylindrical part of the pin had corrosion pits. Pitting corrosion was also seen at the fracture initiation site.

Figure 7.78 *Landing gear pin failure.[1] (Reprinted with the permission of M. Zamanzadeh, ATCO Associates, Pittsburgh, USA)*

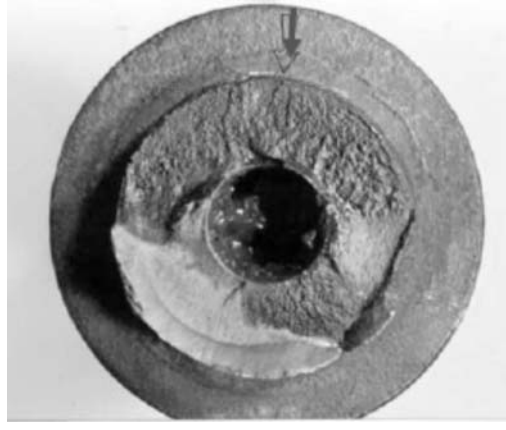

Figure 7.79 *Fracture surface shows convergent chevron patterns as the fracture initiation site.[1] (Reprinted with the permission of M. Zamanzadeh, ATCO Associates, Pittsburgh, USA)*

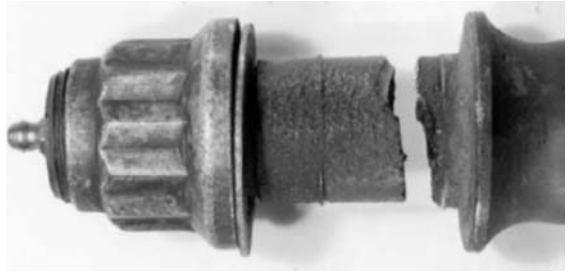

Figure 7.80 *Fracture surface profile shows the presence of a circumferential ridge and depression.*[1] *(Reprinted with the permission of M. Zamanzadeh, ATCO Associates, Pittsburgh, USA)*

The fracture surface profile is shown in Figure 7.80. The presence of a circumferential ridge and depression in the cylindrical surface is to be noted in the case of both the broken and reference pins. By comparing the cylindrical parts of the broken pin with the reference pin it was concluded that the fracture of the broken pin initiated at the circumferential depression. Macroetching with 50% hydrochloric acid for 30 s enabled the identification of fracture initiation site in Figure 7.80.

A transverse cross-section through the fracture initiation site was examined by metallography. The fracture surface profile was found to be relatively flat and there was no crack branching. The microstructure showed dark-etching-tempered martensite. Further no plastic deformation was observed at the fracture initiation site.

It is concluded that the pin failed due to fatigue initiated at the outside cylindrical surface where wear and pitting corrosion occurred. The fracture initiated at a shallow circumferential groove and corrosion of the fracture occurred after the rupture. There was no evidence of stress–corrosion cracking.

Reference

1. M. Zamanzadeh, E. Larkin and D.Gibbon, *A Re-Examination of Failure Analysis and Root Cause Determination*, Matco Associates, Pittsburgh, Pennsylvania, December 2004.

7.17 Hydrogen-induced Cracking

Hydrogen-induced cracking (HIC) is one of several related mechanisms whereby absorbed hydrogen atoms can compromise the integrity of components manufactured from low-strength steels. HIC is a term applied to phenomena which occur at low temperatures (typically less than about 90°C), and must not be confused with high-temperature hydrogen attack of low-strength carbon-manganese and low-alloy steel materials exposed to hot hydrogen-gas-containing environments. Several different names have been used to identify the types of hydrogen-related damage which have been observed in low strength steels:

- *Hydrogen-induced cracking (HIC):* The development of internal cracks in low strength steels as a consequence of the trapping of absorbed hydrogen atoms (H atoms) as gas

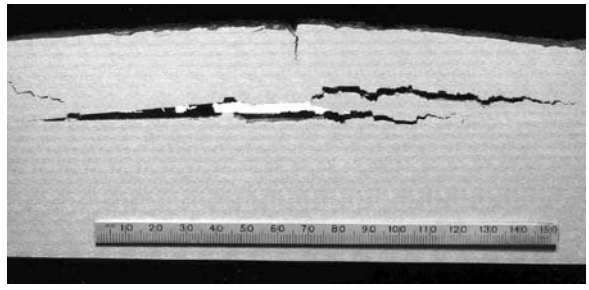

Figure 7.81 *Hydrogen-induced cracking in plate steel exposed to sour gas. (Courtesy of Malcolm Hay)*

molecules (H_2 molecules) at inhomogeneities is termed HIC. The cracks most often (but not always) lie parallel to the rolling plane and the surfaces of the steel component. Residual or applied tensile stress is not needed for HIC development (Figure 7.81).

- *Hydrogen blisters or hydrogen-induced blister cracking (HIBC):* Blisters are a form of HIC in which the build-up of hydrogen gas pressure at the initiated cracks or pre-existing (mill) laminations results in localized deformation and bulging of the steel to the closest surface (or to both surfaces, if mid-wall). Hydrogen gas pressures as high as 2700 psi (18.6 MPa) have been measured inside blisters. Blisters often occur when the hydrogen-induced crack is unable to propagate further parallel to the surface, and is unable to link up with HIC on adjacent planes in the steel. This may be because the hydrogen-atom-trapping inhomogeneity which caused the blister to form has a finite length, or there are no other hydrogen-induced cracks in close proximity (same or adjacent planes, Figure 7.82).
- *Stepwise cracking (SWC):* SWC is a form of HIC in which adjacent cracks on different planes in the steel link-up in a stepwise fashion. This may lead to through-wall cracking and the loss of vessel integrity. Applied or residual stress is not necessary for SWC development. The hydrogen gas pressure inside HIC cracks or blisters can increase to hundreds of atmospheres. This pressure generates internal stress at the tips of the HIC cracks, resulting in localized plastic deformation of the

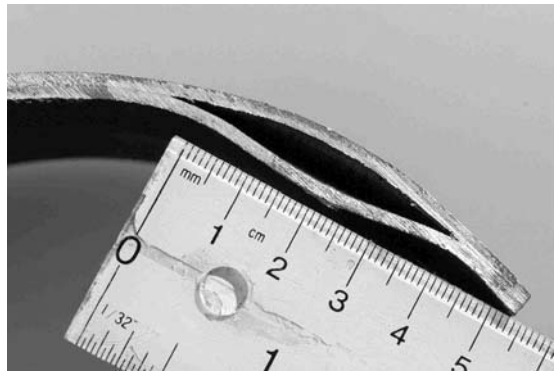

Figure 7.82 *Hydrogen blister in NPS 6 sour gas pipeline (Courtesy of Malcolm Hay)*

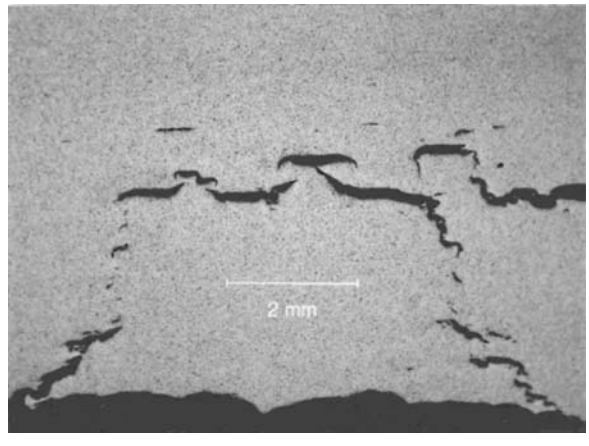

Figure 7.83 *Stepwise cracking in plate steel exposed to sour gas (Courtesy of Malcolm Hay)*

steel. The cold-worked steel is susceptible to hydrogen embrittlement cracking (HEC), which is the mechanism of link-up (Figure 7.83).

- *Stress-oriented hydrogen-induced cracking (SOHIC):* The presence of tensile stress in the component may cause individual ligaments of HIC to form in a stacked, through-thickness array. This is a necessary precursor to what is called SOHIC. This array is oriented perpendicular to the principal applied stress. The HIC may subsequently completely link up to cause through-wall cracking and loss of vessel integrity, i.e., SOHIC. SOHIC, like SWC, is probably a combination of HIC and either hydrogen embrittlement cracking (HEC) or sulfide stress cracking (SSC). HEC and SSC are possible in low-strength steels if the material is highly stressed, especially if it is plastically deformed and there is a stress-concentrating mechanism, and there is a high enough hydrogen atom charging rate. SOHIC is most common in the heat-affected zones (HAZs) of welds in low-strength steels, though can form in the base material (Figure 7.84).

7.17.1 Extent of Problem: Failures due to Hydrogen-induced Cracking

HIC has especially been reported in low-strength steels exposed to sour oil and gas environments. HIC has also been reported in other industries where hydrogen

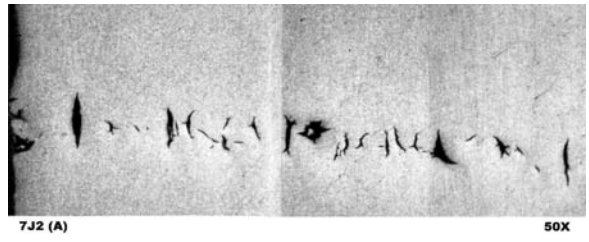

Figure 7.84 *Stress-oriented hydrogen-induced cracking in linepipe (× 50) (Courtesy of Malcolm Hay)*

atom charging is possible, for example in vessels in anhydrous hydrofluoric acid service, in the cathodes of electrochemical cells, and where over-cathodic protection of pipelines has occurred. HIC has been recognized as being a problem in the production and processing of sour hydrocarbons (oil, condensate and gas) for over 50 years. The equipment most commonly affected in the oil and gas industry has been gathering system pipelines, and gas plant and refinery pressure vessels (Table 7.8). Coiled tubing used in sour oil and gas wells is also potentially vulnerable to hydrogen damage mechanisms including HIC and SOHIC. Failures of sweet gas transmission pipelines have been ascribed to over-cathodic protection or other mechanisms in which the hydrogen atom charging is from the outside surface rather than the internal surface.

7.17.2 HIC Development and Failures Occur Predominantly in Welded Pipe

Failures have occurred in both single and double submerged arc-welded (SAW and DSAW) (Figures 7.85, 7.86). Failures have also occurred in electric-resistance-welded

Figure 7.85 *SOHIC failure of NPS 16 spiral-welded linepipe (Courtesy of Malcolm Hay)*

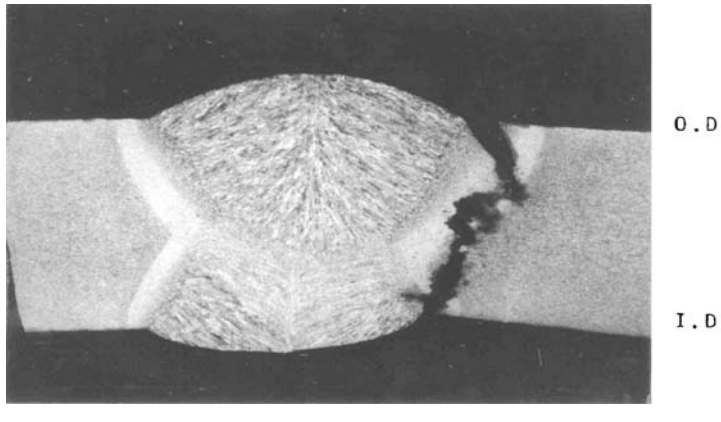

Figure 7.86 *Cross-section through SOHIC in spiral-welded linepipe (Courtesy of Malcolm Hay)*

Table 7.8 *HIC-related damage and failures of linepipes (Courtesy of Malcolm Hay)*

Material				Service and performance					Reference
Specification and type	Grade (MPa)	Size (NPS)	Wall Thickness (mm)	H_2S (mol %)	CO_2 (mol %)	Temperature (°C)	Pressing (MPa)	Comments	
API 5L-X52 DSAW	359	16 and 24	6.88	1.0	15.0		6.9	Uninhibited; several ruptures at blisters	1, 2
API 5L-X52 spiral DSAW	359	16	9.53	2.2	4.0			Inhibited; failed in weld HAZ within 48 h	3
API 5L-X42 ERW	290	16	8.76	1.0	8.7		4.5	Blistering, SWC and rupture after a few months	4
API 5L-X60 SAW	414	30		Sour oil				Failed by SWC after a few months	5
API 5L-X42 spiral SAW	290	24	6.35	3.4	8.8	85	2.4	Three ruptures near spiral weld; HIC over	6, 7
Sour gas pipeline				1.5	8.9	50	0.7	Cracked after 5 yrs	7
API 5L-X52 ERW	359	8	4.78	6.0				Inhibited; ruptured at midwall blister	3
CSA Z245.5 spiral DSAW	386	16	9.53	2.2	4.0		7.6	Rupture/SOHIC in weld HAZ after 30 h	
CSA Z245.5 spiral DSAW	359	16	9.53	15.0	4.3	35	7.5	Rupture/SOHIC in weld HAZ after 40 h	
API 5L-X52 SAW	359	24	12.70	3.0	8.5		9.8	Extensive HIC within months	9
CSA Z245.3 ERW	290	3	3.96	1.6	5.7	17	7.0	Rupture along HIC-damaged during ERW	10
API 5L-X60 SAW	414	24	12.70	8.6	7.8	60	2.8	Crude oil + 140 ppm H_2S; leaked at blister	11

API 5L-X42 ERW	290	12	7.11	3.7	8.8	66	1.7	Blistering at pre-existing (mill) laminations	11
API 5L-X42 ERW	290	8	7.20	23.0	8.5		8.9	SOHIC and rupture after 7.4 yrs	12
API 5L-X60 SAW	414	34	9.25	10 ppm	4.0		4.8	Ruptures at blisters after 12 yrs	13
API 5L-X60 spiral SAW	414	34	7.80	0		20	3.6	Crude oil; over-cathodic protection	14
CSA Z245 ERW	290	4		9.0			8.3	Rupture after 9 yrs	10
ASTM A106 seamless		12	5.99	turned sour				Rupture at SWC after 24 yrs	15
API 5L-B seamless	241	10	9.27	3.2	6.5	20	0.8	Leaked at blister/SOHIC after 41 yr	16,17
CSA Z245.2 DSAW	483	42	12.00	0	0	18	8.3	Rupture at midwall HIC/SWC after 12 yrs	18
CSA Z245 ERW	359	6	4.00	2.0	4.5			Rupture at midwall blisters after 5 yrs	19
API 5L-B seamless	241			'High'		49	5.5	Rupture due to HIC/SOHIC at pits after 1 yr	20

Figure 7.87 *NPS 3 linepipe ruptured during hydrotest due to HIC at ERW (Courtesy of Malcolm Hay)*

(ERW) pipe (Figures 7.87, 7.88). HIC may develop in the base material or in the weldment. The chemical composition and processing that occurs during the manufacturing of the skelp (flat-rolled plate) used to make welded pipe encourages the formation of the inhomogeneities responsible for trapping diffusing hydrogen atoms, leading to HIC damage. The manufacturing route followed does not result in the formation of hydrogen damage initiation sites, or at least does not result in a high density of these inhomogeneities compared with welded pipe. However, a failure of a seamless linepipe (Figures 7.89, 7.90) has been reported by Malcolm Hay (lecture delivered at the Conference of the Metallurgical Society CIM 2003, Vancouver, BC, Canada).

Figure 7.88 *Cleaned pipe: HIC-damaged and inhibitor-protected surfaces (Courtesy of Malcolm Hay)*

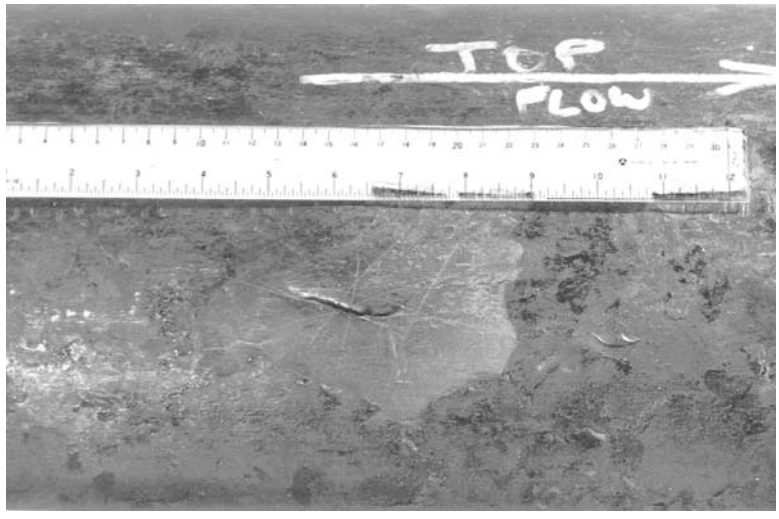

Figure 7.89 *Leak location at blister in seamless linepipe (Courtesy of Malcolm Hay)*

7.17.3 Pipeline Failure

Table 7.8 was constructed from literature sources.[1–20] The table demonstrates the great variety of materials and conditions under which HIC failures have occurred. Although the impetus to understand the HIC phenomenon and develop HIC-resistant linepipe and other materials (e.g., pressure vessel plate) started after several failures in the Middle East in the early 1970s, failures had been reported at least as early as 1954. Despite the availability of adequately HIC-resistant linepipe since the late 1970s, failures are still occurring in pipelines constructed since that time.

7.17.4 Mechanism of Hydrogen-induced Cracking

HIC occurs when H atoms diffusing through a linepipe steel become trapped as H_2 molecules at inhomogeneities in the steel. A planar, gas-filled defect is created, which grows parallel with the vessel surfaces as it traps more diffusing H atoms. If the

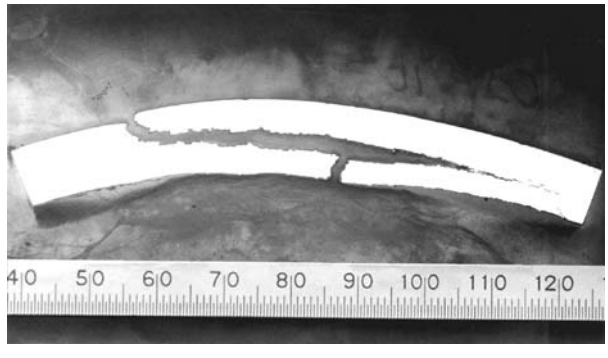

Figure 7.90 *Cross-section through leak location in seamless linepipe (Courtesy of Malcolm Hay)*

defect grows sufficiently large, it may cause blister formation. HIC failure occurs if a mechanism exists for linkage of one or (normally) more nearby defects or blisters with the internal and external vessel surfaces. Possible linkage mechanisms are SWC and SOHIC.

The H atom source is normally the cathodic reaction of an acid corrosion mechanism occurring at the internal vessel surface, i.e., the reduction of hydrogen ions, H^+:

Anodic reaction: $Fe \rightarrow Fe^{2+} + 2e^-$

Cathodic reaction: $2H^+ + 2e^- \rightarrow 2H_{ads}$

The H atoms produced by the cathodic reaction are adsorbed onto the steel surface. They may combine to form a H_2 gas molecule, which enters the internal vessel environment. Alternatively, they may become absorbed into the steel:

H_2 gas formation: $H_{ads} + H_{ads} \rightarrow H_2$ (H_2 evolved from steel surface)

H atom absorption: $H_{ads} \rightarrow H_{abs}$ (H atom enters steel)

The presence of specific chemical species in the corrosive environment 'poisons' or retards the rate of the H_{ads} atom combination reaction, thereby permitting a higher fraction of the H atoms generated by corrosion to become absorbed by (enter into) the steel. Bisulfide ions (HS^-), formed when H_2S molecules are dissolved in water, are very effective H atom combination poisons. Other effective H atom combination poisons are cyanide ions (CN^-) and arsenic ions (As^{3+}).

References

1. F. Paredes and W. W. Mize. Hydrogen Blisters - Their Causes and Methods of Prevention. *Gas* **40**(12) 89 (1954).
2. F. Paredes and W. W. Mize. Unusual Pipeline Failures Traced to Hydrogen Blisters. *Oil and Gas Journal* **52**(12) 99 (1954).
3. D. N. Williams. *Correlation of the Results of Stepwise Cracking Tests with Service Experience in Sour Gas*. Battelle report to NG-18 Line Pipe Research Supervisory Committee of the American Gas Association, October 1983. NG-18 Report 138.
4. I. Class. Report on Investigation of Sulfide Stress Corrosion Cracking of Steels, Particularly of Steels of Comparatively Low Tensile Strength. Second International Conference on Metallic Corrosion, New York, U.S.A., 1963-03-11/15, pp 342–355 (NACE 1966).
5. J. Leslie, J. A. King. Sour Gas Pipelines. Paper OTC 5741, Volume 2, pp 499, 20th Annual Offshore Technology Conference, Houston, Texas, U.S.A., 1988-05-02/05.
6. Nippon Steel Corporation. The Investigation of the Cause of Gas Pipe Failure. NSC Report 1975-10-20.
7. E. M. Moore, D. A. Hansen. Specifying Linepipe Suitable for Safe Operation in Sour, Wet Service. Transactions ASME, Journal of Energy Resources Technology **104**, 134, (1982), and ASME 81-PET-1.
8. E. M. Moore, J. J. Warga. Factors Influencing the Hydrogen Cracking Sensitivity of Pipeline Steels. NACE Corrosion/76 Paper 144, Houston, Texas, U.S.A., 1976-03-22/26, and Materials Performance **15**(6), 17 (1976).
9. I. M. El-Jundi. Qatar NGL-2 Pipeline Problems. Society of Petroleum Engineers Production Engineering **1**(6), 478 (1986).
10. Alberta, Canada, Energy Resources Conservation Board data, including Pipeline Integrity Workshop, 1992-10-08.

11. E. M. Moore. Hydrocarbon-Induced Damage in Sour, Wet Crude Pipelines. SPE 11514, Middle East Oil Technical Conference of the Society of Petroleum Engineers, Manama, Bahrain, 1983-03-14/17.
12. W. Bruckhoff, O. Geier, K. Hofbauer, G. Schmitt, D. Steinmetz. Rupture of a Sour Gas Line Due to Stress Oriented Hydrogen Induced Cracking - Failure Analyses, Experimental Results and Corrosion Prevention. NACE Corrosion/85, Paper 389, Boston, USA, 1985-03-25/29.
13. A. M. Kurdi, M. S. Abougfeefa, A. K. Denney. Rehab Permits Desert Line to Run at Original Pressures. Oil and Gas Journal, **91**(30), 76 (1993). (Fourth European and Middle Eastern Pipeline Rehabilitation Seminar, Abu Dhabi, United Arab Emirates, 1993-04-24/27.)
14. A. Punter, A. T. Fikkers, G. Vanstaen. Hydrogen-Induced Stress Corrosion Cracking on a Pipeline. Materials Performance **31**(6), 24 (1992). (Proceedings of the Pipe Protection Conference, Cannes, France, 1991.)
15. S. Y. Gajam, A. El-Amari. Failure of a Gas/Condensate Line. Materials Performance **31**(10), 55 (1992).
16. M. G. Hay, M. D. Stead. The Hydrogen-Induced Cracking Failure of a Seamless Sour Gas Pipeline. NACE Canadian Region Western Conference, Calgary, Canada, 1994-02-07/10.
17. M. G. Hay, D. W. Rider. Integrity Management of a HIC-Damaged Pipeline and Refinery Pressure Vessel Through Hydrogen Permeation Measurements. NACE Corrosion/98 Paper 395, San Diego, California, U.S.A., 1998-03-22/27.
18. Commodity Pipeline Occurrence Report - Natural Gas Pipeline Rupture. Transportation Safety Board of Canada Report Number P94H0003, 1995-08-23.
19. P. Jones, T. Hetu. A Case Study of Hydrogen Induced Cracking Failure - Investigation, Remedial Action and Maintenance. NACE International, Calgary Section, One Day Seminar on Failure Mechanisms, Calgary, Alberta, Canada, 1998-04-07.
20. B. D. Craig, T. V. Bruno, W. M. Buehler. Complexities of Failure Analyses in Sour Systems. Canadian Welding Society/American Society for Metals conference 'Materials and Welding for Sour Service and Low Temperature Service'. Calgary, Alberta, Canada, 1997-11-20/21.

7.18 Micromechanisms of Liquid and Solid Metal-induced Embrittlement

The importance of this phenomenon is in the development of safe accelerator-driven nuclear reactors/incinerators; heavy liquid metals are used spallation targets, as well as coolants; solid metals are used as protective coatings.

Liquid metal-induced embrittlement (LMIE), particularly solid metal-induced failure result in accelerated brittle failure on normally ductile metals under applied or residual stresses when in contact with liquid or solid low-melting point metal. SMIE was first noted as the delayed failure of steels in solid Cd environments.

7.18.1 Liquid Metal-induced Embrittlement (LMIE)

Typical experimental data on the crack growth rate vs stress intensity factor in LMIE conditions are shown in Figure 7.91. Large cracks are at the top portion (>2 mm) and small cracks (<2 mm) are located at the bottom of the figure and reflect the kinetics of growth of cracks. The micromechanism of crack growth is different in the upper and lower regions.

The two micromechanism of LMIE are: (i) the dissolution–condensation model (DCM); and (ii) the adsorption-induced localized slip model. In the DCM mechanism the crack is filled with melt and grows by dissolution of atoms from the crack tip where the chemical potential is increased due to applied stress.[1,2] In the second model,

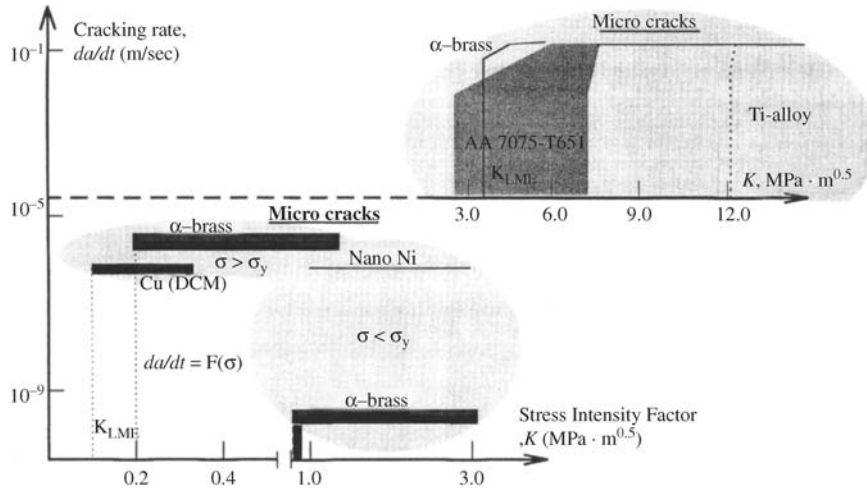

Figure 7.91 *Typical experimental data on CGR vs stress intensity factor K under LMIE Conditions; Liquid metal = Hg*

adsorption of liquid metal atoms ejects dislocations from the crack tip and thus advances the crack.[3] Both the models are depicted in Figure 7.92. The main difference in the two models is the role of dislocations in the process of crack growth. Dislocations are not required for crack extension in the dissolution model while they are directly involved in the adsorption-induced localized-slip model.

Nanocrystalline material (which is free of dislocations) such as nickel was tested for delayed fracture in the presence of mercury. The fracture surface shown in Figure 7.93 has three zones. Zone I shows initial microcrack, and zone III shows the final failure stage. Zone II, of the order of 100 μm width, appears different from zones I and III and shows the path of crack growth. This shows that dislocations are not involved in the crack growth in LMIE conditions of dissolution–condensation model of LMIE is favored.

The dissolution–condensation-model (Figure 7.91) adequately explains the crack growth rate and its dependence on stress, temperature and interfacial energy for short cracks. This model does not account for high crack growth rates and hence a third-party process involving the plastic zone has been involved.

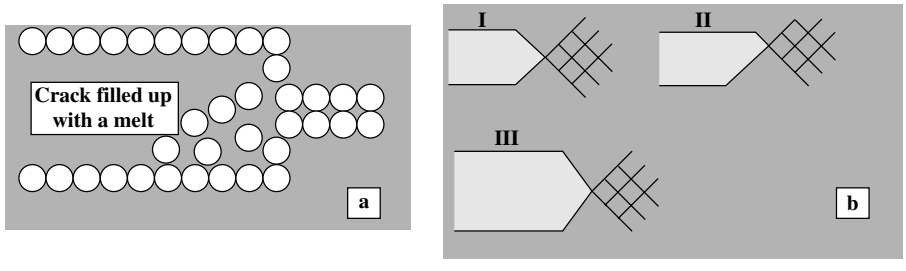

Figure 7.92 *Sketches of (a) dissolution–Condensation and (b) adsorption-induced localized-slip Models of LMIE*

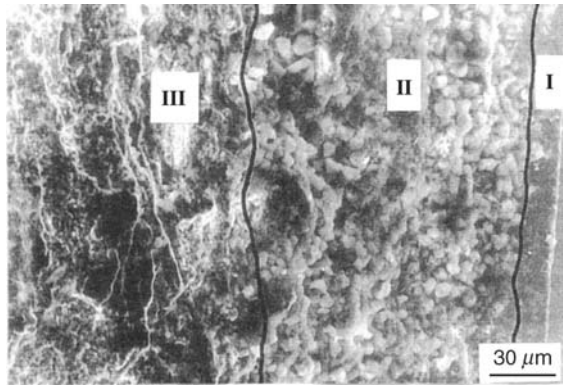

Figure 7.93 *Overall image of the fracture surface of nano-Ni after delayed failure in the presence of Hg*

Experimental data on crack growth rates and conditions such as grain size, grain boundary energy, stress and temperature available for Cu–solid Bi[4] permits the development of a model given in Figure 7.94. According to this model the two major processes for crack growth (failure) under SMIE conditions are: (i) grain boundary sliding (GBS) that occurs because of the applied stress and results in creation of pile-ups of grain boundary dislocations (i.e., permanent stress concentration) at triple junctions. This process reaches a stable state (i.e., a balance between the number of incoming and leaving dislocations) in a short period of time, which leads to sustaining a certain level of local stress concentration σ_{GB} at the joints. (ii) On the other hand, atoms of the low-melting-point metal (metal coating in Figure 7.94) penetrate into the GB by surface self- and/or grain boundary diffusion, i.e., their concentration at the GB, as well as at the triple joints constantly increases.

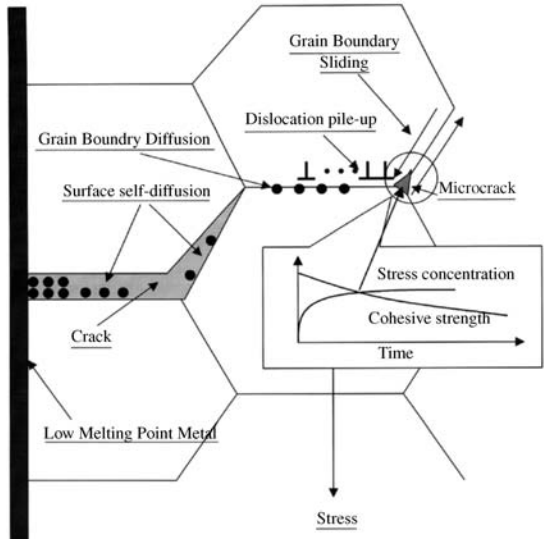

Figure 7.94 *Scheme of the model of SMIE*

Because atoms of LMPM are known to cause an embrittlement of GB, i.e., to reduce their cohesive strength σ_{CH}, this process will constantly weaken the GB. Once the cohesive strength at the triple joint (Figure 7.94) becomes equal to the local stress concentration, nucleation of a microcrack occurs. The microcrack will then propagate backward and coalesce with the main crack.

The kinetics of crack growth under SMIE conditions may be given by:[5]

$$\ell = d[1 - (D_s/D_b)] + 4\alpha^2 D_s \tau/\ell$$

where ℓ is the length of a crack; τ – time; d – grain size; D_s and D_b are coefficients of surface self-diffusion and grain boundary diffusion, respectively. The kinetic coefficient α depends on the level of applied stress, temperature and some parameters of the system such as mutual solubility, interfacial energy, etc. It may be either calculated or established for a system of interest (metal/LMPM) at any given temperature and stress.

The most important achievement of the kinetic model is its capability to describe almost all the experimental data on SMIE available so far.[6–8] It means that the above equation may be used for prediction of the lifetime in industrial applications where LMPM are used, for example as protective coatings.

7.18.2 Conclusion

The brief analysis of the microscopic models of LMIE and SMIE indicates that the dissolution–condensation model of LMIE may be considered as realistic and provides a solid background for its further development. The micromechanism of SMIE seems to be reliable and may be used for prediction of the lifetime.

References

1. W. M. Robertson, Propagation of a Crack Filled with liquid Metal, *Metallurgical Transactions, AIME*, **236**, 1478–1486, (1966).
2. E. Glickman, K. Sarychev, V. Demin and Y. Goryounov, Fracture kinetics and mechanism for Cu under deformation in surface-active melts, Communication IV: The LME macroscopic manifestations and micromechanism, *Soviet Physics Journal*, **7**, 2–29, 1976 (in Russian).
3. V. V. Popovich, Mechanism of Liquid Metal Induced Embrittlement, *Physical-Chemical Mechanics of Materials*, No. **5**, 11–20, (1979) (in Russian).
4. V. I. Igoshev, L. G. Rogova, L. I. Trusov and T. P. Khvostantseva, Embrittlement of Nanocrystalline Nickel by Liquid Metals, *Journal of Materials Science*, **24**, 1569–1574, (1994).
5. E. E. Glickman and V. I. Igoshev, Micromechanism of Solid Metal Induced Embrittlement: Fractography and Kinetic Model, *Surface: Physics, Chemistry, Mechanics*, No. **3**, 104–112, (1989) (in Russian).
6. E. E. Glickman and V. I. Igoshev, Micromechanism of Solid Metal Induced Embrittlement: Comparison of the Model with the Experiment, *Surface: Physics, Chemistry, Mechanics*, No. 128–136 (1989) (in Russian).
7. S. P. Lynch, Solid Metal Induced Embrittlement, *Materials Science and Engineering*, **108**, 203–212, (1989).
8. J. J. lewandowski, Y. S. Kim and N. J. H. Holroyd, Lead-Induced Solid Metal Embrittlement of an Excess Silicon Al-Mg-Si Alloy at Temperatures of −4°C to 80°C, *Metallurgical Transactions A*, **23A**, June, 1679–1689, (1992).

7.19 Nitrate SCC of Carbon Steel in the Heat Recovery Steam Generators of a Co-generation Plant

The carbon steel casings of heat recovery steam generators (HRSGs) in a co-generation plant developed cracks that originated on the inside surfaces. The HRSGs receive hot exhaust gases from the primary gas turbines (GTs), which are fuelled with pipeline natural gas. The GTs were initially operating without any suppression of nitrogen oxides (NO_x).

After about 2 yr, some of the cracks were found to have penetrated right through the ¼-in-thick casings. The casings are fitted with insulation on the inside (hot gas side). Steel samples cut from the casing walls revealed:

(i) fine cracks propagating through the steel from the inside surfaces;
(ii) the presence of relatively large amounts of nitrate ion on the inside surfaces.

The nitrate ions originated from nitric acid that was condensing on the relatively cool walls of the casings behind the insulation. Nitric acid was formed in the GT exhaust gases by the combination of water vapor (formed from combustion of the hydrocarbon fuel and from moisture in the combustion air) and nitrogen oxides.

Figure 7.95 shows a schematic of a typical combined-cycle power plant. High temperatures produced by GTs cause nitrogen and oxygen in the combustion air to combine to form nitrogen oxide gases NO_x. The NO_x levels of around 200 ppm were produced in each GT train.

7.19.1 Materials

ASTM A 36 structural grade carbon steel which analyzed: 0.25% C; 0.04% P; 0.05% S; 0.40% Si; tensile properties of 1/4-inch HRSG plates are: yield point (min) 36 ksi; tensile strength 58–80 ksi and elongation (min) 23%.

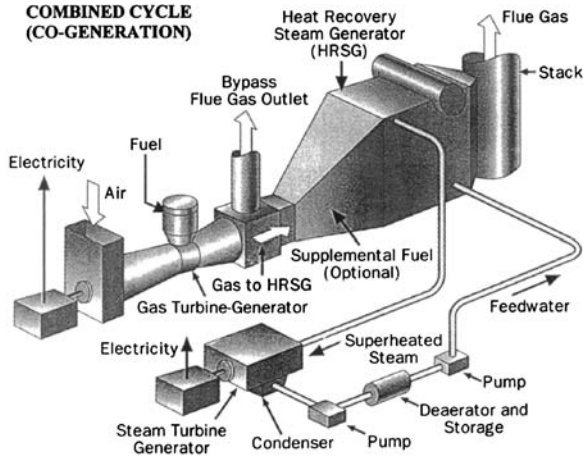

Figure 7.95 *Schematic of a typical combined-cycle power plant*

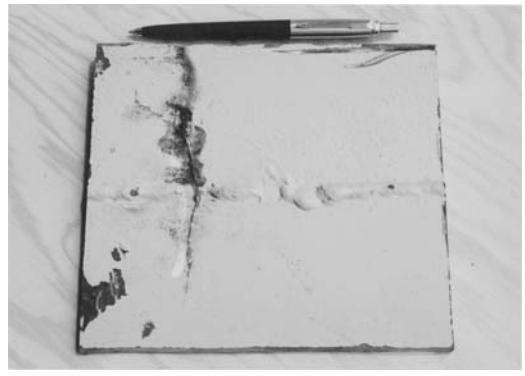

Figure 7.96 *The outer surface of a steel plate cut from an HRSG casing; note the crack running perpendicularly to the butt-weld. (Reproduced from COM'1999 and 2005 with permission from the Metallurgy Society of CIM)*

The sample had a butt-weld across the middle and a crack running perpendicular to the weld. Figure 7.96 shows the outer (painted) surface of the sample plate, and Figure 7.97 shows the inner surface.

The majority of cracks associated with welds joining the plates cracks are perpendicular to the weld and run through the weldment. Repair-welded areas cracked again.

Metallography showed small branched cracks originating at the inner surface and running across the ¼-inch plate (Figure 7.98). Highly branched intergranular cracks leads to the conclusion that the cause is intergranular stress–corrosion cracking (SCC), (Figure 7.99).

Chemical analysis of the following material was carried out:

(i) corrosion products on the inner surface of the casing sample and on the surfaces of the main through-crack;
(ii) material oozing out of cracks on the casing walls;

Figure 7.97 Plate 9 *The inner surface of a steel plate cut from HRSG casing; note the rusty corrosion products and adhering insulation (top). (Reproduced from COM'1999 and 2005 with permission from the Metallurgy Society of CIM)*

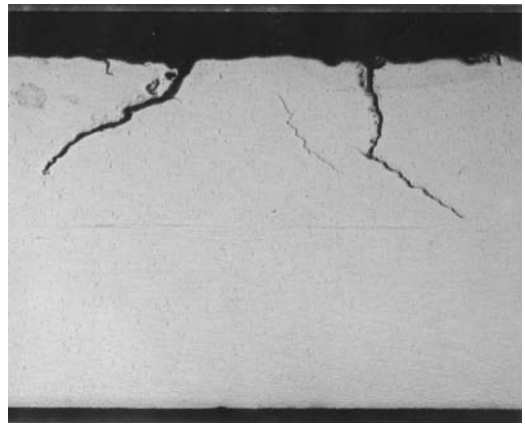

Figure 7.98 *Cross-section through casing plate; small cracks originating from inner surface of the plate (∼ × 8)*

(iii) 'used' thermal insulation material that had been in service immediately adjacent to the inner surface of the casing steel; and

(iv) 'unused' thermal insulation material (the same as the used insulation) that had never been in service, showing the presence of large amounts of nitrate and small amounts of sulfate and chloride (Table 7.9). Concentrations in the original solid samples are given in Table 7.10.

X-ray photoelectron spectroscopy (XPS) performed on corrosion products still adhering both to the inner surface of the casing sample and to the surfaces of the through-crack showed high levels of nitrogen (present as nitrate) along with iron, manganese, oxygen, magnesium, calcium, silicon and some carbon. XPS of the material on the crack surfaces gave very similar results, detecting relatively large amounts of nitrogen (as nitrate) along with iron, manganese, oxygen, magnesium, calcium and carbon.

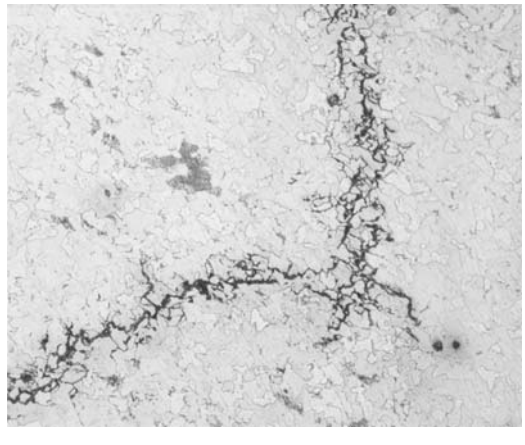

Figure 7.99 *Close-up view of intergranular branched crack (∼ × 300).*

Table 7.9 *Chemical analyses of samples taken from the HRSGs*

Sample	pH	Nitrate (as N) (mg/L)	Sulfate (mg/L)	Chloride (mg/L)
Corrosion products on casing	5.3	760	2	6
Material oozing from cracks	8.5	4540	25	11
'Used' insulation next to casing	6.8	1280	16	4
'Unused' insulation	6.4	<0.05	0.65	0.12

Table 7.10 *Recalculated nitrate results from Table 7.9*

Sample	Nitrate (mg/kg)	Nitrate (%)
Corrosion products on casing	17,660	7.8
Material oozing from cracks	143,600	63.6
'Used' insulation next to casing	16,200	7.2
'Unused' insulation	<2	

The nitrate results from Table 7.9 were recalculated to determine concentrations in the original solid samples. Table 7.10 gives the recalculated data.

7.19.2 Conclusions

Intergranular cracks in the carbon steel casings of heat-recovery steam generators (HRSGs) were caused by nitrate SCC. The relatively cool walls of the casings (behind the thermal insulation) encouraged condensation of the nitric acid that provided the necessary nitrate ions. Nitric acid was formed by the interaction of water vapor with the oxides of nitrogen present in the gas turbine exhaust gases that entered the HRSGs. The butt-welds in the carbon steel plates (1/4-in-thick) which formed the HRSG casings were not stress-relieved after welding. Residual stresses provided the necessary tensile stresses for SCC to occur.

References

1. E. Hamner, *Corrosion Data Survey, Metals Section*, 5th edn, National Association of Corrosion Engineers, Houston, Texas, USA, 1974, 130, 268.
2. *The Metals Handbook*, 9th edn, Vol. 13, Corrosion, ASM International, Metals Park, Ohio, USA, 1987, 146, 326, 328, 365.
3. *The Metals Handbook*, 9th edn, Vol. 11: Failure Analysis and Prevention, ASM International, Metals Park, Ohio, USA, 1986, 210, 211, 214.
4. D.N. Miller, Mass Transfer in Nitric Acid Absorption, *Journal of the American Institute of Chemical Engineers*, **33**(8), 1987, 1351–1358.
5. R.G.I. Leferink and W.M.M. Huijbregts, Nitrate Stress Corrosion Cracking in Waste-Heat Recovery Boilers, *Anti-Corrosion Methods and Materials*, **49**(2), 118–126 (2002).
6. E.D.D. During, *Corrosion Atlas*, 3rd edn, Elsevier, New York, 1997, 34 (Case History 01.01.18.04).

7.20 Performance of Stainless Steel Rebar in Concrete

Corrosion mitigation of steel rebar in concrete can be achieved by:

(i) selection of corrosion-resistant steel;
(ii) use of coatings;
(iii) addition of inhibitors such as calcium nitrite to the concrete;
(iv) addition of concrete sealers;
(v) use of membranes;
(vi) use of thicker concrete overlay;
(vii) cathodic protection.

The first mode of corrosion mitigation involves selection of material such as stainless steel rebar and the merits and demerits of this mode are detailed below.

The mechanical and physical properties of some alloys chosen for rebar in concrete are relevant in the performance of the alloys. The mechanical properties of some reinforcing bar alloys are given in Table 7.11. All the steels except duplex steels were subjected to cold work in order to increase their strength. Duplex S31803 steel in the annealed state exhibits strength levels close to the values of the cold-worked alloys.

Some physical properties such as coefficient of thermal expansion and modulus of elasticity of the alloys are given in Table 7.12. Other factors such as resistance to general and pitting corrosion, pitting resistance equivalent number (PREN) and the relative cost ratios are also given in Table 7.12.

Pitting resistance equivalent number (PREN) is derived from a formula involving chromium, molybdenum and nitrogen contents of the alloys. These numbers are used as a qualitative indication of the pitting resistance of the alloys. The higher the PREN value the greater the resistance of the alloys to corrosion due to chloride.

Table 7.11 *Mechanical properties of some reinforcing bar alloys*

Alloy	Tensile strength, (MPa)	Yield strength, (MPa)	Elongation (%) in 2 in. typical minimum values	Brinell hardness
Steel, cold-worked	540	400 min	25	200
Steel, epoxy-coated	540	400 min	25	200
S30400 stainless ~10%, cold-worked	750	600	37	200
S30453 stainless ~10%, cold-worked	730	500	37	200
S31600 stainless ~10%, cold-worked	810	520	40	220
S31653 stainless ~10%, cold-worked	660	495	40	210
Duplex S31803, annealed	680	480	25	290

Table 7.12 *Physical properties and corrosion resistance of steels*

Alloy	Coefficient of thermal expansion 20–100°C (μm/mm/°C)	Modulus of elasticity $\times 10^3$	Magnetic?	Corrosion resistance general/ pitting	PREN*	Approximate cost ratio
Steel	11.7	205	Yes	poor/poor	—	1.0
Steel epoxy coated	11.7	205	Yes	poor/poor	—	1.7–2.0
S30400	17.0	200	No	good/fair	18	3.8
S30453	16.8	200	No	good/fair	21	4.3
S31600	16.5	200	No	Good/better	25	4.4
S31653	16.5	200	No	Good/better	27	4.7
Duplex S31803	13	190	Yes	Very good/ Very good	36	4.4

*Pitting resistance equivalent number

The results obtained from tests on carbon steel and stainless steels on exposure to 0.5 and 2% chloride for period of two years at 80% relative humidity are noted in Table 7.13. It is obvious from the data that carbon steel failed in 2% chloride along with severe cracking of the concrete sample. The stainless steels did not corrode and the concrete also remained intact without cracking.

Life cycle costs for the Öland Bridge in Sweden were calculated in the case of carbon steel and type 304 and 316 stainless steels for a period of 120 yr. The data are shown in Figure 7.100. For a period of 18 yr the cost of carbon steel is less than type 304 stainless steel which in turn is less than 316 stainless. For a life between 18 to 120 yr the stainless steels cost by far less than carbon steel.

Table 7.13 *80% relative humidity; temperature cycled between 25 and 65°C; steel and stainless steel examined after 2 yrs*

		Concrete sample condition	Rebar condition
Steel	0.5% chloride	No cracking observed	No significant corrosion observed
	0.2% chloride	Severe cracks, all samples broken after 4 months	Severe corrosion on entire rebar
304 Stainless Steel	0.5% Chloride	No cracking observed	No corrosion observed on rebar
	0.2% Chloride	No cracking observed	No corrosion observed on rebar
316 Stainless Steel	0.5% Chloride	No cracking observed	No corrosion observed on rebar
	0.2% Chloride	No cracking observed	No corrosion observed on rebar

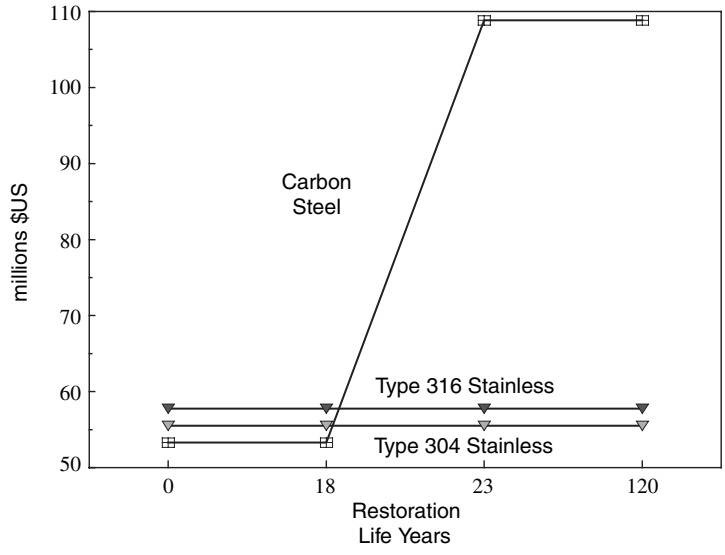

Figure 7.100 *Life cycle cost figures for Öland Bridge*

The standards for stainless steel rebar are available as follows:

- U.K. Standard specification BS6744: 1986 Austenitic Stainless Steel Bars (Type 304, 304L, 316 and 316L)
- ASTM Standard A 955-96, Standard Specification for Deformed and Plain Stainless Steel Bars for Concrete Reinforcement (Type 304, 304L, 316, 316L, 316 LN and duplex 2205)

In the case of carbon steel reinforcement, restoration work is required within a 20-yr period. The restoration work means longer journeys, delivery delay, consumption of more fuel by idling cars, added costs due to drilling, blasting, crushing, and transport of aggregate, cement and the related consumption of energy in the manufacture need to be considered in the calculation of costs. These are indirect costs applicable in the case of carbon steel reinforcements, while stainless steels are free from these indirect costs.

Bibliography

1. Cederquist, S.C., NACE, *Materials Performance*, p. 20, May 1999.
2. The Learning Channel, *Building Better Bridges*, March 25, 2000.
3. Nickel Development Institute, *Building Better Bridges*, **14**(1), September 1998.
4. McDonald, D.B., Sherman, M.R., Pfeifer, D.W., and Virmani, Y.P., *Stainless Steel Reinforcing as Corrosion Protection*, Nickel Development Institute, Reprint Series 14034, August 1995.
5. National Research Council of Canada, *Corrosion Behaviour of Pre-stressed Stainless Steel Embedded in Chloride Contaminated Concrete*, Report A-264 1. 1, December 4, 1997.

6. *Corrosion Evaluation of Epoxy-coated Metallic-clad and Solid Metallic Reinforcing Bars in Concrete*, US Department of Transportation, Federal Highway Administration, Publication FHWA-RD-98-153, December 1998.
7. BS 6744:1986, British Standard Specification for Austenitic Stainless Steel Bars for the Reinforcement of Concrete, British Standards Institution, London, United Kingdom.
8. ASTM A 955M-96, Standard Specification for Deformed and Plain Stainless Steel Bars for Concrete Reinforcement(Metric), American Society for Testing and Materials, West Conshohocken, PA.
9. Smith, F.N., C.P. Cutler, D.J. Cochrane, Stainless Steel Reinforcing Bars, *Proceedings, Conference on Understanding Corrosion Mechanisms* in: *Concrete*, Massachusetts Institute of Technology, Cambridge, MA, July 1997.
10. Kilworth, S.R., J. Fallon, Stainless Steels for Reinforcement, *Concrete Durability in the Arabian Gulf, 2nd Regional Concrete Conference*, Bahrain, 19-21 March 1995.
11. *Case Study, LCC – Life Cycle Costing and Stainless Steels, River Crossing Highway Bridge*, Euro Inox, European Stainless Steel Development & Information Group, Zurich, Switzerland.
12. Wiseman, A., Public Works and Government Services Canada, Nepean, Ontario, Canada, September 5, 1997, private communication.

7.21 Corrosion of an Oil Storage Tank

A 3-mm hole developed at the bottom of an oil storage tank after 25 months of service. This premature failure of the tank raised questions as to the construction material of the tank as well as the possibility of corrosive elements (i.e., water) present in the contents of the tank.

The tank was received with two sections removed for analysis. One section was taken from the top, where minimal corrosion was expected to be seen, while the second section was taken from the bottom, where the tank had failed.

The chemical composition of the steel, determined by spectrographic analysis, is listed in Table 7.14. Based upon this composition, the steel is most likely SAE-AISI 1006 or 1010. The thickness of the steel averaged 1.84 mm.

7.21.1 Sampling

The overall dimensions of the larger section, cut from the bottom of the tank, are 70 cm long by 33 cm wide. The section appears to be about 80% corroded on the surface. The surface corrosion along the edge appears to be smeared and brushed as a result of the cutting. The underlying metal substrate has mill scale attached and is blue-gray in appearance.

Table 7.14 *Spectrographic analysis of tank steel*

Elements	C	Si	Mn	Cr	Ni	Mo	Cu	Al	P	S	Sn
Percentage found	0.05	0.014	0.25	0.02	<0.02	>0.03	0.005	0.014	0.016	0.010	0.001

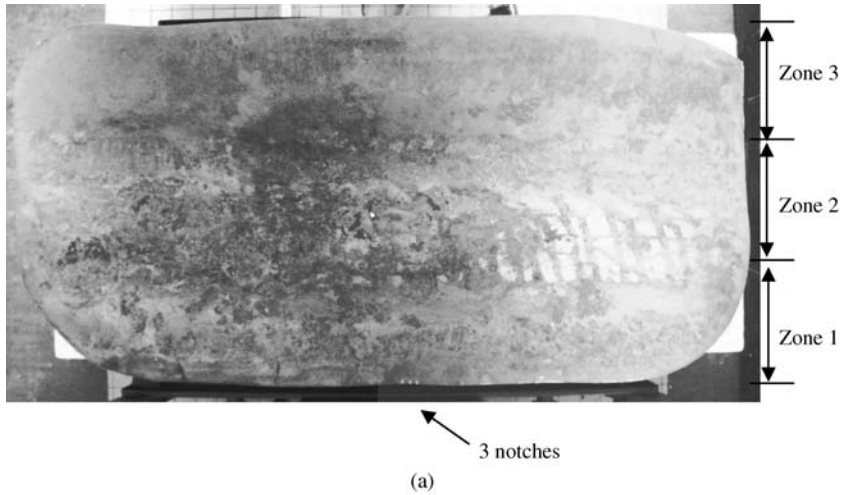

(a)

(b)

Figure 7.101 *Sections showing: (a) the bottom of the tank; (b) the top of the tank. (Copyright of Her Majesty the Queen in Right of Canada, as represented by the Minister of Natural Resources, 2004, 2006)*

Three notches, shown in Figure 7.101, were cut along one of the long edges of the section to mark the orientation. The section was then divided into three imaginary zones. One third of the section (shown in Figure 7.101) is zone 1, the centre third of the section (the very bottom of the tank) is zone 2, and the remaining third of the section is zone 3. Particular attention was paid to zone 2 because the failure occurred at the very bottom of the tank.

7.21.2 Color

The corrosion product seen here is rust. There are areas along zone 1 that are light orange to dark orange, and the rust is uniform. The central band (zone 2) has areas of dark orange to brown. Those areas that are dark in color contain significant sediment on the surface. Zone 3 is light orange to dark red.

7.21.3 Corrosion

About 80% of the surface area is corroded. Some of this corrosion is merely surface corrosion that can be easily rubbed off with a finger. However, there are areas that have deep corrosion that penetrates past the mill scale and into the metal substrate. Once the corrosion has penetrated past the mill scale, pitting occurs, and these areas are generally marked by deep pitting. This can be seen by chipping away the severe corrosion present on the mill scale and revealing the pitting below.

7.21.4 Pitting

Pitting can be seen along the very bottom of the tank. There is severe pitting along the length of the sample where the shiny corrosion exists. The shiny corrosion may involve the mill scale, and there are some areas with severe pitting, one such area being shown in Figure 7.102. Obviously, the area with the hole is the most severely pitted, followed closely by an area on the right-hand side of the sample that was close to developing a second hole.

The smaller section cut from the top portion of the tank was examined and the general features are:

(i) the surface of the sample was clean and free from corrosion;
(ii) the color of the sample ranged from light to dark blue-gray which may be due to surface mill scale; light orange discolouration along one side was present;
(iii) the surface had an adherent mill scale and a small amount of corrosion product was present in one corner of the sample;
(iv) the sample showed a minor (trace) of corrosion; the mill scale is present with any spallation;
(v) the sample showed no pitting.

Figure 7.102 *Close-up image of the section cut from the bottom of the tank, showing the hole that formed, causing the tank to fail. (Copyright of Her Majesty the Queen in Right of Canada, as represented by the Minister of Natural Resources, 2004, 2006)*

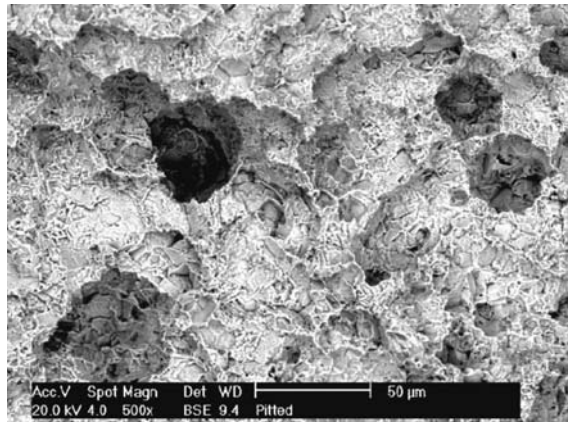

Figure 7.103 *SEM micrograph; SE mode, showing the extent of pitting corrosion. (Copyright of Her Majesty the Queen in Right of Canada, as represented by the Minister of Natural Resources, 2004, 2006)*

7.21.5 Pitted Surface

Examination of the metal surface after removal of the corrosion product showed the extent of the pitting corrosion taking place. At higher magnification, the pits appeared quite deep (~150 µm) with an external surface diameter of ~50 µm (Figure 7.103).

Pitting Phenomenon. Pitting is a deep narrow attack seen in a restricted oxygen environment that often causes rapid penetration of the metal substrate. One characteristic common to all forms of pitting is attack in a localized region that surrounded by a region of very little or no corrosion.[1,2]

The restricted level of oxygen within the pit causes that area to become anodic while the external surfaces then become cathodic. Consequently, the metal at the base of the pit dissolves to form ions. These ions migrate to the mouth of the pit where they are hydrolyzed to form hydroxide deposits. As the hydroxyl ions are consumed at the mouth of the pit, the net acidity within the pit increases.[1]

The following equations demonstrate the primary anodic reaction:

$$Fe^0 - 2e^- \rightarrow Fe^{2+}$$
$$½O_2 + H_2O + 2e^- \rightarrow 2OH^-$$
$$Fe^0 + ½O_2 + H_2O \rightarrow Fe^{2+} + 2OH^-$$
$$Fe^{2+} + 2OH^- \rightarrow Fe(OH)_2$$

Furthermore, the secondary mechanism then causes the pit propagation to become autocatalytic where one of the products formed in the reaction serves to accelerate it. Figure 7.104 describes the following mechanism. Pitting occurs in three stages: initiation, propagation and termination.

Initiation: factors that are believed to contribute to pit initiation are: (1) imperfections or defects in the metal oxide, passive, or protective layer between the metal substrate and its environment; and (2) exposure of the metal substrate to an aggressive medium.

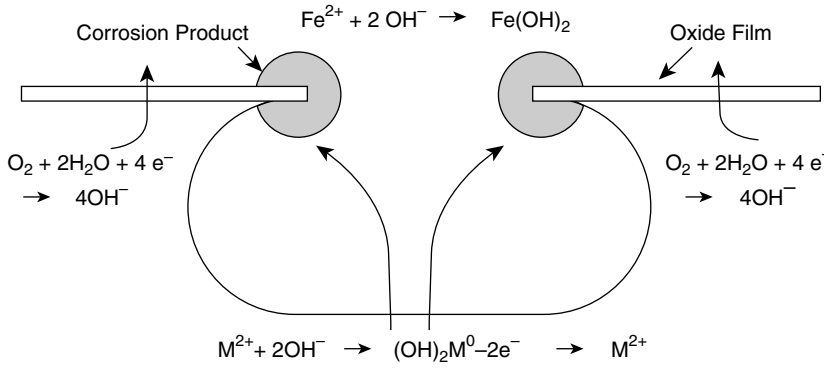

Figure 7.104 *Mechanism of pitting*[2]

Propagation: the corrosion is driven by the potential difference between the anodic base of the pit and the cathodic area surrounding the pit. Furthermore, reaction products formed autocatalyze the propagation reaction and cause the environment within to become even more aggressive.

Termination: the propagation of the pit may terminate due to an increased internal resistance to the local cell. This can be the result of the pit being filled with corrosion product or the cathodic area being filmed with corrosion product. Pitting will also terminate if the metal becomes dry. However, the pits may reinitiate once the metal substrate becomes wet again.

7.21.6 Factors Affecting Pitting

Defects or imperfections in the protective or passive layer between the metal substrate and the environment may affect pitting. Defects may be naturally occurring or the result of mechanical damage. In the case of fluid containers, stagnation of the solution tends to favor pitting. Movement or gentle flow conditions may help to alleviate pitting by preventing the formation of acid and alkaline area.[2,3] The rate of pit penetration seems to decrease as the number of pits increase since adjacent pits must share the same cathodic surface area.[3]

7.21.7 Discussion

The tank failed by pitting corrosion from the inside. Notwithstanding the general corrosion over parts of the tank and the pitting that was observed, the compositions of both the steel and the oil were within specification. The corrosion observed could have been caused by water, but the source of such water and the method by which it entered the tank could not be established.

The premature failure of the tank was most likely caused by water that entered the tank, either before or during service. Regardless of the source of water, the quantity and composition of water in the tank were sufficient for the corrosion to penetrate the tank in 2 yr.

As indicated by EDS analysis, the oxide scale consisted mainly of oxide with some areas containing chlorides and/or sulfides. These sulfides and chlorides were not spread

over the entire surface and did not form a pattern. Sulfur peaks in EDS analysis indicated only trace amounts of sulfur. Chloride, however, was a little higher, but could have resulted from contamination after sectioning the tank. The chloride concentration in the scale in this small amount would not be significant to the corrosion process without the presence of water. There are other factors that could increase the corrosion rate, such as temperature, debris, contamination, etc. However, all these factors have little or no effect on corrosion if there is no water present.

Therefore, it is assumed that there was a small amount of water in the tank as a result of condensation, the water would react with the steel until the water was completely consumed by the reaction. When the water was consumed, the reaction stopped. When more water was available, then the reaction would start again. The rate-determining step was the water supply to the steel.

7.21.8 Conclusions

1. High levels of sulfur and chlorine were found in the partially corroded and severely corroded samples.
2. The pits on the corroded surfaces averaged 50 μm in width and 150 μm in depth.

References

1. *Metals Handbook*, 10th edn, Vol. 1 *Properties and Selection: Irons, Steels and High-performance Alloys*. ASM International, March 1990, p. 150.
2. Van Droffelaar and Atkinson. *Corrosion and its Control*, 2nd edn. NACE International Book Publications, 1995, pp. 25, 33–35.
3. NACE International Basic Corrosion Course. NACE International, 1999, pp. 5:7–5:10.

7.22 Corrosion of a Carbon Steel Tank in a Phosphatizing Process

The phosphatizing of aluminum plates consists of exposure of the plates to: (i) alkali precleaning at pH 9 at 130°F; (ii) water rinse at 110°F; (iii) phosphatizing at pH 4.5, at 130°F; (iv) two stages of water rinse at 100–110°F; and (v) sealer.

The composition of phosphatizing solution and the initial precleaning solution is given in Table 7.15; a schematic of the process is shown in Figure 7.105. The composition of

Table 7.15 *Composition of precleaning and phosphatizing solutions*

Precleaning solutions	Phosphatizing solutions
Alkoxylated alcohol	Phosphoric acid
Block copolymer	Sodium benzoate
Sodium ethylhexyl sulfate	Sodium nitrobenzene sulfonate
Sodium Alkanate	

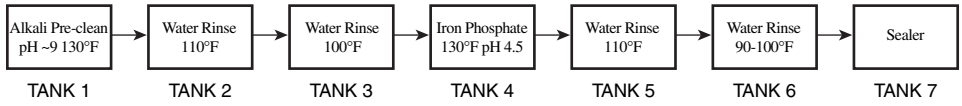

Figure 7.105 *Schematic of the process*

the carbon steel tank and aluminum plates used are given in Tables 7.16 and 7.17 respectively.

Severe corrosion at the bottom of the phosphatizing tank was observed, which led to the failure of the tank through the formation of hole in the tank. Perforation was also observed in the tank, involving rinse cycle operation. During the operations the aluminum plates fall and reach the bottom of the tanks. Considerable corrosion was also observed in the portions of the tanks where the aluminum plates or filings are in close contact with the floor of the steel tank.

Based on studies of optical micrographs and energy dispersive X-ray (EDX) analysis of the deposits on the floor plate and side plate the following mechanism has been proposed.

A porous or cracked mill scale can expose the steel substrate underneath the rinse solution, Table 7.18. The mill scale will then act as a cathode, and the exposed area, which will be an anode, will undergo galvanic corrosion. Due to the large-area cathode compared with the small-area anode (exposed through the cracks in the mill scale), the corrosion rates will be quite high. The presence of copper within the mill scale can increase the cathodic reduction rate, thus accelerating further the corrosion of steel in the exposed regions.

A disbanded mill scale can also result in a situation where the rinse water can flow and fill the gap between the mill scale and the steel substrate through the cracks/pores in the mill scale. This will result in an occluded cell situation where the chemistry of the electrolyte within the occluded cell, usually at a lower pH, will be very different from that of the bulk rinse water. This can result in the corrosion of the steel substrate. The presence of chloride will significantly increase the steel corrosion rate, as chlorides can readily migrate to the occluded region where they can lower the water pH quite readily and can increase the rate of the balancing cathodic reaction. The observation that trace levels of chloride were found within a corrosion perforation supports this discussion.

In the previously stated mechanism the presence of copper in the mill scale has been surmised to accelerate the cathodic reduction rate. Reference to Table 7.19 shows that the concentrations of copper and chloride in the corrosion deposit on the side plate of tanks are twice the concentrations detected in the mill scale located on the bottom plate. But the observed corrosive attack is more severe on the bottom plate than on the side plate.

Table 7.16 *Composition of carbon steel*

Element	Percentage
C	0.12
Mn	0.5
S	<0.02
P	<0.02

Table 7.17 *Composition of aluminum 6063 plates*

Element	Percentage
Si	0.2–0.6
Fe	0.35
Cu	0.10
Mn	0.10
Mg	0.45–0.90
Cr	0.10
Zn	0.10

The chemical environment and the steel composition are constant, but the bottom plate is in intimate contact with the aluminum panel while such a contact is not present in the case of the side plate. Thus, the aluminum plate may have a role in the corrosion process.

7.22.1 Galvanic Corrosion

Since two dissimilar metals are in contact galvanic corrosion may be suspected. When two dissimilar conducting materials in electrical contact with each other are exposed to an electrolyte, a galvanic current flows from one to the other. Galvanic corrosion is that part of the corrosion that occurs at the anodic member of the couple and is directly related to the galvanic current by Faraday's Law. Under a coupling condition, the simultaneous additional corrosion taking place on the anode of the couple is known as the local corrosion.

Factors Involved in Galvanic Corrosion

(a) Potential difference between the coupled metals;
(b) reactions such as dissolution, oxygen reduction, hydrogen evolution;

Table 7.18 *Composition of water used in operations*

	Composition (mg/L)	
Component	Incoming	Stage 4 after one day*
Na	18.8	62.7
K	1.0	-
Mg	18.8	20.6
Ca	32.6	26.4
F	0.21	0.7
Cl	4.6	8.2
Nitrate, as N	0.32	-
Sulfate	0.60	3.6
Hardness, as $CaCO_3$	159	151
pH	8.17	8.01
Conductivity (mho/cm)	364	470
Alkalinity as $CaCO_3$	192	206
Copper	0.26	0.066

*It is useful to analyze the water samples after 1 month of operation specifically for chloride

Table 7.19 *Composition of surface deposit from EDX*

Element	Weight % on stage 3 tank	
	From floor	From side
Copper	0.31, 0.29, 0.46, 0.41, 0.28	0.66, 1.15
Chloride	0.12, 0.41, 0.82, 0.81, 0.27	0.40, 1.40

(c) metallurgical factors such as alloying, heat treatment, mechanical work;
(d) surface conditions such as surface treatments, passive film, corrosion products;
(e) Geometric factors: area, distance, position, shape, orientation;
(f) environmental factors: moisture, wet/dry cycle, climate, solar radiation;
(g) electrolyte properties such as ionic species, pH, conductivity, temperature, volume, flow rate.

Among the factors governing galvanic corrosion, metallurgical and geometric factors are fixed in the present context since the aluminum panels and the steel tanks cannot be changed in the operations. Environmental effects do not apply to the present situation. Thus, the reversible electrode potentials, the reactions occurring at the electrodes, surface conditions such as passive film and corrosion products and electrolyte properties do play a significant role in the present context of galvanic corrosion.

The galvanic series of metals and alloys in seawater is given in Table 7.20. From this series it is clear that steel and 2024 aluminum are in close proximity. From their positions it is inferred that steel is cathodic and aluminum is anodic in seawater. The corrosion potentials of iron and aluminum measured after immersion in various media for 24 h are given in Table 7.21. It is seen from these data that the corrosion potentials of iron and aluminum are very nearly the same in 0.1 *M* sodium chloride. Some studies on the galvanic action of the steel–aluminum couple in fresh waters such as pure, river, lake and underground water and salt solutions are noted in Table 7.22. In one of the studies, the

Table 7.20 *Galvanic series in seawater*

Cathodic ↑	Gold
	Silver
	Copper
	Tin
	Chromium
	stainless steel
	Steel or iron
Anodic ↓	2024 aluminium
	Cadmium
	Pure aluminum
	Zinc
	Magnesium

Table 7.21 *Corrosion potentials (mV) after 24 h immersion*

Metal	0.1 *M* HCl	0.1 *M* NaCl	0.1 *M* Na_2SO_4	0.1 *M* NaOH
Fe	−557	−710	−720	−389
Al	−731	−712	−505	−1351

potential–time curves were obtained in solutions containing different amounts of sodium chloride, as shown in Figure 7.106. It is significant to note that at a sodium chloride concentration of 100 ppm and below aluminum is distinctly cathodic to mild steel, but after a time lapse of 5 days it is slightly cathodic. Potential–time curves for iron and aluminum were also reported in other media such as distilled water, 0.05% sodium sulfate, 0.05% sodium bicarbonate and city water. It is seen from these figures that aluminum is more noble or cathodic to steel. It is clear from this that polarity reversal occurs in this system, resulting in aluminum becoming cathodic and steel becoming anodic.

The polarity reversal is sensitive to temperature. Polarity reversal occurs faster at higher temperature.

Galvanic corrosion rates (mils) of some couples after 16 yr exposure to seawater and fresh water are given in Table 7.23. In the cae of carbon steel/aluminum the data show that in fresh water carbon steel corrodes to a greater extent than aluminum which provides further evidence for polarity reversal of the steel/Al couple in fresh water.

It has been well documented that polarity reversal is due to the formation of passive film and its breakdown. In the case of aluminum it should be noted that the passive oxide, being amphoteric, is stable in the pH range of 4–9 and the film breakdown occurs at very high chloride concentrations (Figure 7.106).

7.22.2 Localized Corrosion

The aluminum panel and the bottom of the steel tank are in intimate contact, separated by a small amount of solution and this might result in crevice corrosion as well as pitting corrosion when the trapped chloride concentration is high. This form of localized corrosion can lead to perforations and eventual failure.

Table 7.22 *Studies on galvanic action*

Example	Measurement, atmosphere		Reference
Steel–Al	Weight-loss measured	Automotive parts	1
Steel–Al	Fresh waters (pure, rivers, lake, underground) Polarity reversal	E_{corr} measured	2
Steel–Al	Salt solutions	Galvanic potential and current measured	3

1. R. Baboian, G. Haynes and R. Turcotte, ASTM STP 978, H.P. Hack (Ed.), American Society for Testing and Materials, Philadelphia, PA, p. 249, 1988.
2. D.R. Gabe and A.M. El-Hassan, *Br. Corr. J.*, **2l**(3), 185, (1986).
3. L.M. Wing, J. Commander, J. O'Grady and T. Koga, SAE Paper 97 1004, 1997.

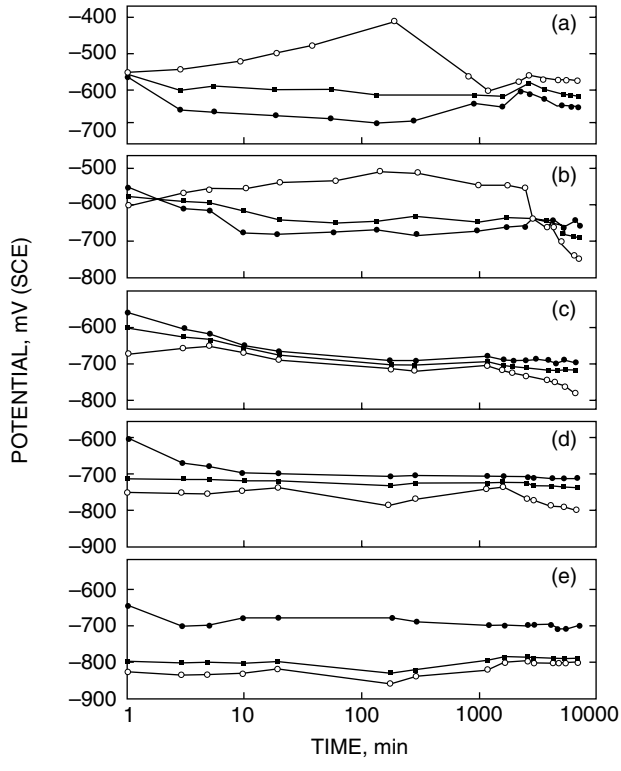

Figure 7.106 *Potential–time curves for mild steel and aluminium couples and uncoupled in saline water. (a) 100 ppm NaCl; (b) 312 ppm NaCl; (c) 10.25% NaCl; (d) 1.0% NaCl; (e) 20.0% NaCl;*

Table 7.23 *Galvanic corrosion rates (mils) of alloys after 16 yrs exposure**

Strip/Plate	Seawater	Fresh water
316 SS. steel/carbon steel	0.1/49.5	0.0/32.4
Carbon steel/aluminum	1.6/7.8	17/9.4
Carbon steel/copper	350/2.9	77.7/0.2
Carbon steel/302 stainless steel	298/0.8	52.7/0.0

*D. Massinon, D. Dauchelle, and J.C. Charbonier, *Mater Science Forum*, **44–45**, 461, (1989).

7.22.3 Overall Corrosion Scenario

It is possible to surmise, based on the foregoing discussion, that either one or all the following processes of corrosive attack may be involved:

(i) galvanic corrosion involving the mill scale as cathode and the steel as anode; in addition disbanded mill scale can lead to occluded cell situation and hence perforation; the high concentrations of copper in the mill scale can accelerate galvanic corrosion;
(ii) polarity reversal of the steel/Al couple was lead to galvanic corrosion of steel; this may be accelerated by the copper although the source of copper is not known since the Al plate contains only 0.1% and the water has 0.3 ppm copper;
(iii) localized corrosion such as crevice and pitting when the electrolyte is trapped between the Al panel and steel bottom plate.

In order to suggest preventive measures it is necessary to identify the corrosive mode in the system. The following outline of laboratory studies should help to identify the major corrosive mode.

1. Measure potential–time curves for steel/Al couple in solutions of interest (tanks 3,4,5 compositions);
2. Potentiodynamic polarization curves for steel and Al in solutions of interest;
3. Simulated laboratory corrosion rates of steel/Al in solutions of interest both with added copper and without copper;
4. EDX analysis of samples from laboratory tests and field samples.

7.23 Underground Corrosion of Water Pipes in Cities

This section summarizes a study to determine the causes and mechanism of water main failures.

7.23.1 Observations

A total of 17 pipe failures and soil samples were studied by metallurgical and analytical evaluation and the following points have been noted.

In almost all the failures, including failure of the service saddle on an asbestos-cement 10-inch water pipe, corrosion from the soil side was to great extent responsible for the failures.

Cast iron pipes give a corrosion rate in the range 0.21–0.58 mm/yr (average rate 0.41 mm/yr) in a typical soil environment. The failure appeared as a localized attack in the form of pitting leading to complete perforation of the pipe walls. Graphitic corrosion involving selective leaching of steel matrix resulting in a loss of strength and mechanical properties, ultimately leading to pipe rupture, was observed. Both localized corrosion and graphitization resulted in gradual wall thinning and produced cracks in the pipe.

Loss in mechanical properties such as reduced tensile strength of cast iron pipes contributed to the pipe failures.

The corrosion rate of ductile iron pipes in soils was in the range 0.62–2.5 mm/yr with an average of 1.11 mm/yr which is twice the rate of cast iron pipe. Failure of ductile iron pipe was solely due to localized pitting corrosion leading to pipe wall perforation.

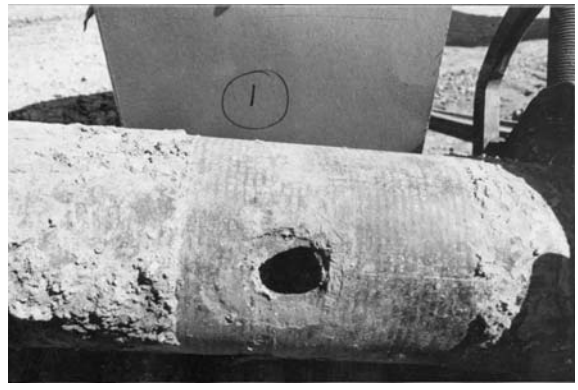

Figure 7.107 *Cast iron pipe: O.D. 176 mm (6 in) by 10 mm (0.4 in) W.T.; single large corrosion hole, ~5 cm (1.97 in) diameter*

There was no indication of pipe failure due to the defects of the pipe material. With the exception of one example corrosion of both ductile iron and cast iron pipes from the water side was negligible.

Deterioration of water pipe fittings such as service saddles contributes to water main failures. This type of failure may be due to galvanic corrosion since the pipe is cast or ductile iron, saddle is either bronze, steel or cast iron and the service line is made of copper.

Chemical and physical analysis of the soils where the failures of pipe were observed showed the soils to be either corrosive or very corrosive. The soils consisted of wet salty clay containing irons with resistivity in the range of 820–4200 Ω cm. A strong relationship between the corrosion rate of buried cast and ductile iron pipes and soil resistivity was found.

Thin bituminous coatings on the ductile and cast iron pipes peeled and flaked. In addition rust spots were also present.

The pipes and fittings were wrapped with polyethylene film and no evidence was found that these pipes were protective from corrosive attack.

Figures 7.107 and 7.108 show the corrosive attack on samples of cast iron pipe and ductile iron pipe buried under the soil for 20 and 9 yrs, respectively. The large hole in

Figure 7.108 *Circumferential failure of the pipe had originated at larger corrosion pit, and progressed in a brittle manner around the circumference in both directions*

cast iron pipe (Figure 7.107) and the corrosion pit and perforation in ductile iron pipe (Figure 7.108) show the severe nature of soil corrosion.

Cathodic protection can reduce the extent of corrosion of iron pipes.

7.24 Corrosion in Drilling and Well Stimulation

Acidizing is the oldest and most commonly used technique for stimulating oil and gas wells.[1-10] The primary purpose of an acid treatment is to dissolve rock or other plugging solids and the choice of acid depends on:

(i) rock-dissolving capacity;
(ii) contact time;
(iii) solubility of reaction products;
(iv) extent of metal corrosion;
(v) compatibility of acid with reservoir fluids; and
(vi) density and viscosity of spent fluids.

In common with any acidification the temperature, acid concentration, amount of acid, velocity of injection, viscosity of acid and fluid loss properties of formation have profound effects on the reaction rate.

Acidizing involves treatment with either mineral acids such as HCl or HF or organic acids such as acetic or formic acid. The acids are used in combination with inhibitors. The general reactions involved are:

$$2HCl + CaCO_3 \longrightarrow CaCl_2 + H_2O + CO_2 \quad (1)$$

$$4HCl + CaMg(CO_3)_2 \longrightarrow CaCl_2 + MgCl_2 + 2H_2O \quad (2)$$

$$SiO_2 + 4HF \longrightarrow SiF_4 + 2H_2O \quad (3)$$

$$2HF + SiF_4 \longrightarrow H_2SiF_6 \quad (4)$$

$$2CH_3COOH + CaCO_3 \longrightarrow Ca(CH_3COO)_2 + H_2O + CO_2 \quad (5)$$

$$2HCOOH + CaCO_3 \longrightarrow Ca(HCOO)_2 + H_2O + CO_2 \quad (6)$$

The various types of acidizing and other additions are detailed below:

Matrix acidizing (acid squeeze). Acid is squeezed into the formation matrix including the pores; acid penetrates and enlarges flow channels and dissolving plugging particles.

Tubing wash. Removes rust, mill scale and precipitates 15% HCl with inhibitor is circulated in the tubing followed backwashing from the well.

Acid soak (acid wash). Acid is directed at the desired location or circulated back and front across perforations. Removes scales from well bore surfaces witout penetration into the formation near wellbore.

Underbalanced acid wash on uncased hole. Acid mixed with nitrogen is jetted against the borehole with coiled tubing as the well is flowing to remove wellbore 'skin' in horizontal wells.

Nonemulsifiers. Surfactants reduce surface tension of acid solutions; disperse and suspend fine solids.

Iron control agents. Citric acid, acetic acid and organophosphorus compounds complex iron and prevent the formation and precipitation of ferric hydroxide.

Anti-sludge agents. During acid treatment, sludge, consisting of asphaltenes, resin, paraffin and other high molecular weight hydrocarbons is formed. Addition of oil-soluble surfactants can prevent the formation of insoluble film.

7.24.1 Materials

The most commonly used metals in drilling and well stimulation[11–13] are low-alloy carbon steel (API Grades J-55, L-80, N-80; coiled tubing); quality tubing (grades QT-70, 80, 1000); chrome alloy steels (ASM Grade Cr-13, duplex steel).

Low-alloys steels are used for wellbore tubulars. Corrosion limits for jointed tubing is arbitrarily set at <0.05 pounds per square foot of tubing surface area which represents a loss of 1/1000 of an inch in wall thickness. Pitting deeper than 0.015 inch (0.381 mm) is not acceptable.

For the low-alloy steel used in coiled tubing the weight loss specification of 0.02 lb/ft^2 and zero pitting tendency should be met.

The guideline for high-alloy tubular materials is set at 0.05 lb/ft^2 chrome and duplex steels are used to fight bottom hole corrosion.

7.24.2 Corrosion Inhibition

Acid corrosion causes significant loss in metal along with pitting. The corrosion reactions are:[14–17]

$$Fe^0 \longrightarrow Fe^{2+} + 2e^- \qquad \text{Anodic oxidation}$$

$$2H^+ + 2e^- \longrightarrow H_2 \qquad \text{Cathodic reduction}$$

The hydrogen ion may be adsorbed on the surface of the metal or may form hydrogen atom which can produce molecular hydrogen by the combination of hydrogen atoms at the cathodic sites.

The inhibitors used in acid systems consist of organic amines which form an inhibitor film due to Fe–N interactions. Other inhibitors used consist of acetylenic alcohols such as propargyl alcohol.

Hexynol or Ethyl Octynol. The mechanism of inhibition by acetylenic alcohols consists of chemisorption followed by subsequent polymerization. For maximum inhibition the hydroxyl group has to be in the β- position to the acetylenic function and the acetylenic function should be terminal.

The synergistic blends consist of amines, acetylenic alcohols, surfactants and oils to make a readily dispersed product.

7.24.3 Corrosion in Underbalanced Drilling Operations

The underbalanced drilling technique minimizes the harmful effects of drilling fluid invasion by reducing the hydrostatic pressure of the drilling fluid.[14–17] This method requires nitrogen which may be accomplished by using nitrogen membranes. When nitrogen membranes are used, the impact of injecting 5–8% of oxygen into the drilling

fluid needs to be considered. The drilling fluids are water-based saline solutions which cause corrosion of casing, drill pipe and bottom hole assembly.

Oxygen, along with CO_2 or H_2S, causes severe corrosion.

$$\text{Fe} \longrightarrow \text{Fe}^{2+} + 2\text{e} \qquad \text{Anodic reaction}$$

$$\text{O}_2 + 2\text{H}_2\text{O} + 4\text{e} \longrightarrow 4\text{OH}^- \qquad \text{Cathodic reaction}$$

Above pH 4, the precipitation of ferric hydroxide can occur. The corrosion due to oxygen may also result in pitting.

Hydrogen cracking may occur when moist hydrogen sulfide is present and the steel is high-strength steel and under tensile stress. Inhibitors such as Nowcorr 800 (consisting of a film-forming amine and a component that reacts with H_2S) combats sulfide stress cracking (SSC).

Batch treatment of the inhibitor is based on the formula:

$$\text{Volume of inhibitor} = 12\,\text{L inhibitor} \times \text{inch diameter} \times \text{mile}$$

An additional 50% volume of inhibitor is added to compensate for the loss due to adsorption on solids.

In continuous treatment Nowcorr 800 is added to the drilling fluid or to the acid blends. The concentration depends on downhole conditions; temperature, total pressure and partial pressure of H_2S.

In the case of underbalanced acid wash treatments in sour environments, Nowcorr 800 is used in addition to the acid corrosion inhibitor such as Nowsco's AI-275 and CI-30.

References

1. Smith, C.F., Dollarhide and F.E., Byth, J.N., *J. Petroleum Technology*, 737–746 (1978).
2. Crow, C.W. and Minor, S.S., *Petroleum Society of CIM*, 1982, Paper No. 82-33-15.
3. Frenier, W.W., *SPE Paper No. 18468*, 1989 p 111–123.
4. Walker, S.M., Dill, R.W. and Bester, R.M., *Petroleum Society of CIM*, 1989. Paper No. 89-40-41.
5. Gidly, J.L., Neely, A.B., Nierode, D.E., Schechter, R.S., 1977. Course organized by Society of Petroleum Engineering of AIME.
6. Delorey, J.R., Taylor, R.S., *Petroleum Society of CIM*, 1985. Paper No. 85-36-38.
7. Dill, W. and Smolarchuk, P., 1988. *J. Canadian Petroleum Technology*, **27**(3), 75–78 (1988).
8. King, G.E., Society of Petroleum Engineers, SPE 14432 (1985).
9. Williams, B.B., Gidley, J.L. and Schechter, R.S., 1979. *Acidizing Fundamentals*; Vol. 6, Soc.Pet. Eng., pp. 100–103, 1979.
10. Nowsco Well Service Ltd., 1996. Acidizing, Service Supervisor Training Program.
11. Vicentini, B., Rondelli, B., Onofrio, G., Lazzari, L. and Cigada, A., *Corrosion*, 1987. Paper No. 43.
12. Burke, P.A., Dawson, J.L., Bailey, G. and Woollam, R.C., *Corrosion*, 1987. Paper No. 41.
13. Growcok, F.B., *Corrosion*, 1988. Paper No. 338.
14. Metcalf, A.S. and Boles, J.L., *Paper presented at the 49th Annual Technical Meeting of The Petroleum Society*, Calgary, Alberta, 8–10 June 1998, Paper No. 98–87.
15. Hausler, R.H., *Proceedings 3rd European Sympsoium Corrosion Inhibitors, Ferrara, Italy*, 1971 pp. 399–410.
16. Hausler, R.H., *Materials Performance*, **13**(9), 16–22 (1974).
17. Hausler, R. H., 1979. American Chemical Society, Chapter 9.

Index

Corrosion Prevention and Protection: Practical Solutions V. S. Sastri, E. Ghali and M. Elboujdaini

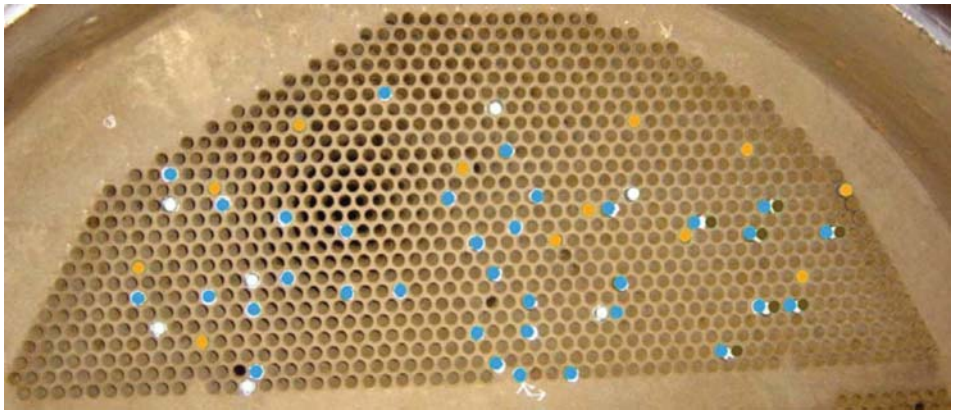

Plate 1 (Figure 7.36) *Top section of a condenser. White indicates tubes plugged with extensive internal corrosion; blue indicates tubes identified with internal corrosion to be monitored; and orange indicates tubes previously replaced. (Reproduced from COM' 1999 and 2005 with permission from the Metallurgy Society of CIM)*

Plate 2 (Figure 7.53) *Dark red and greenish spots on the outside surface*

Plate 3 (Figure 7.54) *Sample did not display the reddish spots on the exterior surface*

Plate 4 (Figure 7.55) *Sample did not display the reddish spots on the exterior surface, even though the surface contained a visible crack*

Plate 5 (Figure 7.56) *Internal surface of pipe is coated with a thick, black, tightly adherent scale*

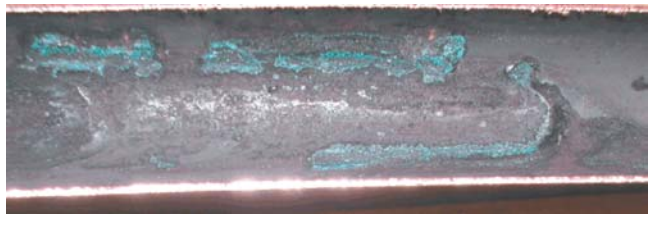

Plate 6 (Figure 7.57) *Internal surface shows green deposits*

Plate 7 (Figure 7.58) *Bright shiny copper can be seen with greenish deposits*

Plate 8 (Figure 7.73) *Section of tube showing the inner surface covered with a mixed black/brown scale that extended over the rolled portion of the tube for ~100 mm. (Reproduced from COM' 1999 and 2005 with permission from the Metallurgy Society of CIM)*

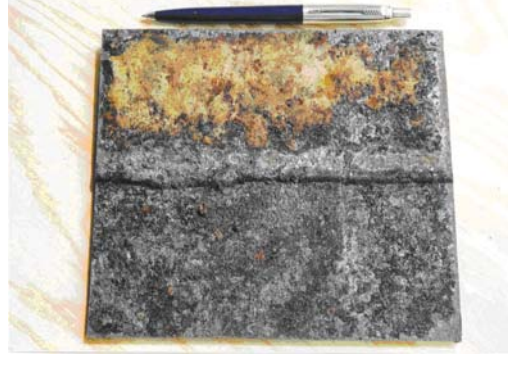

Plate 9 (Figure 7.97) *The inner surface of a steel plate cut from HRSG casing; note the rusty corrosion products and adhering insulation (top). (Reproduced from COM' 1999 and 2005 with permission from the Metallurgy Society of CIM)*